The Washington Climate Change Impacts Assessment

Evaluating Washington's Future in a Changing Climate

A report by

The Climate Impacts Group
University of Washington

June 2009

CLIMATE IMPACTS GROUP
Climate Science in the Public Interest

Recommended citation:
Climate Impacts Group, 2009. *The Washington Climate Change Impacts Assessment*, M. McGuire Elsner, J. Littell, and L Whitely Binder (eds). Center for Science in the Earth System, Joint Institute for the Study of the Atmosphere and Oceans, University of Washington, Seattle, Washington.
Available at: http://www.cses.washington.edu/db/pdf/wacciareport681.pdf

Front cover satellite image credit:

http://visibleearth.nasa.gov/view_rec.php?vev1id=4786
NASA - National Aeronautics and Space Administration
Visible Earth: A catalog of NASA images and animations of our home planet

Provided by the SeaWiFS Project, NASA/Goddard Space Flight Center, and ORBIMAGE

The Pacific Northwest is cloud-free in this SeaWiFS image. Multihued phytoplankton blooms are visible off of Washington's Olympic coast. Also visible in this image are: Fraser River outflow, snowcapped peaks of Mt. Olympus, Mt. Rainier, Mt. Adams, Mt. Hood, Mt. Jefferson, the Three Sisters, the North Cascades, and the Columbia and Snake River watersheds.

Metadata
** Sensor OrbView-2/SeaWiFS*
** Visualization Date 2000-09-26*
** The Visible Earth is part of the EOS Project Science Office located at NASA Goddard Space Flight Center.*

Small images credits:
Wheat: © 2009 www.photos.com
Coast; Seattle skyline: © J. Martin Grassley
McNary Dam: courtesy Bonneville Power Administration
Salmon: courtesy University of Washington News and Information
Forest: courtesy Climate Impacts Group, University of Washington

Report design: Beth Tully, Edit-Design Center, University of Washington

The Washington Climate Change Impacts Assessment

Evaluating Washington's Future in a Changing Climate

A report by

The Climate Impacts Group
University of Washington

June 2009

Edited by: Marketa McGuire Elsner
Jeremy Littell
Lara Whitely Binder

PRINCIPAL INVESTIGATORS:

Edward L. Miles, *Director, Climate Impacts Group and Bloedel Professor of Marine Studies and Public Affairs, School of Marine Affairs, University of Washington*
Dennis P. Lettenmaier, *Professor, Dept. of Civil and Environmental Engineering, University of Washington*

TEAM MEMBERS:

Jeremy Avise, *Atmospheric Modeling and Support Section, California Air Resources Board*
Derek B. Booth, *Stillwater Sciences and Dept. of Civil and Environmental Engineering, University of Washington*
Rick Boydston, *USDA-ARS, Washington State University IAREC*
Jay Brunner, *Tree Fruit Research and Extension Center, Washington State University*
Jeff Burkey, *King County Water and Land Resources Division*
Jack Chen, *Institute for Chemical Process and Environmental Technology, National Research Council Canada*
Serena H. Chung, *Laboratory for Atmospheric Research, Dept. of Civil and Environmental Engineering, Washington State University*
Lan Cuo, *Dept. of Civil and Environmental Engineering, University of Washington*
Meriel Darzen, *Kathy and Steve Berman Environmental Law Clinic, University of Washington*
Jeffrey S. Deems, *Dept. of Civil and Environmental Engineering, University of Washington*
Karen Dyson, *School of Marine Affairs, University of Washington*
Marketa McGuire Elsner, *Climate Impacts Group, University of Washington*
Richard A. Fenske, *Environmental & Occupational Health Sciences, University of Washington*
Cole Fitzpatrick, *Environmental & Occupational Health Sciences, University of Washington*
Thomas F. Graham, *Kathy and Steve Berman Environmental Law Clinic, University of Washington*
Gary Grove, *Irrigated Agricultural Research and Extension Center, Washington State University*
Alan F. Hamlet, *Climate Impacts Group and Dept. of Civil and Environmental Engineering, University of Washington*
David Hartley, *Northwest Hydraulic Consultants*
Marc J. Hershman, *School of Marine Affairs, University of Washington (in memoriam)*
Stewart Higgins, *Dept. of Biological Systems Engineering, Washington State University*
Jeffrey A. Hicke, *Dept. of Geography, University of Idaho*
John Hodges-Howell, *Kathy and Steve Berman Environmental Law Clinic, University of Washington*
Daniel D. Huppert, *School of Marine Affairs, University of Washington*
J. Elizabeth Jackson, *Dept. of Family Medicine and Dept. of Sociology, University of Washington*
Catherine Karr, *Dept. of Pediatrics and Environmental & Occupational Health Sciences, University of Washington*
Patrick W. Keys, *Dept. of Civil and Environmental Engineering, University of Washington*
Jennifer Krencicki Barcelos, *Kathy and Steve Berman Environmental Law Clinic, University of Washington*
Chad Kruger, *Center for Sustaining Agriculture & Natural Resources, Washington State University*
Brian K. Lamb, *Laboratory for Atmospheric Research, Dept. of Civil and Environmental Engineering, Washington State University*
Se-Yeun Lee, *Dept. of Civil and Environmental Engineering, University of Washington*
Dennis P. Lettenmaier, *Dept. of Civil and Environmental Engineering, University of Washington*
L. Ruby Leung, *Atmospheric Sciences and Global Change Division, Pacific Northwest National Laboratory*
Jeremy S. Littell, *Climate Impacts Group, University of Washington*
James A. Lutz, *College of Forest Resources, University of Washington*
Nathan Mantua, *Climate Impacts Group and School of Aquatic and Fishery Sciences, University of Washington*
Jennifer Marlow, *Kathy and Steve Berman Environmental Law Clinic, University of Washington*
Don McKenzie, *Climate Impacts Group and USDA Forest Service Pacific Northwest Research Station*
Kristian E.B. Mickelson, *Dept. of Civil and Environmental Engineering, University of Washington*
Edward L. Miles, *Climate Impacts Group and School of Marine Affairs, University of Washington*
Amber Moore, *School of Marine Affairs, University of Washington*
Philip W. Mote, *Climate Impacts Group and Office of the Washington State Climatologist*
Roger L. Nelson, *Dept. of Biological Systems Engineering, Washington State University*
Robert A. Norheim, *Climate Impacts Group*
Elaine E. Oneil, *Rural Technology Initiative, College of Forest Resources, University of Washington*
Richard N. Palmer, *Dept. of Civil and Environmental Engineering, University of Massachusetts Amherst*
Austin Polebitski, *Dept. of Civil and Environmental Engineering, University of Massachusetts Amherst*
Yun Qian, *Atmospheric Sciences and Global Change Division, Pacific Northwest National Laboratory*
Michael Robinson-Dorn, *Kathy and Steve Berman Environmental Law Clinic, University of Washington*
Eric A. Rosenberg, *Dept. of Civil and Environmental Engineering, University of Washington*
Roger A. Rosenblatt, *Dept. of Family Medicine, University of Washington*
Eric P. Salathé, Jr., *Climate Impacts Group, University of Washington*
Michael Scott, *Pacific Northwest National Laboratory*
Amy K. Snover, *Climate Impacts Group, University of Washington*
Anne C. Steinemann, *Dept. of Civil and Environmental Engineering and Evans School of Public Affairs, University of Washington*
Claudio O. Stöckle, *Dept. of Biological Systems Engineering, Washington State University*
Ingrid Tohver, *Climate Impacts Group, University of Washington*
Julie A. Vano, *Dept. of Civil and Environmental Engineering, University of Washington*
Nathalie Voisin, *Dept. of Civil and Environmental Engineering, University of Washington*
Lara C. Whitely Binder, *Climate Impacts Group, University of Washington*
Mathew Whiting, *Irrigated Agricultural Research and Extension Center, Washington State University*
Michael G. Yost, *Environmental & Occupational Health Sciences, University of Washington*
Yongxin Zhang, *Climate Impacts Group, University of Washington*

Table of Contents

Washington Climate Change Impacts Assessment

Evaluating Washington's Future in a Changing Climate

Executive Summary

Temperature records indicate that Pacific Northwest temperatures increased 1.5°F since 1920. Climate models used in the Intergovernmental Panel on Climate Change (IPCC) Fourth Assessment Report simulate the same historical warming by including both human and natural causes, and point to much greater warming for the next century. **These models project[1] increases in annual temperature of, on average, 2.0°F by the 2020s, 3.2°F by the 2040s, and 5.3°F by the 2080s (compared to 1970 to 1999[2]), averaged across all climate models[3].** Projected changes in annual precipitation, averaged over all models, are small (+1 to +2%), but some models project an enhanced seasonal precipitation cycle with changes toward wetter autumns and winters and drier summers. Increases in extreme high precipitation in western Washington and reductions in Cascades snowpack are key projections that are consistent among different projections of a high-resolution regional climate model.

[1] All changes are benchmarked to 1970 to 1999 unless otherwise stated.
[2] 20 different global climate models for greenhouse gas emissions under a "medium" emissions scenario (A1B) and 19 models for a "low" scenario (B1) - see Box 3 for more information. All statements in this document are for the "medium" scenario (A1B) unless otherwise stated.
[3] We use the term "projections" throughout to minimize confusion with "forecasts" and "predictions", both of which convey levels of certainty inappropriate for future climate. We use "likely" to convey relatively high certainty and "possibly" to convey less certainty.

Probable impacts associated with projected 21st century changes in Northwest climate include the following:

- **April 1 snowpack is projected to decrease by 28% across the state by the 2020s, 40% by the 2040s, and 59% by the 2080s compared with the 1916 - 2006 historical average.** As a result, seasonal streamflow timing will likely shift significantly in sensitive watersheds.
- **The Yakima basin reservoir system will likely be less able (compared to 1970 to 2005) to supply water to all users, especially those with junior water rights.** Historically (1916-2006), detrimental water shortages in the Yakima basin occurred in 14% of years. Without adaptation, shortages would likely occur more frequently: 32% of years in the 2020s, 36% of years in the 2040s, and 77% of years in the 2080s. Due to lack of irrigation water and more frequent and severe prorating, the average production of apples and cherries could decline by approximately $23 million (about 5%) in the 2020s and by $70 million (about 16%) in the 2080s.
- **Rising stream temperatures will likely reduce the quality and extent of freshwater salmon habitat.** The duration of periods that cause thermal stress and migration barriers to salmon is projected to at least double (low emissions scenario, B1) and perhaps quadruple (medium emissions scenario, A1B) by the 2080s for most analyzed streams and lakes. The greatest increases in thermal stress would occur in the Interior Columbia River Basin and the Lake Washington Ship Canal.

- **Due to increased summer temperature and decreased summer precipitation, the area burned by fire regionally is projected to double by the 2040s and triple by the 2080s[4].** The probability that more than two million acres will burn in a given year is projected to increase from 5% (observed) to 33% by the 2080s. Primarily east of the Cascades, mountain pine beetles will likely reach higher elevations and pine trees will likely be more vulnerable to attack by beetles.
- **Although few statistically significant changes in extreme precipitation have been observed to date in the Puget Sound, the Spokane area, or Vancouver/Portland, regional climate model simulations generally predict increases in extreme high precipitation over the next half-century, particularly around Puget Sound.** In that region, existing drainage infrastructure designed using mid-20th century rainfall records may be subject to rainfall regimes that differ from current design standards.
- **Climate change in Washington will likely lead to significantly more heat- and air pollution-related deaths throughout this century.** Projected warming would likely result in 101 additional deaths among persons aged 45 and above during heat events in 2025 and 156 additional deaths in 2045 in the greater Seattle area alone[5]. By mid-century, King County will likely experience 132 additional deaths between May and September annually due to worsened air quality caused by climate change.

The significance of these regional consequences of climate change underscore the fact that historical resource management strategies will not be sufficient to meet the challenges of future changes in climate. Rather, these changes demand new strategies. Options for adapting to climate change vary between sectors (e.g., between water resources and forest ecosystems) and even within sectors (e.g., between watersheds) depending on the unique characteristics of the systems being considered. This assessment highlights some of the likely impacts of future changes in climate in Washington. There is more work yet to be done, however, including (1) continuing work to identify and quantify impacts in these and other sectors, and (2) analyzing the adaptation options appropriate to specific impacts, specific locations, management goals, and jurisdictions. Additionally, the range of projected climates from different global climate models (or regional climate models) could be explored more fully in future work to develop a range of impacts scenarios useful for making decisions under different levels of risk tolerance. Integration between the sectors is also very important because the nature of some impacts is synergistic within and between sectors.

[4] Relative to 1916 - 2006.

[5] Relative to 1980 - 2006.

Box 1: Climate Change, Climate Variability, and Weather

In this assessment, it is necessary to distinguish between climate change (the long term trend), climate variability (year-to-year or decade-to-decade variations), and weather (the daily to seasonal changes with which we are all familiar). Pacific Northwest events – storms, floods, winters that seem colder and summers that seem hotter - need to be put in an appropriate context and time frame. Such events can be associated with climate, but only over many years – a single flood, back-to-back snowy winters, or an extended drought don't necessarily signal a change in climate over longer time frames. Some common questions and their answers help distinguish these sometimes confusing terms.

Q. The last two winters have been cool in the Pacific Northwest. Has global warming stopped?

A. No. Rising greenhouse gases (carbon dioxide, methane, and others) continue to produce increasingly warmer temperatures. Additional upward or downward detours come from other important sources of climate variability. For example, an extremely strong tropical El Niño event helped make 1998 a record warm year, not to be matched until 2005, a year with a mild El Niño event. The 2008 La Niña event produced temporary global cooling, but even so, the National Climatic Data Center still ranked 2008 as the 8th warmest year globally on record. Local cold weather, or heat waves, tell us nothing about global factors in climate like the effects of rising greenhouse gases.

Q. Isn't the climate record dominated by natural variability?

A. Yes, but natural causes and natural variability cannot explain the rapid increase in global temperatures in the last 50 years. Scientists have searched for other explanations – heat from the ocean, solar variability, cosmic rays, instrumental error – and have used sophisticated statistical techniques, and nearly every study concludes that the rising temperature is a result of rising greenhouse gases. Laboratory tests, ground-based instruments, and satellite instruments show that adding greenhouse gases to the atmosphere warms the surface – a simple physical fact.

1. Introduction

The 2007 Fourth Assessment Report of the Intergovernmental Panel on Climate Change (IPCC) states that 20th century warming of our climate is unequivocal and that human activities have contributed to increasing atmospheric greenhouse gas concentrations and therefore warming of the atmosphere and oceans. The IPCC expects global climate to continue warming in the 21st century, with the rate of warming somewhat dependent on the rate of human greenhouse gas emissions.

What are the consequences of a warming climate for the regional systems we rely upon for our livelihood? Certainly, we may no longer rely solely on past events, measurements, and management approaches to understand our natural and human resources. To help answer this question, the Washington State legislature passed House Bill 1303, which mandated the preparation of a comprehensive assessment of the impacts of climate change on the State of Washington. Passed in April 2007, HB 1303 specifically requested that the Departments of Community, Trade, and Economic Development and Ecology work with the University of Washington Climate Impacts Group (in collaboration with Washington State University and Pacific Northwest National Laboratory) to produce this comprehensive assessment.

To assess the future impacts of climate change, we integrate climate model projections into our understanding of the physical, biological, and human responses to climate that will shape Washington's future. This assessment presents the most complete and up to date look yet at the future climate of the Pacific Northwest (PNW) and the potential impacts of projected climate change on important ecological and economic sectors in Washington State, and provides Washington State decision makers and resource managers with information critical to planning for climate change.

This executive summary describes the key findings and conclusions of the Climate Impacts Group's Washington Climate Change Impacts Assessment. The Assessment addresses the impacts of global climate change over the next 50 years or more on eight sectors: Hydrology and Water Resources, Energy, Agriculture, Salmon, Forests, Coasts, Urban Stormwater Infrastructure, and Human Health (Box 2). In addition, the Washington Assessment addresses the need for adaptive planning and adaptation options within each sector. Full technical details are provided in a series of papers that together comprise the Washington Assessment.

Figure 1. Washington State and surrounding Pacific Northwest region. This assessment is focused on impacts of climate change on resources in the state of Washington, but the region as a whole has been considered because the climatic and hydrologic impacts require regional analyses. For example, Columbia River flow is related to conditions across an area much greater than Washington alone, the purple line outlines the Columbia River Basin.

Box 2: Impacts Assessment Sectors Covered in this Summary and Their Main Areas of Focus

- **Climate Scenarios:** changes in future temperature and precipitation for the Pacific Northwest and assessment of sub-regional climate change using regional climate models
- **Hydrology and Water Resources:** changes in the hydrology (streamflow, snowpack, soil moisture) and the water resources (water storage, irrigated agriculture) of Washington
- **Energy:** changes in the demand for and production of hydropower in Washington
- **Agriculture:** changes in the expected production of high-value crops in Washington
- **Salmon:** changes in the quality and quantity of salmon freshwater habitat in Washington
- **Forests:** changes in the productivity, distribution and disturbance of forest ecosystems in Washington
- **Coasts:** impacts in coastal areas of Washington
- **Urban Stormwater Infrastructure:** changes in storms and demands on urban stormwater infrastructure in Washington
- **Human Health:** impacts of heat waves and climate-related air pollution on health in Washington
- **Adaptation:** fundamental concepts for planning for climate change and options for adapting to the impacts identified in the above sectors

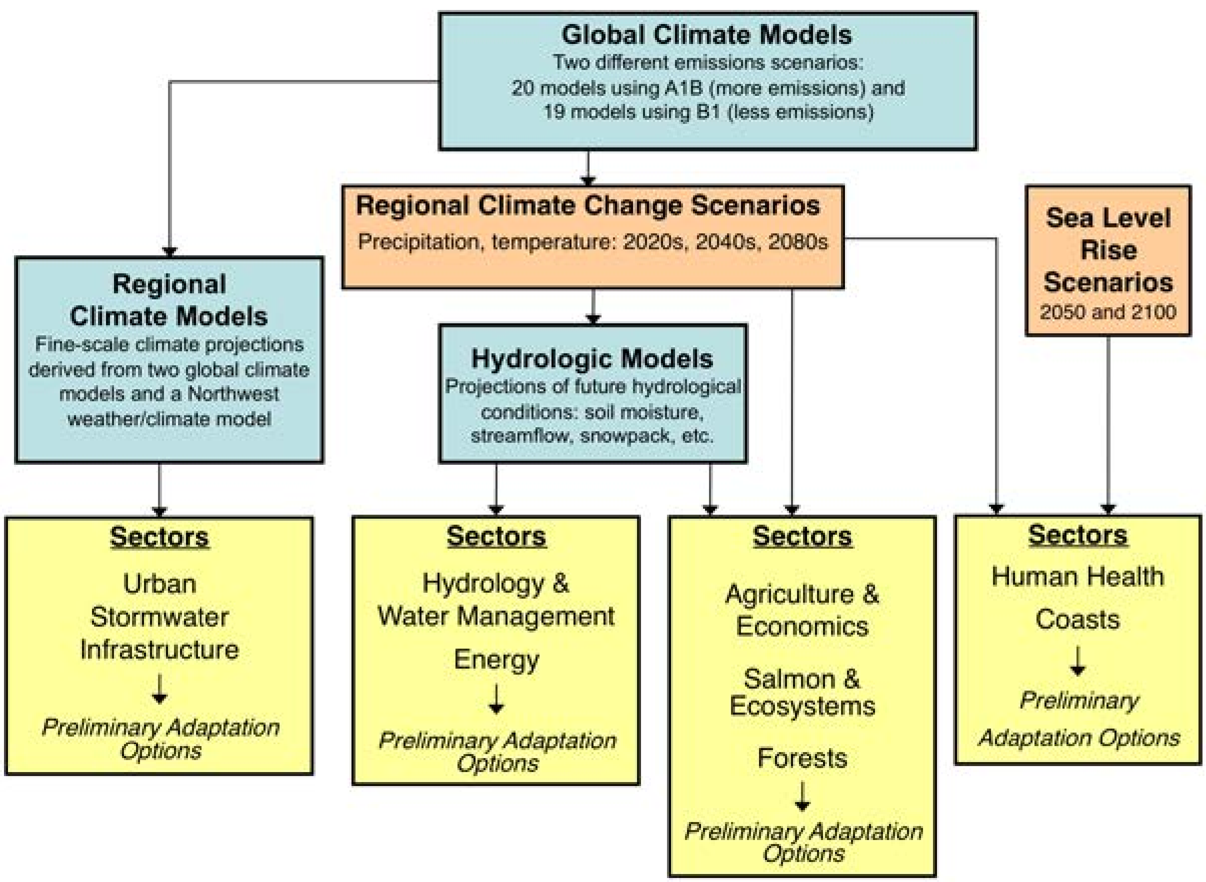

Figure 2. Summary of overall assessment approach. Sectors use one or more pathways in the flowchart above. Global and regional climate change information is related to sector impacts using hydrologic and regional climate models. This allows quantification of impacts at scales more useful for decision making. Adaptation options are developed based on the downscaled impacts.

1.1 Assessment Approach

The climate of the 21st century in Washington State will very likely be quite different from the climate we have witnessed in the past. The changes will in many cases be large, and the ultimate consequences will depend on how well we plan for and manage these changes. Effective planning requires sectorally and geographically specific information on which to base decisions. This assessment provides that information by using global climate model projections from the IPCC Fourth Assessment to develop regionally-specific climate change scenarios and then assessing some of the consequences for eight important sectors (Box 2) in Washington (Figure 1). Figure 2 illustrates the overall approach taken in this study. The sections that follow present the main conclusions for each sector. The Washington Assessment focuses on three 30-year windows in the 21st century, that is, the thirty years centered on the 2020s (2010 to 2039), 2040s (2030 to 2059), and 2080s (2070 to 2099)[6]. Projections for the 2080s are least certain of those presented here[7], because climate, human population growth, and energy use patterns are more difficult to estimate farther into the future.

1.2 Modeling Approach

Translating from projections of global climate change to impacts in Washington State requires making the climate projections more regionally specific and, in many cases, using those climate projections to develop other important information such as hydrologic projections (Figure 2). The process begins with 20 climate models from research groups around the world (models that were used in the 2007 IPCC Fourth Assessment). For each of these global climate models, two IPCC greenhouse gas emissions scenarios were used to represent different assumptions about future global development (see Box 3 for description of the emissions scenarios).

Six average climate change scenarios (called "composites") were created for the Pacific Northwest by averaging the model output for the region for each of the model runs during each time period of interest, i.e., 2020s medium emissions scenario (A1B), 2020s low emissions scenario (B1), 2040s medium emissions scenario (A1B), 2040s low emissions scenario (B1), and so on for the 2080s. In order to make the composite climate scenarios suitable for locally-specific climate impacts analysis, they were "downscaled" to create higher resolution climate projections in the Pacific Northwest. Each downscaled climate change scenario was used as input into a hydrologic model (Hydrology chapter) that uses climate and other information to develop projections of future hydrologic conditions, soil moisture and streamflow. In addition, a regional

Box 3: Future Emissions Scenarios: Low (B1) and Medium (A1B)

Greenhouse gasses are the main cause of 21st century climate change, and they stem from human choices in many arenas. They are by no means the only influence on climate, nor are they the only forcings considered by the IPCC. This assessment uses two future scenarios that differ in their assumptions about future greenhouse gas emissions and other factors influencing climate. The two scenarios are called "B1" and "A1B" – these letters refer to emissions scenario "families" developed for the IPCC, and described fully in the IPCC Special Report on Emissions Scenarios (SRES). A1B refers to a future where global population peaks mid-century and there is very rapid economic growth and a balanced portfolio of energy technologies including both fossil fuels and high efficiency technology that is adopted rapidly. B1 refers to a future where population is the same as A1B, but there are rapid economic shifts toward a service/information economy, the introduction of clean and resource-efficient technologies and emphasis on global solutions to economic, social, and environmental sustainability. A1B results in warmer future climates by the end of the century and can be considered a "medium" scenario in terms of warming, (it is not the warmest of all the IPCC scenarios). B1 has less warming (see section 2, Future scenarios), and could be considered the "low" warming scenario. The emissions scenarios were used by the IPCC as input into global climate models to project climate changes for 20 (scenario A1B) or 19 (scenario B1) climate models (Figure 2).

---

[6] The overlap between the 2020s and 2040s is due to the focus on time frames most useful for decision-making (first half of the 21st century) and also the need to have sufficient numbers of years (~30) for projection purposes.

[7] Uncertainty about future projections is dealt with in several ways in the climate modeling and impacts sectors. Uncertainty about future climate is addressed by using many (20) climate models, two emissions scenarios, and two approaches for "downscaling" climate projections specifically for the Pacific Northwest. This allows a range of possible futures, i.e., different climates, different rates of change, and different levels of detail to be considered in the impacts assessments. The models are also "weighted" by their ability to track observed changes, with better models receiving higher importance when calculating the average changes ("composite delta") projected by the climate models. Uncertainty about future impacts is addressed in the individual chapters when necessary.

climate model (Regional Climate chapter) was used to better understand the influence of sub-regional geographic variability (such as mountains) on future climate. Both downscaling and regional climate models provide increased resolution for future projections by accounting for the influence of smaller features than can be resolved in a global climate model. Detailed descriptions of how the future climate scenarios were used to generate sector-specific results are available in each sector chapter (Box 2).

This assessment is the first to combine such a diverse set of climate models, fine spatial resolution, and hydrologic modeling into an integrated climate impacts assessment. It is also the first to examine impacts on human health, agriculture, and urban stormwater infrastructure in the Northwest. In each of the following sections, the most important projections of future impacts are presented for each sector. Further details are in the sector chapters that follow this summary.

2. Future Climate Scenarios

Using 20 different climate models (see Scenarios chapter) to explore the consequences of two different greenhouse gas emissions scenarios results in a wide range of possible future climates for the Pacific Northwest. All of the models indicate that this future climate will be warmer than the past and together, they suggest that Pacific Northwest **warming rates will be greater in the 21st century than those observed in the 20th century**. All changes below are relative to the period 1970-1999 unless noted, and all are regionally averaged changes that apply to the Pacific Northwest including the state of Washington.

- **Climate models project increases in annual average temperature** of 2.0°F (range of projections from all models: +1.1°F to +3.3°F) by the 2020s; 3.2°F (range: +1.5°F to +5.2°F) by the 2040s; and 5.3°F (range: +2.8°F to +9.7°F) by the 2080s (Table 1).
- Climate models are able to match the observed 20th century warming (+1.5°F since 1920, or +0.2°F per decade for 1920 to 2000) in the Northwest, and foresee a warming rate of roughly +0.5°F per decade of warming in the 21st century (Figure 3).
- **Projected changes in annual precipitation vary considerably between models, but averaged over all models are small (+1 to +2%).** Changes early in the 21st century may not be noticeable given the large natural variations between wetter and drier years. Some models show large seasonal changes, especially toward wetter autumns and winters and drier summers. Regional modeling additionally points out areas and seasons that get drier even as the region gets wetter (Figure 4).
- **Warming is expected to occur during all seasons** with most models projecting the largest temperature increases in summer. The models with the most warming also produce the most summer drying.
- **Medium projections of sea level rise for 2100 are 2 inches to 13 inches (depending on location) in Washington State.** Substantial variability within the region exists due to coastal winds and vertical land movement[8]. The small possibility of substantial sea level rise from the melting of the Greenland ice cap lead to projections as high as 35 inches to 50 inches for 2100 (depending on location).
- **Regional climate models project some changes that are similar across global models, namely increases in extreme high precipitation in western Washinton and reductions in Cascade snowpack.** Regional climate models project a larger increase in extreme daily heat and precipitation events in some locations than the global climate models suggest.
- **Regional climate models suggest that some local changes in temperature and precipitation may be quite different than average regional changes projected by the global models.** For example, the two global models examined suggest winter precipitation will increase in many parts of the Pacific Northwest, but potentially decrease in the Cascades. Future research is required to understand if this is a trend consistent across many global models.

[8] Sea level rise projections for specific coastal areas can be found in: Mote et al. 2008. Sea-level rise in the coastal waters of Washington: A report by the Climate Impacts Group, University of Washington, and the Washington Department of Ecology.

	Temperature Change (F°)	Precipitation Change (%)
2020s	+2.0 (+1.1 to +3.3)	+1.3 (-9 to +12)
2040s	+3.2 (+1.5 to +5.2)	+2.3 (-11 to +12)
2080s	+5.3 (+2.8 to +9.7)	+3.8 (-10 to +20)

Table 1. Average and range of projected changes in temperature and precipitation for the Pacific Northwest. Reported averages are changes relative to 1970-1999, for both medium (A1B) and low (B1) scenarios and all models (39 combinations averaged for each cell in the table). The ranges for the lowest to highest projected change are in parentheses.

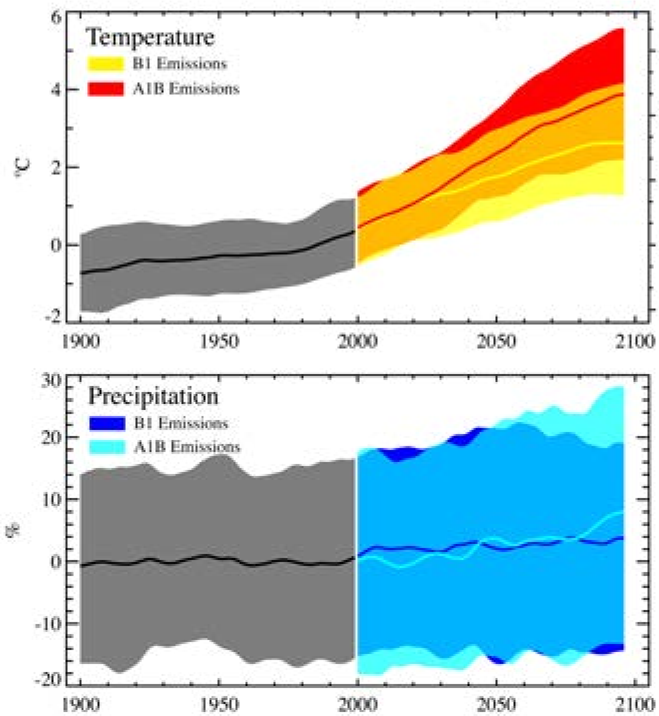

Figure 3. Simulated temperature change (top panel) and percent precipitation change (bottom panel) for the 20th and 21st century global climate model simulations. The black curve for each panel is the weighted average[9] of all models during the 20th century. The colored curves are the weighted average of all models in that emissions scenario ("low" or B1, and "medium" or A1B) for the 21st century. The colored areas indicate the range (5th to 95th percentile) for each year in the 21st century. All changes are relative to 1970-1999 averages.

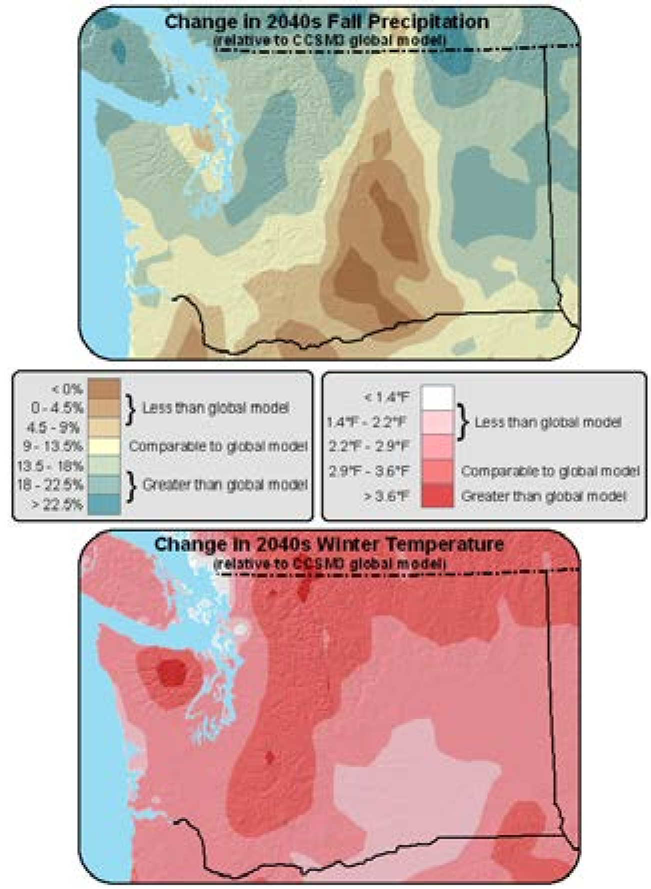

Figure 4. Differences between a regional climate model (WRF) and a global climate model (CCSM3) for projected changes in fall precipitation (September to November top) and winter temperature (December to February, bottom) for the 2040s. The global model produces a regionally averaged 11.7% increase in precipitation, but the regional model provides more detail (top), projecting some areas of increase (green) and some of decrease (brown) compared to the global model. Note that large increases are seen on windward (west and southwest) slopes and smaller increases on leeward (east and northeast) slopes. The global model produces a 3.6°F statewide averaged increase in winter temperature, while the regional model produces a statewide average 2.6°F warming. There are greater increases (darker red) at higher elevations and windward slopes, particularly the Olympic Mountains, North Cascades, and central Cascades. These differences illustrate the value of regional climate models for identifying sub-regional patterns and differences. The patterns of climate change differ depending on the global model being downscaled (we present only one here); nevertheless, the local terrain has a consistent influence on the results.

[9] The global climate models used by the IPCC were weighted by their ability to model observed regional Pacific Northwest data, with better performing models weighted more highly than those that had significant bias for the last half of the 20th century. See Scenarios chapter for more detail.

3. Hydrology and Water Resources

Projected hydrologic changes across the state are closely linked with future projections of precipitation and temperature. This assessment evaluated the hydrologic implications of climate change over the State of Washington as a whole, and in addition focused on several watersheds that are of particular importance from a water resources management standpoint. Impacts of climate change on Washington's water resources are herein divided into three parts: regional hydrology (snowpack, soil moisture, streamflow); water management in the Yakima River basin; and water management in the Puget Sound region.

Washington snowpacks are among the most sensitive to warming in the West because of their relatively low elevation. The impact of warming temperature on snowpack will differ with the type of river basin. There are three important types: *rain dominant* (precipitation falls primarily as rain, usually in low elevations, such as the Chehalis River), *snowmelt dominant* (precipitation falls primarily as snow and is released as snowmelt, usually in higher elevation basins or large river systems with mountainous headwaters like the Columbia River, and *transient* (mixed rain and snowmelt dominant, usually in mid elevations, such as the Yakima River). Especially in transient basins, a relatively small increase in temperature can significantly increase the fraction of winter precipitation falling as rain and decrease the amount of water stored in snowpack.

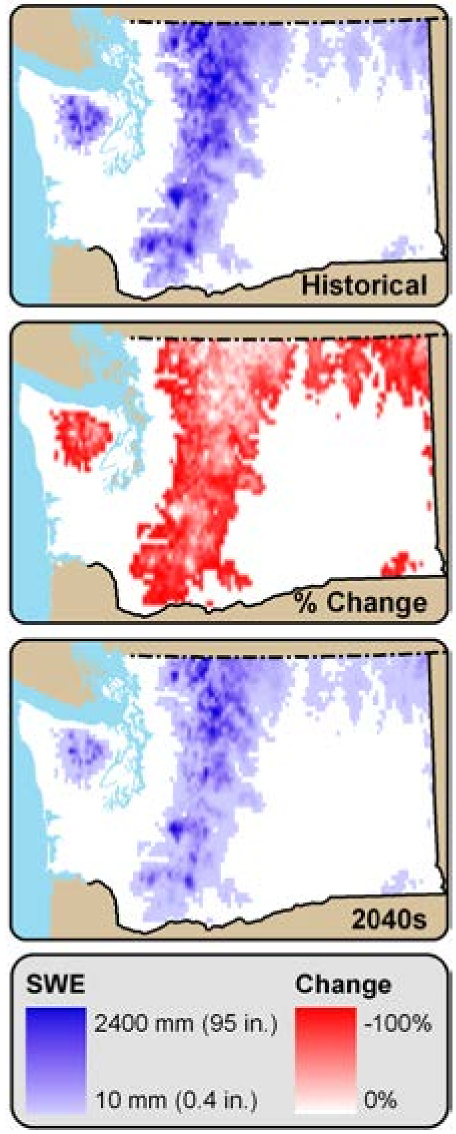

Figure 5. Summary of projected April 1 snow pack (measured as snow water equivalent, or SWE) and changes in April 1 snow pack for the 2040s, medium emissions scenario (A1B). Projected statewide decline relative to 1916-2006 is 37% to 44%. Snow water equivalent is simply the amount of water the snowpack would yield if it were melted.

3.1 Regional Hydrologic Impacts

- **April 1[10] snow water equivalent (snow water content) is projected to decrease** by an average of 28% to 29% across the state by the 2020s, 37% to 44% by the 2040s and 53% to 65% by the 2080s compared with the 1916 – 2006 historical mean (Figure 5).
- **By the 2080s, seasonal streamflow timing in snowmelt-dominated and transient rain-snow watersheds would shift significantly due to the decrease in snowpack and earlier melt (Figure 6).** Snowmelt-dominated watersheds will likely become transient, resulting in reduced peak spring streamflow, increased winter streamflow and reduced late summer flow. Transient basins will likely experience significant shifts, becoming rain dominant as winter precipitation falls more as rain and less as snow. Watersheds that are rain dominated will likely experience higher winter streamflow because of increases in average winter precipitation, but overall will experience relatively little change with respect to streamflow timing. These changes are important because they determine when water is available and how it must be stored.
- **For Washington State as a whole, projected changes in runoff depend strongly on season.**

[10] In watersheds that accumulate significant snowpack, SWE on April 1 is a common indicator of summer water supply.

- Average cool season (October to March) runoff is projected to increase 10% to 13% by the 2020s, 16% to 21% by the 2040s, and 26% to 35% by the 2080s, corresponding with reduced snowpack and increased precipitation falling as rain.
- Average warm season (April to September) runoff is projected to decrease 16% to 19% by the 2020s, 22% to 28% by the 2040s, and 34% to 43% by the 2080s, although warm season runoff is historically about half of cool season runoff so the magnitude of these changes is smaller.
- Annual runoff (water into streams) across the state is projected to increase 0% to 2% by the 2020s, 2% to 3% by the 2040s, and 4% to 6% by the 2080s. These changes are mainly driven by projected increases in winter precipitation.

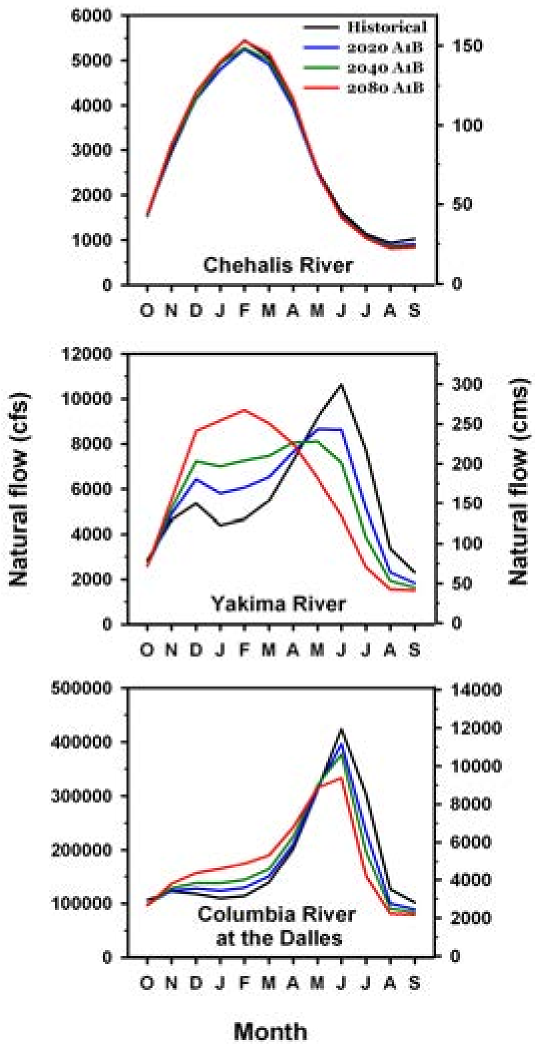

Figure 6. Historical and projected future hydrographs for three rivers under the medium emissions scenario (A1B). The Chehalis River represents a rain-dominated watershed, the Yakima River represents a transient watershed (mixed rain and snow), and the Columbia River represents a snowmelt-dominated watershed. Projected climate changes will influence the timing of peak streamflow differently in different types of hydrologic basins. The timing of peak streamflow does not change in rain-dominated basins because most of the precipitation falls as rain, both currently and in the future, and is therefore available for runoff as it falls. Timing of peak flow shifts earlier as climate warms in the transient and snowmelt-dominated basins because precipitation that historically fell as snow later falls as rain – snowpack melting ceases to dominate the timing of peak flow as the snowpack declines.

3.2 Water Management - Puget Sound

According to the 2000 census, the Puget Sound region contains almost 70% of Washington State's population. The water supply that is required to sustain the regional environment and more than 4 million people depends heavily on both natural and artificial means of storage. Puget Sound watersheds, like other basins that receive both rain and snow, are highly sensitive to changes in climate. Key findings on the implications of climate change for water management in the Puget Sound include the following:

- **The primary impact of climate change on Puget Sound natural water supply will be a shift in the timing of peak river flow from late spring (driven by snowmelt) to winter (driven by precipitation).** Puget Sound water supply systems will generally be able to accommodate changes through the 2020s in the absence of any significant demand increases. Projected changes in system reliability are small for the Everett, Seattle, and Tacoma systems in the 2020s. Even with future increases in demand, only the Tacoma system is projected to experience substantial reductions in reliability by the 2040s, primarily because water allocations within that system are closer to current system capacity.
- **Other aspects of system performance, such as reduced levels of summer and fall storage, occur as early as the 2020s.** Seasonal patterns of reservoir storage will be affected to varying degrees in all three systems. The amount of water stored in reservoirs will be lower from late spring through early fall, affecting water supply for municipal use and other

operating objectives such as hydropower production and the ability of the systems to augment seasonal low flows for fish protection. For example, in the Seattle system, October storage levels below 50% active capacity occurred historically 34% of the time, but are projected to increase to 58% in the 2020s, 67% in the 2040s, and 71% in the 2080s (scenario A1B).

3.3 Water Management and Irrigated Agriculture – Yakima

Crops in the Yakima Valley, most of which are irrigated, represent about a quarter of the value of all crops grown in Washington. The watershed's reservoirs hold 30% of streamflow annually and rely heavily on additional water storage in winter snowpack to meet water demand for agriculture. As in other watersheds across Washington, climate change is projected to cause decreases in snowpack and changes in streamflow patterns, making active management of water supply critical for minimizing negative impacts. Agricultural production increases caused by warming temperatures will likely be undermined by lack of water for irrigation.

- **The Yakima basin reservoir system will be less able (compared to 1970-2005) to supply water to all users, especially those with junior water rights.** Historically (1916-2006)[11], the Yakima basin has been significantly water short[12] 14% of the time. Without adaptations, current projections of the medium (A1B) emissions scenario estimate this value will increase to 32% (15% to 54% range) in the 2020s and will increase further to 36% in the 2040s and 77% in the 2080s.
- **Due to increases in temperature and changes in the timing and quantity of snowmelt and runoff, the irrigation season will likely be shorter, the growing season will likely be earlier by about two weeks, and crop maturity will likely be earlier by two to four weeks by the 2080s.**
- **Under the medium (A1B) emissions scenario, average apple and cherry yields are likely to decline by 20% to 25% (2020s) and by 40% to 50% (2080s) for junior water rights holders.** These declines are due to lack of irrigation water and more frequent and severe prorating, even though the direct effect of warming and CO_2 (carbon dioxide) would be to increase production (see Agriculture chapter).
- **The value of apple and cherry production in the Yakima basin is likely to decline by approximately \$23 million (about 5%) in the 2020s and by \$70 million (about 16%) in the 2080s.** These declines are buffered by senior irrigators and by price responses to smaller production. Overall, the risk of net operating losses for junior irrigators is likely to increase substantially.

[11] Simulation models for the historical period 1916-2006 were used to determine the frequency of water short years – see chapter 3, Hydrology and Water Resources, for details. Prorating began on the Yakima system in 1970.

[12] "Water short" is defined as 75% prorating (effectively, a legal loss of 25% of water rights during drought) for junior water rights holders.

4. Energy Supply and Demand

Hydropower accounts for roughly 70% of the electrical energy production in the Pacific Northwest and is strongly affected by climate-related changes in annual streamflow amounts and seasonal streamflow timing. Heating and cooling energy demand in Washington will be affected by both population growth and warming temperatures. Other factors influence energy supply and demand, but this assessment focuses on (1) the effects of projected warming and precipitation change on regional hydropower production, and (2) the effects of warming on energy demand, expressed in terms of heating energy demand (population times heating degree days, or the demand for energy for heating structures) and residential cooling energy demand (population times cooling degree days times the amount of air conditioning use, or the demand for energy for cooling structures).

- **Annual hydropower production (assuming constant installed capacity) is projected to decline by a few percent due to small changes in annual stream flow, but seasonal changes will be *substantial* (Figure 7).** Winter hydropower production is projected to increase by about 0.5% to 4.0% by the 2020s, 4.0% to 4.2% by the 2040s, and 7% to 10% by the 2080s (compared to water year 1917-2006) under the medium (A1B) emissions scenario. The largest and most likely changes in hydropower production are projected to occur from June to September, during the peak air conditioning season. Summer (JJA) energy production is projected to decline by 9% to11% by the 2020s, 13% to 16% by the 2040s, and 18% to 21% by the 2080s
- **Despite decreasing heating degree days with projected warming, annual heating energy demand**

is projected to increase due to population growth[13] (Figure 8). In the absence of warming, population growth would increase heating energy demand in WA by 38% by the 2020s, 68% by the 2040s, and 129% by the 2080s. For fixed 2000 population, projected warming would reduce heating energy demand by 11% to 12% for the 2020s, 15-19% for the 2040s, and 24% to 32% for the 2080s due to decreased heating degree days. Combining the effects of warming with population growth, heating energy demand for WA is projected to increase by 22% to 23% for the 2020s, 35% to 42% for the 2040s, and 56% to 74% for the 2080s. Increases in annual heating energy demand will affect both fossil fuel use for heating and demand for electrical power.

- **Residential cooling energy demand is projected to increase rapidly due to increasing population, increasing cooling degree days, and increasing use of air conditioning (Figure 8).** In the absence of warming, population growth would increase cooling energy demand in WA by 38% by the 2020s, 69% by the 2040s, and 131% by the 2080s. For fixed 2000 population, warming would increase cooling energy demand by 92% to 118% for the 2020s, 174-289% for the 2040s, and 371% to 749% by the 2080s due to the combined effects of increased cooling degree days, and increased use of air conditioning. Combining the effects of warming with population growth, cooling energy demand would increase by 165% to 201% (a factor of 2.6-3.0) for the 2020s, 363-555% (a factor of 4.6-6.5) for the 2040s, and 981-1845% (a factor of 10.8-19.5) by the 2080s. Increases in cooling energy demand are expected to translate directly to higher average and peak electrical demands in summer.
- **Taken together the changes in energy demand and regional hydropower production suggest that adaptation to climate change in cool season will be easier than in warm season.** Increases in hydropower production in winter will at least partially offset projected increases in heating energy demand due to population growth. Adapting to projected increases in cooling energy demand (which would result in increased electrical energy demand) will be more difficult because of reductions in hydropower production in the peak air conditioning season. These effects in summer will put additional pressure on other sources of energy.

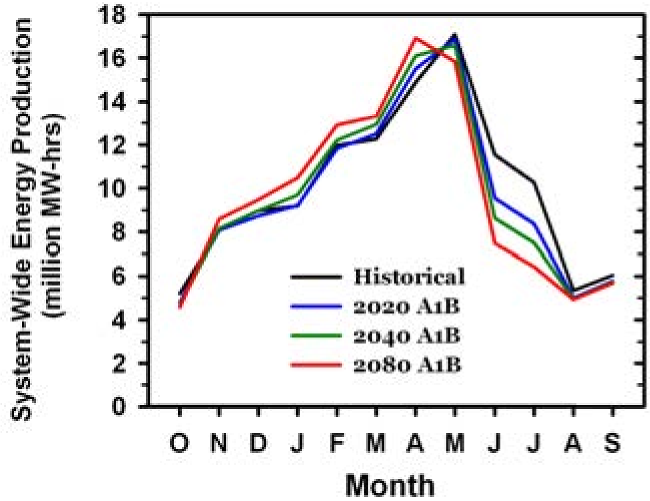

Figure 7. Long-term average system-wide energy production from the Columbia River hydro system for historical 20th century climate (1917-2006) by month, compared to future scenarios for the 2020s, 2040s, and 2080s for the medium (A1B) emissions scenario.

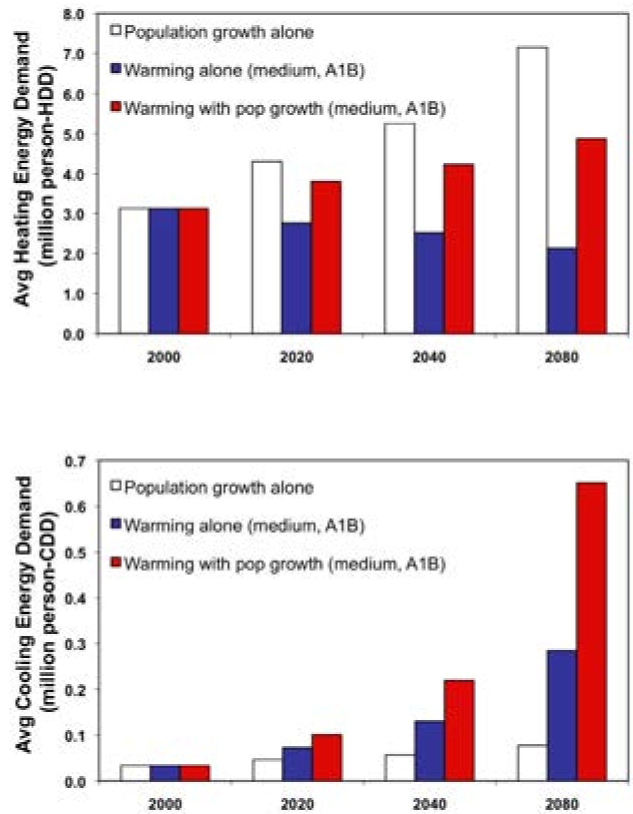

Figure 8. Heating energy demand (top) and cooling energy demand (bottom) for projected population growth and regional warming averaged over Washington. Units: million person-heating degree days (HDD) or million person-cooling degree days (CDD).

[13] Population estimates in this study used information from both the Washington Growth Management Act estimates and global estimates. See Energy chapter for details.

5. Agriculture

The impact of climate change on agriculture in eastern Washington State is assessed in this study by focusing on the major commodities in terms of output value: apples, potatoes, and wheat. Agricultural impacts depend on the direct effects of climate, but they also depend on increasing atmospheric carbon dioxide (CO_2) independent of CO_2's influence on climate. Increased CO_2 in the atmosphere can increase crop yields for some plants and also increase water use efficiency, which in turn may provide additional benefits in dryland crop yields. Projections presented assume that plants have adequate supply of nutrients and are well protected from pests and weeds, and for irrigated crops they assume adequate availability of water for irrigation (see section 3.2, Water Management and Irrigated Agriculture). Crop response to climate change[14] is assessed based on changes for 2020, 2040, and 2080 scenarios with respect to a baseline climate (1975-2005).

- **The impact of climate change on these crops in eastern Washington is projected to be mild in the short term (i.e., next two decades), but increasingly detrimental with time, with potential yield losses reaching 25% for some crops by the end of the century**. However, increased atmospheric CO_2 will likely offset some of the direct effects of climate and result in important yield gains for some crops. There is some debate about whether the CO_2 effect on plants will be temporary (perennial plants may adapt to new conditions or growth of plants in natural environments may be limited by other factors), but mounting experimental evidence involving agricultural crops show a definite beneficial effect of "CO_2 fertilization" on growth and yield of many crops, even for perennial crops such as fruit trees that are expected to be in production for many years.
- **Yields of dryland winter wheat are projected to increase (2% to 8%) for the 2020s and remain unchanged or increase slightly for the 2040s because earlier maturity in response to warming will allow plants to avoid some water stress.** However, yield reductions (4% to 7%) are projected for the 2080s in the higher precipitation region. When CO_2 increase is added, yields are projected to increase by 13% to 15% (2020s), 13% to 24% (2040s), and 23% to 35% (2080s), with the larger gains in drier sites. No change in spring wheat yields is projected for the 2020s, but declines of 10% to 15% for the 2040s, and 20% to 26% for the 2080s are projected due to climate change. Increased CO_2 will compensate for decreased yields, leading to increases of 7% and 2% for the 2020s and 2040s at Pullman, but a 7% increase (2020s) followed by a 7% reduction (2040s) at Saint John. Earlier planting combined with CO_2 elevation is projected to increase yields by 16% for the 2020s.
- **Yields of fully irrigated potatoes are projected to decline by 9%, 15%, and 22% for the 2020s, 2040s, and 2080s, respectively, with smaller losses of only 2% to 3% for all scenarios when the effect of CO_2 is included.** The development of varieties with a longer duration of green leaf area, combined with elevated CO_2, could potentially result in yield gains of ~15%. However, tuber quality is a concern due to tuber growth limitations under warmer conditions.
- **Without the effect of elevated CO_2, future climate change is projected to decrease fully irrigated apple production by 1%, 3%, and 4% for the 2020s, 2040s, and 2080s, respectively.** When the effect of CO_2 is added, yields are projected to increase by 6% (2020s), 9% (2040s), and 16% (2080s). Realizing potential yield gains and maintaining fruit quality standards at higher yields will require management adaptations.

Caveats of the projection of impacts on agriculture presented in this study are: a) possible changes in the frequency and persistence of extreme temperature events (both frosts and heat waves) are not well represented in current climate projections, which could adversely affect crop yields, b) the extent to which the potential benefits of elevated CO_2 will be realized is moderately uncertain, c) changes in impacts by pests, weeds, and invasive species could affect agriculture in ways not described here, and d) although water supply was assumed to be sufficient for irrigated crops, other studies (see Water Resources - Irrigated Agriculture) indicate that it may decrease in many locations as a result of climate change, adding additional stress.

[14] Climate change scenarios in the Agriculture sector used future scenarios from four global climate models with contrasting future conditions, rather than the average of many scenarios. These models were PCM1 (a model that projects less warming and more precipitation for the Pacific Northwest), CCSM3 (a model that projects more warming and less precipitation for the Pacific Northwest), and ECHAM5 and CGCM3 (models that project intermediate changes compared to the first two). All modeling used medium (A1B) CO_2 emission scenarios.

6. Salmon Production and Distribution

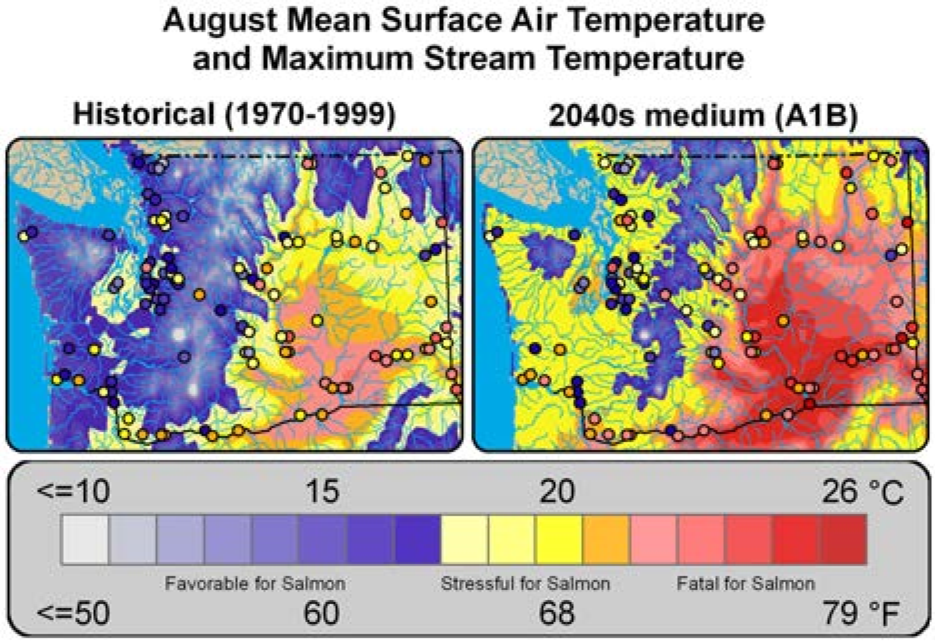

Figure 9. August mean surface air temperature (colored patches) and maximum stream temperature (dots) for 1970-1999 (left) and the 2040s (right, medium emissions scenario, (A1B)). The area of favorable thermal habitat for salmon declines by the 2040s in western Washington, and in eastern Washington many areas transition from stressful to fatal for salmon. Circles represent selected stream temperature monitoring stations used for modeling stream temperatures.

Climate plays a crucial role in salmon ecology at every stage of their life cycle. Key limiting factors for freshwater salmon reproductive success depend on species, their life history, watershed characteristics, and stock-specific adaptations to local environmental factors. The overarching questions addressed here are: (1) How will climate change alter the reproductive success of salmon and steelhead in freshwaters of Washington State? and (2) Where and under what conditions will salmon habitat be most vulnerable to climate change (increasing water temperatures and changes in the timing and amount of streamflow)?

- **Rising stream temperature will reduce the quality and quantity of freshwater salmon habitat substantially.** Since the 1980s the majority of waters with stream temperature monitoring stations in the interior Columbia Basin have been classified as stressful for salmon (where annual maximum weekly water temperatures exceed 60°F). Water temperatures at these stations are projected to become increasingly hostile for salmon under both medium (A1B) and low (B1) emissions scenarios. The duration of temperatures[15] causing migration barriers and thermal stress in the interior Columbia Basin are projected to quadruple by the 2080s. Water temperatures for western Washington stations are generally cooler, and projected increases in thermal stress are significant but less severe - the duration of temperatures greater than 70°F will increase but such temperatures are still projected to be relatively rare for all but the warmest water bodies in Washington (Figure 9).

- **In the major river systems of Puget Sound and lower elevation basins in the interior Columbia Basin, flood risk will likely increase, which in turn increases the risk of streambed scouring of spawning habitat.** In snowmelt-dominated watersheds that prevail in the higher altitude catchments and in much of the interior Columbia Basin, flood risk will likely decrease. Summer low flows will decrease in most rivers under most scenarios (Figure 10), leading to reduced habitat capacities for rearing juveniles that must spend at least one summer in freshwater.

- **Consequences of these changes will vary with different populations and with where they spend the different parts of their life cycles.** Salmon populations that typically inhabit freshwater during summer and early fall for either spawning migrations, spawning, or rearing will experience significant thermal stress. For spawning migrations, effects of warming are projected to be most severe for adult summer steelhead, sockeye, and summer Chinook populations in the Columbia Basin, sockeye and Chinook in the Lake Washington system, and summer chum in Hood Canal. For rearing habitat, impacts of warming will likely be greatest for coho and steelhead (summer and winter run) throughout western Washington. Reductions in summer and

[15] Thermal stress for salmon in streams can be of several types. Salmon suffer physical stress when stream temperatures are too warm, but warm waters also present thermal barriers to migration because the water is too warm for salmon to pass through. Where weekly water temperatures exceed 70°F, both physical stress and thermal barriers to migration are very likely.

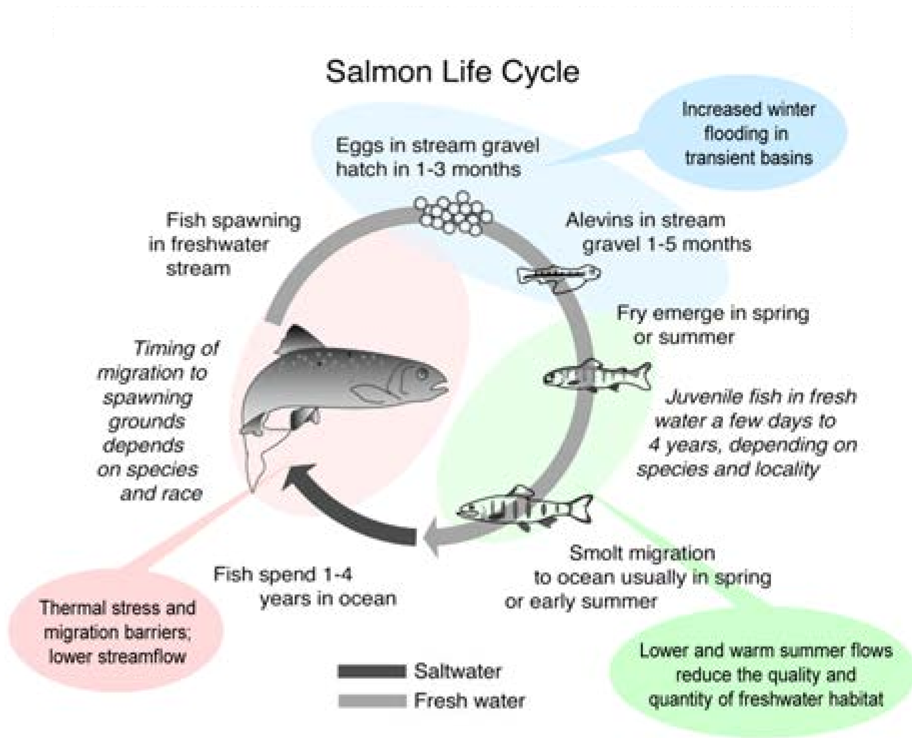

Figure 10. Life cycle assessment and impacts mechanisms for salmon and steelhead in Washington.

fall flows will likely negatively impact the rearing capacities and for coho, steelhead, and stream type Chinook because they all have a life history pattern that requires at least one year of juvenile rearing in freshwater.

7. Forests

Climate influences nearly all aspects of forest ecosystems. Forest fires, insect outbreaks, tree species' ranges and forest productivity are closely tied to climate. Profound changes in forest ecosystems are possible given the magnitude of projected climate changes. The combined climate change impacts on tree growth, regeneration, fire, and insects will fundamentally change the nature of forests, particularly in ecosystems where water deficits are greatest. Many impacts will likely occur first in forests east of the Cascade crest, but forests west of the Cascades will likely experience significant changes in disturbance regime and species distribution before the end of the 21st century.

- **Due to changes in summer precipitation and temperature, the area burned by fire regionally (in the U.S. Columbia Basin) is projected to double or triple (medium scenario, (A1B)), from about 425,000 acres annually (1916-2006) to 0.8 million acres in the 2020s, 1.1 million acres in the 2040s, and 2.0 million acres in the 2080s.** The probability that more than two million acres will burn in a given year is projected to increase from 5% (1916-2006) to 33% by the 2080s. Fire regimes in different ecosystems in the Pacific Northwest have different sensitivities to climate, but most ecosystems will likely experience an increase in area burned by the 2040s. Year-to-year variation will increase in some ecosystems.
- **Due to climatic stress on host trees, mountain pine beetle outbreaks are projected to increase in frequency and cause increased tree mortality.** Mountain pine beetles will reach higher elevations due to a shift to favorable temperature conditions in these locations as the region warms. Conversely, the mountain pine beetle will possibly become less of a threat at middle and lower elevations because temperatures will be unfavorable for epidemics. Other species of insects (such as spruce beetle,

Douglas-fir bark beetle, fir engraver beetle, and western spruce budworm) will possibly also emerge in areas that are no longer suitable for the mountain pine beetle.

- **The amount of habitat with climate ranges required for pine species[16] susceptible to mountain pine beetle will likely decline substantially by mid 21st century (Figure 11).** Much of the currently climatically suitable habitat is in places unlikely to have future climatic conditions suitable for pine species establishment and regeneration, and established trees will be under substantial climatic stress. The regeneration of pine species after disturbance will likely be slowed, if the species can establish at all.
- **The area of severely water-limited forests[17] will increase a minimum of 32% in the 2020s, and an additional 12% in both the 2040s and 2080s (Figure 11, medium scenario, (A1B)).** Douglas-fir productivity varies with climate across the region and will potentially increase in wetter parts of the state during the first half of the 21st century but decrease in the driest parts of its range. Geographic patterns of productivity will likely change; statewide productivity will possibly initially increase due to warmer temperatures but will then decrease due to increased drought stress. It is important to note that changes in species mortality or regeneration failures will possibly occur before the point of severe water limitation (as it is defined here) is reached.

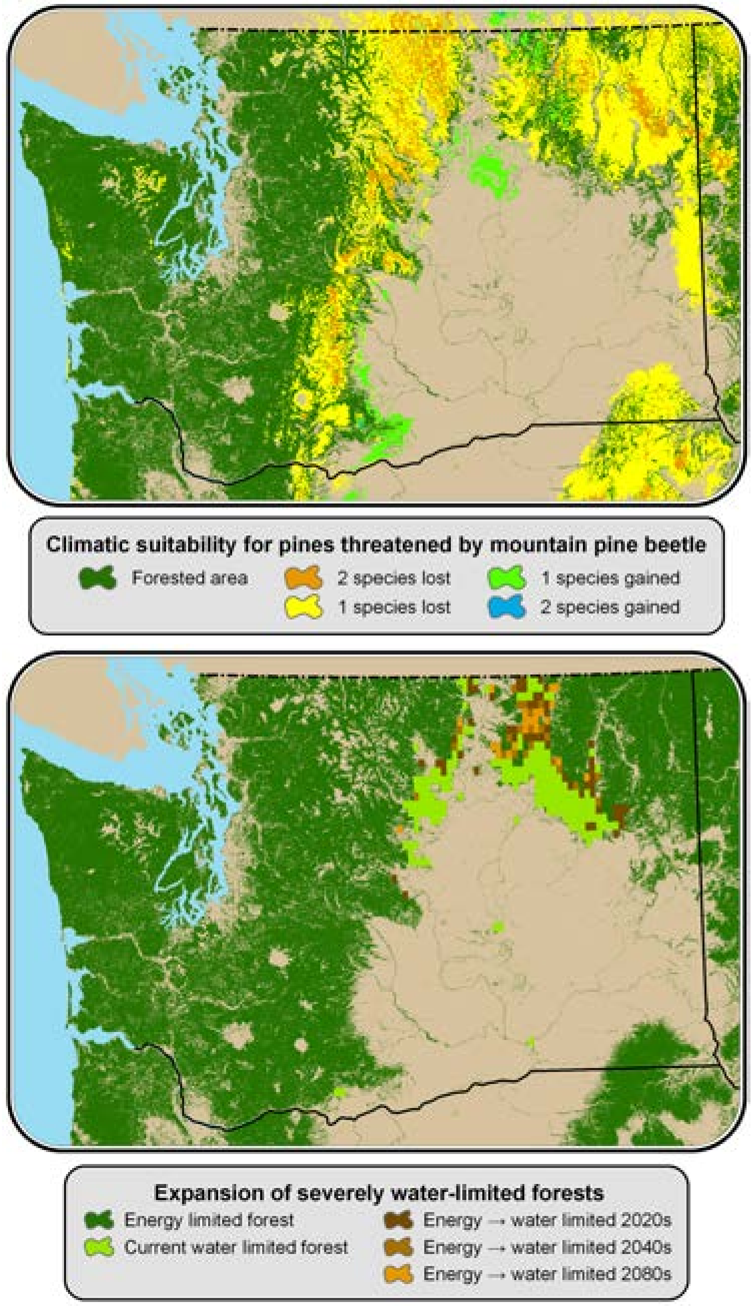

Figure 11. Changes in areas of potential pine species' ranges for 2060 (top panel) and severely water limited forest (bottom panel) in Washington. Areas of orange and yellow in the top panel indicate areas where one or more species of pines will possibly have difficulty re-establishing after disturbance (fire, insect attack, etc.) because the climate is beyond the ranges to which they are adapted (Data: Rehfeldt et al. 2006, multiple IPCC emissions scenarios[18]). Hydrologic modeling suggests that many forested areas on the northern edge of the Columbia basin will become severely water limited (bottom, scenario A1B), defined conservatively as those forests where summer environmental water demand exceeds annual precipitation. The area of water limited forests would increase substantially if the definition is expanded to a more general definition where forests are water limited if annual water demand exceeds annual precipitation (not shown).

---

[16] Ponderosa pine, lodgepole pine, and whitebark pine were considered in this study.

[17] Severely water limited forests occur where the annual supply of water does not meet the summer environmental demand for water. Specifically, when summer potential evapotranspiration exceeds annual precipitation, there is severe water limitation.

[18] The data (from Rehfeldt et al. 2006) used for this analysis were developed by researchers using similar emissions scenarios in an older generation of global climate models to model tree species' ranges in western North America. The ranges of projected future climate changes used in Rehfeldt are comparable to those developed for this assessment.

8. Coasts

Washington State's approximately 3000 miles of coastline (Figure 12) are diverse, ranging from the sandy beaches and shallow waters of Willapa Bay to the steep rocky shores in the San Juan Islands, to the heavily populated but relatively unstable bluffs of the Puget Sound region. While global climate change will drive the same basic physical changes throughout the region, each shore area, and the human activities in those areas, will respond in specific ways depending upon substrate (sand versus bedrock), slope (shallow versus steep cliffs), and the surrounding conditions (exposed versus sheltered from storms). Because Washington's coasts are heavily utilized for ports, home sites, public recreation, wildlife habitat, and shellfish aquaculture, these physical effects of climate change will pose significant challenges. The summary of coastal impacts, and related threats posed to homes, infrastructure, and commerce, are derived from examination of several specific sites and physical threats. Some of the specific sites examined include Willapa Bay, Bainbridge Island, Whidbey Island, the San Juan Islands, and the Ports of Seattle and Tacoma. This assessment does not examine impacts on wildlife habitat, which climate change could possibly affect through sea level rise, bluff erosion, water temperature, and other impacts.

Figure 12. Washington State coastal areas.

Overall, this brief survey of climate impacts on the coasts of Washington State has identified possible routes by which climate can interfere with typical human uses of the coast and has raised many questions requiring additional research.

- **Sea level rise will shift coastal beaches inland and increase erosion of unstable bluffs, endangering houses and other structures built near the shore or near the bluff edges (see Scenarios section for sea level rise information).** On Whidbey Island, future possible impacts include increased bluff erosion and landslides and inundation. On Bainbrige Island, inundation and, to a lesser extent, bluff erosion are possible. Willapa Bay would see possible increases in shoreline erosion.
- **Shellfish will possibly be negatively impacted by increasing ocean temperatures and acidity, shifts in disease and growth patterns, and more frequent harmful algal blooms.** Further, inter-tidal habitat for shellfish aquaculture will likely be slowly shifting shoreward as sea level rises. Health risks due to harmful algal blooms will possibly be a increasing concern, leading to more frequent closures of both recreational and commercial shellfishing.
- **The major ports of Seattle and Tacoma are only slightly above existing sea level, and both have some plans to raise the height of piers, docks and terminals in response to sea level rise.** Both ports also rely on access to highway and railroad transportation to move freight, but key railroad tracks and much of the container yards will possibly be subject to flooding without more extensive construction of dikes or land filling. Protecting the port lands and transportation networks will be a challenge for these and other ports throughout the state.
- **These conclusions extend to other coastal structures and facilities in the Puget Sound region which must accommodate to sea level rise or retreat to higher ground.**

Adapting to these effects will possibly involve both innovative property boundary laws to accommodate the shifting high tide lines and genetic research to select more resilient sub-species of shellfish. Further research will be a necessary element of any longer-term, adaptive strategy for climate change in the region.

9. Urban Stormwater Infrastructure

Washington's urban infrastructure elements are not equally vulnerable to weather and climate. This assessment focuses on stormwater management facilities in urban areas because the relationship to potential climate change (particularly precipitation extremes on which much of their design is based) is obvious, the consequences of inadequate facilities are severe, and the economic impact of increasing the capacity of stormwater facilities (or more severe flooding) would be substantial. Three specific areas – the central Puget Sound, Spokane, and Portland-Vancouver – were chosen for detailed analyses because they are the most populous in the state.

- **Few statistically significant changes in extreme precipitation have been observed to date in the state's three major metropolitan areas.** Nonetheless, drainage infrastructure designed using mid-20th century rainfall records may be subject to a future rainfall regime that differs from current design standards.
- **Projections from two regional climate model (RCM) simulations generally indicate increases in extreme rainfall magnitudes throughout the state over the next half-century, but their projections vary substantially by both model and region (see Figure 13).**
- **Hydrologic modeling of two urban creeks in central Puget Sound suggest overall increases in peak annual discharge over the next half-century, but only those projections resulting from one of the two RCM simulations are statistically significant.** Magnitudes of projected changes vary widely, depending on the particular basin under consideration and the choice of the underlying global climate model.

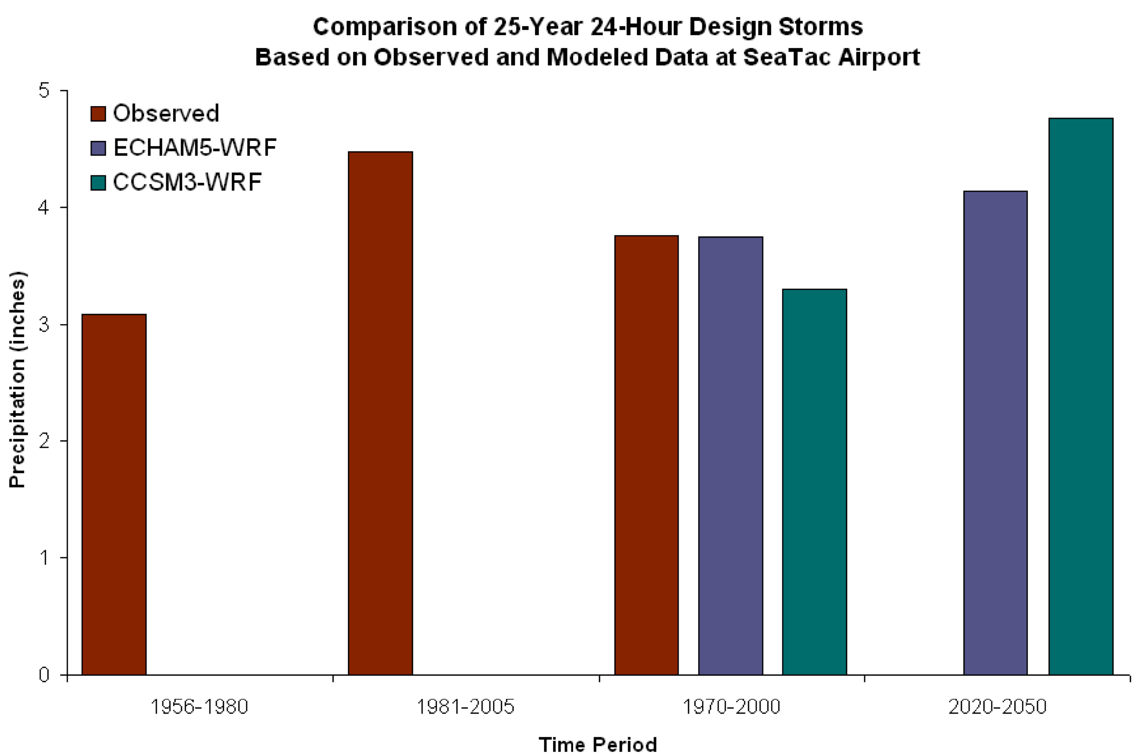

Figure 13. Comparison of 25-year, 24-hour design storms[18] based on observed and modeled (regional climate model) data at SeaTac airport. Projected changes under one climate model[19] are greater than those under another climate model, although both project increases. The historical range is similar to the range of projected changes. Note that the two time periods at left (1956 to 1980 and 1981 to 2005) overlap the third time period (1970 to 2000).

[18] 25-year, 24-hour design storm is a typical design standard for storm sewer capacity. The 25-year 24-hour design storm is the amount of precipitation falling over a 24 hour period that has a 1 out of 25 (4%) chance of being exceeded in any given year.
[19] ECHAM5 and CCSM3 are global climate models, and in this assessment, these global models were the two used to provide input conditions to a much more detailed regional climate model (WRF) – see Scenarios chapter for details.

10. Human Health

Illness and mortality related to heat and worsening air quality are core public health concerns associated with climate change projections. First, the historical relationship between mortality rates and heat events in the greater Seattle area (King, Pierce and Snohomish counties), Spokane County, the Tri-Cities (Benton and Franklin counties) and Yakima County from 1980 through 2006 are examined for different ages of people and causes of mortality. Second, increased mortality from projected heat events is estimated for 2025, 2045, and 2085. Third, increased mortality due to ozone pollution caused by climate change is estimated for mid century (2045-2054) in King and Spokane Counties. We focused on these impacts because they are among the more direct effects of climate on human health. It is possible that impacts related to communicable diseases, changes in disease vector habits, extreme weather events, and other factors would also become problematic in the future, but these were not addressed in this study.

- **Washington State residents were more likely to die during heat waves than during more temperate periods (baseline 1980-2006).** Risks increased during heat waves lasting two or more days, and were greatest for older adults. Among residents of the greater Seattle area (King, Pierce and Snohomish Counties) aged 65 and above, heat waves of two to four days' duration were associated with a 14% to 33% increase in the risk of death from non-traumatic causes. Greater Seattle residents aged 85 and above were 31% to 48% more likely to die during heat waves of two to four days (Figure 14).
- **Climate change in Washington State will likely lead to larger numbers of heat-related deaths. The greater Seattle area in particular can expect substantial mortality during future heat events due to the combination of hotter summers and population growth.** Considering just the effects of climate, a medium (A1B) climate change scenario projects 101 additional deaths among persons aged 45 and above during heat events in 2025. By 2045, approximately a 50% increase in additional deaths could be attributed directly to climate change; even more excess deaths could be expected if population continued to grow beyond 2025 projections. Nearly half of these are expected to occur among persons 85 years of age and older.
- **Although better control of air pollution has led to improvements in air quality, warmer temperatures threaten some of the sizeable gains that have been made in recent years.** The estimated number of summer deaths due to ozone pollution in 1997-2006 is 69 in King County and 37 in Spokane County. Ground-level ozone concentrations are projected to increase in both counties. Using projections of the future population size[20] and ozone concentrations, this would increase to 132 deaths in King County and 74 deaths in Spokane County by the 2040s.

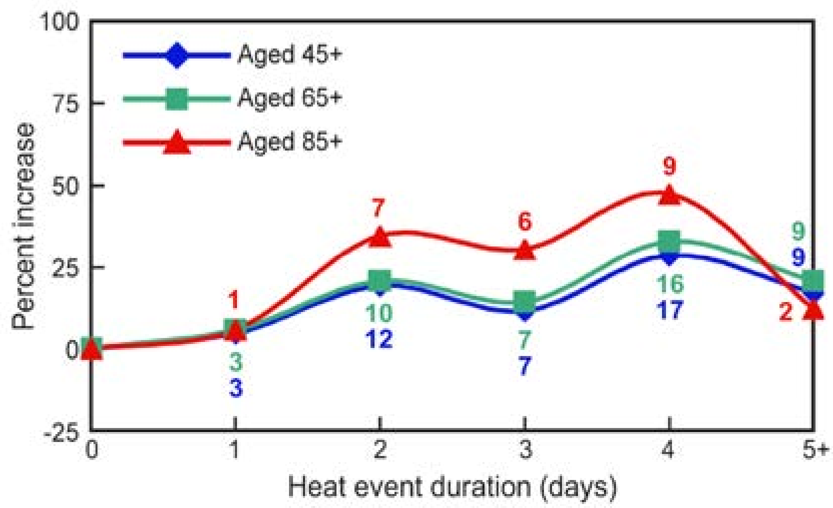

Figure 14. Percent increase in risk of death, and number of deaths each day for all non-traumatic causes by heat event duration, greater Seattle area, 1980-2006. Given 2006 population levels, residents of the greater Seattle area aged 65 and above could be expected to experience, on average, 3 additional deaths on day 1 of a heat event, 10 additional deaths on day 2, and so forth; over a 5 day heat event this age group would incur a total of 45 additional deaths, and during an average heat event of 2.2 days' duration, they would experience an additional 14 deaths. Persons aged 85 and above could be expected to experience 25 additional deaths during a 5 day heat event and 9 additional deaths during a typical heat event.

[20] Population estimates from Washington State's Office of Financial Management.

11. Adaptation

Climate change will affect many aspects of Washington's natural, institutional, economic, cultural, and legal landscape. Furthermore, because of lags in the global climate system and the long lifetime for key greenhouse gasses in the atmosphere, climate change impacts over the next few decades are virtually certain. Impacts in the second half of the 21st century are also certain, but the magnitude of those changes will be greatly influenced by the success or failure of efforts to reduce greenhouse gas concentrations both in the near-term and over time.

Preparing for (or adapting to) the impacts of climate change is necessary to minimize the negative consequences of climate change in Washington State, including an increased risk for drought, forest fires, habitat loss, and heat stress. Adapting to climate change also creates opportunities to maximize the benefits of climate change, such as a longer growing season and increased winter hydropower production. Additional reasons for preparing for climate change at the state and local level are provided in Box 4.

Box 4. Why Preparing for Climate Change Is Required at the State and Local Level

1. Significant regional-scale climate change impacts are projected.
2. State and local governments, businesses, and residents are on the "front line" for dealing with climate change impacts.
3. Decisions with long-term impacts are being made every day, and today's choices will shape tomorrow's vulnerabilities.
4. Significant time is required to develop adaptive capacity and implement changes.
5. Preparing for climate change may reduce the future costs of climate impacts and responses.
6. Planning for climate change can benefit the present as well as the future.

Navigating Washington's changing future will require regulatory, legal, institutional, and cultural changes to reduce the barriers that limit building a more climate resilient Washington. Washington's commitment to adapting to climate change was formalized on February 7, 2007, when Governor Christine Gregoire signed the Washington Climate Change Challenge (Executive Order 07-02). In addition to establishing greenhouse gas reduction goals for the state, Executive Order 07-02 committed the state to determining what steps the State could take to prepare for the impacts of climate change in five key sectors: public health, agriculture, coasts and infrastructure, forestry, and water supply. Adaptation recommendations from the Preparation/Adaptation Working Groups (PAWGs) were presented to the Governor in February 2008.

The Washington Climate Change Impacts Assessment complements the State's effort with the PAWGs by providing updated and expanded details on the potential impacts of climate change in Washington. It is important to note that the adaptation discussion in the Washington Assessment should be viewed as starting point for initiating a more systematic look at the adaptation needs identified by the PAWGs in addition to other potential options. This could be done with continued involvement from the PAWGs and/or through a combination of intra- and inter-agency working groups (and public input) convened to evaluate what adaptation options are needed and how they can be implemented.

As Washington's state and local governments begin considering how to address climate change impacts, three fundamental principles must be recognized. **First, there is no "one size fits all" solution for adapting to climate change.** Options for adapting to climate change vary among sectors (e.g., between water resources and forest ecosystems) and even within sectors (e.g., between watersheds) depending on the unique characteristics of the systems being considered. Adapting to climate change will require multiple actions implemented over varying time frames based on projected impacts, resources, and risks.

Second, adapting to climate change is not a one-time activity. Climate will continue to change as will Washington's communities, economies, social preferences, and policies and regulations. The assumptions that shape adaptive planning must be revisited periodically and adjusted to reflect these changes. Thus, adapting to climate change must be seen as a continuous series of decisions and activities undertaken by individuals, groups, and governments rather than a one-time activity.

Third, effective adaptation will require more regulatory flexibility and systematic integration of governance levels, science, regulation, policy, and economics. Increased flexibility and integration is needed to accommodate uncertainties of climate change as well as the uncertainties in non-climatic stresses, such as population growth, changing resource demands, and economic trends. More general options for increasing flexibility in Washington State policy-making include, but are not limited to, building social capital (increasing knowledge and engagement); broader use of market mechanisms, conditional permitting, adaptive management, and the precautionary principle; and increasing legislative flexibility in the courts. Implementing no-regrets, low-regrets, and win-win (co-benefit) strategies are also effective ways of moving forward with adaptation in the face of uncertainty. Without more integration and flexibility, the institutions, laws, and policies used to govern human and natural systems could become increasingly constrained in their ability to effectively manage climate change impacts.

Implementing the PAWG recommendations and adaptation options identified in this report will require a concerted effort on the part of state and local decision makers, working in partnership with federal agencies, tribal governments, and the private sector, to make needed changes in how human and natural systems are governed in Washington. Washington State faces unprecedented economic challenges, however. A significant budget deficit looms and deep cuts will be required to balance the state budget.

Despite these challenges, preparing for climate change can continue from its important beginnings in the 2007 PAWG process. Many of the actions recommended by the PAWG process as well as others provided within this report require nominal fiscal resources. Furthermore, many adaptive actions may create cost savings through damage avoidance or delayed infrastructure upgrades, for example. Finally, many of the changes required to develop a more climate-resilient Washington will take time to implement. Waiting for climate change to "arrive" will be too late in some cases and could be significantly more costly in other cases.

12. Conclusion

Climate plays a strong role in many of the resources and the quality of human life in Washington State. Projected increases in temperature and accompanying variability in precipitation point to a very different future for Washington's people and resources than that of the recent past. All sectors examined in this study project quantifiable impacts of climate change on important resources, and the projections of future climate indicate that these impacts are very likely to grow increasingly strong with time.

- **Adaptation to the changes in climate and their impacts on human, hydrological and ecological systems is necessary because the projected impacts of climate change are large.** There is enough current scientific information to plan and develop strategies for future projected climate changes and impacts even though information is not always complete. For example, "no regrets" strategies that provide benefits now and potential flexibility later are a good place to start. However, adaptation could be costly in some cases where the rate of change is very fast or where severe impacts are spread over large areas. Finally, significant impacts are projected in some sectors as early as the 2020s and certainly by the 2040s – these are not "far in the future" impacts.
- **To the extent that it can be identified, quantified, and mitigated, uncertainty is a component of planning, not a reason to avoid planning.** Many sectors report different impacts in different systems (e.g., snowpack response in low vs. high elevations, fire response in the western Cascades vs. Blue Mountains, different salmon populations and different crops etc.), but the **natural complexity (variability in geographic space and in time, such as decadal climate variability) of these systems is a key part of planning for the future.** Better climate information, better monitoring, and better awareness of complexity are all required to anticipate future impacts and to develop adaptation strategies that are likely to be successful.
- While there is compelling evidence that climate in the next century will differ markedly from that of the past, the exact nature of those differences are impossible to predict with precision. Our sensitivity to the inherent uncertainty of future climate change can be evaluated through an examination of multiple future climate scenarios and their associated impacts. **By understanding the likely direction and magnitude of future climate changes and impacts, we can manage risks and exploit opportunities in an informed and systematic way.**

1: Scenarios

Future Climate in the Pacific Northwest

Philip W. Mote[1,2] and Eric P. Salathé Jr.[1]

Abstract

Climate models used in the Intergovernmental Panel on Climate Change (IPCC) Fourth Assessment Report (AR4) on the whole reproduce the observed seasonal cycle and 20th century warming trend of 0.8°C (1.5°F) in the Pacific Northwest, and point to much greater warming for the next century. These models project increases in annual temperature of, on average, 1.1°C (2.0°F) by the 2020s, 1.8°C (3.2°F) by the 2040s, and 3.0°C (5.3°F) by the 2080s, compared with the average from 1970 to 1999, averaged across all climate models. Rates of warming range from 0.1 to 0.6°C (0.2° to 1.0°F) per decade. Projected changes in annual precipitation, averaged over all models, are small (+1 to +2%), but some models project an enhanced seasonal cycle with changes toward wetter autumns and winters and drier summers.

Changes in nearshore sea surface temperatures, though smaller than on land, are likely to substantially exceed interannual variability, but coastal upwelling changes little. Rates of 21st century sea level rise will depend on poorly known factors like ice sheet instability in Greenland and Antarctica, and could be as low as 20th century values (20cm, 8”) or as large as 1.3m (50”).

[1]JISAO Climate Impacts Group, University of Washington, Seattle, Washington 98195-5672
[2]Oregon Climate Change Research Institute, College of Oceanic and Atmospheric Sciences, Oregon State Univ., Corvallis, Oregon 97331-5503

1. Global Climate Models

Envisioning global climate in a future with much higher greenhouse gases requires the use of physically based numerical models of the ocean, atmosphere, land, and ice, often called global climate models (GCMs) or climate system models. A common set of simulations using 21 GCMs was coordinated through the Intergovernmental Panel on Climate Change (IPCC), described in the IPCC 2007 report (Randall et al. 2007), and archived by the Program for Climate Model Diagnostics and Intercomparisons (PCMDI). These models typically resolve the atmosphere with between 6,000 and 15,000 grid squares horizontally, and with between 12 and 56 atmospheric layers. All GCMs in the PCMDI archive include a fully resolved global ocean model, usually with higher resolution than the atmospheric model, and nearly all include models of sea ice dynamics and models of the land surface. By calculating energy fluxes between the sun, atmosphere, and surface, these models compute surface temperature distributions that compare well with observations. Details of the models, as well as references, can be found in Table 8.1 of Randall et al. 2007.

Simulations of 21st century climate require projections of future greenhouse gases and sulfate aerosols (which reflect sunlight and also promote cloud formation, thereby offsetting greenhouse gases locally), more than 40 of which were produced under the auspices of the IPCC (SRES, Nakicenovic et al. 2000) after considering a wide range of future socioeconomic changes. Three of these "SRES" scenarios were commonly chosen for forcing the GCMs: B1, A1B, and A2. The climate forcing of all scenarios, including B2 and the older IS92a used in the Second Assessment report (Figure 1) is similar until about 2020 owing primarily to the long lifetime of coal fired electric power plants and of the major greenhouse gases. A2 produces the highest climate forcing by the end of the century, but before mid-century, none of the scenarios is consistently the highest. Because more modeling groups ran A1B than A2, and since our focus for this study was on mid-century change, we chose A1B as the higher emissions scenario and B1 as the low emissions scenario for our analysis of 21st century PNW climate. We have analyzed available A2 runs as well, as shown in Figures 8, 11, and 12, but we emphasize A1B and B1. Though B1 is the lowest of the IPCC illustrative scenarios, it still produces changes in climate that many scientists call "dangerous" (Schellnhuber et al. 2006) — a threshold that a growing number of political leaders have stated their intention to avoid. At the high end, scenario A1FI (not shown) results in even higher climate forcing by 2100 than A2 or A1B. Mid-2000s global emissions of CO_2 exceeded even the A1FI scenario (Raupach et al. 2007). Whether these exceedingly high emissions will continue into the future is beyond our expertise to judge.

On the PCMDI web site (esg.llnl.gov), all modeling centers provided simulations of 20th century climate using observed solar, volcanic, and greenhouse gas forcing. Twenty modeling centers provided simulations of 21st century climate with the A1B scenario, 19 with B1, and 17 with A2, for a total of 56 runs. These form the basis for the analysis presented in most of the other chapters in this assessment report. In some cases several different model runs were provided for each scenario; we chose Run 1

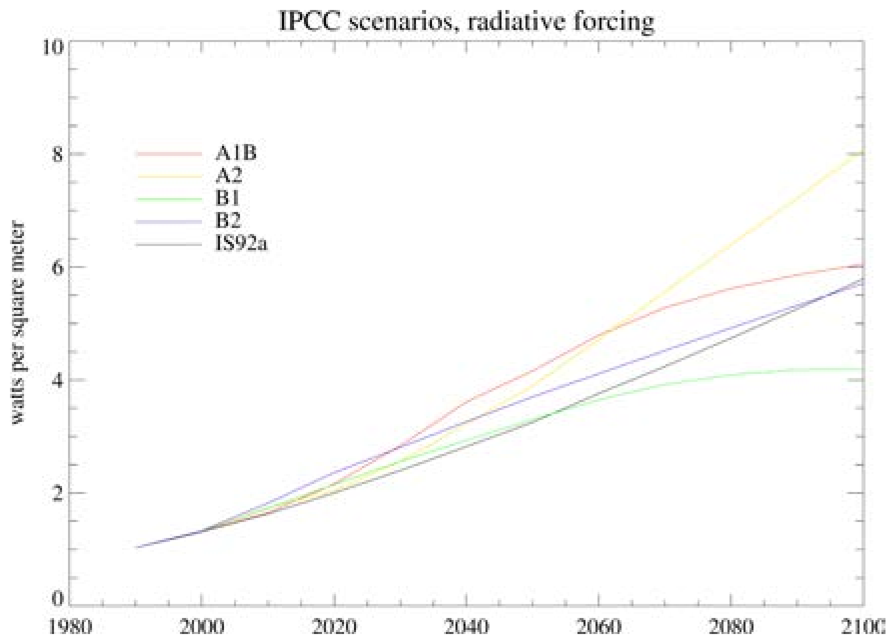

Figure 1. Globally averaged radiative forcing by greenhouse gases and sulfate aerosols, for four of the six illustrative scenarios plus the older IS92a scenario, from IPCC (2001) Appendix II.3. In this study we use A1B and B1. Differences between scenarios grow after about 2020.

except as noted in Appendix A. This set of models is larger than the set available in 2005 when similar analysis was performed for the Northwest (Mote et al. 2005, 10 models) and California (Cayan et al. 2007, 12 models but emphasizing two).

Randall et al. (2007) and CCSP (2008) evaluated the models' fidelity in simulating various aspects of global climate, and also calculated each model's climate sensitivity. The modeled climate sensitivity is a measure of the model's response to doubled CO_2, and has historically been calculated in two ways: either the "equilibrium climate sensitivity" or the "transient climate response" (TCR, ibid.). The equilibrium climate sensitivity is defined as the globally averaged temperature change in a simulation with a doubling of CO_2, in which the simulation is long enough for the global temperature to reach equilibrium. Because the climate system takes a long time to come into equilibrium, the calculation of the equilibrium climate sensitivity was typically performed only in models with a very simple ocean component, which was standard before the mid-1990s. By the late 1990s, most models included a sophisticated ocean, and running such a model to equilibrium would require a great deal of computer resources. The TCR was a more practical metric of models' sensitivity. The TCR is defined as the global mean temperature change at the time of CO_2 doubling in a simulation in which the CO_2 increased at 1%/year (roughly IS92a, the black curve in Figure 1). The range of values of TCR reported by Randall et al. (2007) was 1.2-2.6°C (their Table 8.2).

2. Model Evaluation: 20th Century Climate of the Northwest

The domain used in the rest of the chapters in this study is the state of Washington. However, because the state is represented by only a few grid points in a typical GCM, for examining the GCMs we use the larger domain of the Pacific Northwest, defined as the region between 124° and 111°

west longitude, 41.5° to 49.5° north latitude: Washington, Oregon, Idaho, western Montana, and a small slice of adjacent states and British Columbia. Models have different spatial resolutions, but the number of model grid points enclosed in this latitude-longitude box is between 6 and 91.

In any prediction exercise the first question should be, how well can the predictive model simulate the past? In this section we examine the 20 models' simulation of 20th century climate in the Pacific Northwest, a step not discussed by Cayan et al. (2007) in their two-model study of climate change in California. We use a regionally averaged time series formed by averaging the temperature and precipitation values at all the Northwest grid points. The reason for such averaging is that variations in model climate on scales smaller than a few grid cells is not meaningful. Put another way, the models represent the variations of climate that would occur on a smooth planet with similar land-sea distributions and large smooth bumps where Earth has major mountain ranges.

Besides model resolution, another consideration in comparing global models with observations is that there are different ways to calculate "observed" regionally averaged temperature and precipitation. A common approach is to average weather station data into latitude-longitude boxes or into geographically defined "climate divisions" and combine these areas into a state or regional average with area weighting; this was how Mote et al. (2005) compared climate models with observations. The drawback of this approach is that it does not account for the contribution to a regional average of high terrain, which has very few weather stations. A better estimate interpolates (horizontally) and extrapolates (vertically) observations to a uniform, high-resolution grid (e.g., Hamlet and Lettenmaier 2005). Such an estimate, however, would be unsuitable for comparing with climate model output, which lacks the vertical relief.

A third approach is to assimilate observed data into a weather prediction model at the spatial resolution of climate models, as has been done for the NCEP/NCAR reanalysis (Kalnay et al. 1996). This approach processes observations in a manner most similar to a global climate model, or in other words constrains a model twice a day to be consistent with observations, and hence it is perhaps the fairest comparison with climate models and is the one we used previously (Mote and Salathé 2009). However, in this analysis we use 0.5°-0.5° (latitude-longitude) gridded data of the University of East Anglia Climatic Research Unit (CRU) version 2.02 (Mitchell et al. 2004). We area-average the data over the same domain as the climate models and use monthly means for 1901-2000.

We begin with a comparison of the annual mean difference, or bias, between models and CRU for 1970-99. Most models have a slight cold bias, and both the mean and median bias is 1.8°C (3.3°F) (Figure 2). The models with least bias in annual average temperature are GISS-ER, MIROC-hi, INMCM3, and CNRM. For precipitation (Figure 3), all models have a wet bias, and for some the bias exceeds 50%. The mean bias is 6.0 cm/month (41%). Models with lowest bias are BCCR, GISS_er, HadCM, PCM1, and CGCM_T47. Note that no model falls in the best five for both temperature and precipitation, and likewise no model falls in the worst five for both temperature and precipitation. Comparing these results with those obtained using NCEP, the NCEP regional average temperature was

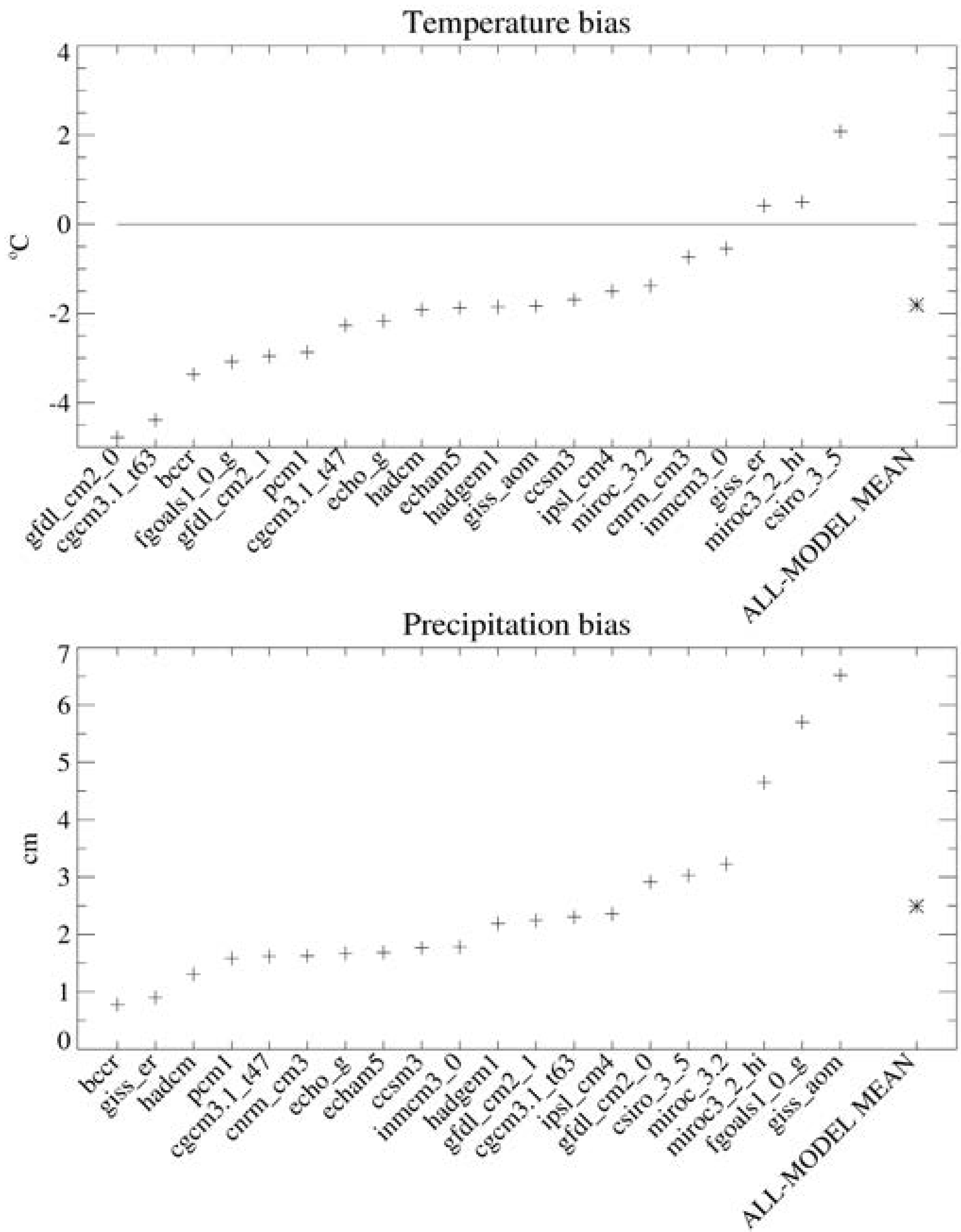

Figure 2. Differences (biases) between each model's mean annual (top) temperature and (bottom) precipitation from gridded CRU data, averaged over the Pacific Northwest, for 1970-99.

slightly lower and precipitation quite a bit higher (Mote and Salathé 2009) than the CRU averages, so the average biases were smaller and in the case of temperature the list of models with lowest bias was different.

The models' simulated seasonal cycles for the PNW are shown in Figure 3. For temperature, the multi-model average is consistently 1-3°C cooler than CRU for each month, and six models (led by MIROC-hi) have a lower root-mean-square (rms) difference from CRU than the multi-model average. With NCEP, the multi-model mean was consistently within 1°C of NCEP monthly means and no model had a smaller rms difference.

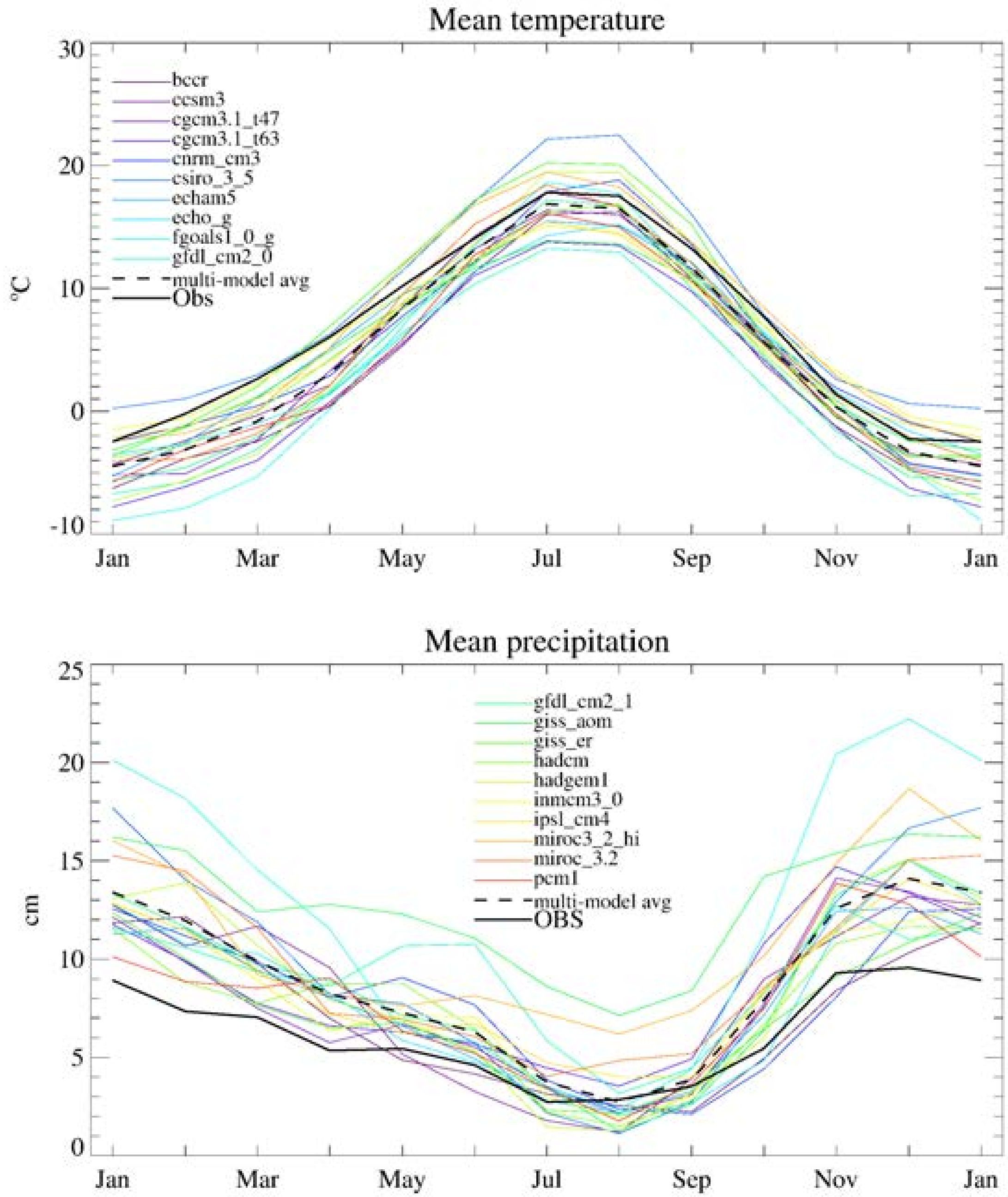

Figure 3. Mean seasonal cycle for each climate model from its 20th century simulation, compared with the CRU data (black), averaged over the PNW. All 20 models are shown in both panels but the legend is split between the panels. The black dashed line shows the average of all the models, which is quite close to the observations for temperature and a bit too wet for precipitation, but with approximately the right contrast between wet and dry seasons.

For precipitation, all models reproduce the contrast between wet winters and dry summers, though a few produce summers that are only slightly drier than winters. The multi-model average is 30-50% wetter than CRU in most months. Twelve of the models have a lower rms difference from observed than the multi-model average, with GISS_er the closest and FGOALS the farthest owing to its very wet summers.

Another facet of 20th century climate that can be evaluated is the trend in temperature. For the global average, many models simulate a warming rate similar to the 0.6°C increase in global temperature observed in the 20th century. At the regional scale (Figure 4), the warming rate could be dominated by changes in atmospheric circulation rather than greenhouse forcing; nonetheless, eight of the models simulate a warming for 1900-2000 in the Northwest within 0.2°C of the observed warming of 0.8°C

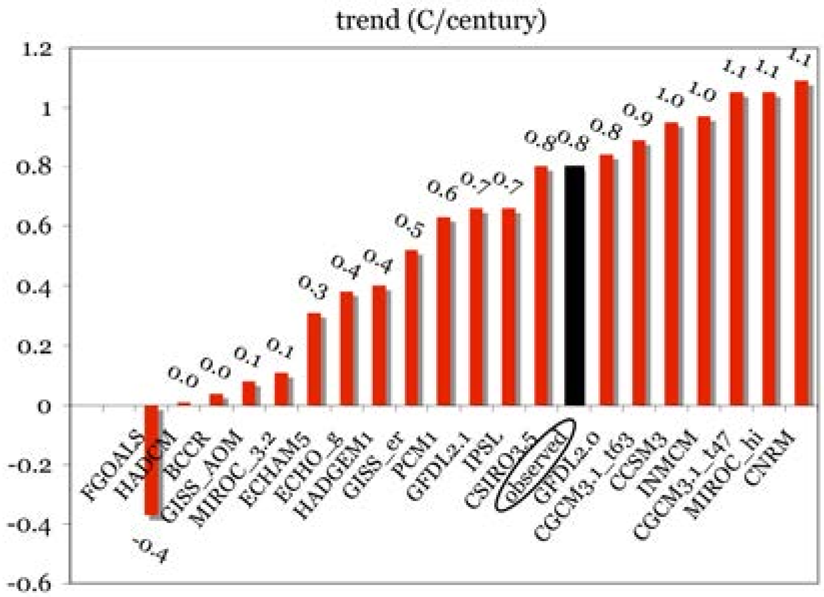

Figure 4. Trend in each model's annual mean temperature for the PNW during the 20th century, and the observed trend calculated from the USHCN data. Note that the observed trend is close to the median trend from the models.

during the same period, calculated using regionally averaged, area-weighted Historical Climate Network data (Mote 2003, updated). We do not perform the same comparison for precipitation since there is no evidence that precipitation responded to greenhouse forcing in the 20th century, either globally or in the zonal mean at these latitudes (Zhang et al. 2007). The time series of regional precipitation is characterized by high interannual variability, and the direction of linear trends depend on the start and end point, unlike temperature, for which linear trends are robustly upward.

Finally, we examine aspects of 20th century climate that pertain to the mesoscale modeling that will be reported elsewhere (Salathé et al. 2009, this report). Since the GCMs provide the global context for the regional modeling, the GCM fields over the domain of the mesoscale model help determine the quality of the mesoscale model simulation; in particular the moisture flux into the region provided by the GCM plays a crucial role in determining both the amount and the distribution of precipitation by the regional model.

For each model, we mapped the precipitation, sea level pressure (SLP), and temperature over roughly the domain for which we ran the mesoscale model (results of which will be reported elsewhere). Figure 5 shows the maps for one of these models, the CGCM_T47, compared with the NCEP/NCAR reanalysis. This model was chosen for display because it scores the best in comparisons with the reanalysis (Figure 6). In both instances we show the annual mean for 1950-99. All models reproduce the basic features of each field: the heavy precipitation over the coastal mountains of British Columbia, the swath of high precipitation in the lower left corner, the Aleutian low and Pacific high pressure features in the top panel, and the low temperatures over the mountainous West and the strong gradient of sea surface temperature over the eastern Pacific.

An efficient method of quantitatively comparing fields is the Taylor diagram (Taylor 2000). Values are plotted in radial coordinates with the radius being the ratio of the modeled area-averaged variance to the

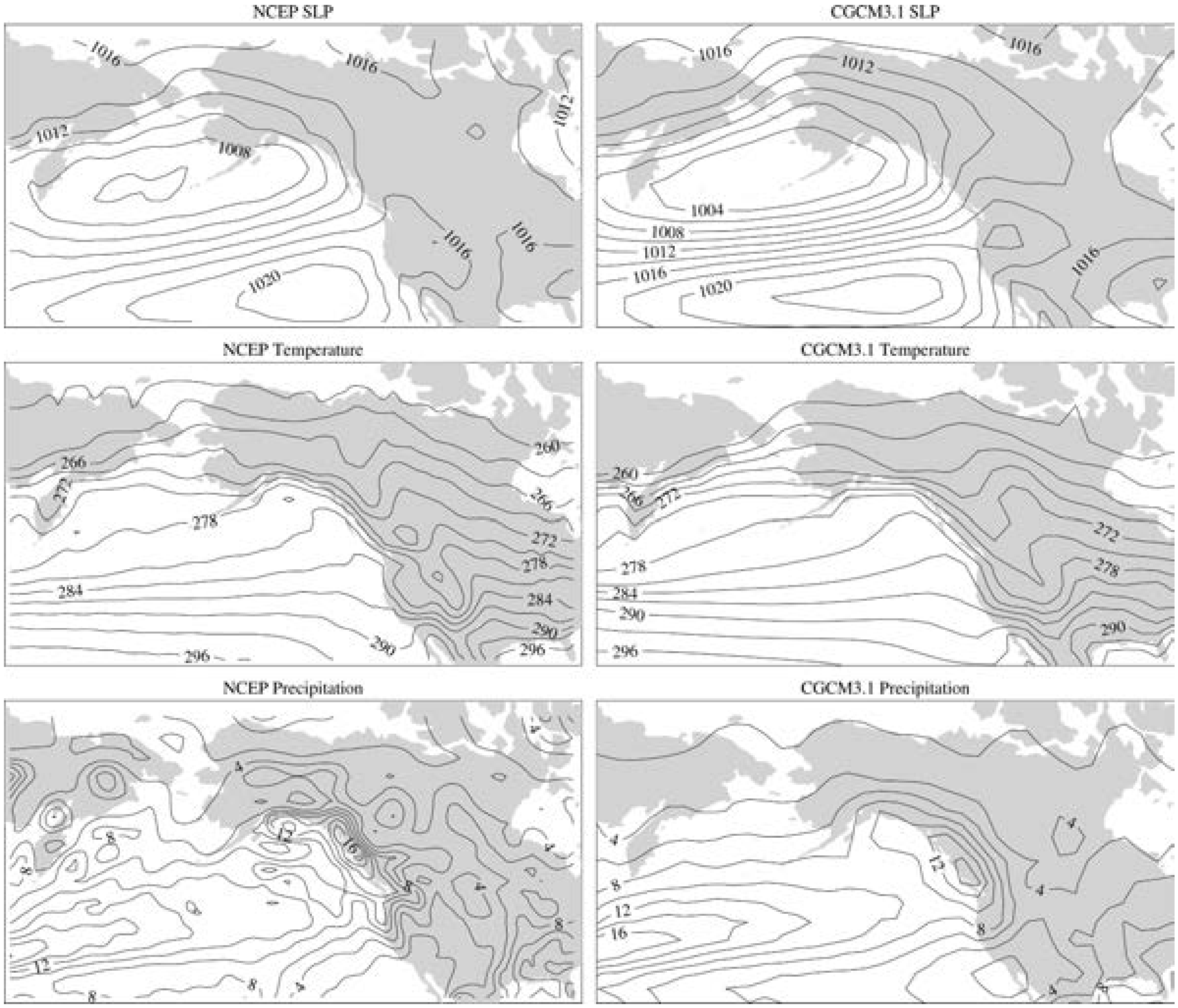

Figure 5. Annual mean patterns from (left column) CGCM-T47 and (right column) NCEP-NCAR reanalysis, for years 1950-99. Top row shows sea level pressure in hPa, middle row temperature in Kelvin (273.16K=0°C=32°F), and bottom row precipitation in mm/day.

observed area-averaged variance, where the variance is calculated at each grid point using 50 years (1950-99) of monthly data. The angle represents the spatial correlation between the 50-year mean fields. Figure 6 shows the Taylor diagram for all 20 models, evaluated over the domain shown in Figure 5. As with global mean fields (Randall et al. 2007), of the three fields shown here temperature is best simulated by the models, with a correlation typically >0.97. Sea level pressure is next best simulated, followed by precipitation, except that for GISS-ER the SLP is worse than any model's precipitation field, owing largely to an Aleutian Low that is much too far to the west. In the Taylor diagram, the distance of a point to (1,1) represents the rms error, and we can use this distance to rank the models for each field and to average the distances to rank the models overall (Fig. 6 lower). Of all the models, CGCM-T47 (shown in Fig. 5) ranks the best.

3. Projected Changes in Temperature and Precipitation

Some years ago it was common practice in impacts research to present the results of one or two global climate models. With greater opportunities and technical abilities for analyzing multiple model simulations, ensembles are now the state of the science. Climate model simulations provide

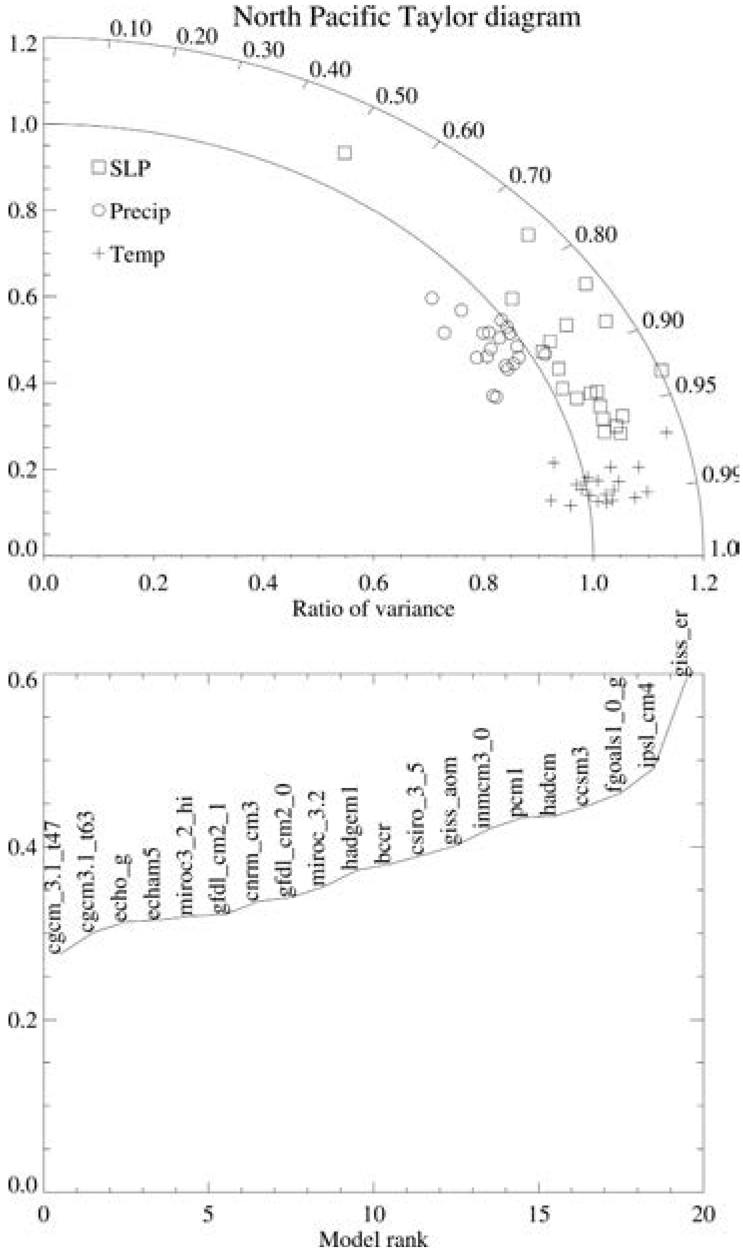

Figure 6. Evaluation of model performance over the domain shown in Figure 5. Top panel shows the correlation (angle) and ratio of variance (radius) for each model and each field. The root-mean-square difference from the observed field is just the distance on the diagram. Bottom panel ranks the models by mean distance for the three fields. Most models simulate temperature fairly well, sea level pressure less well, and precipitation still less well, but there is a wide range in performance especially for sea level pressure. The model that scores the best overall is shown in the right hand panels in Figure 5.

"ensembles of opportunity" (Meehl et al. 2007) whereas what we really need are statistical distributions of future changes – e.g., estimates of the likelihood of changes in temperature above a certain value by a certain date. It is common practice to presume that the distribution of future changes is well represented by an ensemble of future climate model projections, though massive distributed climate experiments through climateprediction.net offer one possible way to characterize statistical distributions (e.g., Stainforth et al. 2005) and the authors of this chapter are engaged in a project to produce regional climate simulations using the climateprediction.net framework. Here, we follow common practice and present the range of projected changes from model simulations as well as a weighted average.

The new, weighted average follows the reliability ensemble averaging "REA" (Giorgi and Mearns 2002) approach. In this approach, the REA value

Figure 7. Smoothed traces in temperature (top) and precipitation (bottom) for the 20th and 21st century model simulations for the PNW, relative to the 1970-99 mean. The heavy smooth curve for each scenario is the REA value, calculated for each year and then smoothed using loess. The top and bottom bounds of the shaded area are the 5th and 95th percentiles of the annual values (in a running 10-year window) from the ~20 simulations, smoothed in the same manner as the mean value. Mean warming rates for the 21st century differ substantially between the two SRES scenarios after 2020, whereas for precipitation the range is much wider than the trend and there is little difference between scenarios.

for each season and decade is calculated by weighting each model's output by its bias and distance from the all-model average. Multi-model averages in weather forecasting, seasonal forecasting, and climate simulations often come closer to observations than single models (see Figure 3a above), and REA may produce better results for the future than an unweighted average by giving more weight to models that perform well in simulating 20th century climate. For details on the REA calculation, see Appendix B. The weights assigned to each model for the REA calculations are listed in Table 1. In this document, "2020s" denotes the 2010-2039 average, 1980s denotes the 1970-1999 average, and likewise for 2040s and 2080s.

3.1. 21st Century Trends in the Annual Mean

The regionally averaged temperature and precipitation for all B1 and A1B simulations are shown in Figure 7, along with the REA value for each year. To calculate the REA weighting, each model's projected temperature is smoothed by regressing temperature on the logarithm of the atmospheric concentration of CO_2, an approximation (IPCC 2001) of global radiative forcing (see Figure 1). The same is done for precipitation. This approach,

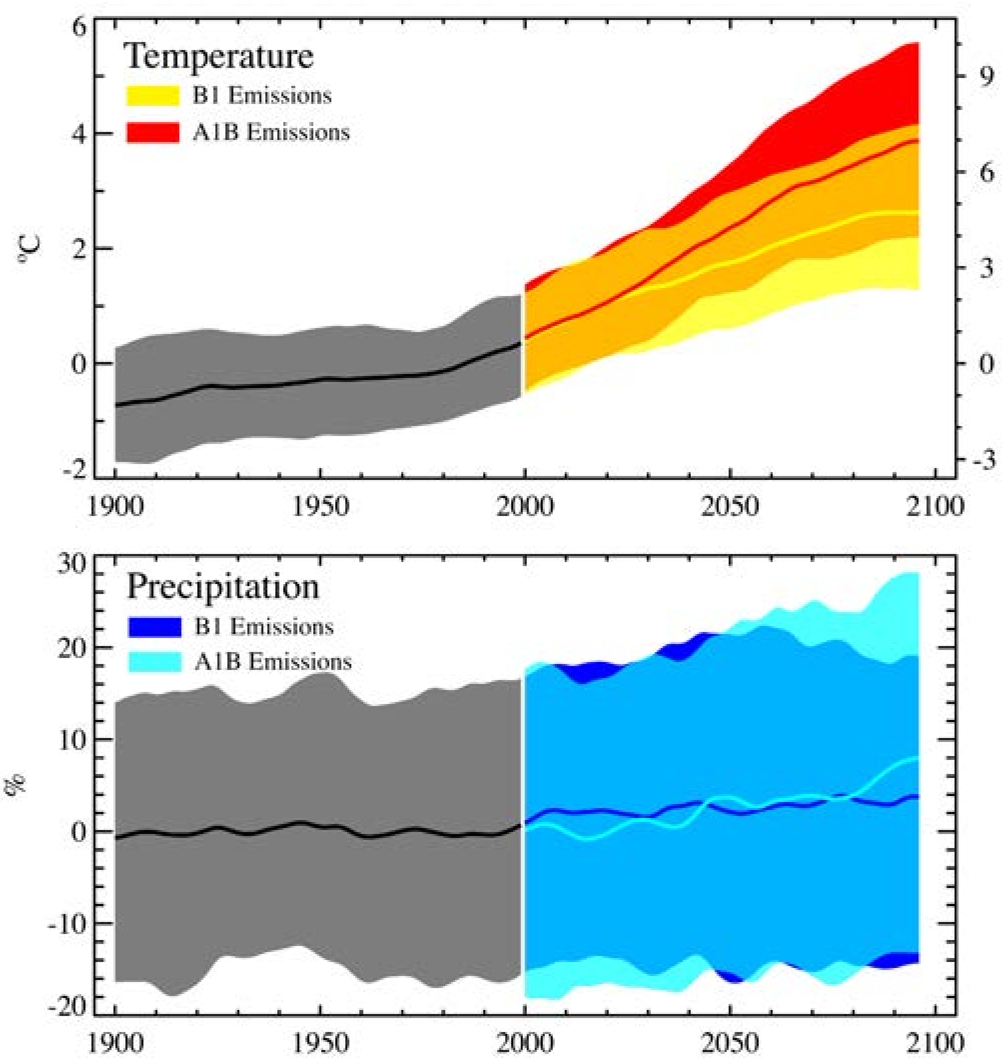

which is used only to calculate the annual REA values shown in Figure 7, highlights the region's response to the forcing on century timescales, masking model interdecadal variability which, while interesting, can confound the detection of forced change, especially for precipitation. Note how different the evolution of temperature is after about 2050 for the two scenarios, owing to the markedly different radiative forcing produced by different concentrations of greenhouse gases. By the 2080s the REA value of temperature change is almost 3.4°C (6.1°F) for A1B and only 2.5°C (4.5°F) for B1. The range just for these two scenarios is 1.5 to 5.8°C (2.8-9.7°F); other IPCC emissions scenarios would produce more warming by 2100, but B1 produces the least.

The observed trend in regional mean temperature is statistically significant, that is, it exceeds what would be expected from a time series with no trend and the same amount of interannual variability (Mote 2003). Likewise, the projected future trends, even for the very lowest of the scenarios, is substantially greater than observed in the 20th century.

Model results for changes in precipitation are equivocal (Figure 7). In the maps of late-21st century changes in precipitation presented by Christensen et al. (2007), nearly all climate models project increases in annual mean precipitation in the northern third of North America and nearly all project decreases in the southern third, and the PNW lies in the vague area in between. Consistent with those maps, the annual mean REA change for the PNW is practically zero throughout the 21st century, though individual models produce changes of as much as -10% or +20% by the 2080s. It should be noted that the REA weighting emphasizes past performance and

Table 1. REA weights (bias factor times distance factor) for the A1B scenario. Seasonal weights are computed separately and do not sum to the total.

	Temperature					Precipitation				
	DJF	MAM	JJA	SON	annual	DJF	MAM	JJA	SON	annual
bccr	0.2	0.3	0.3	0.3	0.2	1.0	1.0	1.0	1.0	0.9
ccsm3	0.3	0.5	1.0	0.4	0.4	1.0	1.0	1.0	1.0	1.0
cgcm3.1_t47	0.2	0.4	0.5	0.5	0.3	1.0	1.0	0.7	1.0	0.4
cgcm3.1_t63	0.1	0.2	0.2	0.2	0.1	1.0	1.0	1.0	1.0	1.0
cnrm_cm3	1.0	0.5	1.0	1.0	0.9	1.0	1.0	1.0	1.0	0.7
csiro_3_5	0.2	1.0	0.2	0.6	0.3	1.0	1.0	1.0	1.0	1.0
echam5	0.2	1.0	0.3	0.4	0.3	0.8	1.0	1.0	1.0	0.9
echo_g	0.6	0.3	0.2	1.0	0.3	1.0	1.0	0.6	0.7	0.5
fgoals1_0_g	0.1	0.2	1.0	0.6	0.2	1.0	1.0	1.0	1.0	1.0
gfdl_cm2_0	0.1	0.3	0.1	0.1	0.1	1.0	1.0	0.7	1.0	0.7
gfdl_cm2_1	0.2	0.3	0.5	0.2	0.2	1.0	1.0	1.0	1.0	1.0
giss_aom	0.8	1.0	0.2	0.4	0.4	1.0	1.0	0.4	0.6	0.3
giss_er	0.5	1.0	0.2	1.0	1.0	0.4	0.6	0.6	0.5	0.2
hadcm	0.3	0.6	0.4	0.3	0.3	1.0	1.0	0.4	0.6	0.4
hadgem1	0.1	0.3	0.6	1.0	0.4	0.4	0.7	0.4	0.5	0.2
inmcm3_0	0.6	1.0	0.3	1.0	1.0	1.0	1.0	0.6	0.9	0.4
ipsl_cm4	1.0	0.8	0.3	0.4	0.4	1.0	1.0	1.0	1.0	0.5
miroc3_2_hi	1.0	1.0	0.4	0.8	1.0	0.5	0.8	0.7	0.9	0.2
miroc_3.2	0.3	0.4	1.0	0.7	0.5	0.5	1.0	1.0	0.8	0.3
pcm1	0.2	0.3	0.3	0.4	0.2	1.0	1.0	0.6	1.0	0.4

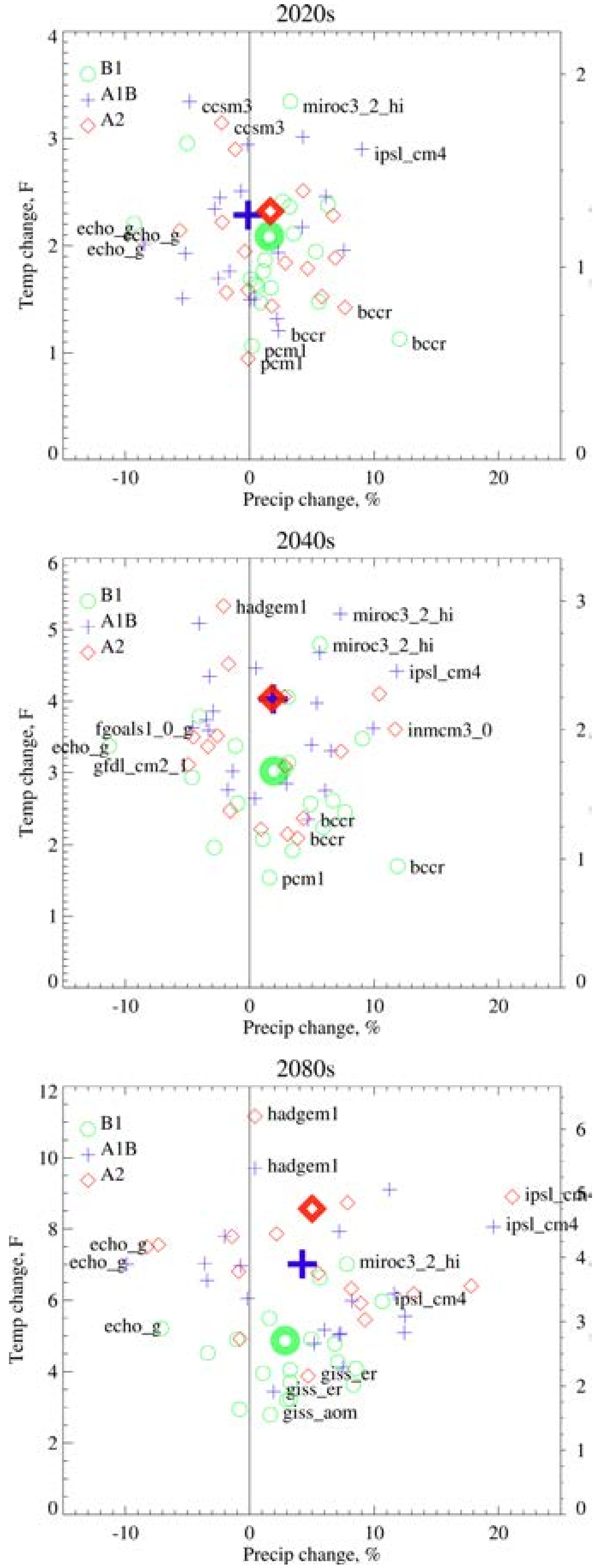

Figure 8. Scatterplot of change in annually averaged PNW temperature and precipitation for each of the 20 models and 3 SRES scenarios, for the decades indicated. Green circles indicate B1, blue crosses A1B, and red diamonds A2. Large bold symbols indicate the REA value for each scenario and decade. Model names label the four extremes for each scenario.

closeness to the multi-model mean, which are no guarantee of responding correctly to future greenhouse forcing; but it could also be argued that the models with poor performance in simulating observed annual mean or seasonal precipitation may have the storm track at the wrong latitude and hence respond incorrectly to future greenhouse forcing.

Another way to view the scenarios is to plot the change in temperature on one axis and the change in precipitation on another axis (Figure 8). Figure 8 roughly shows the sensitivity of the models to forcing, with different magnitudes of forcing applied by the three SRES scenarios and in different quantities for the three decades. The ranking of models is similar for each decade and SRES scenario: HadGEM1, MIROC3_ 2_hi, or CCSM3 tend to be the warmest in each scenario and each decade, IPSL_CM4 or BCCR the wettest, and so on. Unlike the situation in the global mean, where the precipitation change and temperature change of models tend to be correlated, there seems to be no correspondence between temperature change and precipitation change in the Pacific Northwest. Differences among the scenarios are small in the 2020s but are substantial by the 2040s. In the coolest scenario, regional temperature rises 0.6°C (1.1°F) by the 2020s, 0.9°C (1.5°F) by the 2040s, and 1.6°C (2.8°F) by the 2080s. In the warmest scenario, annually averaged warming is roughly a factor of three higher than the lowest scenario: 1.9°C (3.3°F) by the 2020s, 2.9°C (5.2°F) by the 2040s, and 5.4°C (9.7°F) by the 2080s.

3.2. Seasonality of Changes in Climate

For some applications the changes of climate in a given season may be more important than the changes in annual mean. In this section we present the changes in climate by season. Figures 9 and 10 show changes in temperature and precipitation for the 2020s, 2040s, and 2080s relative to the 1980s. For both B1 and A1B, warming is projected to be largest in summer. In most seasons B1 has the lowest projected change and A1B the highest, but this is not always true in the 2020s when the radiative forcing of the two scenarios is very similar.

On the seasonal scale the most consistent changes in precipitation appear in the summertime, with a large majority of models (68-90% depending on decade and SRES scenario) projecting decreases and the REA value reaching -14% by the 2080s. Some models foresee reductions of as much as 20-40% in summer precipitation, though these large percentages only translate to 3- 6 cm over the season, 3-6% of the all-model annual mean 20th century value (102 cm). While small hydrologically in the Northwest, summer precipitation and its associated cloudiness nonetheless has an impact on evaporative demand and hence, for example, on urban water use (Palmer and Hahn 2002) and forest fires (McKenzie et al. 2004).

In winter, by contrast, a majority (50-80% depending on decade and SRES scenario) of models project increases in precipitation. The REA value reaches +8% (about 3cm) by the 2080s for the A1B scenario, still small relative to interannual variability. And although some of the models predict modest reductions in fall or winter precipitation, some predict very large increases (up to 42%). Changes of this magnitude would substantially alter regional hydrology.

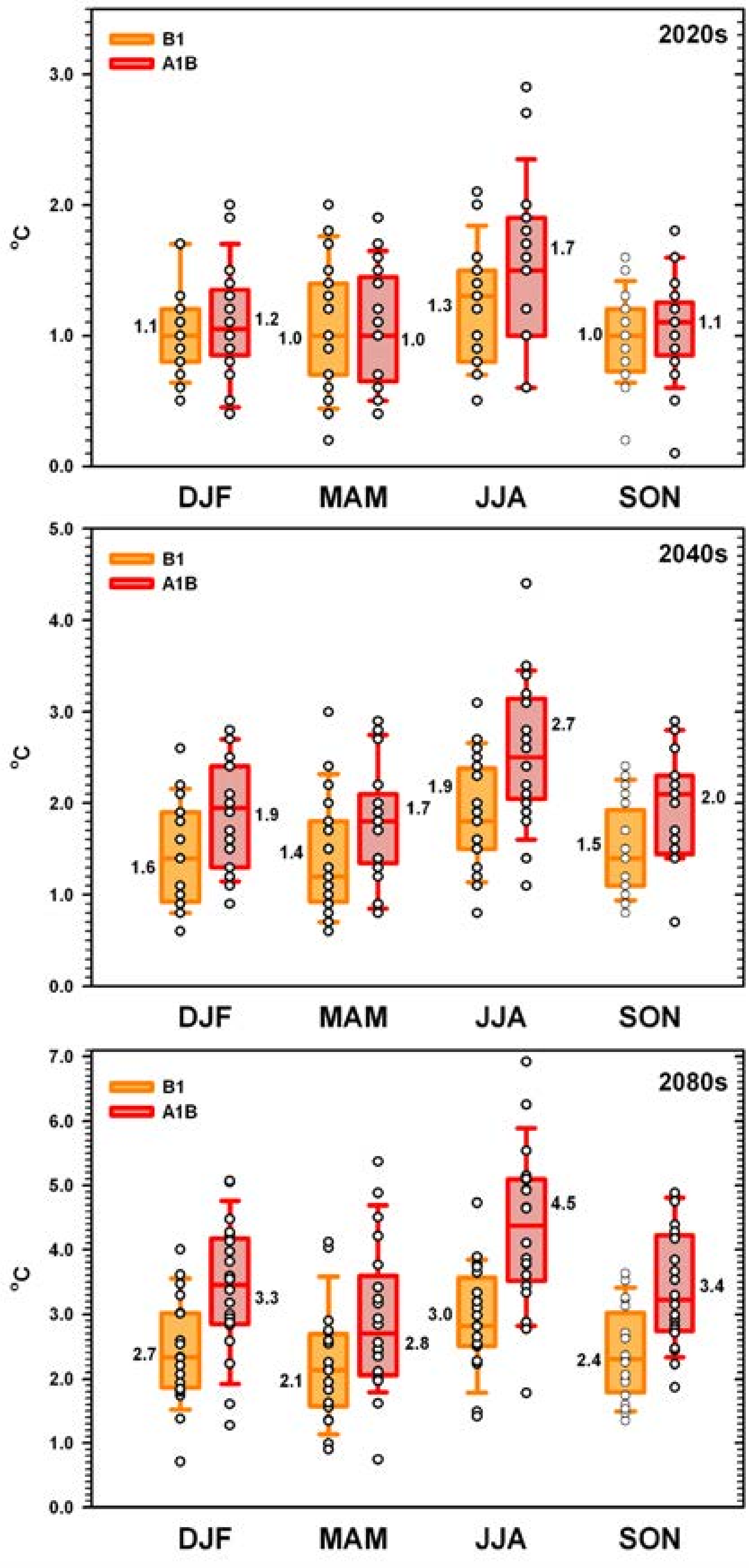

Figure 9. Range (lowest to highest) of projected changes in temperature for each season (DJF=winter, etc.), relative to the 1970-99 mean. In each pair of box- and-whiskers, the left one is for SRES scenario B1 and the right is A1B; circles are individual model values. Box-and-whiskers plots indicate 10th and 90th percentiles (whiskers), 25th and 75th percentiles (box ends), and median (solid middle bar) for each season and scenario. Not all values are visible due to symbol overlap. Printed values are the weighted Reliability Ensemble Average of all GCMs for the season and scenario.

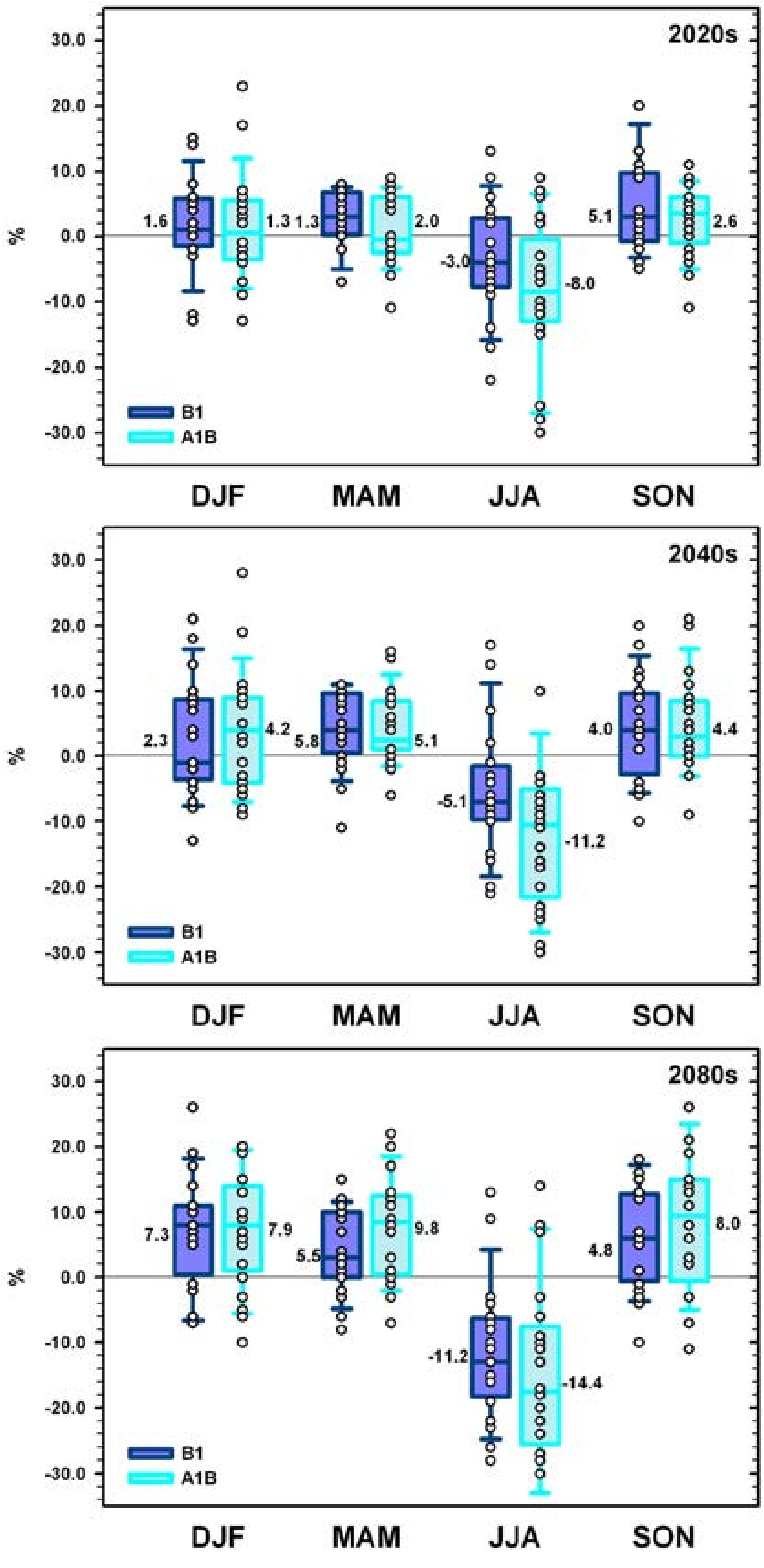

Figure 10. As in Figure 9, but for precipitation. The height of the bars indicates actual water precipitation but the percentages are calculated with respect to a reference value for that season, so that -11% in JJA is much less than -11% in DJF. The reference values for the extremes are that model's 20th century mean for that season (or annual mean), and for the REA average the reference is the all-model 20th century value. Unlike for temperature, for any season some models project increases and some project decreases, though the vast majority project decreases for summer and increases for winter by the 2080s

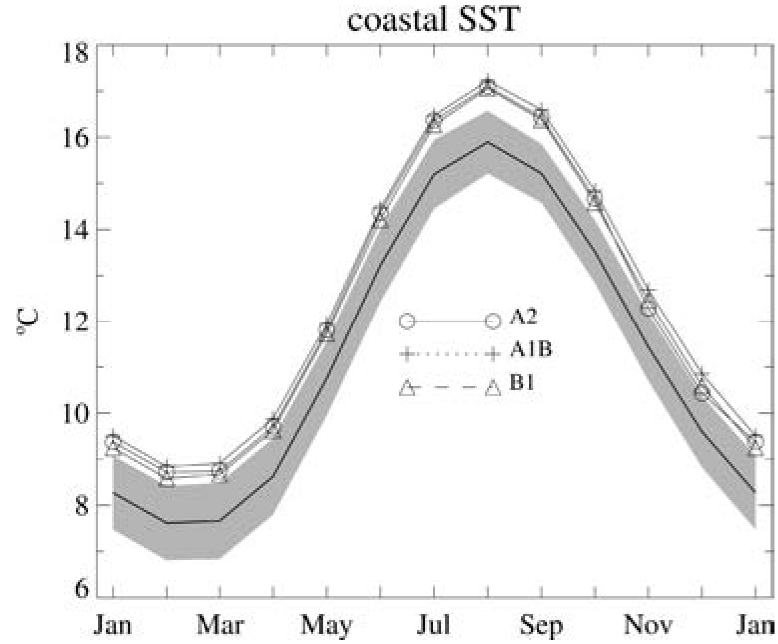

Figure 11. Simulated annual cycle of sea surface temperature (SST) averaged over 1970-99 for all available models. Grey shading represents ±1 standard deviation of the multimodel ensemble about the 1970-99 mean, shown as a solid black line, and the three curves above the grey shaded area show the means for 2030-2059 for the three scenarios. Though small, the 1.2°C warming is substantially outside the 20th century variability.

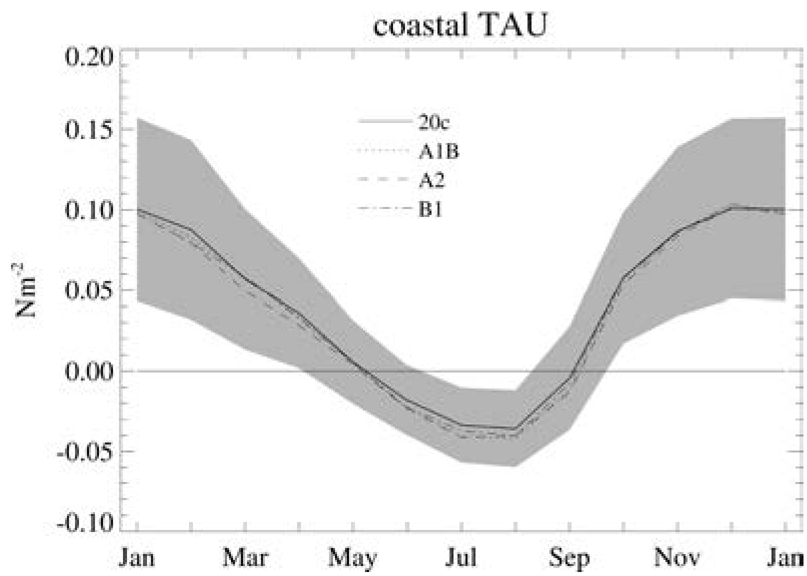

Figure 12. As in Fig. 11 but for alongshore wind stress, which changes very little in the future scenarios.

For some applications one may want to choose a few GCM scenarios to represent a "medium" (closest to REA average), "worst case", and "best case". The worst and best case will depend very much on application, and certain seasons may matter most. For example, the worst case scenario might be the one with the largest winter or spring warming and small or negative change in winter precipitation: for 2040s, MIROC 3.2 A1B has 2.8°C (5.0°F) spring warming, only 3% increase in spring precipitation and no change in winter precipitation. The best case may be BCCR-B1 with a 17% increase in winter precipitation, 8% increase in spring precipitation, and warming of only 0.9°C (1.6°F) in winter and 0.5°C (0.9°F) in spring. Another dimension of impacts centers on how warm-dry summers are: the mean is +2.1°C (3.8°F) and -12% for A1B, worst-case +4.4°C (7.9°F) and -30% in HadCM, and best-case +0.85°C (1.5°F) and +7% for PCM1 B1.

4. Changes in Coastal Water Properties

Coastal sea surface temperature (SST) helps determine the biological and physical conditions of the marine environment and the estuaries of the Northwest. Each of the 20 models examined here has a detailed ocean model with higher spatial resolution than the atmosphere model, and simulates SST. Owing however to the still relatively coarse resolution of the ocean model and the complexity of nearshore circulations, simulated coastal SST and especially its seasonal cycle may bear little resemblance to observed SST. Figure 11 shows the mean annual cycle for the 1970-99 and 2030-59 periods for coastal grid points between 46° and 49°N. Modeled change in SST is about 1.2°C (2.2°F), somewhat less than for the PNW land areas (2.0°C, 3.6°F) but a significant change relative to the small interannual variability of the ocean.

Along the west coast of each continent, summertime equatorward winds pull water offshore and water must upwell from depth to replace it. This nutrient-rich water serves as the basis for very high biological productivity. Our earlier analysis of two climate models (Mote and Mantua 2002) indicated little change in coastal upwelling in any of the major regions of upwelling. For the 20 models used in this study, the mean change is also quite small (Figure 12).

Another important aspect of change in the coastal ocean is local sea level rise (SLR), which is produced by the combined effects of global sea level rise and local factors such as vertical land deformation (e.g., tectonic movement, isostatic rebound) and seasonal ocean elevation changes due to atmospheric circulation effects. We previously (Mote et al. 2008) reviewed available projections of these factors for the coastal waters of Washington and provided low, medium, and high estimates of local SLR for 2050 and 2100. These are summarized here.

The Fourth Assessment Report of the IPCC projects global SLR over the course of this century to be between 18 and 38 cm (7-15") for their lowest (B1) emissions scenario, and between 26 and 59 cm (10-23") for their highest emissions scenario. Based on the current science, our "medium" estimate of 21st century SLR in Washington is that in Puget Sound, local SLR will closely match global SLR. On the northwest Olympic Peninsula, very little relative SLR will be apparent due to rates of local tectonic uplift that currently exceed projected rates of global SLR. On the central and southern Washington coast, the number of continuous monitoring sites with sufficiently long data records is small, adding to the uncertainty of SLR estimates for this region. Available data points suggest, however, that uplift is occurring in this region, but at rates lower than that observed on the NW Olympic Peninsula.

The application of SLR estimates in decision making will depend on location, time frame, and risk tolerance. For decisions with long timelines and low risk tolerance, such as coastal development and public infrastructure, users should consider low-probability high-impact estimates that take into account, among other things, the potential for higher rates of SLR driven by recent observations of rapid ice loss in Greenland and Antarctica, which though observed were not factored into the IPCC's latest global SLR estimates. Combining the IPCC high emissions scenario with 1) higher estimates of ice loss from Greenland and Antarctica, 2) seasonal changes in atmospheric circulation in the Pacific, and 3) vertical land deformation, a low-probability high-impact estimate of local SLR for the Puget Sound Basin is 55 cm (22") by 2050 and 128 cm (50") by 2100. Low-probability, high impact estimates are smaller for the central and southern Washington coast (45 cm [18"] by 2050 and 108 cm [43"] by 2100), and even lower for the NW Olympic Peninsula (35 cm [14"] by 2050 and 88 cm [35"] by 2100) due to tectonic uplift.

5. Downscaling Methods

Two approaches are commonly used to map coarse-scale climate model output to finer-scale local detail: statistical downscaling and regional modeling. Statistical downscaling methods use the empirical relationship between an observed climatology, say precipitation, at the higher resolution and coarse-scale model fields, like the altitude of the 700 hPa pressure level, from global climate models. The empirical relationship is derived using the observations as predictand and a simulation from a global climate model for the observed period, and may use a number of modeled fields as predictors in the empirical relationship. For example, often atmospheric circulation and moisture variables are used to downscale regional precipitation.

For this project, we applied statistical downscaling based on 1/16-degree gridded historic observed temperature and precipitation (Elsner et al. 2009, this report) using two methods. The first is a simple "delta method" where the observed daily temperature and precipitation from the period 1970-1999 are perturbed to produce fine-scale projections of the future (e.g. Loáiciga 2000; Lettenmaier and Gan 1990), by computing monthly mean changes in average PNW temperature and percent change in precipitation for the 2020s, 2040s, and 2080s. We then apply these perturbations, or deltas, to the 1/16-degree historic data to form future climate change scenarios. At each grid point, the regional temperature delta is added to the observed daily maximum and minimum temperatures and the regional precipitation delta is multiplied by the daily precipitation. In this way, we produce 30-year daily temperature and precipitation sequences and spatial patterns that are physically consistent but modified by different scenarios of climate change for each future time period and each global climate model. This method has the advantage of preserving the observed sequence of weather and natural climate variability, which allows easy comparison to the past. However, if anthropogenic influence on climate includes a change in higher statistical moments – variance, skewness – this method will miss such changes.

The second and more sophisticated statistical downscaling method is based on methods described by Wood et al. (2002), Widmann et al. (2003), and Salathé (2005). This approach preserves the observed statistical properties of temperature and precipitation during the 20th century while allowing these to change in future projections. As in Wood et al., the monthly-mean global climate model data are bias-corrected. The bias-corrected climate model is then downscaled to 1/16-degree grid spacing. For precipitation, the "dynamical scaling" method presented in Widmann et al. (2003) is used. This method accounts for the effects of both large-scale precipitation processes and changes in atmospheric circulation on the local precipitation. For temperature, a simple spatial disaggregation is applied (Wood et al. 2002). Finally, the monthly mean data are disaggregated to daily time steps using the method described in Salathé (2005).

The important differences between the transient statistical downscaling and delta method are 1) the trends in the climate projection are preserved and 2) modes of climate variability and shifts in climate variability in the global model are preserved in the transient downscaling. In some applications, for example in water resource planning, these issues are not important and make the interpretation of results more difficult (Salathé et al. 2007). In other applications, for example in modeling ecologic systems, climate trends and variability are important to consider.

Regional climate models are another tool for downscaling and provide a physically-based representation of the interactions between the large-scale atmospheric features simulated by global models and the fine-scale regional features such as terrain, land-use, and water bodies. These interactions can produce local rates of change of temperature and precipitation that are quite different from those simulated by global climate models (Salathé et al. 2008). Salathé et al (2009) present results from a regional climate model applied to downscale two global climate models.

The relative merits of downscaling methods for the Pacific Northwest are discussed in Salathé et al. (2007). Statistical downscaling has an important advantage over a regional model in that it is computationally efficient and allows the consideration of a large set of climate scenarios. Over the next 50 years, projections differ much more among various models than among emissions scenarios. Therefore, to fully account for this uncertainty, a multi-model ensemble is the most appropriate approach and statistical downscaling is well suited to many applications that require projections only of temperature and precipitation. Statistical methods can also tune the statistical properties of climate simulations, eliminating biases and adjusting the variance, to better match observed statistics. Regional climate models, however, can better represent the local responses to climate change, which may be critical to applications in regions of complex terrain and land-water contrasts. Regional simulations also open up a broad range of impacts applications that are not suited to statistical downscaling, such as air quality modeling (Avise et al. 2006).

6. Discussion and Conclusions

Most GCMs reproduce key features of observed PNW climate including the sharp contrast between wet winters and dry summers, the 20th century warming of about 0.8°C, and the mean atmospheric circulation over the North Pacific. These successes provide some confidence in their projected changes in future climate. For the SRES scenarios examined here, all models produce annual mean warming of at least 0.1°C per decade with some prospect of stabilizing climate by 2100 in the B1 scenario. For the A1B scenario the warming by the 2080s could be as high as 5.7°C (9.7°F) according to one model. Even the mean warming rate of 0.3°C (0.5°F) per decade could produce profound changes in the hydrology and environment of the Northwest, as discussed in later chapters.

Annual mean precipitation changes little when averaged over all the models, but individual models produce substantially wetter or drier futures. For all of the 30-year means considered here, a majority of models produce wetter winters and drier summers, though the average shifts are small and not statistically significant.

Changes in the coastal zone include large projected warming relative to 20^{th} century variability but little change in coastal along-shore wind stress and coastal upwelling.

Other important aspects of climate change are more suitable for investigation by regional models, which can better resolve daily-scale as well as fine spatial-scale variability. Leung et al. (2004) using a regional model forced by an earlier version of the PCM found reductions (not significant) in precipitation west of the Cascades, especially in winter, but increases throughout the PNW in extreme daily precipitation. Salathé et al. (2009, this report) provide additional analysis of changes at smaller scales.

Acknowledgments

We are grateful to the Program for Climate Model Diagnosis and Intercomparison for making available the model output, and to the State of Washington for funding this work. Emily Jump assisted in processing the GCM output.

Appendices

Appendix A

In a few instances the data available from Run 1 appeared not to be complete (e.g., missing variable or decade) so we used Run 2. The models for which this occurred were CCSM3 A2 and B1, and PCM1 B1.

Appendix B

Reliability ensemble averaging (REA) uses a bias factor and a distance factor to weight each model's output. Each factor is calculated by averaging quantities over the Pacific Northwest, for each season and for the annual mean, following these steps.

1. Compute the difference δ between the model mean and CRU mean, for the 1970-99 period.
2. Calculate the tolerance factor ε to allow for variability of 30-year means relative to the century timescale. First, using regionally averaged CRU data for 1901-2000, detrend (subtract the linear fit from) the 20^{th} century time series, then calculate the standard deviation ε of the running 30-year mean. The tolerance factor is used in computing both the bias factor and the distance factor.
3. Calculate the bias factor. For models with a δ less than ε, the bias factor is 1; if δ is greater than ε, the bias factor is reduced to ε/δ.
4. Looking now at 21^{st} century simulations, regress the quantity in question (e.g., annual mean temperature) on the log of CO_2 (see Figure 1). For purposes of calculating the distance factor, take the

value of the resulting fit at year 2045 minus the value at year 2000, di, for model i. This is the only step in which we depart from the method of Giorgi and Mearns, and we do so in order that each model has a single weighting factor for each of the time periods considered (2020s, 2040s, 2080s).

5. Calculate the all-model mean value d of the individual model distances d_i. Then weight each model d_i by its distance from the mean d and recompute the all-model mean d. Only one or two iterations is needed to converge.
6. Calculate the distance factor in the same manner as the bias factor: for di less than ε, the distance factor is 1; for d_i greater than ε, the distance factor is ε/d_i.
7. For each season, decade, scenario, and variable, compute an REA value by summing over all available models the product of the model's projected change, its bias factor, and its distance factor.

References

Cayan DR, Maurer EP, Dettinger MD, Tyree M, Hayhoe K (2007) Climate change scenarios for the California region. Clim Chang, doi 10.1007/s10584-007-9377-6

CCSP (2008) Climate Models: An Assessment of Strengths and Limitations. A Report by the U.S. Climate Change Science Program and the Subcommittee on Global Change Research [Bader D.C., C. Covey, W.J. Gutowski Jr., I.M. Held, K.E. Kunkel, R.L. Miller, R.T. Tokmakian and M.H. Zhang (Authors)]. Department of Energy, Office of Biological and Environmental Research, Washington, D.C., USA, 124 pp

Christensen JH, et al. (2007) Regional climate projections. In: Climate Change 2007: The physical science basis. Contribution of working group I to the fourth assessment report of the Intergovernmental Panel on Climate Change [Solomon S, Qin D, Manning M, Chen Z, Marquis M, Averyt KB, Tignor M, Miller HL (eds.)]. Cambridge University Press, Cambridge, United Kingdom and New York, NY, USA

Elsner MM, Cuo L, Voisin N, Hamlet AF, Deems JS, Lettenmaier DP, Mickelson KEB, Lee SY (2009) Implications of 21st century climate change for the hydrology of Washintgon State. Clim Chang, in preparation

Giorgi F, Mearns LO (2002) Calculation of average, uncertainty range, and reliability of regional climate changes from AOGCM simulations via the reliability ensemble averaging (REA) method. J Clim 15: 1141–1158

Hamlet AF, Lettenmaier DP (2005) Production of temporally consistent gridded precipitation and temperature fields for the continental United States. J Hydrometeorol, 6: 330-336

Kalnay E, et al. (1996) The NCEP/NCAR 40-year reanalysis project. Bull Amer Meteorol Soc 77: 437–471

Lettenmaier DP, Gan TY (1990) Hydrologic sensitivities of the Sacramento-San Joaquin River basin, California, to global warming. Water Resour Res 26: 69–86

Leung LR, Qian Y, Bin X, Washington WM, Han J, Roads JO (2004) Mid-century ensemble regional climate change scenarios for the western United States. Clim Chang 62: 75–113

Loáiciga HA, Maidment DR, Valdes JB (2000) Climate-change impacts in a regional karst aquifer, Texas, USA. J Hydrol 227: 173-194

McKenzie D, Gedalof ZM, Peterson DL, and Mote PW (2004) Climatic change, wildfire, and conservation. Conserv Biol 18(4):890-902

Meehl, GA, Stocker TF, Collins WD, Friedlingstein P, Gaye AT, Gregory JM, Kitoh A, Knutti R, Murphy JM, Noda A, Raper SCB, Watterson IG, Weaver AJ, and Zhao Z-C (2007) Global climate projections. in Climate change 2007: The Physical science basis. Contribution of working group I to the fourth assessment report of the Intergovernmental Panel on Climate Change [Solomon, S, et al., (eds)]. Cambridge University Press, Cambridge, United Kingdom and New York, NY, USA.

Mitchell TD, Carter TR, Jones PD, Hulme M, and New M (2004) A comprehensive set of climate scenarios for Europe and the globe: the observed record (1901-2000) and 16 scenarios (2001-2100). Tyndall Centre Working Paper No. 55, University of East Anglia, Norwich, UK.

Mote PW (2003) Trends in temperature and precipitation in the Pacific Northwest. Northwest Science 77: 271–282.

Mote PW, Mantua NJ (2002) Coastal upwelling in a warming future. Geophys Res Lett 29(23)

Mote PW, Salathé EP (2009) Future climate in the Pacific Northwest. Chapter 1 in The Washington Climate Change Impacts Assessment: Evaluating Washington's Future in a Changing Climate, Climate Impacts Group, University of Washington, Seattle, Washington.

Mote PW, Salathé EP, and Peacock C (2005) Scenarios of Future Climate for the Pacific Northwest. Climate Impacts Group, Joint Institute for the Study of the Atmosphere and Ocean, University of Washington. 13pp.

Mote PW, Peterson A, Reeder S, Shipman H, Whitely Binder L (2008) Sea level rise in the coastal waters of Washington state. Climate Impacts Group, Joint Institute for the Study of the Atmosphere and Ocean, University of Washington. 11pp

Nakićenović N, Swart R (eds.) (2000) Special report on emissions scenarios. A special report of working group III of the Intergovernmental Panel on Climate Change. Cambridge University Press, Cambridge, United Kingdom and New York, NY, USA, 599 pp

Palmer RN, Hahn MA (2002) The impacts of climate change on Portland's water supply: An investigation of potential hydrologic and management impacts on the Bull Run system. Report prepared for the Portland Water Bureau, University of Washington, Seattle. 139 pp

Randall DA, Wood RA, Bony S, Colman R, Fichefet T, Fyfe J, Kattsov V, Pitman A, Shukla J, Srinivasan J, Stouffer RJ, Sumi A, Taylor KE (2007) Climate models and their evaluation. In: Climate change 2007: The Physical science basis. Contribution of working group I to the fourth assessment report of the Intergovernmental Panel on Climate Change [Solomon, S, et al., (eds)]. Cambridge University Press, Cambridge, United Kingdom and New York, NY, USA

Raupach MR, Marland G, Ciais P, Le Quéré C, Canadell JG, Klepper G, Field CB (2007) Global and regional drivers of accelerating CO2 emissions. Proc Natl Acad Sci doi 10.1073/pnas.0700609104

Salathé EP (2005) Downscaling simulations of future global climate with application to hydrologic modeling. Int J Clim 25:419-436

Salathé EP, Mote PW, and Wiley MW (2007) Review of scenario selection and downscaling methods for the assessment of climate change impacts on hydrology in the United States pacific northwest. Int J Clim 27:1611-1621

Salathé EP, Steed R, Mass CF, and Zahn P (2008) A high-resolution climate model for the U.S. Pacific Northwest: Mesoscale feedbacks and local responses to climate change. J Clim 21:5708-5726

Salathé EP, Leung LR, Qian Y, Zhang Y (2009) Regional climate model projections for the State of Washington. Clim Chang, in preparation

Schellnhuber HJ, et al. (eds) (2006) Avoiding dangerous climate change. Cambridge University Press, New York, NY

Stainforth, D.A., et al., 2005: Uncertainty in predictions of the climate response to rising levels of greenhouse gases. Nature, 433, doi: 10.1038/nature03301.

Taylor KE (2000) Summarizing multiple aspects of model performance in a single diagram. Report No. 55 of the Program for climate model diagnosis and intercomparison, Lawrence Livermore National Laboratory

Widmann M, Bretherton CS (2000) Validation of mesoscale precipitation in the NCEP reanalysis using a new gridcell dataset for the northwestern United States. J Clim 13: 1936-1950

Widmann M, Bretherton CS, and Salathé EP (2003) Statistical precipitation downscaling over the Northwestern United States using numerically simulated precipitation as a predictor. J Clim 16:799-816

Wood AW, Maurer EP, Kumar A, and Lettenmaier DP (2002) Long-range experimental hydrologic forecasting for the eastern United States. J Geophys Res-Atmos 107:4429-4443

Zhang, X., Zwiers, F.W., Hegerl, G.C., Lambert, F.H., Gillett, N.P., Solomon, S., Stott, P.A, and Nozawa, T. 2007. Detection of human influence on twentieth-century precipitation trends. Nature: 06025, DOI:10.1038, 1-5.

Photo credit, page 23: iStockphoto.com

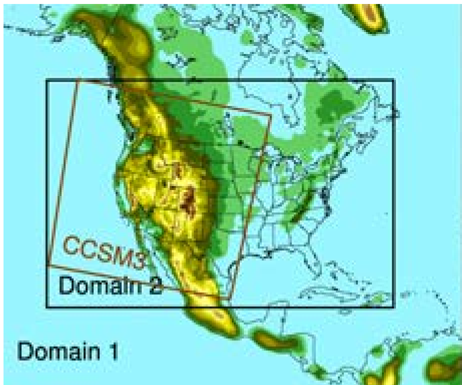


2: Regional Climate Models

Regional Climate Model Projections for the State of Washington

Eric P Salathé Jr[1], L Ruby Leung[2], Yun Qian[2], and Yongxin Zhang[1]

Abstract

Global climate models do not have sufficient spatial resolution to represent the atmospheric and land surface processes that determine the unique regional heterogeneity of the climate of the State of Washington. If future large-scale weather patterns interact differently with the local terrain and coastlines than current weather patterns, local changes in temperature and precipitation could be quite different from the coarse-scale changes projected by global models. Regional climate models explicitly simulate the interactions between the large-scale weather patterns simulated by a global model and the local terrain. We have performed two 100-year climate simulations using the Weather and Research Forecasting (WRF) model developed at the National Center for Atmospheric Research (NCAR). One simulation is forced by the NCAR Community Climate System Model version 3 (CCSM3) and the second is forced by a simulation of the Max Plank Institute, Hamburg, global model (ECHAM5). The mesoscale simulations produce regional changes in snow cover, cloudiness, and circulation patterns associated with interactions between the large-scale climate change and the regional topography and land-water contrasts. These changes substantially alter the temperature and precipitation trends over the region relative to the global model result or statistical downscaling. To illustrate this effect, we analyze the changes from the current climate (1970-1999) to the mid 21st century (2030-2059). Changes in seasonal-mean temperature, precipitation, and snowpack are presented. Several climatological indices of extreme daily weather are also presented: precipitation intensity, fraction of precipitation occurring in extreme daily events, heat wave frequency, growing season length, and frequency of warm nights. Despite somewhat different changes in seasonal precipitation and temperature from the two regional simulations, consistent results for changes in snowpack and extreme precipitation are found in both simulations.

[1] JISAO Climate Impacts Group, University of Washington, Seattle, Washington
[2] Atmospheric Science and Global Change Division, Pacific Northwest National Laboratory, Richland, Washington

1. Introduction

The climate of the State of Washington is exceptional in its range of variability. Geographical climate zones range from temperate coastal rain forests to glaciated mountain ranges to arid scrublands. Temporally, the state experiences a large range in precipitation over the annual cycle and significant year-to-year variability associated with the El Niño-Southern Oscillation and modulated by the Pacific Decadal Oscillation. The region is characterized by its complex terrain, coastlines, varied ecological landscapes, and land use patterns. These features interact at all spatial and temporal scales with weather systems from the North Pacific and continental interior to establish the regional climate of the state. To understand how climate change will affect the state, we must understand how these interactions modulate the large-scale global climate change patterns simulated by global climate models.

Global climate models do not account for the atmospheric processes that determine the unique spatially heterogeneous climatic features of Washington. Elsewhere in this report (Elsner et al., 2009, this report), climate datasets with high spatial resolution (on a 6km grid) are produced using a combination of global climate simulations and gridded observations by way of statistical downscaling methods (Mote et al., 2009, this report). Statistical methods have been successfully employed in the Pacific Northwest (Salathé, 2003, 2005; Widmann et al., 2003; Wood et al., 2004) and other regions (Giorgi et al., 1999). Statistical downscaling is based on fine-scale data derived using assumptions about how temperature and precipitation vary over complex terrain in order to interpolate the sparse station network (about 50-km spacing) to a 6-km grid. Information simulated by the coarse-resolution global models (with output on a 100-to-300 km grid) is then used to project the future climate. This approach represents the mean climate and local regimes quite well but does not take into account how the terrain influences individual weather systems. Mesoscale process involving land and water surface characteristics, such as orographic precipitation, convergence zones, snow-albedo feedbacks, and cold air drainage, are likely to respond to the changing large-scale climate (see, for example, Leung et al., 2004 and Salathé et al., 2008). Since mesoscale processes are not explicitly represented in global models and statistical downscaling, their role in determining regional climate change is not fully accounted for with these methods. The motivation for applying regional climate models, therefore, is to simulate these processes and to understand their role in regional climate change. In the typical regional climate modeling design, as used here, mesoscale processes do not feedback onto the global climate simulation, and large-scale features that depend on these feedbacks cannot be properly represented. However, many important feedbacks operate at the local scale, such as snow-albedo feedback, and these can substantially modify the regional climate projection.

A regional climate model is similar to a global climate model in that it simulates the physical processes in the climate system. Regional climate models cover a limited area of the globe and are run at much finer spatial resolution – 1-50 km grid spacing as opposed to 100-300 km grid spacing in a global model – thus they can simulate the interactions between large-scale weather patterns and the local terrain. Global model output data are used to force the regional model at its boundaries and the regional model downscales the global model by producing fine-scale weather patterns consistent with the coarse-resolution features in the global model. The disadvantages of a regional climate model are that it is computationally expensive and cannot explicitly remove systematic differences (biases) between the global model and observations as statistical methods can. Thus, for many applications, some bias correction must be applied to the results, to remove the combined biases of the global and regional model. This approach is used in Rosenberg et al (2009, this report) using data from the WRF simulations presented here.

In this paper we report results from two 100-year simulations with a regional climate model using two different global models to provide forcing at the boundaries. Both regional simulations use the Weather Research and Forecasting (WRF) model developed at the National Center for Atmospheric Research (NCAR). This model includes advanced representations of cloud microphysics and land-surface dynamics to simulate the complex interactions between atmospheric processes like precipitation and land surface characteristics such as snow cover and soil moisture. One simulation is forced by the NCAR Community Climate System Model version 3 (CCSM3) and will be referred to as CCSM3-WRF and the second is forced by a simulation of the Max Plank Institute, Hamburg, global model (ECHAM5), referred to as ECHAM5-WRF. The WRF model configuration is very similar for both simulations, with modifications described below. The ECHAM5-WRF simulation was performed on a 36-km grid while the CCSM3-WRF simulation was on a 20-km grid. Thus, differences between the two simulations are primarily attributable to the forcing models and the grid spacing used. The ECHAM5-WRF grid encompasses the continental US while the CCSM3-WRF grid covers the western US. Here we analyze results only for the Pacific Northwest. We base our analysis on differences in the regional simulations for the present climate, defined as the 30-year period 1970 to 1999, and the mid 21st century, the 30-year period 2030-2059.

High spatial resolution in the regional model is critical to simulating mesoscale processes and adding value over the global model. For example, Leung and Qian (2003) showed substantial improvement in simulating precipitation and snowpack for the Pacific Northwest when reducing the grid spacing in a regional model. The 20-km grid CCSM3-WRF and 36-km ECHAM5-WRF grid spacing is sufficient to resolve the major mountain ranges and coastlines of the Pacific Northwest that are important to the climate of Washington.

2. Model Configuration

2.1. Forcing Models

The two models used to force the regional climate model (CCSM3 and ECHAM5) are compared with a set of 19 global models in Mote and Salathé (2009, this report), who show that both models provide realistic simulations of the 20th century climate. Compared to the multi-model average for the Pacific Northwest (Table 1), ECHAM5 projects a low temperature increase and a high precipitation increase while CCSM3 projects a relatively warmer and drier future.

Table 1. Pacific Northwest annual mean changes in temperature and precipitation from 1970-1999 to 2030-2059 for ECHAM5 and CCSM3 compared to a 19-model average.

Change	ECHAM5	CCSM3	19-model avg
Temperature (B1)	1.25°C	2.10°C	1.68°C
Temperature (A1B)	1.58°C	2.41°C	2.24°C
Precipitation (B1)	5.9%	-4.0%	2.0%
Precipitation (A1B)	3.0%	-3.2%	1.9%

The atmospheric component of ECHAM5/MPI-OM is the fifth-generation general circulation model developed at the European Centre for Medium-Range Weather Forecasts and the Max Planck Institute for Meteorology (Roeckner et al., 1999; Roeckner et al., 2003), and the ocean component is the Max Planck Institute Ocean Model (MPI-OM) (Marsland et al., 2003). Here we will refer to the coupled model simply at ECHAM5. For the present climate (1970-1999), we used an ECHAM5 simulation of the 20th century with historical forcing; for the 21st century, we used a simulation with the Special Report on Emissions Scenarios (SRES) A1B emissions scenario (Nakicenovic et al., 2000). ECHAM5 was run at T63 spectral resolution, which corresponds to a horizontal grid spacing of approximately 140x210 km at mid-latitudes, and 32 levels in the vertical. Model output at 6-hourly intervals was obtained from the CERA WWW Gateway at <http://cera-www.dkrz.de/CERA/index.html>; the data are managed by World Data Center for Climate <http://www.mad.zmaw.de/wdcc/>.

The NCAR Community Climate System Model Version 3 (CCSM3) consists of the Community Atmospheric Model (CAM), the Parallel Ocean Program (POP), the Community Land Model (CLM), and the Community Sea Ice Model (CSIM) coupled through a flux coupler to simulate the atmosphere, ocean, cryosphere, and land processes, and their interactions (Collins et al., 2006). The atmospheric model (CAM) that provides boundary conditions to CCSM3-WRF was run at a horizontal grid resolution of T85, which corresponds roughly to a grid spacing of 150 km in the mid-latitudes, with 26 vertical levels. For the present climate (1970-1999), CCSM3-WRF was forced with one of the 10 ensemble CCSM3 simulations of the 20th century with historical radiative forcing. For the future climate, we used one of five ensemble simulations prepared for the IPCC AR4 using the SRES A2 emission scenario. Model output at 6-hour intervals is available from the NCAR mass storage, the Program for Climate Model Diagnostic and Intercomparison (PCMDI) AR4 global simulation archives (http://www-pcmdi.llnl.gov/), and the Earth System Grid (ESG).

Since CCSM3 was run for an ensemble of simulations, we can compare the simulation used here to the full ensemble. Differences among ensemble members reflect the inherent variability in the simulated climate given the same radiative forcing, and each simulation can be taken as an equally likely projection of the climate. Of the parameters discussed here, precipitation shows by far the greatest variation across the ensemble, consistent with the large observed natural variability in regional precipitation. While precipitation from the global model is not used in forcing the regional model, the winds and moisture fields are used, and this ensures an overall compatibility of the global and regional precipitation simulation. The ensemble member used for this study differs from the ensemble mean most significantly in November precipitation over the Pacific Northwest. The CCSM3 SRES A2 ensemble mean shows a modest increase in autumn and spring precipitation with decreases in the winter and summer, which is generally consistent with the multi-model ensemble mean discussed in Mote and Salathé (2009, this report). For the ensemble member used to force WRF, the 1970-1999 November mean Pacific Northwest precipitation is the lowest and the 2030-2059 mean is the highest in the ensemble. Thus, the change in November precipitation is high compared to the ensemble mean. In the results below, we find that this increase in precipitation has a marked influence on the simulated regional climate change; these results must be interpreted as the combined influence of systematic climate change and internal climate variability.

2.2. Regional Model

The WRF model is a state-of-the-art mesoscale numerical weather prediction system designed to serve both operational forecasting and atmospheric research needs (http://www.wrf-model.org). This model has been developed and used extensively in recent years for regional climate simulation (Leung et al., 2006). WRF is a non-hydrostatic model with multiple choices for physical parameterizations suitable for applications across scales ranging from meters to thousands of kilometers. The physics package includes microphysics, convective parameterization, planetary boundary layer (PBL), land surface models (LSM), and longwave and shortwave radiation

In this work, the microphysics and convective parameterizations used were the WRF Single-Moment 5-class (WSM5) scheme (Hong et al., 2004) and the Kain-Fritsch scheme (Kain et al., 1993). The WSM5 microphysics explicitly simulates water vapor, cloud water, rain, cloud ice, and snow. The Kain-Fritsch convective parameterization utilizes a simple cloud model with moist updrafts and downdrafts that includes the effects of detrainment and entrainment. The land-surface model used was the NOAH (National Centers for Environmental Prediction - NCEP, Oregon State University, Air Force, and Hydrologic Research Lab) LSM (Chen et al., 2001). This is a 4-layer soil temperature and moisture model with canopy moisture and snow cover prediction. It includes root zone, evapotranspiration, soil drainage, and runoff, taking into account vegetation categories, monthly vegetation fraction, and soil texture. A modification is included so that soil temperatures vary at the lower boundary of the soil column (8-m depth) in accordance with the evolving climatological surface temperature. The PBL parameterization used was the YSU (Yonsei University) scheme (Hong et al., 1996). This scheme includes counter-gradient terms to represent heat and moisture fluxes due to both local and non-local gradients. Atmospheric shortwave and longwave radiation were computed by the NCAR CAM (Community Atmospheric Model) shortwave scheme and longwave scheme (Collins et al., 2004).

There are minor differences in the WRF model configurations used at Pacific Northwest National Laboratory for the CCSM3-WRF and used at the University of Washington for the ECHAM5-WRF simulations. First, the CCSM3-WRF simulation used the SRES A2 scenario while

ECHAM5-WRF used the SRES A1B emissions scenario. The effect of these different emissions scenarios on the simulated climate is insignificant since the two emissions scenarios do not begin to diverge until the mid 21st century. Secondly, the ECHAM5-WRF simulation follows the methods of the MM5-based mesoscale climate modeling described in Salathé et al. (2008): Nested grids and interior nudging are used to match the WRF simulation to the global model. The CCSM3-WRF uses a single model domain with a wider buffer zone for the lateral boundaries to increase the constraints from the global climate simulation. The relaxation coefficients of the nudging boundary conditions follow a linear-exponential function to smoothly blend the large-scale circulation from the global simulation and the regional simulation. As seen below, both simulations closely follow the forcing model, so both nudging and the extended buffer zone are successful methods of constraining the regional simulation.

3. Model Evaluation

To establish whether the regional climate simulations can reproduce the observed climate of the Pacific Northwest, we compared the two simulations for the winter (December-January-February, DJF) and summer (June-July-August, JJA) to gridded observations averaged for the period 1970-1999, in a similar manner to Leung et al. (2003). The gridded data consist of station observations interpolated to a 1/16-degree grid using an empirical model for the effects of terrain on temperature and precipitation (Daly, 2004; Elsner et al., 2009, this report). Since the CCSM3 and ECHAM5 simulations are from free-running climate models, the observed temporal sequence (i.e. at daily to interannual time scales) is not reproduced. However, for averages over a period of 30 years, most natural and internal model variability should be removed and we expect any differences among the simulations and gridded observations to be the result of model deficiencies and, to some degree, differences in grid resolutions. It is important to note that a regional model does not explicitly remove any bias in the forcing model, except where such bias is due to unresolved processes, and may introduce additional biases. This comparison, therefore, evaluates both the regional model and the global forcing model. Some uncertainty in the evaluation is introduced in using gridded observations as opposed to station observations since the gridding procedure interpolates between the sparse station network based on a simple terrain model for temperature and precipitation. An alternative method for evaluation of the WRF regional climate simulation, based on station observations, may be found in Zhang et al. (2009), who use a WRF simulation forced by an atmospheric reanalysis in order to isolate deficiencies in the mesoscale model from errors in the forcing model. That study found that Tmax and Tmin simulated by WRF compare well with the station observations. Warm biases of Tmax are noted in WRF simulations between February and June with cold biases during the rest of the year. Warm biases of Tmin prevail in throughout the year. The temporal correlation between the simulated and observed daily precipitation is low; however, the correlation increases steadily for longer averaging times, showing good representation of seasonal and interannual variability.

Figure 1 shows the winter (DJF) and summer (JJA) temperature simulated by CCSM3-WRF (left) and ECHAM5-WRF (middle) simulation in comparison

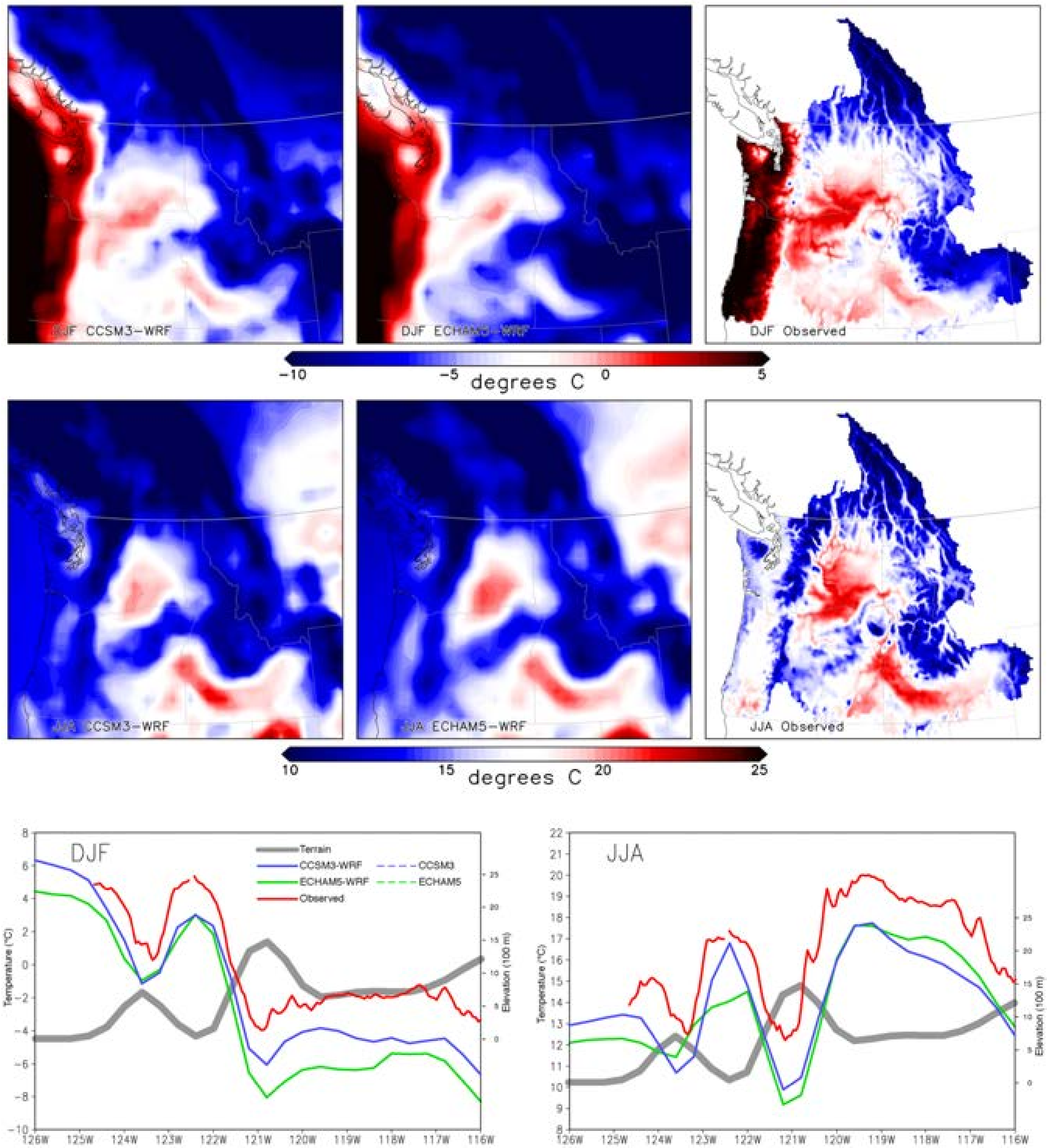

Figure 1. 1970-1999 seasonal mean temperature (°C) for DJF (top row) and JJA (middle row) from CCSM3-WRF (column 1), ECHAM5-WRF (column 2) and gridded observations (column 3). Bottom row: observed temperature and simulated temperature from both regional models and global forcing models along a West-East transect of the State of Washington at 47.8°N latitude. Terrain height is indicated by the thick gray line.

to the gridded observations (right). The bottom two panels show simulated and observed temperature and the ECHAM5-WRF terrain along a transect of Washington at 47.8°N; observed precipitation has been averaged over a latitude band to reflect the model resolution. Overall, the temperature is well represented in the simulations: the influence of the major geographical features is captured, and the seasonal cycle is reproduced. Both models exhibit a substantial cold bias relative to the gridded observations. In DJF, this bias is evident over the Cascade crest and Southeast Washington. Any bias in the global forcing models is inherited by the WRF simulation, so this comparison depends on combined deficiencies in the forcing model and regional model.

Figure 2 shows the corresponding results for simulated and observed 1970-1999 precipitation. Again, the overall magnitude of precipitation and its geographical distribution are well characterized by the simulations for both seasons. Both models are unable to resolve the large precipitation peak over the Olympics, but do represent the maximum over the Cascades. The finer grid spacing in the CCSM3-WRF simulation reproduces the intensity along the crests of the Cascades and Olympics better than the ECHAM5-WRF simulation although precipitation is over estimated in the southern Cascades of Oregon. Both models also do well in producing the peak precipitation on the windward slopes of the Cascade Range with a rapid drop in the lee. The CCSM3-WRF result produces comparable peaks for each range while the ECHAM5-WRF simulation produces a somewhat smaller maximum over the Olympics due to its coarser grid spacing. As shown in Leung and Qian (2003), as model resolution improves, the maximum over the Olympics becomes larger than that over the Cascades, in accordance with observations.

Figure 3, top panels, shows the 1970-1999 average April 1 snowpack from the two regional models expressed as millimeters of snow-water equivalent (SWE). The SWE follow the spatial pattern of the precipitation, with the CCSM3-WRF (left) clearly showing more tightly localized and higher SWE values than the ECHAM5-WRF (right) simulation. For comparison, we include two baseline snow climatologies. Figure 3, bottom left, shows the 1970-1999 average April 1 SWE computed from the VIC hydrologic model (McGuire et al, 2009, this report) using the temperature and precipitation shown in Figures 1 and 2. Figure 3, bottom right, shows April average snow water equivalent for the period 1979-1996 from a product employed operationally at the Canadian Meteorological Centre (CMC). This 0.25-degree gridded dataset combines in situ daily observations from ~8,000 U.S. cooperative stations and Canadian climate stations and first-guess fields with an optimum interpolation scheme developed by Brown et al. (2003). Only the monthly-means are available for the CMC data; the April average from the WRF simulations is qualitatively similar to the April 1 field, so we use this for comparison. While the geographical extent of snow cover is well represented in the WRF simulations, there is clearly an underestimate at mid elevations. This deficiency is consistent with the coarse topographic resolution in the regional models, and the CCSM3-WRF simulation, which has finer grid spacing, does somewhat better than the ECHAM5-WRF simulation. The CMC data also compares better to the WRF simulations than the VIC simulation, consistent with the similar spatial resolution of the models and this gridded data product.

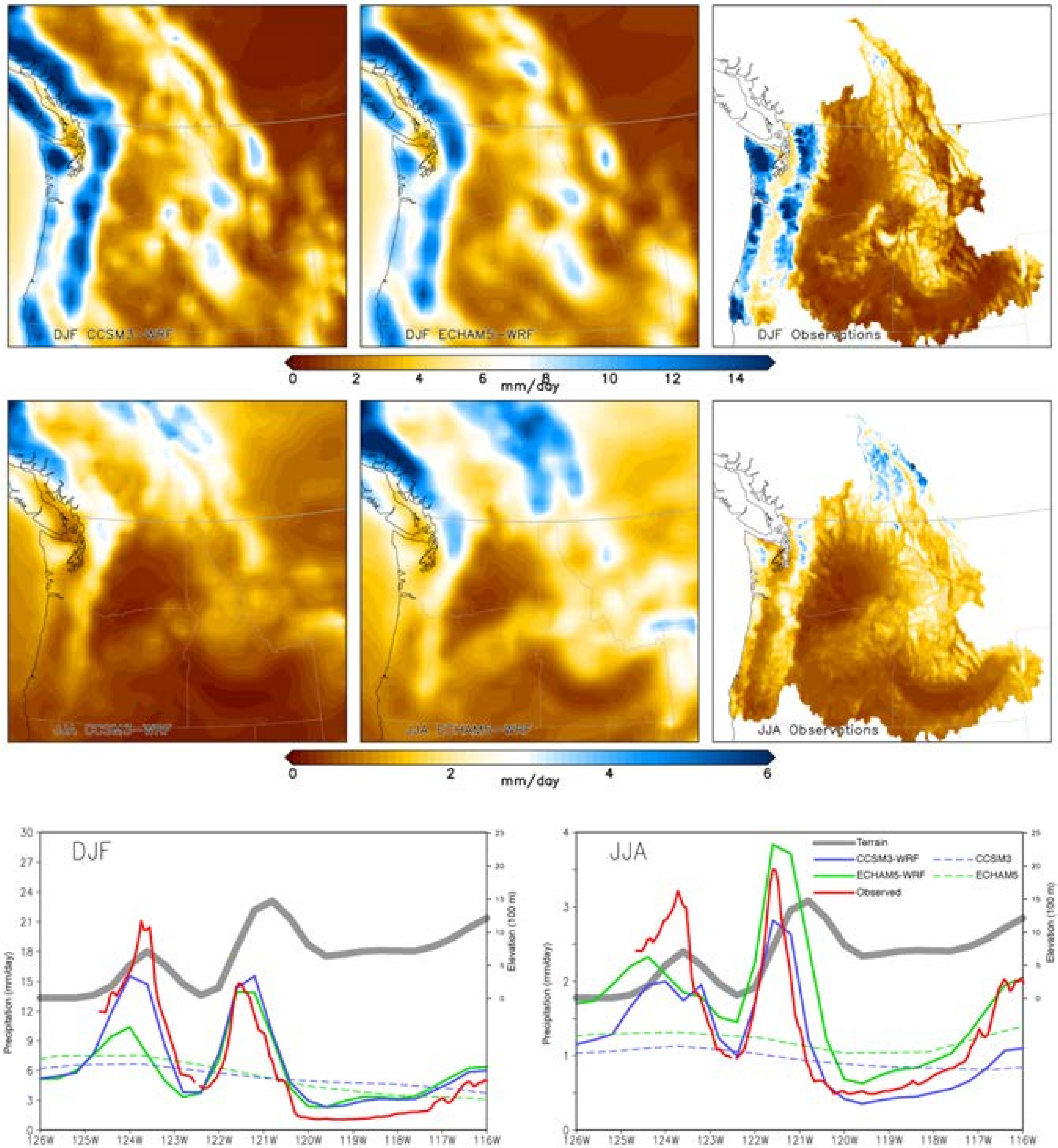

Figure 2. 1970-1999 seasonal mean precipitation (mm/day) for DJF (top row) and JJA (middle row) from CCSM3-WRF (column 1), ECHAM5-WRF (column 2) and gridded observations (column 3). Bottom row: Observed precipitation and simulated precipitation from both regional models and global forcing models along a West-East transect of the State of Washington at 47.8°N latitude. Terrain height is indicated by the thick gray line.

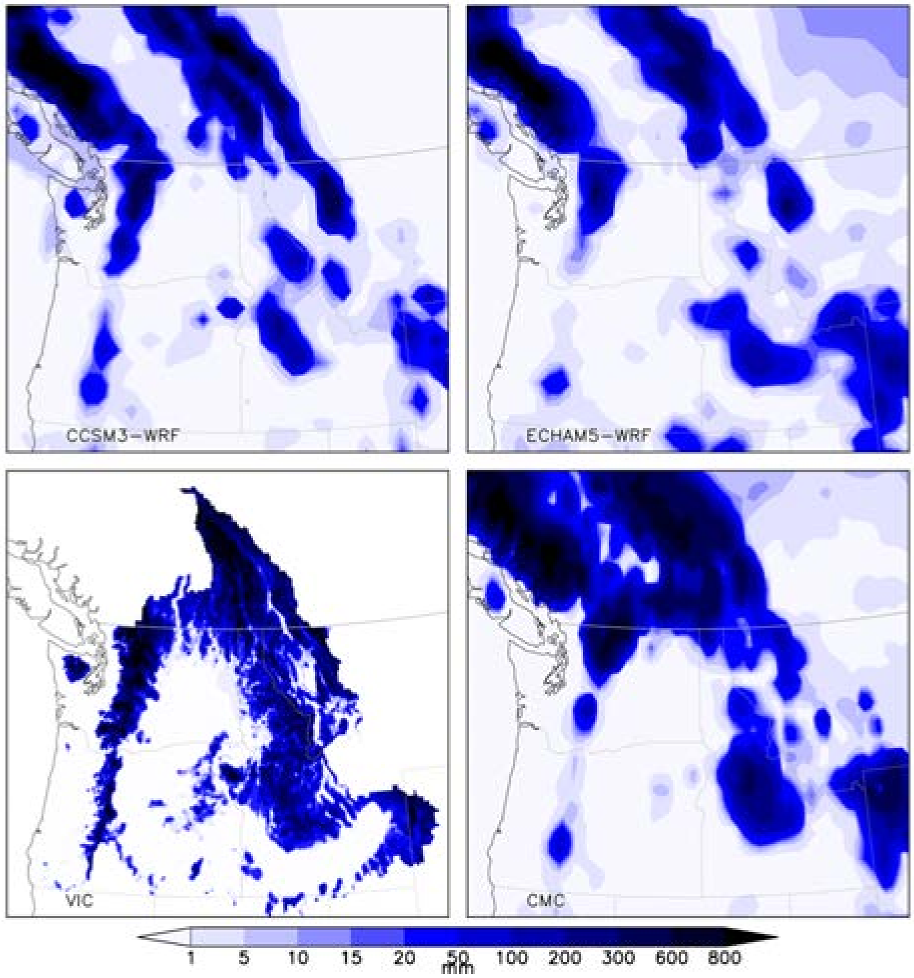

Figure 3. 1970-1999 simulated April 1 snow water equivalent (mm) from CCSM3-WRF (top left), ECHAM5-WRF (top right), the VIC model forced by the gridded observations in Figs 1 and 2 (bottom left). 1979-1997 average April SWE from the Canadian Meteorological Centre snow analysis (bottom right).

4. Seasonal Patterns of Climate Change for 2030-2059

4.1. Precipitation

Precipitation changes in the regional simulations for 2030-2059 include a pronounced seasonality and considerable variation across the region (Figure 4). Both CCSM3-WRF and ECHAM5-WRF produce substantial decreases in DJF precipitation over the Cascade Range and Olympic Mountains and modest increases east of the Cascades. The two simulations produce opposite responses in spring (MAM), with ECHAM5-WRF producing increased precipitation and CCSM3-WRF a substantial decrease; in both cases the change is of the same sign across Washington, with larger magnitudes over the mountain ranges. For summer, the ECHAM5-WRF simulation shows very little change in rainfall while the CCSM3-WRF shows substantial decreases along the mountain ranges. For autumn, both models predict substantial increases in precipitation over the mountain ranges. As we show below, the increases in autumn precipitation result in more intense daily precipitation events.

When compared with the precipitation pattern simulated by the global models, the regional model results are generally consistent with the forcing model. This similarity is due to the dominant role that large-scale storms and moisture flux plays in controlling regionally averaged precipitation. The regional model maintains the large-scale weather systems from the forcing

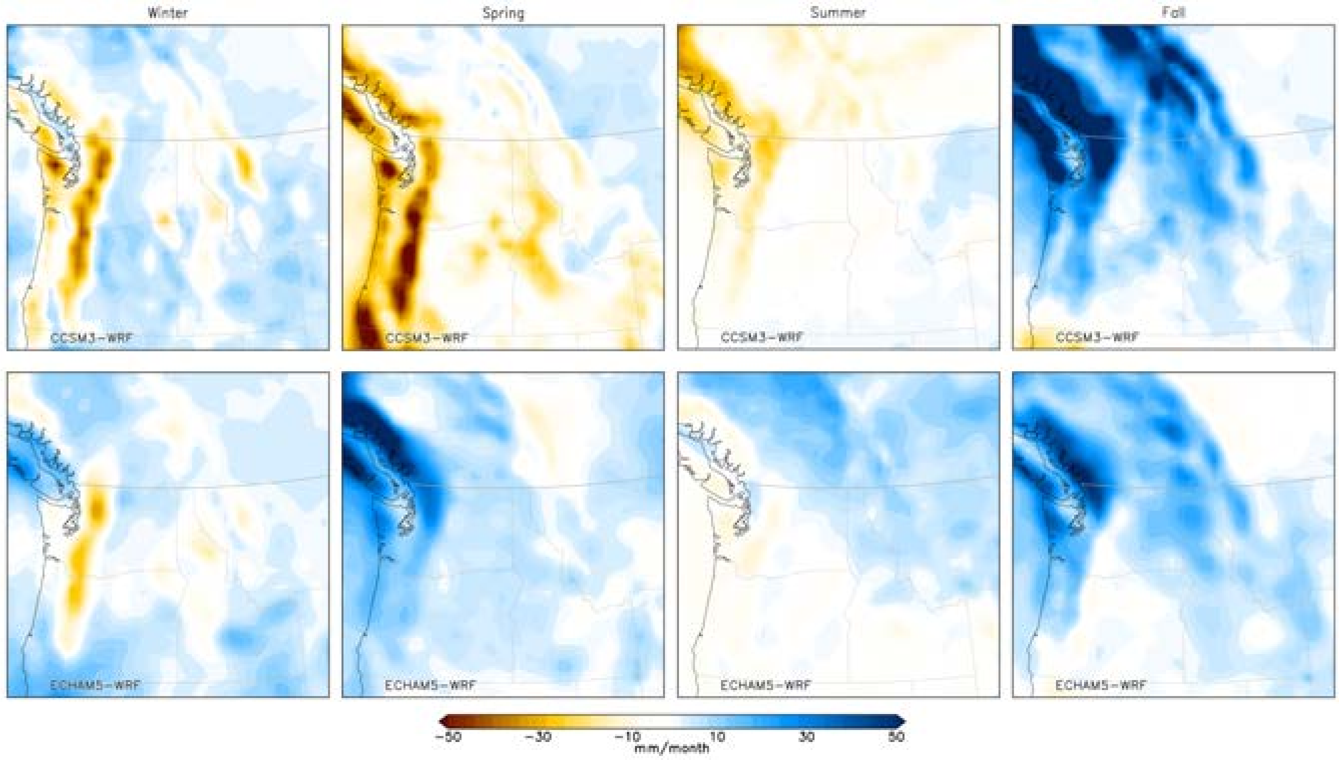

Figure 4. Change in precipitation (mm/month) from 1970-1999 to 2030-2059 for CCSM3-WRF (top row) and ECHAM5-WRF (bottom row) for the four seasons.

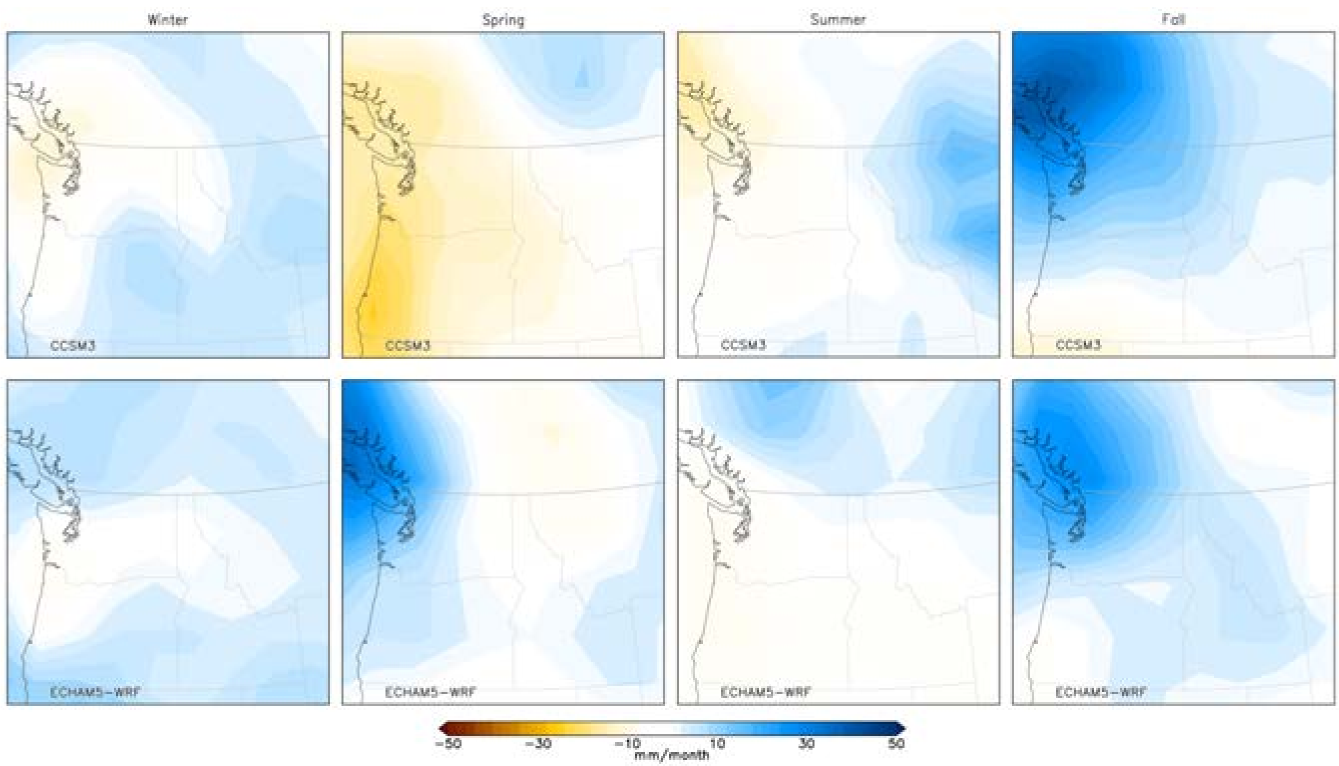

Figure 5. As for Fig. 4 except for the CCSM3 (top) and ECHAM5 (bottom) global forcing models.

model and simulates fine scale features that derive from interactions with the land surface and mesoscale weather processes. These mesoscale processes yield important differences in the magnitude and distribution of the precipitation changes around the regional topography, which are seen by comparing the global climate model changes (Fig. 5) to the regional model changes (Fig. 4). In general, the precipitation changes in the regional model follow the sign of the changes in the global model but with intensification over complex terrain. Thus, the modest reduction in DJF precipitation in western Washington in both CCSM3 and ECHAM5 is considerably amplified in the Cascade Range and Olympics. Likewise, increases in SON precipitation in both models and in MAM precipitation in ECHAM5 are amplified along the windward sides of the terrain in the regional simulations.

In some cases, the regional model produces precipitation changes of the opposite sign from the forcing model. For example, for DJF, both ECHAM5 and CCSM3 show decreases in precipitation over nearly the entire domain, including eastern Washington. However, both regional models, and especially CCSM3-WRF, show an increase in precipitation for eastern Washington. This difference in sign between anomalies east and west of the Cascade Range is also seen in natural climate variability associated with El Niño-Southern Oscillation (ENSO) (Leung et al., 2003). The circulation patterns that generate a decrease in precipitation over the Cascades generally reduce the intensity of the rainshadow, allowing more moisture transport to eastern Washington and consequently more precipitation. For DJF, both simulations produce strong reductions in precipitation throughout the west of the domain despite negligible precipitation changes in the forcing models. This suggests that, while the large-scale moisture flux may increase in a warmer climate, the changes in the circulation patterns are not favorable to orographic precipitation.

To illustrate the importance of the topography on regional precipitation under climate change, we examine a transect across Washington along the latitude 47.8°N, which crosses both the Olympics and North Cascades. Figure 6 shows the percentage change in precipitation for each of the four seasons and the ECHAM5-WRF topography. The fractional change in precipitation in the regional models varies considerably around the topography in the climate change projections. Using the percentage change removes the large background variation in precipitation along the transect and more clearly shows the climate change signal. For DJF (Fig. 6, top left), both simulations show the largest reductions in precipitation on the windward sides of the Olympics and Cascades. The changes become sharply positive in both cases immediately in the lee of the Cascades. For MAM (Fig. 6, top right), the two simulations are quite different. The ECHAM5-WRF simulation shows substantial increases on the windward slopes but also in the lee of the Cascades. It is likely that different synoptic conditions are responsible for the changes across the transect, but that an overall increase in moisture availability allows increased precipitation under favorable of weather patterns. The CCSM3-WRF simulation shows a more uniform decrease in precipitation, with a maximum on the windward slope of the Olympics. Results for both models in SON (Fig. 6, bottom right) are similar to the MAM results for ECHAM5-WRF. Peak precipitation increases are found not only on the windward slopes, but also in Eastern Washington, where the fractional increase is comparable to the increases over the mountains. These results give clear evidence that the effect of climate change on precipitation is tightly coupled to the interaction of increased moisture availability and various synoptic weather patterns with the regional topography.

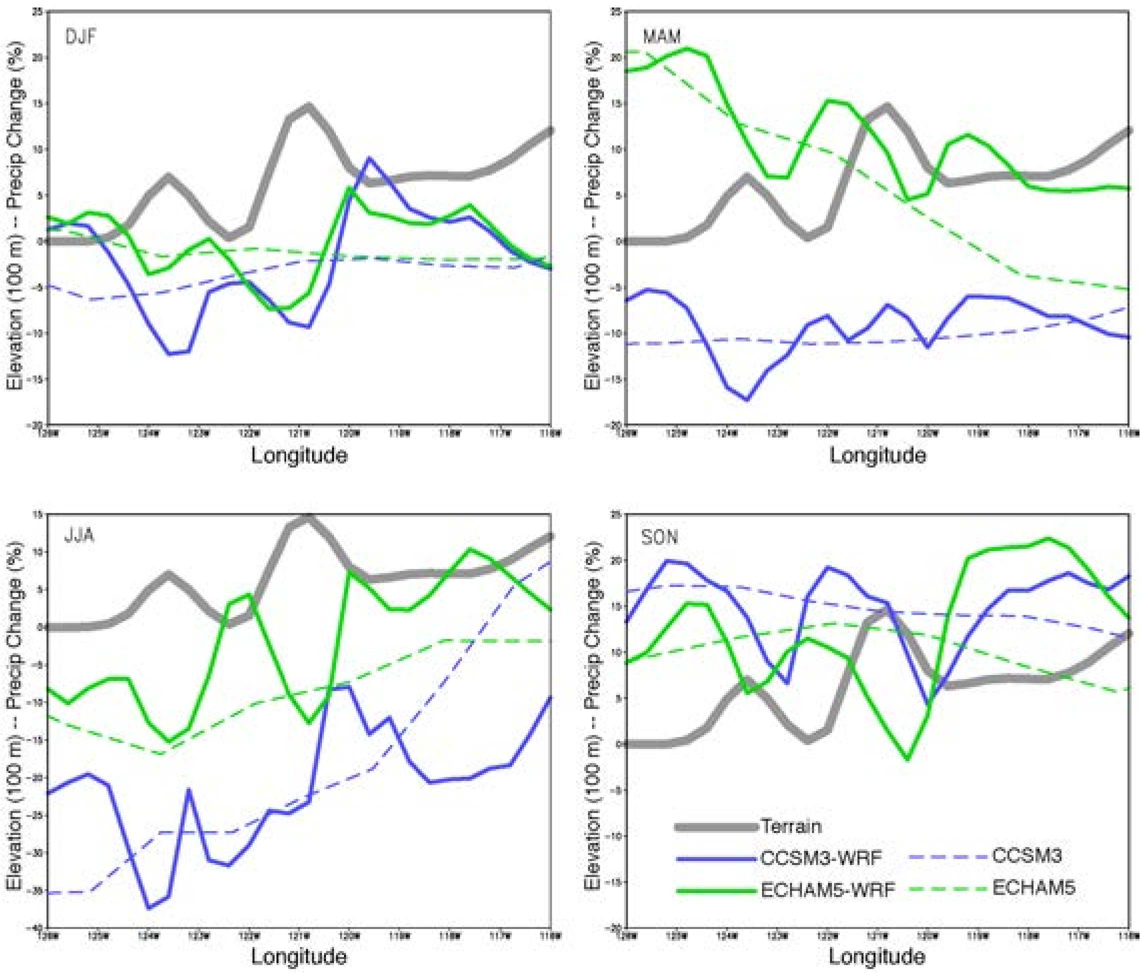

Figure 6. Percent change in precipitation from 1970-1999 to 2030-2059 for each season as simulated by the regional models and forcing globalmodels along a West-East transect of the State of Washington at 478°N latitude. Terrain height is indicated by the thick gray line.

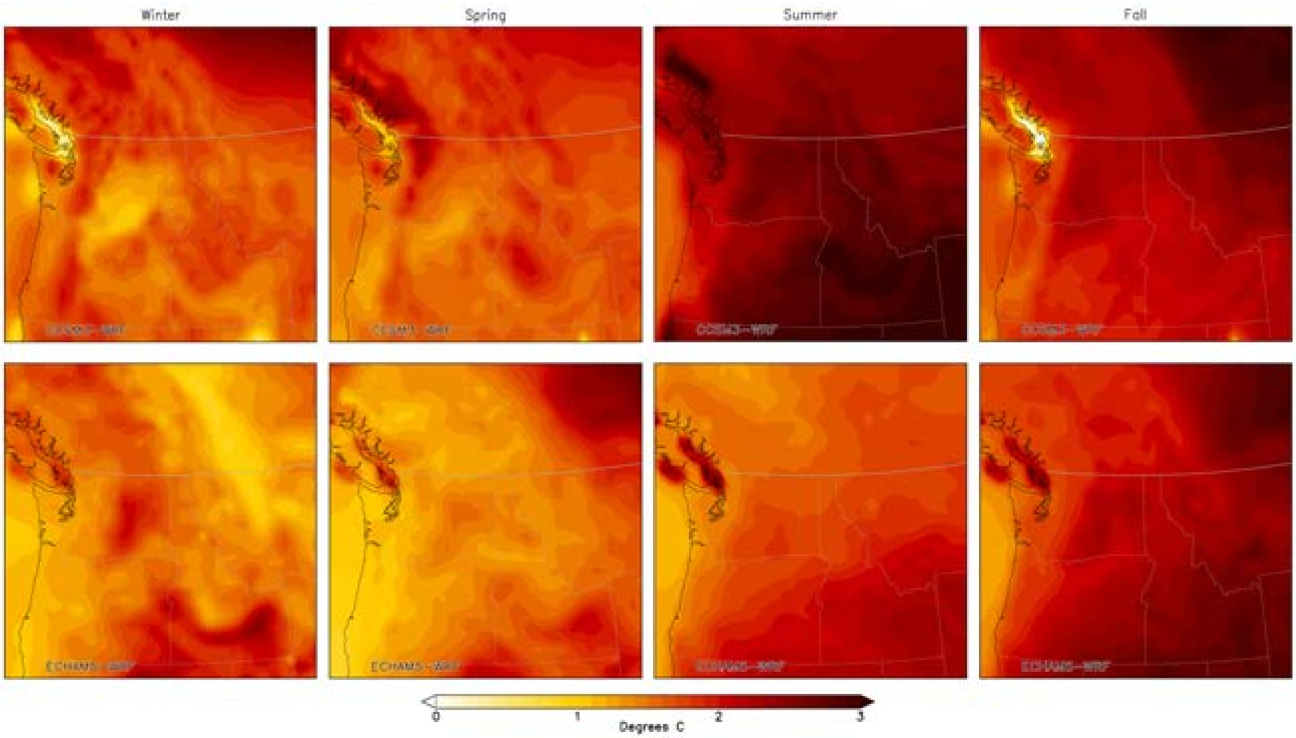

Figure 7. Change in temperature (°C) from 1970-1999 to 2030-2059 for CCSM3-WRF (top row) and ECHAM5-WRF (bottom row) for the four seasons.

4.2. Temperature

Figure 7 shows the temperature change for 2030-2059 in the regional model simulations for the four seasons. There is considerable difference in the temperature response between the two models and with season. These changes are largely the result of the global forcing model and feedbacks within the regional model driven by changes in precipitation, cloudiness, and surface radiation. In the cool season, the spatial pattern of warming in a regional model is strongly linked to changes in snowpack and cloud cover, which alters the surface radiation (Leung et al., 2004; Salathé et al., 2008). For example, where snowpack is lost, either due to warmer temperatures or less precipitation, the albedo is decreased, more solar radiation is absorbed at the surface, and the warming is amplified. For DJF, the CCSM3-WRF simulation (Fig. 7, 1st column, top row) shows amplified warming over the Washington Cascades. This warming exceeds the projection from global forcing model (Fig. 8), but coincides with the region of significant reduction in precipitation (Fig. 4). Thus, the warming is amplified by the loss of precipitation and less frequent snow and clouds over the Cascades. The very different pattern found for DJF in the ECHAM5-WRF simulation (Fig. 7, 1st column, bottom row) follows from the much smaller warming in the ECHAM5 forcing model and smaller decrease in precipitation. In eastern Washington, the CCSM3-WRF simulation shows less warming than the ECHAM5-WRF simulation. This result is consistent with the differences in the forcing from the two models, with ECHAM5 producing more warming along a southeast-northwest axis and the CCSM3 warming mostly in the western portion of the domain. Furthermore, precipitation increases over eastern Washington in the CCSM3-WRF simulation, which implies

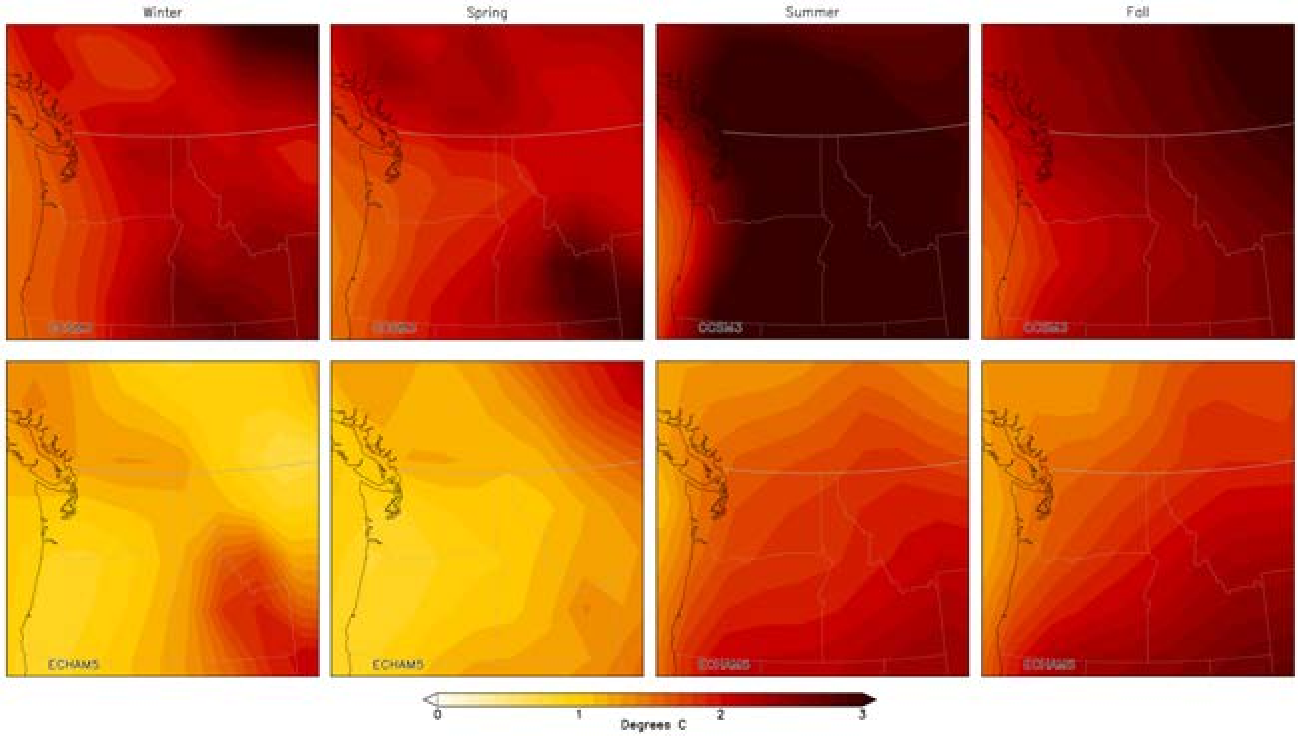

Figure 8. As for Fig. 7 except for the CCSM3 (top) and ECHAM5 (bottom) global forcing models.

increased cloud cover and reduced solar heating of the surface.

For MAM (Fig. 7, 2nd column), the differences between the two simulations seen for DJF are accentuated due to the very different precipitation results, with considerable loss of precipitation in CCSM3-WRF and considerable increase in ECHAM5-WRF. For JJA, both regional models closely follow the global model, which suggests that mesoscale processes are not as critical to the summer temperature sensitivity. In spring and summer, both the global and regional models indicate less warming in coastal areas than inland. In some cases, the regional models reduce the coastal warming relative to the global model. Nevertheless, warming is still substantial in western Washington and, as shown below, heat waves are projected to become more frequent. For SON, the global forcing models and regional precipitation response are very similar and thus the temperature changes are similar.

4.3. Snowpack

Substantial losses of snowpack are found in both regional simulations. Figure 9 shows the change in average spring (MAM) snowpack from the present to future climate. When averaged over Washington, CCSM3-WRF projects a 71% loss of SWE while ECHAM5-WRF projects a 32% loss. Since spring snowpack is a good predictor of summertime streamflows, changes for this season indicate the magnitude of the impacts of regional climate change on water resources (see Vano et al. 2009a, this report). The CCSM3-WRF simulation (Fig. 9, left) yields much larger snow loss than ECHAM5-WRF (Fig. 9, right) over the entire domain, but particularly for the Cascade and Olympic mountains. In part, this may be due to the finer grid spacing in CCSM3-WRF, allowing better representation of smaller terrain

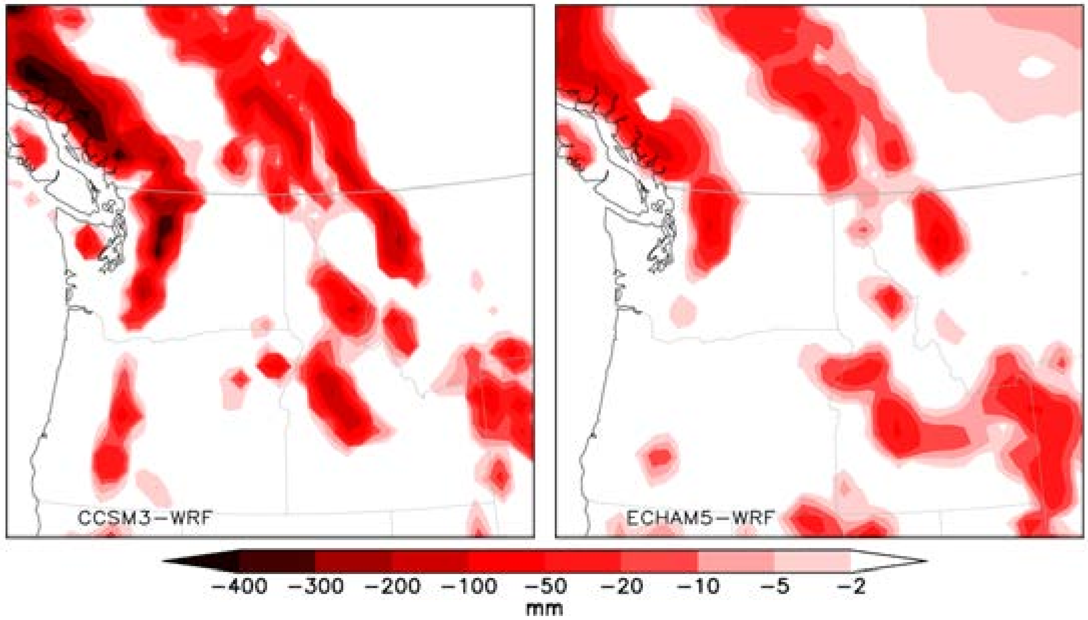

Figure 9. Change in April 1 snow water equivalent (mm) from CCSM3-WRF (left) and ECHAM5-WRF (right).

features such as the Olympics. However, the 1970-1999 snowpack (Fig. 3) is more similar between the two models than the simulated changes, so model resolution is not the most important effect.

Most of the difference between the two simulations is due to the forcing models and the resulting regional precipitation. Snowpack changes are a result of both changes in precipitation and changes in temperature (Mote et al., 2008). While CCSM3-WRF show somewhat more warming than ECHAM5-WRF and both models show increased autumn precipitation, the dominant effect on the differences in simulated spring snowpack is the difference in precipitation projections. Figure 4 shows a larger reduction in winter and spring precipitation in CCSM3-WRF than in ECHAM5-WRF, and this result dominates the snowpack results. The consensus among global climate models (Mote and Salathé 2009, this report) is for modest increases in cool-season precipitation, so the CCSM3 results presented here are not necessarily characteristic. Nevertheless, despite the increase in cool-season precipitation in ECHAM5-WRF, snowpack decreases over a similar geographical extent as in the much drier CCSM3-WRF projection and about half the magnitude. Thus, while the disparity in precipitation projections in the two models modulates the magnitude of snow loss, warming plays a prominent role in determining future snowpack, counteracting potential increases in precipitation.

5. Changes in Extreme Events

A key motivation for using regional climate models in climate impacts research is the ability to represent extreme events. By nature, extreme weather occurs rapidly and over a small geographical extent. Extreme seasonal conditions, such as drought, occur more slowly and with larger geographical extent, and typically depend on fine-scale interactions between the atmosphere and land surface features such as topography that are not well resolved in global models. Thus, regional climate models are especially well suited to studying these events. Here we present summary statistics for several types of extreme events related to temperature and precipitation. Our analysis follows the

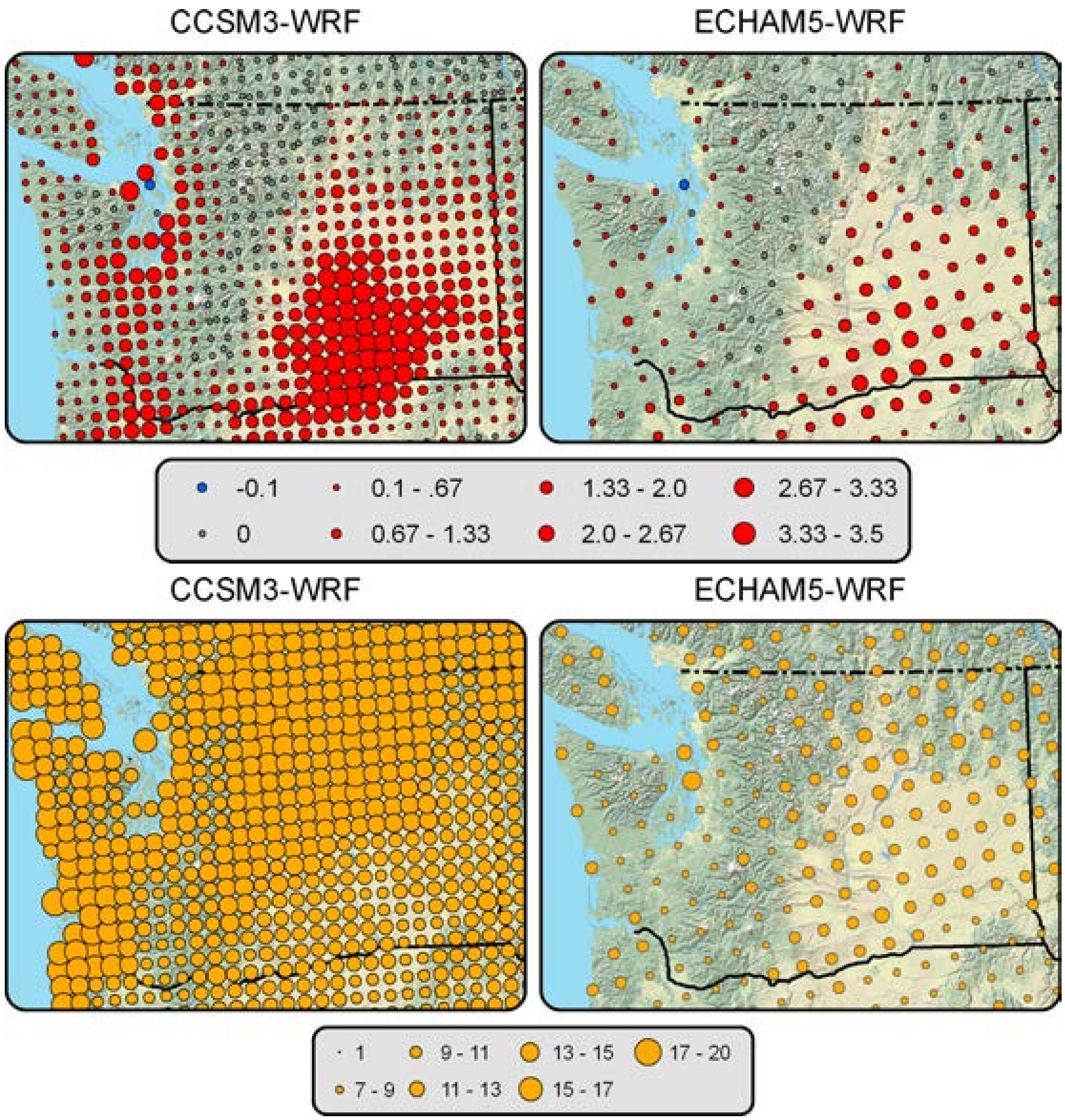

Figure 10. Top: change in the number of heat wave events from CCSM3-WRF (left) and ECHAM5-WRF (right). Bottom: change in the frequency of warm nights (Tmin>90th percentile).

approach of Tebaldi et al. (2006) for global climate model analysis and uses parameters defined in Frich et al. (2002).

5.1. Heat Waves and Warm Nights

Climate change is predicted to have significant human health consequences due to heat stress in vulnerable individuals. This issue is discussed in detail in Jackson et al (2009, this report) where the quantitative relationship between heat events and mortality is analyzed, showing that mortality rises significantly after heat waves last for three or more days. Future heat wave frequencies are represented in Jackson et al (2009, this report) by a uniform perturbation to the historic record since the global climate models do not give good information on the geographic signature of warming or changes in daily variability. Here we use output from the regional models to compute the frequency of heat waves for present and future time periods. We define a heat wave as an episode of three or more days where the daily heat index (HUMIDEX) exceeds 32°C. Figure 10, top panel, shows the change in the number of heat waves simulated by the two regional models from 1970-1999 to 2030-2059. Both models show a larger increase in heat wave frequency in south-central Washington than elsewhere in the state. The CCSM3-WRF simulation (Fig. 10, left) also shows considerable increase in heat waves in the lowlands of western Washington, following the more widespread warming in the CCSM3 scenario. Note that this increase in heat waves occurs despite relatively less seasonal-average warming here than the interior. This result suggests that effects that would moderate coastal warming, such as marine cloudiness, are intermittent and have little effect on the frequency and duration of extreme heat events. Although the heat index includes the effect of relative humidity, the large increase in heat wave frequency in south-central Washington is a result of an increase only in temperature since summertime relative humidity remains nearly constant for this region under climate change.

The frequency of warm nights is another measure of persistent heat stress with important impacts. To analyze the change in the frequency of warm nights, we computed the 90th percentile minimum temperature (Tmin) for each calendar day at each grid point for the 20th century simulations. The change in the percentage of days where Tmin exceeds the 90th percentile is then computed from the 21st century simulation as shown in Figure 10, bottom panel. In comparison to the change in heat-wave frequency, the frequency of warm nights does not show as marked a geographical pattern, but rather closely follows the pattern of summertime warming (Fig. 7).

5.2. Extreme Precipitation

We use two parameters to analyze changes in extreme precipitation, which yield somewhat different results. An increase in these parameters indicates that more of the precipitation is coming in extreme events. The first parameter, precipitation intensity, is defined as the annual total precipitation divided by the number of wet days (precipitation exceeding 1 mm). Precipitation intensity increases when the annual precipitation increases more rapidly than the number of wet days. The second parameter, R95, is the fraction of precipitation falling on days with precipitation exceeding the 95th percentile for that location, where the 95th percentile is calculated from the 20th century simulation. An increase in R95 indicates that precipitation in events exceeding the threshold increases more than total precipitation.

For precipitation intensity (Fig. 11), both regional models produce similar results. The change from the current to the future period is positive or very small over the entire state with considerable increases only over the northwestern portion of the state. The increase appears to follow the southwest, windward flanks of the North Cascades, Olympics, Vancouver Island, and BC Coast Range. The changes in R95 (Fig. 12) are much more widespread, owing in part to the geographical dependence of the threshold. The pattern in the ECHAM5-WRF (Fig. 12, right) simulation is more spatially uniform, with increases in the western and eastern portions of the state and slight decreases in central Washington, along the lee of the Cascades. The CCSM3-WRF (Fig. 12, left) simulation shows much more spatial heterogeneity, likely due to its finer spatial grid and better topographic resolution. In addition, it is interesting to note that in CCSM3-WRF, both precipitation intensity and R95 increase substantially on the

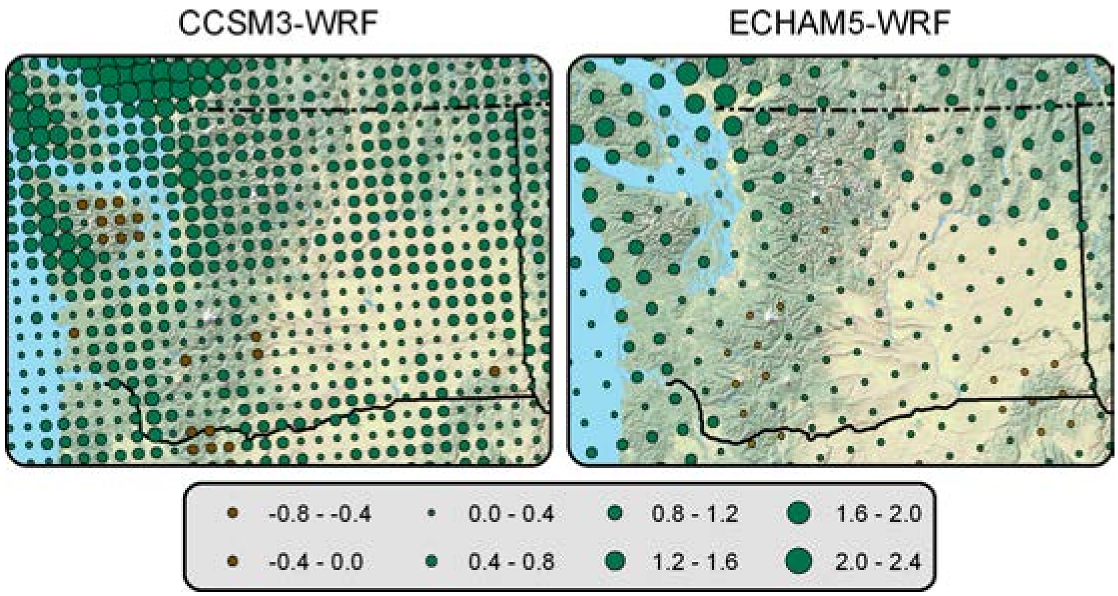

Figure 11. Change in precipitation intensity from CCSM3-WRF (left) and ECHAM5-WRF (right).

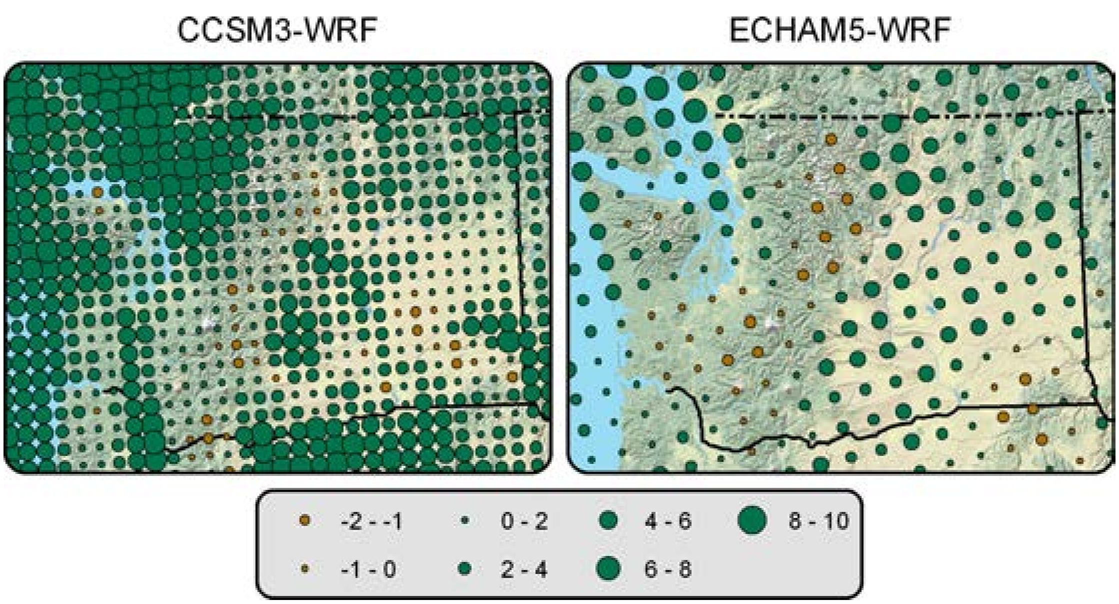

Figure 12. Change in the fraction of daily precipitation exceeding the 20th century 95th percentile (R95) from CCSM3-WRF (left) and ECHAM5-WRF (right).

windward slopes of the coastal mountains despite reductions in the total annual precipitation shown in Figure 4.

As discussed above, the CCSM3 ensemble member used to force the CCSM3-WRF simulation has an uncharacteristic increase in November precipitation. To test how critical this result is in determining the change in extreme precipitation, we repeated the above analysis using only data for the months December through February. This restriction makes very little difference for the ECHAM5-WRF simulation, although there is a more pronounced reduction in extremes along the lee of the Cascade Range and a larger increase elsewhere. For the CCSM3-WRF simulation, the increase in extremes for western Washington remains but is reduced; the increase east of the Cascade Range, however, is amplified. Qualitatively, the results based on all months are consistent with the results for the winter months, with some geographical differences.

Consistent with previous findings (e.g., Leung et al. 2004), these results suggest that extreme precipitation changes are more related to increased moisture availability in a warmer climate than to increases in climate-mean precipitation. Although changes in the mean large-scale circulation may not favor precipitation in a climatological sense, increased atmospheric moisture availability under intermittent synoptic conditions favorable for precipitation can lead to increased precipitation intensity and extreme precipitation. This finding has important implications as it suggests that extreme precipitation can increase regardless of the change in total precipitation, which has larger uncertainty as shown in Figure 4.

6. Conclusion

Regional climate models provide important insight into how the regional climate may respond to global climate change. We have presented two long simulations from a mesoscale climate model forced by two global climate model simulations. The object of regional climate modeling is to understand how fine scale weather and land-surface processes respond to the large-scale forcing generated by global models, and how that may alter the local climate change patterns. In overall details, both simulations presented here are quite consistent with the global forcing models used, which is expected. Furthermore, due to the unique characteristics of the forcing models, the fine scale features simulated are substantially different, accentuating differences in the forcing scenarios and underscoring the need for extended simulations using a large ensemble of forcing models and regional models

The most profound difference between the two simulations is in the cool-season precipitation, which is closely related to the simulated changes in snow pack and temperature. The CCSM3-WRF model shows substantial decreases in winter and spring precipitation. This, combined with a strong warming signal, yields substantial decreases in snow pack along the Cascade Crest and Olympic mountains. Where snow cover is reduced, the warming is locally amplified, suggesting a feedback between precipitation, snowpack, and temperature.

Despite these differences, there are important areas of agreement between the two simulations, suggesting that some local responses to global climate change are robust. Most clear is the loss of snowpack in both simulations. Despite substantial differences in the precipitation simulations, both simulations project a similar geographic extent of snow loss and a substantial net loss of snowpack for the state. The reduced snowpack and earlier snowmelt will alter the timing and amount of river runoff in the summer, although changes in annual runoff will depend on annual precipitation changes, which can differ noticeably from one scenario to another.

Changes in extreme events are also similar in the two simulations. Despite modest annual-mean precipitation changes in the CCSM3 and ECHAM5 global climate models, local terrain effects amplify the changes in the regional simulations, with locally opposite signs of changes in some seasons between ECHAM5-WRF and CCSM3-WRF. Yet, both simulations yield an increase in the measures of extreme precipitation even though the CCSM3-WRF simulation produced mostly reductions in total precipitation during winter and spring. Our results show that extreme precipitation increases over the north Cascades and over eastern Washington in both simulations. The geographical distribution of this increase clearly follows the terrain indicating the important role of topography in producing increased precipitation under favorable synoptic conditions with increase moisture availability in a warmer climate.

Our results show that, with increased spatial resolution relative to global models, regional climate models can represent the local forcing from the complex terrain to produce more realistic spatial and temporal variability of temperature, precipitation, and snowpack in the State of Washington. With the ability to resolve topographic effects, more robust changes in mountain snowpack and extreme precipitation emerge. These changes are consistent between the two regional simulations despite differences in seasonal precipitation and temperature changes in the global and regional model results. While the regional models contain substantial biases in their 20th century simulation, these results give good guidance to interpreting the results of statistical downscaling, for example, by showing whether orographic precipitation effects are suitably represented in the statistical downscaling. It is clear that changes in the seasonal climate and the frequency of extreme events may be locally much more intense than can be inferred from statistical methods. The implication is that, while a valuable tool for regional climate impacts assessment, multi-model ensembles of global climate projections and statistical methods may under represent the local severity of climate change.

References

Brown RD, Brasnett B, and Robinson D (2003) Gridded North American monthly snow depth and snow water equivalent for GCM evaluation. Atmos-Ocean 41:1-14

Chen F, Dudhia J (2001) Coupling an advanced land surface-hydrology model with the Penn State-NCAR MM5 modeling system. Part I: Model implementation and sensitivity. Mon Weather Rev 129:569-585

Collins W, et al. (2006) The Community Climate System Model version 3 (CCSM3). J Clim 19:2122-2143

Collins WD, Rasch PJ, Boville BA, Hack JJ, McCaa JR, Williamson DL, Kiehl JT, Briegleb B, Bitz C, Lin S-J, Zhang M, and Dai Y (2004) Description of the NCAR Community Atmospheric Model (CAM 3.0). NCAR Tech. Note, NCAR/TN-464+STR, 226

Daly C, Neilson RP, and Phillips DL (1994) A Statistical Topographic Model for Mapping Climatological Precipitation over Mountainous Terrain. J Appl Meteorol 33:140-158

Elsner MM, Cuo L, Voisin N, Deems JS, Hamlet AF, Vano J, and Lettenmaier DP (2009) Implications of IPCC 4th Assessment Report climate projections for the hydrology of Washington State in the 21st century. Washington Climate Change Impacts Assessment: Evaluating Washington's future in a changing climate. In press

Frich P, Alexander LV, Della-Marta P, Gleason B, Haylock M, Tank A, and Peterson T (2002) Observed coherent changes in climatic extremes during the second half of the twentieth century. Clim Res 19:193-212

Giorgi F and Mearns LO (1999) Introduction to special section: Regional climate modeling revisited. J Geophys Res-Atmos 104:6335-6352

Hong SY, Pan HL (1996) Nonlocal boundary layer vertical diffusion in a Medium-Range Forecast Model. Mon Weather Rev 124:2322-2339

Hong SY, Dudhia J, and Chen SH (2004) A revised approach to ice microphysical processes for the bulk parameterization of clouds and precipitation. Mon Weather Rev 132:103-120

Jackson JE, Yost MG, Karr C, Fitzpatrick C, Lamb BK, Chung S, Chen J, Avise J, Rosenblatt RA, Fenske RA (2009) Public health impacts of climate change in Washington State: projected mortality risks due to heat events and air pollution. Washington Climate Change Impacts Assessment: Evaluating Washington's future in a changing climate. In press

Kain JS and Fritsch JM (1993) Convective parameterization for mesoscale models: The Kain-Fritsch scheme. In: (ed) The representation of cumulus convection in numerical models. Amer Meteor Soc

Leung LR and Qian Y (2003) The sensitivity of precipitation and snowpack simulations to model resolution via nesting in regions of complex terrain. J of Hydrometeorol 4:1025-1043

Leung LR, Qian Y, and Bian X (2003) Hydroclimate of the western United States based on observations and regional climate simulation of 1981-2000. Part I: Seasonal statistics. J Clim 16:1892-1911

Leung LR, Kuo YH, Tribbia J (2006) Research needs and directions of regional climate modeling using WRF and CCSM. B Am Meteorol Soc 87:1747-1751

Leung LR, Qian Y, Bian X, and Hunt A (2003) Hydroclimate of the western United States Based on observations and regional climate simulation of 1981-2000. Part II: Mesoscale ENSO anomalies. J Clim 16:1912-1928

Leung LR, Qian Y, Bian X, Washington WM, Han J, and Roads JO (2004) Mid-century ensemble regional climate change scenarios for the western United States. Clim Chang 62:75-113

Marsland SJ, Haak H, Jungclaus JH, Latif M, and Roske F (2003) The Max-Planck-Institute global ocean/sea ice model with orthogonal curvilinear coordinates. Ocean Model 5:91-127

Mote P, Salathé E (2009) Future climate in the Pacific Northwest. Washington Climate Change Impacts Assessment: Evaluating Washington's future in a changing climate. In press

Mote P, Hamlet A, Salathé E (2008) Has spring snowpack declined in the Washington Cascades? Hydrol Earth Syst Sci 12:193-206

Nakicenovic N, et al. (2000) IPCC special report on emissions scenarios. Cambridge University Press

Roeckner E, Bengtsson L, Feichter J, Lelieveld J, and Rodhe H (1999) Transient climate change simulations with a coupled atmosphere-ocean GCM including the tropospheric sulfur cycle. J Clim 12:3004-3032

Roeckner E, Bäuml G, Bonaventura L, Brokopf R, Esch M, Giorgetta M, Hagemann S, Kirchner I, Kornbleuh L, Manzini E, Rhodin A, Schlese U, Schulzweida U, and Tomkins A (2003) The atmospheric general circulation model ECHAM5, Part I: Model description, Max-Planck-Institute for Meteorology Report No. 349

Rosenberg, E.A., P.W. Keys, D.B. Booth, D. Hartley, J. Burkey, A.C. Steinemann, D.P. Lettenmaier, 2009. Precipitation Extremes and the Impacts of Climate Change on Stormwater Infrastructure in Washington State. Washington Climate Change Impacts Assessment: Evaluating Washington's Future in a Changing Climate. In Press.

Salathé EP (2003) Comparison of various precipitation downscaling methods for the simulation of streamflow in a rainshadow river basin. Int J Clim 23:887-901

—— (2005) Downscaling simulations of future global climate with application to hydrologic modeling. Int J Clim 25:419-436

Salathé EP, Steed R, Mass CF, and Zahn P (2008) A high-resolution climate model for the U.S. Pacific Northwest: Mesoscale feedbacks and local responses to climate change. J Clim 21:5708-5726

Tebaldi C, Hayhoe K, Arblaster JM, and Meehl GA (2006) Going to the extremes. Clim Chang 79:185-211

Vano JA, Voisin N, Cuo L, Hamlet AF, Elsner MM, Palmer RN, Polebitski A, Lettenmaier DP (2009a) Multi-model assessment of the impacts of climate change on water management in the Puget Sound region, Washington, USA. Washington Climate Change Impacts Assessment: Evaluating Washington's future in a changing climate. In press

Widmann M, Bretherton CS, and Salathé EP (2003) Statistical precipitation downscaling over the Northwestern United States using numerically simulated precipitation as a predictor. J Clim 16:799-816

Wood AW, Leung LR, Sridhar V, and Lettenmaier DP (2004) Hydrologic implications of dynamical and statistical approaches to downscaling climate model outputs. Clim Chang 62:189-216

Image credit, page 47: Climate Impacts Group, University of Washington

3: Hydrology and Water Resources

Implications of 21st Century Climate Change for the Hydrology of Washington State

Marketa M Elsner[1], Lan Cuo[2], Nathalie Voisin[2], Jeffrey S Deems[2], Alan F Hamlet[1,2], Julie A Vano[2], Kristian EB Mickelson[2], Se-Yeun Lee[2], and Dennis P Lettenmaier[1,2]

Abstract

The hydrology of the Pacific Northwest (PNW) is particularly sensitive to changes in climate because seasonal runoff is dominated by snowmelt from cool season mountain snowpack, and temperature changes impact the balance of precipitation falling as rain and snow. Based on results from 39 global simulations performed for the Fourth Assessment Report of the Intergovernmental Panel on Climate Change (IPCC AR4), PNW temperatures are projected to increase an average of approximately 0.3°C per decade over the 21st century, while changes in annual mean precipitation are projected to be modest, with a projected increase of 1% by the 2020s and 2% by the 2040s. Based on IPCC AR4 projections, we updated previous studies of implications of climate change on the hydrology of the PNW. In particular, we used results from 20 global climate models (GCMs) and two emissions scenarios from the Special Report on Emissions Scenarios (SRES): A1B and B1. PNW 21st century hydrology was simulated using the full suite of GCMs and 2 SRES emissions scenarios over Washington, as well as focus regions of the Columbia River basin, the Yakima River basin, and those Puget Sound river basins that supply much of the basin's municipal water supply. Using two hydrological models, we evaluated projected changes in snow water equivalent, seasonal soil moisture and runoff for the entire state and case study watersheds for A1B and B1 SRES emissions scenarios for the 2020s, 2040s, and 2080s. We then evaluated future projected changes in seasonal streamflow in Washington. April 1 snow water equivalent (SWE) is projected to decrease by an average of approximately 27-29% across the State by the 2020s, 37-44% by the 2040s and 53-65% by the 2080s, based on the composite scenarios of B1 and A1B, respectively, which represent average effects of all climate models. In three relatively warm transient watersheds west of the Cascade crest, April 1 SWE is projected to almost completely disappear by the 2080s. By the 2080s, seasonal streamflow timing will shift significantly in both snowmelt dominant and transient, rain-snow mixed watersheds. Annual runoff across the State is projected to increase by 0-2% by the 2020s, 2-3% by the 2040s, and 4-6% by the 2080s; these changes are mainly driven by projected increases in winter precipitation.

[1]JISAO Climate Impacts Group, University of Washington, Seattle, Washington
[2]Department of Civil and Environmental Engineering, University of Washington, Seattle, Washington

1. Introduction

The Fourth Assessment Report (AR4) of the Intergovernmental Panel on Climate Change (IPCC) states that warming of Earth's climate is unequivocal and that anthropogenic use of fossil fuels has contributed to increasing carbon dioxide concentrations and thereby warming of the atmosphere (IPCC, 2007). The hydrology of the Pacific Northwest (PNW - which typically includes the Columbia River basin and watersheds draining to the Oregon and Washington coasts) is particularly sensitive to changes in climate because of the role of mountain snowpack on the region's rivers. In this paper, we utilize archived climate projections from the IPCC AR4 to evaluate impacts on regional hydrology, with focus on Washington, which includes the lower Columbia River basin in the eastern and southern part of the State, as well as coastal drainages, including the Puget Sound basin (Figure 1).

Washington is partitioned into two distinct climatic regimes by the Cascade Mountains. The west side of the Cascades on average receives approximately 1,250 mm of precipitation annually, while the east side receives slightly more than one-quarter of this amount. Washington, like much of the western US, relies on cool season precipitation (defined as October through March) and resulting snowpack to sustain warm season streamflows (defined as April through September). Approximately 75% of the annual precipitation in the Cascades falls during the cool season (Snover and Miles, in review). A changing climate affects the balance of precipitation falling as rain and snow and therefore the timing of streamflow over the course of the year. Figure 2 illustrates simulated historical mean annual runoff over the period 1916-2006 using the Variable Infiltration Capacity hydrologic model (further described below) and shows the importance of the State's mountainous regions with respect to water supply for various natural resources.

Small changes in temperature can strongly affect the balance of precipitation falling as rain and snow, depending on a watershed's location, elevation, and aspect. Washington, and the Pacific Northwest as a whole, is often characterized as having three runoff regimes: snow-melt dominant, rain dominant, and transient (Hamlet and Lettenmaier 2007). In snowmelt dominant watersheds, much of the winter precipitation is stored in the snowpack, which melts in the spring and early summer resulting in low streamflow in the cool season and peak streamflow in late spring or early summer (May-July). Rain dominant watersheds are typically lower in elevation and mostly on the west side of the Cascades. They receive little snowfall. Streamflow in these watersheds peaks in the cool season, roughly in phase with peak precipitation (usually November through January). Transient watersheds are characterized as mixed rain-snow due to their mid-range elevation. These watersheds receive some snowfall, some of which melts in the cool season and some of which is stored over winter and melts as seasonal temperatures increase. Rivers draining these watersheds typically experience two streamflow peaks: one in winter coinciding with seasonal maximum precipitation, and another in late spring or early summer when water stored in snowpack melts. Hydrographs of simulated average historic streamflow, which are representative of the three watershed types, are shown in Figure 3.

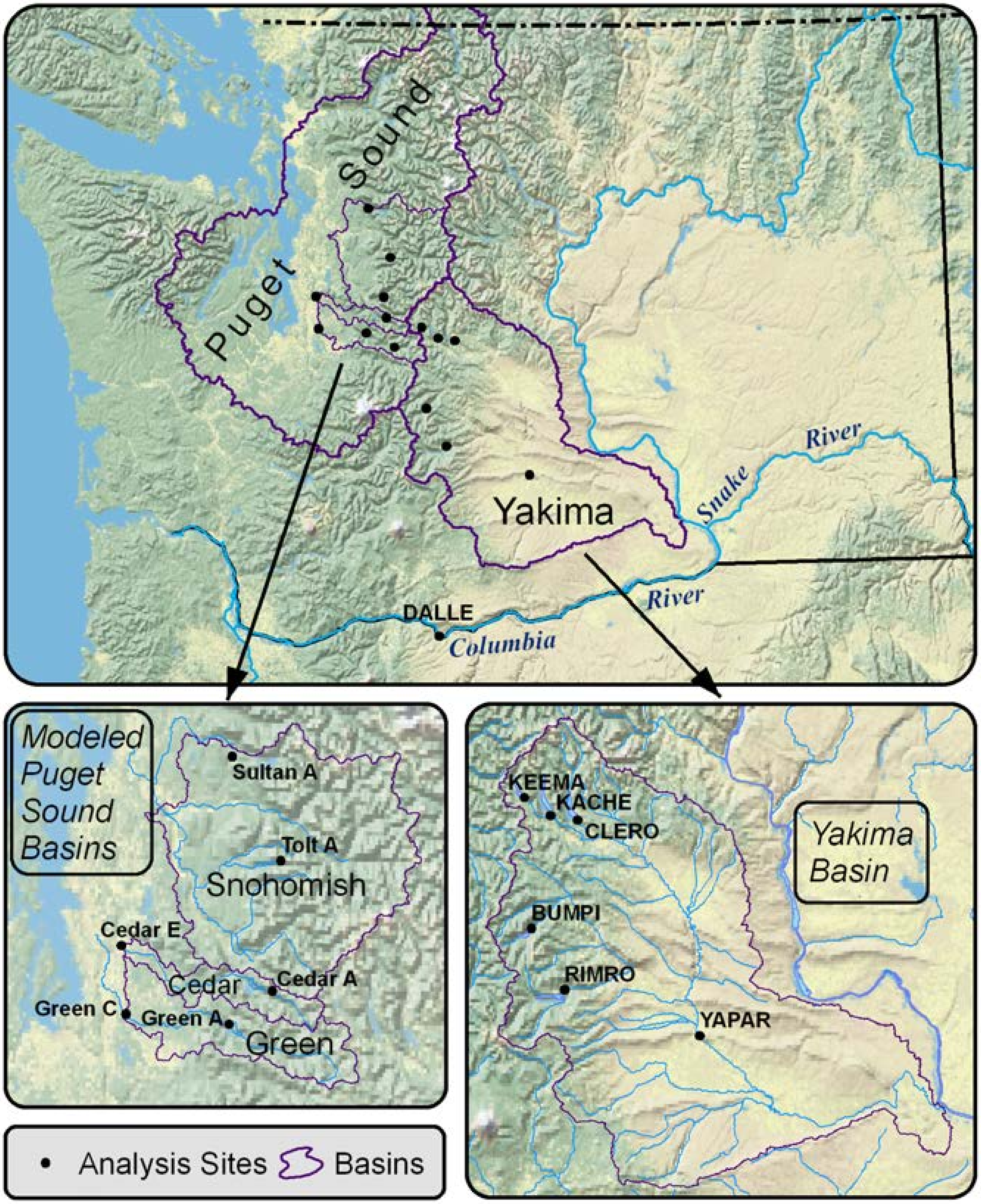

Figure 1. Overview figure of Washington state, Puget Sound and Yakima case study basins, and significant analysis locations.

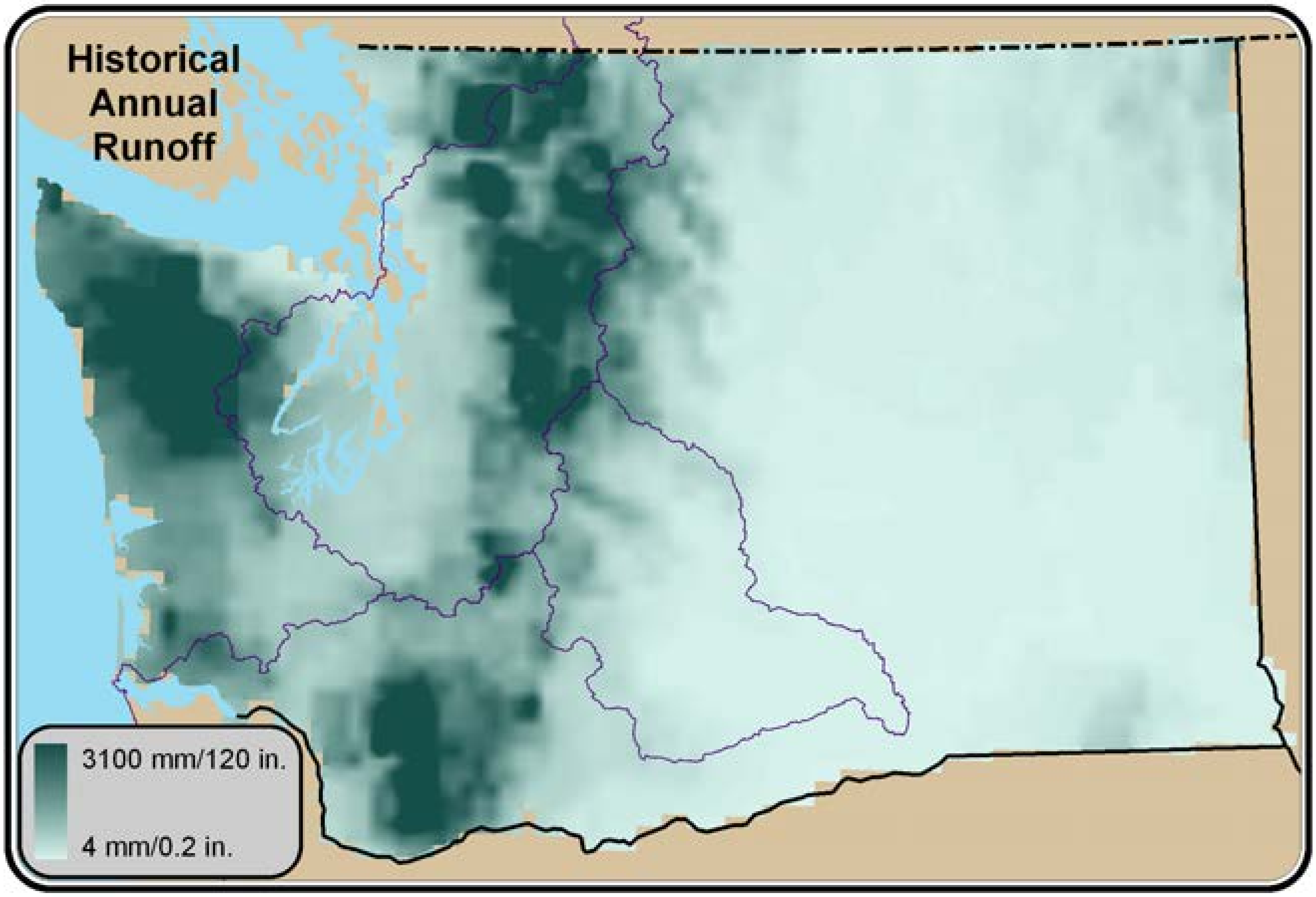

Figure 2. Simulated mean annual runoff over Washington state by the Variable Infiltration Capacity (VIC) model over the historic period from 1916-2006.

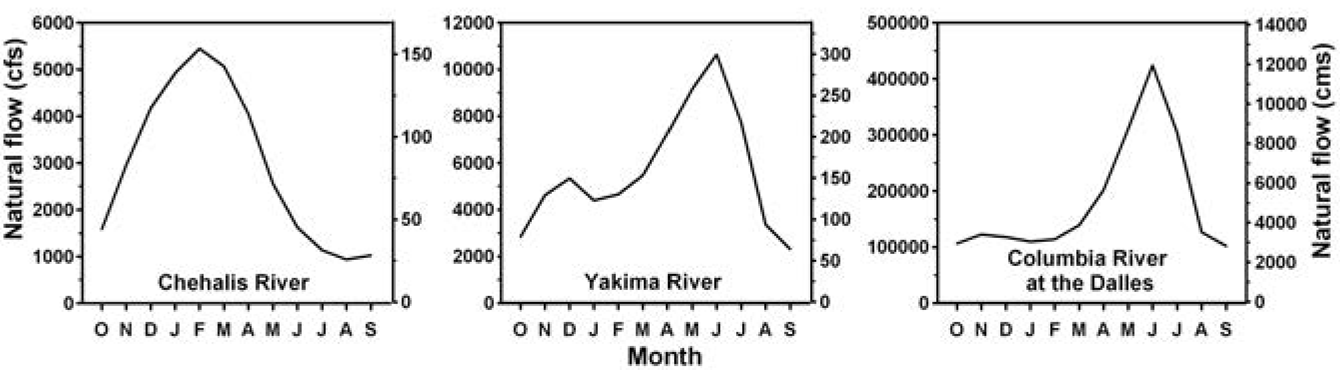

Figure 3. Simulated monthly historic streamflow hydrographs for three representative watershed types in Washington, namely rain dominant (Chehalis River at Porter), transient rain-snow (Yakima River at Parker), and snowmelt dominant (Columbia River at the Dalles). Hydrographs represent monthly averages of simulated daily streamflow by the VIC model for 1916-2006.

Hydrologic simulations from which these hydrographs were developed are fully described in Section 2.2 below. The Chehalis River, which drains to the Washington coast (Figure 3), is a characteristic rain dominant watershed, while the Yakima River, which drains to the Columbia River (Figure 3), is a characteristic transient watershed, and the Columbia River, which drains from mountainous regions in mainly Canada, Idaho, Oregon, and Washington, is a characteristic snowmelt dominant watershed.

Previous studies have presented metrics which can be used to define watershed type. Barnett et al. (2005) suggested a metric which they defined as the ratio of peak snow water equivalent (SWE) to total cool season (October-March) precipitation. SWE is defined as the liquid water content of the snowpack. Barnett et al. (2008) also showed that SWE to precipitation ratios have been declining in the historic record due to observed warming, and that these changes are predominantly related to human influence on the climate. Hamlet and Lettenmaier (2007) characterized the three types of watersheds over the Pacific Northwest by temperature. Snowmelt dominant watersheds have average winter temperatures of less than -6°C., while completely rain dominant watersheds have average temperatures above 5°C. Their analysis explored changes in flood characteristics over basins of varying scale for these watershed categories. Hamlet (2007) and Mantua et al. (2009, this report) also applied the SWE to precipitation ratio metric to the Hydrologic Unit Code (HUC) 4 regions in the PNW as a means to catalogue high-disturbance areas. In Figure 4, we show the SWE to precipitation ratio computed for 1/16th degree grid cells over the PNW. Rain-dominant regions generally have ratios less than 0.1; transient regions are in the range of about 0.1-0.4; and, snowmelt dominant regions generally have ratios greater than 0.4 (see additional figures and discussion in Mantua et al., 2009, this report). Locations at which the historic streamflow hydrographs shown in Figure 3 were simulated are noted in Figure 4. Figure 4 shows that the urban water supply systems for the state's major metropolitan areas in the Puget Sound basin and the Yakima area are located in transient regions. As shown in accompanying papers by Vano et al. (2009a; b, this report), shifts in seasonal streamflow in these regions toward higher winter flow and lower summer flow have strong implications for water management. This paper focuses on hydrologic impacts of climate change and relates those to the three watershed categories discussed above.

2. Approach and Methods

We applied a range of climate change projections from the IPCC AR4 (IPCC, 2007) to hydrologic model simulations and evaluated the impact of climate change on the hydrology of Washington with additional focus on the Columbia River basin, which is a major source of hydropower energy (Hamlet et al. 2009, this report), the Yakima River basin (Vano et al. 2009a, this report), which supports irrigation of high-valued crops such as orchards, and those Puget Sound watersheds that supply water to a majority of the state's population (Vano et al. 2009b, this report). We performed hydrologic simulations using the Variable Infiltration Capacity (VIC) macroscale hydrology model (Liang et al., 1994; Nijssen et al., 1997) at 1/16th degree latitude by longitude spatial resolution over the entire state. We also applied the DHSVM, the Distributed Hydrology Soil and Vegetation Model (Wigmosta et al, 1994), at 150 meter spatial resolution over the Puget Sound watersheds. We used these models to explore sensitivity of runoff to changes in precipitation and temperature over our focus regions. We then evaluated implications of projected changes in snowpack and soil moisture over the same domains.

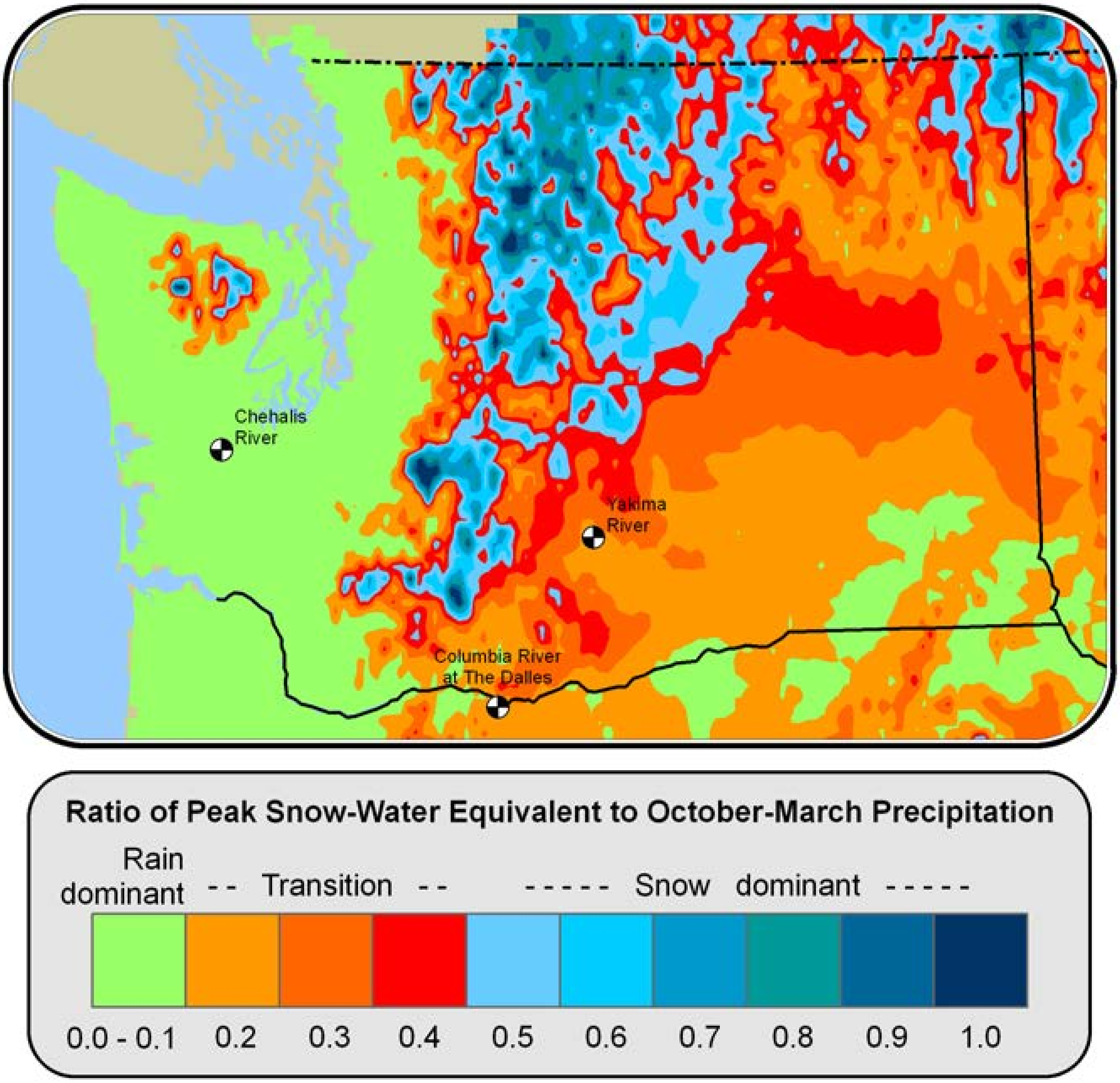

Figure 4. The average ratio of peak VIC model simulated snow water equivalent (SWE) to October – March precipitation for the historical period (1916-2006).

2.1. Hydrologic Simulations

Studies of the impacts of climate change on regional hydrology are becoming increasingly common (Maurer, 2007; Maurer and Duffy, 2005; Hayhoe et al., 2007; Christensen and Lettenmaier, 2007; Christensen et al., 2004; Payne et al., 2004; Van Rheenen et al., 2004; Miller et al., 2003; among others). Many of these studies use a scenario approach which evaluates projections of hydrological variables, like streamflow, using a hydrology model forced with downscaled ensembles of projected climate from GCMs. These future climate simulations are then compared with a baseline hydrological simulation using historical climate (see e.g. Christensen and Lettenmaier, 2007; Maurer 2007; Hayhoe et al., 2007; among others). This approach is sometimes termed "off-line" forcing of a hydrological model, because it does not directly represent feedbacks between the land surface and climate system. An alternative approach, based on regional climate models, represents land-atmosphere feedbacks; however, complications arise due to bias in the climate model simulations (see Wood et al., 2004 for a detailed discussion), and computational requirements which generally preclude the use of multi-model ensemble methods. For this reason, we used the off-line simulation approach.

We used climate change scenarios to force two hydrology models – the VIC Model (Liang et al., 1994; Liang et al., 1996; Nijssen et al., 1997) and DHSVM (Wigmosta et al. 1994). The VIC model is a macroscale model, meaning it is intended for application to relatively large distributed areas, typically ranging from 10,000 km^2 or so, up to continental and even global scales. A key underlying model assumption is that sub-grid scale variability (in vegetation, topography, soil properties, etc.) can be parameterized, rather than represented explicitly. We evaluated VIC model simulations over all of Washington (and over the entire PNW to evaluate streamflow in the lower Columbia basin), including the Yakima River basin, which covers 15,850 km^2.

DHSVM is an explicitly distributed hydrology model, intended for application at much higher spatial resolution (and hence to smaller areas) than VIC. In this study, we applied DHSVM to relatively small rivers flowing to the Puget Sound basin at a 150 m spatial resolution. These watersheds range from 52 – 1055 km^2 in area. Both VIC and DHSVM are described in more detail below.

2.1.1. Variable Infiltration Capacity (VIC) Model

The VIC model (Liang et al., 1994; Liang et al., 1996; Nijssen et al., 1997) has been used to assess the impact of climate change on U.S. hydrology in a number of previous studies. Hamlet and Lettenmaier (1999) studied the implications of GCM projections from the second IPCC assessment (1995) over the Columbia River Basin. Following the third IPCC Assessment Report (2001), Payne et al. (2004) studied climate change effects on the Columbia River Basin, Christensen et al. (2004) studied effects on the Colorado River, and Van Rheenen et al. (2004) studied effects on California. Similarly, recent studies by Vicuna et al. (2007) and Maurer (2007) analyzed the effects of IPCC AR4 projections on hydrologic systems in California, Christensen and Lettenmaier (2007) on the Colorado River basin, and Hayhoe et al. (2007) on the northeastern U.S., all using the VIC model.

Although predictions of winter precipitation changes over the PNW have differed somewhat among recent IPCC reports (the 1995 report suggests an increase, whereas the 2001 report indicates only modest changes), warmer temperatures in all previous assessments have led to projections of reduced snowpack, and hence a transition from spring to winter runoff (Hamlet and Lettenmaier, 1999; Payne et al., 2004). Other impacts common to previous studies of hydrological impacts of climate change in the PNW include earlier spring peak flow and lower summer flows.

In this paper, we used GCM simulations archived for the IPCC AR4 and increased the spatial resolution of the hydrological model over the PNW from 1/8th degree (used in all previous studies cited above) to 1/16th degree. An historical input data set including daily precipitation, maximum and minimum daily temperature, and windspeed was developed for this study at 1/16th degree spatial resolution and its unique features are described in section 2.2.1. Model calibration at routed streamflow locations included use of initial parameters for the 1/8th degree VIC model (Matheussen et al., 2000), transferred to the 1/16th degree model. These parameters were evaluated at 1/16th resolution at two calibration locations (Table 1a). Further calibration was performed over the Yakima River basin. Model calibration and validation statistics for the VIC model used in this study are provided in Table 1a and include relative error in mean annual streamflow and Nash Sutcliffe efficiencies. A well calibrated model typically yields a relative error less than 10% and a Nash Sutcliffe efficiency higher than 0.7 (Liang et al., 1996; Nijssen et al., 1997). Calibration and validation periods were chosen to include a range of streamflow conditions with which to test model performance. Other parameters (e.g. simulated SWE or soil moisture) were not used to further constrain model parameters. However, previous studies comparing VIC simulated SWE with observations (Andreadis et al., 2009 in review) and soil moisture with observations (Maurer et al., 2002), indicate that the model successfully simulates grid level processes. In addition to increasing the VIC model resolution for this study, the number of GCMs from which the ensembles are formed was increased substantially relative to previous studies.

We also adapted the model to allow output of potential evapotranspiration (PET) for each model grid cell. PET is the amount of water that would be transpired by vegetation, provided unlimited water supply, and is often used as a reference value of land surface water stress in characterizations of climate interactions with forest processes (e.g., Littell et al., 2009, this report). PET is calculated in the VIC model using the Penman-Montieth approach (Liang et al., 1996) and the user may choose to output PET of natural vegetation, open water PET, as well as PET of certain reference agricultural crops.

2.1.2. Distributed Hydrology Soil Vegetation Model (DHSVM)

DHSVM was originally designed for application to mountainous forested watersheds, and includes explicit representations of the effects of forest vegetation on the water cycle, in particular the role of vegetation as it intercepts liquid and solid precipitation, and on snow accumulation and

Table 1a. Summary statistics of model calibration and validation for the Variable Infiltration Capacity (VIC) model in units of cubic meters per second (cms). The relative error is defined as the ratio of the difference between mean annual simulated flow (sim.) and mean annual observed natural flow (nat.) to the mean annual observed natural flow. The Nash Sutcliffe efficiency is a coefficient which is commonly used to define hydrologic predictive power, where a coefficient of one is a perfect match between simulated and observed natural flow.

Basins (gage)	Annual mean			N-S model efficiency	
	Nat. (cms)	Sim. (cms)	Rel. error (%)	Calibration (monthly)	Validation (monthly)
Yakima (12505000) *Calibration period (1986-2000)* *Validation period (1971-1985)*	132.8	142.8	7	0.71	0.65
Columbia (14105700) *Calibration period (1986-1999)* *Validation period* (1970-1985)	5132	5375	4.5	0.85	0.83

ablation under forest canopies. Early applications of the model addressed how forest harvest affected flood frequency in the PNW (Bowling, 2000, La Marche and Lettenmaier, 2001; Bowling et al., 2001). The model represents runoff primarily via the saturation excess mechanism and explicitly represents the depth to water table at each model pixel, which has typically ranged from 10-200 m in past applications of the model (in our application to the Puget Sound basins, we used 150 m spatial resolution).

Some DHSVM model parameterizations are similar to those in Topmodel (Beven and Kirkby, 1979); a key difference is the explicit, rather than statistical representation of downslope redistribution of moisture in the saturated zone. In addition to its representation of the water table and downslope redistribution of moisture, DHSVM represents the land surface energy balance (in a manner similar to VIC), unsaturated soil moisture movement, saturation overland flow, and snowmelt and accumulation. DHSVM simulates snow accumulation and ablation, using the same snow model used by VIC, which is described by Cherkauer et al. (2003). In brief, it uses a two-layer snow algorithm, in which the top layer is used to solve an energy balance with the atmosphere, including effects of vegetation cover, while the bottom layer is used as storage to simulate deeper snowpack.

Using a 150 m resolution digital elevation model (DEM) as a base map (US Department of Interior/US Geological Survey, http://seamless.usgs.gov), DHSVM explicitly accounts for soil and vegetation types and stream channel network and morphology. Wigmosta et al. (1994; 2002) provide a detailed description of the model. The model also uses a soil class map based on the STATSGO soil map produced by the U.S. Department of Agriculture. The land cover map was derived from Alberti, et al. (2004). The model is forced by climate inputs including precipitation and temperature, (at daily or shorter time steps), downward solar and longwave radiation, surface humidity, and wind speed. Using the historical 16th degree dataset developed for the VIC model (described below) and procedures developed by Nijssen et al. (2001), daily forcings were disaggregated to 3-hour

Table 1b. Summary statistics of model calibration and validation for the Distributed Hydrology Soil and Vegetation Model (DHSVM) in units of cubic meters per second (cms). The relative error is defined as the ratio of the difference between mean annual simulated flow (sim.) and mean annual observed natural flow (nat.) to the mean annual observed natural flow. The Nash Sutcliffe efficiency is a coefficient which is commonly used to define hydrologic predictive power, where a coefficient of one is a perfect match between simulated and observed natural flow.

Basins (gage)	Annual mean			N-S model efficiency		
	Nat. (cms)	Sim. (cms)	Rel. error (%)	Calib. (daily)	Calib. (monthly)	Valid. (monthly)
Snohomish (12141300) *Calibration period (1993-2002)* *Validation period (1983-1993)*	35.5	36.1	2	0.50	0.79	0.75
Cedar (12115000) *Calibration period (1982-1992)* *Validation period (1992-2002)*	6.85	6.18	-10	0.61	0.81	0.81
Green (12104500) *Calibration Period (1973-1983)* *Validation Period (1983-1993)*	9.79	9.76	0	0.54	0.72	0.71
Tolt (12147600) *Calibration period (1983-1993)* *Validation period (1993-2002)*	1.52	1.39	-9	0.45	0.70	0.75

intervals as described in detail by Cuo et al. (2008b), who applied DHSVM to the entire Puget Sound basin. Model calibration and validation statistics for the DHSVM used in this study are provided in Table 1b. Similar to VIC, a well calibrated DHSVM model typically yields a relative error less than 10% and a Nash Sutcliffe efficiency higher than 0.7 (Wigmosta et al., 1994; Leung et al.,1996). Calibration and validation periods were chosen to include a range of streamflow conditions with which to test model performance.

2.2. Model Input Variables

2.2.1. Historical Inputs

Both VIC and DHSVM require as forcing variables precipitation (Prcp) and temperature at a sub-daily time step, as well as downward solar and longwave radiation, surface wind, and vapor pressure deficit. All simulations described in this paper are based on a 1/16th degree spatial resolution data set of daily historical Prcp and daily temperature maxima and minima (Tmax, Tmin) developed from observations following methods described in Maurer et al. (2002) and Hamlet and Lettenmaier (2005), adapted as described below. Variables other than daily precipitation and temperature maxima and minima are derived from the daily temperature range or mean temperature following methods outlined in Maurer et al. (2002). One exception is surface wind. Daily wind speed values for 1949-2006 were downscaled from National Centers for Environmental Prediction-National Center for Atmospheric Research (NCEP-NCAR) reanalysis products (Kalanay et al., 1996). For years prior to 1949, daily wind speed climatology was derived from the 1949-2006 reanalysis.

We used the National Climatic Data Center Cooperative Observer (Co-Op) network and Environment Canada (EC) daily station data as the primary sources for precipitation and temperature values. We used a method described by Hamlet and Lettenmaier (2005) that corrects for temporal inhomogeneities in the raw gridded data using a set of temporally consistent and quality controlled index stations from the U.S. Historical Climatology Network (HCN) and the Adjusted Historical Canadian Climate Database (AHCCD) data. This approach assures that no spurious trends are introduced into the gridded historical data as a result of inclusion of stations with records shorter than the length of the gridded data set. The data are adjusted for orographic effects using the PRISM (Daly et al., 1994; 2002) climatology (1971-2001) following methods outlined in Maurer et al. (2002).

Daily station data from 1915 to 2006 were processed as in Hamlet and Lettenmaier (2005), but using only Co-Op, EC, HCN, and AHCCD stations within a 100 km buffer of the domain. Quality control flags included in the raw Co-Op data set for each recorded value were used to ensure accuracy and to temporally redistribute "accumulated" Prcp values. We used the Symap algorithm (Sheppard, 1984; as per Maurer et al., 2002) to interpolate Co-Op/EC station data to a 1/16th degree.

We then adjusted the daily Prcp, Tmax, and Tmin values for topographic influences by scaling the monthly means to match the monthly PRISM climate normals from 1970-2000. In the temperature rescaling method used for this study, Tmax and Tmin were adjusted by the same amount to avoid introducing a bias into daily mean temperatures and the daily temperature range. First, the average of the Tmax and Tmin values were computed for each of the monthly PRISM and monthly mean Co-Op time series. The difference between these values was applied as an offset to the average of the daily Tmax and Tmin in the appropriate month, thereby explicitly preserving the daily temperature range. For days where Tmin exceeds Tmax due to interpolation errors in the initial regridding step, we offset the average of these inverted Tmax and Tmin values and applied a climatological daily range from PRISM Tmax and Tmin.

2.2.2. Regional Climate Change Projections

As part of the IPCC AR4, results from a common set of simulations of 21st century climate were archived from 21 global climate models (GCM) (Mote and Salathé 2009, this report), using greenhouse gas emissions scenarios as summarized in the IPCC's Special Report on Emissions Scenarios (SRES) (Nakićenović, 2000). Simulations were archived predominantly for three SRES emissions scenarios (A1B, B1, and A2) for most of the 21 GCMs, with A2 following the highest trajectory for future CO2 emissions at the end of the 21st century. We focus on A1B and B1 emission scenarios because these were simulated by the most GCMs and our study focuses on mid-century change, at which point none of the scenarios is consistently the highest. Following Mote and Salathé (2009, this report), we used output from 20 of the GCMs for which monthly gridded precipitation, temperature, and other variables were archived for SRES emissions scenario A1B, and

19 for which the same variables were archived for emissions scenario B1. Mote and Salathé (2009, this report) summarize the GCM predictions of 21st century precipitation and temperature over the Pacific Northwest, and evaluate performance of the GCMs in reconstructing 20th century climate. The spatial resolution of the 20 models varies, but is generally about three degrees latitude by longitude; therefore, we downscaled the climate model output to the spatial resolution of a regional hydrology model as described below.

2.2.3. Downscaling Procedures

In general, the GCM output is at too coarse a spatial resolution to be meaningful for hydrological studies. Therefore, we downscaled the GCM output to 1/16th degree spatial resolution and applied a delta method approach to develop climate change scenarios with which to evaluate impacts (see e.g. Hamlet and Lettenmaier, 1999; Snover et al., 2003). In the delta method, projected changes in precipitation and temperature, as determined by GCM simulations, are applied to the historical record at the resolution of hydrologic models. We used regional projected monthly changes derived from a total of 39 climate ensembles (described in Section 2.2.2). We performed hydrologic simulations using the historical record perturbed by these monthly changes and then evaluated impacts of climate change on a number of hydrologic variables.

There are three previously established ways to develop climate change scenarios based on GCM output and may be used in off-line hydrologic simulations. As noted above, the delta method simply applies changes in temperature and precipitation from the GCM to historical inputs or inputs derived from historical data, which in turn are used to force the hydrological model in the same way that simulations using historical forcings are performed. This approach was used by Hamlet and Lettenmaier (1999). The second approach uses transient projections of future climate from GCMs statistically downscaled to the spatial resolution of the watershed model and from a monthly to daily time step. This approach was used by Christensen et al., 2004 and Christensen and Lettenmaier (2007) in the Colorado River basin, Van Rheenen et al. (2004), Maurer and Duffy (2005) in the Sacramento and San Joaquin basins of California, Payne et al. (2004) in the Columbia River basin, and Hayhoe et al. (2007) over the northeastern U.S. All of these studies followed the bias correction and statistical downscaling (BCSD) approach described by Salathé et al. 2007, Wood et al. (2004), and Wood et al. (2002). The third approach is to utilize regional climate model simulations constrained by GCMs to drive hydrologic models. Significant resources are required to implement this approach, which have limited its use.

The advantage of the BCSD approach is that it makes direct use of transient climate change scenarios and, therefore, incorporates projected changes in climate variability. There are, however, some key assumptions in the spatial and temporal downscaling that can complicate interpretation of results at sub-monthly (e.g., daily or weekly) time steps. In addition, evaluation of transient scenarios is complicated by the stochastic element of the transient climate variability. Full analysis of this effect requires a large number of ensemble members; however, most GCMs archive only a single transient run, and even for those that archive multiple ensembles, the number is generally quite small. The primary advantage of the delta method approach is that it provides realistic temporal sequencing associated with the historic record, while avoiding bias in the GCM simulations. Another advantage is that climate change impacts may be evaluated in the context of historical events. However, the primary disadvantage is that we do not incorporate projected changes in climate variability by the GCMs into the hydrologic simulations. The delta method approach is arguably more appropriate for this study to evaluate water resource system performance at a sub-monthly timestep in a changing climate, as reported in companion papers by Hamlet et al. 2009 (this report) and Vano et al. 2008a; b (this report).

We performed hydrologic simulations to evaluate the impacts of climate change on statewide hydrology in the 2020s, 2040s and 2080s. The delta values represent monthly average changes for each future period over the whole PNW and were applied to Washington. The PNW is arguably the smallest area that the GCMs are able to resolve and, therefore, potential differences in rates of climate change across the State are not incorporated. Each future period represents a 30-year average of projected climate, for instance, the 2020s are represented by the 30-year average climate between 2010 and 2039. Likewise for the 2040s and 2080s, these represent the average climate over 30-year periods 2030-2059 and 2070-2099, respectively. Six composite scenarios were formed following methods outlined by Mote and Salathé, 2009 (this report). In particular, for each 30-year time period and each month, we computed domain-average precipitation and temperature changes. Unlike Mote and Salathe (2009, this issue), we assume equal weighting of each climate change scenario for this study because, as similarly found by Brekke et al. (2004), the weighting of scenarios is largely dependent on the criteria used. In accordance with the delta method approach, we perturbed the entire spatially gridded record of observed historical daily precipitation and temperature (1916-2006) by the projected change for the corresponding month (12 values for each of precipitation and temperature), for each of the three future periods.

In addition to performing hydrology simulations over the Washington using composite scenarios, we also performed simulations using 39 individual scenarios of 2020s climate over focus watersheds of the Yakima River basin and the Puget Sound for each of the GCMs. These focus watersheds are further described below.

2.3. Focus Watersheds

We evaluated in more detail the impacts of projected future climate change on the hydrology of three key areas: The Puget Sound drainage basin, the Yakima River basin, and the Columbia River basin. The three focus regions are shown in Figure 1.

The Columbia River basin is one of our focus basins because it drains the eastern 2/3 of the state, as well as much of Idaho, part of British Columbia, and 2/3 of Oregon. In addition, roughly 70 percent of the electrical energy consumption within the State of Washington is derived from hydropower, most of which comes from the Columbia River (Bonneville Power Administration 1994). Detailed analysis of impacts on the Columbia River in the context of hydropower production are presented in a companion paper, Hamlet et al. (2009, this report).

The Puget Sound basin is bounded to the east by the Cascades and to the west by the Olympic Mountains, and covers an area of approximately 30,000 km^2. Its elevation ranges from sea level to 4,400 m. Substantial winter snowfall occurs at high elevations, but rarely in the lowlands. Annual precipitation ranges from 600 to over 3,000 mm, depending on elevation, most of which falls from October to March. The watersheds that make up the Puget Sound basin are generally characterized as transient. The Puget Sound basin includes more than 69% of the State's population (based on 2000 census). Quantification of the region's future water supply is therefore critical to the region's future growth and ecosystem conservation. We focus here on four Puget Sound watersheds that are managed primarily for water supply: the Cedar River basin, Green River basin, Tolt River basin, and Sultan River basin (Figure 1). In a companion paper (Vano et al., 2008a, this report), we use the hydrological sequences described herein as input to reservoir simulation models. In this paper, we limit our attention to the hydrological projections.

The Yakima River, which drains east through an arid lowland area, supplies water to over 180,000 irrigated hectares (450,000 acres). Agriculture in the Yakima River basin has changed over time. Land used to grow annual crops (e.g. wheat) has decreased, while that used to grow perennial crops including apples and grapes has increased. This shift toward perennial crops has increased dependence by agricultural producers on reliable water supplies (EES, Inc. 2003). Vano et al. (2008b) use the hydrological sequences described herein in conjunction with a reservoir simulation model of the Yakima River basin to evaluate potential climate change impacts on agricultural production in the basin.

3. Model Sensitivities to Changes in Climate

By the 2040s, future regional temperatures are projected to be out of the range of historic variability (Mote at Salathé 2009, this report). Further, we lack observations to evaluate the sensitivity of hydrologic models to projected changes in climate, which makes evaluating confidence in predicting impacts difficult. The need for "validation" of hydrological models is widely accepted in the hydrological literature, and it is usually performed by using split sample methods first to estimate model parameters, and then to evaluate model performance (see e.g. Refsgaard and Storm, 1996). However, a similar structure for evaluation of model sensitivities, such as how much runoff will change for a given amount of warming, is often lacking. Dooge (1992) suggested a framework for assessing hydrological sensitivity to climate change, via what is referred to as elasticity, or the fractional change in runoff compared to the fractional change in precipitation (precipitation elasticity) or potential evapotranspiration (PET elasticity). Here we focus on precipitation elasticity, which can be evaluated, on an annual basis, from historical observations of streamflow (or runoff) and precipitation. Simulated runoff may be used as a surrogate for streamflow in calculation of elasticity because, on an annual basis, the difference introduced by the time lag of streamflow routing is negligible. Previous studies show that precipitation elasticities performed on the same watershed using different hydrologic models can lead to different results. For example, the results from Nash and Gleick (1991) and Schaake (1990) for the Colorado River differ in their precipitation elasticities by a factor of about two.

Sankarasubramanian et al. (2001) suggested a non-parametric, robust, and unbiased elasticity estimator which summarizes sensitivity of streamflow to changes in precipitation, which yields similar results for a wide range of hydrologic model structures. Their estimator of the streamflow elasticity to precipitation is:

$$e_P = median\left(\frac{Q_t - \overline{Q}}{P_t - \overline{P}} * \frac{\overline{P}}{\overline{Q}}\right) \quad (1)$$

where Q_t and P_t are annual streamflow and precipitation, respectively, and and are the long-term mean annual streamflow and precipitation.

A result of the Sankarasubramanian et al. (2001) work was a contour map for the continental U.S. of (annual) streamflow elasticities to precipitation. The map shows streamflow elasticities in the range 1.0-2.0 for much of Washington State. In other words, a given fractional change in precipitation would result in a one- to two-fold fractional increase in streamflow. Using eq. 1, we evaluated observed and simulated runoff elasticities to precipitation for 6 locations within the Yakima watershed and 6 in the Puget Sound basin. These locations are noted in Figure 1 (overview map) and are defined in Table 1. Elasticities for the Yakima River watersheds were calculated using results from the VIC model, while elasticities for the Puget Sound were calculated using the DHSVM model.

Analysis of temperature sensitivities is slightly more complicated. In the Dooge (1992) formulation, streamflow elasticities to precipitation and potential evaporation are described and these are used as a measure of model sensitivity. However, potential evaporation is a computed, rather than observed, quantity. In general, it depends on net radiation, vapor pressure deficit, wind, and land surface properties such as roughness length. Several of these quantities are temperature dependent. Furthermore, hydrological sensitivities to temperature are generally much more subtle than to precipitation, and they are difficult to estimate from observations because precipitation effects dominate the results. Instead, we computed runoff sensitivity to temperature in two ways. The first is a fixed temperature increase, in which both daily maximum and minimum temperature were increased by 1°C. In the Maurer et al. (2002) formulation of land surface forcing variables, downward solar radiation is indexed to the daily temperature range, hence for the same increase in Tmin and Tmax, downward solar radiation is constant (however, net longwave radiation, as well as vapor pressure deficit, both change). Such a fixed temperature increase was used to develop delta method scenarios in this study.

The second computation also changes the daily average temperature by 1°C, but leaves Tmin unchanged, while increasing Tmax by 2°C. This has the effect of increasing downward solar radiation, but leaving the dew point (which is directly related to the daily minimum temperature in the model) unchanged. Meehl et al. (2007) summarizes projected changes in the global diurnal temperature range (i.e. difference between Tmax and Tmin). Although this range is expected to change over parts of the globe, there is no consensus among GCMs over the direction of change for the

Pacific Northwest. Therefore, we decided that it is most appropriate to apply the delta method approach using fixed change in Tmax and Tmin.

We analyzed precipitation elasticity and temperature sensitivities for six locations in the Yakima River basin, which correspond to the five basin reservoir locations, in addition to the Yakima River at Parker (USGS ID 12505000), which is a key reference station for water management in the basin. Observed and simulated precipitation elasticities calculated from the historical record for these sites are in close agreement and are summarized in Table 3. They range from 1.08 to 1.42 in the Yakima watershed. A 10% increase in precipitation causes an increase in runoff of a factor of 1.59 for the entire basin (at Parker) to 1.87 for Bumping Lake, which has a small contributing area (184 km^2) and is at a relatively high elevation (1,030 m). An average daily temperature increase of 1°C, applied by increasing both minimum and maximum temperature (downward solar radiation unchanged), reduces basin runoff by approximately 2.45 (Rimrock) to 5.77% (Bumping Lake) (refer to Table 2, Temperature Sensitivity a). Alternatively, the same average daily increase, by altering maximum temperature only (constant dew point), reduces runoff by 5.15% (Parker) to 9.81% (Bumping Lake) (refer to Table 2, Temperature Sensitivity b).

In the Puget Sound basin, we analyzed six catchments including the Cedar River at Renton, (Cedar E), the Cedar River near Cedar Falls (Cedar A), Green River near Auburn (Green C), the Green River above Howard Hanson Dam (Green A), the Sultan River (Sultan A) and the South Fork Tolt River near Index (Tolt A) (see Figure 1 for locations). These points are generally located near water supply reservoirs. Precipitation elasticity of observed and simulated historical periods at the six sites are in agreement (See Table 2) with values ranging from 1.0 – 1.4. An increase in precipitation of 10% for the same simulated watersheds (with temperature remaining unchanged) causes an increase in runoff by a factor of 1.17 to 1.63 in the Puget Sound basin. An average temperature increase of 1°C, by increasing both maximum and minimum temperature by 1°C (see Table 3, Temperature Sensitivity a), results in approximately a 0.7-2.4% decrease in the Puget Sound basin streamflows. The same average increase in daily temperature applied by increasing the maximum temperature by 2°C and leaving the minimum temperature unchanged (see Table 3, Temperature Sensitivity b) results in decreases in runoff by 1.5-5.6%.

Runoff sensitivity to temperature change is expected to be higher when only Tmax is increased as compared with increasing both the Tmax and Tmin. This is expected because the algorithm used to estimate downward solar radiation is based on the daily temperature range, and therefore downward solar radiation, remains constant when both the maximum and minimum temperature are increased. As a result, the change in net radiation is generally smaller than when the minimum temperature is left unchanged. The basis for different precipitation elasticities and temperature sensitivities across sites is less clear. Elasticities are generally higher for Yakima River basin sites than for Puget Sound sites, but it is not entirely clear whether these differences are related to watershed characteristics or to potentially different sensitivities of the two hydrologic models. Precipitation and temperature sensitivities calculated above are based on annual changes and runoff responses will vary depending on the seasonality of change.

Table 2. Summary of analysis locations. Sites with USGS ID of "NA" indicate these are not USGS gage locations.

Site ID	Description	Basin Area (km2)	USGS ID
Yakima Basin			
BUMPI	Bumping River near Nile	184	12488000
RIMRO	Tieton River at Tieton Dam near Naches	484	12491500
KACHE	Kachess River near Easton	166	12476000
KEEMA	Yakima River near Martin	142	12474500
CLERO	Cle Elum River near Roslyn	526	12479000
YAPAR	Yakima River near Parker	6,889	12505000
Columbia Basin			
DALLE	Columbia River at the Dalles	613,827	14105700
Puget Sound Basin			
Cedar E	Cedar River at Renton	469	12119000
Green C	Green River Outlet near Auburn	1032	NA
Cedar A	Cedar River near Cedar Falls	106	12115000
Green A	Green River above Howard Hanson Dam	573	NA
Sultan A	Sultan River	178	NA
Tolt A	South Fork Tolt River near Index	17	12147600

Table 3. Summary of precipitation elasticity and temperature sensitivity at analysis locations. Precipitation elasticity is defined as the ratio of the fractional change in runoff to the fractional change in precipitation. Temperature sensitivities are defined as the percent change in runoff per 1°C of warming. Temperature sensitivity (a) considers increased daily minimum and maximum temperature, while temperature sensitivity (b) considers increased daily maximum temperature.

Site	Observed (and Simulated) Precipitation Elasticity	Precipitation Elasticity (10% increase)	Temperature Sensitivity (a), %/oC	Temperature Sensitivity (b), %/oC
Yakima Basin				
BUMPI	1.42 (1.12)	1.87	-5.77	-9.81
RIMRO	1.37 (1.08)	1.65	-2.45	-6.26
KACHE	1.16 (1.23)	1.67	-3.70	-6.36
KEEMA	1.15 (1.19)	1.78	-5.19	-7.56
CLERO	1.12 (1.13)	1.61	-4.01	-6.73
YAPAR	1.32 (1.32)	1.59	-2.84	-5.15
Puget Sound Basin				
Cedar E	1.38 (1.22)	1.36	-1.11	-2.99
Green C	1.33 (1.43)	1.63	-2.33	-5.57
Cedar A	1.08 (1.17)	1.28	-1.05	-2.77
Green A	1.42 (1.37)	1.61	-2.42	-5.64
Sultan A	1.06 (1.12)	1.17	-0.69	-1.69
Tolt A	1.12 (1.00)	1.20	-0.66	-1.50

4. Results and Discussion

Projections of 21st century climate of the PNW summarized in Mote and Salathé (2009, this report) indicate that temperatures will increase an average of 0.3°C (0.5°F) per decade. Changes in annual mean precipitation are projected to be modest, with a projected increase of 1% by the 2020s and 2% by the 2040s. However, the range of projected precipitation shows a decrease of almost 11% to an increase of almost 20% by the 2080s, underscoring the uncertainty in projections of future precipitation. Projected temperature increases, along with changes in seasonal precipitation have important implications for hydrologic variables across Washington. In this section we summarize impacts of projected changes in climate on a state level, as well as the Columbia River watershed, and then provide a more focused evaluation of watersheds within the Puget Sound and Yakima drainage basins.

4.1. Statewide Climate Change Impacts

4.1.1. Implications of Changes in April 1 Snow Water Equivalent

Many past studies demonstrated that changes in snowpack are a primary impact pathway associated with regional warming in the PNW (Lettenmaier et al., 1999; Hamlet and Lettenmaier, 1999; Snover et al., 2003). Changes in snowpack are affected by both precipitation and temperature, although in the 20th century, temperature has been the more important driver (Mote et al., 2005; Hamlet et al., 2005; Mote, 2006; Mote and Salathé, 2009, this report), particularly in relatively warm areas such as the Cascades. SWE on April 1 is an important metric for evaluating snowpack changes because in the PNW, the water stored in the snowpack on April 1 is strongly correlated with summer water supply.

Figure 5 shows projected changes in April 1 SWE for the 2020s, 2040s, and 2080s for the composite A1B and B1 climate conditions, as simulated using the VIC model. Results from these hydrologic simulations are consistent with previous studies, such as the climate impacts study conducted for King County, Washington, which projected a decrease in snowpack over the 21st century (Casola et al. 2005). Generally, results using the B1 emissions scenario project less significant impacts than those using the A1B scenario. Based on composite scenarios for the B1 and A1B scenarios respectively, April 1 SWE is projected to decrease by 27 to 29% across the state by the 2020s, 37 to 44% by the 2040s and 53 to 65% by the 2080s.

Changes in SWE vary by elevation, as Figure 5 suggests. We summarized these changes over three bands of elevation, specifically elevations below 1,000 meters, between 1,000 and 2,000 meters, and above 2,000 meters (see Table 4). The results show that the lowest elevations will experience the largest decreases in snowpack, with reductions for B1 and A1B emissions scenarios, respectively, of 36 to 37% by the 2020s to 62 to 71% by the 2080s. The reduction of snowpack in the regions of highest elevation is projected to be less significant.

Projected changes in snowpack are directly correlated with temperature. The greatest sensitivity of snowpack to warming is at temperatures near

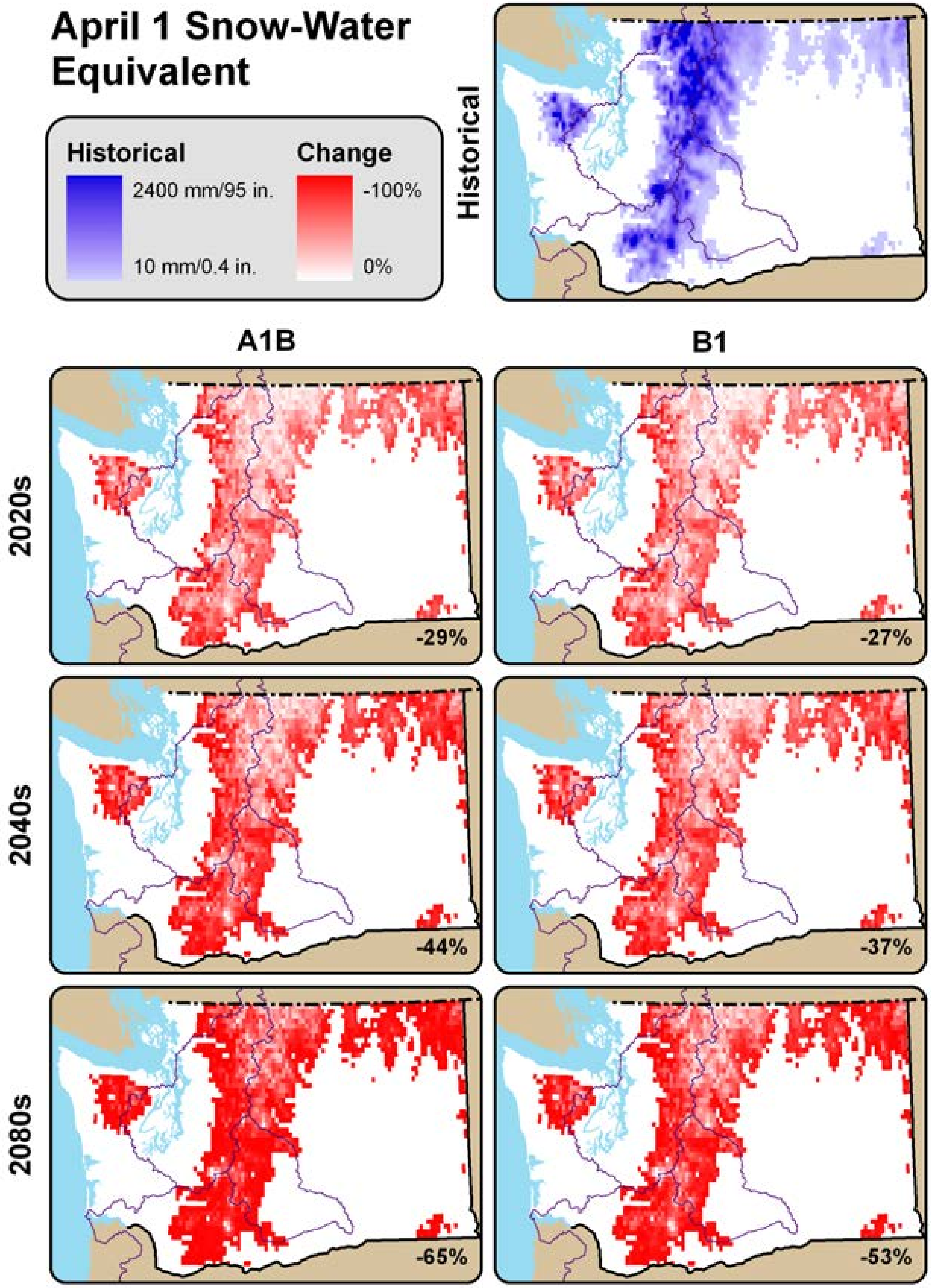

Figure 5. Summary of projected April 1 snow water equivalent (SWE) for the 2020s, 2040s and 2080s (A1B and B1 SRES scenarios) by the VIC model. Percent change values represent spatially averaged April 1 SWE across Washington State.

Table 4. Projected changes (%) in April 1 snow water equivalent (SWE) according to elevation using delta method composite climate change scenarios (30-year average changes not weighted) for the 2020s, 2040s, and 2080s.

	2020s		2040s		2080s	
% Change in	(2010-2039)		(2030-2059)		(2070-2099)	
April 1 SWE	A1B	B1	A1B	B1	A1B	B1
< 1,000m (< 3,280ft)	-37%	-36%	-54%	-46%	-71%	-62%
1,000 m - 1,999 m (3,280 ft – 6,558 ft)	-27%	-25%	-42%	-34%	-63%	-51%
>= 2,000 m (>= 6,558 ft)	-17%	-15%	-29%	-23%	-54%	-39%
Overall	-29	-27%	-44%	-37%	-65%	-53%

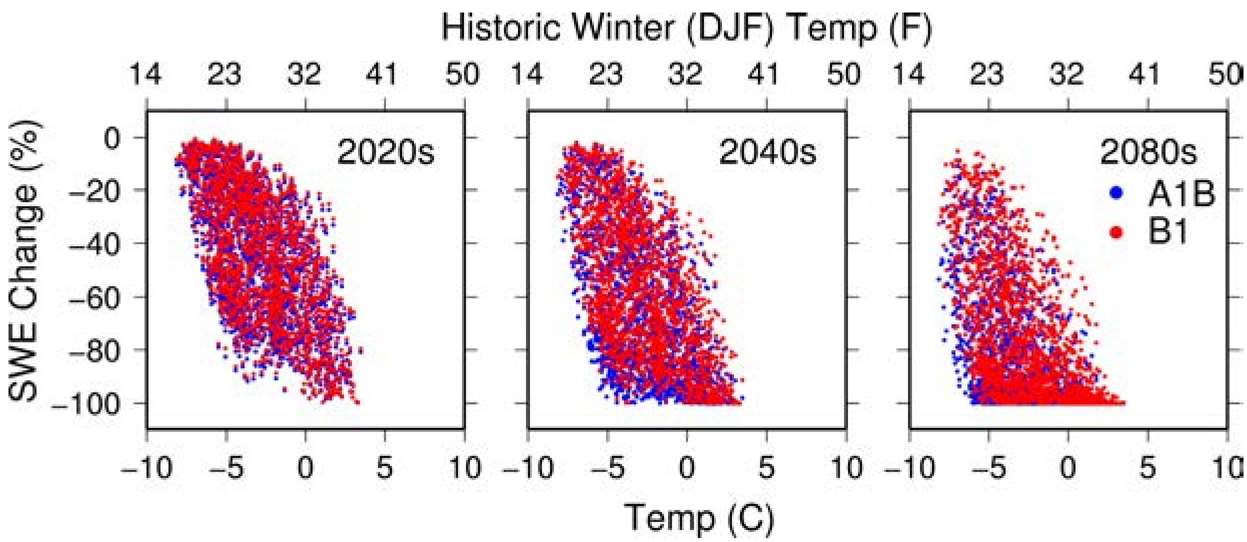

Figure 6. Projected change in April 1 snow water equivalent (SWE) for the 2020s, 2040s, and 2080s plotted against mean historical winter temperature (1916-2006). Individual points represent April 1 SWE for each of the 91 years simulated by the VIC model. Projected values are derived using a delta method approach, where historical temperature and precipitation are perturbed by the projected average monthly changes in these vales for the 2020s (average change from 2010-2039), 2040s (average change from 2030-2059), and 2080s (average change from 2070-2099).

freezing. Locations with a warmer mean historical winter temperature (defined as December through February) are projected to experience the greatest reduction of snowpack, while locations with cooler winter temperatures are projected to experience more modest reductions (Figure 6). Projections using the A1B emissions scenario generally show greater reductions in snowpack than those using the B1 scenario, especially for the 2080s simulations

4.1.2. Implications of Changes in July 1 Soil Moisture

Vegetation and dry land agriculture rely heavily on soil moisture, in addition to precipitation, particularly in the arid region of the state (east of the Cascades in the Columbia River basin) where summer precipitation is low. Soil moisture in snow dominated watersheds (like the Columbia River basin overall) tends to peak in spring or early summer, in response to melting mountain snowpack. In the summer, lower precipitation (along with clearer and longer days) and increased vegetative activity cause depletion of soil moisture, resulting in minimum soil moisture values in September.

Simulated soil moisture by hydrologic models is strongly determined by model assumptions (Liang et al., 1998), but when expressed as percentiles, many of these differences are removed (Wang, 2008). For this reason, we present projected soil moisture changes across the state as percentiles of simulated historic mean soil moisture (1916-2006), where a projected decrease in soil moisture is represented by percentiles less than 50 and a projected increase is represented by percentiles greater than 50. Specifically, we summarize projections of July 1 soil moisture from the VIC model, as this is the typical period of peak soil moisture which is critical for water supply in the State's arid regions.

Projections of July 1 total soil moisture change for the composite A1B and B1 scenarios are modest but generally show decreases across the State. Projected decreases are greater for A1B scenario simulations compared with B1 simulations. For the three future periods, soil moisture is projected to be in the 38th to 43rd percentile (A1B and B1, respectively) by the 2020s, 35th to 40th percentile by the 2040s, and 32nd to 35th percentile by the 2080s, with 50% being equal to mean historical values. However, projected soil moisture changes vary on either side of the Cascade Mountains. In the mountains and coastal drainages west of the Cascades, warming of the climate tends to enhance soil drying in the summer and, in combination with reduced winter snowpack and earlier snowmelt, causes decreases in summer soil moisture (Figure 7). East of the Cascades, summer soil moisture is primarily driven by recharge of snowmelt water into the deep soil layers. Increased snowpack at the highest elevations in some parts of the Cascades (tied to projected increases in winter precipitation) and subsequently increased snowmelt, are likely to cause greater overall infiltration. Similar trends east and west of the Cascades were found in the study of PNW regional climate change impacts (Casola et al., 2005).

4.1.3. Implications of Changes in Mean Annual Runoff and Streamflow

As noted by Mote and Salathé (2009, this report), there is a wide range in projections of future precipitation across GCMs and SRES emissions scenarios. Across the 39 scenarios considered in this study (20 GCMs and 2 SRES emissions scenarios for all but one GCM), projected annual precipitation changes over the PNW range from -9% to +12% for the 2020s, -11% to +12% for the 2040s, and -10% to +20% for the 2080s, with modest increases projected for the composite scenarios for A1B and B1 (Table 5). Although projected increases of annual precipitation are modest, projections of seasonal precipitation change indicate increased winter precipitation and decreased summer precipitation (Tables 6 and 7). With 75 % of the annual precipitation falling between October and March (Snover and Miles, in review), cool season precipitation is the primary driver of hydrologic processes in Washington and the PNW. Projections of cool season precipitation for the composite B1 and A1B scenarios, respectively, range from +2.3% to +3.3% for the 2020s, +3.9% to 5.4% for the 2040s, and +6.4% to +9.6% for the 2080s (Table 6). Table 5 summarizes the composite projected changes in annual precipitation and corresponding state-wide changes in runoff simulated by the VIC model. The importance of cool season precipitation to the state's runoff is evident: even with increased temperatures and modest, as opposed to significant, annual precipitation increases (and in the case of the 2020s for emissions scenario A1B, a slight decrease in annual precipitation) runoff

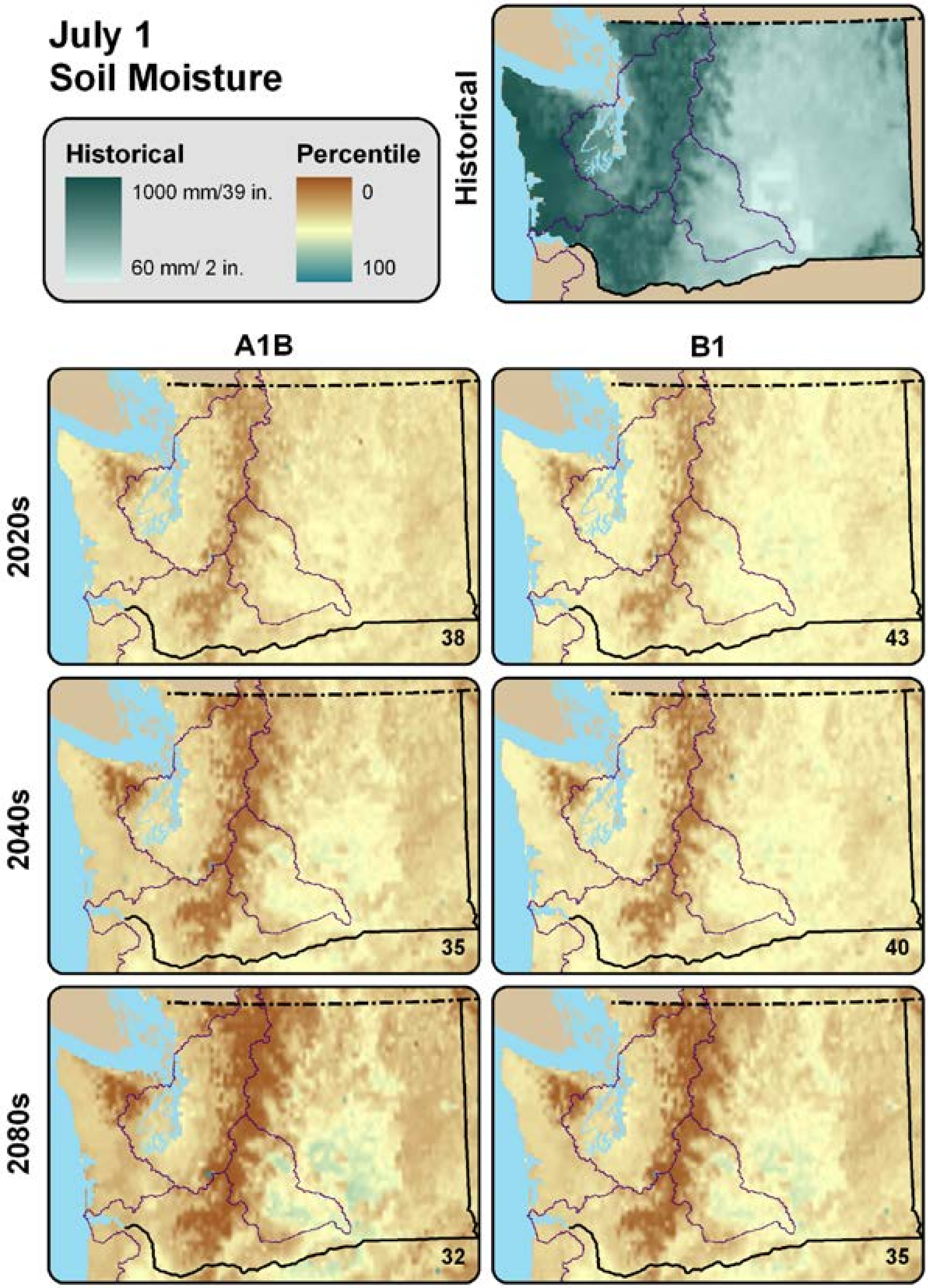

Figure 7. Summary of projected July 1 soil moisture for the 2020s, 2040s, 2080s (A1B and B1 SRES scenarios) as percentile of simulated historical mean from 1916-2006 (using the VIC model). Percentiles less than 50 represent a decrease in soil moisture, while percentiles greater than 50 show an increase in soil moisture. Reported values represent spatially averaged percentile across Washington State.

Table 5. Summary of composite changes in annual precipitation and runoff across Washington using delta method composite climate change scenarios (30-year average changes not weighted) for the 2020s, 2040s, and 2080s for SRES A1B and B1 global emissions scenarios.

	2020s		2040s		2080s	
	(2010-2039)		(2030-2059)		(2070-2099)	
	A1B	B1	A1B	B1	A1B	B1
Change in Temperature	+1.2°C	+1.1°C	+2.1°C	+1.6°C	+3.5°C	+2.5°C
% Change in Precipitation	+0.2%	+1.9%	+2.1%	+2.2%	+4.9%	+3.4%
% Change in Runoff	0.0%	+2.3%	+2.7%	+2.2%	+6.4%	+4.2%

Table 6. Summary of composite changes in cool season (October through March) precipitation and runoff across Washington using delta method composite climate change scenarios (30-year average changes not weighted) for the 2020s, 2040s, and 2080s for SRES A1B and B1 global emissions scenarios.

	2020s		2040s		2080s	
	(2010-2039)		(2030-2059)		(2070-2099)	
	A1B	B1	A1B	B1	A1B	B1
Change in Temperature	+1.1°C	+1.0°C	+1.8°C	+1.4°C	+3.2°C	+2.3°C
% Change in Precipitation	+2.3%	+3.3%	+5.4%	+3.9%	+9.6%	+6.4%
% Change in Runoff	+10.9%	+12.6%	+20.5%	+16.1%	+34.6%	+25.6%

Table 7. Summary of composite changes in warm season (April through September) precipitation and runoff across Washington using delta method composite climate change scenarios (30-year average changes not weighted) for the 2020s, 2040s, and 2080s for SRES A1B and B1 global emissions scenarios.

	2020s		2040s		2080s	
	(2010-2039)		(2030-2059)		(2070-2099)	
	A1B	B1	A1B	B1	A1B	B1
Change in Temperature	+1.3°C	+1.2°C	+2.3°C	+1.7°C	+3.8°C	+2.7°C
% Change in Precipitation	-4.2%	-0.9%	-5.0%	-1.3%	-4.7%	-2.2%
% Change in Runoff	-19.1%	-15.8%	-28.6%	-22.1%	-43.2%	-33.4%

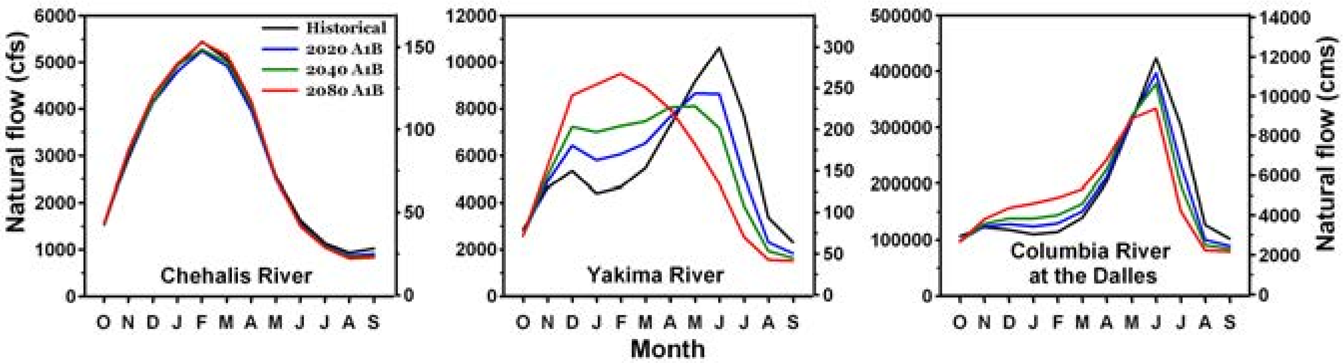

Figure 8. Projected average monthly streamflow for a rain dominant watershed (Chehalis River at Porter), transient rain-snow watershed (Yakima River at Parker), and snowmelt dominant watershed (Columbia River at The Dalles). Hydrographs represent monthly averages of simulated daily streamflow by the VIC model for the historic period (1916-2006) and three future periods (2020s, 2040s, and 2080s) using the A1B SRES scenario.

increases in all cases. This contrasts with results for precipitation elasticity and temperature sensitivities (Table 3) to the extent that on an annual basis, the modest precipitation changes coupled with temperature increases should have led to runoff reductions. The reason this is not the case is that in the Table 3 experiments, precipitation changes are uniform over the year, whereas in the GCM output (at least for the composites), cool season precipitation, which is much more efficient than summer precipitation in terms of runoff production due to higher soil moisture storage and lower vegetative water demand, increases while summer precipitation decreases.

These results differ from the projected changes in runoff presented by Milly et al. (2005), who summarized average changes in runoff over Water Resources Regions across the continental U.S. and Alaska, defined by the U.S. Water Resources Council for the period 2041-2060, relative to 1901-1970. Their projections are based on output from 12 IPCC AR4 GCMs and the A1B SRES scenario, and showed slight decreases in runoff of 2-5% across the PNW. The 12 GCMs they used are a subset of the 21 (IPCC AR4) models used in this study. Milly et al. (2005) average over 24 ensembles from the 12 models (i.e. for some GCMs, multiple experiments were conducted on the same model); however, the number of ensembles was not the same for each GCM, which effectively weights some models more heavily than others. In addition, Milly et al. (2005) used land surface schemes embedded in the GCMs, which are at coarser resolution than the VIC model and do not resolve the topography of the PNW.

Projections of streamflow differ from those of runoff because runoff is a spatial quantity that is an integral part of the water balance at each hydrologic model grid cell and does not incorporate the time lag effects that contribute to streamflow. Runoff is useful for evaluating projected basin-wide changes as a direct effect of precipitation and snow storage or melt. Streamflow, however, is the culmination of hydrologic processes evaluated at a given location over time. Figure 8 shows projected mean hydrographs for the example rain-dominant, transient, and snow-dominant watersheds in Figure 4. In the Chehalis River, projected changes to the mean hydrograph are minimal. Changes in the mean hydrograph at The Dalles are more apparent, including reduced peak flow in the late spring and early summer and increased cool season flow in connection with reduced snowpack. Changes in the Yakima watershed, a transient rain-snow watershed, are significant, indicating a shift to a characteristic rain-dominant watershed by the 2080s. Vano et al. (2009b, this report) describes the implications of this change on water management in the basin.

4.2. Hydrologic Case Studies

We evaluated impacts of climate change on three focus regions, namely the Columbia River Basin, the Puget Sound, and the Yakima River basin. Because the Columbia River basin covers approximately 2/3 of Washington State, discussion of impacts in this region is incorporated into the discussion of statewide impacts above. The other two case study watersheds, the Puget Sound and Yakima River basin, are discussed here. They are both transient watersheds, meaning they are highly sensitive to climate change; however, they differ with respect to their climatic regime – precipitation is generally much higher in the Puget Sound basin than in the Yakima, particularly its lower reaches. As noted in Section 2.2, we used the high resolution DHSVM hydrologic model in the relatively small Puget Sound basins, and we used the VIC model in the Yakima.

4.2.1 Implications of Climate Change on Puget Sound Catchments

We examined SWE predictions in the headwaters of the Cedar, Sultan, Tolt, and Green river basins. Figures 10 and 11 show simulated historical April 1 SWE and predicted change of SWE in the 2020s, 2040s and 2080s for A1B and B1 SRES scenarios (See Figure 9 for historical April 1 SWE). In both Figures 10 and 11, the top left illustrates the upper part of the Sultan River basin, the top right shows the upper Tolt River basin, the middle right shows the upper Cedar River basin, and the lower shows the upper Green River watershed.

In the 2020s, 2040s and 2080s, the largest decrease in SWE occurs in the watershed valleys as temperature rises. Upper Cedar and Green watersheds have approximately 90% reductions in SWE in the valleys starting from the 2020s, while the Sultan and Tolt River basins, which are located in higher elevations, have smaller reductions in the 2020s. SWE decreases more substantially in the upper parts of all four basins in the 2040s, and by the 2080s, SWE is projected to disappear. Generally, simulations using the A1B SRES scenario show greater reductions in SWE (Figure 10) than those using B1 (Figure 11).

Projected weekly time series of basin-averaged SWE in the four Puget Sound basins from the six composite scenarios described earlier for the 2020s, 2040s, and 2080s, as well as from all 39 ensemble scenarios for the 2020s, are summarized in Figure 12. We summarize the ensemble projections through use of a gray swath which spans the range of results from the 39 ensembles. Weekly values are summarized according to water year, October to September. The figure shows reduction of SWE throughout the winter months, compared to historical simulations. Peak SWE is projected to shift in all watersheds from near week 26 (late March), which is the average historical peak, to near week 23 (early March) by the 2020s and 2040s to near week 20 (mid-February) by the 2080s.

Simulated streamflow at the reservoirs in the four basins shows a consistent shift in the hydrograph toward higher runoff in cool season and lower runoff in warm season (Figure 13). The winter peaks become higher but summer peaks become lower in the 2020s, 2040s and 2080s compared to the historical simulation. Into the future, the double-peak hydrograph

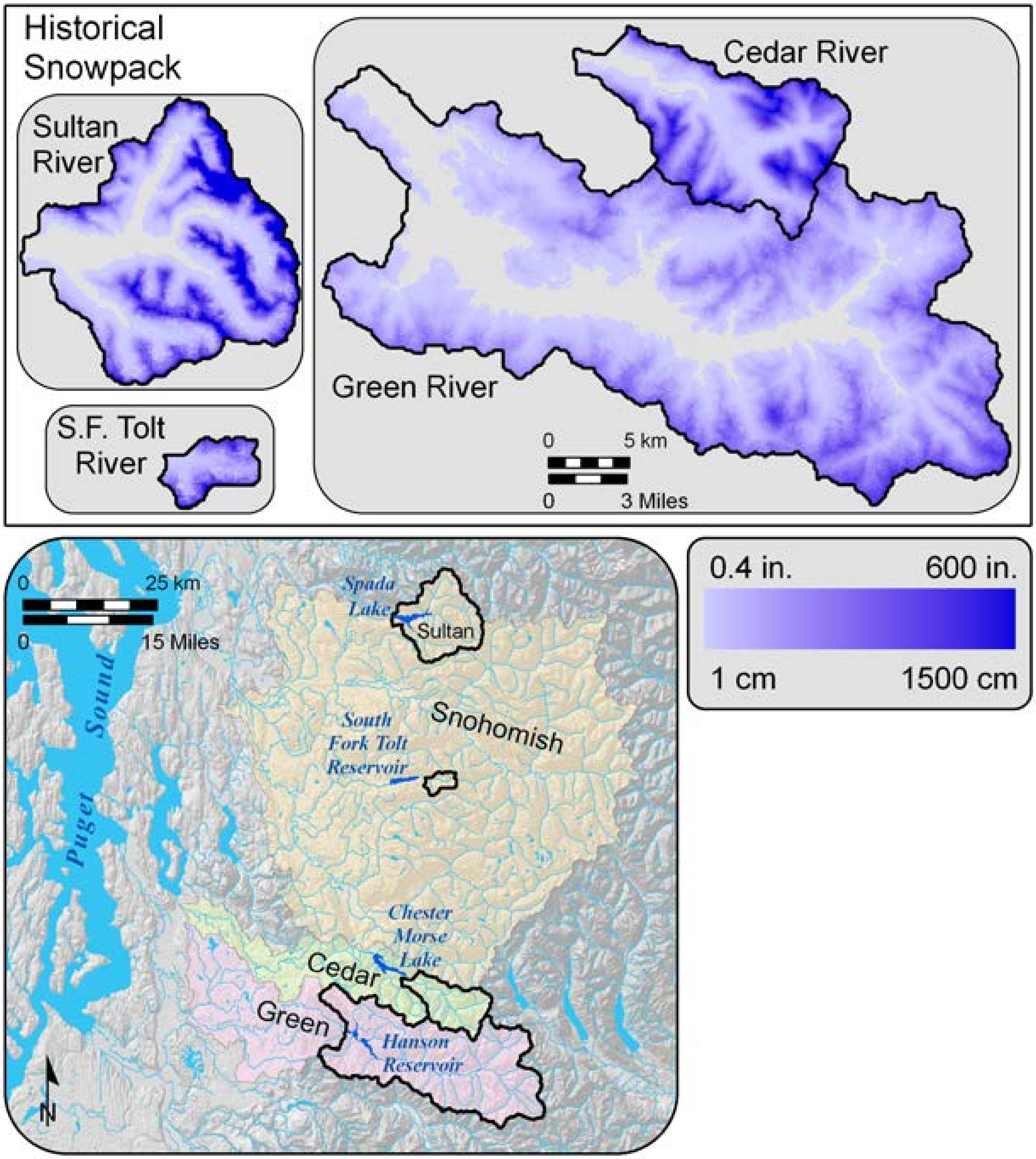

Figure 9. Historical simulated April 1 snow water equivalent (SWE) in four Puget Sound watersheds (1916-2006) as simulated by the DHSVM. Watersheds are located in the overview map (smallest watershed is Tolt; Sultan, the northernmost watershed is located in the upper left corner; Green watershed is the largest; and, the Cedar watershed is in the upper right corner).

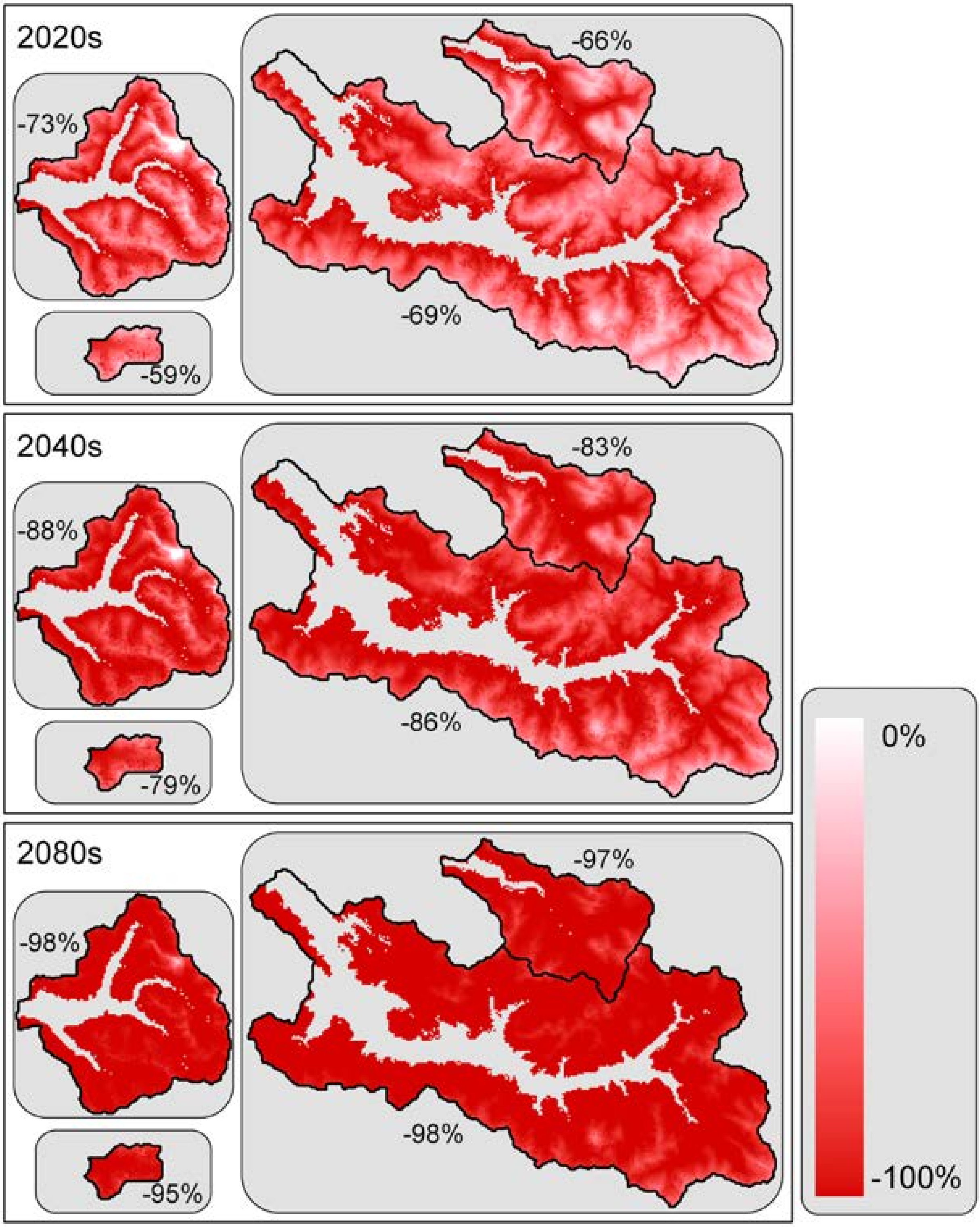

Figure 10. Projected changes in snow water equivalent (SWE) in four Puget Sound watersheds for the 2020s, 2040s, and 2080s (A1B SRES scenario) compared with simulated mean historical April 1 SWE (1916-2006) as simulated by the DHSVM. Watersheds are located in the overview map in Figure 9 (smallest watershed is Tolt; Sultan, the northernmost watershed is located in the upper left corner; Green watershed is the largest; and, the Cedar watershed is in the upper right corner).

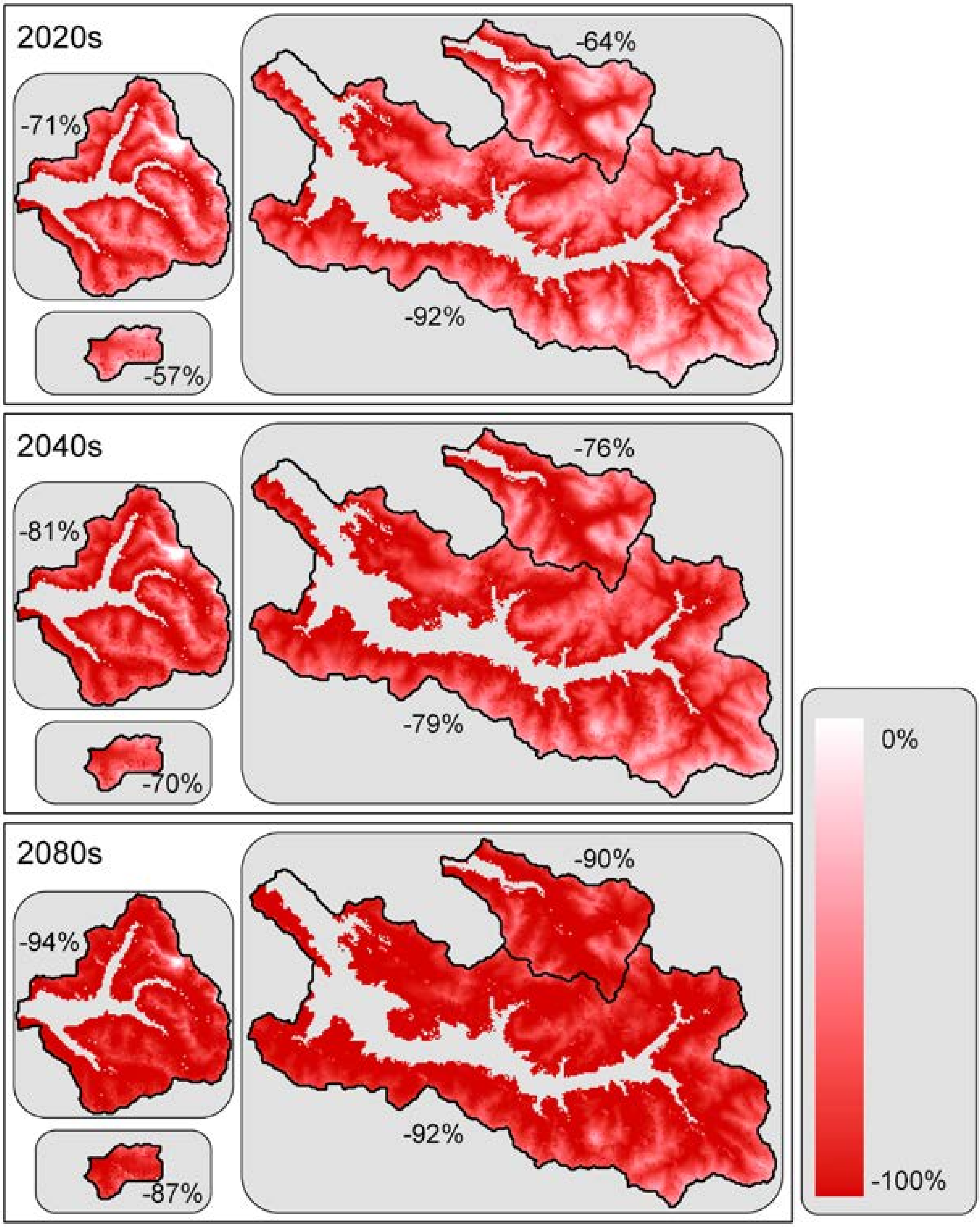

Figure 11. Projected changes in snow water equivalent (SWE) in four Puget Sound watersheds for the 2020s, 2040s, and 2080s (B1 SRES scenario) compared with simulated mean historical April 1 SWE (1916-2006) as simulated by the DHSVM. Watersheds are located in the overview map in Figure 9 (smallest watershed is Tolt; Sultan, the northernmost watershed is located in the upper left corner; Green watershed is the largest; and, the Cedar watershed is in the upper right corner).

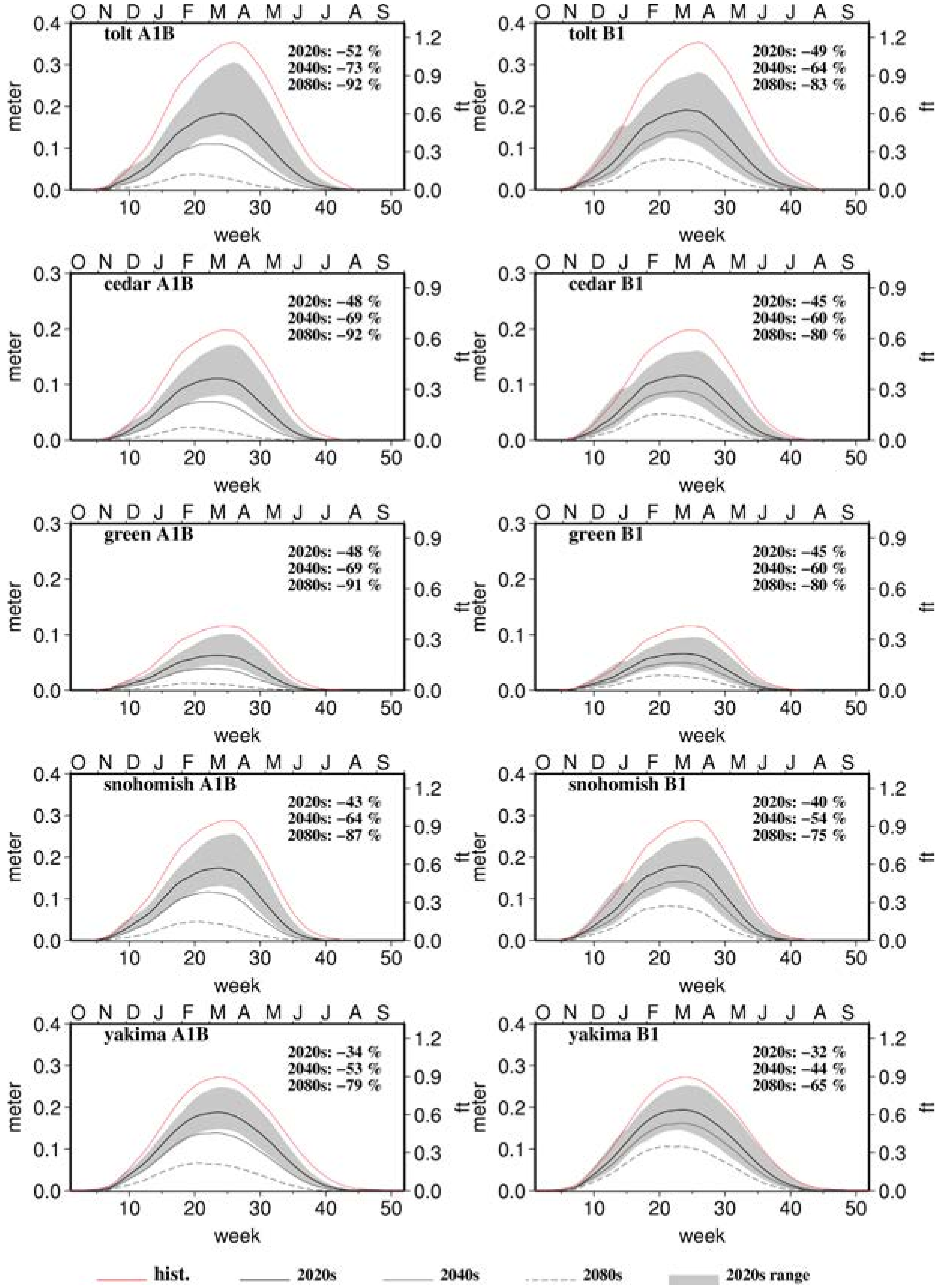

Figure 12. Projected changes in weekly snow water equivalent (SWE) for the 2020s, 2040s, and 2080s (according to water year). Results in the top four pairs of panels are based on DHSVM simulations, while the bottom pair of panels are based on VIC model simulations. Units are meters.

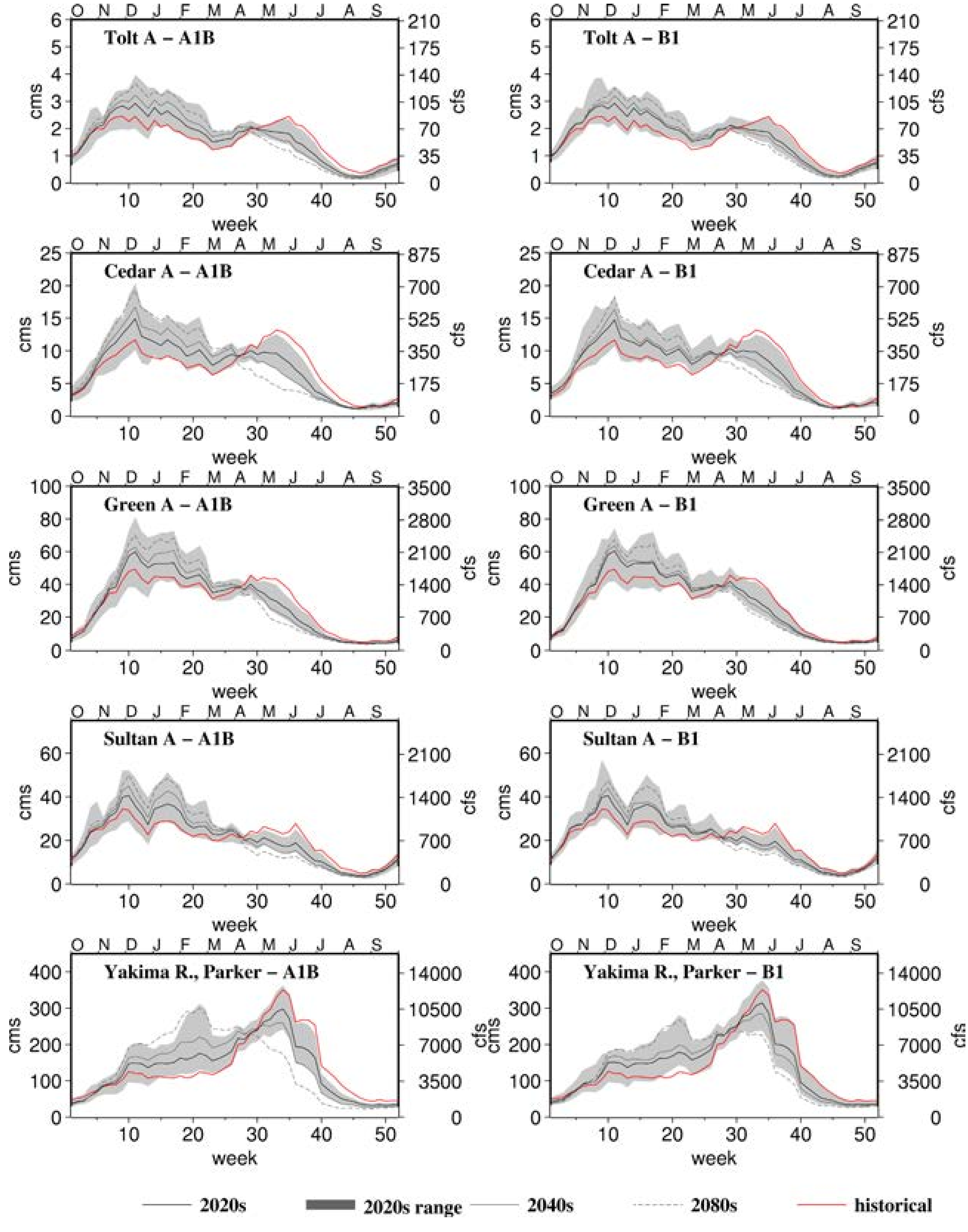

Figure 13. Projected changes in weekly streamflow for the 2020s, 2040s, and 2080s (A1B and B1 SRES scenarios). Results in the top four pairs of panels are based on DHSVM simulations, while the bottom pair of panels are based on VIC model simulations. Units are cubic meters per second (cms).

Table 8. Centroids of streamflow timing based on weekly means for the historical period (water year 1917-2006), 2020s, 2040s and 2080s. The centroid is calculated as the time of year at which half of the annual (water year) flow has passed.

		Puget Sound				*Yakima Basin*
		Sultan A	**Cedar A**	**Tolt A**	**Green A**	YAPAR
	Hist	**21**	**24**	**22**	**21**	**30**
AIB scenarios	**min 2020s**	17	17	17	17	25
	avg 2020s	18	19	18	19	27
	max 2020s	20	21	20	20	29
	2040s	17	18	17	18	24
	2080s	16	16	16	17	21
B1 scenarios	**min 2020s**	16	18	17	18	25
	avg 2020s	18	20	19	19	27
	max 2020s	20	22	20	20	29
	2040s	17	19	18	18	26
	2080s	16	17	17	17	23

* Values indicate week numbers within the water year, where:

Week 15 is Jan 7
Week 20 is Feb 11
Week 25 is Mar 18
Week 30 is Apr 22

transforms into a single-peak hydrograph associated with increasingly rain-dominant behavior. The streamflow timing shift is mainly due to the less frequent snow occurrence, and faster and early snow melt in these historically snow-rain mixed watersheds.

To assess the extent climate change might impact the timing of flow, and thus annual reservoir storage, we compared the time of year at which half of the annual (water year) flow has passed (centroid of timing, see Stewart et al, 2005). The centroid of timing (CT) values were computed from the 1917- 2006 (water year) weekly average flows. The seasonal shift is visible in the CT values (Table 8), which for the A1B emissions scenario and 2020s are about 2 weeks earlier for inflows into the Howard Hanson Reservoir on the Green River, 5 weeks earlier for Chester Morse Reservoir inflows on the Cedar River, and 3 weeks earlier for Spada Lake Reservoir on the Sultan River for the 2020s period. CT changes are smaller for B1 emissions scenarios. Given the small size (relative to mean annual inflow) of all three water supply systems, these shifts suggest that there will be increasing challenges in meeting water management objectives (Vano et al. 2009a, this report).

4.2.2. Implications of Climate Change on the Yakima Watershed

Projections of change in April 1 SWE over the Yakima River basin are summarized in Figure 14 and indicate that for A1B and B1 emissions scenarios, respectively, SWE will decrease by 31 to 34% by the 2020s, 43 to 53% by the 2040s and 65 to 80% by the 2080s. Changes in snowpack projected for the Yakima basin are higher than projected average changes over the State as a whole (Figure 5). Weekly SWE was calculated for the Yakima watershed using results from the VIC model and are summarized in the bottom panel of Figure 12. The bottom panel of Figure 12 shows historical and projected weekly SWE for the entire Yakima River watershed. The peak weekly SWE historically occurs near week 24 (mid-March). Projections of weekly SWE for the 2020s indicate that SWE will be reduced by an average of 39 to 41% according to A1B and B1 scenarios, respectively. The peak week is projected to shift earlier to near week 23 (early to mid-March). By the 2040s, SWE will be reduced by 50 to 58% (with a peak projected to occur near week 22, or early March), and by 67 to 80% by the 2080s (with a peak projected to occur near week 20, or mid-February).

We also summarized projections of weekly streamflow in the bottom panel of Figure 13 for the same suite of scenarios evaluated with respect to SWE. Peak streamflow historically occurs near week 34 (mid-May) in the Yakima River at the USGS gage at Parker. The suite of projections for the 2020s indicate that the peak streamflow will not shift significantly; however, increased streamflow in winter is expected. By the 2040s, the spring peak streamflow is projected to shift earlier near week 30 (mid- to late April) and a significant second peak flow is projected in the winter, which is characteristic of historically lower elevation transient watersheds. By the 2080s, a significant shift in the hydrologic characteristics of the watershed are projected, as the spring peak is lost and peak streamflow is projected to occur in the winter near week 20 (mid-February) which is more characteristic of rain dominant watersheds. Thus warming through the 21st century will result in increasingly rain-dominant behavior in the Yakima basin.

Similar to our analysis for the Puget Sound watersheds, we evaluated the shift in the CT of flow. CT values were computed from the 1917- 2006 (water year) weekly average flows for the unregulated flow of the Yakima River at Parker, which provides a representation of naturalized flow throughout the basin. Historically, the CT occurs in mid-April (week 30). In the 2020s scenarios, the CTA seasonal shift is visible in the CT values, which for the A1B emissions scenario and 2020s is about 3 weeks earlier for both A1B and B1 scenarios. In the 2040s and 2080s for the A1B scenarios, flows shift by 6 and 9 weeks respectively. For the B1 scenarios, these shifts are 4 weeks earlier for the 2040s and 7 weeks for the 2080s. These results are summarized in Table 8. These hydrologic changes will have important implications for irrigated agriculture in WA (Vano et al., 2009b, this report).

5. Conclusions and Recommendations

Climate change will impact Washington's hydrologic resources significantly over the next century. Sensitive areas, such as transient watersheds will experience substantial impacts by the 2020s. Annual runoff across the state is projected to increase by 0-2% by the 2020s, 2.2-2.7% by the 2040s, and

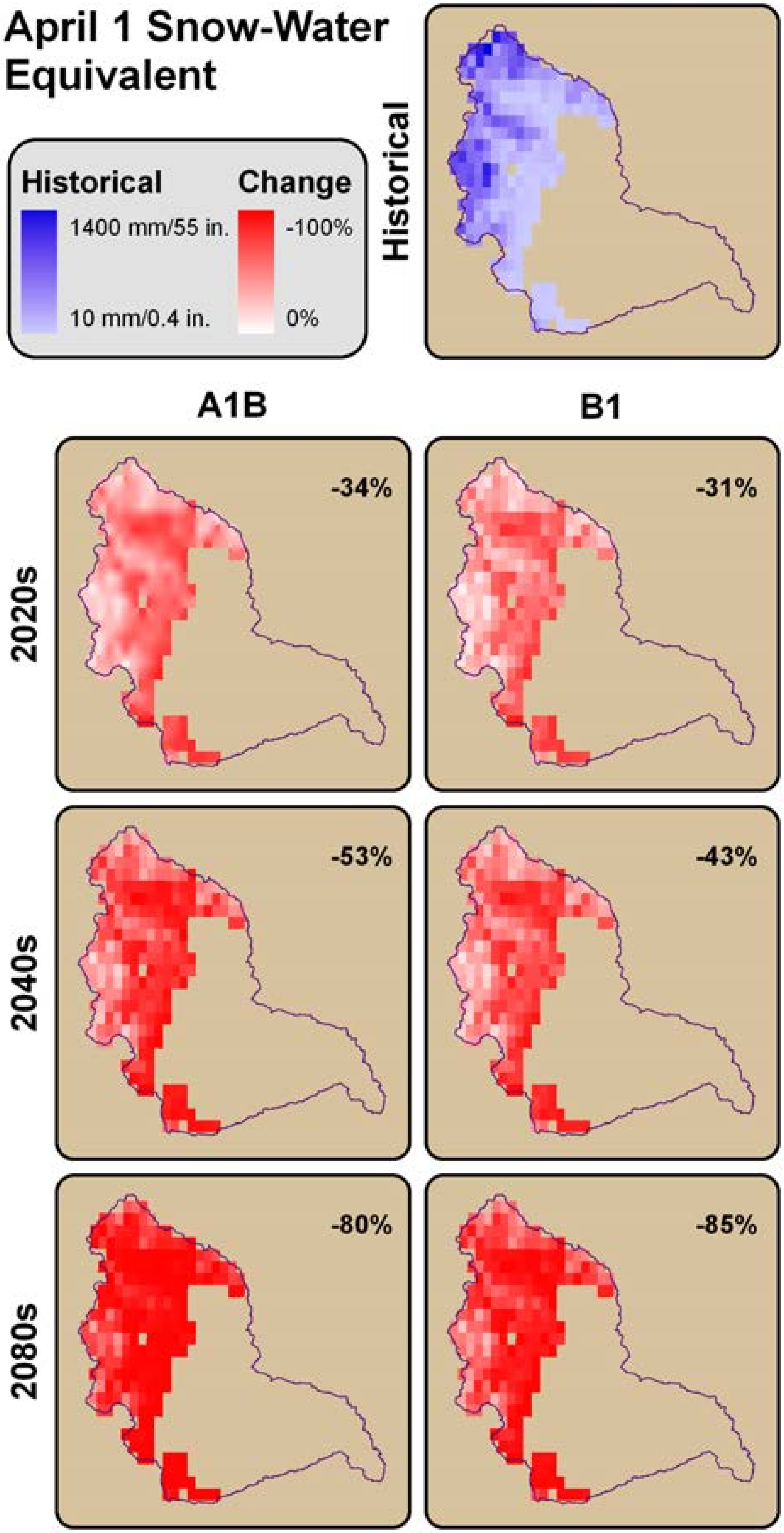

Figure 14. Projected changes in April 1 snow water equivalent (SWE) in the Yakima River basin for the 2020s, 2040s, and 2080s (A1B and B1 SRES scenarios) compared with mean historical April 1 SWE (1916-2006) as simulated by the VIC model.

4.2-6.4% by the 2080s. These changes are primarily driven by projected increases in winter precipitation. April 1 SWE is projected to decrease by an average of approximately 27-29% across the state by the 2020s, 37-44% by the 2040s and 53-65% by the 2080s, based on composite changes in temperature and precipitation as summarized by Mote and Salathé (2008). Soil moisture is projected to be in the 38th to 43rd percentile by the 2020s, 35th to 40th percentile by the 2040s, and 32nd to 35th percentile by the 2080s, with 50% being equal to mean historical values.

The effects of climate change on the urban water supply basins of Puget Sound and the agriculturally rich area of the Yakima basin will be significant. In the watersheds of the Puget Sound, which are characterized as transient rain-snow watersheds, snowpack is projected to decrease and seasonal streamflow is projected to shift from the characteristic double-peak to a single-peak, characteristic of rain-dominant watersheds. By the 2080s, April 1 snowpack in the watersheds will be almost entirely absent.

Projections of weekly SWE over the Yakima basin indicate that it will decrease by an average of 39% by the 2020s, 50% by the 2040s, and 70% by the 2080s. The suite of projections for the 2020s indicate increased streamflow in winter but no significant change in the timing of the peak. Yet, by the 2040s, the spring peak streamflow is projected to shift toward a characteristic lower elevation transient watershed with two streamflow peaks (defined in Section 1). And by the 2080s, the streamflow regime will become rain dominant.

This study utilizes climate change projections from the full suite of 39 scenarios based on A1B and B1 SRES scenarios using a delta method approach. However, further refinement of the statistical downscaling of the transient daily climate change projections such that results from coupled hydrologic simulations are robust at sub-monthly time scales would be beneficial to evaluate the potential changes in the relative variability of temperature and precipitation and other related variables. The combination of spatial and temporal statistical downscaling can introduce unrealistic storm events in the future period. One possible method to eliminate this problem is to maintain the historic sequencing of daily variability in the transient scenarios through development of a hybrid delta method and BCSD approach. These climate change projections would provide a better understanding of the uncertainty of future climate and the variability of hydrologic processes. Barriers to widespread use of climate change projections in water resources studies include the availability of data and the knowledge to effectively and appropriately use this information for specific watershed studies. The ability to educate the public about the implications of climate change is crucial, as our climate system is non-stationary and we can no longer rely on historical information alone to plan for the future.

Acknowledgments

The authors would like to thank Shraddhanand Shukla at the University of Washington for his VIC model calibration work and consultation with respect to the 1/16th degree VIC model implementation. We would also like to thank Tazebe Kiros Beyene and Elizabeth Clark at the University of

Washington for their assistance with data analysis and troubleshooting. We also thank Rob Norheim at the Climate Impacts Group for his assistance with data analysis and graphics, and the four anonymous reviewers who provided valuable input for improving this work.

References

Alberti M, Weeks R, Coe S (2004) Urban land-cover change analysis in central Puget Sound. Photogramm Eng Remote Sens 70: 1043-1052

Barnett TP, Adam JC, Lettenmaier DP (2005) Potential impacts of a warming climate on water availability in snow-dominated regions. Nature 438: 303-309

Beven KJ, Kirkby, MJ (1979) A physically based, variable contributing area model of basin hydrology. Hydrol Sci Bull 24(1): 43-69

Bonneville Power Administration, U.S. Army Corps of Engineers(USACE), NPD, U.S. Bureau of Reclamation (USBR), PNR, (1994) The Columbia River System: The inside story. Report DOE/BP-1689, published by the USACE and USBR

Bowling LC, Lettenmaier DP (2001) The effects of forest roads and harvest on catchment hydrology in a mountainous maritime environment, in land use and watersheds: human influence on hydrology and geomorphology in urban and forest areas. Wigmosta MS, Burges, SJ (ed), AGU Water Sci Appl 2:145-164

Bowling LC, Storck P, Lettenmaier DP (2000) Hydrologic effects of logging in western Washington. United States. Wat Resour Res 36: 3223-3240

Brekke LD, Miller NL, Bashford KE, Quinn NWT, Dracup JA (2004) Climate change impacts uncertainty for water resources in the San Joaquin river basin, California. J Am Water Res Assoc 40(1):149-164

Casola JH, Kay JE, Snover AK, Norheim RA, Whitely Binder LC, Climate Impacts Group (2005) Climate impacts on Washington's hydropower, water Supply, forests, fish, and agriculture. A report prepared for King County (Washington) by the Climate Impacts Group, Center for Science in the Earth System, Joint Institute for the Study of the Atmosphere and Ocean, University of Washington, Seattle

Cherkauer KA, Lettenmaier DP (2003) Simulation of spatial variability in snow and frozen soil. Field J Geophy Res (108)D22: 8858

Christensen NS, Wood AW, Voisin N, Lettenmaier DP, Palmer RN (2004) The effects of climate change on the hydrology and water resources of the Colorado River basin. Clim Change 62:337–363

Christensen N, Lettenmaier DP (2007) A multimodel ensemble approach to assessment of climate change impacts on the hydrology and water resources of the Colorado River basin. Hydrol Earth System Sci 11: 1417-1434

Cuo L, Lettenmaier DP, Mattheussen BP, Storck P, Wiley M (2008) Hydrological prediction for urban watersheds with the Distributed Hydrology-Soil-Vegetation Model. Hydrol Proc (22)21: 4205-4213

Daly C, Neilson RP, Phillips DL (1994) A statistical-topographic model for mapping climatological precipitation over mountainous terrain. J Appl Meteorol 33: 140-158

Daly C, Gibson WP, Taylor G, Johnson GL, Pasteris P (2002) A knowledge-based approach to the statistical mapping of climate. Clim Res 22: 99-113

Dooge JC (1992) Hydrologic models and climate change. J Geophys Res (97): D3 2677-2686

Economic and Engineering Services, Inc. (2003) Watershed management plan, Yakima River basin, for Yakima River watershed planning unit and Tri-County water resources agency

Hamlet AF, Lettenmaier DP (1999) Effects of climate change on hydrology and water resources of the Columbia River basin. J Am Water Resour Assoc 35:1597–1624

Hamlet AF, Mote PW, Clark M, Lettenmaier DP (2005) Effects of temperature and precipitation variability on snowpack trends in the western United States. J Clim 18(21): 4545-4561

Hamlet AF, Lettenmaier DP (2005) Production of temporally consistent gridded precipitation and temperature fields for the continental United States. J Hydrometeorol, 6: 330-336

Hamlet AF, Lettenmaier DP (2007) Effects of 20th century warming and climate variability on flood risk in the western US. Water Resour Res 43: W06427

Hamlet AF, Lee SY, Mickleson KEB, Elsner MM (2009) Effects of projected climate change on energy supply and demand in the Pacific Northwest. Washington Climate Change Impacts Assessment: Evaluating Washington's future in a changing climate. In press

Hayhoe K, Cayan D, Field C, Frumhoff P, Maurer E, Miller N, Moser S, Schneider S, Cahill K, Cleland E, Dale L, Drapek R, Hanemann RM, Kalkstein L, Lenihan J, Lunch C, Neilson R, Sheridan S, Verville J (2004) Emissions pathways, climate change, and impacts on California. Proc Natl Acad Sci USA 101 (34):12422–12427

Hayhoe K, Wake C, Huntington TG, Luo L, Schwartz MD, Sheffield J, Wood EF, Anderson B, Bradbury J, DeGaetano TT, Wolfe D (2007) Past and future changes in climate and hydrological indicators in the U.S. Northeast. Clim Dyn 28: 381-407

IPCC (2007) Summary for policymakers. In: Climate Change 2007: The physical science basis. Contribution of working group I to the fourth assessment report of the intergovernmental panel on climate change. Solomon S, Qin D, Manning M, Chen Z, Marquis M, Averyt KB, Tignor M Miller HL (eds) Cambridge University Press, Cambridge, United Kingdom and New York, NY, USA

Kalaney E, et al. (1996 The NCEP/NCAR 40-year reanalysis project. Bull Am Meteorol Soc 77: 437-471

Lamarche J, Lettenmaier DP (2001) Effects of forest roads on flood flows in the Deschutes River basin, Washington. Earth Surf Proc Landf 26: 115-134

Liang X, Lettenmaier DP, Wood EF, Burges SJ (1994) A simple hydrologically based model of land surface water and energy fluxes for GSMs. J Geophys Res (99)D7: 14,415-14,428

Liang X, Wood EF, Lettenmaier DP (1996) Surface soil moisture parameterization of the VIC-2L model: Evaluation and modifications. Glob Planet Chang 13: 195-206

Liang X, Wood EF, Lohmann D, Lettenmaier DP, and others (1998) The project for intercomparison of land-surface parameterization schemes (PILPS) phase-2c Red-Arkansas River basin experiment: 2. Spatial and temporal analysis of energy fluxes J Glob Planet Chang 19: 137-159

Littell JS, Oneil EE, McKenzie D, Hicke JA, Lutz J, Norheim RA, Elsner MM (2009) Forest ecosystems, disturbance, and climatic change in Washington State, USA. Washington Climate Change Impacts Assessment: Evaluating Washington's future in a changing climate. In press

Leung L. R., Wigmosta M. S., Ghan S. J., Epstein D. J., Vail L. W. (1996) Application of a subgrid orographic precipitation/surface hydrology scheme to a mountain watershed. J Geopgys Research 101(D8): 12803-12817

Matheussen B, Kirschbaum RL, Goodman IA, O'Donnell GM, Lettenmaier DP (2000) Effects of land cover change on streamflow in the interior Columbia basin. Hydrol Proc 14(5): 867-885

Maurer EP, Wood AW, Adam JC, Lettenmaier DP, Nijssen B (2002) A long-term hydrologically based dataset of land surface fluxes and states for the conterminous United States. J Clim 15: 3237-3251

Maurer EP (2007) Uncertainty in hydrologic impacts of climate change in the Sierra

Nevada, California under two emissions scenarios. Clim Chang 82(3-4): 309-325

Maurer EP, Duffy PB (2005) Uncertainty in projections of streamflow changes due to climate change in California. Geophys Res Let 32(3): L03704

Meehl G.A., Stocker T.F., Collins W.D., Friedlingstein P., Gaye A.T., Gregory J.M., Kitoh A., Knutti R., Murphy J.M., Noda A., Raper S.C.B., Watterson I.G., Weaver A.J., Zhao Z.-C. (2007) Global Climate Projections. In: Climate Change 2007: The Physical Science Basis. Contribution of Working Group I to the Fourth Assessment Report of the Intergovernmental Panel on Climate Change [Solomon, S., D. Qin, M. Manning, Z. Chen, M. Marquis, K.B. Averyt, M. Tignor and H.L. Miller (eds.)]. Cambridge University Press, Cambridge, United Kingdom and New York, NY, USA.

Mekis E, Hogg WD (1999) Rehabilitation and analysis of Canadian daily precipitation time series. Atmos Ocean 37: 53-85

Miller NL, Bashford KE, Strem E (2003) Potential impacts of climate change on California hydrology. J Am Water Res Assoc 39: 771-784

Milly PCD, Dunne KA, Vecchia AV (2005) Global pattern of trends in streamflow and water availability in a changing climate. Nature 438: 347-350

Mote PW, Hamlet AF, Clark M, Lettenmaier DP (2005) Declining mountain snowpack in western North America. Bull Am Meteorol Soc 86(1):39-49

Mote PW (2006) Climate-driven variability and trends in mountain snowpack in western North America. J of Clim 19(23): 6209-6220

Mote PW, Salathé Jr EP (2009) Future climate in the Pacific Northwest. Washington Climate Change Impacts Assessment: Evaluating Washington's future in a changing climate. In press

Nakićenović N, Swart R (eds.) (2000) Special report on emissions scenarios. A Special report of working group III of the Intergovernmental Panel on Climate Change. Cambridge University Press, Cambridge, United Kingdom and New York, NY, USA, 599

Nash LL, Gleick PH (1991) The sensitivity of streamflow in the Colorado Basin to climatic changes. J Hydrol 125: 221-241

Nijssen BN, Lettenmaier DP, Liang X, Wetzel SW, Wood EF (1997) Streamflow simulation for continental-scale river basins. Water Resour Res 33(4): 711-724

Nijssen BN, O'Donnell GM, Lettenmaier DP, Lohmann D, Wood EF (2001) Predicting the discharge of global rivers. J Clim 14: 3307-3323

Payne JT, Wood AW, Hamlet AF, Palmer RN, Lettenmaier DP (2004) Mitigating the effects of climate change on the water resources of the Columbia River basin. Clim Change 62:233–256

Refsgaard JC, Storm S (1996) Distributed hydrologic modeling. Chapter 3: Consturction, calibration, and validation of hydrological models. Kluswer Academic Publishers.

Salathé EP, Mote PW, Wiley MW (2007) Review of scenario selection and downscaling methods for the assessment of climate change impacts on hydrology in the United States Pacific Northwest. Int J Climatol 27(12): 1611-1621

Sankarasubramanian A, Vogel RM, Limbrunner JF (2001) Climate elasticity of streamflow in the United States. Water Res Res 37(6): 1771-1781

Schaake JC (1990) From climate to flow. In: Climate change and US water resources. Waggoner, PE (ed) John Wiley, New York, USA pp177-206

Shepard DS (1984) Computer mapping: The SYMAP interpolation algorithm. Spatial Statistics and Models Gaille, GL Willmott CJ (eds) Reidel, 133-145

Snover AK, Miles EL (In review) Regional integrated climate impacts assessment. In: Chapter 2, Snover, AK, Miles EL, and the Climate Impacts Group, Rhythms of change: An integrated assessment of climate impacts on the Pacific Northwest, Cambridge, Massachusetts, MIT Press

Snover AK, Hamlet AF, Lettenmaier DP (2003) Climate change scenarios for water planning studies: Pilot applications in the Pacific Northwest. Bull Am Meteorol Soc 84(11):1513-1518

Stewart IT, Cayan DR, Dettinger MD (2005) Changes toward earlier streamflow timing across western North America. J Clim 18: 1136-1155

Vano JA, Voisin N, Cuo L, Hamlet AF, Elsner MM, Palmer RN, Polebitski, A, Lettenmaier DP (2009a) Multi-model assessment of the impacts of climate change on water management in the Puget Sound region, Washington, USA. Washington Climate Change Impacts Assessment: Evaluating Washington's future in a changing climate. In press

Vano JA, Voisin N, Scott M, Stöckle CO, Halmet AF, Mickleson KEB, Elsner MM, Lettenmaier DP (2009b) Multi-model assessment of the impacts of climate change on water management and agriculture of the Yakima River basin, Washington, USA. Washington Climate Change Impacts Assessment: Evaluating Washington's future in a changing climate. In press

Van Rheenen NT, Wood AW, Palmer RN, Lettenmaier DP (2004) Potential implications of PCM climate change scenarios for California hydrology and water resources. Clim Chang 62:257–281

Vincent LA, Zhang X, Bonsal BR, Hogg WD (2002) Homogenization of daily temperatures over Canada. J Clim 15: 1322-1334

Vicuna S, Maurer EP, Joyce B, Dracup JA, Purkey D (2007) The sensitivity of California water resources to climate change scenarios. J Am Water Res Assoc 43(2): 482 –498

Wigmosta MS, Vail LW, Lettenmaier DP (1994) A distributed hydrology: Vegetation model for complex terrain. Can J For Res 30: 1665-1679

Wang A, Bohn TJ, Mahanama SP, Koster RD, Lettenmaier DP (2008) Multimodel ensemble reconstruction of drought over the continental United States. J Clim (accepted)

Wood AW, Leung LR, Sridhar V, Lettenmaier DP (2004) Hydrologic implications of dynamical and statistical approaches to downscaling climate model outputs. Clim Chang 62(1-3): 189-216

Wood AW, Maurer EP, Kumar A. Lettenmaier DP (2002) Long range experimental hydrologic forecasting for the eastern U.S. J Geophys Res 107(D20): 4429

Photo credit, page 71: Ron Nichols, USDA Natural Resources Conservation Service

Climate Change Impacts on Water Management in the Puget Sound Region, Washington, USA

Julie A. Vano[1], Nathalie Voisin[1], Lan Cuo[1,2], Alan F. Hamlet[1,2], Marketa McGuire Elsner[2], Richard N. Palmer[3], Austin Polebitski[1], and Dennis P. Lettenmaier[1,2]

Abstract

Climate change is projected to result, on average, in earlier snowmelt and reduced summer flows, patterns that are not well represented in the historical observations used for planning and reliability analyses by water utilities. We extend ongoing efforts in the Puget Sound basin cities of Everett, Seattle, and Tacoma to characterize differences between historic and future streamflow and the ability of the region's water supply systems to meet future demands. We use future streamflow simulations for the 2020s, 2040s, and 2080s from the Distributed Hydrology-Soil-Vegetation Model (DHSVM), driven by climate simulations archived by the 2007 Fourth Assessment Report (AR4) of the Intergovernmental Panel on Climate Change (IPCC). We use ensembles of streamflow predictions produced by DHSVM forced with multiple downscaled ensembles from the IPCC climate models as inputs to reservoir system models for the Everett, Seattle, and Tacoma water supply systems. Over the next century, under average conditions all three systems are projected to experience a decline and eventual disappearance of the springtime snowmelt peak in their inflows. How these shifts impact water management depends on the specifics of the reservoir system and their operating objectives, site-specific variations in the influence that reductions in snowmelt have on reservoir inflows, and the adaptive capacity of each system. Without adaptations, average seasonal drawdown of reservoir storage is projected to increase in all of the systems throughout the 21st century. The reliability of the three water supply systems in the absence of demand increases is, however, generally robust to climate changes through the 2020s, and in the 2040s and 2080s reliability remains above 98% for the Seattle and Everett systems. With demand increases, however, system reliability is progressively reduced by climate change impacts.

1. Introduction

The Puget Sound basin receives most of its precipitation in the winter, whereas municipal water use is greatest in the summer. Most of this incremental increase in demand is for residential and commercial landscape irrigation. In the Pacific Northwest, heavy winter precipitation poses challenges in managing floods while extended periods of low precipitation in summer and early fall pose challenges in meeting municipal water demands and in maintaining instream flows for environmental purposes. Water managers rely on reservoirs and storage of winter precipitation in mountain snowpack to provide inflows into reservoirs and to maintain instream flows in the summer and fall. Climate change is predicted to result in warmer temperatures that will reduce snowpack and cause earlier snowmelt runoff, reduced summer flows, higher winter flows (Mote et al. 2005, Milly et al. 2005, Knowles et al., 2006, IPCC, 2007, Cuo et al. 2008a) and a general loss of stationarity of the climate system (Milly et al., 2008). Therefore, managing water supply systems to provide sufficient water throughout the summer may become more challenging.

Municipal water suppliers in the Puget Sound basin have already taken steps to evaluate the implications of possible future climate conditions on the reliability of their systems (Palmer, 2007; SPU, 2007). Wiley and Palmer (2008) used downscaled output from four IPCC (2007) General Circulation Models (GCMs), specifically ECHAM4, HadCM3, GFDL_R30, and PCM models, to evaluate the potential impacts of climate change in the 2020s, and 2040s on the Seattle water supply system. Traynham (2007) used downscaled output from three different IPCC (2007) GCMs (GISS_B1, ECHAM5_A2, and IPSL_A2 models) to evaluate the potential impacts of climate change on the Seattle, Tacoma, and

[1]Department of Civil and Environmental Engineering, University of Washington, Seattle, Washington
[2]Climate Impacts Group, University of Washington, Seattle, Washington
[3]Civil and Environmental Engineering, University of Massachusetts Amherst, Amherst, Massachusetts

Everett water supply systems (Figure 1). Polebitski et al. (2008) extended this work to include the proposed White River water source that would use Lake Tapps water to serve members of the Cascade Water Alliance, which includes municipalities in the rapidly growing areas east of Seattle, and would assume some of Seattle's future water demand. Taken together, the results of these three studies suggest that projected climate change may impact the yield of each system, that each system will respond differently, and that changes in system operating policies can help to mitigate impacts of climate change.

We build on these previous efforts to include more information about the range of potential effects of climate change on water supply systems in the Puget Sound basin and compare these potential hydrologic changes with changes in water demand. A major advance in this study as compared with previous efforts is the use of the full suite of GCM output that was archived by the IPCC (2007). Previous studies in general have not had access to such a large number of simulations of future climate, and therefore have not been able to incorporate the range of uncertainty represented by climate model simulations. For instance, Payne et al. (2004), Christensen et al. (2004), and Van Rheenen et al. (2004) all used downscaled output from a single GCM. More recent studies, prepared as the 2007 IPCC output began to be archived, have used what is sometimes termed a multi-model ensemble approach – that is, hydrologic, and water resources simulations, are performed using multiple climate model output sequences, or ensembles. Maurer (2007), in a study of hydrologic impacts of climate change in California, used 11 models and 2 global emissions scenarios. Christensen and Lettenmaier (2007) used essentially the same GCM ensembles and emissions scenarios in a study of the hydrologic and water resources sensitivity to climate change in the Colorado River basin. Hayhoe et al. (2007) used nine GCM ensembles and three emissions scenarios in a study of the hydrologic sensitivity to climate change in the northeastern U.S. In this analysis, we use A1B and B1 IPCC emissions scenarios with 20 and 19 GCM models for A1B and B1 respectively. Mote and Salathé (2009, this report) provide details of IPCC emissions scenarios and discuss why these emission scenarios were selected. The larger number of GCM ensembles that we were able to include here allows us to develop a better understanding of the variability and especially the range of uncertainties of simulations of hydrology that may accompany future climate emissions scenarios, and the resulting impacts on water management. The ensemble members are taken as equally likely representations of future climate. In that respect, they are our best current basis for characterizing the uncertainty in future climate simulations, although they do not necessarily cover the entire range of future possibilities. For a further discussion of this point, the reader is referred to Mote and Salathé (2009, this report).

Our study follows closely on the work of Traynham (2007). We use the same reservoir system models for the Everett, Seattle, and Tacoma water supply systems and the same hydrological model (Distributed Hydrology-Soil-Vegetation Model). However, we have enhanced the long-term data sets used to force the hydrologic models considerably. The distributed spatial resolution is higher (we use a 1/16th degree latitude-longitude daily historical data set), and the base period is much longer than was previously available (1917 to 2006). Furthermore, adjustments to the data have been

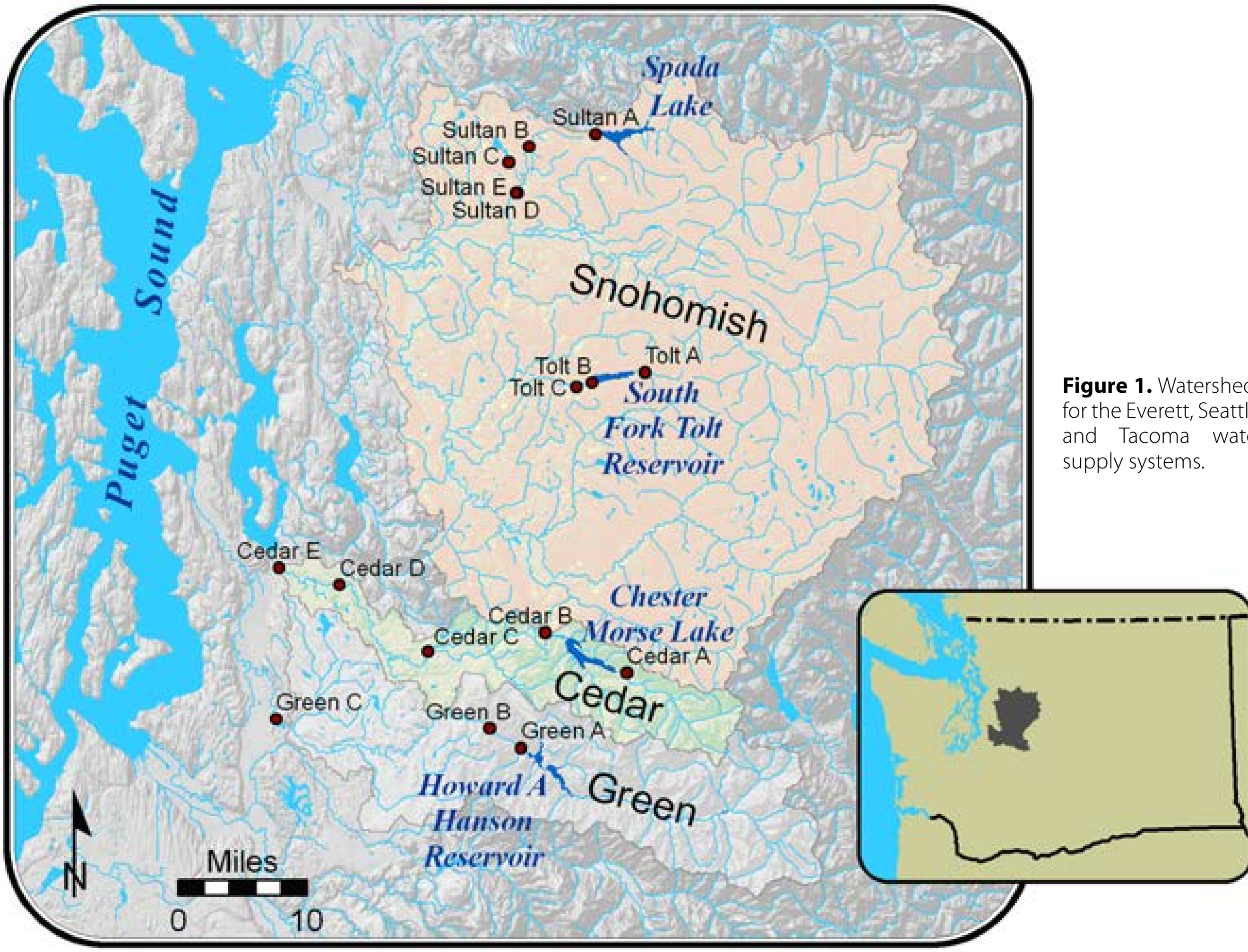

Figure 1. Watersheds for the Everett, Seattle, and Tacoma water supply systems.

incorporated to avoid spurious trends in the historic record. Elsner et al. (2009, this report) describe these improvements in an accompanying paper.

In this paper, we first describe briefly the three water supply systems that were analyzed, and water management models of each of the three systems. We then use the models to explore how without adaptations the performance of the three systems is expected to respond to changes in climate over the next century and to changes in water demand.

2. Site Descriptions

Cascade Mountain precipitation is the source of most of the water used by the major population centers of the Puget Sound, including King County (Seattle and Bellevue), Pierce County (Tacoma), and Snohomish County (Everett). In all three systems snowpack plays an important role in shaping the seasonal cycle of reservoir inflows. The Snohomish (including the Sultan and Tolt Rivers), Cedar, and Green River basins (Figure 1, Table 1), provide water to Everett (Sultan River), Seattle (South Fork Tolt and Cedar Rivers), and Tacoma (Green River). These three water supply systems each have unique physical characteristics, management histories, and operating objectives. These factors also determine how these basins are impacted by and may be able to adapt to climate change. One important indicator

Table 1. Reservoir system statistics.

Reservoir	total capacity ($1000m^3$)	total capacity (acre-ft)	active capacity (m3)	active capacity (acre-ft)	ratio of storage to demand	people served	firm yield in 2006[B] (cms)	firm yield in 2006[B] (mgd)
Everett								
Spada	188,700	153,000	169,500	137,400	1.56	550000 [C]	8.8	200
Seattle								
Chester Morse	104,400	84,600	59,800	48,500 [A]	0.42	1,350,000	7.5	171
South Fork Tolt	71,400	57,900	52,000	42,200 [A]	0.85			
Tacoma								
Howard Hanson	130,700	106,000	68,600	55,600[A]	1.46	302,000	4.6	105

[A] active capacity as parameterized in reservoir model without adaptations

[B] data from Miller (2008)

[C] personal communication with Jim Miller, January 2009.

of the susceptibility of these systems to climate change is how strongly the seasonal runoff cycle is affected by snow accumulation and melt. For strongly snow-affected basins, the extent to which the basin is likely to transition along the continuum from snow-dominated to mixed rain-snow to rain-dominated (see Elsner et al. 2009, this report) suggests how average seasonal hydrographs may shift. The size of the reservoir storage capacity relative to mean annual inflow, the relative amount of spring and summer inflow, the municipal and industrial (M&I) and instream flow demands, and the overall adaptive capacity of the water system, including the system's decision-makers, are also key determinants of how each of the systems might respond to climate change. Systems within the Puget Sound basin, compared to reservoirs elsewhere in the western U.S., have little carry-over storage from year-to-year. Characteristics for each of the systems are summarized below.

2.1. Everett Supply System

The Jackson Hydroelectric Project is the source of most of the city of Everett's water supply. The City of Everett and the Snohomish County Public Utility District #1 (SnoPUD) are co-managers of the system. SnoPUD operates the Jackson projects for a variety of purposes during different times of the year, including hydropower production, water supply, flood control, and maintenance of environmental flow targets. Water is diverted from Spada Lake through a 13 km tunnel system to the 112 MW capacity Jackson Powerhouse. A portion of this water is provided to Lake Chaplain for Everett's water demand. They are currently providing 3.9 cms (cubic meters per second) (88 million gallon days (mgd)) and are anticipated to increase in the future (Traynham, 2007; SnoPud, 2008)). Under the system's recent FERC relicensing (Snohomish Public Utility Dist 1 and City of Everett, 2006), the system must be operated to protect and enhance instream fish habitat, and to mitigate turbidity effects of the reservoir and hydropower systems. Recently, Jackson Hydropower Project operators partnered with the University of Washington to assess methods for optimizing hydroelectric generation with climate and energy forecasts in real time (Alemu, 2008).

2.2. Seattle Water Supply System

The Seattle water supply system consists of the Chester Morse reservoir on the Cedar River, and the South Fork Tolt reservoir, as well as several relatively small groundwater sources. The system is managed by Seattle Public Utilities (SPU) for various objectives, the most important of which are municipal and industrial water supply and environmental flows (SPU, 2007). About 70% of the system's demand is provided by Chester Morse Reservoir, and the balance by the South Fork Tolt and other sources. The system currently serves over 1.3 million people. Despite population growth, total water use has declined from 7.5 cms (171 mgd) in 1989 due to system savings, aggressive conservation programs and price increases for both water supply and wastewater treatment (wastewater treatment charges for residential customers are linked to water consumption, and typically are about double the cost of water). System-wide demand is projected to stay below 6.6 cms (150 mgd) through mid-century due to expected reduction in wholesale sales to a group of suburban water users known as the Cascade Water Alliance and a policy commitment to pursue additional conservation programs to be implemented through 2030 that are projected to save an additional 0.7 cms (15 mgd). The Cascade Water Alliance expects to develop its own supplies that will ultimately satisfy 1.1 cms (25 mgd) by 2049 (Traynham, 2007). In addition to water supply, the Cedar River and South Fork Tolt River reservoir systems are operated to meet minimum in-stream flows to support salmon spawning and rearing (SPU, 2007).

2.3. Tacoma Supply System

Tacoma receives its water supply primarily from the Green River, a portion of which can be stored in the Howard Hanson Reservoir, with groundwater providing about 10% of water deliveries on an annual average basis. The reservoir, built in 1962, is operated by the U.S. Army Corps of Engineers, primarily for flood control purposes. The Green River drainage to Howard Hanson is much larger than that of any of the other systems. The first water right for flows in the Green River is for municipal water supply so water is passed through the reservoir for that purpose. The First Diversion Water Right (FDWR) of 3.2 cms (113 cfs) was supplemented in 1995 with a Second Diversion Water Right (SDWR) for a maximum of 2.8 cms (100 cfs) also for consumptive use. The SDWR has instream flow limitations, although both diversion rights are constrained by the guarantee of minimum instream flows at Auburn (Green C in Figure 1). The capacity of Howard Hanson Reservoir is 131 million cubic meters (mcm), or 106 thousand acre-feet (taf), of which conservation is allocated 41 mcm (33.2 taf) for sustaining fish populations and the ecologic health of the river. Whereas, the city of Tacoma and its partners are allocated a total of 24.7 mcm (20 taf) for water supply. An ongoing project is intended to raise the pool 3.3 m (10 ft) to an elevation of 359 m (1,177 ft) to provide additional water storage for municipal water supply (USACE, 2008). Like the other systems, because of water conservation measures, Tacoma experienced its demand peak in 1989. In the future, Tacoma projects gradually increasing demands after the 2020s (Traynham, 2007). The project also includes increases in storage and fish enhancements to improve habitat and fish passage (USACE, 2008).

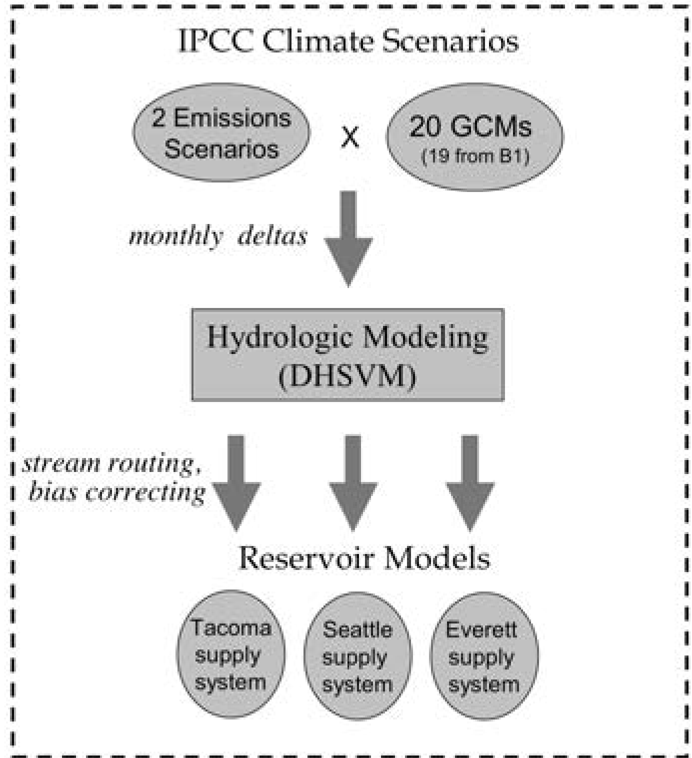

Figure 2. Multi-model process. Schematic of how climate model projections, hydrologc model, and water management models are connected.

3. Approach

We extended the multi-model ensemble approach as previously implemented by Christensen and Lettenmaier (2007), Hayhoe et al. (2007), and Maurer (2007) to explore climate impacts on the three reservoir systems (Figure 2). We used a physically-based hydrologic model driven by atmospheric forcings (precipitation, temperature) downscaled from GCM output as described in further detail in Elsner et al. (2009, this report). Our downscaling method consisted of the so-called delta method, in which the (daily) historic record of observations is perturbed by an additive (daily temperature maxima and minima) or multiplicative (daily precipitation) amount that is constant for each month in the 2020s (representing monthly averages from the transient GCM records from 2010-2039 for both A1B and B1 emission scenarios), 2040s (2030-2059) and 2080s (2070-2099) respectively. We removed bias attributable to uncertainties in the hydrological model, parameters and meteorological forcings (see Elsner et al., 2009, this report) using the quantile mapping method described in Snover et al. (2003) and Wood et al. (2002). Elsner et al. (2009, this report) describe the hydrologic simulations resulting from application of the delta method to develop inflow sequences for the Distributed Hydrology-Soil-Vegetation Model (DHSVM) for each of the three watersheds, all of which were based on the historical period from 1916 to 2006 (water years).

Simulations were performed for six composite delta scenarios (in which the delta values were averaged over all 20 (A1B) and 19 (B1) emissions scenarios for the 2020s, 2040s, and 2080s). Simulations were also performed for the 39 individual GCMs in the 2020s time period. The A1B emissions scenario is similar to what is sometimes termed a ‘business as usual’, whereas the B1 emissions scenarios represents the effects of more resource-efficient technologies intended eventually to stabilize greenhouse gas emissions at 550 ppm by 2100 (IPCC, 2007). However, for practical purposes, through about 2050, the two emissions scenarios are quite similar.

It is important to recognize that the delta method for downscaling results in hydrologic simulations that are quasi-stationary for the climate of the reference year – that is, a 2020s A1B simulation is effectively a 1916-2006 period with perpetual 2020s climate with A1B emissions. While this is artificial (and is to be contrasted with the transient approach used in other recent studies, such as Christensen and Lettenmaier (2007), Maurer (2007), and Hayhoe et al. (2007), it does have the advantage that transient changes in hydrology are not confounded with natural variability. For each water management model, simulations were evaluated by comparing historical flow (simulated flow using observed climate) with observed streamflow for the historical period, and then by comparing simulated reservoir storage generated using both historical and observed inflows as input to the water management (reservoir) model. Once we were satisfied that reservoir model performance for the historical period was comparable using simulated and observed flows (Section 4.1.1), we performed reservoir model simulations with the hydrology model output produced using the downscaled climate change forcings (Section 4.1.2).

3.1. Hydrologic Simulations

Historical and future streamflow simulations for the 2020s, 2040s, and 2080s were performed using the Distributed Hydrology-Soil-Vegetation Model (DHSVM) as described in Elsner et al. (2009, this report) and Mote and Salathé (2009, this report). Future climate is projected to have additive temperature and multiplicative precipitation changes as summarized in (Table 2) that result in hydrologic changes.

Water management models that require daily inflows are particularly sensitive to small biases that may be introduced by hydrologic simulations. For example, an unrealistic sequence of low flows may result in system shortfalls, whereas if actual flows have more variability the system can recover before shortfalls occur. For this reason, simulated inflows were bias corrected at locations used in the management models in such a way that the probability distributions of the historical simulated values matched those of the observations. This adjustment was performed for all reservoir inflow values, which included two inflows in the Green River basin, five in the Cedar, three in the Tolt, and five in the Sultan. Elsner et al. (2009, this report) provide more details on how well historical runs represent hydrology prior to bias correction. After bias correction, reservoir inflows closely match observations (Figure 3).

As described in Elsner et al. (2009, this report) DHSVM was calibrated for a 10-year period at upstream gages in the Cedar (USGS Gage 12115000, Cedar River near Cedar Falls), Green (USGS Gage 12104500, Green River near Lester), Snohomish (USGS Gage 12141300, Middle Fork Snoqualmie River near Tanner), and S.F. Tolt River (USGS Gage 12147600, South Fork Tolt River near Index). When observed values were not available, historic records were reconstructed. During the calibration period, the relative error in annual mean streamflow ranged from -10 to 2% (See Elsner et al. 2009, this report).

Table 2. Climatic changes in annual precipitation and temperature.

	2020s (2010-2039)		2040s (2030-2059)		2080s (2070-2099)	
	A1B	B1	A1B	B1	A1B	B1
% Change in Annual Precipitation	+0.2%	+1.9%	+2.1%	+2.2%	+4.9%	+3.4%
% Change in Cool Season Precipitation	+2.3%	+3.3%	+5.4%	+3.9%	+9.6%	+6.4%
% Change in Warm Season Precipitation	-4.2%	-0.9%	-5.0%	-1.3%	-4.7%	-2.2%

Notes: Cool season defined as October through March, while warm season is defined as April through September.

	2020s (2010-2039)		2040s (2030-2059)		2080s (2070-2099)	
	A1B	B1	A1B	B1	A1B	B1
Change in Annual Temperature (°C)	+1.18	+1.08	+2.05	+1.57	+3.52	+2.49
Change in Cool Season Temperature (°C)	+1.05	+1.01	+1.83	+1.42	+3.24	+2.33
Change in Warm Season Temperature (°C)	+1.31	+1.16	+2.26	+1.71	+3.79	+2.66

3.2. Water Management Modeling

Daily streamflow (1916-2006) from the DHSVM simulations was used as input to water resources models (WRMs) that simulate the operations of the three reservoir systems. Water year 1916 was used as spinup for the WRMs and 1917-2006 was used for the analysis. The models are essentially the same as in Palmer (2007), Traynham (2007), and Polebitski et al. (2007).

All WRMs run at a daily time step using GoldSim software. GoldSim is an object-orientated language tailored to represent reservoir systems that serve diverse needs such as municipal supply, flood control, environmental flows, and hydroelectric power. Inputs to the reservoir models include flows into the reservoirs as well as intervening flows to the system between the upstream inflow points and specified downstream control points (Figure 1). In the case of the Tacoma system, there are two inflows: flows into Howard Hanson Reservoir (Green A) and the difference between Green C and Green B. The Seattle model has two inflows above its two reservoirs (Tolt A and Cedar A) and four intervening flows on the Cedar and two on the Tolt. The Everett model has two reservoir inflows (Sultan A and Sultan C) and three intervening flows. A description of these inflow locations and information from the Water Supply Planning Process for the Puget Sound region is contained in O'Neill and Palmer (2007). More detailed descriptions of each model have been prepared by the Water Resources Management and Drought Planning Group for the Seattle system (Traynham and Palmer, 2006), for

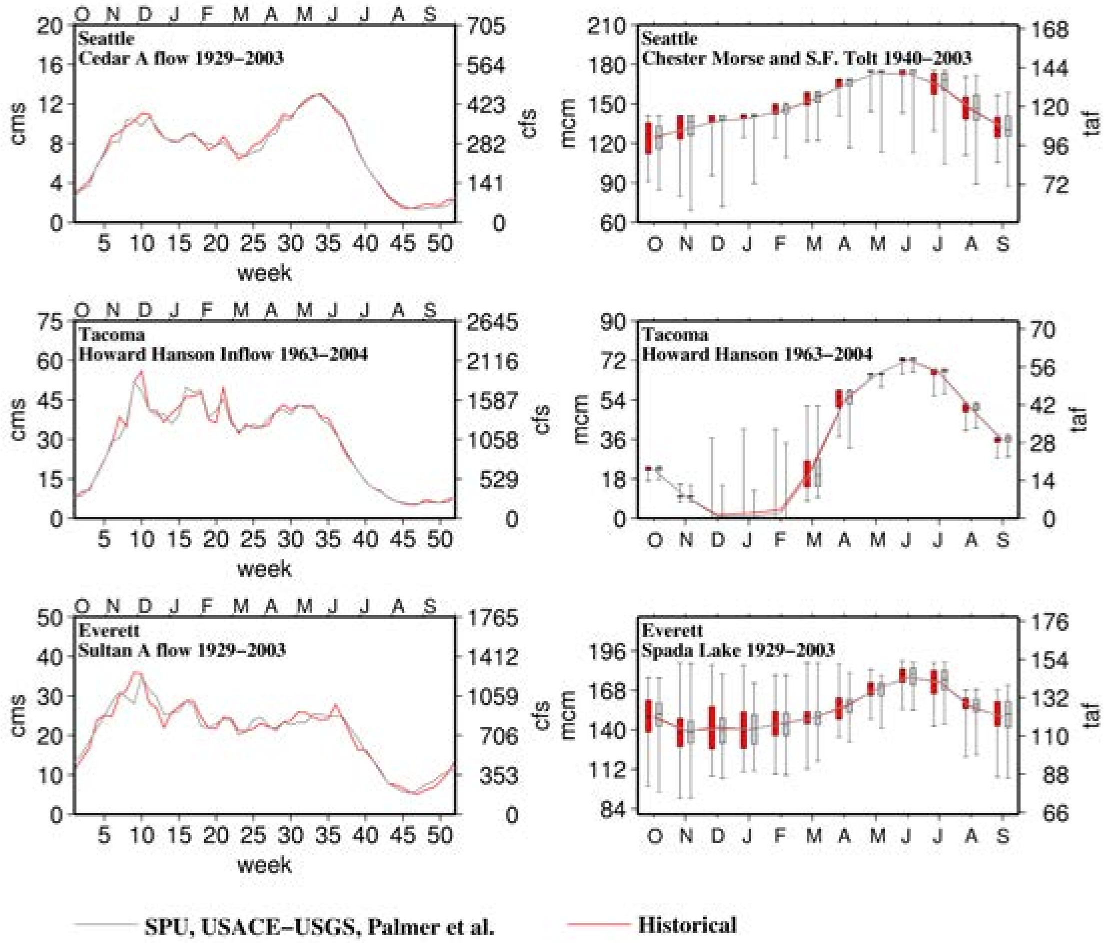

Figure 3. Historical reservoir inflows and storage. Reservoir inflows (left) and reservoir storage (right) for the three municipalities. In both graphs, the lines represent weekly averages. Bars on the right indicate box and whisker plots for individual months.

the Everett system (Enfield and Palmer, 2006), and for the Tacoma system (King, 2006).

Our focus in this study is on the effects of changes in supply and demand as related to a reference (current climate, defined as 1917-2006) simulation. For this reason, the existing reservoir models were used as described in the above references, aside from limited alterations to allow batch mode processing to automate the multiple runs for the three water management models. It is important to note that adaptations and alterations of reservoir operating policies is an ongoing process; the representations of the three systems, as detailed in Section 2, does not include various alternatives being considered by the water utilities (i.e. optimizing hydroelectric generation with climate and energy forecasts). In addition to investigation of changes in reservoir inflows, the impact of concurrent changes in customer-driven demands was also evaluated. Techniques used to forecast future water demands may be significantly impacted by water pricing policies, water conservation efforts, changing technologies, and water reuse. Therefore, to investigate demands, we did not explicitly represent these changes but rather looked at the sensitivity of each system by increasing and decreasing current demands by 10%, 25% and 50% (Table 3). These values can then be compared with ongoing efforts by Central Puget Sound Water Suppliers' Forum (2009) to assess future demands.

To assess the performance of DHSVM inflow locations for the water

Table 3. Current and future water demands in cms (and mgd), as simulated in reservoir models.

	50%	75%	90%	**2000s**	110%	125%	150%
Everett	1.9 (44)	2.9 (660	3.5 (79)	3.9 **(88)**	4.2 (96)	4.8 (110)	5.8 (132)
Seattle	3.2 (74)	4.8 (110)	5.8 (132)	6.4 **(147)**	7.1 (162)	8.1 (184)	9.7 (221)
Tacoma	1.4 (32)	2.1 (49	2.5 (58)	2.8 **(65)**	3.1 (71)	3.1 (81)	4.2 (97)

* Values for the 2000s provided by utilities as outlined in Traynham (2007).

management models, in the Green River basin we used flows provided by the U.S. Army Corps of Engineers and U.S. Geological Survey from 1962 through 2004. In the Cedar and Tolt River basins we used observed and intervening flows estimated by the U.S. Geological Survey and Seattle Public Utilities for October 1928 through September 2003. In the Sultan River basin we used flows that were simulated as part of the Water Supply Planning Process for the Puget Sound region for the Sultan River from October 1928 through September 2003 (Palmer, 2007). As shown in Figure 3, reservoir system performance, simulated using the two sets of reservoir inflows, is quite similar not only in terms of (weekly) average values but also as indicated by interannual monthly storage variability. Reliability measures, not shown, are also in close agreement.

Table 4. Week number designations.

week number	date
1	1-Oct
5	29-Oct
10	3-Dec
15	7-Jan
20	11-Feb
25	18-Mar
30	22-Apr
35	27-May
40	1-Jul
45	5-Aug
50	9-Sep

Following performance evaluation for the historical reference periods, the water management models were run with inflows that resulted from forcing DHSVM with downscaled output from the various climate change models (20 A1B and 19 B1 models for 2020s, and composite flows for both A1B and B1 for the 2020s, 2040s, and 2080s). Hereafter we refer to a simulation using a water resources model forced with simulated historical flows as the "historical" simulation. We refer to "observations" as the simulation model output when forced with observed flows, and "climate change" runs as simulations when forced by predicted flows for a given climate change scenario. Output metrics for each reservoir system are quite different. While comparisons of relative changes across water systems adds insights into their susceptibility to climate change, it is important not to compare absolute values between systems because they all differ significantly in their operations and management goals.

In our presentation of results, years indicate water years (October - September). Most analyses are on weekly time steps with seasonal values reported as weekly averages. When weeks are numbered, they start on October 1 (see also Table 4).

4. Results

4.1. Seasonal Timing

In reservoir systems that depend on snowpack to enhance reservoir storage, delayed snowmelt results in greater effective storage capacity. In a warming climate, seasonality of streamflow may shift substantially, with more flow occurring on average in the winter due to precipitation falling as rain rather than snow, and a decline and possible disappearance of the spring snowmelt peak. Elsner et al. (2009, this report, Figure 10) provide a more detailed description of how the rivers that provide water for the Seattle, Tacoma, and Everett water supply systems are likely to respond to changes in snowpack in a warming climate.

4.1.1. Historic Reservoir Inflows and Storage

Figure 3 compares historical flows and simulated reservoir storage using both historical observed streamflows and historical simulations from DHSVM. In the Seattle system, seasonal average flows from 1929 to 2003 into the Chester Morse Reservoir have a well-defined double peak or "mixed" hydrograph as defined by Elsner et al. (2009, this report) with the first peak occurring on average in early December and the second, larger peak in mid-May. The double peak is captured in both the observed and simulated historical flows. Simulated storage (total of Chester Morse and South Fork (S.F.) Tolt Reservoirs) tracks the rule curve closely in both cases, but has less interannual variability in July through November for simulated historic, as compared with observed historical flows. Simulated inflows have higher minimum values as compared with observations, although maximum, 75th percentile, median, and 25th percentile comparisons of interannual variability across these 75 years are quite similar. In simulations using DHSVM-generated inflows, minimum storages tend to be higher than storage levels simulated using the observed inflows. Therefore, DHSVM inflows generate storage levels that are somewhat more conservative in a relative (simulation comparison) sense. Total interseasonal storage variations in Chester Morse and S.F. Tolt Reservoirs combined, as simulated by the reservoir model, average approximately 9.3 mcm (40 taf). In the more rain-dominated Tacoma system, seasonal average inflows into the Howard Hanson Reservoir from 1964 to 2004 are more variable throughout the year than in the Cedar and S.F. Tolt. Because this system is primarily operated for flood control, the active storage simulated by the reservoir model represents only the amount in the system allocated to conservation and municipal uses. Not surprisingly given the relatively small storage relative to mean annual inflows, seasonal and interannual variability of simulated storage for these purposes is quite similar for reservoir simulations that use observed and DHSVM inflows. Most interannual variability occurs in February and March, with 14 mcm (60 taf) of storage drawn down for wintertime flood control.

Average inflows from1929 to 2003 into Spada Lake, the largest reservoir within the Everett system, have a double peak hydrograph with the largest peak occurring on average in early December, and the second, less well-defined, peak occurring in early June in both inflow datasets. The system has only been in operation since 1965, however, inflow values have been estimated from 1929; therefore, the system was simulated for the longer period. Simulated storage is more variable between years than for the Seattle and Tacoma management systems. These variations reflect operating procedures that are less constrained by limited supply and high demand, and are determined more by operating considerations for hydropower production.

4.1.2. Future Reservoir Inflows and Storage

Figure 4 summarizes simulated future climate reservoir inflows and reservoir storage. In the Seattle system, the ensemble of climate change projections indicates a transition from a double peak hydrograph to one that peaks primarily in December. A similar trend in the Cedar and S.F. Tolt River hydrographs was reported by Wiley and Palmer (2008). By the 2020s, composite inflows into Chester Morse Reservoir (black line) already have an average December peak that exceeds the spring peak, and the range between the minimum and maximum scenario (gray area) deviates most during the December peak (by roughly 8.5 cms (300 cfs) as compared with 4.2 cms (150 cfs) for the mid-May peak). Shifts in the hydrograph become more pronounced throughout the 21st century, and by the 2080s, the second, snowmelt peak has disappeared entirely. Hydrograph shifts are more pronounced in the A1B emission scenarios, however differences for A1B and B1 scenarios are generally similar. In the end of March, all future scenario flows transition from being greater than historical to less than historical, primarily because of earlier snowmelt. These changes translate into an overall decline in simulated storage, especially in June to December. On average, without operational adaptations, the summer-fall decline (June-October) in storage is 7.4 mcm (6 taf) (ranging from 1.2 to 17 mcm (1 to14 taf) for the various ensembles) for the 2020s, 9.9 mcm (8 taf) for the 2040s, and 18.5 mcm (15 taf) for the 2080s.

On average, the Tacoma system undergoes flow shifts similar to the Seattle system (Figure 4, Howard Hanson graphs). However, because snowpack in the Green River above the reservoir are smaller in the current climate, the hydrographs are altered less. As with the Seattle system, in the future climate simulations flows switch from being greater than historic to less at the end of March. The wintertime peak increases about 24 cms (850 cfs) in the 2080s, whereas summer flows decline by about 1 cms (35 cfs). These flows result in simulated storage decreases between June to October by 3.2 mcm (2.6 taf) for the 2020s composite with a range of 1.7 to 6.8 mcm (1.4 to 5.5 taf) over ensemble members, 5.6 mcm (4.5 taf) for the 2040s composite, and 9.5 mcm (7.7 taf) for the 2080s composite. In early spring when conservation and water supply pools are allowed to fill, however, future reservoir storage may increase. The largest projected increases in storage are in March with increases of 4 mcm (3.3 taf) for the 2020s composite with a range of 0.25 to 11.3 mcm (0.2 to 9.2 taf) range over all ensemble members), and increases of 6.3 mcm (5.1 taf) for the 2040s composite and 8.8 mcm (7.1 taf) for the 2080s composite. Because the Tacoma system is managed in the winter for flood control, storage is drawn down quickly until March. For this reason, storage differences between A1B and B1 scenarios are slight, although as expected B1 mean storage is slightly closer to historic than is A1B.

The Everett system has the same general hydrograph shifts in seasonal reservoir inflows as Seattle and Tacoma. The early December peak increases by as much as 17 cms (600 cfs) and the snowmelt peak declines by as much as 14 cms (500 cfs) by the 2080s resulting in a primarily winter-flow driven system. The shift from flows being greater than historic to less occurs in early April. As a result, simulated future storage values in the Spada Reservoir transition from being greater than historic to being

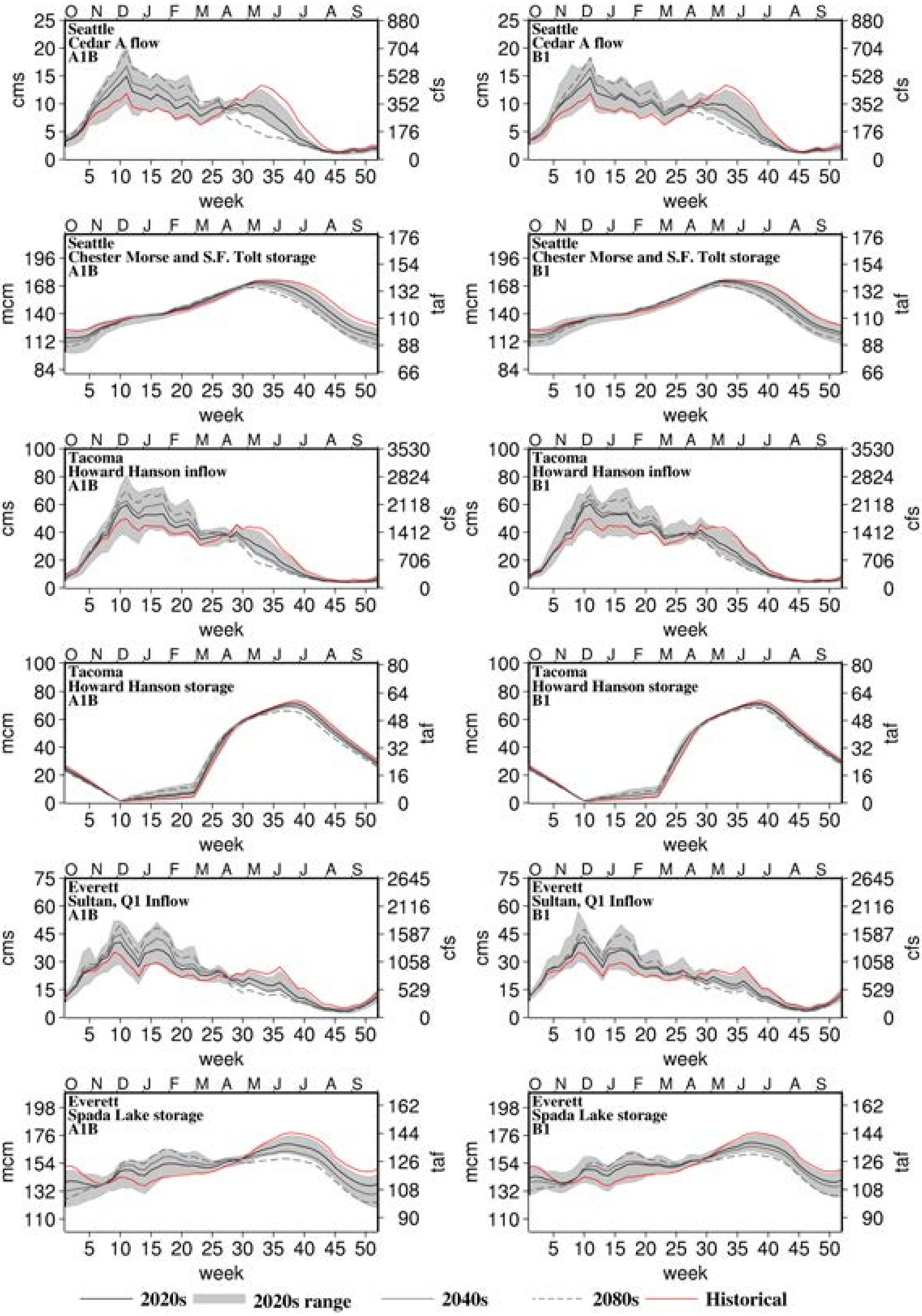

Figure 4. Future projections of reservoir inflows and storage. The red line indicates historical weekly averages from 1917-2006. Future projections are weekly averages across a similar time period that is representative of the 2020s (black line is the composite and the gray area represents the range of the in ensembles), the 2040s (gray line), and 2080s (dotted gray line). Week one begins on October 1.

less than historic at the end of April. Projected future reservoir inflows are greater than historic values by a maximum annual difference of 10.5 mcm (8.5 taf) in the 2020s A1B composite, 16.2 mcm (13.1 taf) in the 2040s, and 22.0 mcm (17.8 taf) in the 2080s. B1 scenarios have slightly smaller future changes, but again, the differences between A1B and B1 scenarios are slight. Winter storage in this system is more variable than for the Seattle or Tacoma systems as a result of the multiple reservoir operating purposes and generally large storage relative to water supply demand. For instance, as shown in Figure 3, Spada Reservoir storage in the month of January varies by as much as 76.4 mcm (61.9 taf) in the simulated 90-year period with typical year-to- year variations in the 125.8 to 150.5 mcm (102 to 122 taf) range (the 25^{th} and 75^{th} quantiles).

4.2. Municipal and Industrial Water Supply

Each of the three systems is impacted by shifts in its average seasonal inflow pattern, although the magnitude of the impact depends on numerous conditions including reservoir capacity, systems demands, the extent to which each system relies on a gradually melting snowpack to retain water from the winter to the summer, the adaptive capacity of each system, and specifics system operations (including objectives other than water supply). We explored the interaction of some of these factors as they are related to system reliability and reservoir storage change. We first analyze how the reliability of the systems change with water demand held constant at 2000s values (Section 4.2.1). We then compare these results with simulations when demands increase and decrease by 10%, 25%, and 50% for each climate change scenario (Section 4.2.2).

4.2.1. System Reliability

A system's ability to meet its demands, whether for instream flow requirements or consumptive use by water users, is necessary for long-term water planning. We calculate reliability on an annual basis to reflect the likelihood of meeting all demands during a water year (Tables 5a and 5b). In the Seattle system, we measure reliability as the percent of years within the model of which there were no municipal and industrial delivery shortfalls. The Tacoma system is operated with water allocated for multiple goals from multiple sources. The first diversion water right (FDWR) for municipal water supply and the minimum instream flow at Palmer (MIF), an existing requirement that the Corps of Engineers provides 3.1 cms (110 cfs) at the Palmer gage (Figure 1, Green B) with 98% reliability. When Tacoma's demands are not met by surface water, simulations allow for groundwater to be used as outlined by King (2006). In the Everett system, we investigate shortfalls for municipal water, which is allocated prior to hydropower.

Historical simulations show a reliability of 100% for Seattle's M&I, Everett's M&I, and Tacoma's FDWR and 99% reliability for Tacoma's MIF at Palmer. With 2000s water demands, we found that in all three systems, the only time reliability dropped below 98% (excluding Tacoma's MIF) in the 2020s B1 simulations was for the warmest and driest 2020s climate scenarios CCSM3 and ECHO_G. In the Seattle and Tacoma systems, 2 of 20 of the A1B ensembles and 2 of 19 for the B1 ensembles have reliability

Table 5a. Reliability and storage for A1B emissions scenarios.

AIB	Reliability			Seattle system: likelihood active capacity in October will drop below		
	Seattle	Tacoma FDWR	Tacoma MIF	**50% full** 55.9 mcm *(45328 af)*	**25% full** 28.0 mcm *(22664 af)*	**10% full** 11.2 mcm *(9067af)*
historical simulation	100%	100%	99%	34%	1%	0.0%
warmest and wetter:						
hadcm	99%	98%	92%	66%	11%	1.6%
miroc_3.2	100%	97%	82%	64%	11%	0.2%
miroc3_2_hi	100%	99%	89%	55%	5%	0.1%
ipsl_cm4	99%	99%	90%	61%	6%	0.3%
inmcm3_0	99%	99%	92%	72%	12%	0.3%
cgcm3.1_t47	100%	99%	92%	43%	3%	0.0%
warmest and drier:						
ccsm3	96%	95%	81%	80%	32%	7.8%
hadgem1	99%	96%	90%	58%	9%	0.0%
gfdl_cm2_1	99%	98%	96%	67%	12%	0.6%
warmer and drier:						
echo_g	96%	99%	93%	74%	19%	3.2%
fgoals1_0_g	99%	99%	90%	59%	11%	1.0%
pcm1	99%	99%	97%	58%	9%	0.0%
gfdl_cm2_0	100%	100%	96%	61%	6%	0.1%
giss_er	99%	98%	93%	52%	7%	0.7%
warmer and wetter:						
csiro_3_5	100%	100%	91%	51%	5%	0.1%
cgcm3.1_t63	100%	100%	92%	38%	2%	0.0%
giss_aom	100%	99%	95%	50%	5%	0.0%
cnrm_cm3	100%	99%	99%	58%	7%	0.0%
echam5	100%	99%	93%	43%	4%	0.1%
bccr	100%	99%	99%	43%	2%	0.0%
Composites						
2020	100%	99%	92%	58%	8%	0.2%
2040	99%	96%	79%	67%	11%	0.3%
2080	99%	93%	63%	71%	18%	1.6%

* Delta categories of warming and dry/wet are based on annual deltas.

**First Diversion Water Right=FDWR, Minimum Instream Flow=MIF

Table 5b. Reliability and storage for B1 emission scenarios.

B1 (wetter than A1B)	Reliability			Seattle system: likelihood active capacity in October will drop below		
	Seattle	Tacoma FDWR	Tacoma MIF	**50% full** 55.9 mcm *(45328 af)*	**25% full** 28.0 mcm *(22664 af)*	**10% full** 11.2 mcm *(9067af)*
historical simulation	100%	100%	99%	34%	1%	0.0%
warmest and wetter:						
miroc_3.2	100%	98%	90%	59%	7%	0.1%
miroc3_2_hi	100%	98%	82%	59%	7%	0.2%
ipsl_cm4	100%	99%	91%	42%	4%	0.1%
cgcm3.1_t47	100%	99%	90%	48%	3%	0.0%
cgcm3.1_t63	100%	100%	90%	52%	3%	0.0%
warmest and drier, or less wet:						
ccsm3	98%	95%	85%	71%	18%	3.0%
echo_g	97%	99%	88%	72%	19%	2.8%
hadcm	100%	98%	97%	45%	5%	0.0%
warmer and drier, or less wet:						
fgoals1_0_g	100%	99%	91%	44%	4%	0.1%
pcm1	100%	100%	97%	42%	1%	0.0%
echam5	100%	98%	96%	46%	5%	0.2%
gfdl_cm2_0	100%	100%	95%	55%	4%	0.1%
gfdl_cm2_1	100%	100%	97%	44%	3%	0.0%
warmer and wetter:						
csiro_3_5	100%	100%	96%	35%	1%	0.0%
giss_aom	100%	99%	95%	52%	5%	0.1%
giss_er	99%	99%	93%	53%	5%	0.2%
cnrm_cm3	100%	99%	98%	48%	2%	0.0%
bccr	100%	100%	98%	31%	1%	0.0%
inmcm3_0	100%	99%	93%	58%	8%	0.2%
Composites						
2020	100%	99%	92%	49%	4%	0.0%
2040	100%	99%	91%	57%	7%	0.2%
2080	99%	96%	75%	65%	12%	0.4%

* Delta categories of warming and dry/wet are based on annual deltas.

**First Diversion Water Right=FDWR, Minimum Instream Flow=MIF less than 98%). In the 2040s, the composite A1B scenario for the Tacoma system has a FDWR reliability of 96% and in the 2080s the reliability is 93% for A1B and 96% for B1, respectively. The MIF Palmer reliability for Tacoma is less; the 99% reliability in the historical simulation declines to 92% in the 2020s (81-99% range over ensemble members), 79% in the 2040s, and 63% in the 2080s for A1B emissions scenarios. Performance is slightly more robust in the B1 scenario, declining to 75% in the 2080s (see Table 5b). In the Everett system, because the system's water supply capacity is much greater than current demands, the reliability in all simulations is 100%.

Because changes in reliability are only sensitive to conditions when shortfalls occur, another measure of how likely the system is to fully meet delivery requirements is minimum reservoir storage, which provides a measure of system stress. For the Seattle system, we therefore used as a performance measure the fraction of years when there was any occurrence of current active capacity storage (Table 1) dropping below 50%, 25%, and 10% in the month of October, which is typically when reservoir storage in this system is lowest.

Assessed in this way, reservoir performance under the A1B emissions scenarios is always degraded relative to historic. In the B1 scenarios, this is also true except for the 2020 BCCR GCM climate scenario, which has a smaller likelihood of lower reservoir values in October than the historical simulation. For the composite scenarios, performance is progressively degraded through the century, i.e., 2040s performance is worse than 2020s, and 2080s is worse than 2040s. In the historical simulations, there is a 34% likelihood that reservoirs drop below 50% of active capacity in October. In the 2020s for A1B, this increases to 58% (38 to 80% range over ensemble members), which increases further to 67% in the 2040s and 71% in the 2080s for composite scenarios for the latter two periods. For B1 scenarios, these values are smaller, with a 49% (range over ensemble members of 31 to 72%) probability of October storage levels being less than 50% of capacity in the 2020s, and for the 2040s and 2080s composites, 57% in the 2040s, and 65% in the 2080s. The likelihood of reservoirs dropping below 25% and 10% active capacity reflects similar patterns. Performance for the dry and warm CCSM3 GCM simulation has the lowest 2020s performance with a 7.8% likelihood of storage less than 10% minimum for A1B emissions and 3% for B1 emissions. Again, all simulations reported in this section are for water demand at 2000s values.

4.2.2. Future Water Demands

Results thus far have focused on reservoir system performance associated with a changing future climate with water demand fixed at 2000s values, and with current reservoir operating practices. Water demands are, however, likely to change over the study period, so we investigated the effects of these changes as well. We run simulations of both increases and decreases in demand of 10%, 25%, and 50% (Table 3) of 2000s values for the historic and composite 2020s, 2040s, and 2080s climate projections. We compare reliability measures, as assessed in Section 4.2.1, in each reservoir system model for all the demand projections (Table 6). The reliability, as predicted by each reservoir model, reflects system-specific components that are not

Table 6. System reliability with variations in demand.

	Reliability (historic)				Reliability (2020s)				Reliability (2040s)				Reliability (2080s)			
	Seattle	Tacoma (FDWR)	Tacoma (Palmer MIF)	Everett	Seattle	Tacoma (FDWR)	Tacoma (Palmer MIF)	Everett	Seattle	Tacoma (FDWR)	Tacoma (Palmer MIF)	Everett	Seattle	Tacoma (FDWR)	Tacoma (Palmer MIF)	Everett
					AIB											
50%	100%	100%	99%	100%	100%	99%	97%	100%	100%	97%	90%	100%	100%	95%	68%	100%
75%	100%	100%	99%	100%	100%	99%	96%	100%	100%	97%	88%	100%	100%	93%	66%	100%
90%	100%	100%	99%	100%	100%	99%	96%	100%	100%	97%	84%	100%	100%	93%	64%	100%
100% (current demand)	**100%**	**100%**	**99%**	**100%**	**100%**	**99%**	**92%**	**100%**	**99%**	**96%**	**79%**	**100%**	**99%**	**93%**	**63%**	**100%**
110%	99%	100%	99%	100%	97%	99%	92%	100%	98%	96%	79%	100%	94%	91%	63%	100%
125%	96%	100%	99%	100%	88%	97%	92%	100%	81%	93%	78%	100%	73%	91%	62%	100%
150%	74%	100%	99%	100%	57%	97%	92%	100%	49%	92%	77%	100%	38%	90%	62%	100%
					B1											
50%					100%	99%	97%	100%	100%	99%	95%	100%	100%	97%	82%	100%
75%					100%	99%	97%	100%	100%	99%	93%	100%	100%	96%	82%	100%
90%					100%	99%	95%	100%	100%	99%	91%	100%	100%	96%	77%	100%
100% (current demand)					**100%**	**99%**	**92%**	**100%**	**100%**	**99%**	**91%**	**100%**	**99%**	**96%**	**75%**	**100%**
110%					98%	99%	92%	100%	98%	98%	91%	100%	98%	96%	75%	100%
125%					93%	99%	92%	100%	88%	98%	89%	100%	82%	95%	75%	100%
150%					68%	98%	91%	100%	59%	98%	89%	100%	46%	95%	73%	100%

First Diversion Water Right=FDWR, Minimum Instream Flow=MIF

comparable across systems.

The current firm yield of the Seattle system as calculated by Seattle Public Utilities (2007) is 7.5 cms (171 mgd), which is 1.1 cms (24 mgd) greater than current demands. As a result, reliability with current demands is greater than 98% in the 2020s, 2040s, and 2080s for both A1B and B1 scenarios (Table 6). When demand increases, differences in reliability between the 2020s, 2040s, and 2080s climate projections become more apparent. With a 10% demand increase, reliability in the 2080s drops by 5% in A1B and 1% in B1 emissions scenarios, whereas with a 50% demand increase 2080s reliability decreases by 36%. These values are relatively close to the reliability Traynham (2007) reported (98.7% for a 2050 climate as simulated by IPSL_A2 GCM with projected future demands of 6.4 cms (145 mgd). These changes compare with 2075 reliability for 3 GCMs reported by Traynham of 86.8%, 93.4%, and 77.6% with simulated demands of 8.2 cms (187 mgd). Our results indicate for a 125% increase in demand (8.1 cms or 184 mgd), reliability in the 2080s would be near 73% in A1B and 82% in B1 emission scenarios (Table 6). Because managers regularly assess future conditions and make adjustments accordingly, operating near capacity is rare. For example, SPU's 2007 Water System Plan (2007) notes that, given current firm yield estimates for existing supply resources and demand forecasts, a new source of supply will be needed sometime after 2060 and the plan provides more details on these new supply alternatives.

In Tacoma's system, water allocations differ considerably from Seattle's and projects for increasing capacity are underway (these projects are not reflected in our reservoir model). Therefore, simulated effects of climate change on the current reservoir system and with current operations are more likely to lead to shortfalls. Because the system, as simulated by the reservoir model, is less buffered by a large difference between supply and demand, changes from climate and population growth are both evident as early as the 2020s (Table 6). With increases in water demand of 50%, the first diversion water right (FDWR) reliability of the Tacoma system decreases the reliability in the 2020s by 2%, in the 2040s by 4%, and in the 2080s by 3% for the A1B emissions scenario and by only 1% in all composite runs in the B1 scenarios. Simulated minimum instream flow at Palmer (MIF) reliability changes less when demands are incorporated into the model, as a result of reservoir operations which is based on various allocation pools. The metrics we use in this respect are not the same used as those used by Traynham (2007) who instead used a measure of Tacoma M&I reliability. Our values however capture the same relative trend. In general, the effects of changing climate and hydrology are problematic in the fall because the reservoir rules draw down flows before there is enough water in the reservoir to insure that fish flow targets can be met.

Everett's system is less sensitive to shortfalls in municipal and industrial demand than the other two systems because reservoir capacity and inflows are larger relative to water demands. Current firm yield is 8.8 cms (200 mgd), more than twice 2000s demands. Changes in demand of 50% in a 2080s climate are still not enough to create a shortfall. When current demand is doubled to 7.7 cms (175 mgd), it is only in the 2080s with impacts from both climate change and water demands increases that shortfalls occur, resulting in decreased reliability to 99% with the A1B and 99% for the B1 emission scenarios. Traynham (2007) reported 65.8%, 93.4%, and 63.2% reliability with 3 GCMs in 2075, with demand values of 8.6 cms (195.5 mgd). A demand level that is greater than twice the current demand.

In our analysis, the impact of 50% increases in demand on the Seattle system are more substantial than the same percentage demand increase on the Tacoma and Everett systems (Table 3). It is important to note, however, that changing future demands will depend not only on population growth, but also on water pricing policies, water conservation efforts, changing technologies, and that these factors will inevitably vary across the three systems as well.

4.3. Flood Control

The Howard Hanson Reservoir is primarily operated for flood control, with events of most concern occurring between October and March. To investigate how climate change may impact Tacoma's flood control, and thus impact summertime storage potential, we evaluated the average number of days per year when the system is under flood control operations in the 2020s, 2040s, and 2080s (Figure 5) relative to historical simulations. It is important to note that as in all other simulations, we used the delta method of producing reservoir inflows, and therefore, while the future climate inflows reflect the effects of changes in temperature and precipitation, they do not reflect possible changes in precipitation patterns (e.g., changes in precipitation frequency, and/or duration of storms).

Flood conditions in the reservoir model occur on days when flows at the Auburn gage are predicted to reach 12,000 cfs, which is specified in the water management model as when the inflows upstream plus the difference between Palmer (Figure 1, Green B) and Auburn (Green C) gages total 12,000

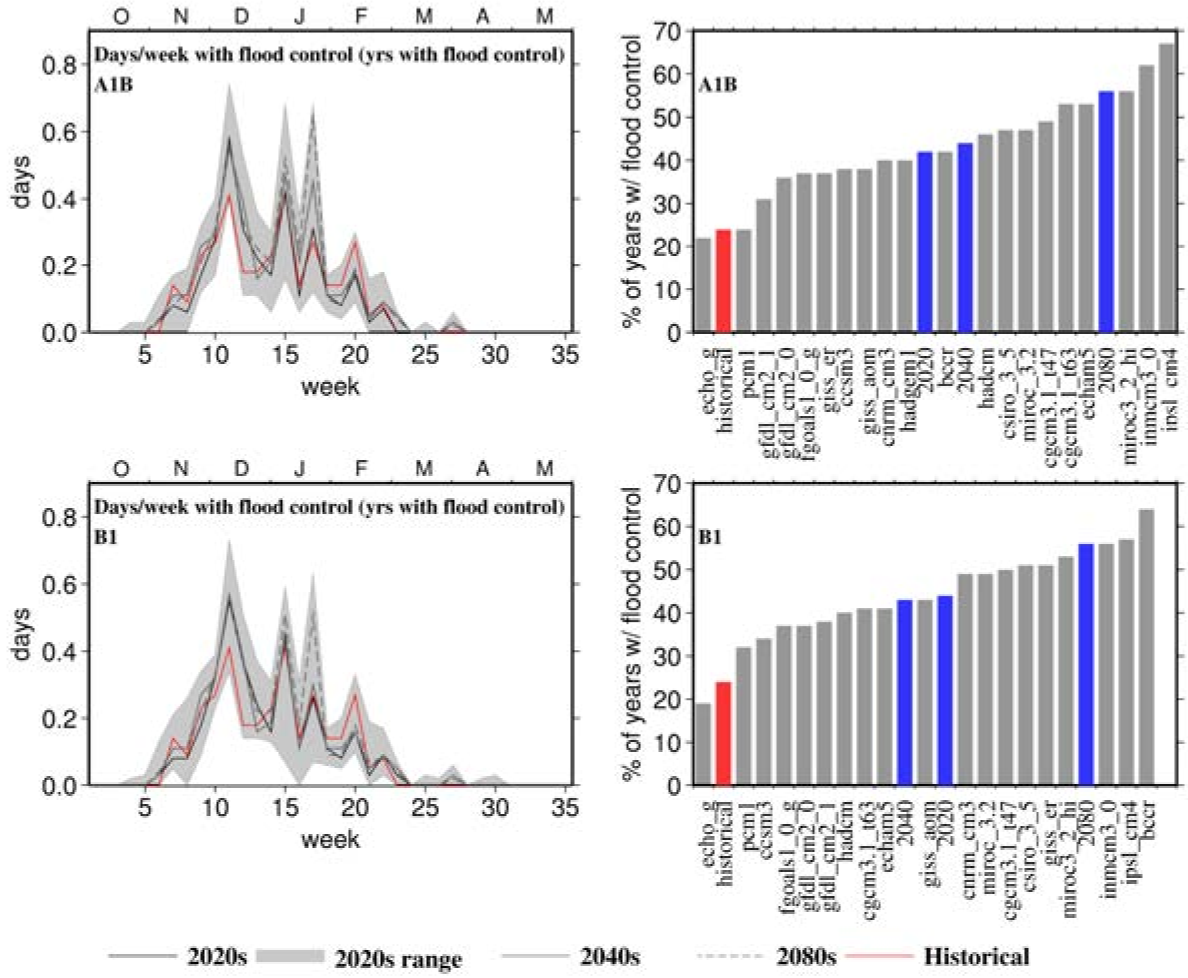

Figure 5. Flood control days (Tacoma).

cfs. Once this occurs, storage for flood control is allocated (King, 2006).

Figure 5, left panels show the change in seasonality of when flood conditions occur. The system is under flood control operations most frequently in December-May. As the climate warms, there is a shift in timing. This includes both a decrease in frequency of flood control in April-May and an increase in frequency in January-March, and these changes occur progressively from the 2020s through the 2080s.

The right panels of Figure 5 indicate the likelihood that flood conditions occur at least once in a year for all water management simulations (historic and all climate change projections). Simulations indicate that flood conditions may occur more frequently, with all but one 2020s scenario (ECHO_G) having a higher likelihood of flood conditions. The range between the models varies from less than 20% to more than 60% for the 2020s ensembles. The 2020s and 2040s composite runs have similar likelihoods of flood control conditions, related to the similarities in their peak flow. The 2040s B1 scenario is associated with less frequent flood conditions than the 2020s B1 scenario (by 1%). This is likely because of surface processes transitioning toward more winter-dominated flow. In the 2080s, however, the frequency with which flood operating conditions occur is considerably higher than in the 2020s and 2040s, with occurrence of more than one flood control day likely in more than 50% of years.

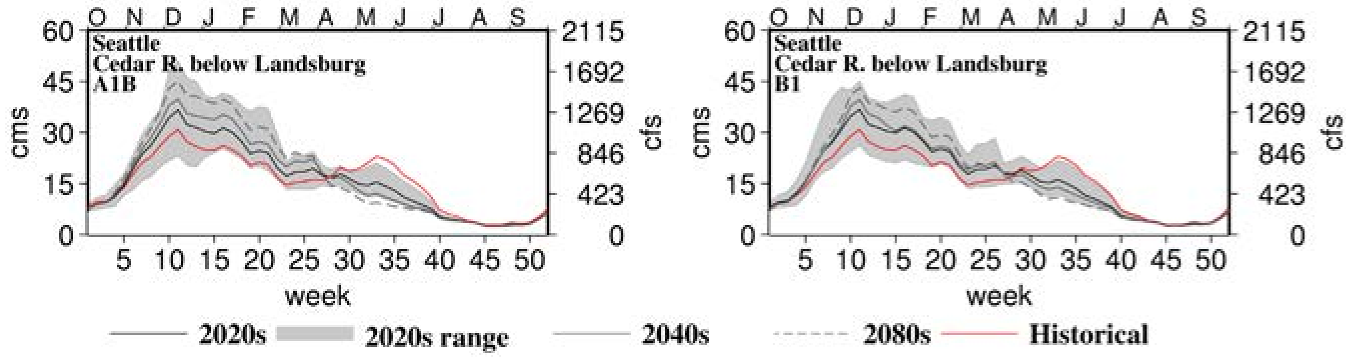

Figure 6. Environmental flows.

4.4. Environmental Flows

As an example of multiple-management objectives, in the Seattle system, priorities are given to instream flows over other water allocations. Within the Cedar, Landsburg (Figure 1, Cedar C) has been an important location in efforts to enhance fish habitat, especially for salmonids. To evaluate how the ability to meet environmental flow targets may change with climate, we compare changes in regulated flows at Landsburg as simulated by the Seattle system model using normal instream flow requirements (Traynham and Palmer, 2006) with current 2000s water demands (Figure 6). These flows do not account for potential adaptations such as accounting for flows for the supplemental block requirements curtailments and pumping dead storage. Normal and critical instream flow requirements, as instituted by the Habitat Conservation Plan (SPU, 2000), have been set according to studies on the needs salmonids present in the river system. These flows are lower than typical flows, never exceeding 8.2 cms (288 cfs) and declining in August and September to less than 3.0cms (108 cfs). Therefore shortfalls only occur in the most extreme climate change simulations in the 2020s and in the 2040s and 2080s for A1B. Shortfalls occur to a lesser extent in B1 emission scenarios, with shortfalls occurring only in the 2020s with the most extreme ensemble simulations and in the 2080s. These limited shortfalls occur in the late fall and early winter when instream flow requirements are greater than 6.1 cms (216 cfs) and shortfalls generally do not exceed 0.02 cms (0.9 cfs). These results are similar to those of Wiley and Palmer (2004, 2008) who showed that minimum instream flows at Landsburg were not dramatically impacted in near-term climate change simulations. There are, however, other effects such as increasing water temperature that warrant serious attention as discussed inBattin et al. (2007) and Mantua et al. (2009, this report).

4.5. Hydroelectric Power

Hydropower production, a key consideration in reservoir operations in the Everett system, generates flows through the Jackson power tunnel that are a function of the price of power, fish needs, and potential flooding. We simulated these future flows with yield constrained by the head, friction loss, and cavitation boundary of the Chaplain reservoir (Enfield and Palmer, 2006). Our simulations did not reflect the price of power or flood forecasts. Changes in inflow hydrographs are evident in the power tunnel

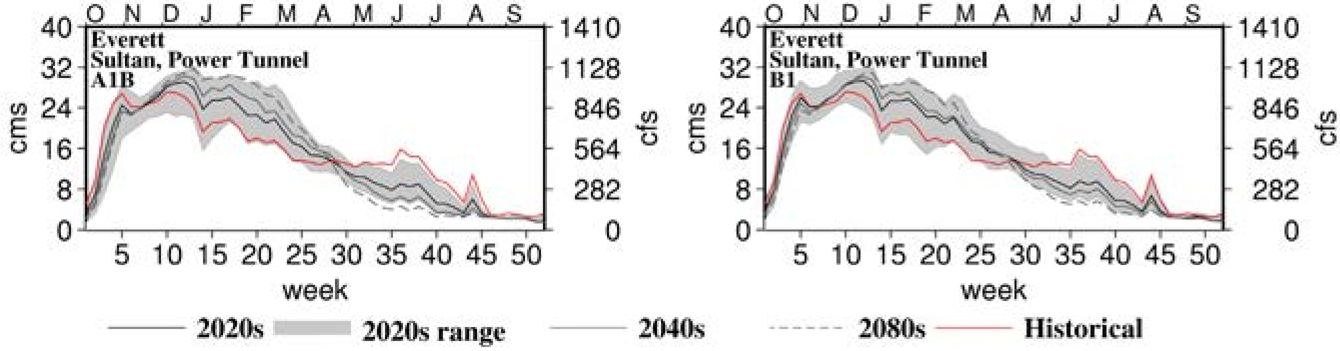

Figure 7. Hydroelectric power (Everett).

flow simulations (Figure 7). Generally, future climate change projections with current 2000s demands indicate there may be more power generation in the winter and less in the summer, which coincides with trends in energy production on the Columbia River basin (Hamlet et al., 2009, this report). Currently, the flows are highest in early December and peak slightly again in June. Peaks remain at approximately the same time of year, but the magnitude of the already large wintertime peak increases by 2 cms (70 cfs) with a range over ensemble members of 2.5 cms declines to 5 cms increases (-90 to 180 cfs) in the 2020s, 2 cms (110 cfs) in the 2040s, and 4.5 cms (160 cfs) in the 2080s (Figure 7). The peak in June, alternatively, declines by 6.8 cms (240 cfs) with a range over ensemble members of 2 to 10 cms (70 to 350 cfs) in the 2020s, 9.3 cms (330 cfs) in the 2040s, and 11.3 cms (400 cfs) in the 2080s for A1B emission scenarios. Changes relative to the historical simulation are slightly less in the B1 scenario.

5. Conclusions

The primary hydrological manifestation of climate change, which will affect each of the three major Puget Sound water supply systems to varying degrees, will be the decline and eventual disappearance on average of the springtime snowmelt hydrograph peak, and its replacement with an elevated winter runoff peak. These shifts are projected to become more pronounced throughout the century, although year-to-year variability in weather and inflows should still be expected. There will be years with snowmelt that is similar to current conditions, but years with high springtime snowmelt are projected to progressively become less frequent. The three water supply systems, with current operating policies and in the absence of demand increases, may be generally robust to changes through the 2020s, with reliabilities projected to remain above 98% in all cases. However, other aspects of system performance, such as reduced levels of summer and fall storage, may occur as early as the 2020s.

The primary reason for current robustness in the systems is that system demand has been reduced in recent years, particularly in the Seattle system. With increases in demands, the systems become less robust to impacts from climate change, notwithstanding that the changes in demand are modest aside from large demand increases late in the study period. For example, if Seattle's demand increases by 10%, reliability for the 2080s drops by 5% in A1B and 1% in B1 emissions scenarios relative to historic conditions, whereas with a 50% demand increase climate change impacts in the

2080s decreases reliability by 36%. Seasonal patterns of reservoir storage are affected to varying degrees in all three systems. Reservoir storage is generally projected to be lower from late spring through early fall, and ancillary operating objectives, such as hydropower production by the Everett system, flood control in Tacoma, and the ability of the systems to augment seasonal low flows, may be impacted. All of the analysis reported here, use current operating policies. Some mitigation of the effects we have identified can likely be achieved by changes in reservoir operating policies.

Acknowledgments

The authors would like to thank people at Seattle Public Utilities, Tacoma Water, the City of Everett, the USACE Howard Hanson project, and Snohomish County Public Utility District for their insights into system specific goals and operating procedures. Three anonymous reviewers provided helpful feedback on earlier drafts. Thanks also go to Rob Norheim and Kristian Mickelson at the University of Washington for their help with paper preparations.

References

Alemu ET (2008) A decision support system for optimizing reservoir operations at the Jackson Hydropower Project. Thesis (M.S.C.E.)--Univ of Washing

Battin J, Wiley MW, Ruckelshaus MH, Palmer RN, Korb E, Bartz KK, Imaki H (2007) Projected impacts of climate change on salmon habitat restoration. Proceedings of the Natl Acad of Sci 104:6720-6725

Central Puget Sound Water Suppliers' Forum (2009) Accessed January 15, 2008 at http://www.cpswatersuppliersforum.org/Home/Default.asp?ID=3

Christensen NS, Wood AW, Voisin N, Lettenmaier DP, Palmer RN (2004) The effects of climate change on the hydrology and water resources of the Colorado River basin. Clim Chang 62:337–363

Christensen N, Lettenmaier DP (2007) A multimodel ensemble approach to assessment of climate change impacts on the hydrology and water resources of the Colorado River basin. Hydrol Earth System Sci 11: 1417-1434

Cunnane C (1978) Unbiased plotting positions – a review, Journal of Hydrol 37(3/4): 205-222

Cuo L, Lettenmaier DP, Alberti M, Richey JE (2008a) Effects of a century of land cover and climate change on the hydrology of Puget Sound basin. Hydrol Process (accepted)

Cuo L, Lettenmaier DP, Mattheussen BV, Storck P, Wiley M (2008b) Hydrological prediction for urban watersheds with the Distributed Hydrology-Soil-Vegetation Model, Hydrol Process DOI: 10.1002/hyp7023

Enfield B. and R. Palmer (2006) Snohomish County Water Supply Model: Documentation. White paper prepared by the University of Washington Water Resource management and Drought Planning Group and used in the Climate Change Technical Subcommittee of the Regional Water Supply Planning Process

Elsner MM, Cuo L, Voisin N, Hamlet AF, Deems JS, Lettenmaier DP, Mickelson KEB, Lee SY (2009) Implications of 21st century climate change for the hydrology of Washington State. Washington Climate Change Impacts Assessment: Evaluating Washington's future in a changing climate. This report

Hamlet AF, Lee SY, Mickelson KEB, Elsner MM (2009) Effects of projected climate change on energy supply and demand in the Pacific Northwest. Washington Climate Change Impacts Assessment: Evaluating Washington's future in a changing climate. This report

Hashino T, Bradley AA, Schwartz SS (2007) Evaluation of bias correction methods for ensemble streamflow forecasts, Hydrol and Earth Sys Sci 11: 939-950

Knowles N, Dettinger MD, Cayan DR (2006) Trends in snowfall verse rainfall in the western United States. J Clim 19:4545-4559

Hayhoe K, Wake C, Huntington TG, Luo L, Schwartz MD, Sheffield J, Wood EF, Anderson B, Bradbury J, DeGaetano TT, Wolfe D (2007) Past and future changes in climate and hydrological indicators in the U.S. Northeast Clim Dyn 28: 381-407

IPCC (2007) Summary for policymakers. In: Climate Change 2007: The physical science basis. Contribution of working group I to the fourth assessment report of the intergovernmental panel on climate change. Solomon S, Qin D, Manning M, Chen Z, Marquis M, Averyt KB, Tignor M Miller HL (eds) Cambridge University Press, Cambridge, United Kingdom and New York, NY, USA

King, K. (2006). The Green River System and Howard Hanson Dam. White paper prepared by the University of Washington Water Resource management and Drought Planning Group and used in the Climate Change Technical Subcommittee of the Regional Water Supply Planning Process

Leung LR, Hamlet AF, Lettenmaier DP, Kumar A (1999) A.: Simulations of the ENSO hydroclimate signals in the Pacific Northwest Columbia River basin, Bull Am Meteorol Soc 80: 2313–2328

Lins HF, Stakhiv EZ (1996) Managing the nation's water in a changing climate. J Am Water Resour Assoc 34:1255-1264

Mantua N, Tohver IM, Hamlet AF (2009) Impacts of climate change on key aspects of freshwater salmon habitat in Washington State. Washington Climate Change Impacts Assessment: Evaluating Washington's future in a changing climate. This report

Maurer EP (2007) Uncertainty in hydrologic impacts of climate change in the Sierra Nevada, California under two emissions scenarios. Clim Chang 82(3-4): 309-325

Miller, Jim, (2008) Impact of Climate Change on Water Supplies of Everett, Seattle, and Tacoma. Presentation for the AWWA-PNWS Annual Conference, Vancouver, WA, May 2008 Available online at: http://www.pnws-awwa.org/Page.asp?NavID=299

Milly PCD, Dunne KA, Vecchia AV (2005) Global pattern of trends in streamflow and water availability in a changing climate. Nature 438: 347-350

Milly PCD, Betancourt J, Falkenmark M, Hirsch RM, Kundzewicz ZW, Lettenmaier DP, Stouffer RJ (2008) Stationarity is dead: Whither water management? Sci 319(5863) 573-574

Mote PW, Hamlet AF, Clark MP, Lettenmaier DP (2005) Declining mountain snowpack in western North America. Bull Am Meterol Soc 86(1): 39-49

Mote PW, Salathé Jr EP (2009) Future climate in the Pacific Northwest. Washington Climate Change Impacts Assessment: Evaluating Washington's future in a changing climate. This report

O'Neill C, Palmer RN (2007) Technical memorandum #3: Online database functionality and design for climate impacted data. A report prepared by the Climate Change Technical Subcommittee of the Regional Water Supply Planning Process, Seattle, WA. http://www.climate.tag.washington.edu

Panofsky HA, Brier GW (1968) Some applications of statistics to meteorology. The Pennsylvania State Univy, Univ Park, 224pp

Palmer RN, Polebitski A, Traynham LE, King K, Enfield B (2006) Review of Seattle's new water demand model. Report for King County Deparment of Natural Resources and Parks, July 7, 2006

Palmer RN (2007) Final report of the Climate Change Technical Committee. A report prepared by the Climate Change Technical Subcommittee of the Regional Water Supply Planning Process, Seattle, WA

Payne JT, Wood AW, Hamlet AF, Palmer RN, Lettenmaier DP (2004) Mitigating the effects of climate change on the water resources of the Columbia River basin. Clim Chang 62:233–256

Polebitski A, Traynham L, Palmer RN (2007) Technical Memorandum #5:

Approach for developing climate impacted streamflow data and its quality assurance/ quality control. A report prepared by the Climate Change Technical Subcommittee of the Regional Water Supply Planning Process, Seattle, WA. http://www.climate.tag.washington.edu/

Public Utility Dist 1 Snohomish County and City of Everett (2006). Revised Study Plans

and Studies Not Proposed, Henry M. Jackson Hydroelectric Project FERC No. 2157 September 12, 2006

Seattle Public Utilities (2007) 2007 Water System Plan. Accessed December 18, 2008 at http://www.seattle.gov/util/About_SPU/Water_System/Plans/2007WaterSystemPlan/SPU01_002126.asp

Snohomish County Public Utilities (2008) Accessed December 15, 2008 at http://www.snopud.com/water/jhp.ashx?p=1819

Snover AK, Hamlet AF, Lettenmaier DP (2003) Climate-change scenarios for water planning studies, Bull Am Meteorol Soc 84(11): 1513-1518

Storck P, Bowling L, Wetherbee P, Lettenmaier DP (1998) Application of a GIS-based distributed hydrology model for prediction of forest harvest effects on peak stream flow in the Pacific Northwest. Hydrol Proc 12: 889-904

Traynham LE (2007) Impacts of future climate conditions and forecasted population growth on water supply systems in the Puget Sound Region. Thesis (M.S.C.E.)--Univ of Washington

Traynham, LE and R Palmer (2006). GoldSim Regional Water Supply Model: Seattle System. White paper prepared by the University of Washington Water Resource management and Drought Planning Group and used in the Climate Change Technical Subcommittee of the Regional Water Supply Planning Process

USACE (2008) Howard Hanson Dam additional storage project. Accessed December 18, 2008 at http://www.mytpu.org/tacomawater/water-system/supply/regional-water-supply/howard-hanson-dam.html

Van Rheenen NT, Wood AW, Palmer RN, Lettenmaier DP (2004) Potential implications of PCM climate change scenarios for California hydrology and water resources. Clim Chang 62:257–281

Wiley MW (2004) Analysis techniques to incorporate climate change information into Seattle's long range water supply planning. Thesis, Univ of Washing

Wiley MW, Palmer RN (2008) Estimating the impacts and uncertainty of climate Change on a municipal water supply system. J Water Resourc Plan Manage 134(3):239-246

Wiley MW, Palmer RN, Salathé (2007) The development of GCM based climate scenarios for use in water resource system impact evaluations. J Water Resourc Plan Manage

Vano, JA, Scott M, Voisin N, Stöckle CO, Halmet AF, Mickelson KEB, Elsner MM, Lettenmaier DP (2009b) Multi-model assessment of the impacts of climate change on water management and agriculture of the Yakima River basin, Washington, USA. Washington Climate Change Impacts Assessment: Evaluating Washington's future in a changing climate. This report

Wood AW, Maurer EP, Kumar A, and Lettenmaier DP (2002) Long-range experimental hydrologic forecasting for the eastern United States, J Geophys Res - Atmosphere 107: 4429

Climate Change Impacts on Water Management and Irrigated Agriculture in the Yakima River Basin, Washington, USA

Julie A. Vano[1], Michael Scott[2], Nathalie Voisin[1], Claudio O. Stöckle[3], Alan F. Hamlet[1,4], Kristian E. B. Mickelson[1], Marketa McGuire Elsner[4], and Dennis P. Lettenmaier[1,4]

Abstract

The Yakima River Reservoir system supplies irrigation water to over 180,000 irrigated hectares (450,000 acres). Runoff is derived mostly from winter precipitation in the Cascade Mountains, much of which is stored as snowpack and runs off in the spring and early summer. Five reservoirs within the basin have cumulative reservoir storage of approximately 30% of the river's mean annual flow. Climate change during the 21st century is expected to result in earlier snowmelt runoff, and reduced summer flows. The effects of these changes on irrigated agriculture in the basin were simulated using a hydrological model driven by downscaled climate scenarios from 20 climate models, output of which was archived by the 2007 IPCC Fourth Assessment Report. In general, we find that the basin transitions to earlier and reduced spring snowmelt as the century progresses, which results in increased curtailment of water deliveries, especially to junior water rights holders. Historically, the Yakima basin has experienced water shortages (years in which substantial prorating of deliveries to junior water users was required) in 14% of years. Without adaptations, for the A1B emission scenarios, water shortages that occur in 14% of years historically increase to 32% (15% to 54% range) in the 2020s, to 36% in the 2040s, and to 77% of years in the 2080s. For the B1 emissions scenario, water shortages occur in 27% of years (14% to 54% range), in the 2020s, 33% for the 2040s and 50% for the 2080s. Furthermore, the historically unprecedented condition in which the senior water rights holders suffer shortfalls occurs with increasing frequency in both the A1B and B1 climate change scenarios. Economic losses include lost value of expected annual production in the range of 5% to 16%, with significantly greater probabilities of annual net operating losses for junior water rights holders.

1. Introduction

The Yakima River basin is an agriculture-rich region in central Washington State (Figure 1) that contains the largest agricultural economy in the state (US Bureau of Reclamation , 2002). Most crops in the basin are irrigated. Thirty-four percent of the irrigated land in the three counties included within the basin is planted in tree crops and vineyards. The remainder is mostly planted in forage, pasture, and annual vegetable and field crops, but also includes specialty crops such as mint and hops (USDA, 2004). The U.S. Bureau of Reclamation (USBR) operates a system of five reservoirs (Figure 1; Table 1) that supply water to the basin. Much of the basin's runoff is derived from mountain snowpack and the reservoirs are small enough that they generally fill in the springtime of most years (USBR, 2002).

Climate change is expected to cause continued decline in snowpack and earlier snowmelt resulting in reduced water supplies. Analysis of past observations suggests that this process is already underway (Mote et al, 2005). Previous studies have shown that the Washington Cascade Mountains, from which the Yakima River drains, are likely to lose about 20% of their April 1st snowpack with 1°C (1.8°F) of warming (Casola et al, 2008), and an accompanying study (Elsner et al, 2009, this report) suggests that for the Yakima basin, a similar temperature-snowpack sensitivity can be expected. Using +1ºC and +2ºC warming scenarios, Mastin (2008) showed a 12 and 27% decrease, respectively, in snowmelt within the basin over a base period 1981-2005. Because the reservoir system is relatively small (total reservoir storage is about 30% of the mean annual flow of the river), and because the snowpack is highly sensitive to even modest warming, water deliveries from the reservoir system have been sensitive to even small departures from

[1]Department of Civil and Environmental Engineering, University of Washington, Seattle, Washington
[2]Pacific Northwest National Laboratory, Richland, Washington
[3]Department of Biological Systems Engineering, Washington State University
[4]Climate Impacts Group, University of Washington, Seattle, Washington

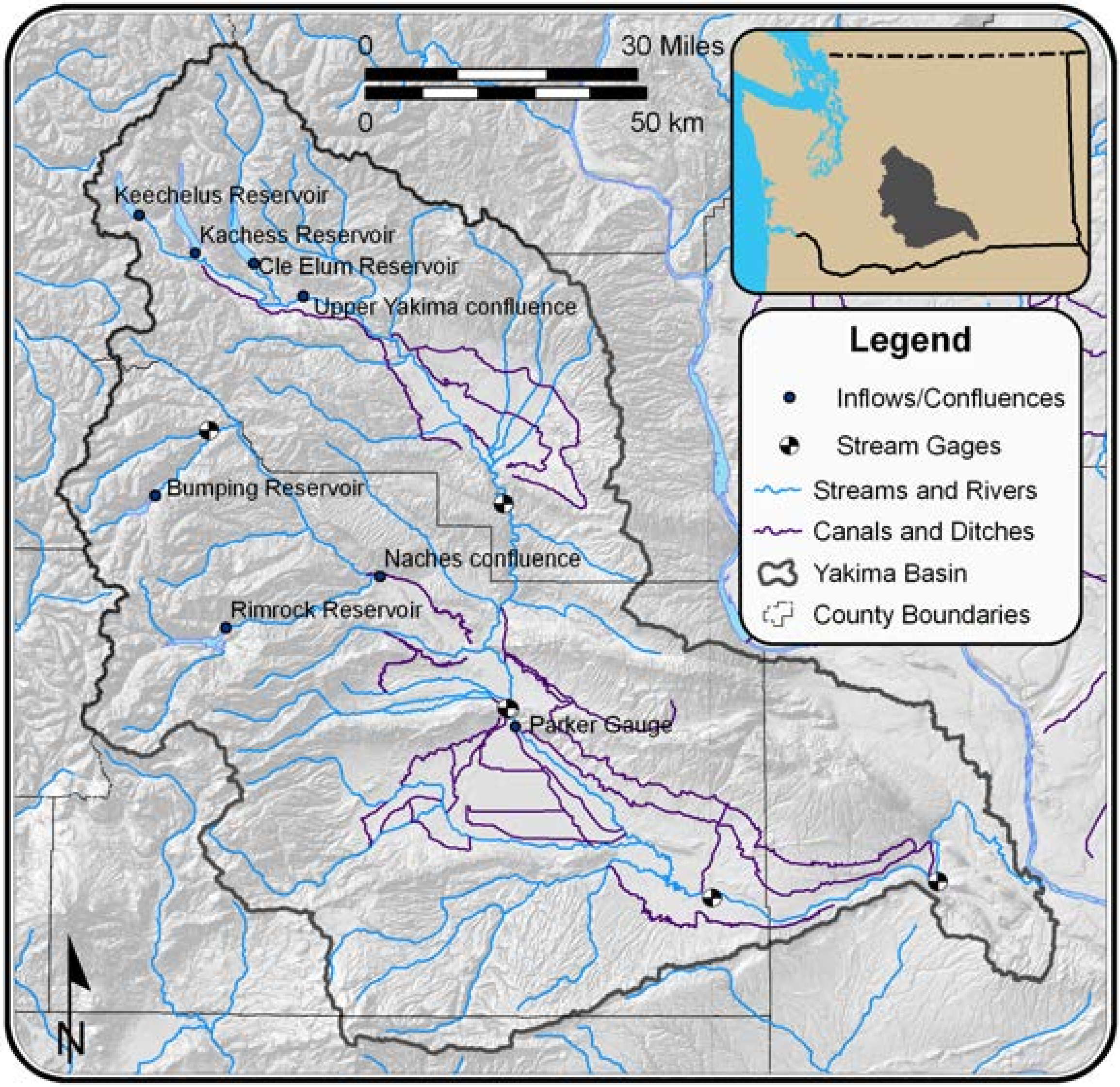

Figure 1. Yakima watershed. Reservoir inflow locations used in the water management model are specified, including five reservoirs, two confluences, and the gage near Parker.

Table 1. Physical properties of the Yakima River reservoir system

	Elevation of Reservoir Sill (ft)	Drainage Area (miles^2)	Reservoir Capacity (AF)	Percent of Total Water Supply (%)	Ratio of average runoff to reservoir capacity
Bumping	3426	70.7	33700	13	6.2:1
Cle Elum	2223	203	436900	42	1.5:1
Kachess	2254	63.6	239000	12	0.9:1
Keechelus	2427	54.7	157800	13	1.5:1
Rimrock	2766	187	198000	20	1.8:1

*Values provided by Reclamation (USBR, 2002) average historic conditions.

Most assessments of climate change impacts on agriculture have focused on annual crops, although some studies have addressed impacts on perennial crops as well, and are relevant to the high-valued tree crops and vineyards of the Yakima basin. Using a statistical model, Lobell et al. (2006) found that climate change would reduce yields of four California perennials (almond, walnut, avocado, and table grape) by 2050, even without consideration of climate change impacts on irrigation water availability. Projected losses ranged from 0 to more than 40% depending on the crop and the particular climate change scenario.[1] Scott et al. (2004a, b) analyzed effects of periodic droughts in the Yakima basin, and found substantial reductions in crop yields and increases in economic risk both in dry years with current climate, and in a future climate with 2°C warming and no change in annual precipitation.

Since the 1970s, water managers in the Yakima Basin have managed water supply using regression-based forecasts of Total Water Supply Available (TWSA). TWSA is defined by the USBR as "the total water available for the Yakima River basin above Parker for the period April through September" (USBR, 2002). It accounts for a combination of measures including forecasted runoff, reservoir storage contents, and projected return flow. These forecasts are issued by the USBR Yakima regional field office starting in the beginning of March and are updated every month (USBR, 2002). This management strategy implicitly assumes that the historic conditions - on which regression parameters for their water supply forecasts are based - will persist in the future. As indicated by Milly et al. (2008), assumptions based on a stationary climate may no longer be tenable.

To provide a better understanding of how the Yakima River reservoir system may respond to climate change, we used future climate scenarios that were archived as part of the Fourth Assessment Report of the Intergovernmental Panel on Climate Change (IPCC, 2007). The methodology of selecting general circulation models (GCMs) is described in detail by Mote and Salathé (2009, this report). The scenarios are based on two global emissions scenarios A1B and B1. B1 has lower CO_2 emissions than A1B and therefore results in less projected warming for the region. The emissions scenarios are quite similar until about mid-century, with differences evolving mostly thereafter (SRES, 2007; Mote and Salathé, 2009, this report). Climate change projection departures from the 1970-1999 climatology were averaged over the 2020s (average of 2010-2039), 2040s (average of 2030-2059), and 2080s (average of 2070-2099). A delta method approach incremented historical precipitation and temperature on a monthly basis to produce scenarios of future climate that were used as input to a hydrology model, which produced scenarios of future Yakima River streamflow at selected reservoir inflow points for the climate of the 2020s, 2040s, and 2080s. Elsner et al. (2009, this report) describe the approach in more detail. We specifically focus here on how the projected hydrologic changes in the Yakima River basin affect reservoir operations and alter water availability for junior and senior water rights users (Section 4). We then investigate how these shifts in reservoir system performance impact economic crop value by application of crop

[1]They did not model CO_2 fertilization effects or any adaptation measures on the part of farmers. Note that the uptake of adaptive actions like adopting heat-tolerant varieties is likely to proceed more slowly in long-lived crops than in annual crops.

models to projected irrigation water releases for future climate scenarios (Section 5).

2. Site Description

The Yakima River basin drains the east side slope of the central Washington Cascade Mountains (Figure 1). Climate varies strongly within the basin. Mean-annual precipitation averaged over 1970-2000 ranged from 203 to 356 cm (80 to 140 inches) along the Cascade Crest headwaters to less than 25 cm (10 inches) at the basin outlet. Most of the annual precipitation (61-81% depending on the particular year) falls in the cool season between October and March (USBR, 2002; WRCC, 2007).

The five major USBR reservoirs in the system are Bumping Lake [established 1910], Cle Elum [1933], Kachess [1912], Keechelus [1917], and Rimrock/Tieton Dam [1925] (USBR, 2002). They have a combined total capacity of 1.2 billion cubic meters (bcm) (1.07 million acre-feet, maf), which is approximately one-third of the average annual unregulated flow of the Yakima River basin at its mouth at the Columbia River. Annual discharge is estimated to be 4.2 bcm (3.4 maf) per year, as averaged from 1961-1990. The reservoirs vary in their upstream drainage area, capacity, and contributions to total basin water supply as shown in Figure 1 and Table 1; however, the capacity of the system is such that the reservoirs generally refill every year. In managing the refill cycle, USBR must carefully balance reservoir outflow to avoid potential flooding while still capturing water for use throughout the dry summer months. The irrigation season begins in April (some water use starts in March), therefore in the early spring and summer, the snowpack effectively acts as a sixth reservoir, which augments the reservoir storage so that reservoirs do not need to be drawn down until June (USBR, 2002). However, in some low snowpack years, such as 1992-1994, 2001, and 2005, reservoir storage has been insufficient to meet demands, and in these years, water was allocated to junior users based on prorating according to the seniority of their water rights and the TWSA, a process described in more detail below.

Notwithstanding consideration of possible spring flooding and maintenance of instream flows in the operating policies that dictate reservoir releases, the system's primary operating purpose is to supply irrigation water. Maintenance of in-stream flows for protection and enhancement of native and anadromous fish, however, has changed reservoir operating policies somewhat in recent years. In 1994, legislation was enacted for a river basin water enhancement project with approximately $200 million allocated for fishery and irrigation system efficiency improvements including fish ladders and other infrastructure projects. Since then, various other management actions have been proposed and/or implemented to enhance storage, recreation, and fish and wildlife habitat. The final planning report for the Yakima River Basin Water Storage Feasibility Study (2008) provides an overview of these water management policies and projects.

Water withdrawals typically begin in March, but reservoirs generally do not reach their maximum storage volumes until June. Reservoir storage at Cle Elum and Keechelus is usually lowest in September when outflows are reduced to the instream flow maintenance levels. Kachess and Rimrock usually continue to draft into October in order to maintain specific flow levels throughout the winter months on reaches of the Cle Elum and Teanaway Rivers to increase the likelihood of successful spawning of several endangered species of salmon (USBR, 2006). This management strategy, implemented as a component of the 1980 Quackenbush Decision, is intended to encourage spring Chinook salmon to spawn at relatively low flows, so that lower flows are required to keep redds (egg nests) covered in winter (USBR, 2002). This is primarily accomplished by limiting irrigation releases from the Cle Elum Reservoir and increasing flows from Rimrock Reservoir to compensate. This switch in reservoir releases in early September is commonly known within the basin as "flip-flop."

Water allocations within the basin are based on seniority according to the 1945 Consent Decree by the District Court of Eastern Washington (as referenced in USBR, 2002). In low runoff years, not all water demands can be met; therefore water is first allocated to the senior (non-proratable, indicating they receive their total entitlement every year) water right holders and then to junior (proratable)water users. Therefore, water availability for irrigators with junior water rights is a measure of how well the system meets its nominal water demands. The system's total reservoir capacity is 1.25 bcm (1.07 maf), whereas the annual diversions allocated by the Consent Decree is approximately 2.57 bcm (2.2 maf), of which about half is allocated to senior, non-proratable water users. Because the reservoirs historically capture only about 30% of the annual unregulated flow of the Yakima River near Parker, this discontinuity is typically compensated by unregulated flow, much of which is derived from snowpack.

Between 1970 and 2005, water allocations have been restricted for junior water users in 13 years. The lowest prorating levels for junior water users, defined as the portion of their water right they can expect to receive in the upcoming irrigation season, was in 1977 with prorating of 6-26% in May and 13-50% in June; these ranges proved controversial and increased later in the season when reservoir inflow forecasts were revised (Glantz, 1982; USBR, 2002). This drought resulted in a court ruling (Acquavella Adjudication, Case No. 77-2-0148-5 in the Superior Court of Yakima County) that continues to impact water management in the basin (Glantz, 1982; Kent, 2004). In general, when prorating levels are greater than 75%, shifting the start and end of the irrigation season can compensate for water limitation impacts. When prorating levels drop below 75%, however, decisions become more challenging at the farm level in terms of how to apportion limited water to specific crops.

The Yakima basin currently has a water-trading program that began in 2001 and is activated in drought emergencies as declared by the state of Washington. It is intended to relieve the impact of drought on junior water rights holders by providing a mechanism for voluntary transfers of water from interruptible or low-valued to higher-valued uses. The water-trading program is supervised by the Washington State Department of Ecology and was active in both the 2001 and 2005 drought years (Scott et al. 2004, Anderson et al. 2006). The program generally has the effect of creating an economic market that diverts water in low runoff years from low-valued annual crops (which are fallowed), to high-valued perennial crops. There are nonetheless numerous institutional and "plumbing" complications in the application of this program. These include the inability to move water to junior water rights holders in some parts of the basin. Furthermore, legally, water trades must not adversely affect outflow from the basin (as measured near Parker), and must not have adverse third-party impacts such as reduced flows for fish (Yakima River Basin Conservation Advisory Group 2002, Isley 2001). Finally, only irrigation districts can purchase water on behalf of irrigators. Nonetheless, the Sunnyside Valley Irrigation District, which has a mix of senior and junior water rights holders, and the Roza Irrigation District, which has primarily junior water rights holders, have been able to make good use of the water trading program. The Washington Department of Ecology Yakima Basin website (2009) provides background and discussion of current water-trading and water-banking activities in the basin.

3. Approach

We use a multi-model ensemble approach similar to that described in the accompanying papers by Elsner et al. (2009, this report) and Vano et al. (2009a, this report) to explore climate impacts on the Yakima River reservoir system (Figure 2). Spatially and temporally complete daily records of historic and future streamflows were simulated using the Variable Infiltration Capacity (VIC) macroscale hydrology model, forced with both gridded historical observation data, and downscaled future climate scenarios. Both historical data and future climate scenarios are described in accompanying papers by Mote and Salathé (2009, this report) and Elsner et al. (2009, this report). Note that each downscaled scenario in fact consists of the historical (daily) precipitation and temperature for 1916-2006, but adjusted on a monthly basis to reflect predicted changes for the 2020s, 2040s or 2080s (delta method); these adjusted precipitation and temperature sequences were then used as forcings to a hydrology model to produce daily streamflow sequences as described in Elsner et al (2009, this report). Summary statistics and information about the climate scenarios are included in Table 2. The streamflows simulated by the hydrological model for both historical and future climate were used as input to the water management model described in Section 3.2. The water management model computes the amount of prorating (if any) that is required at each model time step (daily). These prorating values are then used in the subsequent agricultural and economic analysis (Section 5).

3.1. Climate and Hydrologic Information

Inflow sequences for the historical period from 1916 to 2006 as well as selected future climate periods were simulated using the VIC hydrology model as described in Elsner et al (2009, this report). Streamflows were produced at locations shown in Figure 1, which are required by the water management model. In general, these points represent inflows to the five reservoirs, as well as inflows below the reservoirs. Future streamflow were provided as quasi-stationary sequences as projected by climate models for the 2020s, 2040s, and 2080s, with more focus on the near-term 2020s simulations. For the 2020s, we ran the water management model with each of 20 streamflow sequences downscaled from individual GCMs for IPCC emissions scenario A1B, and 19 for B1. We also use composites that effectively represent the best estimate of 2020s, 2040s, and 2080s climate

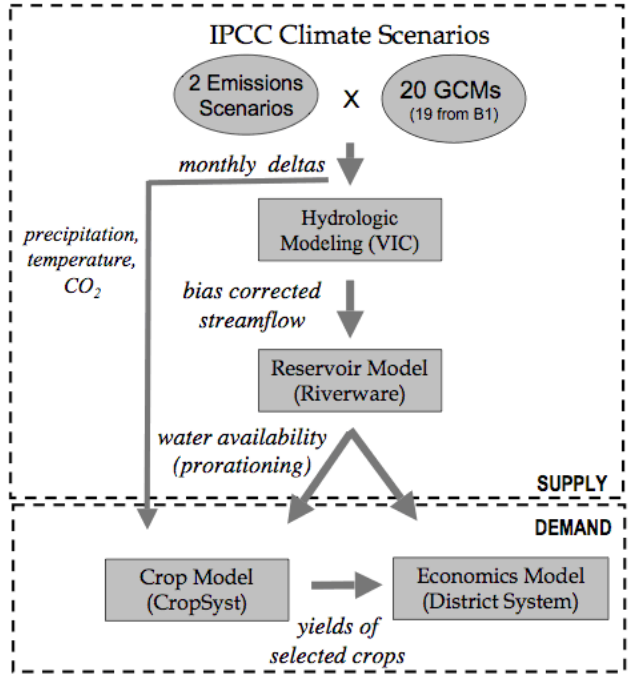

Figure 2. Multi-model process. Schematic of how climate model projections, hydrologic model, and water management models are connected.

Table 2. Annual temperature and precipitation for climate change scenarios.

	2020s (2010-2039)		2040s (2030-2059)		2080s (2070-2099)	
	A1B	B1	A1B	B1	A1B	B1
% Change in Annual Precipitation	+0.22%	+1.9%	+2.1%	+2.2%	+4.9%	+3.4%
% Change in Cool Season Precipitation	+2.3%	+3.3%	+5.4%	+3.9%	+9.6%	+6.4%
% Change in Warm Season Precipitation	-4.2%	-0.9%	-5.0%	-1.3%	-4.7%	-2.2%

Notes: Cool season defined as October through March, while warm season is defined as April through September.

	2020s (2010-2039)		2040s (2030-2059)		2080s (2070-2099)	
	A1B	B1	A1B	B1	A1B	B1
Change in Annual Temperature (°C)	+1.18	+1.08	+2.05	+1.57	+3.52	+2.49
Change in Cool Season Temperature (°C)	+1.05	+1.01	+1.83	+1.42	+3.24	+2.33
Change in Warm Season Temperature (°C)	+1.31	+1.16	+2.26	+1.71	+3.79	+2.66

averaged for the GCMs for each of the two emissions scenarios.

We removed remaining systematic biases in the calibrated streamflow simulations by applying a bias correction procedure trained on historical observations (e.g. the historical period VIC simulation was corrected to match, on a probabilistic basis, reservoir inflows reconstructed from observations by the USBR, referred to in the Hydromet dataset as ‘Computed Natural Flowí). The same bias correction procedure was then applied to future flows. The bias correction method is a quantile mapping technique discussed by Wood et al (2002) and Snover et al (2003). In brief, the technique involves a mapping procedure that matches the statistics of the unregulated flow record with observations at monthly time scales. Simulated daily flows are subsequently rescaled to match the bias-corrected monthly values.

For this study, simulated VIC streamflows were bias corrected to correspond with inflows used by the USBR in their water planning. In this comparison, we use only unregulated (or ‘naturalized’) streamflow, meaning that these flows represent ‘natural’ conditions prior to management alterations. The USBR provided 24-year records of unregulated streamflow for water years 1982-2005. The data included reservoir inflows and local inflows downstream of reservoirs that are required by their water management model. To extend data records beyond 24-years, we used a closely related set of daily unregulated flows (http://www.usbr.gov/pn/hydromet/yakima) for the period 1930-2006. These two sets of unregulated flows differ primarily in the accounting of routing time lags and irrigation return flows. We adjusted the 77-year records to be comparable to the 24 year records using a quantile-mapping bias correction procedure similar to the one outlined above. The longer record was used as the basis for bias correcting VIC output.

The monthly-daily adjustment procedure discussed above does not by construct preserve annual totals. Therefore, as a second step, we bias adjusted the annual total flows at each site, and then made second stage adjustments to monthly flows to add to the annual total, and of daily flows to sum to monthly. We also adjusted to assure that mass balance was preserved over sites by moving from the lowest site (Yakima near Parker), upstream to higher locations. In general, the adjusted 1930-2006 record was similar to the original record, matching both the shape of the hydrograph and its magnitude. During the Autumn and Winter months this process adjusted the VIC’s higher streamflow to match the historic mean by minimizing the late Autumn rain dominated runoff. In the Spring, flows shifted from peak flow in June to peak flows in May, which corresponds to the historical record. Elsner et al. (2009, this report) provides more details on how well historical runs represent the hydrology prior to bias correction. The process followed for adjustment of future climate flows generally paralleled the one outlined above for historical flows. Procedures similar to those outlined above were also implemented to assure mass balance of monthly and annual flows, and across sites.

3.2. Water Management Model

We used a modified version of the reservoir operations model used by USBR in their operational planning, referred to as the ‘water management model' throughout this paper. The model is written in RiverWare™ software (see Zagona et al (2001) for a RiverWare overview) and is one component of the Watershed and Rivers System Management Program (WARSMP), a collaborative effort to simulate water management in the Yakima basin between the U.S. Geological Survey and USBR (Mastin and Vaccaro, 2002). Within the model, simulated system operations are primarily focused on agriculture, however constraints provided by minimum instream flow and other operating requirements are also represented. Because we are focused on capturing the average response of the management system to climate change, reservoirs are operated with the same rules each year regardless of year-to-year maintenance concerns.

To allow the water management model to run with VIC simulated flows (1915-2006 for the historical run, and adjusted 1915-2006 following the delta method for future streamflow projections), we made several modifications to the original model. The version of RiverWare we used was originally constrained to an operations period 1981 to 2003. Because RiverWare saves all variables internally, simulations longer than 25 years are computationally cumbersome. To improve performance, we effectively concatenated simulations of 20-year segments with 5 years of overlap (spin-up). These runs covered periods 1915-1940, 1935-1960, 1955-1980, 1975-2000 and 1981-2006, where the first five years of each sequential run was discarded as spin-up and the 1981 run had more spin up to keep runs a consistent length for batch processing. Because the reservoirs typically refill each year, the spin up period proved more than adequate, and test comparisons using explicit model initialization showed little difference from simulations performed using the spin-up procedure.

Another modification of the water management model was that we used eight inflow locations as shown in Figure 1, including five reservoir inflows (Bumping, Cle Elum, Kachess, Keechelus, Rimrock), and two confluences (Upper Yakima, Naches) and the Yakima River gage at Parker. The operational USBR model has 15 inflow locations, eight of which are intervening flows that include smaller inflow locations such as the American River. We aggregated the intervening flows to three, by subtracting upstream from downstream flows, with negative values set to zero. Intervening flows were inferred from those estimated for the historical period of record. In locations where VIC did not directly produce intervening inflow values, we used the proportion of 1981-2003 long-term averages of these flows to distribute between multiple intervening locations. We compared simulations produced using our simplified setup (5 upstream flow locations and 3 intervening flows) with the USBR setup for the historical period 1981-2003 and found no significant differences in model predictions of water apportionment to the irrigation districts, primarily because the key water allocation decisions in the model are keyed to predicted flows near Parker, which are constrained in our approach to be the same as in the more detailed USBR version of the model. One additional consideration is that the USBR operational model requires forecasts of reservoir inflows through the end of the water year. In our simulations, we assumed perfect knowledge of future streamflows, which allowed prorating values to align with water availability exactly. In the operational setting, managers must make forecasts of how much water will be available based on external streamflow forecast measures.

Prior to this study, the water management model had been run primarily for conditions in 1981 to 2003, and we found several instances in the longer historical record where flow conditions were outside the bounds of the model, a problem that was exacerbated for some of the future climate simulations. To allow the model to run with these new flow conditions, we made several alterations including allowing allocations to junior water users to go to zero, extending the interpolation of anticipated September flow at the Keechelus Reservoir (by linear extrapolation), and disabling computations for the Chandler Canal which is below the Parker gage and therefore was not a factor in this study. With these revisions, all simulations were completed except for one GCM run, the BCCR B1 scenario, which failed in the 1915-1940 period because of an inability of the model to account properly for operations of the Cle Elum Reservoir in these particular sequences of inflows (second warmer and wetter scenario for B1).

The prorating of water is calculated in the water management model for junior and senior water rights according to their monthly prorating entitlements as determined by the Consent Decree of 1945. The water supply available within their allocation is divided by the total amount remaining to obtain a prorating ratio. In the management model, water demands are taken as constant across all projections according to water rights, e.g. the simulations do not allow for the possibility that water demands might change in a future climate.

Results of the historic water management simulation, specifically regulated flow near Parker, reservoir storage and outflow at the Cle Elum Reservoir (the largest reservoir which contributes 42% of the total basin storage), and prorating are shown in Figure 3 and discussed in Section 4. In our presentation of results, years indicate water years (October-September). Most analyses are aggregated to a weekly time step for ease of presentation, where week 1 starts on October 1 (see also Table 3).

Table 3. Week number designations.

week number	date
1	1-Oct
5	29-Oct
10	3-Dec
15	7-Jan
20	11-Feb
25	18-Mar
30	22-Apr
35	27-May
40	1-Jul
45	5-Aug
50	9-Sep

4. Results: Water Supply

In reservoir systems that depend on snowpack to enhance reservoir storage, the more delayed the snowmelt, the greater the effective storage capacity of the reservoir system. As warming progresses, the seasonal peak of simulated reservoir inflows in the Yakima system shift progressively earlier in the year, as more winter precipitation occurs as rain and less as snow (Elsner et al., 2009, this report). To assess how these altered hydrologic conditions impact water supplies, we first evaluate how well water-management-model simulations represent historical operations (Section 4.1). Then in Section 4.2 we show how water deliveries are projected to respond to climate-change scenarios. We subsequently discuss variability of inflows, storage, and outflows in future years and between various locations in the basin (Section 4.3).

4.1. Reservoir System Historical Operations

Figure 3 compares reservoir system historical operations between (1) water management model simulations run using 1917-2006 VIC historical

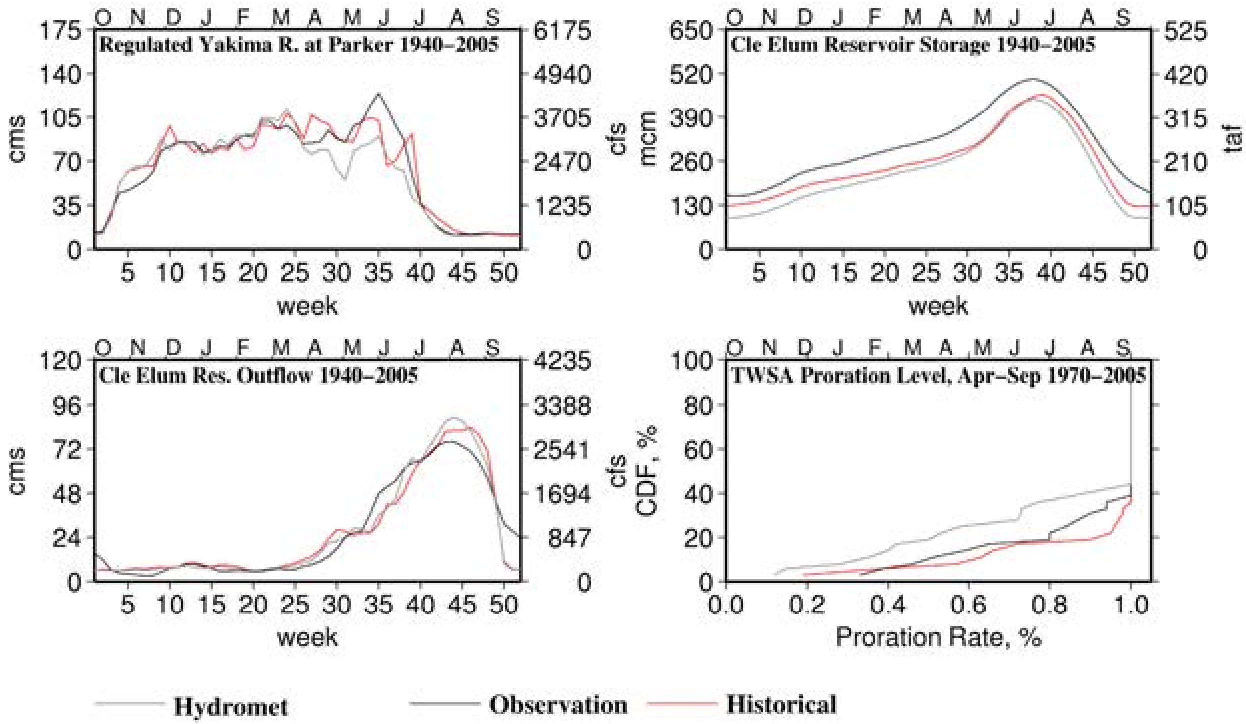

Figure 3. Historic comparisons. Historical regulated flows near Parker, reservoir storage and outflow for Cle Elum reservoir (largest reservoir in the basin) and prorating levels. Years begin on October 1st and end on September 30th.

bias-corrected streamflow (termed '*Historical*') (2) water management model simulations run using the adjusted reconstructed USBR 'Computed Natural Flowí for the period 1930-2006 as discussed in Section 3.2. (termed '*Hydromet*'), and (3) USBR observations of streamflows, reservoir storage, and prorationing values (termed '*Observation*'). *Historical* and *Hydromet* simulated values assume current irrigation demands and operating policies. *Observation* values alternatively reflect actual year-to-year management operations from 1940 to 2005, which differ from the consistent model representation of current operating policies (USBR, 2002; USBR, 2008).

The upper left panel on Figure 3 shows Yakima River regulated flows near Parker from 1940 to 2005. The current reservoir system was in place by 1940, therefore comparisons of simulations with observed flows and storage is only appropriate, with caveats mention above, after 1940. Seasonal average flows are lowest between mid-July and mid-October. They increase gradually from October until December and then increase more rapidly from about 85 cubic meters per second (cms) to 115 cms (3000 to 4000 cubic feet per second (cfs)) in May. In May, flows reach their highest weekly averages before declining as the irrigation season progresses. *Observation*, *Hydromet*, and *Historical* regulated flows have similar seasonality, with the largest divergence occurring in mid-April through May. More regulated flow in the irrigation season for the *Observation* flow is realistic given that reservoir operations and irrigation demands have changed since 1940.

The Cle Elum Reservoir is the largest in the basin (representing 42% of the total basin storage), and we therefore focus on simulated and observed storage at this location (Figure 3, upper right panel). Results for other reservoirs (not shown) were qualitatively similar. Seasonal average storage (units in mcm, or million cubic meters, or taf, thousands of acre feet) in Cle Elum Reservoir peaks at about 490 mcm (400 taf) at the end of May and then declines until September to about 0.123 mcm (100 taf). Storage then increases gradually until April-May, when the rate of reservoir refill increases. On average, throughout the year the Cle Elum Reservoir *Observation* storage is greater by about 61.2 mcm (50 taf) than simulated storage. The difference is not unexpected because reservoir operating procedures and water demands have changed considerably over the last 60 years. Simulated *Hydromet* and *Historical* storage are generally closer to each other than to *Observation* storage, because these simulations reflect the same reservoir operating rules. It is worth noting that *Historical* storages tend to be somewhat higher than *Hydromet*, and our interpretation is therefore somewhat conservative for simulated results in terms of the implications of climate effects on reservoir system performance.

With *Historical* simulations, average weekly reservoir outflows from Cle Elum Reservoir begin to increase in March, peak in July at ~80 cms (~2800 cfs), and decline quickly to ~7 cms (~250 cfs) by the beginning of September (Figure 3, lower left panel). They then remain at about this level through the fall and winter until mid-March. These changes in outflows are largely determined by target instream flows for fish, as outlined in Section 2. In particular, during the low flow months the target is to keep flows relatively low so as to encourage spawning at low flows.

Comparisons between *Observation* reservoir releases and the simulated *Hydromet* and *Historical* reservoir outflows show similar seasonality, however *Observation* outflows have a longer, lower peak than simulated reservoir outflows (see Figure 3, lower left panel). Reservoir outflows are heavily constrained at the end of September at the point of transition in the operating policy (sometimes termed "flip-flop" as described in Section 2), when the source of water deliveries changes from Cle Elum to Rimrock.

As discussed in Section 2, in dry years, not all water allocations can be fulfilled and proratable entitlements are the first to be reduced. To compare prorating levels, we evaluated the cumulative probability distribution of water supplied (Figure 3, lower right panel), which is a way to compare the frequency and the severity of simulated proratings between simulations. Our water management model plausibly reproduces monthly total water supply available (TWSA) water prorating rates that have been set in practice by USBR since 1970. *Observation* prorating has occurred in 13 of 35 years (~37% of the years on the ordinate in Figure 3). This compares closely with our *Historical* (VIC-based) simulations in which prorating occurs in 12 of 35 years. Prorating occurs in 15 of 35 years (~42% of the time) in Hydromet simulations. Prorating values, which we have assessed as annual averages from April to September, have similar trends in all three simulations (Figure 3, lower right); *Observation* prorating values are highly correlated with *Historical* (r=0.96) and *Hydromet* simulations (r=0.96). Actual TWSA observations (*Observation*) only drop to ~37% of prorating, whereas *Hydromet* simulations decline to ~17% and *Historical* simulations decline to ~20%. Year-to-year variability in simulated prorating values are similar to the actual *Observation* prorating values designated by the USBR, especially significant dry years including drought years in the early 1990s, 2001, and 2005. Generally, the water management model run with VIC inflows has more conservative prorating values than predicted by model runs using Hydromet values.

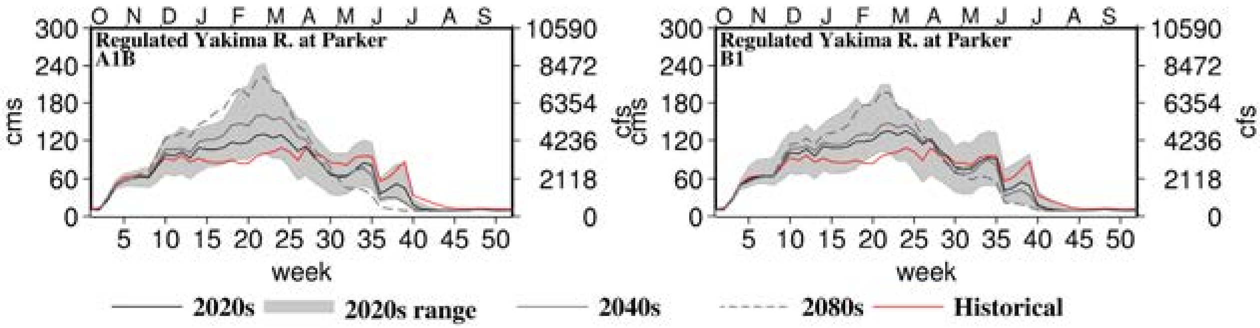

Figure 4. Regulated flow. Simulated regulated flow of the Yakima River near Parker for historical, 2020s, 2040s, and 2080s climate conditions.

Because *Observation* values, which reflect actual operating policies, are not consistent from year to year, we use simulated historical reservoir storages and releases to compare values simulated from the climate change experiments in subsequent sections. Our climate change comparisons are between VIC simulated (rather than actual) historical conditions, and simulated future conditions.

4.2. Water Supply for Agriculture

Figure 4 shows the simulated regulated flow for the Yakima River near Parker for historical, 2020s, 2040s, and 2080s climate conditions. The regulated flows at Parker are key indices of reservoir system performances because they are used in determining TWSA, which in turn determines the proportion of water that is available to junior and senior water right users. Historically, on average regulated flows near Parker are highest in April (115 cms (4000 cfs)) however in simulated historical record they were over 566 cms (20,000 cfs) 40 days in 90 years in December and January and a maximum flow of approximately 50,000 cfs. In the future scenarios, streamflows are higher during the fall and winter seasons and streamflow peaks earlier in the year. For the A1B emission scenarios, in the last week of February flows increase on average to 129.4 cms (4570 cfs) (ensemble range from 103.1 cms (3640 cfs) to 243.2 cms (8590 cfs)) in the 2020s, 160.6 cms (5670 cfs) in the 2040s, and 220.6 cms (7790 cfs) in the 2080s. Then, in June, climate projected flows are less than historical flows until November when reservoirs begin to refill. For B1 scenarios, these trends and timing of changes are similar, although the differences from historical values are smaller. The February average flow is 135.1 cms (4770 cfs) (ensemble range from 103.6 cms (3660 cfs) to 209.2 cms (7390 cfs)) for the 2020s, 147.2 cms (5200 cfs) for the 2040s, and 196.8 cms (6950 cfs) for the 2080s.

In the water management model, when there is insufficient supply for all water users, once junior water rights supply reaches zero, senior water rights are prorated. Subsequent to implementation of TWSA prorating in the 1970s, senior water rights users have always received 100% of their allocation. In our historical simulations with current water demands, infrastructure, and operating rules, junior water rights would have been prorated (less than 100% allocation) in 30% of years, and in just 1% of years (one year, 1941) for senior water rights (top of Table 4a or 4b).

Figure 5 and Tables 4a and 4b show how water rights for junior water

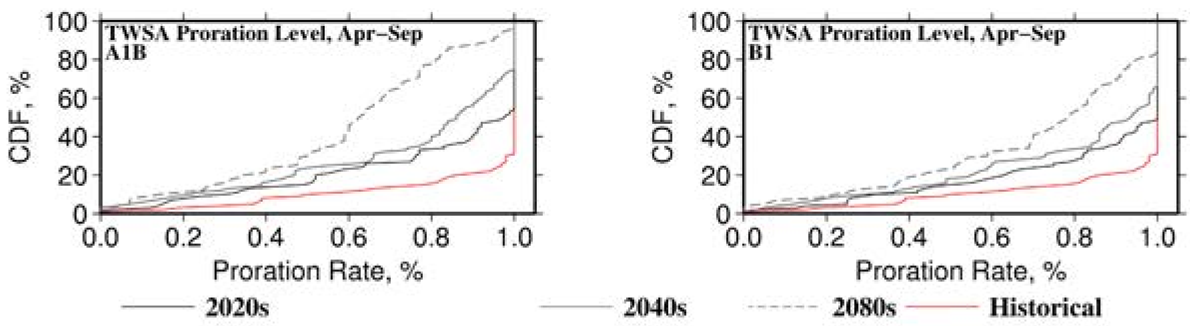

users are simulated to be impacted by climate change. Junior water users experience prorating considerably more frequently. Historically, prorating declines to values below 75% (a approximate threshold beyond which water shortages can no longer be handled without significant impacts to agricultural production and costs) in 14% of years. For the A1B emission scenarios, the fraction of years with prorating values less than 75% increases in the 2020 to 32% for the composite simulation (ensemble range 15% to 54%). These fractions increase to 36% in the 2040s, and 77% in the 2080s. The B1 emission scenario is projected to have a slightly smaller impact on water shortages than A1B. In the 2020s, the fraction of years with prorating values of 75% or less is 27% for the composite simulation, with ensemble range from 14% to 54%. The equivalent fractions for B1 composite case increase to 33% in the 2040s and 50% in the 2080s.

Figure 5. Total Water Supply Available Proration Levels. Cumulative distribution function (CDF) of water supply prorating for junior water users for historical, 2020s, 2040s, and 2080s conditions ranks the likelihood of water supply availability for Junior water users from 0 to 100% of the time (horizontal axis) for April to September average annual values. For example, historically, Junior water users receive 80% or less of their water supply (horizontal axis), 20% of the time (vertical axis). Whereas, they receive 40% or less of their allocated water supply about 8% of the time.

Water deliveries to senior water users drop below 100% for a few climate scenarios and below 75% in the driest scenarios of the 2020s ensembles (1 of 20 for A1B and 2 of 20 for B1). The increased likelihood of senior water user shortfalls indicates that the system will be impacted in ways not previously encountered in the past. Failure to meet senior water rights occurs in 2% of years in the 2020s composite (ensemble range from 0 to 8%) and increases to 3% in the 2040s and 2080s for A1B emission scenarios. For B1 emissions scenarios, the frequencies are slightly less.

4.3. Future System Inflows, Storage, and Outflow

The April 1 snow water equivalent analysis in Elsner et al. (2009, this report) indicates that 78% of the Yakima basin is in what is commonly termed the transition zone, where precipitation transitions many times each winter between rain and snow. Because much of the basin is in the transition zone, it is highly sensitive to temperature changes as discussed further in Elsner et al (2009, this report).

Although natural flow varies throughout the basin, we assess unregulated simulated flow near Parker, which is representative of the basin as a whole (Figure 6). Changes in unregulated flow near Parker and upstream flows have similar trends. It is important to note that these are bias-adjusted flows taken directly from the hydrologic model and represent unregulated conditions. The water management model incorporates these flows at the specific locations indicated in Figure 1 using differences between downstream and upstream locations to generate intervening flows. Unregulated flows in the Yakima basin historically peak in the end of May

Table 4a. Summary of reservoir simulation results for A1B emissions scenario: prorating

AIB	Junior water right prorating: likelihood of having September value drop below					Senior water right prorating: likelihood of having September value drop below		
	100%	**75%**	**50%**	**25%**	**10%**	**100%**	**95%**	**75%**
historical simulation	30%	14%	10%	3%	1%	1%	1%	0%
warmest and wetter:								
hadcm	56%	33%	17%	9%	4%	3%	2%	0%
miroc_3.2	70%	35%	21%	8%	5%	2%	1%	0%
miroc3_2_hi	62%	30%	15%	6%	4%	1%	0%	0%
ipsl_cm4	53%	20%	10%	2%	1%	0%	0%	0%
inmcm3_0	52%	21%	11%	4%	1%	1%	0%	0%
cgcm3.1_t47	50%	24%	13%	3%	2%	0%	0%	0%
warmest and drier:								
ccsm3	80%	54%	33%	14%	10%	6%	6%	0%
hadgem1	69%	39%	25%	14%	6%	4%	4%	0%
gfdl_cm2_1	58%	37%	25%	10%	8%	4%	4%	0%
warmer and drier :								
echo_g	67%	54%	40%	19%	9%	8%	8%	1%
fgoals1_0_g	68%	44%	30%	14%	8%	6%	6%	0%
pcm1	59%	44%	28%	12%	7%	3%	3%	0%
gfdl_cm2_0	58%	35%	20%	9%	2%	1%	0%	0%
giss_er	48%	29%	14%	8%	2%	2%	1%	0%
warmer and wetter:								
csiro_3_5	51%	26%	14%	8%	2%	1%	0%	0%
cgcm3.1_t63	50%	18%	10%	4%	1%	0%	0%	0%
giss_aom	50%	28%	14%	6%	2%	1%	0%	0%
cnrm_cm3	41%	22%	13%	7%	2%	1%	1%	0%
echam5	45%	24%	13%	3%	2%	1%	0%	0%
bccr	33%	15%	11%	4%	2%	0%	0%	0%
Composites								
2020	52%	32%	17%	9%	2%	2%	1%	0%
2040	74%	36%	24%	11%	6%	3%	3%	0%
2080	95%	77%	33%	13%	9%	3%	2%	0%

* Delta categories of warming and dry/wet are based on annual deltas.
* More information on GCM properties and selection can be found in Mote and Salathˇ (2009, this report).

Figure 6 (right). Basin-average reservoir inflow. Simulated unregulated flow (flow that would occur in the absence of reservoirs and irrigation withdrawals) near Parker for historical, 2020s, 2040s, and 2080s conditions.

Table 4b. Summary of reservoir simulation results for B1 emissions scenario: prorating

B1	Junior water right prorating: likelihood of having September value drop below					Senior water right prorating: likelihood of having September value drop below		
	100%	**75%**	**50%**	**25%**	**10%**	**100%**	**95%**	**75%**
historical simulation	30%	14%	10%	3%	1%	1%	1%	0%
warmest and wetter:								
miroc_3.2	57%	29%	13%	7%	3%	1%	0%	0%
miroc3_2_hi	74%	34%	18%	8%	5%	2%	0%	0%
ipsl_cm4	52%	22%	11%	3%	2%	0%	0%	0%
cgcm3.1_t47	58%	28%	14%	8%	2%	1%	0%	0%
cgcm3.1_t63	64%	32%	17%	8%	5%	2%	0%	0%
warmest and drier, or less wet:								
ccsm3	77%	54%	37%	15%	12%	8%	7%	1%
echo_g	74%	58%	39%	21%	12%	10%	9%	1%
hadcm	48%	28%	15%	7%	2%	2%	1%	0%
warmer and drier, or less wet :								
fgoals1_0_g	54%	33%	17%	9%	3%	1%	0%	0%
pcm1	39%	25%	14%	4%	2%	0%	0%	0%
echam5	47%	25%	14%	7%	2%	1%	1%	0%
gfdl_cm2_0	50%	32%	17%	9%	2%	0%	0%	0%
gfdl_cm2_1	50%	32%	15%	8%	2%	1%	1%	0%
warmer and wetter:								
csiro_3_5	30%	15%	7%	4%	1%	0%	0%	0%
giss_aom	50%	25%	13%	7%	2%	1%	0%	0%
giss_er	46%	25%	13%	3%	2%	1%	0%	0%
cnrm_cm3	39%	14%	10%	3%	1%	0%	0%	0%
bccr	NA	NA	NA	NA	NA	NA	NA	NA
inmcm3_0	40%	19%	11%	4%	2%	1%	0%	0%
Composites								
2020	48%	27%	15%	6%	2%	2%	1%	0%
2040	65%	33%	18%	9%	6%	2%	1%	0%
2080	82%	50%	26%	11%	7%	3%	1%	0%

* Delta categories of warming and dry/wet are based on annual deltas.

* More information on GCM properties and selection can be found in Mote and Salathˇ (2009, this report).

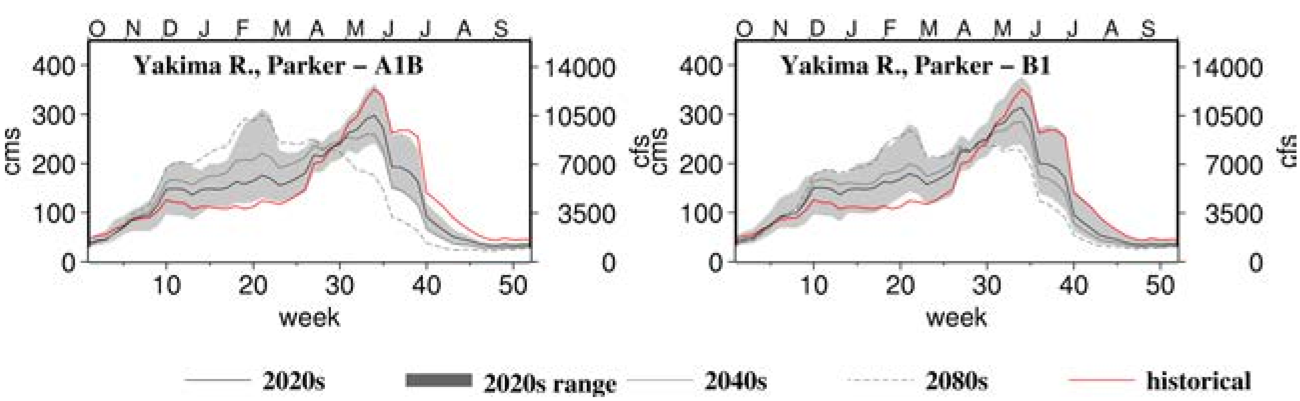

at an average of 340 cms (~12,000 cfs) and they are at their lowest in September at ~55 cms (~2000 cfs).

In the A1B emission scenarios, the May peak flow declines in the 2020s composite run to ~280 cms (~10000 cfs) (ensemble range from ~225 cms (~8000 cfs) to 370 cms (~13000 cfs)), then declines further to 255 cms (~9000 cfs) in the 2040s composite and further declines and shifts earlier to mid-February at 225 cms (~8000 cfs) in the 2080s composite (Figure 6). In the B1 emissions scenarios, the peak streamflow declines in the 2020s composite to ~310 cms (~11000 cfs) (ensemble range from ~225 cms (~8000 cfs) to 370 cms (~13000 cfs)), ~280 cms (~10000 cfs) in the 2040s composite, and 255 cms (~9000 cfs) in the 2080s composite with the 2080s peak shifting to February (Figure 6). Low flows in both A1B and B1 emissions scenarios decrease slightly, but not dramatically.

Figure 7 shows how reservoir storage varies throughout the basin as the climate changes. Total system storage (Figure 7, top panel) is, on average, highest historically at the end of June at 1,140 mcm (~ 923 taf). In A1B emission scenarios, the peak in storage occurs 2 weeks earlier for the 2020s composite at 1.098 mcm (890 taf) (ensemble range from 941 to 1,114 mcm, or 763 to 968 taf), 4 weeks earlier in the 2040s at 1.122 mcm (910 taf), and 5 weeks earlier in the 2080s at 1.131 mcm (917 taf). In all future projections, storage is less than historical storage levels from mid-June through January. Between January and June future storage values increase. With the B1 emission scenarios, changes in basin-wide storage are less substantial, especially in the 2080s. The peak in storage occurs 2 weeks earlier in 2020s composite run at 1,118 mcm (906 thousands af) (ensemble range 940 to 1,176 mcm, or 762 to 953 taf,) and 3 weeks earlier in the 2040s at 1.120 mcm (908 taf), and 4 weeks earlier in the 2080s at 1.130 mcm (916 taf).

In addition to the combined reservoir flows, storage in each of the five reservoirs changes, more or less in concert with total system storage (Figure 7), although reservoir storage varies between reservoirs according to specific management goals as well as the capacity and inflows of each reservoir. In general, summer reservoir storage declines and winter storage increases, although the magnitude and extent of these differences are most notable in winter storage in Bumping Reservoir and through much of the year in Kachess. Bumping has the smallest reservoir capacity to annual runoff ratio (0.2), whereas Kachess has the largest (1.1), effectively, this means that Kachess does not fill even in years of "normal" flow, whereas Bumping can refill multiple times throughout a year.

Tables 5a and 5b summarize projected storage changes for the five major reservoirs in October, the month when the entire system capacity is at its lowest. Under historical conditions, reservoirs drop below 10% of their capacities on average, ranging from 53% of the time for Keechelus to 7% of the time for Bumping. In the 2020s A1B ensembles, for the warmest and driest ensemble members, storage is likely to drop below current levels. The warmer and wetter scenarios are closest to historical values, but are still substantially more likely to drop below 10% of capacity. Considering all of the 2020s ensemble members, there is a substantial incidence of lower early fall reservoir storage. For example, historically Cle Elum Reservoir drops below 10% of capacity 1 out of every 3 years, whereas in

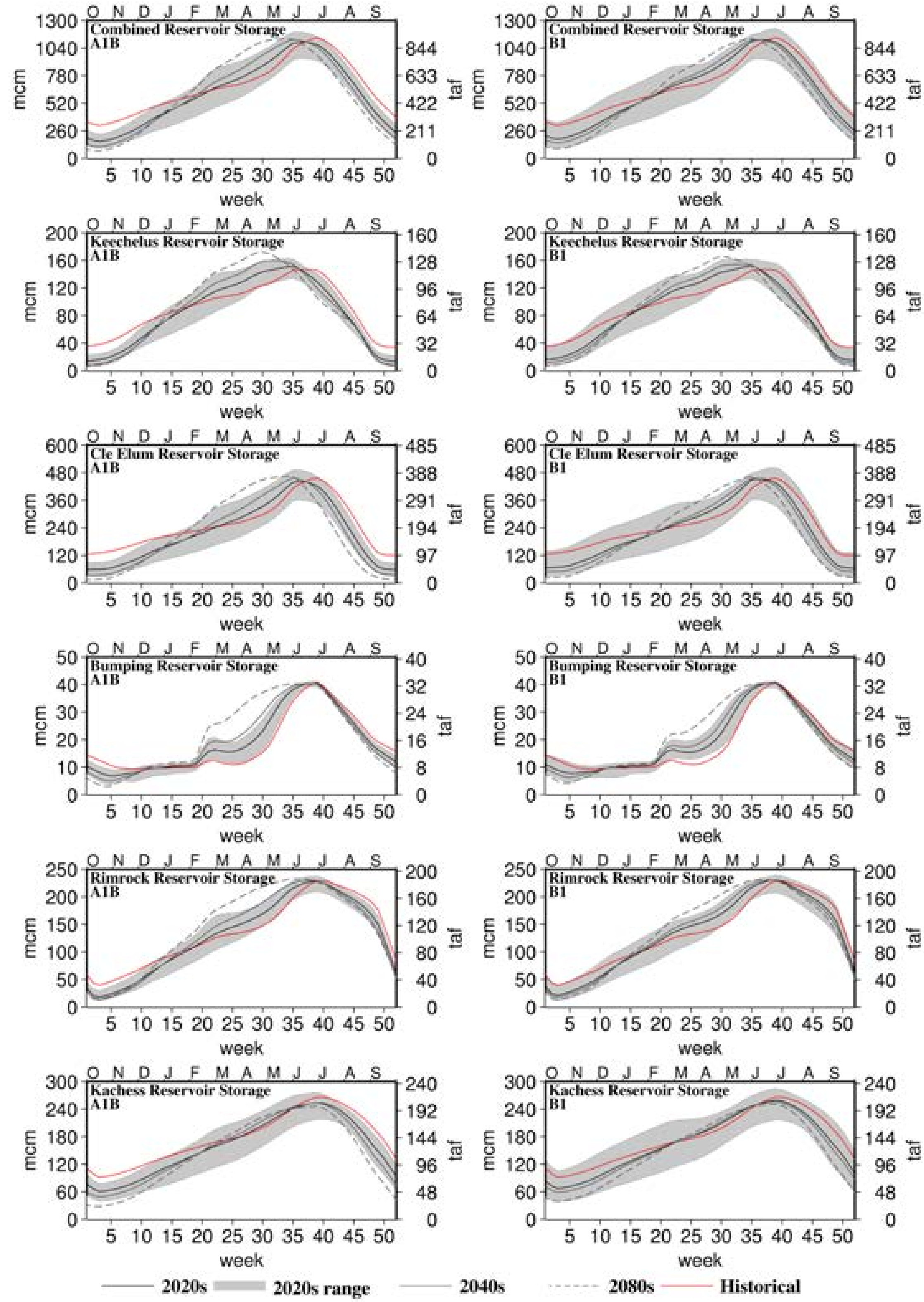

Figure 7. Reservoir storage. Simulated reservoir storage for the combined system (top panel) and for each of the five major reservoirs (lower five panels) for historical, 2020s, 2040s, and 2080s conditions.

Table 5a. Summary of reservoir simulation results for A1B emissions scenario: reservoir storage

AIB	Likelihood of October Reservoir Storage dropping below 10%				
	Cle Elum	**Keechelus**	**Bumping**	**Rimrock**	**Kaches**
historical simulation	33%	53%	7%	34%	19%
warmest and wetter:					
hadcm	60%	80%	27%	63%	37%
miroc_3.2	69%	84%	28%	64%	40%
miroc3_2_hi	68%	81%	25%	59%	38%
ipsl_cm4	59%	80%	20%	60%	26%
inmcm3_0	59%	82%	23%	61%	28%
cgcm3.1_t47	54%	73%	16%	48%	31%
warmest and drier:					
ccsm3	78%	94%	42%	71%	52%
hadgem1	62%	78%	25%	59%	39%
gfdl_cm2_1	67%	81%	27%	60%	43%
warmer and drier :					
echo_g	73%	85%	35%	69%	57%
fgoals1_0_g	72%	84%	31%	65%	50%
pcm1	66%	79%	26%	58%	48%
gfdl_cm2_0	63%	76%	22%	52%	37%
giss_er	49%	71%	19%	50%	33%
warmer and wetter:					
csiro_3_5	54%	77%	21%	56%	34%
cgcm3.1_t63	59%	72%	16%	51%	26%
giss_aom	57%	76%	18%	54%	38%
cnrm_cm3	46%	72%	19%	55%	28%
echam5	47%	69%	12%	40%	26%
bccr	44%	68%	12%	49%	25%
Composites					
2020	63%	79%	23%	60%	37%
2040	76%	88%	34%	70%	41%
2080	91%	93%	53%	65%	67%

* Delta categories of warming and dry/wet are based on annual deltas.
* More information on GCM properties and selection can be found in Mote and Salathé (2009, this report).

Table 5b. Summary of reservoir simulation results for B1 emissions scenario: Reservoir storage

B1	Likelihood of October Reservoir Storage dropping below 10%				
	Cle Elum	**Keechelus**	**Bumping**	**Rimrock**	**Kaches**
historical simulation	33%	53%	7%	34%	19%
warmest and wetter:					
miroc_3.2	62%	81%	25%	60%	36%
miroc3_2_hi	73%	84%	32%	63%	40%
ipsl_cm4	59%	73%	19%	50%	29%
cgcm3.1_t47	59%	74%	22%	51%	36%
cgcm3.1_t63	62%	80%	26%	58%	39%
warmest and drier, or less wet:					
ccsm3	77%	90%	35%	65%	51%
echo_g	77%	90%	40%	70%	58%
hadcm	52%	72%	19%	53%	35%
warmer and drier, or less wet :					
fgoals1_0_g	62%	74%	20%	58%	37%
pcm1	43%	65%	13%	50%	31%
echam5	53%	72%	17%	56%	33%
gfdl_cm2_0	56%	73%	20%	60%	38%
gfdl_cm2_1	59%	77%	21%	57%	37%
warmer and wetter:					
csiro_3_5	42%	69%	10%	46%	21%
giss_aom	56%	75%	19%	54%	31%
giss_er	49%	70%	16%	47%	27%
cnrm_cm3	43%	71%	13%	52%	19%
bccr	NA	NA	NA	NA	NA
inmcm3_0	44%	71%	15%	52%	27%
Composites					
2020	55%	76%	20%	55%	34%
2040	63%	81%	26%	58%	39%
2080	86%	91%	41%	70%	47%

* Delta categories of warming and dry/wet are based on annual deltas.
* More information on GCM properties and selection can be found in Mote and Salathé (2009, this report).

the 2020s composite (A1B emissions), it drops below this level in 63% of years (ensemble range 44% to 78%) of the time. This percentage increases to 76% in the 2040s and to 91% in the 2080s. B1 emission scenarios have similar trends, although the frequency of low storage is somewhat less than for A1B.

Unlike the municipal systems in the Puget Sound basin (Vano et al, 2009a, this report), in the Yakima system demands are reduced substantially until the beginning of the irrigation season the following spring. However, low carry-over at the end of the irrigation season can impact the system's ability to meet instream flows due to hydraulic capacity limitations or insufficient volumes to supplement natural flows. [2] Therefore the increase in the frequency of this condition shows that the system may be under increased water stress with progressing climate change. Furthermore, USBR attempts to maintain some reservoir storage carry-over, especially in the Kachess Reservoir, which has a relatively high storage to inflow ratio. Carry-over storage is especially important when the upcoming fall and winter are dry. Reservoir outflows (Figure 8) reflect similar variations in the total system and in particular storage components within the system.

5. Economic Impacts on Irrigated Agriculture

An economic analysis of the impacts of climate change on Yakima basin perennial crops was conducted using two models: the CropSyst model (Stöckle and Nelson, 1996; Stöckle, et al., 2003) (which simulates irrigated crop response to climate change) and the Irrigation District System Model (which projects economic impacts), briefly described in this paper. The perennial crops analyzed include apples and sweet cherries, which represent 48 percent of the region's crop value. For this analysis, we used the A1B and B1 emissions scenarios and the composite model runs for the 2020s, 2040s and 2080s. Comparisons over time were performed with composite model runs. For each time period, potential fertilization effects CO_2 were simulated for the average CO_2 levels expected in both the A1B and B1 scenarios for each time step. Higher future average CO_2 levels are believed likely by many researchers to increase the future effectiveness of photosynthesis in many crops as well as reduce the plants' loss of water in transpiration. The strength and longevity these effects are still a matter of both some controversy and active field research. (The likely effects of CO_2 on plants are described in Stöckle et al. (2009, this report) and methods for incorporating CO_2 effects in Cropsyst in Stöckle et al. 2003). The Cropsyst analysis for this paper was done both with and without CO_2 fertilization effects for both the A1B and B1 scenarios. The Cropsyst yield estimates include the effects of changed growing weather and the impacts of prorationing resulting from projected climate change for the composite scenario for the 2020s, 2040s, and 2080s. (See Table 6.) They are discussed in Section 5.2.

[2] Future considerations such as additional mandated fish flows or additional endangered species designations could make winter flows a larger consideration.

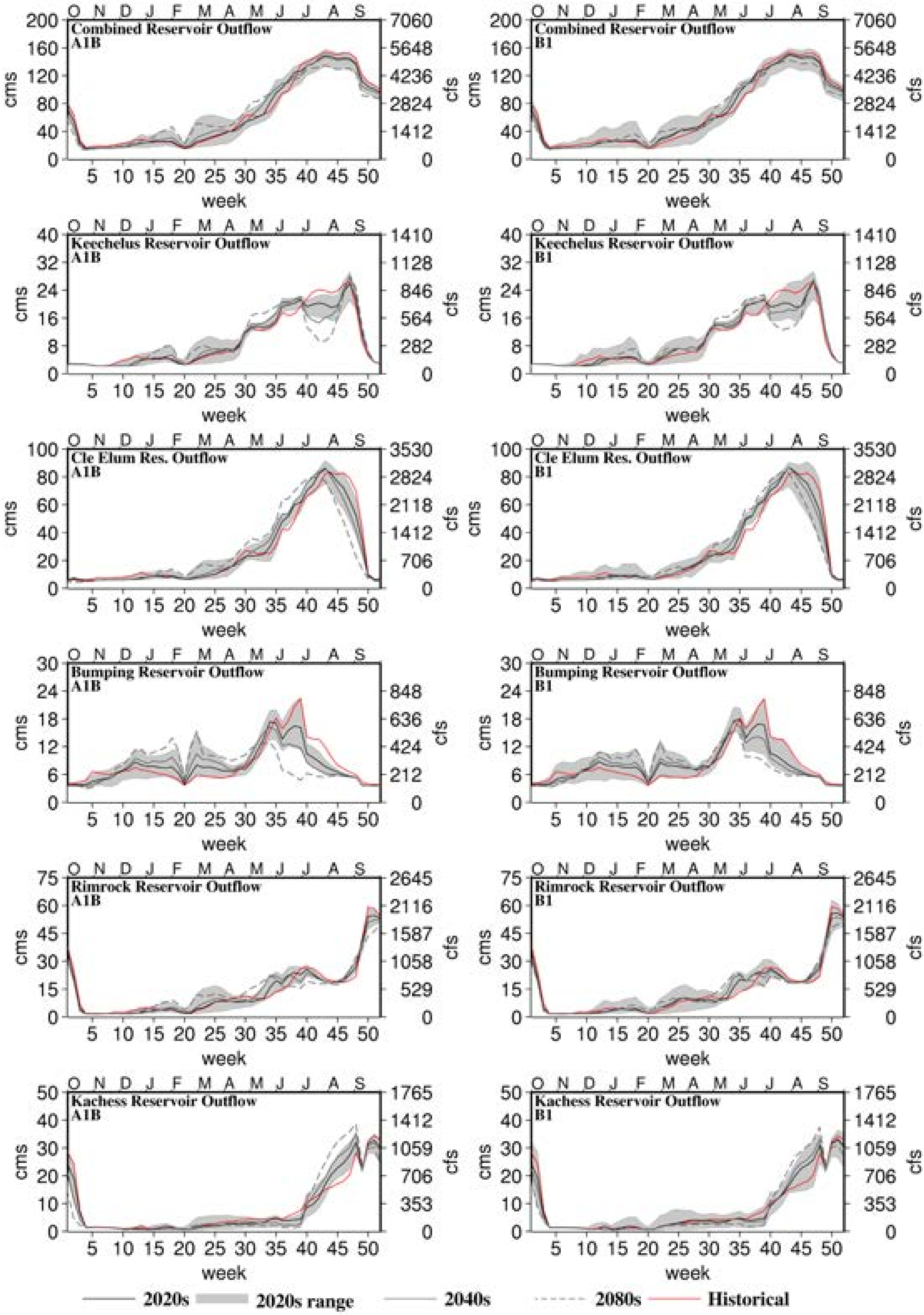

Figure 8. Reservoir outflow. Projected reservoir outflow for the combined system (top panel) and for each of the five major reservoirs (lower five panels) for historical, 2020s, 2040s, and 2080s conditions.

Table 6. Agricultural economics assumptions and data for apples and sweet cherries

		Apples				Sweet Cherries			
Statewide Yields 1995-2007, Tons/Acre (Junior and Senior Lands Combined)									
	Mean	17.2				4.61			
	Standard Deviation	1.74				0.72			
Cropsyst Model Scenario Composite Case Yields, by Time Period and Scenario, with and without CO2 Fertilization									
		Mean (senior)	Mean (junior)	Std Dev (senior)	Std Dev (junior)	Mean (senior)	Mean (junior)	Std Dev (senior)	Std Dev (junior)
	Historical	22.2	20	1.2	5.3	8.9	8.1	0.9	1.9
2020 A1B	No CO2	19.7	15.8	0.9	6.1	7.4	6	0.8	2.2
	CO2	21	17	1	6.6	8	6.4	0.9	2.3
B1	No CO2	19.7	16.4	0.9	5.8	7.4	6.2	0.8	1.9
	CO2	20.8	17.4	0.9	6.1	7.8	6.5	0.9	2.2
2040 A1B	No CO2	19.1	15.7	1	5.1	7	5.5	0.7	2.1
	CO2	21.6	17.8	1	5.6	8	6.2	0.9	2.5
B1	No CO2	19.3	15.9	0.9	5.4	7.2	5.8	0.8	2.2
	CO2	21.2	17.5	0.9	5.8	8	6.5	0.9	2.4
2080 A1B	No CO2	17.9	12.4	1.2	4.6	6.3	4	0.8	2.1
	CO2	22.2	15.7	1.4	5.5	7.9	5	1	2.5
B1	No CO2	18.6	14.6	1.1	5	6.8	4.9	0.8	2.1
	CO2	21.5	16.9	1.1	5.6	7.9	5.8	0.9	2.5
Statewide Prices (Dollars/Ton)									
	Historical Average Price per Ton (2000-2007)	$401				$1,741			
	Standard Deviation in Price (1995-2007)	$109				$309			
	Price Sensitivity to Yield	= Random Normal(0, $109)+$795-$25.008 x Yield				Random Normal ($1,741, $309)			
Production Cost Data (2007 Dollars per Acre)									
	Total Variable Production Cost per Acre	$6,543				$5,188			
	Picking Labor and Transportation per Acre	$1,526				$2,176			
Estimated Acreages of Crops (Yakima Irrigation Project)									
	Senior	22,842				3,138			
	Junior	39,267				6,370			
	Total	62,109				9,508			

5.1. Economic Analysis Approach

The economic simulations calculate the impact of climate change on value of farm output and net profit for apple and cherry growing operations in Yakima basin that are similar to those prevailing in 2007. Therefore, the simulations reflect the potential impacts of climate change on Yakima basin farm operations for today's economic conditions, not those that might evolve over the next 20, 40, or 80 years.

Economic risks associated with changes in yield were evaluated with a spreadsheet-based model of Yakima River Basin irrigated agriculture called the Irrigation District System Model (IDSM). The IDSM takes as input statistical distributions of per- acre yields of apples and cherries shown in Table 6 for the historical simulation from 1975-2004, with delta method climate change projections applied to this 30 year period as described earlier for the 2020s (2010-2039), 2040s (2030-2059), and 2080s (2070-2099). The model sampled values from these distribution of crop yields from Cropsyst using Crystal Ball® (Oracle 2009) and multiplied the per-acre yields times the estimated acreage of apples and cherries operated by junior and senior irrigators in the Yakima basin irrigation districts to obtain statistical distributions of total production for each time period for junior and senior irrigators. It also multiplied sampled per-acre yields times sampled values of 2000-2007 crop prices from Table 6 to obtain statistical distributions of per acre value of output, and subtracted estimated year 2007 operating costs per acre to obtain statistical distributions of net operating profit per acre. Both these values are multiplied times the affected acreages to obtain estimates of the total impact on value of production and net operating profit. Acreages are shown in Table 6.

Crop price can be either statistically associated with local yields or may be somewhat independent, depending on market circumstances. For example, there is a statistically significant negative correlation in Washington between statewide average yields and prices, with prices declining about $25 per ton of increase in yield during the period 1995-2007[3]. That relationship has been included in the economic projections. Analysis of prices for cherries showed highly variable prices, but did not show a similar statistically significant historical relationship to yields[4], so cherry prices were allowed to vary independently. Operating costs came from Washington State University crop budget information for apples and sweet cherries.[5] They vary with yield. In water-short years, a smaller or non-existent harvest would result in savings of costs closely related to harvest such as picking labor and transportation (Table 6).

Most water charges in Yakima Valley irrigation districts are fixed charges (since these charges are primarily levied by irrigation districts for retirement of capital debt and maintenance of distribution systems), so those costs would not be saved in water-short years. Many farmers that have proratable water supplies also have emergency wells that they use during droughts. Because wells take more energy to operate than gravity-fed irrigation district water, water costs can actually increase (this would have added to the production costs, but also would have reduced crop losses in water-short years).

5.2. Economic Impacts

Table 6 shows the Cropsyst-estimated impact of climate change on yields for A1B and B1 emissions scenarios for apples and for sweet cherries grown

[3]Statewide apple yields varied from 14.6 tons per acre to 19.9 tons per acre during the period, and prices ranged from $230 to $580 per ton. Also, see Table 6.
[4]Statewide sweet cherry yields varied from 3.35 to 5.48 tons per acre, and prices varied from $1310 to $2440 per ton, but there was no relationship noted between price and yield based on historical statewide data. Also see Table 6.
[5]Crop budgets were supplied by Suzette Galinato, IMPACT Center, Washington State University, on September 22, 2008.

by senior and junior water users, compared with the corresponding yields for historical conditions (1975-2004). While there are other important crops in the Yakima River basin (for example, timothy hay in the upper part of the basin in Kittitas County, wine grapes in Yakima and Benton Counties, and mint and hops in Yakima County), apples and cherries have among the highest dollar yields (regionally and statewide in 2007), and have among the highest values per acre. Both are also perennial crops, which are rarely modeled in climate impacts work, both are sensitive to growing weather and water shortages, and they span the growing season (cherries are an early crop, harvested in June, and apples are a late crop, harvested in September or October). The means and standard deviations shown in Table 6 are for individual crop years for the 30-year periods indicated and do not account for potential carryover losses associated with potential loss of entire trees, or for any additional effects of persistent drought. The analysis also ignores effects of climate on fruit size, quality, and marketability.

The adverse effect of climate change on yield is apparent in these Cropsyst runs. While the impacts differ substantially by year, it is apparent that, notwithstanding a positive CO_2 fertilization effect, warmer future climate generally results in lower yields than in the historical period, mostly due to water stress. This is apparent for both crops, both scenarios, and with and without CO_2 fertilization effects. Junior water users (whose irrigation water is sometimes prorated and prorated more frequently as the century progresses) experience more steeply declining yields than do senior water users. CO_2 fertilization effects potentially offset many of the effects of higher temperatures and reduced water availability. An example of this occurs in Table 6 for apples between 2020 and 2040 for junior water users in the A1B scenario. In 2020 no-CO_2 case the average yield for junior water users is 15.8 tons per acre, whereas in the CO_2 case it is 17.0 tons per acre. In addition, between 2020 and 2040 in the no-CO_2 case the average yield falls from 15.8 tons to 15.7 tons, whereas in the CO_2 case, higher average CO_2 in 2040 leads to an increase in yields from 17.0 tons to 17.8 tons. This effect does not persist, however. In the 2080 period the lack of water dominates, with average yields falling back to the 15.7 ton level, even with CO_2 fertilization.

A secondary effect of warming is an earlier and reduced growing season and a reduction in the need for irrigation. Table 7 shows the effect of warming with and without the CO_2 fertilization effect on reducing season length and net requirement for irrigation, By the end of the century, the growing season begins 10 to 20 days earlier and ends up to 30 days earlier for apples, shortening the growing season by between 3 days and two weeks. With climate change and earlier and shorter season irrigation requirements, water demands are reduced by as much as 37% for apples and 47% for cherries in the 2080s in the A1B case without a CO_2 fertilization effect. The additional amount of water saved with CO_2 fertilization is about 4% for apples and 2% for cherries. However, in the absence of adaptation, the increasing frequency and severity of water shortages as the century progresses increases the number and severity of water stress days, and yields decline on average, as shown in Table 6.

The negative impact on yields adversely affects growers' incomes. Figure 9 shows the impact of the warming scenarios on the cumulative probability

Table 7. Season length in days and net requirements for irrigation for apples and cherries in the A1B and B1 emissions scenarios for the 2020s, 2040s, and 2060s (mm/season)

			Average Season Length			Net Required Irrigation	
			Bud Break (day)	Maturity (day)	Season Length (day)	Average (mm/season)	Std Dev (mm/season)
Apples							
		Historical	89	243	151	656	166
2020	**A1B**	**No CO2**	81	228	146	529	182
		CO2	81	227	146	524	182
	B1	**No CO2**	81	227	147	537	170
		CO2	81	228	147	530	167
2040	**A1B**	**No CO2**	79	222	143	515	159
		CO2	79	222	143	501	155
	B1	**No CO2**	80	225	145	524	167
		CO2	80	225	145	512	161
2080	**A1B**	**No CO2**	76	213	138	415	143
		CO2	76	213	138	384	130
	B1	**No CO2**	78	219	141	478	155
		CO2	78	219	141	462	149
Sweet Cherries							
		Historical	88	209	121	448	118
2020	**A1B**	**No CO2**	74	197	124	333	136
		CO2	74	197	124	333	134
	B1	**No CO2**	73	198	125	344	124
		CO2	73	198	125	343	128
2040	**A1B**	**No CO2**	70	192	122	311	127
		CO2	70	192	122	312	131
	B1	**No CO2**	71	195	124	323	134
		CO2	71	195	124	325	134
2080	**A1B**	**No CO2**	65	175	118	239	124
		CO2	65	183	118	226	110
	B1	**No CO2**	68	189	121	285	129
		CO2	68	189	121	287	132

distributions of per-acre value of crop yields for apples and cherries in the period of the 2020s, 2040s, and 2080s (in the absence of adaptation) at 2000-2007 prices and 2007 costs . The figure indicates a substantial shift toward lower yields and therefore, lower values per acre. For apples it also shows the effect of CO_2 fertilization and the inverse effect of lower yields causing higher prices. Cherries do not have a price effect in this analysis, and are an early seasonal crop that may not be able to take advantage as apples do of higher CO_2 in the 2040s. As a consequence, in Table 6 yields and values of cherry production in Figure 9 fall between the 2020s and the 2040s for those with junior water rights. For senior irrigators, CO_2 fertilization appears to increase yields and warmer weather appears to produce less negative effects on yields, as shown in Table 6.

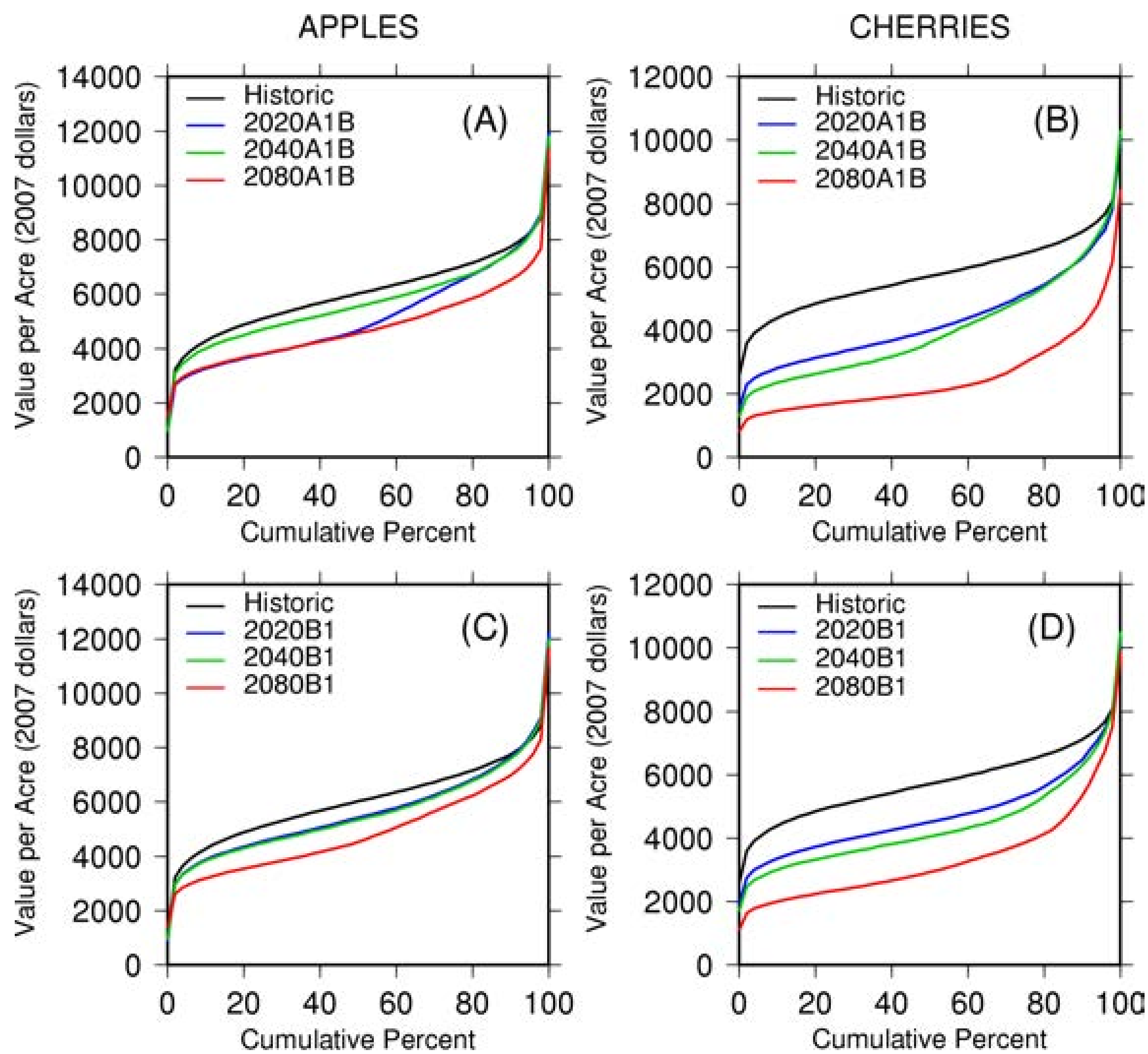

Figure 9. Impact of climate change for junior irrigators of apples A1B (A), cherries A1B (B), apples B1 (C), and cherries B1 (D) on value of production per acre in the 2020s, 204s, and 2080s.

Table 8 shows the impact of climate change on average physical yields and on the mean and standard deviations of per-acre value of production, per-acre operating profit, and overall value of production for apples and cherries in the Yakima River basin. The table shows that in all three future time periods (2020s, 2040s, and 2080s) and for both crops, lower water availability substantially reduces the per-acre average value of production as well as net operating profit. In addition, there is an increasing probability of poor harvest years, leading to greater and more frequent operating losses. Table 8 shows that the expected annual operating profit on junior land raising cherries goes from a net profit to a net loss in both the A1B and B1 scenarios and that apples become increasingly unprofitable. These losses can be attributed to lack of water. With full water availability, as Table 6 shows, the projected climate change would not be harmful. These negative results for water-limited apple production indicate why there is the difference from the generally positive results for fully irrigated apples reported by Stöckle et al. (2009, this report).

The estimated expected average loss of annual value of production for these two crops from climate change ranges between \$23 million (2020s, B1 scenario) and \$70 million (2080s, A1B scenario) per year, even with CO_2

Table 8. Impact of climate change (A1B and B1 scenarios) on value of production, operating profit, and aggregate value of production for irrigated apples and cherries in the Yakima River basin, 2020s, 2040s, and 2080s

		Historical Conditions (1975-2004)	A1B 2020s	B1 2020s	A1B 2040s	B1 2040s	A1B 2080s	B1 2080s
Average and Standard Deviation of Value Per Acre, Junior Water Rights Growers (2007 Dollars)								
Apples	Expected Value	$6,017	$5,118	$5,599	$5,659	$5,531	$4,763	$4,867
	Standard Deviation	$1,357	$1,694	$1,501	$1,399	$1,486	$1,277	$1,504
Cherries	Expected Value	$5,733	$4,311	$4,729	$4,028	$4,364	$2,492	$3,325
	Standard Deviation	$1,073	$1,394	$1,266	$1,601	$1,342	$1,204	$1,420
Average and Standard Deviation of Annual Operating Profit/Acre, Junior Water Rights Growers (2007 Dollars)								
Apples	Expected Value	($14)	($729)	($367)	($291)	($403)	($914)	($867)
	Standard Deviation	$1,357	$1,470	$1,394	$1,332	$1,371	$1,148	$1,317
Cherries	Expected Value	$1,163	$128	$432	($79)	$166	($1,197)	($590)
	Standard Deviation	$1,046	$1,151	$1,091	$1,275	$1,118	$936	$1,119
Average and Standard Deviation of Total Annual Value of Production (Million 2007 Dollars)								
Apples	Expected Value	$379,392	$344,102	$362,963	$365,343	$360,297	$330,148	$334,228
	Standard Deviation	$96,157	$100,173	$97,931	$95,280	$96,906	$86,114	$92,834
Cherries	Expected Value	$61,663	$52,616	$55,272	$50,813	$52,953	$41,038	$46,343
	Standard Deviation	$11,127	$11,911	$11,493	$12,810	$11,680	$10,166	$11,593
Total	Expected Value	$441,055	$396,718	$418,235	$416,156	$413,250	$371,187	$380,571

fertilization. This decline is between 5% and 16% of historical averages for these crops and between 2% and 5% of the total value of the $1.3 billion of crops and animal products produced in the three counties (Yakima, Benton, and Kittitas) that correspond to the Yakima basin (USDA 2004). It does not account for additional economic losses that may arise from loss of or permanent damage to trees, from carryover effects on yields, or from effects on fruit size, quality, or marketability. It also does not account for the impacts on other crops. An average 5% to 16% decline in the $913 million in (mostly irrigated) crops produced annually in the three counties would range from $46 million to $146 million per year.

6. Conclusions

Climate change is projected to impact water supply within the Yakima River basin, especially for water users with junior water rights and - in the most extreme years – users with senior water rights. Due to changes in seasonal patterns of runoff, the system is projected to become increasingly unable to meet deliveries to junior water rights, and these increased occurrences of curtailments for junior water users may be substantial even in the 2020s. In the recent historical record, the Yakima basin has been significantly water short (as defined by 75% or less of prorating for junior water users) 14% of the years. Without adaptations, projections of the A1B emission scenarios indicate that this value may increase to 32% (with a range of 15% to 54%

over ensemble members) in the 2020s, and may increase further to 36% in the 2040s, and 77% in the 2080s. The B1 emissions scenario would likely have a slightly smaller impact on water shortages than A1B. In the 2020s, our projections show chances of prorating may occur in 27% of years for the composite runs (with an ensemble range from 14% to 54%), 33% for the 2040s and 50% for the 2080s.

Assuming current water rights and operating policies, these changes in system performance may result in decreases in economic value of crop production. Even with earlier crop development, which may somewhat reduce the impacts of summer water shortages, the expected value of production on junior lands may decline substantially as early as the 2020s. Without adaptation, the expected annual profits of perennials on junior land are much more likely to be negative, putting the success of many farm operations in doubt. In addition, the total annual value of farm production for the two crops discussed may decline anywhere from about $23 million to $70 million, depending on the time period and scenario, about 2% to 5% of total current farm production in the three counties that correspond to the Yakima River basin. Because many junior acres in the Yakima are devoted to other crops that would also be harmed by water shortages, the reductions in economic value could be larger. Additionally, shortages to senior water rights, although small, remove elasticity in the system and therefore impact the ability to transfer water in those years. Economic costs in those years may be more extreme because of lasting damage to perennial crops. Future planning within the basin must consider this, in addition to other changes as water rights are further adjudicated and because of legal mandates for instream flows.

Additional research should explore adaptations to future changes. By changing reservoir operation rules and allowing water to move between water users, as discussed further in Whitely Binder et al. (2009, this report), impacts may be reduced. How to adapt to future change requires careful consideration, especially because winter reservoir storage is projected to increase, therefore narrowing the time period between when managers decide to release water to prevent floods and to store water for summertime irrigation.

Acknowledgments

The authors would like to thank Chris Lynch at the USBR for his insights into system operating procedures for the USBR Yakima Project and Lance Vail and Andre Coleman at Pacific Northwest National Laboratory for their assistance with RiverWare simulations. Three anonymous reviewers also provided helpful feedback on earlier drafts.

References

Adams, RM, Carl BA, Mearns LO (2003) The Effects of Spatial Scale of Climatic Scenarios on Economic Assessments: An Example from U.S. Agriculture. Clim Chan 60: 131-148

Anderson, B, Gibbs M, Hart C, Inman R, McChesney D, Slattery K (2006) 2005 Drought Response Report to the Legislature. Publication 06-11-001. Washington State Department of Ecology, Water Resources Program, Olympia Washington, pp 48

Casola JH, Cuo L, Livneh B, Lettenmaier DP, Stoelinga MT, Mote PW (2009) Assessing the Impacts of Global Warming on Snowpack in the Washington Cascades, J Clim, In Press

Elsner MM, Cuo L, Voisin N, Hamlet AF, Deems JS, Lettenmaier DP, Vano, JA, Mickelson KEB, Lee SY (2009) Implications of 21st century climate change for the hydrology of Washington State. Washington Climate Change Impacts Assessment: Evaluating Washington's future in a changing climate. In press

Cherkauer KA and Lettenmaier DP (2003) Simulation of spatial variability in snow and frozen soil. J of Geophys Res 108(D22): 19:1-13

Glantz MH (1982) "Consequences and responsibility in drought forecasting: the case of Yakima, 1977," Water Resour Res 18, 3-13

Isley S (2001) Memorandum to the Drought Water Transfers Group, May 19,2001: Proposed Methodology for Calculating TWSA Water Budget Neutral Water Transfer Quantities Using Consumptive Use Calculations. http://www.roundtableassociates.com/xfer/docs/ConsumpUseMethod.htm Accessed 10 April 2006

Jacobs K and Pulwarty R (2003) "Water Resource Management: Science, Planning and

Decision-Making." In: Water: Science, Policy and Management - Challenges and Opportunities, Lawford, R., D. Fort, H. Hartmann, and S. Eden (Eds.), Water Resources Monograph 16, Am Geophy Union, Washing, D.C.

Jones JW, Hoogenboom G, Porter CH, Boote KJ, Batchelor WD, Hunt LA, Wilkens PW, Singh U, Gijsman AJ, Ritchie JT (2003) Eur J of Agron 18(3): 235-265

Kent CA (2004) Water Resource Planning in the Yakima River Basin: Development vs. Sustainability. APCG Yearbook (2004) 66: 27-60

Liang X., Lettenmaier DP, Wood EF, Burges SJ (1994) "A simple hydrologically based model of land surface water and energy fluxes for general circulation models," J. Geophys. Res., 99(14), 415-14, 428

Liang X, Wood EF, Lettenmaier DP (1996) Surface soil moisture parameterization of the VIC-2L model: Evaluation and modification. Global Planet Change, 13: 195-206

Lobell DB, Field CB, Cahill KN, Bonfils C (2006) Impacts of future climate change on California perennial crop yields: Model projections with climate and crop uncertainties. Agric and For Meteorol 141(2-4), 208-218

Lohmann D, Raschke E, Nijssen B, Lettenmaier DP (1998) Regional scale hydrology:II. Application of the VIC-2L model to the Weser river, Germany, Hydrol Sci 43(1), 143-158

Mastin MC , Vaccaro JJ (2002) Watershed Models for Decision Support in the Yakima River Basin, Washington. US Geological Survey Open-File Report 02-404, Tacoma, WA

Mastin MC (2008) Effects of potential future warming on runoff in the Yakima River Basin, Washington: U.S. Geological Survey Scientific Investigations Report, 2008-5124, 12p. It is available on line at : http://pubs.usgs.gov/sir/2008/5124/

Milly PCD, Betancourt J, Falkenmark M, Hirsch RM, Kundzewicz ZW, Lettenmaier DP, Stouffer RJ (2008) Stationarity is dead: Whither water management? Sci 319(5863) 573-574

Mote PW (2006) "Climate-driven variability and trends in mountain snowpack in Western North America," J of Clim 19(23): 6209-6220

Mote PW, Salathé EP, Dulière V, Jump E (2008) Scenarios of Future Climate Change for the Pacific Northwest. Report prepared by the Climate Impacts Group, Center for Science in the Earth System, Joint Institute for the Study of the Atmosphere and Oceans, Univ of Washing, Seattle

Northwest Economic Associates (NEA) (1997) The Economic Benefits of Enhanced Water Supplies in the Yakima River Basin. Prepared for the Tri-County Water Resources Agency, Yakima, Washington. Northwest Economic Associates, Vancouver, WA

Nijssen BN, Lettenmaier DP, Liang X, Wetzel SW, Wood EF (1997) Streamflow simulation for continental-scale river basins, Water Resour. Res. 33(4), 711-724

Oracle. (2009) "Oracle Crystal Ball." http://www.oracle.com/appserver/business-intelligence/crystalball/crystalball.html Accessed 30 January 2009

Scott MJ, Vail LW, Jaksch JA, Stöckle CO, Kemanian AR (2004a) Water Exchanges: Tools to Beat El Niño Climate Variability in Irrigated Agriculture. J of the Water Resour Assoc40(1):15-31

Scott MJ, Vail LW, Jaksch JA, Stöckle CO, Kemanian AR (2004b) Climate Change and Adaptation in Irrigated Agriculture – A Case Study of the Yakima River. In Proceedings of the UCOWR/NIWR Annual Conference, July 20-22, 2004, Portland, Oregon. PNWD-SA-6448. Pacific Northwest National Laboratory, Richland, WA

Snover AK, Hamlet AF, Lettenmaier DP (2003) Climate change scenarios for water planning studies: Pilot applications in the Pacific Northwest, Bulletin of the American Meteorological Society 84(11):1513-1518. online supplement at: http://www.hydro.washington.edu/Lettenmaier/permanent_archive/hamleaf/bams_paper/technical_documentation.pdf

Stöckle CO, Nelson R (1996) CropSyst User's Manual (Version 2.0). Biological Systems Engineering Dept., Washing State Univ, Pullman, WA, USA

Stöckle CO, Donatelli M, Nelson R (2003) CropSyst, a cropping systems simulation model. Eur J of Agron 18:289-307

Stöckle CO, Nelson R, Higgins S, Brunner J, Grove G, Boydston R, Whiting M, and Kruger C (2009). Assessment of climate change impact on Eastern Washington agriculture. Washington Climate Change Impacts Assessment: Evaluating Washington's Future in a Changing Climate. In Press

U.S. Department of Agriculture (2004) 2002 Census of Agriculture. Washington State and County Data, Volume 1, Geographic Area Series, Part 47. AC-02-A-47. U.S. Department of Agriculture, Washington, D.C., pp 483

U.S. Bureau of Reclamation (2002) "Interim Comprehensive Basin Operating Plan for the Yakima Project, Washington." Yakima, WA; Yakima Field Office.

U.S. Bureau of Reclamation (2008) "Yakima River Basin Water Storage Feasibility Study" Final Planning Report/Environmental Impact Statement. online supplement at: http://www.usbr.gov/pn/programs/storage_study/reports/eis/final/index.html. Accessed 4 January 2009.

U.S. Geological Survey (USGS) (2008) Watershed and River Systems Management Program: Application to the Yakima River Basin, Washington. http://wa.water.usga.gov/projects/yakimawarsmp/warsmp/index.html. Accessed 4 April 2008

Vano JA, Voisin N, Cuo L, Hamlet AF, Elsner MM, Palmer RN, Polebitski A, Lettenmaier DP (2009a) Multi-model assessment of the impacts of climate change on water management in the Puget Sound region, Washington, USA. Washington Climate Change Impacts Assessment: Evaluating Washington's Future in a Changing Climate. In Press

Washington State Department of Ecology (2009) Yakima River Basin water management. http://www.ecy.wa.gov/programs/wr/cro/yakimabasin.html. Accessed 24 February 2009

Western Region Climate Center (WRCC) (2007) Monthly Climate Summaries. http://www.wrcc.dri.edu/summary/Climsmwa.html. Accessed13 December 2007

Whitely Binder LC, Barcelos JK, Booth DB, Darzen M, Elsner MM, Graham TF, Hamlet AF, Hodges-Howell J, Huppert DD, Jackson JE, Karr C, Keys PW, Littell JS, Mantua N, Marlow J, McKenzie D, Robinson-Dorn M, Rosenberg EA, Stöckle CO, Vano JA (2009) Preparing for climate change in Washington State. Washington Climate Change Impacts Assessment: Evaluating Washington's Future in a Changing Climate. In Press

Wood AW, Maurer EP, Kumar A, Lettenmaier DP(2002)Long-range experimental hydrologic forecasting for the eastern United States, J of Geophyl Res 107(D20): 6:1-15

Yakima River Basin Conservation Advisory Group (CAG) 2002. Yakima River Basin Water Transfers 2001 Drought Year and 2002 Pilot Transfer Process. March 2002. Prepared by CAG facilitator, Roundtable Associates, Seattle WA, pp 13

Zagona EA, Fulp TJ, Shane R, Magee T, Goranflo HM (2001) RiverWare: A Generalized Tool for Complex Reservoir System Modeling, Journal of the AWRA, 37(4): 913-929

4: Energy

Effects of Projected Climate Change on Energy Supply and Demand in the Pacific Northwest and Washington State

Alan F. Hamlet [1,2], Se-Yeun Lee [1], Kristian E.B. Mickelson [1], Marketa M. Elsner [1,2]

Abstract

Climate strongly affects energy supply and demand in the Pacific Northwest (PNW) and Washington State (WA). We evaluate potential changes in the seasonality and annual amount of PNW hydropower production and changes in energy demand in a warming climate by linking simulated streamflow scenarios produced by a hydrology model to a simulation model of the Columbia River hydro system. Energy demand, and potential changes therein, are assessed estimates of heating degree days (HDD) and cooling degree days (CDD) for both the 20th century climate and projections of climate in three future periods (2010-2039, 2030-2059, and 2070-2099) and two emissions scenarios (IPCC A1B and B1). The gridded HDD and CDD values are then combined with population projections to create energy demand indices that respond both to climate, future population, and changes in air conditioning market penetration. We find that substantial changes in the amount and seasonality of energy supply and demand in the PNW are likely to occur over the next century in response to warming, precipitation changes, and population growth. In the 2020s, regional hydropower production increases by 0.5-4% in winter, decreases by 9-11% in summer, with annual reductions of 1-4%. Slightly larger increases in winter, and summer decreases, are projected for the 2040s and 2080s. In the absence of warming, population growth is projected to result in considerable increases in heating energy demand, however, the combined effects of warming and population growth are projected to result in net increases that are approximately one-half those associated with population growth alone. On the other hand, population growth combined with warming greatly increases the projected demand for cooling energy, notwithstanding that by the 2080s, total cooling energy requirements will still be substantially lower than heating energy demand.

[1]Department of Civil and Environmental Engineering, University of Washington, Seattle, Washington
[2]JISAO Climate Impacts Group, University of Washington, Seattle, Washington

1. Introduction

Approximately 70 percent of electrical energy consumption in the Pacific Northwest (PNW) is generated by hydropower (Bonneville Power Administration 1994). Because streamflow, mostly within the Columbia River basin, is the main power source, its climatic sensitivity has been a concern, and has been the topic of several previous studies (Hamlet and Lettenmaier 1999; Payne et al. 2004; NWPCC 2005). Regional hydropower production in the Columbia River basin has a profound impact on Washington's energy supply. A number of Public Utility Districts (PUDs) in Washington, for example, receive the majority of their power from the Bonneville Power Administration (BPA), which markets ,most of the Columbia River's hydropower production. Snohomish County PUD, to give one example, currently receives about 88% of its electrical energy resources from the BPA (URL-1). Less attention has been given to the climatic sensitivity of energy demand in the PNW, although links between climate and the demand for fossil fuels and electric power are evident, and have been explored in past studies (e.g. Sailor and Munoz 1997; Sailor and Pavlova 2003; Voisin et al. 2006; NWPCC 2005; Westerling et al. 2008).

In addition to direct effects to energy supply (for instance, changes in the seasonality and annual volume of streamflow entering hydropower reservoirs), there are a number of indirect effects of climate on hydropower supply and demand. These include a) changes in hydropower production related to climate change adaptation for other water management objectives (e.g. changes in flood control or attempts to adapt to losses of instream flow in summer), b) climate related effects to fossil fuel costs or availability, c) climate related effects to renewable energy resources such as wind turbines or photovoltaic cells, and d) shifts in population that may be partly related to changes in climate or water supply.

In this paper, we analyze projected future changes in energy supply and demand in the PNW that specifically affect Washington State (WA). In particular, we address the following research questions:

- How will seasonal and annual total hydropower production from the Columbia River basin change over the next century in response to projected warming and changes in precipitation?
- How will heating and cooling energy demand change over the next century in response to warming and population growth?
- How do electrical peak energy demand sensitivities to temperature compare in the PNW and California, and how can this information be used to understand potential changes in peak energy demand in the region related to warming?

Following methods common to the other investigations in this report, we examine the effects of climate change projected for future conditions in the 2020s (2010-2039), 2040s (2030-2059), and 2080s (2070-2099) for two IPCC greenhouse gas emissions scenarios (A1B and B1) (Nakićenović et al. 2000; Mote and Salathé 2009, this report).

Table 1 Summary of temperature and precipitation changes for six composite climate change scenarios

Temperature change relative to late 20th century values (˚C)

Scenario	J	F	M	A	M	J	J	A	S	O	N	D
2020A1B	1.22	0.99	1.11	0.99	1.01	1.28	1.59	1.60	1.37	1.00	0.83	1.17
2020B1	1.10	1.08	1.11	1.03	1.01	1.06	1.34	1.30	1.21	0.99	0.79	1.01
2040A1B	1.99	1.75	1.90	1.74	1.68	2.13	2.79	2.72	2.50	1.86	1.56	1.94
2040B1	1.49	1.41	1.46	1.45	1.37	1.44	2.05	2.05	1.90	1.37	1.17	1.65
2080A1B	3.59	3.25	3.22	2.87	2.69	3.66	4.59	4.73	4.20	3.15	2.85	3.40
2080B1	2.53	2.39	2.27	2.23	2.04	2.49	3.07	3.22	2.91	2.14	2.12	2.53

Precipitation change as a fraction of late 20th century values

Scenario	J	F	M	A	M	J	J	A	S	O	N	D
2020A1B	1.00	1.00	1.02	1.01	0.99	0.94	0.90	0.90	0.91	1.02	1.06	1.03
2020B1	1.01	0.99	1.03	1.03	1.00	0.99	0.99	0.97	0.94	1.07	1.06	1.04
2040A1B	1.04	1.01	1.06	1.06	0.99	0.90	0.85	0.88	0.87	1.07	1.08	1.06
2040B1	0.99	1.00	1.06	1.03	1.02	0.99	0.95	0.91	0.94	1.05	1.07	1.07
2080A1B	1.06	1.07	1.11	1.09	1.00	0.89	0.82	0.78	0.92	1.13	1.11	1.11
2080B1	1.05	1.03	1.03	1.06	1.03	0.93	0.89	0.84	0.95	1.07	1.09	1.09

2. Methods

We summarize briefly in this section the main aspects of the methods used to address the research questions outlined above.

2.1. Temperature and Precipitation Scenarios

We used composite temperature and precipitation scenarios which are spatial (regional) and temporal (monthly) averages of climatic changes simulated by 20 Global Climate Models (GCMs) for three future time periods (2010-2039, 2030-2059, and 2070-2099) and two emissions scenarios (A1B and B1) (Mote and Salathé 2009, this report). The combination of three time periods and two emissions scenarios results in six climate change scenarios, which we will refer to as composite scenarios. The composite monthly average temperature and precipitation projections for each time period and each emissions scenario are given in Table 1. Around these mean projections of future climate there is a range of temperature and precipitation changes simulated by different climate models for different time periods due to both differing GCM sensitivity to greenhouse forcing and simulated decadal sequencing of precipitation and temperature variability (Mote and Salathé 2009, this report). These uncertainties notwithstanding, the composite scenarios represent a consensus prediction of systematic changes in climate, which form the basis for our attempt here to understand systematic changes in PNW energy supply and demand.

2.2. Estimates of Regional Scale Hydropower Production

To estimate hydropower resources in the Columbia River hydro system, streamflow impacts for the entire Columbia River basin must be estimated. Here we use results produced by a 1/16th degree implementation of the

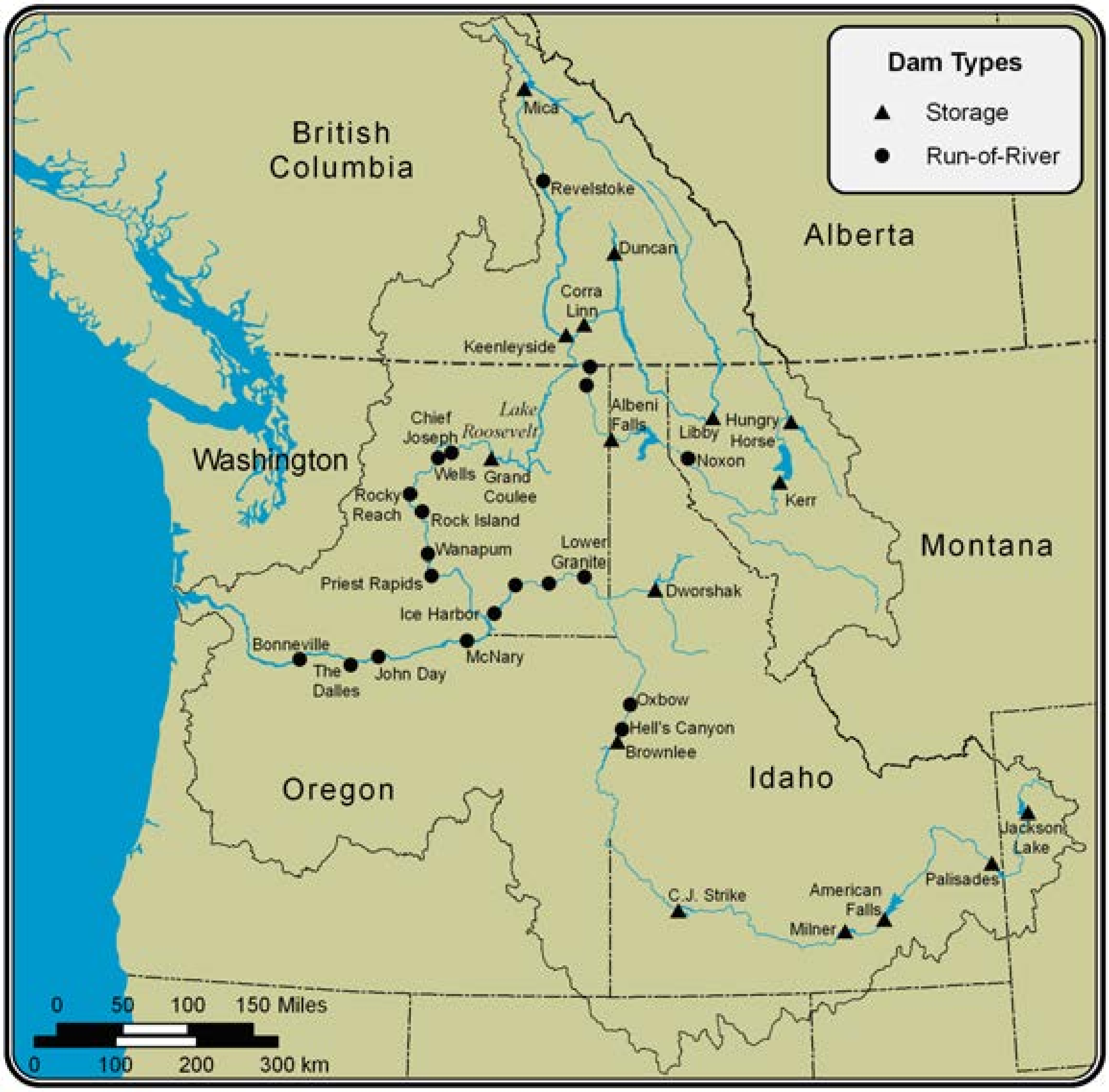

Figure 1. Columbia River basin projects incorporated in the ColSim reservoir model (note Snake River projects are aggregated in the model).

VIC hydrologic model (Liang et al. 1994) implemented over the Columbia River basin to predict changes in streamflow over the next century relative to a baseline 1916-2006 period. Elsner et al. (2009, this report) describe the VIC model implementation, and the model forcing data sets. VIC streamflow simulations were bias adjusted at monthly time scales using methods described by Snover et al. (2003). Historical "modified" streamflow data sets (which are estimates of the flows that would have occurred in the absence of the reservoir system, adjusted for a consistent level of consumptive water use for irrigation), used to train the bias adjustment process, were originally prepared for the BPA and cover the period 1928-1999 (BPA 2004).

To estimate hydropower production, the ColSim reservoir simulation model (Hamlet and Lettenmaier 1999; see also Figure 1) was used to simulate reservoir operations resulting in energy production at 20 major projects in the basin for a historic baseline period of 1917-2006 (one year, 1916, required for spin-up), and the same group of water years extracted from the future delta-method scenarios described above. Hamlet and Lettenmaier

(1999) describe the model in more detail, but in brief it simulates the operation of the multi-objective reservoir system, including hydropower production, flood control, irrigation withdrawals in the Snake Basin, and instream flow augmentation for fish in the mainstem and tributaries. By linking the model to different streamflow scenarios, the effects of altered hydrologic variability on system-wide energy production are estimated. The model includes some basic adaptive responses associated with flood control (i.e. the amount of flood evacuation is automatically adjusted in the model as a function of changing summer flow volumes), but in general the reservoir operating policies (including monthly energy targets for "firm" and "non-firm" energy in the model, which are derived from historic analyses) are held fixed in these experiments. Thus the simulation framework represents very limited adaptive responses related primarily to improved streamflow forecasting that takes into account ongoing warming in estimating summer streamflow volumes. Other potential adaptation alternatives are discussed by Whitely Binder et al. (2009, this report).

The effects of potentially changing seasonal energy demand on the reservoir model simulations merits some further discussion. Currently, hydropower resources supply approximately 70% of the electrical energy demand in the PNW (BPA 2004). Because hydropower usually represents the least expensive source of energy, the amount of energy that is extracted from the Columbia River hydro system is not strongly related to year-to-year demand variations, but is instead controlled primarily by water availability (i.e. the "fuel" of a hydropower resource is the limiting factor). To be sure, in a given operational year, seasonal variations in demand may play a significant role in the way the reservoir system is operated. Here, however, where long-term averages of hydropower production over a 90-year simulation period (1917-2006) are reported, these short-time-scale operational effects can probably be neglected without affecting the outcomes in any material way. The same cannot be said for conventional fuel-based energy resources that must supply the remaining demand for power over and above what can be supplied by hydropower and other renewable resources.

2.3. Estimates of Heating and Cooling Energy Demand Drivers

In many previous analyses (e.g. NWPCC 2005; Sailor and Munoz 1997; Voisin et al. 2006), energy demand has been estimated using aggregated population, temperature (or heating/cooling degree days) and energy use data for large urban centers. While this approach certainly make sense given the concentration of PNW population in urban centers (Figure 5), here we take the more fundamental approach of estimating population, heating and cooling degree days, and air conditioning market penetration in a gridded format at $1/16^{th}$ degree latitude by longitude resolution (about 5 by 6.5 km, or roughly 32.5 km^2 area). These gridded data are then used to create a gridded heating energy demand index (HEDI) and cooling energy demand index (CEDI) for each grid cell. HEDI is a function of population and heating degree days (HDD), and CEDI is a function of population, cooling degree days (CDD), and air conditioning market penetration (A/C_Pen, defined below). The indices are defined as follows:

$$HEDI = \text{Population} * (\text{Annual Heating Degree Days}) \quad (1)$$

$$CEDI = \text{A/C\_Pen} * \text{Population} * (\text{Annual Cooling Degree Days}) \quad (2)$$

where A/C_Pen is the estimated total residential air conditioning market penetration (i.e. the fraction of the population that has access to either central or window air conditioning) for each grid cell, estimated as a function of annual CDD (Sailor and Pavlova 2003, eq 4):

$$A/C\_Pen\ (CDD) = (0.944 - 1.17 * \exp(-0.00298*\text{CDD}) \quad (3)$$

A minimum value of A/C_Pen of 0.08 was imposed to reflect the fact that at relatively low CDD values air conditioning market penetration is less strongly determined by CDD and is generally not zero (Sailor and Pavlova 2003).

This overall approach has several advantages. First, the climate sensitivity of the indices are primarily physically based, which avoids assumptions of parameter stationarity for future projections (unlike regression-based approaches trained on observed data). Second, it facilitates aggregation of the data in different ways after the fact: allowing, for example, an assessment of rural areas or smaller towns as well as large urban centers. Third, it facilitates the use of more detailed representations of changing population, or changes in energy use patterns that have substantial geographic variations. Separating the influence of population and climate on energy demand also facilitates a clearer representation of the changes related to each, and facilitates the construction of qualitative scenarios that explore a range of uncertainties (a few simple variations of which we will explore in this paper). We note that effects of potentially changing energy use efficiency are not included in the analysis, although this would be a beneficial analysis in the future to evaluate the effectiveness of various adaptation strategies related to conservation and demand management (see Whitely Binder et al. 2009, this report).

We computed gridded estimates of long-term average heating and cooling degree days for a baseline period of 1970-1999, and then performed the same calculations for six future scenarios (discussed above) based on the same group of years. Daily average temperatures (approximated as the average of maximum and minimum daily temperature extremes) were extracted from a gridded 1/16th degree meteorological driving data set. These data are derived from gridded station data, and topographic adjustments were made using products from the Precipitation Regression on Independent Slopes Method (PRISM) (Daly et al. 1994). The methods used in producing these meteorological data sets are described in more detail by Hamlet and Lettenmaier (2005) and Elsner et al. (2009, this report).

Heating degree days (HDD) and cooling degree days (CDD) are calculated in the usual manner for each day as follows:

$$HDD = \max\left(0, 18.33 - \left[\frac{t\max + t\min}{2}\right]\right) \quad (4)$$

$$CDD = \max\left(0, \left[\frac{t\max + t\min}{2}\right] - 23.89\right) \quad (5)$$

where tmax and tmin are maximum and minimum daily temperatures in degrees Celsius, respectively.

These daily values are then aggregated to annual values. Summary results for WA alone were compiled by averaging HEDI and CEDI values for all cells in WA. At the time of this writing gridded 1/16th degree meteorological data were not available for part of the domain in the Puget Sound Lowlands (primarily Island County and San Juan County), and these areas were excluded from the analysis.

Although providing a transparent and largely physically based approach for estimating fundamental energy demand drivers, a number of potential limitations associated with the methods outlined above should be mentioned. HDD and CDD are imperfect measures of per capita energy demand for space heating and cooling, which varies with economic status, building size and design, solar and appliance loads, efficiency of end-use technology, and other factors. Temperature thresholds for calculating HDD and CDD may not be stationary in time, and there is some evidence of acclimatization to warmer conditions which may influence the interpretation of these data (Sailor and Pavlova 2003). Estimates of air conditioning market penetration, although shown to be strongly related to CDD, are subject to many different factors including variations in economic status, cost of energy, prevalence of new construction in a given area, etc. The estimates included here may underestimate market penetration in relatively affluent areas such as the major population centers west of the cascades and in the Spokane and Tri-Cities metropolitan areas, and overestimate market penetration in less affluent areas. Changes in air conditioning market penetration may not progress steadily through time (as we assume here), and instead may emerge in response to extreme heat waves or other factors.

2.4. Population Data

Several sources of future population projections are available for WA. At the county level, population projections have been prepared in support of the WA Growth Management Act (GMA) (URL-2, medium estimates) to 2030. These data are arguably the most carefully prepared projections of changing population in WA, but proved cumbersome given their relatively coarse spatial resolution (roughly 60 km). Therefore, we used a hybrid approach based on gridded 1/16th degree global population estimates for 2000, which we rescaled to match the GMA county estimates of population for 2000 and 2025 over WA. Gridded 2000 population estimates were extracted from high resolution Gridded Population of the World, version 3 (GPWv3) global data sets (CIESIN 2005; Balk and Yetman 2004) and were regridded and aggregated to the 1/16th degree spatial resolution of the climate data (described above). Population growth rates for each county were estimated by comparing medium GMA 2000 population estimates to medium GMA 2025 population estimates. Population estimates for 2045 and 2085 were then projected as a linear extension of the estimated population growth rate from 2000 to 2025 for each county using the medium estimate GMA data sets. Finally, the gridded population data at 1/16th degree for 2000 were rescaled to match the new population estimate in each county for each future time period. Qualitative scenarios of population growth after 2025 are based on: a) a simple assumption of continued linear growth using the rate calculated above through the end of the century, and b) a scenario in which we assume that population continues to grow linearly until 2045, but stays at this level through the end of the century. We should note that population estimates are very uncertain at these long time scales and also lack an appropriate scientific basis (the practical limits of trend extension methods are perhaps one or two decades). Nonetheless, these qualitative scenarios are instructive in the context of a sensitivity analysis, which is their intended use.

2.5. Estimates of Peak Electrical Energy Demand as a Function Temperature

Using multiple linear regression approaches, Voisin et al. (2006) estimated electrical energy demand in the PNW and California (CA), using population-weighted temperature data as the primary explanatory variable. Westerling et al. (2008) refined these methods to produced nonlinear relationships between temperature and regional peak electrical energy demand in both the PNW and CA. In both cases, the relationships are based on hourly electrical energy data supplied by utilities to the Federal Energy Regulatory Commission (FERC) under its 714 reporting requirements. We will primarily use these relationships as a means to understanding potentially changing peak energy demands (related particularly to increased use of air conditioning) in the PNW which may accompany systematically warmer temperatures.

3. Results and Discussion

3.1. Changes in Regional Hydropower Production

As discussed by Elsner et al. (2009, this report), changes in temperature and precipitation (Table 1) expected in the 21st century will have profound implications for the timing and volume of streamflow in the PNW. Changes in streamflow will have important implications for regional-scale electrical energy supply. As discussed above, we examine these changes using model simulations of Columbia River basin hydropower production.

Hydropower production in the Columbia River basin is strongly correlated with modified streamflow in the Columbia River at The Dalles, OR. Figure 2 shows simulated monthly average mean flow at The Dalles, associated with 20th century climate and the three A1B and B1 scenarios. Consistent with many previous studies (Hamlet and Lettenmaier 1999; Payne et al. 2004; NWPCC, 2005), warming produces increased flow in winter, reduced and earlier peak flows, and systematically lower flows in summer (Figure 2). Although the seasonal shifts in streamflow timing are strongly related to warming alone (Elsner et al. 2009, this report), the projected increases in cool season (Oct-March) precipitation and decreases in warm season precipitation in the scenarios (see Mote and Salathé 2009, this report) exacerbate these seasonal effects. On annual time scales, however, the effects of warming and increasing winter precipitation on streamflow are opposed. In the absence of warming, increases in cool season precipitation would increase annual flow (Hamlet and Lettenmaier 1999; Elsner et al. 2009, this report). In the streamflow scenarios, however, small reductions

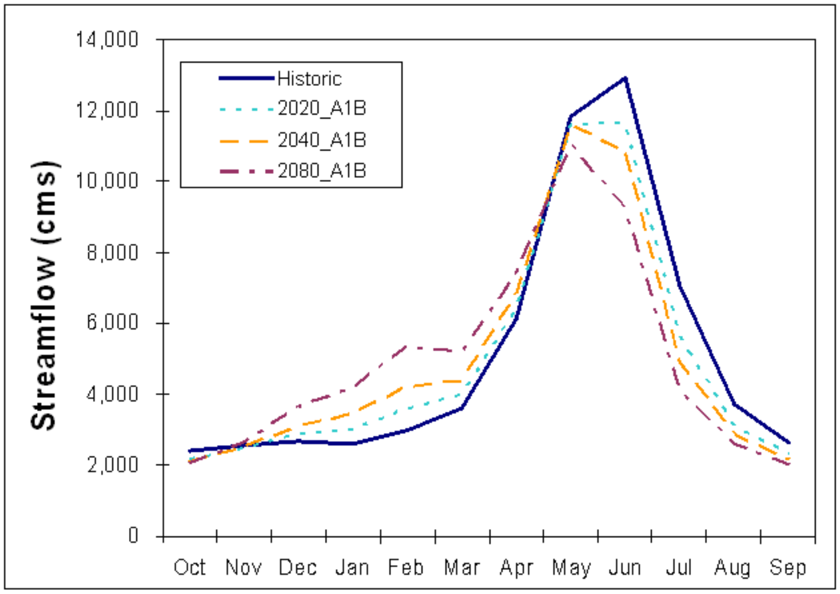

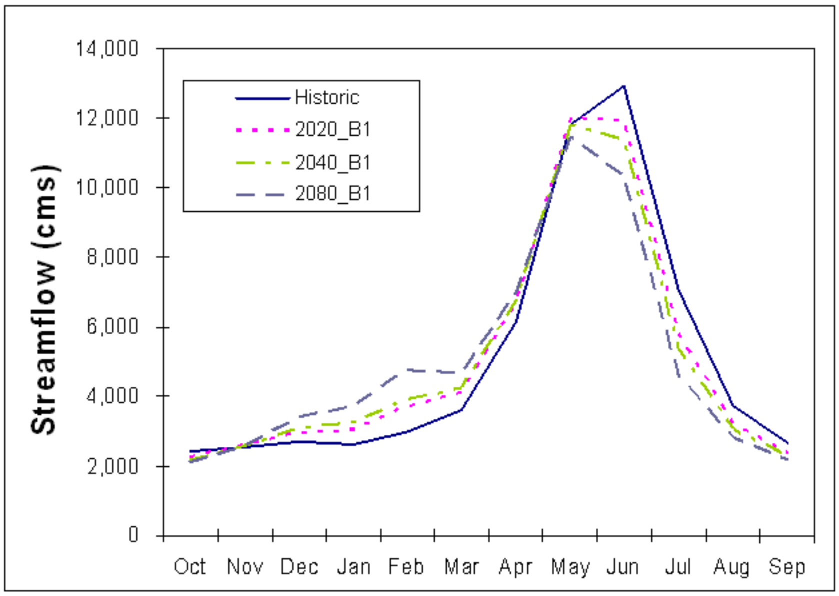

Figure 2. Simulated long-term mean modified streamflow for the Columbia River at The Dalles, OR for six climate change scenarios. Top panels show results for the A1B scenario. Bottom panels show results for the B1 scenario.

in annual flow at The Dalles (2-4% by mid-21st century) result from the combination of warmer temperatures (increased annual evaporation) and increased cool season precipitation.

Simulated changes in system-wide energy production (without substantial adaptive responses to reservoir operations) largely follow the patterns of altered annual flow and streamflow seasonality. Figure 3 shows long-term mean system-wide energy production for the 20th century climate compared to the A1B and B1 climate change scenarios (note that each trace in the plot is an average, by month, over 91 simulated years). These results broadly corroborate the findings of previous studies (Hamlet and Lettenmaier 1999; NWPCC 2005).

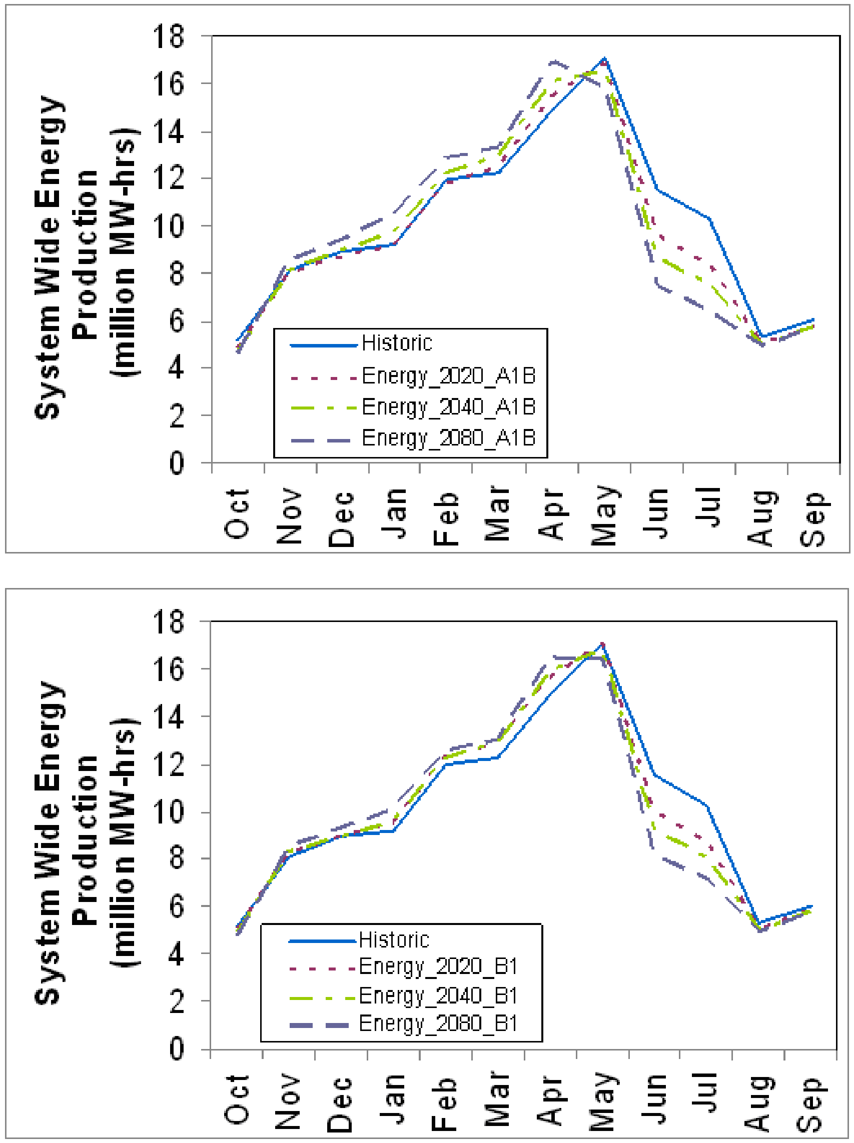

Figure 3. Simulated long-term mean, system-wide hydropower production from the Columbia River basin for six climate change scenarios. Top panels show results for the A1B scenario. Bottom panels show results for the B1 scenario.

Table 2. Summary of simulated hydropower production (percent of historic base case)

	Annual	OND	JFM	AMJ	JAS
Historic	100.00	100.00	100.00	100.00	100.00
2020A1B	96.18	97.01	100.40	96.30	88.56
2020B1	98.83	100.25	103.97	98.08	90.96
2040A1B	96.13	98.09	104.19	94.94	84.05
2040B1	97.57	99.65	104.04	96.57	87.44
2080A1B	96.48	101.63	109.78	92.46	78.73
2080B1	97.05	101.60	106.95	94.38	82.48

Table 2 summarizes the changes in long-term mean hydropower production by season as a percentage of the 20th century values. As expected, the simulations show increased hydropower production in cool season and decreases in warm season. Changes in annual hydropower production are relatively modest (a few percent) and essentially follow the small reductions in simulated annual flow at The Dalles. The largest changes in hydropower production occur in the period July-Sept, which coincides with peak seasonal air conditioning loads (Voisin et al. 2006; Westerling et al. 2008).

3.2. Changes During Drought Years

Changes in extremes during drought are also evident in the simulations, and largely follow the changes in mean energy production in each month discussed above. For simulations of critical drought years (e.g. water years 1937, 1977, 2001), cool season hydropower production under climate change scenarios is comparable to the 20th century simulation, whereas the warm season (defined as April-September) hydropower production is lower than in the 20th century drought years. These results support the hypothesis that the impacts of future droughts in cool season will be comparable to those in the 20th century (mitigated both by use of storage, increased cool season precipitation, and a shift toward increased winter runoff due to reduced snowpack). Drought impacts in spring and summer, however, are exacerbated in the simulations, with lower energy production occurring for these seasons for warmer conditions. Loss of runoff from glacial melt (which is not included in the VIC simulations) may exacerbate impacts to late summer low flow and energy production, especially during critical drought years.

3.3. Uncertainties Related to Decadal Precipitation Variability

Mote and Salathé (2009, this report) have shown that systematic changes in annual precipitation PNW are projected to be modest over the next century (also see Table 1). Furthermore these systematic changes are relatively small in comparison with observed decade-to-decade variations in 20th century precipitation. One can conclude that precipitation variability at decadal time scales are therefore an important source of uncertainty in the assessment of impacts for any given decade in the future. Although 21st century patterns of decadal variability may be different than the 20th century ones, nonetheless 20th century patterns of decadal variability provide a useful basis for assessing these kinds of uncertainties. An analysis of simulated hydropower production for the 2020A1B scenario for the relatively wet period (1947-1976) associated with the cool phase of the Pacific Decadal Oscillation (PDO) (Mantua et al. 1997), compared to the relatively dry period (1977-2004) associated with the warm phase of the PDO showed that only the changes in energy production in June, July, and August were consistently different from the historic base case when decadal variations were considered. As warming intensifies in the 21st century, however, the importance of decadal precipitation uncertainties declines and streamflow timing shifts associated with warming become the dominant effect. This change in the importance of precipitation uncertainties occurs around the 2040s in our analysis (see also Hamlet and Lettenmaier 1999 for a similar analysis of decadal climate variations on future projections).

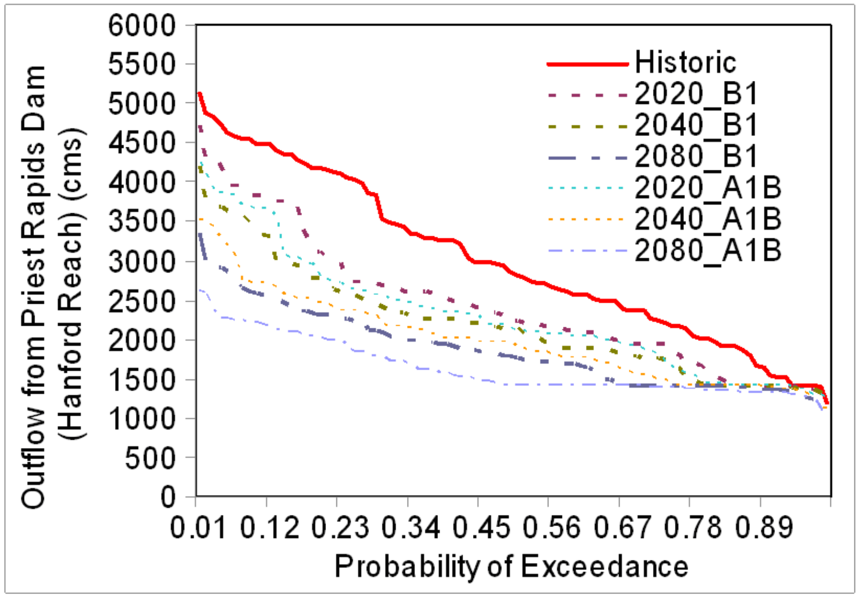

Figure 4. Probability of exceedance plot of simulated regulated flow in the Hanford Reach of the Columbia River for historic conditions and six climate change scenarios.

3.4. Tradeoffs Between Impacts to Hydropower Production and Impacts to Other System Objectives

In some past studies (e.g. NWPCC 2005) the performance of the Columbia River hydropower system in response to climate change scenarios has been largely dissociated from impacts to other system objectives (such as flood control, or instream flow augmentation for fish). This analysis is potentially misleading, because it ignores the potential for future adaptation in response to other system impacts that may indirectly impact energy production. As an illustration of this point, Figure 4 shows a probability of exceedance plot of simulated regulated monthly outflows in August at Priest Rapids Dam from ColSim model simulations. (Flows at this location are associated with instream habitat in the ecologically important Hanford Reach of the Columbia River). As warming increases, regulated summer streamflow becomes increasingly impacted as the streamflow timing shifts. Although the model is using more storage on a limited basis to support minimum monthly flow targets at this location (~1420 cms) more substantial adaptive responses to mitigate these impacts would require a much larger increase in the use of reservoir storage on a basin-wide scale, which in turn would impact energy production. Payne et al. (2004) showed, for example, that there were unavoidable tradeoffs between increasing storage allocation to support fish flows and "firm" energy resources in winter due to impacts on reservoir storage levels.

Changes in flood control operations are also expected in response to generally reduced flood risks in the Columbia main stem and streamflow timing shifts towards earlier peak flows (Lee et al. 2009; Mantua et al. 2009, this report). Lee et al. (2009) demonstrate that the use of current flood control rule curves in warmer conditions will impact reservoir refill, and propose optimization approaches for rebalancing flood control and reservoir refill in a changing climate. Improving reservoir refill ultimately

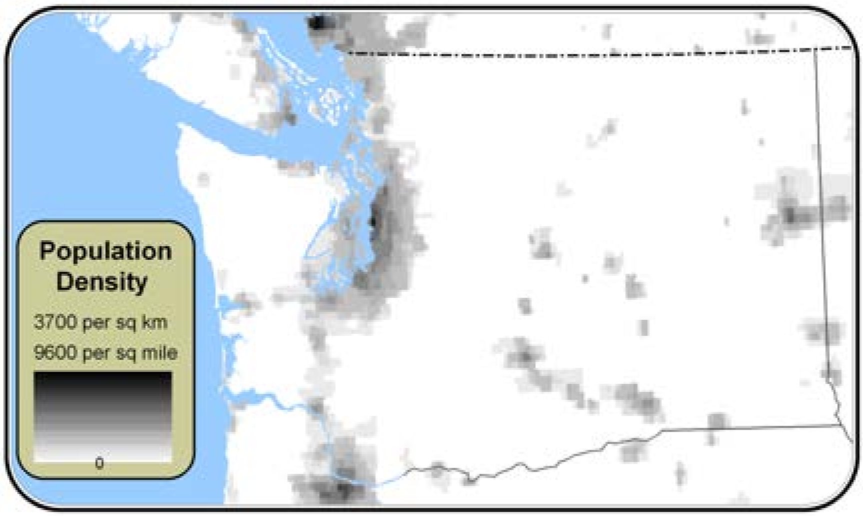

Figure 5. Gridded population estimates for Washington for the year 2000. Units: population density in persons per square km. Each grid cell is approximately 32 km^2.

benefits both hydropower production (by increasing volumetric efficiency of energy production) and instream flow augmentation for fish.

Research to develop more fully integrated adaptation strategies in response to these complex tradeoffs between hydropower production and other system objectives is needed to better understand the combined impacts to regional energy supply. Such tradeoffs will also materially affect transboundary relationships between Canada and the US associated with the Columbia River Treaty (Hamlet 2003), and improved tools to assess these tradeoffs will be needed to inform the negotiations between Canada and the U.S. regarding the future of the Treaty.

3.5. Population

Figure 5 shows gridded estimates of year 2000 population in WA. Most of the population is localized in urban centers in the Interstate-5 corridor in western WA, the Tri-Cities metropolitan area in south-central WA, and Spokane metropolitan area in the eastern-most part of the state. Thus the dominant climatic influences on state-wide energy demand are focused in a few relatively small geographic areas. Projections of population change are uncertain and vary throughout the state by county according to the GMA assessments discussed above, but projected changes are relatively consistent in the large population centers in WA, where projected changes vary from about 13-17% per decade from 2000-2025. Population is assumed to grow only in currently populated areas in the gridded data sets.

It is worth noting that projections of population past the 2020s lack a credible scientific basis and are an important source of uncertainty in energy analysis at time scales relevant to climate change investigations. Future research using new approaches and methods will be needed to address these concerns.

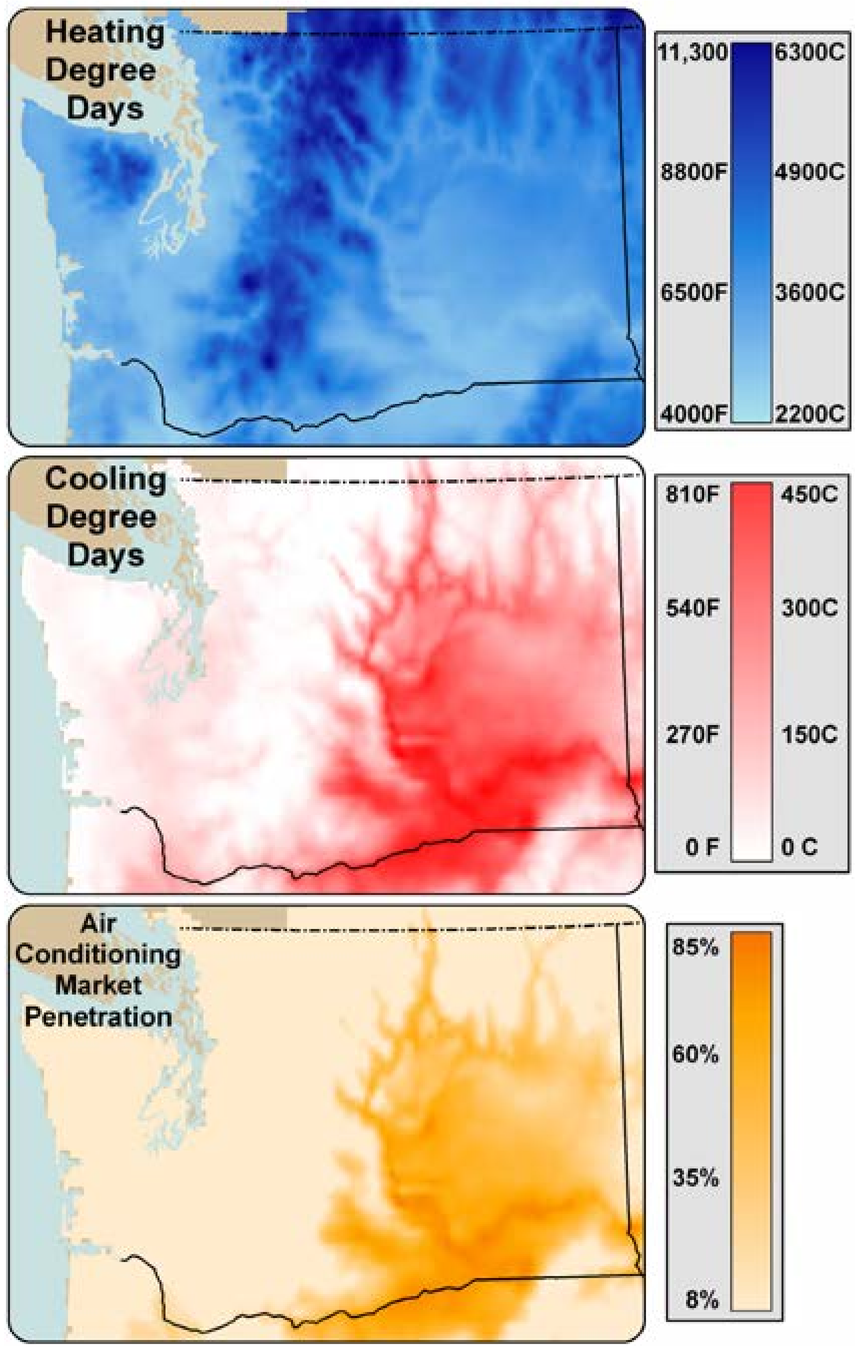

Figure 6. Long-term average historic heating degree days (top panel), cooling degree days (middle panel), and estimated saturation air conditioning market penetration (bottom panel) for Washington (1970-1999). Heating degree days are in units of degree C based on a threshold of 18.33 degrees C (65 degrees F). Cooling degree days are based on a threshold of 23.89 degrees C (75 degrees F). Air conditioning market penetration is expressed as fraction (%).

3.6. HDD, CDD, and Air Condition Market Penetration

Figure 6 shows long term average HDD, CDD, and A/C penetration calculated for historic data (1970-1999) for WA. Figures 7-9 show the same estimates for WA for six climate change scenarios (three time periods and two emissions scenarios discussed above). HDD estimates show relatively homogeneous changes throughout the region as winter temperatures warm (Figure 7). CDD estimates, however, show more localized changes in central WA (Figure 8). A/C penetration, which is a non-linear function of CDD, largely follows the changes in CDD. CDD and A/C penetration in western WA are relatively insensitive to warming

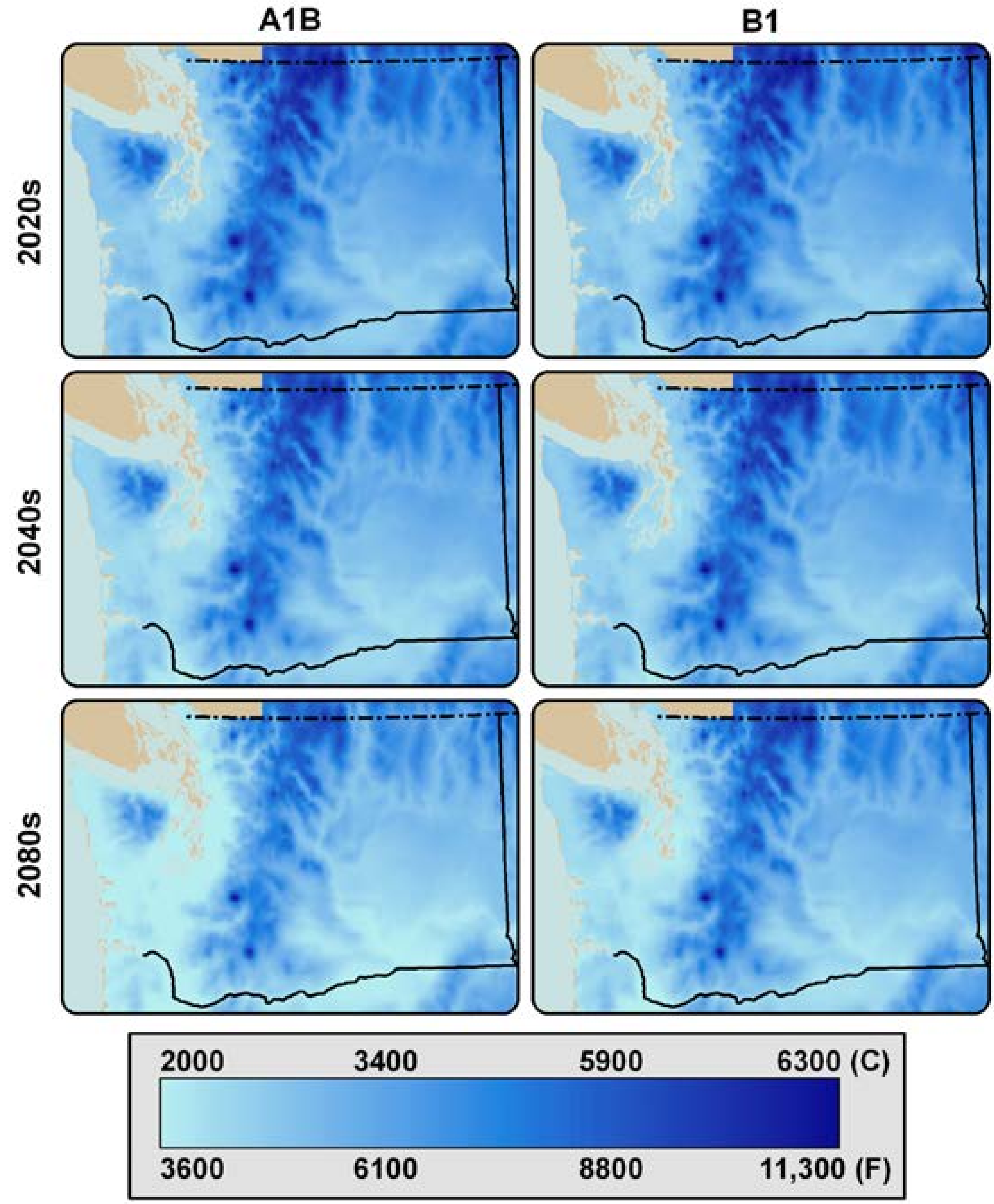

Figure 7. Long-term average annual total heating degree days for Washington, for three future time periods and two emissions scenarios. Heating degree days are in units of degrees C based on a threshold of 18.33 degrees C (65 degrees F).

in the 2020s and 2040s, because temperatures mostly remain below the daily average CDD threshold of 18.3˚C (75˚F), even for a warmer climate. By the 2080s, however, substantial changes in CDD and A/C market penetration are apparent even in the cooler areas of WA.

3.7. Scenarios of HEDI and CEDI

In this section we estimate the sensitivity of HEDI and CEDI to population growth and factors related to warming (changing HDD, CDD and air conditioning use), and then project the combined effects of population growth and warming. Given the great uncertainties related to population

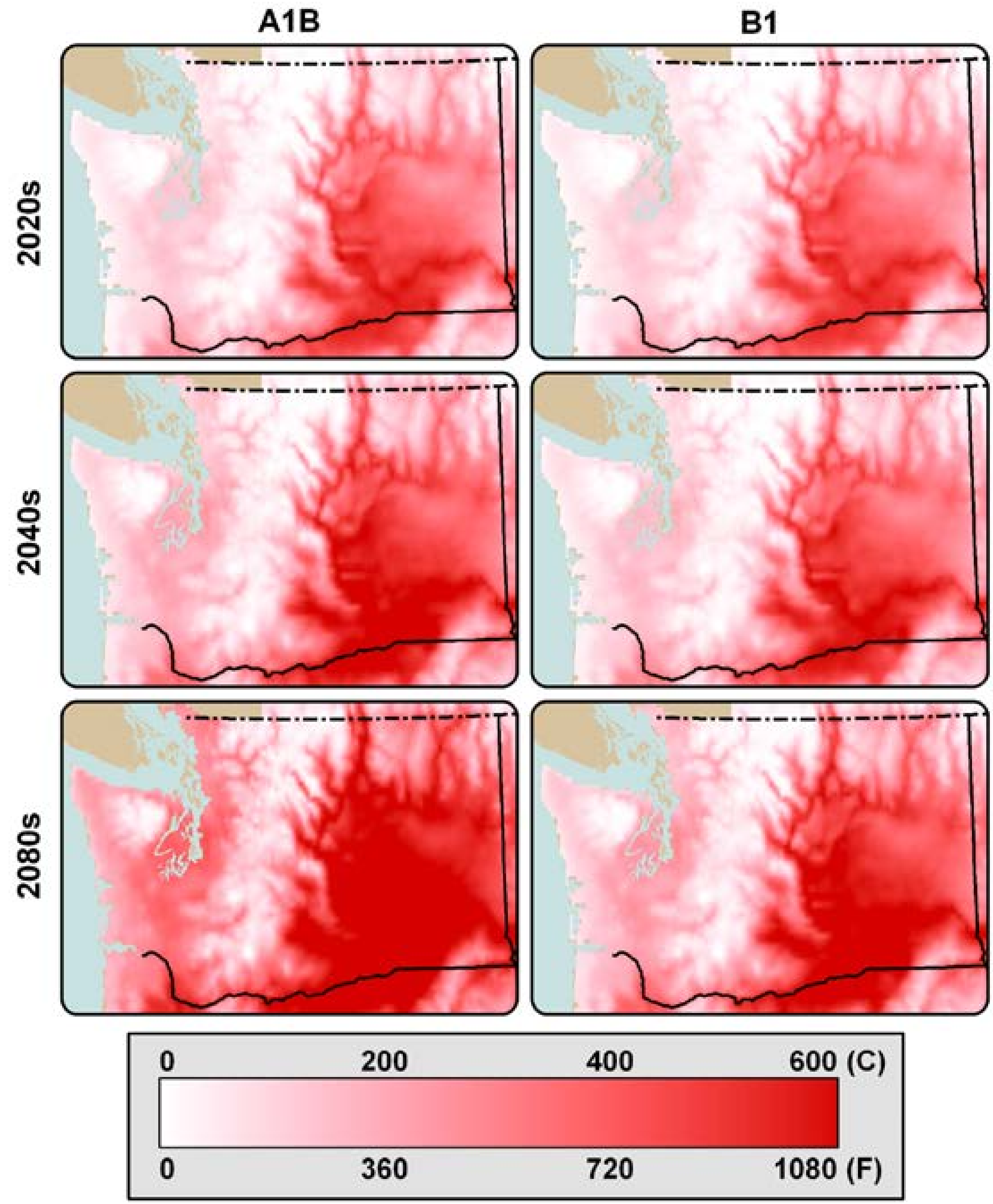

Figure 8. Long-term average annual total cooling degree days for Washington, for three future time periods and two emissions scenarios. Cooling degree days are based on a threshold of 23.89 degrees C (75 degrees F).

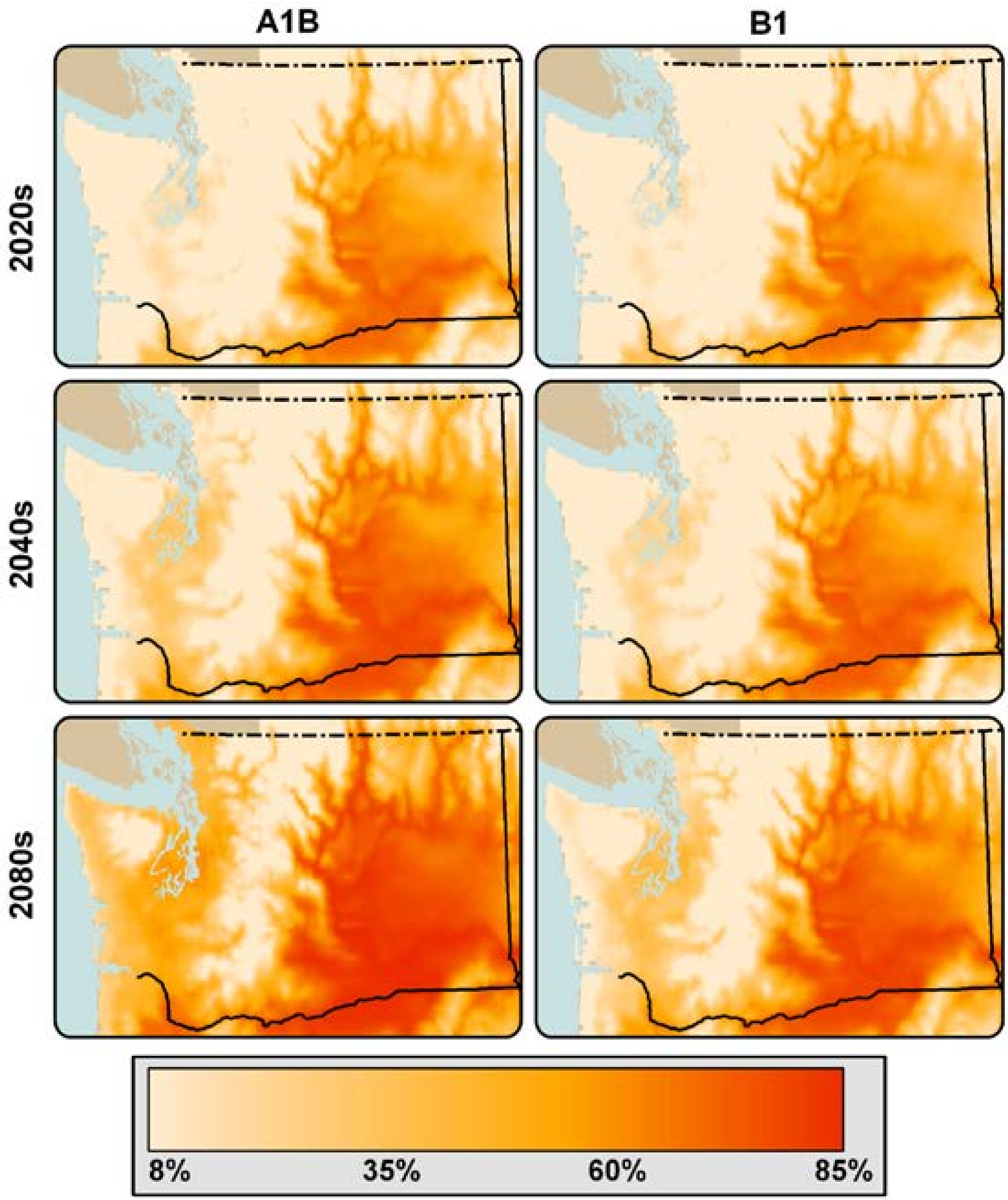

Figure 9. Projected saturation air conditioning market penetration (expressed as a fraction) for three future time periods and two emissions scenarios. (Note that a lower bound of 0.08 has been imposed)

projections at the end of the 21st century, we also estimate HEDI and CEDI using a qualitative scenario-based approach introduced above (Table 3).

Table 3. Matrix summary of Washington State HEDI and CEDI estimates for different combinations of PNW climate (rows) and population (columns) for A1B and B1 emissions scenarios. (HEDI units: million person-HDD, CEDI units: million person-CDD)

A1B scenario				
HEDI				
population	**2000**	**2025**	**2045**	**2085**
Climate				
1980s	3.12	4.31	5.26	7.15
2020s	2.76	3.81	4.64	6.32
2040s	2.51	3.47	4.23	5.76
2080s	2.13	2.94	3.59	4.88
CEDI				
population	**2000**	**2025**	**2045**	**2085**
Climate				
1980s	0.033	0.046	0.057	0.077
2020s	0.073	0.101	0.123	0.168
2040s	0.130	0.180	0.219	0.298
2080s	0.284	0.392	0.478	0.651
B1 scenario				
HEDI				
population	**2000**	**2025**	**2045**	**2085**
Climate				
1980s	3.12	4.31	5.26	7.15
2020s	2.78	3.84	4.68	6.37
2040s	2.64	3.65	4.45	6.05
2080s	2.38	3.28	4.00	5.45
CEDI				
population	**2000**	**2025**	**2045**	**2085**
Climate				
1980s	0.033	0.046	0.057	0.077
2020s	0.064	0.089	0.108	0.148
2040s	0.092	0.127	0.155	0.211
2080s	0.158	0.218	0.266	0.362

Figure 10 shows the sensitivity of HEDI to population growth alone and decreasing HDD alone (fixed 2000 population) and projects the combined effects of warming and linear population growth until the end of the 20th century for the A1B and B1 scenarios. Table 3 tabulates the values in a matrix format for different combinations of warming scenario and population growth. For HEDI, because the effects of changing population and changing climate are in opposite directions, the effects of population growth alone are associated with the greatest increases to HEDI (+38% by the 2020s), whereas the effects due to climate alone are associated with decreases to HEDI (-12% by the 2020s). The combined effects result in impacts between the two extremes in the sensitivity analysis. Changes in HEDI will affect both demand for fossil fuels for space heating and electrical power demand.

Figure 11 shows the sensitivity of CEDI to population growth alone, increasing CDD alone (fixed 2000 population and A/C penetration), and the combined effects of increasing CDD and A/C penetration (fixed 2000 population), and projects the combined effects of warming and linear population growth until the end of the 21th century for the A1B and B1 scenarios. Table 3 tabulates the values in a matrix format. The response of CEDI is fundamentally different from that for HEDI, because in this case the effects of increasing population, increasing CDD, and increasing use of A/C on CEDI are all in the same direction. Thus the greatest effects are shown to occur for combined effects of population growth and warming. Changes in CEDI are especially important in the context of planning for electrical energy needs, because energy use associated with CEDI is associated primarily with electrical energy for air conditioning loads. In the next section we will discuss the potential effects of warming on peak electrical energy demand.

As noted above, large population uncertainties at the end of the 21st century play an important role on the uncertainties in the 2080s projections of HEDI and CEDI. We explore these uncertainties by calculating HEDI and CEDI for the 2080s climate, assuming that population has stabilized

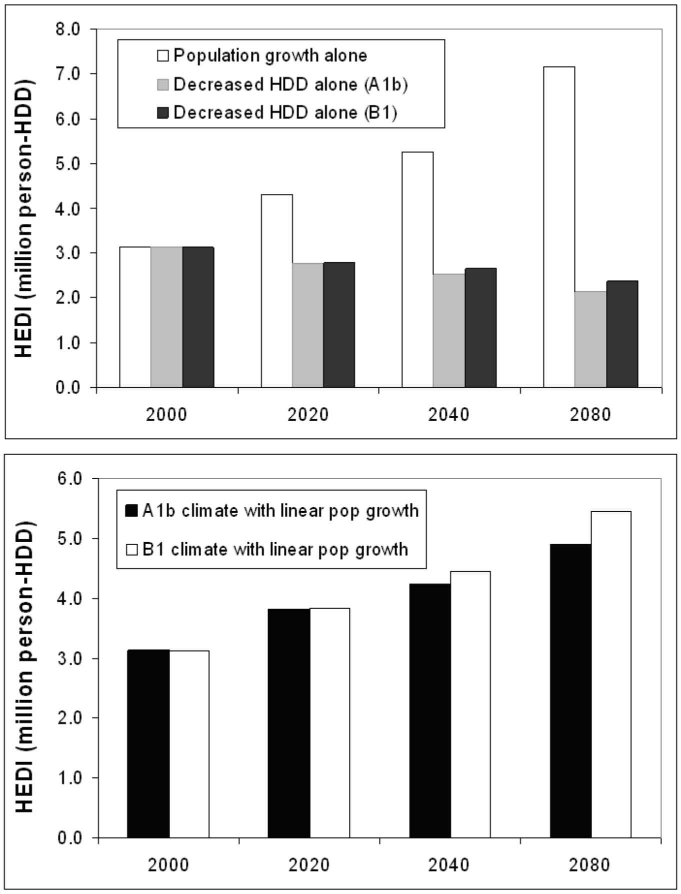

Figure 10. The top panel shows sensitivity of HEDI to population growth alone, and decreasing HDD alone. The bottom panel shows the combined effects of population growth and decreasing HDD on HEDI for two emissions scenarios. (see Table 3 for full matrix of values)

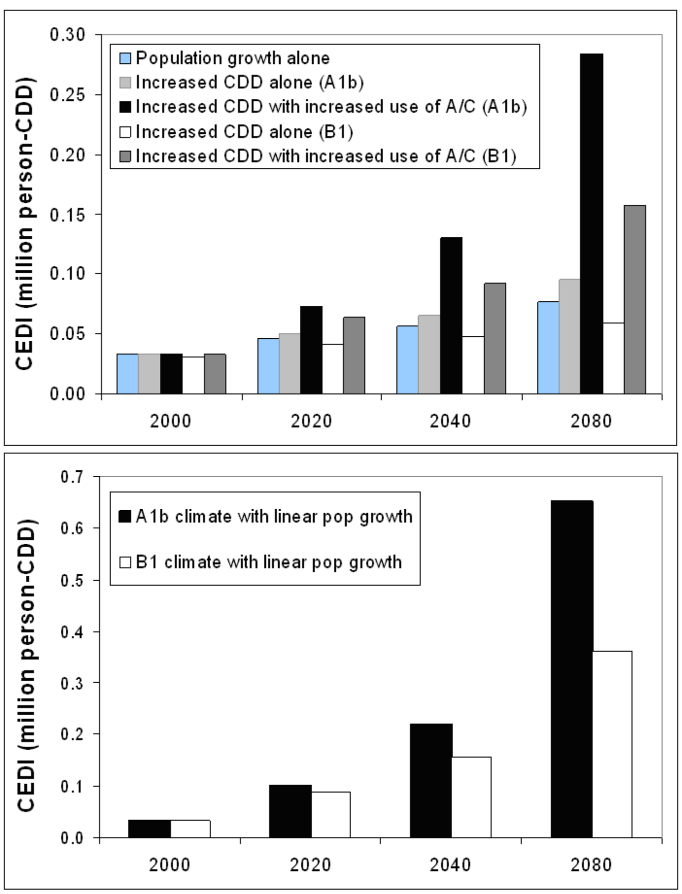

Figure 11. The top panel shows sensitivity of CEDI to population growth alone, increasing CDD alone, and the combined effects of increasing CDD and increasing A/C penetration alone. The bottom panel shows the combined effects of population growth, increasing CDD, and increasing A/C penetration on CEDI for two emissions scenarios. (see Table 3 for full matrix of values)

Table 4. Percentage of estimated total residential electrical energy demand associated with HEDI and CEDI respectively.

Scenario	A1B		B1	
	Percent of Total Demand Associated with HEDI	Percent of Total Demand Associated with CEDI	Percent of Total Demand Associated with HEDI	Percent of Total Demand Associated with CEDI
Historic	99.2	0.8	99.2	0.8
2020s	98.0	2.0	98.3	1.7
2040s	96.2	3.8	97.4	2.6
2080s	90.9	9.1	95.2	4.8

at projected 2045 level (Table 3). For this population growth scenario HEDI is lower in the 2080s than in the 2040s, due to stable population and decreased HDD. This shows that, depending on population growth, heating energy demand could potentially peak in mid-21st century. CEDI, however, continues to strongly increase from the 2040s to the 2080s (roughly doubling) even with the assumption of a stable population, because CDD and A/C penetration continue to increase dramatically with warming.

We close this section with a discussion of the relative magnitude of the changes in HEDI and CEDI. As discussed above, changes in CEDI are very large on a percent basis, but for the historic baseline and early 21st century the absolute magnitude of CEDI is small in comparison with HEDI. Direct comparison of energy demand associated with HEDI and CEDI is somewhat complex, because the sources of energy that supply these fundamental drivers of space heating and cooling demand, and the efficiency of end-use technology in each case is not directly comparable. Residential energy demand associated with HEDI, for example, is supplied by both fossil fuels (about 47% averaged for the 1990s, URL-3) and electric power (53%), and efficiencies of end-use technology range from about 0.75-1.00 depending on the source. Energy demand associated with CEDI is supplied primarily by electrical power for air conditioning, which typically has a higher end-use coefficient of performance of 2.0-3.0.

For the purpose of discussion, we consider only residential heating and cooling load supplied by electrical power. To facilitate this comparison, HEDI is multiplied by 0.53 to account for the fraction of heating energy demand that is taken by electrical power, and end-use efficiency is assumed to be 1.0 (electrical resistance heating). CEDI is assumed to be supplied entirely by electrical power, with an end-use coefficient of performance of 2.5. Using these adjustments, Table 4 shows estimates of the percentage of total residential space heating demand supplied by electric power associated with heating and cooling demand respectively. For the historic condition, cooling energy demand is estimated to account for less than 1% of the total residential electrical demand. For the 2020s, 2040s, and 2080s respectively, cooling energy demand accounts for 1.7-2.0 %, 2.6-3.8%, and 4.8-9.1% of the total residential demand. Relative to the historic baseline for total residential demand, cooling energy rises from 0.8 % of

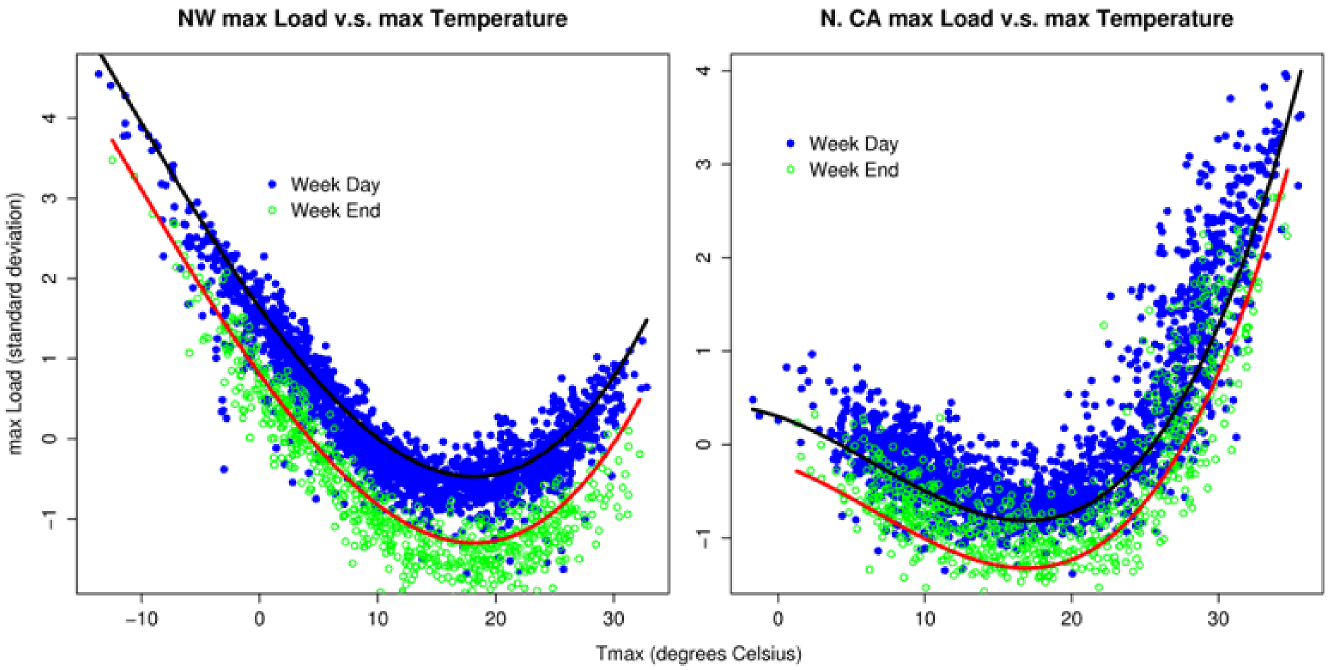

Figure 12. Non-linear relationships between daily maximum temperature and daily peak electrical energy demand in the PNW (left) and northern CA (right). Source: Westerling et al. 2008.

total demand for the base condition to 2.1-2.4%, 3.7-5.3%, 8.7-15.6% for the 2020s, 2040s, and 2080s respectively. Thus for the future scenarios, residential heating energy demand remains the dominant portion of the load, despite dramatic increases in cooling load on a percent basis.

It is important to note that impacts at smaller spatial scales (e.g. small PUDs in eastern WA) and to other elements of the load mix not considered here may behave very differently. Energy demands associated with cooling needs for commercial computer resources, for example, are probably negatively correlated with HEDI, and positively correlated with CEDI and are likely to have a very different sensitivity to warming. More detailed studies will be needed to assess the impacts in different sectors of the energy market and different geographic areas of the state.

3.8. Changes in Peak Electrical Demand in Summer

In the PNW, peak electrical demand in summer is currently relatively low (reflecting low values of CEDI), and the sensitivity of peak demand to warming is modest. In northern CA, by comparison, a much more substantial portion of the observed electrical demand is associated with warm temperatures in the summer, and the sensitivity to increasing temperature is larger (Voisin et al. 2006; Westerling et al. 2008).

Figure 12 shows non-linear relationships between daily tmax and regional peak electrical energy demand in the PNW and northern CA. Although the 20th century summer climate in CA is not a perfect analogue for warmer conditions in the PNW, the differences between these relationships in the PNW and CA provide important information about the kinds of changing peak electrical demand patterns that should be expected to accompany adjustments to systematically warmer conditions (such as increased use of air conditioning). Sensitivity to warmer climate is broadly interpreted as a move to the right along the x-axis in Figure 12. Thus the slope of the fitted lines in plots (i.e. the first partial derivative of demand with respect to temperature) characterizes the demand sensitivity to warming. Note that the slope of the fitted line is much steeper in CA than in the PNW for a given temperature. This supports the argument that changes in the PNW summer electrical energy demand will probably be much larger than would be suggested by historic patterns of use in the PNW. We note, however, that changes in tmax could potentially be different than the projections of the daily average temperature changes we consider here. If tmin increases strongly but tmax does not increase appreciably, for example, peak electrical demand related to space cooling needs may be relatively insensitive to warming.

Monthly regression-based models of daily average regional scale energy demand in CA and the PNW developed by Voisin et al. (2006) also provide useful quantitative guidance on potential changes in end-use technology in the PNW in response to warming. In CA in July for example, the coefficient in the regression equation associated with population weighted temperature (i.e. the first partial derivative ∂(Demand)/∂(Temperature)) is 53% percent higher than that for the PNW at the same time of year. These observed differences between the two regions support the hypothesis that increased temperatures and increased A/C market penetration will result in strongly increased sensitivity to warmer conditions on daily time scales. These issues have been noted in earlier studies as well (e.g. NWPCC 2005), but more research is needed to understand the capacity and distribution impacts of these kinds of effects.

3.9. Future Research Needs

In closing this section, we list a number of specific research needs, beyond the scope of the current investigation, which have emerged in the course of preparing this paper:

1. Population projections over long time horizons (> 20 years) are very uncertain and lack a credible scientific basis. New approaches and methods are needed to provide credible population forecasts on time scales that are relevant to climate change studies.
2. More detailed projections of specific impacts to daily maximum and minimum temperature are needed to facilitate better projections of daily average and peak loads.
3. We have focused here on climate sensitivities related primarily to residential and commercial space heating and cooling needs. Additional analyses estimating climate-related energy demand impacts in the larger commercial, industrial, and transportation sectors are needed to extend these results.
4. The combined effects of hydrologic changes and climate change adaptation on the Columbia River hydro system are only partially understood, and more resources need to be focused on this problem. In particular the combined effects of adaptation for hydropower production, flood control, and instream flow for fish are needed. More sophisticated tools will be needed to explore and prioritize the full range of adaptation alternatives, and to understand the

implications for the transboundary relationship between Canada and the US in the Columbia River basin.

5. Linkages between water availability and conventional energy production (e.g. via power plant cooling needs) have been established in other studies, but projections of constraints on conventional resources that incorporate altered water availability in summer are not currently available. These effects should be incorporated in estimates of warm-season energy supplies from conventional resources.
6. The potential for increased use of renewable energy (such as residential solar water heating) should be considered in future work to estimate both supply and demand, particularly in summer when these technologies are most effective in the PNW.
7. There is a need to better understand the potential conjunctive management strategies with other western regions, and to assess the infrastructure needs associated with these strategies.
8. A quantitative assessment of the effects of glacial melt on summer low flows and late summer hydropower production is needed, particularly in the context of critical drought years.

4. Conclusions

Hydropower production in the Columbia River basin is projected to decline slightly on an annual basis by mid-21st century, but is projected to increase in winter and decline in summer. By the 2020s, regional hydropower production is projected to increase by 0.5-4% in winter, decrease by 9-11% in summer, with annual reductions of 1-4%. By the 2040s hydropower production is projected to increase by 4.0-4.2% in winter, decrease by about 13-16% in summer, with annual reductions of about 2.5-4.0%. By the 2080s hydropower production is projected to increase by 7-10% in winter, decrease by about 18-21% in summer, with annual reductions of 3.0-3.5%. The largest and most robust changes in hydropower production are projected to occur from June-Sept, during the peak air conditioning season.

Despite decreasing HDD with projected warming, heating energy demand is projected to increase due to population growth. In the absence of warming, population growth is projected to increase heating energy demand in WA by 38% by the 2020s, 68% by the 2040s, and 129% by the 2080s. For fixed 2000 population, projected warming would reduce heating energy demand by 11-12% for the 2020s, 15-19% for the 2040s, and 24-32% for the 2080s due to decreased heating degree days. Combining the effects of warming with population growth, heating energy demand for WA is projected to increase by 22-23% for the 2020s, 35-42% for the 2040s, and 56-74% for the 2080s. Increases in HEDI will have important impacts on both demand for fossil fuels such as natural gas and demand for electrical power.

Cooling energy demand is projected to increase rapidly due to increasing population, increasing cooling degree days, and increasing air conditioning market penetration. In the absence of warming, population growth is projected to increase cooling energy demand in WA by 38% by the 2020s, 69% by the 2040s, and 131% by the 2080s. For fixed 2000 population, warming would increase cooling energy demand by 92-118% for the 2020s, 174-289% for the 2040s, and 371-749% by the 2080s due to the combined effects of increased CDD and increased air conditioning market penetration. Combining the effects of warming with population growth, cooling energy demand would increase by 165-201% (a factor of 2.6-3.0) for the 2020s, 363-555% (a factor of 4.6-6.5) for the 2040s, and 981-1845% (a factor of 10.8-19.5) by the 2080s. Increases in CEDI are very tightly coupled to increasing electrical energy demand, because air conditioning technology is powered primarily by electricity. Although increases in CEDI are very large on a percent basis, in absolute terms the increases are relatively small in comparison with increases in HEDI. For residential heating and cooling energy demand, for example, cooling energy demand is projected to increase from less than 1% of the total energy demand in the late 20th century to about 4.8-9.1% of the total demand in the 2080s.

Taken together the changes in energy demand and regional hydropower production suggest that energy adaptation to climate change in the cool season will be easier than in the warm season. Increases in hydropower production in cool season will at least partially offset increases in HEDI. Adapting to changes in warm season energy supply and demand will be more difficult because increases in CEDI (which are also more directly coupled to electrical energy demand) will accompany systematic losses of hydropower resources in the same months. These effects in summer will put additional pressure on other sources of energy. Peak electrical loads for air conditioning are also likely to increase, creating potential capacity, distribution, or voltage stability problems.

The ability to transfer electrical energy from the PNW to other regions is likely to decrease in May, June, July, and August due to reduced hydropower supplies and increased local demand. Excess capacity in other regions (e.g. CA and the SW) in winter (due to reduced winter heating demand and increased capacity needed to cope with summer demand) is likely to make more capacity available to the PNW. These changes in conjunctive management opportunities will impact not only supply and capacity considerations in both regions, but also revenue projections, because power exports from the PNW to CA in summer are currently associated with high market values.

Acknowledgments

Particular thanks to Rob Norheim at the Climate Impacts Group for maps and figures and GIS assistance in preparing county population data bases. Thanks also to Tony Westerling for permission to use peak power demand figures for PNW and northern CA from Westerling et al. (2008). The authors also wish to acknowledge the contributions of three anonymous reviewers, whose comments resulted in substantial improvements to the paper.

References

Balk D, Yetman G (2004) The global distribution of population: evaluating the gains in resolution refinement, Center for International Earth Science Information Network, Columbia University, Palisades, NY (http://sedac.ciesin.columbia.edu/gpw/docs/gpw3_documentation_final.pdf)

Bonneville Power Administration, U.S. Army Corps of Engineers(USACE), NPD, U.S. Bureau of Reclamation (USBR), PNR, (1994) The Columbia River system: The Inside Story. Report DOE/BP-1689, published by the USACE and USBR

Bonneville Power Administration (2004) 2000 Level Modified Stream flow, 1928-1999; Bonneville Power Administration, May

Center for International Earth Science Information Network (CIESIN), Columbia University, Centro Internacional de Agricultura Tropical (CIAT) (2005) Gridded Population of the World Version 3 (GPWv3): Population Grids. Palisades, NY: Socioeconomic Data and Applications Center (SEDAC), Columbia University. Available at http://sedac.ciesin.columbia.edu/gpw. (11/2008)

Daly C, Neilson R, Phillips D (1994) A statistical-topographic model for mapping climatological precipitation over mountainous terrain, J Appl meteorol 33: 140-158

Elsner MM, Cuo L, Voisin N, Hamlet AF, Deems JS, Lettenmaier DP, Mickelson KEB, Lee SY (2009) Implications of 21st century climate change for the hydrology of Washintgon State. Washington Climate Change Impacts Assessment: Evaluating Washington's future in a changing climate. In press

Hamlet AF, Lettenmaier DP (1999) Effects of climate change on hydrology and water resources in the Columbia River basin. J. Am Water Resour Assoc 35 (6): 1597-1623

Hamlet AF (2003) The role of transboundary agreements in the Columbia River basin: An integrated assessment in the context of historic development, climate, and evolving water policy, climate and water: transboundary challenges in the Americas, H. Diaz and B. Morehouse (ed), Kluwer Press, Dordrecht/Boston/London

Hamlet, AF, Lettenmaier, DP (2005) Producing temporally consistent daily precipitation and temperature fields for the continental U.S., J. of Hydrometeorology, 6(3): 330-336

Nakićenović N, Swart R (eds.), (2000) Special report on emissions scenarios. A special report of working group III of the Intergovernmental Panel on Climate Change. Cambridge University Press, Cambridge, United Kingdom and New York, NY, USA, 599 (http://www.grida.no/publications/other/ipcc%5Fsr/?src=/climate/ipcc/emission/)

Lee SY, Hamlet AF, Fitzgerald CJ, Burges SJ, Lettenmaier DP (2009) Optimized flood control in the Columbia River basin for a global warming scenario, ASCE J Water Resources Planning and Management (in review)

Liang X, Lettenmaier DP, Wood EF Burges SJ (1994) A simple hydrologically based model of land surface water and energy fluxes for General Circulation Models, J Geophys. Res, 99 (D7): 14,415-14,428

Mantua N, Hare S, Zhang Y, Wallace JM, Francis R (1997) A pacific interdecadal climate oscillation with impacts on salmon production, Bull Am Meteorol Soc, 78 (6): 1069-1079

Mantua N, Tohver IM, Hamlet AF (2009) Impacts of climate change on key aspects of freshwater salmon habitat in Washington State. Washington Climate Change Impacts Assessment: Evaluating Washington's future in a changing climate. In press

Mote PW, Salathé Jr EP (2009) Future climate in the Pacific Northwest. Washington Climate Change Impacts Assessment: Evaluating Washington's future in a changing climate. In press

NWPCC (2005) Northwest Power and Conservation Council, The fifth Northwest electric power and conservation plan, appendix N, Effects of climate change on the hydroelectric system, May (http://www.nwcouncil.org/energy/powerplan/5/Default.htm)

Payne JT, Wood AW, Hamlet AF, Palmer RN, Lettenmaier DP (2004) Mitigating the effects of climate change on the water resources of the Columbia River basin, Clim Chang, 62 (1-3): 233-256

Sailor DJ, Munoz JR (1997) Sensitivity of electricity and natural gas consumption to climate in the U.S.A.--methodology and results for eight states, Energy, 22 (10): 987-998

Sailor DJ, Pavlova, AA (2003) Air conditioning market saturation and long-term response of residential cooling energy demand to climate change, Energy, 28 (2003): 941-951

Snover AK, Hamlet AF, Lettenmaier DP (2003) Climate change scenarios for water planning studies, BAMS, 84 (11): 1513-151

Voisin N, Hamlet AF, Graham LP, Pierce DW, Barnett TP, Lettenmaier DP (2006) The role of climate forecasts in western U.S. power planning, J Appl Meteorol 45(5): 653-673

Westerling A, Barnett T, Gershunov A, Hamlet AF, Lettenmaier DP, Lu N, Rosenberg E, Steinemann AC (2008) Climate forecasts for improving management of energy and hydropower resources in the western U.S., California Energy Commission, PIER Energy-Related Environmental Research Program. CEC-500-2008-XXX

Whitely Binder LC, Barcelos JK, Booth DB, Darzen M, Elsner MM, Graham TF, Hamlet AF, Hodges-Howell J, Huppert DD, Jackson JE, Karr C, Keys PW, Littell JS, Mantua N, Marlow J, McKenzie D, Robinson-Dorn M, Rosenberg EA, Stockle CO, Vano JA (2009) Preparing for climate change in Washington State. Washington Climate Change Impacts Assessment: Evaluating Washington's Future in a Changing Climate. In Press

URL-1 (12/13/08) http://www.snopud.com/energy/pwrsource.ashx?p=1878#fuelmix

URL-2 (12/13/08) http://www.ofm.wa.gov/pop/gma/projections07.asp

URL-3 (1/5/09) http://www.cted.wa.gov/site/533/default.aspx

Photo credit, page 169: McNary Dam: courtesy Bonneville Power Administration

5: Agriculture

Assessment of Climate Change Impact on Eastern Washington Agriculture

Claudio O. Stöckle[1], Roger L. Nelson[1], Stewart Higgins[1], Jay Brunner[2], Gary Grove[3], Rick Boydston[4], Mathew Whiting[3], and Chad Kruger[5]

Abstract

An assessment of the potential impact of climate change and the concurrent increase of atmospheric carbon dioxide (CO_2) concentration on eastern Washington State agriculture was conducted. Climate projections from four selected general circulation models (GCM) were chosen to evaluate impacts for the periods 2010-2039, 2030-2059 and 2070-2099, identified as 2020, 2040, and 2080 scenarios, respectively. All climate projections reflect a warming future climate, but the individual GCMs vary with respect to precipitation changes – some models reflect wetter conditions and some drier. The assessment included the crops with larger economic value for the state at selected representative locations: irrigated apples at Sunnyside; irrigated potatoes at Othello; dryland wheat at Pullman (high precipitation), Saint John (intermediate precipitation), and Lind and Odessa (low precipitation). To evaluate crop performance, a cropping system simulation model (CropSyst) was utilized using historical (1975-2005) and future climate sequences, including simulations with and without concurrent elevation of atmospheric CO_2 concentration as given by the IPCC A1B CO_2 emission projection. Crops were assumed to receive adequate water (irrigated crops) and nutrient supply and possible negative impacts from pests and diseases were not accounted for. Simulation results project that the impact of climate change on selected but economically significant crops in eastern Washington will be generally mild in the short term (i.e., next two decades), but increasingly detrimental with time (potential yield losses reaching 25% for some crops by the end of the century). However, the projected CO_2 elevation is expected to provide significant mitigation of climate change effects, and in fact result in yield gains for some crops. Yields of winter wheat, without CO_2 effect, are projected to increase 2% to 8% for the 2020 scenario, tending to decline with further warming in high precipitation locations, but continue increasing to reach a 12% gain by the 2080s in low precipitation locations. With CO_2 elevation, winter wheat yields are projected to increase by 15% for the 2020 scenario, with larger increases later in the century. Spring wheat yields are projected not to change for the 2020 scenario, and decline 10% to 15% (2040), and 20% to 26% (2080) without CO_2 effect. However, earlier planting combined with CO_2 elevation is projected to increase yields by 16% for the 2020 scenario.

[1] Department of Biological Systems Engineering, Washington State University, Pullman, Washington
[2] Tree Fruit Research and Extension Center, Washington State University, Wenatchee, Washington
[3] Irrigated Agricultural Research and Extension Center, Washington State University, Prosser, Washington
[4] USDA-ARS at WSU IAREC, Prosser, Washington
[5] Center for Sustaining Ag & Nat Res, Washington State University, Wenatchee, Washington

Yields of irrigated potatoes are projected to decline 9%, 15%, and 22% for the 2020, 2040, and 2080 scenarios, respectively, but these losses are significantly smaller (2 to 3%) with CO_2 elevation. Varieties with a longer duration of green leaf area, combined with elevated CO_2, could potentially result in yield gains of 15%. However, reductions of tuber quality are a concern under warmer conditions. Apple yields are projected to decline 1%, 3%, and 4% for the 2020, 2040, and 2080 scenarios, respectively, but with projected yields increasing 6% (2020), 9% (2040), and 16% (2080) with CO_2 effect. Growers will need to adapt management to benefit from possible yield increases while maintaining fruit quality standards. Lack of good representation of the frequency and persistence of extreme temperature and precipitation events in current climate projections, which could adversely affect crop yields, and the extent to which the beneficial effects of elevated CO_2 on future crop productivity will be expressed are sources of some uncertainty to the projections in this study.

1. Introduction

The increasing concentration of atmospheric carbon dioxide (CO_2), and concurrent changes in temperature and precipitation patterns are expected to affect many aspects of human activities (IPCC, 2007). Because agriculture is widely exposed to these variables, the potential exists for perturbations in response to these changes in the next few decades and beyond.

The availability and capture of solar radiation, water, and nutrients are basic factors for plant growth and survival. Temperature plays an important role in general biological activity, defining in the case of plants the length of the available season suitable for growth, the speed of phenological development, the incidence of heat or freezing stresses, and the level of enzymatic activity associated with photosynthesis and respiration. Plant growth and development are reduced or halted at low temperatures, cells are damaged by freezing temperatures, and high temperatures can be devastating during flowering and initial stages of yield formation. The interaction of these factors will determine the impact on crop productivity, management, and economics of agriculture under climate change.

The objective of this study was to assess the potential impact of climate change and elevated CO_2 on eastern Washington agriculture, which produces most of the state's agricultural output value. The agriculture of the state is highly diversified with some 300 commodities produced commercially, ranking first in the US for production of 11 commodities, and with a value of production for crops and livestock reaching $6.7B in 2006. The state's food and agriculture industry contributes 11% of the state's economy (WSDA, 2008).

This assessment of climate change impact on agriculture focuses on crops that are most economically significant: apples, potatoes, and wheat (winter and spring varieties). Apples and potatoes are irrigated. For this study, we looked only at dryland wheat, which is the dominant dryland crop.

This assessment relied on computer simulation models and their careful interpretation. Work based on computer simulation has been done to assess climate change impact on agriculture during the last several decades (e.g., Rosenzweig et al., 1996; Brown and Rosenberg, 1999; Tubiello et al., 2002; Thompson et al, 2005). These assessments utilize a variety of climate change and agricultural models, including or not the effect of increasing CO_2. This diversity combined with the large variation in climatic conditions and agricultural crops around the US and the world makes it difficult to apply directly this information to a particular region. Overall, assessments by the Intergovernmental Panel on Climate Change (IPCC) have indicated that global agricultural production will not be seriously affected by climate change as projected by several general circulation models (GCMs), but the regional distribution of change is uncertain and current agricultural production in some areas will be vulnerable and adaptations will be necessary (Thompson et al., 2005). A comprehensive climate change impact study by Parry et al. (2004) also concluded that global production appears stable, but regional differences in crop production are likely to grow stronger through time.

Schlenker and Roberts (2008) related temperature patterns and yields of corn, soybeans, and cotton for the period 1950-2005 and most counties in the US by calculating the length of time a crop is exposed to each 1-degree Celsius temperature interval in each day of the growing season. They found that yields as a function of temperature increased modestly up to a critical temperature and then decreased sharply. Using these functions and climatic predictions from the Hadley 3 model, these authors projected nationwide average yields for corn, soybeans and cotton for the years 2070-2099 to decline by 43%, 36%, and 31%, respectively, under a slow warming scenario, and by 79%, 74%, and 67% under a rapid warming scenario. However, because effects from elevated CO_2 were not included, these results are likely overstating the potential negative climate impact. Nevertheless, for the most northern US latitudes results were more benign, with yields being slightly reduced or neutral and even responding positively to temperature increase, a finding of interest for Washington State.

Tubiello et al. (2002) evaluated the effect of climate change on US crop production with a focus on wheat, maize, potato, and citrus, concluding that although model results suggested that current US food production systems will not be at risk in this century, regional production differences are important to consider, with regional results showing that climate change favors northern areas and can worsen conditions in southern areas. A similar difference in response is expected when comparing northern and southern Europe locations (Olesen and Bindi, 2002).

Assessment efforts worldwide have focused mostly on wheat and corn, while much less is known about possible effects of climate change on potatoes and other crops. We did not find studies addressing the effect of climate change on spring wheat, which is cultivated in high to intermediate precipitation dryland areas of eastern WA, and on apples or other temperate tree fruit crops grown in the region.

Thompson et al. (2005) summarized a US national assessment where crop yields were simulated under a suite of climate change scenarios from three GCMs at two levels of global mean temperature increase, +1 and +2.5 ^{o}C, and two levels of CO_2, 365 and 560 ppm. A regional analysis that included Yakima, WA, projected winter wheat yield increases for all scenarios, fluctuating from 8 to 37%, with some increase in yields due to temperature, and largely enhanced by CO_2 increase. Simulations for temperate climates elsewhere have also indicated climate change being neutral or beneficial for winter wheat production (Harrison and Butterfield, 1996; Nonhebel, 1996; Favis-Mortlock et al., 1991).

Information of climate change effects on potatoes is scarce. Rosenzweig et al (1996) reported computer simulations for Yakima, WA projecting yield reductions of 1.4, 3.8, and 18.5% with temperature increases of 1.5, 2.5, and 5 ^{o}C above the baseline. Increased CO_2 resulted in yield increases of 5 to 10% at 1.5 ^{o}C increase, compensated for yield losses or resulted in marginal gains at 2.5 ^{o}C, and reduced somewhat the losses at 5 ^{o}C. Another study by Tubiello et al. (2002) estimated potato yields at Yakima, WA to increase 2 to 5% by 2030 while yields projected in 2090 were estimated to decrease by 10% in two of the three major production sites in the Northwest.

Compensation for the negative effect of climate warming by increasing CO_2 has been projected in many studies (e.g., Favis-Mortlock et al., 1991; Nonhebel, 1996; Hatfield et al., 2008; Thompson et al., 2005; Brown and Rosenberg, 1999). However, a better understanding of the likely beneficial effects of the projected CO_2 increase is needed to properly assess possible compensatory effects for yield declines resulting from warming. There is abundant experimental evidence indicating that elevated CO_2 increases plant growth, biomass accumulation, and yields, the latter depending on increases of sink (e.g., grains, tubers) strength proportional to gains in total biomass. The beneficial effect of elevated CO_2 is more significant for crops with the C_3 photosynthetic pathway (e.g., wheat, potatoes, soybeans, and the majority of domesticated plants) and minor for crops with C_4 photosynthetic pathway (e.g., corn and sorghum). In addition, elevated CO_2 causes partial stomatal closure thus reducing crop water losses by transpiration, which coupled with biomass gains result in some gains on water use efficiency, providing advantages to rainfed crops.

Perhaps the most comprehensive review of crop responses to CO_2 is given by Kimball et al. (2002). These authors summarized crop performance under free-air CO_2 enrichment (FACE) experiments, which render results that are closer to field conditions than greenhouse and other controlled environment experiments. All experimental results were normalized to represent crop responses to a CO_2 change from 360 to 550 ppm. Overall, yields of wheat and rice increased by an average of 12% while tuber yields from potatoes increased by a substantial 28%. The boll yields of cotton were increased by 40%. In the only FACE study conducted with grapevines thus far, Bindi et al. (2001) observed increases of 40-50% in both vegetative and fruit biomass with little change in fruit and wine composition. No information is available regarding elevated CO_2 effects on apples and other temperate tree fruit crops.

A more recent evaluation of FACE experiments (Long et al., 2004) concluded that production is increased by about 20% in C_3 plants with similar increase in seed production, and only a modest increase of a few percent points for C_4 plants. It has been argued, however, that the growth stimulation resulting from increased CO_2 would be transient. Oechel et al. (1994), conducted an experiment on an undisturbed patch of tussock tundra at Toolik Lake, Alaska, enclosed in greenhouses in which the CO_2 level was controlled to ambient (340 ppm) and elevated (680 ppm) levels of CO_2 and temperature was kept ambient or elevated 4 °C. For a doubled

CO_2 level alone, initial growth stimulation was lost within three years, but it was sustained when combined with temperature elevation providing better growth conditions. One possible inhibitory mechanism is that when enhanced photosynthesis exceeds the capacity for carbohydrate export from leaves and utilization (plant organs growth cannot accommodate excess carbohydrate), starch accumulates in leaves and photosynthesis is reduced. Plants in FACE experiments have shown both increased biomass production and increased levels of carbohydrates in leaves, but the transient effect has not been duplicated (Long et al., 2004). A long-term study (13 years) exposing sour orange trees to 300 ppm CO_2 concentration above ambient showed a large increase in biomass production during the early years of tree establishment, decreasing afterwards and stabilizing during the last four years at biomass and fruit production levels of 1.8 times those of trees exposed to ambient CO_2 (Idso and Kimball, 2001). Although still of limited duration, this is the best evidence yet of the permanent nature of CO_2 elevation beneficial effect on growth of a managed crop.

Nutrient supply to crops is assumed to be a non-limiting factor in this study. It has been shown that plants exposed to elevated CO_2 have reduced tissue N concentration compared to plants in ambient conditions (e.g., Cotrufo et al., 1998). However, biomass gains from CO_2 elevation can be preserved if ample N is supplied to crops. Kim et al. (2001) grew rice in a FACE experiment and found that, to maximize rice grain yield under elevated CO_2, it was important to supply sufficient N over the whole season. The implication for agriculture is the need to increase crop fertilization to ensure that growth enhancement by CO_2 will not be limited by nutrient supply.

In the simulations presented in this study, we have assumed a gain of 20% in biomass production for a CO_2 increase from 370 to 600 ppm. When evaluating the results presented, it must be kept in mind that the magnitude of projected benefits of CO_2 increase are very likely but not guaranteed. In addition, increases in overall biomass production can be offset by heat stress reducing reproductive development of grains in cereals or tuber growth in potatoes or any other sink representing harvestable portions, or by the inability of harvestable portions to increase in number or size and absorb the additional amount of carbohydrate production. Thus, caution must be used in the interpretation of simulation results that include elevated CO_2.

2. Approach

This study is based on computer simulations of crop yields of selected crops and representative locations in Washington State as follows: Winter wheat (Pullman, Saint John, Lind, and Odessa), spring wheat (Pullman and Saint John), potatoes (Othello), and apples (Sunnyside). In addition, disease (grape and cherry powdery mildew) and insect (codling moth) models were run to provide insight into potential changes in the incidence of pests and diseases under future climate. Weed models were not available and we relied on literature review for the assessment of weed impacts.

Figure 1 shows a generalized agricultural land use map for the State of Washington and the locations included in the study; specific commodity land use maps are not available.

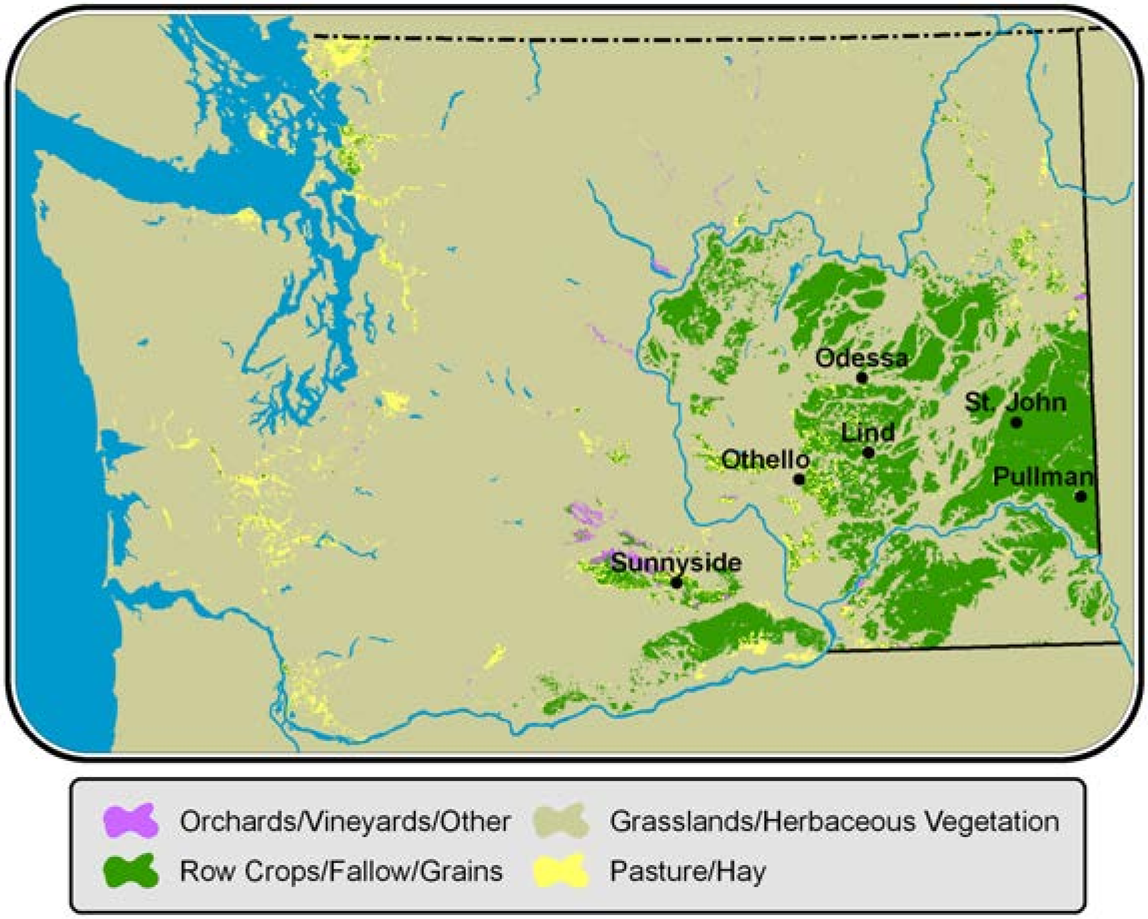

Figure 1. Agricultural land use patterns for Washington state. Locations of simulations are noted on map.

2.1. Simulations

Simulations of crop response to climate change and elevated CO_2 were performed using CropSyst Version 4.12.10 (Stöckle et al, 1994; Stöckle et al, 2003), a cropping system simulation model that represents the response to weather and management of an array of annual and perennial crops and tree fruit crops. Parameters for the simulation of wheat (Pannkuk et al., 1998), potatoes (Peralta and Stöckle, 2002), and apples (Scott et al., 2004) for the region were taken from previous studies and were further refined using available information about crop phenology and morphological, physiological, and biophysical characteristics. The effect of CO_2 on biomass accumulation and crop transpiration was calculated as described by Stöckle et al. (1992). Simulated crops were assumed to receive adequate water (irrigated crops) and nutrient supply. Possible negative impacts from pests and diseases were not accounted for.

2.2. Weather Data

To establish baselines, historical daily weather data for the years 1975-2005 were used in each location. Selected future climate projection scenarios were chosen to evaluate climate impacts for the periods 2010-2039 (2020 scenario), 2030-2059 (2040 scenario) and 2070-2099 (2080 scenario). The climate projections for future scenarios were based on four GCMs: PCM1 (a GCM that projects less warming and more precipitation for eastern WA), CCSM3 (a GCM that projects more warming and less precipitation), ECHAM5 and CGCM3 (GCMs that project intermediate changes compared to the first two).

All daily baseline and future precipitation and temperature data were extracted from a 1/16th degree grid data set available for the region, downscaled from the GCM projections (Mote and Salathé, 2009, in this report). Solar radiation and air humidity were determined from temperature and precipitation using the climate generator ClimGen (Castellvi and Stöckle, 2001; Stöckle et al., 2004), using generation parameters calibrated for stations in an existing agricultural weather network in eastern WA (AgWeatherNet). Climate characteristics for selected locations and GCMs are given in Table 1. Potential evapotranspiration was calculated using the Penman-Monteith model as proposed by Allen et al. (1998).

Table 1. Baseline (current) and projected climate characteristics for precipitation (Precip), temperature (T), and potential evapotranspiration (ETo). Data are for the two extreme GCMs and are presented for the indicated time intervals (annual, seasonal, non-seasonal) at the future periods of interest (2020, 2040, 2080) for each of 3 eastern Washington locations (Pullman, Lind, Sunnyside).

		Baseline	CCSM3			PCM1		
Pullman			**2020**	**2040**	**2080**	**2020**	**2040**	**2080**
Annual	Precip (mm)	535.8	549.9	543.9	588.3	560.2	568.9	589.5
	Mean T (°C)	8.5	10.2	11.2	12.0	9.6	10.5	11.4
	Mean Tmax (°C)	14.5	16.1	17.1	18.0	15.6	16.5	17.3
	Mean Tmin (°C)	2.4	4.2	5.2	6.0	3.6	4.4	5.4
	ET_o (mm)	914.4	966.6	998.8	1023.6	943.3	971.7	994.2
Seasonal	Precip (mm)	181.7	187.6	183.1	192.9	186.9	196.6	188.5
(Apr 1 – Sep 30)	Mean T (°C)	14.8	16.4	17.7	18.5	15.9	16.5	17.5
	Mean Tmax (°C)	22.6	24.0	25.4	26.2	23.6	24.4	25.1
	Mean Tmin (°C)	7.0	8.7	10.0	10.7	8.1	8.6	9.8
	ET_o (mm)	725.8	760.5	791.2	809.8	749.6	767.2	787.1
Non-seasonal	Precip (mm)	352.6	358.9	359.8	396.5	370.8	371.8	399.6
(Oct 1 – Mar 31)	Mean T (°C)	2.1	4.0	4.7	5.5	3.3	4.5	5.0
	Mean Tmax (°C)	6.3	8.2	8.9	9.7	7.6	8.7	9.2
	Mean Tmin (°C)	-2.1	-0.3	0.4	1.3	-0.9	0.2	0.9
	ET_o (mm)	188.3	204.7	209.5	213.4	196.1	204.1	206.9

Table 1 continued on next page.

Table 1 continued

		Baseline	CCSM3			PCM1		
Lind			**2020**	**2040**	**2080**	**2020**	**2040**	**2080**
Annual	Precip (mm)	232.3	249.9	244.3	265.5	246.3	250.1	257.2
	Mean T (°C)	10.1	11.5	12.4	13.3	10.9	11.8	12.7
	Mean Tmax (°C)	16.9	18.4	19.4	20.1	17.8	18.8	19.5
	Mean Tmin (°C)	3.2	4.6	5.5	6.4	4.0	4.9	5.8
	ET_o (mm)	975.9	1030.2	1063.9	1086.4	1006.2	1037.3	1068.1
Seasonal	Precip (mm)	76.7	83.2	79.7	84.9	78.2	81.7	85.6
(Apr 1 – Sep 30)	Mean T (°C)	17.3	18.6	19.8	20.6	18.1	18.7	19.6
	Mean Tmax (°C)	26.2	27.3	28.6	29.5	26.9	27.7	28.4
	Mean Tmin (°C)	8.5	9.8	11.0	11.7	9.2	9.8	10.9
	ET_o (mm)	798.6	828.9	856.9	874.3	818.8	836.4	855.5
Non-seasonal	Precip (mm)	156.1	165.4	164.6	180.9	167.2	167.9	174.8
(Oct 1 – Mar 31)	Mean T (°C)	2.8	4.4	5.1	5.9	3.8	4.9	5.5
	Mean Tmax (°C)	7.6	9.3	10.1	10.7	8.7	9.8	10.3
	Mean Tmin (°C)	-2.1	-0.6	0.1	1.0	-1.1	0.0	0.7
	ET_o (mm)	177.7	200.0	208.8	212.9	188.9	200.4	205.0

Sunnyside			**2020**	**2040**	**2080**	**2020**	**2040**	**2080**
Annual	Precip (mm)	184.5	194.1	188.4	202.2	191.8	192.7	199.1
	Mean T (°C)	10.5	12.4	13.3	14.1	11.8	12.7	13.5
	Mean Tmax (°C)	18.1	20.0	20.9	21.7	19.5	20.4	21.1
	Mean Tmin (°C)	2.9	4.8	5.6	6.5	4.2	5.0	5.9
	ET_o (mm)	1045.1	1113.1	1146.1	1168.0	1089.1	1119.1	1149.3
Seasonal	Precip (mm)	60.4	64.1	61.7	62.7	60.6	60.6	62.7
(Apr 1 – Sep 30)	Mean T (°C)	17.5	19.3	20.4	21.3	18.8	19.4	20.3
	Mean Tmax (°C)	26.6	28.5	29.7	30.5	28.1	28.9	29.5
	Mean Tmin (°C)	8.3	10.1	11.2	12.1	9.5	10.0	11.1
	ET_o (mm)	820.9	866.6	893.6	907.3	853.4	870.1	885.1
Non-seasonal	Precip (mm)	125.3	128.8	126.8	140.0	130.5	131.9	136.8
(Oct 1 – Mar 31)	Mean T (°C)	3.6	5.4	6.1	6.8	4.9	5.9	6.5
	Mean Tmax (°C)	9.6	11.4	12.1	12.8	10.9	11.9	12.5
	Mean Tmin (°C)	-2.4	-0.6	0.1	0.8	-1.1	-0.1	0.6
	ET_o (mm)	223.6	246.3	254.4	261.4	236.8	248.8	254.6

3. Results

3.1. Climate Change

Table 1 summarizes baseline and projected climate characteristics including precipitation, temperature, and potential evapotranspiration. Given space limitations, only projections from the two extreme GCMs included in this study for three distinctive locations in the state are presented.

Table 1 shows annual precipitation increasing by about 10% to 14% and 8% to 10% for the CSSM3 and PCM1 projections, respectively, but with the spring-summer precipitation becoming a smaller fraction of the total increase. The changes in atmospheric evaporative demand (evapotranspiration) are roughly similar to precipitation changes but with a larger proportion of the increase during the spring-summer period.

Annual temperature increase for the CCSM3 GCM is projected as 1.4, 2.3 and 3.2 °C at Lind, and ~1.7, 2.7, and 3.5 °C at Pullman and Sunnyside for the 2020, 2040 and 2080 scenarios, respectively. For the PCM1 projection, the temperature change is expected to be 0.8, 1.7, and 2.6 °C at Lind, 1.1, 2.0, and 2.9 °C at Pullman, and 1.3, 2.2, and 3 °C at Sunnyside for the 2020, 2040, and 2080 scenarios, respectively. The increase is slightly larger for the spring-summer period and CCSM3 projection with changes of 3.3, 3.7, and 3.8 °C for the 2080 scenario at Lind, Pullman, and Sunnyside, respectively, but slightly lower for the PCM1 projection (2.3, 2.7, and 2.8 °C). Overall, the changes for the average maximum and minimum temperatures are similar to those projected for average temperatures.

The projected warming trend will increase the length of the frost-free period throughout the state (Fig. 2), increasing the available growing season for crops, which will continue to be limited in eastern WA by water availability, and likely by extreme heat events in some instances. This will continue the trend observed from 1948 to 2002, during which the frost-free period has lengthened by 29 days in the Columbia Valley (Jones, 2005). The warming trend may also create opportunities for better adaptation of C_4 crop species (e.g., corn). On the other hand, temperate tree fruits grown in the state require a minimum accumulation of chilling units during the winter for adequate and uniform budbreak

Figure 2. Changes in the length of the frost free period (days), based on the CCSM3 climate projection, for the indicated future periods of interest.

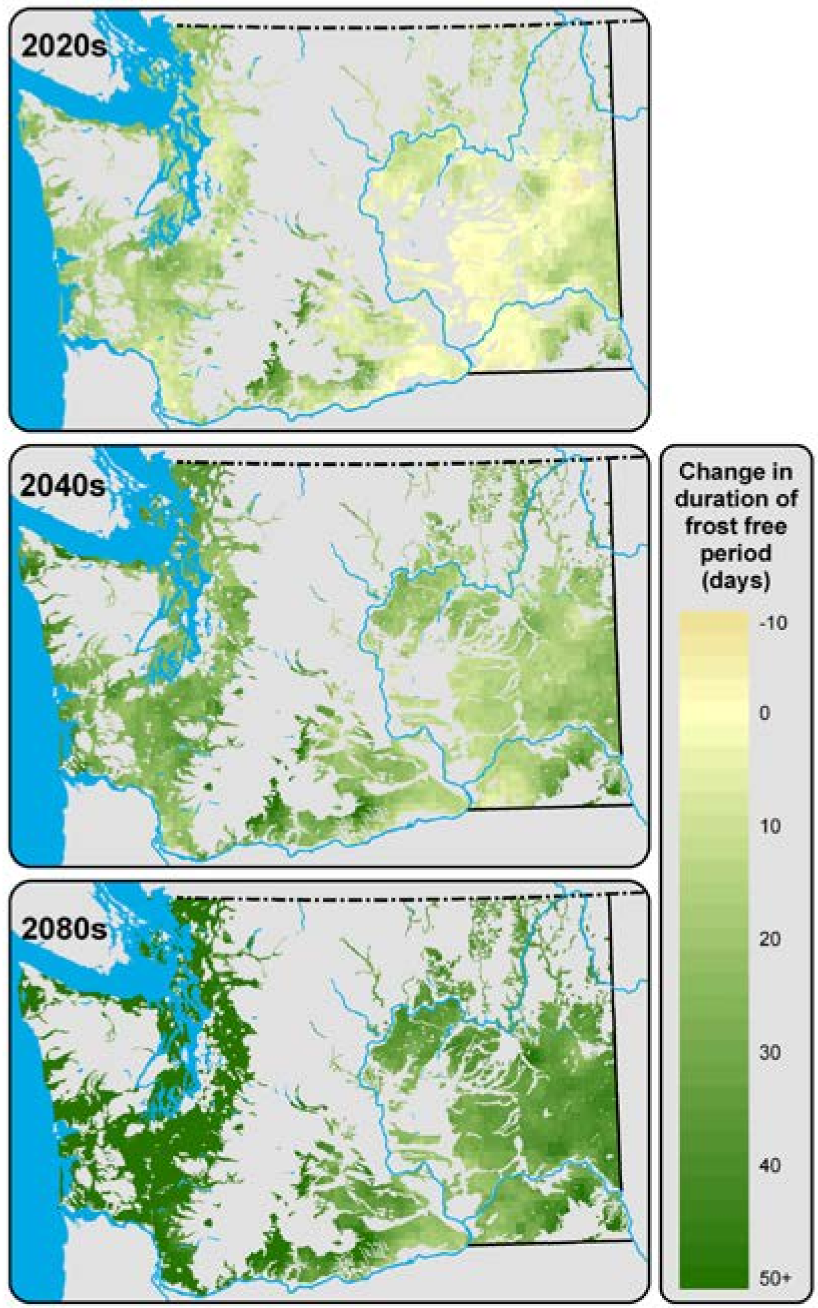

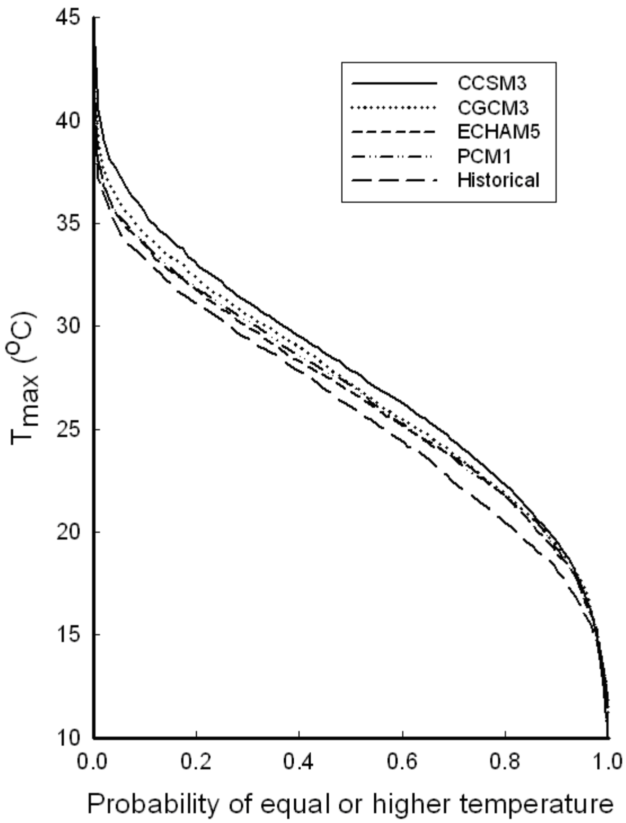

Figure 3. Probabilistic distribution of maximum June/July temperature for Pullman for the 2020 scenario.

and flowering. The opportunity to meet this requirement will be reduced as the climate becomes warmer. Weeds and insects will adapt to the longer season with more favorable conditions.

3.2. Wheat Projections

The impact of climate change on wheat was analyzed for three distinct production regions: a higher precipitation annual cropping region (Pullman site); an intermediate cropping zone in which winter wheat is typically grown in a rotation of summer fallow, winter wheat, and a spring grain (St. John site); and two lower precipitation zones in which winter wheat follows summer fallow in a two-year rotation (Lind and Odessa sites).

Table 2 summarizes simulated winter wheat yields at four locations in response to current and projected climate, with and without inclusion of elevated CO_2 effects on plant growth. At all locations, future climate is beneficial for winter wheat production, with yields increasing by 2% to 8% compared to the baseline for the 2020 scenario. As warming continues to increase, however, yields at Pullman (high rainfall) are projected to drop 4% below current values and yields at Saint John (intermediate rainfall) are maintained at current levels for the 2040 scenario, while yields at Lind and Odessa (low rainfall) continue to increase to 12% by the 2080 scenario. Higher yields are the result of earlier crop maturity while the duration of the grain filling period remains unchanged. The earlier maturity provides a degree of avoidance of the terminal water stress that is typical of the region. As climate warming continues, high temperature events during flowering will negatively affect grain formation, counteracting the effect of water stress avoidance. Figure 3 shows the probabilistic distribution of maximum temperatures in June/July in Pullman for the 2020 scenario, showing an increase in probability of temperatures above 30 °C from a baseline of 22% to 35% depending on the GCM considered. Ferris et al. (1998) showed that increasing the number of hours of exposure to temperatures above 31 °C resulted in reduction of grain numbers and lower grain biomass at harvest.

When the effect of elevated CO_2 is added, a positive picture emerges for winter wheat at all locations, time scenarios and GCM predictions, with yields increasing steadily as the century progresses. For the short-term future (2020 scenario) yields are projected to increase by 12% to 15%, increasing to gains of 23% to 35% by the end of the century. Limitations in the number and size of grains could impede a proportional expression of increased biomass production caused by elevated CO_2 on yields of future varieties. In addition, changes in the frequency of extreme high temperature events, which are not well represented by GCM projections, could limit yield formation. On the other hand, there is sufficient plasticity in photoperiod and vernalization requirements of winter wheat varieties to adapt to warming conditions (Masle et al., 1989).

Table 2. Baseline (current) and simulated dry winter wheat yields (kg/ha) at four eastern Washington locations. Scenarios were run for indicated future periods of interest (2020, 2040, 2080) under the indicated climate projection with (CO_2) and without (no CO_2) the effects of elevated CO_2 on plant growth.

Location baseline yield	CO_2 effects	Scenario		Weather projection			Average yield	Ratio of future to baseline yield
			CCSM3	CGCM3	ECHAM5	PCM1		
			Yield (kg/ha)					
Pullman								
5713 kg/ha	No CO_2	2020	6022	6374	5996	5846	6060	1.061
		2040	5116	6376	5040	5398	5483	0.960
		2080	5209	5752	5187	5002	5288	0.926
	CO_2	2020	6546	6952	6515	6367	6595	1.154
		2040	6034	7503	5881	6430	6462	1.131
		2080	7033	7887	7105	6863	7222	1.264
St. John								
4647 kg/ha	No CO_2	2020	4878	5062	4464	4637	4760	1.024
		2040	4338	4975	4640	4573	4631	0.997
		2080	4275	4749	4469	4377	4468	0.961
	CO_2	2020	5156	5862	5130	5305	5363	1.154
		2040	5491	6187	5722	5776	5794	1.247
		2080	5353	6116	5656	5724	5712	1.229
Lind								
3975 kg/ha	No CO_2	2020	4261	4503	4415	4025	4301	1.082
		2040	4363	4801	4255	4212	4408	1.109
		2080	4332	4610	4564	4296	4451	1.120
	CO_2	2020	4522	4818	4759	4255	4588	1.154
		2040	4867	5308	4645	4571	4848	1.220
		2080	5216	5667	5688	4920	5373	1.352
Odessa								
3728 kg/ha	No CO_2	2020	4000	4003	3935	3808	3937	1.056
		2040	4087	4255	3807	3969	4029	1.081
		2080	4086	4265	4353	4021	4181	1.122
	CO_2	2020	4260	4273	4224	4024	4195	1.125
		2040	4527	4664	4139	4289	4405	1.182
		2080	4896	5083	5445	4490	4979	1.336

Table 3 shows current and projected yields for spring wheat. For the 2020 scenario, no changes are projected compared to current yields. However, yields are projected to show declines, becoming progressively larger for the 2040 and 2080 scenarios. The main factors leading to these yield declines are high temperatures that reduce grain biomass as previously discussed, and a small reduction of grain filling duration. Again, elevated CO_2 is projected to counteract most of the negative effects, with yields being relatively stable or showing a small reduction throughout the century. A possible adaptation for spring cereals will be earlier planting. As shown in Table 3, a two-week earlier planting will reduce the effect of climate change alone, and will result in important yield increases (~17%) for the 2020 scenario when the CO_2 effect is added, with the benefit declining later in the century. Planting dates could be adjusted earlier than two weeks later in the century.

3.3. Potato Projections

Projections for potatoes (Table 4) indicate significant yield declines due to warming, with losses of 9%, 15%, and 22% for the 2020, 2040, and 2080 scenarios, respectively, with a larger decline for the GCM with larger warming prediction (CCSM3). Rosenzweig et al. (1996) projected potato yields in Yakima WA to decline by 1.4%, 3.4% and 18.5% with temperature increases of 1.5, 2.5 and 5.0 ^{o}C, respectively, with elevated CO_2 assumed to have a low beneficial impact on growth and yields, compensating for losses only at temperature increases of 2.5 ^{o}C or lower. In our simulations, increasing CO_2 compensated significantly for temperature increases, but still resulted in 2% yield declines for the 2020 scenario, increasing to 3% later in the century.

Two main factors contributed to the projected decline of potato yields. The first is a shorter growing season of up to 9 days by the end of the century due to the accelerated development and earlier leaf area senescence that accompany warmer temperatures. The second is an increasing occurrence of high temperatures during tuber bulking, which reduces the translocation of carbohydrates from the aboveground canopy to the tubers (Timlin et al., 2006). Although not simulated by the model, high temperature during tuber bulking may contribute to lower tuber quality (Alva et al., 2002), affecting market value.

One possible adaptation is to modify planting dates to decrease the exposure to high temperature during tuber growth and to obtain a longer duration of leaf area. However, in our simulations we tested 2 and 4 weeks planting delay without benefits. We also tried earlier planting without benefit. Similar results were obtained by Rosenzweig et al. (1996), who concluded that changes in planting date will not alleviate the negative trend in potato yields associated with higher temperatures.

Another possible adaptation is to utilize later maturity class cultivars that maintain a green leaf area for a longer period thus taking advantage of the longer available growing season. Simulations performed assuming a variety able to maintain green leaf area for an extra 9 to 10 days (Table 4) resulted in yield increases of 7% and 1%, for the 2020 and 2040 scenarios, respectively, declining to an 8% loss by 2080. With the addition of CO_2 effects, yields with this strategy increased 15% for all time scenarios.

Table 3. Baseline (current) and simulated dry spring wheat yields (kg/ha) at two eastern Washington locations. Scenarios were run for indicated future periods of interest (2020, 2040, 2080) under conditions of standard (baseline) planting date or adaptation, which was planting two weeks earlier, under the indicated climate projection, and either with (CO_2) or without (no CO_2) the effects of elevated CO_2 on plant growth.

Location/ baseline yield	Condition	Scenario	Weather projection				Average yield	Ratio of future to baseline yield
			CCSM3	CGCM3	ECHAM5	PCM1		
			Yield (kg/ha)					
Pullman	**Standard**							
4085	No CO_2	2020	3845	4500	3983	3913	4060	0.994
kg/ha		2040	3289	4164	3712	3495	3665	0.897
		2080	3135	3540	3213	3078	3241	0.794
	CO_2	2020	4159	4902	4327	4240	4407	1.079
		2040	3720	4774	4235	3994	4181	1.024
		2080	3946	4456	4016	3863	4070	0.997
	Adaptation							
	No CO_2	2020	4225	4696	4306	4188	4354	1.066
		2040	3429	4530	3928	4026	3978	0.974
		2080	3284	3792	3591	3280	3487	0.854
	CO_2	2020	4579	5121	4680	4551	4733	1.159
		2040	3879	5208	4495	4632	4554	1.115
		2080	4194	4870	4542	4147	4438	1.087
St John	**Standard**							
3381	No CO_2	2020	3345	3618	3224	3334	3381	1.000
kg/ha		2040	2637	3268	2771	2751	2857	0.845
		2080	2652	2704	2387	2275	2505	0.741
	CO_2	2020	3564	3885	3451	3557	3614	1.069
		2040	2895	3643	3057	3026	3155	0.933
		2080	3179	3306	2852	2726	3016	0.892
	Adaptation							
	No CO_2	2020	3644	3889	3669	3717	3729	1.103
		2040	2738	3535	3086	3207	3142	0.929
		2080	2520	3010	2869	2388	2696	0.798
	CO_2	2020	3878	4162	3926	3965	3983	1.178
		2040	3021	3960	3408	3548	3484	1.031
		2080	3049	3694	3452	2889	3271	0.967

Table 4. Simulated dry yields of potatoes at Othello, Washington using a cultivar adapted to baseline conditions (standard) and a cultivar with a longer duration of green leaf area of 9 to 10 days (adaptation). Scenarios were run for indicated future periods of interest (2020, 2040, 2080) either with (CO_2) or without (no CO_2) the effects of elevated atmospheric CO_2 concentration on plant growth. Baseline yield for potato is 16207 kg/ha. Fresh yields are obtained by dividing by 0.2.

Condition	Scenario		Weather projection			Average yield	Ratio of future to baseline yield
		CCSM3	CGCM3	ECHAM5	PCM1		
		Yield (kg/ha)					
Standard							
No CO_2	2020	14042	14748	15353	15014	14789	0.913
	2040	12654	14260	14208	14289	13853	0.855
	2080	11899	12888	12562	13081	12607	0.778
CO_2	2020	15024	15792	16437	16068	15831	0.977
	2040	14371	16205	16144	16240	15740	0.971
	2080	14817	16041	15639	16301	15700	0.969
Adaptation							
No CO_2	2020	16656	17399	17976	17596	17407	1.074
	2040	15160	16868	16781	16800	16402	1.012
	2080	14261	15282	14856	15534	14983	0.924
CO_2	2020	17824	18633	19248	18834	18635	1.150
	2040	17220	19170	19069	19095	18639	1.150
	2080	17761	19022	18491	19356	18658	1.151

3.4. Apple Projections

Without considering the possible effect of elevated CO_2, future climate is predicted to slightly decrease the production of apples by 1%, 3%, and 4% for the 2020, 2040, and 2080 scenarios (Table 5). Under a warmer climate, the seasonal phenological development will proceed at a faster rate, and the period from budbreak to harvest will be shortened reducing the opportunity for biomass gain. This has already been observed in Alsace (eastern France) where the period between budbreak and harvest in grapes has become shorter and ripening of fruit occurs under warmer conditions (Duchene and Schneider, 2005). When the effect of CO_2 is added, yields are projected to increase by 6%, 9%, and 16% for 2020, 2040, and 2080 scenarios compared to current levels. Growers will need to adapt crop load management targets to maintain fruit quality standards at the higher yields.

Table 5 also shows apple yields that would be potentially attainable given the extended favorable conditions for growth due to warming. These are given as a reference of hypothetical potential benefits of climate change for apple growers in eastern WA, assuming the availability of varieties able to use the extended season or assuming that other adaptive technologies not currently available are developed. Depending on conditions, apple yields could potentially increase 5% to 11% for the 2020 scenario, and reaching

Table 5. Simulated dry yields of apples at Sunnyside, Washington. Scenarios were run for indicated future periods of interest (2020, 2040, 2080) either with (CO_2) or without (no CO_2) the effects of elevated atmospheric CO_2 concentration on yield. Fresh yields are obtained by dividing by 0.30.

Crop/ baseline yield (kg/ha)	Condition	Scenario	Weather projection				Average yield	Ratio of future to baseline yields
			CCSM3	CGCM3	ECHAM5	PCM1		
			Yield (kg/ha)					
Apples 18153								
	Standard							
	No CO_2	2020	17856	18215	18183	17880	18034	0.99
		2040	17251	18239	17682	17520	17673	0.97
		2080	17165	17806	17650	17360	17495	0.96
	CO_2	2020	18987	19367	19299	19010	19166	1.06
		2040	19363	20449	19807	19638	19814	1.09
		2080	20744	21345	21158	20850	21024	1.16
	Adaptation							
	No CO_2	2020	19101	19384	19027	18777	19072	1.05
		2040	18645	19617	18869	18729	18965	1.04
		2080	18537	19175	18980	18773	18866	1.04
	CO_2	2020	20305	20549	20146	19952	20238	1.11
		2040	20823	21455	20996	20882	21039	1.16
		2080	21541	21600	21565	21562	21567	1.19

19% for the 2080 scenario with elevated CO_2.

Even under reduced duration of the period from budbreak to harvest, warming may provide an extended period postharvest that may be beneficial for carbohydrate accumulation by trees –flowering and early growth in the subsequent season utilize stored carbohydrate and nutrient reserves. Greer et al. (2002) reported greater carbohydrate reserves and crop yields in 'Braeburn' apple trees exposed to higher temperatures after harvest. Moreover, bud winter hardiness in apple is positively related to tissue carbohydrate content (Raese et al., 1978), another potential benefit.

Wolfe et al. (2005) reported advances in spring phenology (days to bloom and days to first leaf) ranging from 2 to 8 days for grapes and apples in northeastern USA for the period 1965 to 2001. Although average temperatures are projected to increase for all climate scenarios, minimum temperatures during early spring will still provide conditions for damaging frost events, with added vulnerability due to earlier flowering. Figure 4 shows the distribution of minimum temperature for the month of April for current climate and the 2020 projections of each of the four GCMs included in this study, showing ~20% probability of minimum temperatures below freezing for the latter, not much different from the current condition. Under the projected climate change, flowering will tend to occur about 3 days earlier in the 2020 scenario, which will tend to increase slightly the exposure to frost events of flowers and fruits in initial stages of formation. This could increase current levels of yield loss from frost damage or increase the need and expense for frost protection, factors that are not simulated by the model.

Another factor not accounted for in the model is the effect on quality of apples of decreasing chill hours during the dormant period. Sufficient exposure to cold winter weather is required for uniform budbreak and flowering. This is not likely to be a significant problem since accumulation of sufficient chilling is usually satisfied for most apple cultivars by January.

3.5. Disease, Insect and Weed Pressure Projection

It is of interest to address possible changes in pest and disease pressures on agriculture in response to climate change because they can cause yield reductions and/or increase the cost of control. Only a generalized assessment is presented here, using projections from a few disease and insect models as an indication of possible overall effects. Models of weed-crop competition are very scarce and not suitable for this assessment, so we rely on empirical evidence to offer a projection of changes on weed pressure.

3.5.1. Diseases

One of the most problematic diseases of cherries and grapes in the irrigated production regions of Washington State are the powdery mildews. Powdery mildews are unique aerial plant pathogens because they are less reliant on free water than other fungal pathogens. The powdery mildews of cherry (Grove and Boal, 1991) and grape (Grove, 2004) have an early-season wetting requirement. Once wetting requirements are met, temperature becomes the factor limiting to the incidence and severity of powdery mildew epidemics. In general these powdery mildews reproduce most rapidly between 18 and 29 ^{o}C. Temperatures above 35 ^{o}C are lethal and below 18 ^{o}C are inhibitory (Gent et al., 2008).

Seasonal increases in precipitation could promote the establishment of diseases previously undocumented or considered minor in Eastern Washington. Examples include the downy mildew of grapevines, black rot of grapevines, and cherry leafspot. The emergence or increased importance of these diseases could potentially result in increases in disease management costs.

Projections of risk of infection for cherry and grape powdery mildew at Sunnyside are presented in Fig. 5. Cherry powdery mildew is predicted to increase under the CCSM3 (2020 only) and the CGCM3 projected climate. Small increases or no change in the risk from grapevine powdery mildew were predicted for all climate projections. Overall, warmer climate but with small changes in precipitation during the growing season will tend to maintain and eventually reduce the incidence of these diseases, unless there is an increase in precipitation early in the growing season.

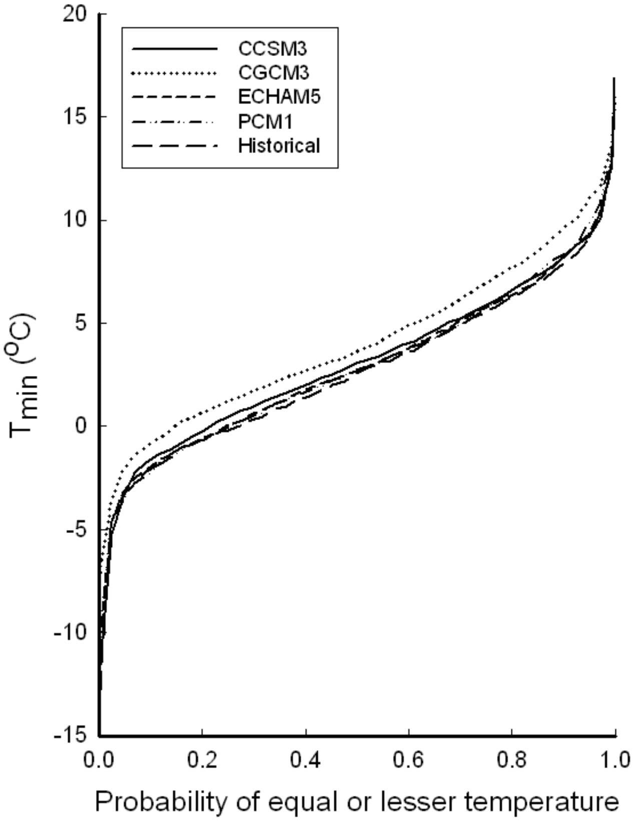

Figure 4. Probabilistic distribution of minimum April temperature for Sunnyside for the 2020 scenario.

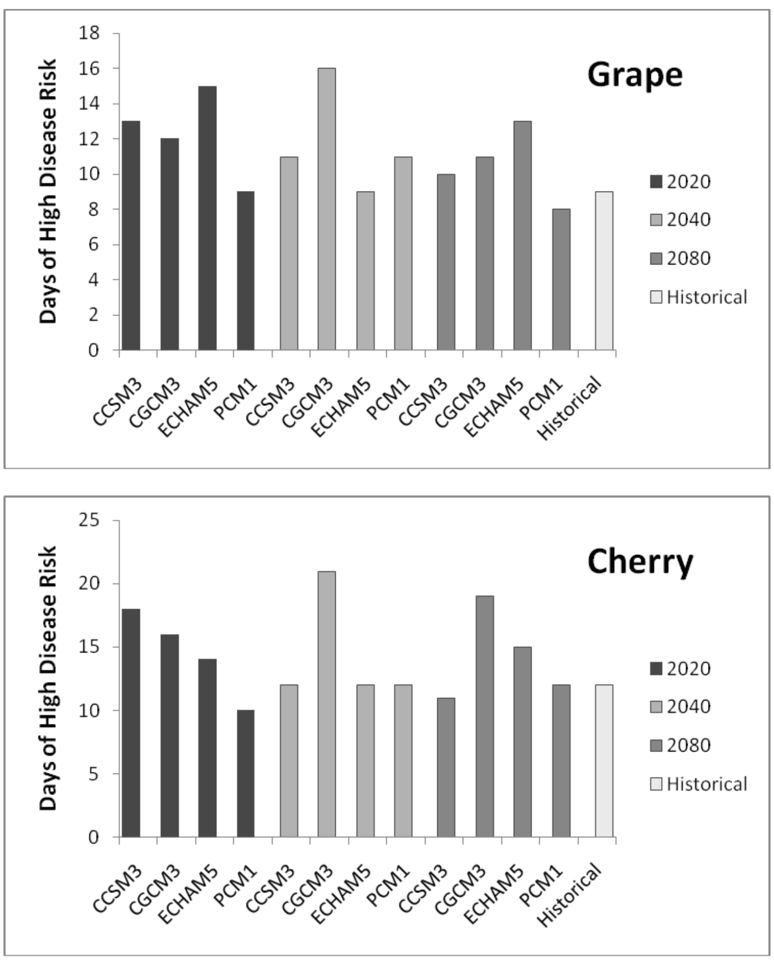

Figure 5. Influence of various climate change scenarios on the predicted risk of powdery mildew infection for grapes and cherries.

3.5.2. Insects

As a model for insects, we selected the codling moth, Cydia pomonella (L.), which is the most important pest of apples in Washington State (Beers et al. 1993). More insecticide applications and quantity of insecticide are applied per acre to control the codling moth than any other pest in Washington (NASS 2006). A model was developed to predict the seasonal life history of codling moth using an accumulation of degree-days (Riedl et al. 1976, Welch et al. 1978, Beers and Brunner 1992). Insect development is governed primarily by temperature so changes in precipitation are not expected to contribute to changes in pest status for most insects. The codling moth model has been primarily used to help growers time the first applications against the first and second generation of this pest and to predict the percent of third generation egg hatch, providing growers some indication of late season risk of crop damage.

The codling moth model was run for Sunnyside using baseline climate and the projection of the four GCMs in this study. Results of these simulations (Table 6) showed first adult flights occurring 6, 9, and 14 days earlier on average than the baseline for the 2020, 2040, 2080 scenarios. The beginning of the first generation egg hatch was advanced by 6, 8, and 13 days, and the beginning of the second generation egg hatch was advanced by 10, 14, and 21 days for the 2020, 2040, and 2080 scenarios.

The predicted fraction of third generation egg hatch was increased dramatically with warming. Earlier emergence of adults in the spring coupled with warmer temperatures in the summer would result in most apple-growing locations in the state experiencing a complete third generation egg hatch. Pheromones used as a control for codling moth would not last the entire season unless more pheromone was added to dispensers, which would increase the cost to growers. In addition, an increase in one to two additional sprays per season would most likely be needed to protect fruit late in the fall, especially on later maturing varieties. Warmer winter temperatures could result in an extended emergence pattern for codling moth making it more difficult to precisely time control applications, further increasing control costs for growers.

3.5.3. Weeds

Weeds account for $7 to 10 billion dollars in agricultural losses in the U.S. (Bridges, 1992) and economic losses from all weeds in the U.S. exceed $36 billion each year (Pimental et al. 2000). Weed species, weed/crop competition, and weed control vary widely among cropping systems and geographic regions. Uncontrolled weeds in annual crops can result in anywhere from 15% to total crop loss depending on weed and crop species present and their density. Weed management in annual crops is necessary to prevent or reduce yield losses.

Currently, few climate models consider the impact of weeds on crop yield as it is generally assumed weeds must be controlled to produce a crop. Estimates of yield stimulation by elevated CO_2 might need to be reduced if effects from competition with weeds are ignored, unless growers adapt accordingly. Most studies on climate change predict that pests

Table 6. Simulated codling moth response to indicated climate projections at Sunnyside, Washington. Scenarios were run for indicated future periods of interest (2020, 2040, 2080).

Weather projection	Scenario	First adult flight	First generation	Second generation	Fraction of third generation
		(day of year)			
Historical		113	142	206	6.0
CCSM3	2020	106	137	195	46.4
	2040	104	134	189	73.8
	2080	97	127	182	90.8
CGCM3	2020	102	132	195	43.4
	2040	98	130	193	54.7
	2080	95	128	186	80.4
ECHAM5	2020	109	139	200	22.3
	2040	108	137	194	44.3
	2080	98	128	187	79.5
PCM1	2020	108	137	197	32.7
	2040	107	136	194	45.4
	2080	104	133	188	70.7
Average	2020	107	136	197	35.9
	2040	104	134	192	54.8
	2080	98	129	186	81.0

will become better able to expand their geographic ranges in a changing climate. An expansion of pest populations may require increased use of agricultural chemicals, implying health, ecological, and economic costs (Rosenzweig et al. 2000). Weeds and other crop pests are projected to expand to higher latitudes (Dahlsten and Garcia 1989; Sutherst 1990).

Anticipated warmer and wetter fall and winter will result in greater numbers and growth of winter annual weeds and require additional herbicide or cultivations to control these weeds. Many winter annual weeds germinate in the late fall and small increases in rainfall and temperature could have large impacts on weed germination and growth during the fall and winter. Volunteer potato, a serious weed in climates with mild winter temperatures, would likely become more abundant with elevated winter temperatures as more tubers would survive in warmer soils. Control of volunteer potato in wheat and corn is accomplished with multiple herbicide applications and cultivation (Boydston, 2004, Steiner et al., 2005).

Overall, there are strong empirical reasons for expecting changes in temperature and CO_2 to have significant effects on weed biology, growth, and weed management. Elevated CO_2 will enhance growth of C_3 weeds allowing them to better compete with C_4 crops, which will obtain only marginal benefits from CO_2 elevation (Ziska, 2003). Stinson and Bazzaz (2006) showed that for a mixed population with two species, the smaller plant might benefit from CO_2 enrichment to a greater extent than the larger plant because of light interception properties, which would give weeds a competitive advantage. The physiological plasticity of weeds and their high degree of intraspecific genetic variation could provide weeds with a competitive advantage in a changing environment. New weed species and more competitive and prolific weeds may require improved timing of weed management practices, improved weed identification and scouting, and more frequent weed control practices (herbicide, mowing, and cultivation).

4. Avenues for Adaptation and Recommendations for Research

Our assessment indicates that, with the possible exception of winter wheat, the main agricultural commodities in eastern Washington State could be affected negatively by future climate warming, even as soon as the next few decades. However, the concurrent elevated atmospheric CO_2 is projected to compensate for the effect of warming and result in yield gains. To cope with the effect of warming and capture the potential benefits of elevated CO_2, adaptation of agricultural cropping systems and management to changing conditions will be critical. Research will play an important role by providing technologies for adaptation.

It is difficult to predict the economic environment under which agriculture will operate as we progress into this century, except that we know that an increasing population projected to reach nine billion people by mid century and the rapid development of highly populated countries such as China and India will ensure high demand for agricultural products. The state's diversified agriculture is likely to be an important factor of adaptation to changing conditions under global climate change. In addition, consequences of climate change appear less severe for higher than lower latitudes, which may favor the relative competitive position of the agriculture of the state and facilitate adaptation.

As shown in Fig. 6, winter wheat yields in the Palouse region around Pullman WA have increased from 3,300 to 5,400 kg ha^{-1} from 1972 to 2003 (perhaps including minor help from CO_2 increase during the period) while yields were only 1,300 kg ha^{-1} 90 years ago (Sievers and Holtz, 1922). This indicates that the contribution of technology (e.g., plant breeding, biotechnology, better crop management) to yield increases should be counted for as a factor that could contribute to mitigate the economic effect of negative climate change impacts, although it is uncertain if the pace of technology improvement will be the same in the future as it has been in the past.

Apples and other temperate tree fruits are projected to benefit from warmer weather combined with elevated CO_2, but management and varieties

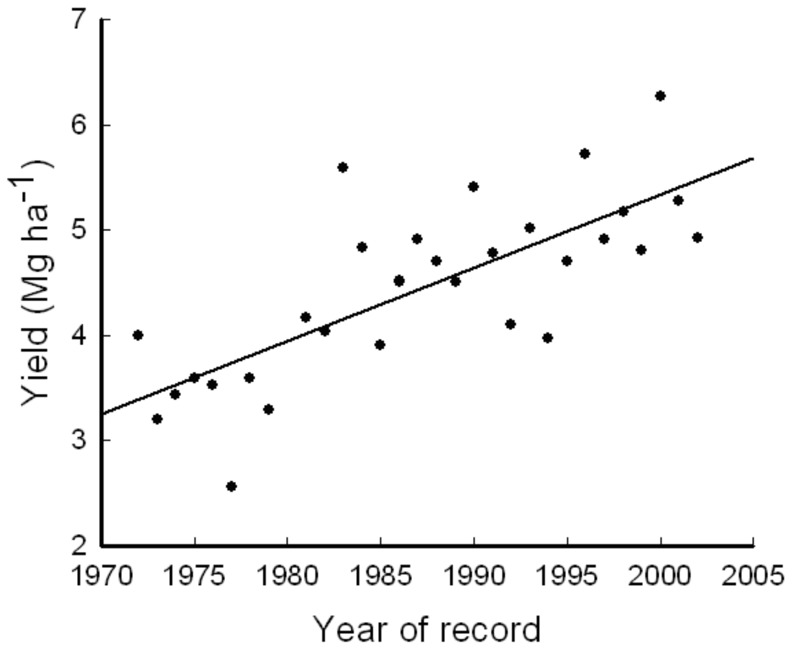

Figure 6. Winter wheat production in Whitman County (based on historic records).

will need to constantly adapt to harvest the benefits of future conditions. Eventually, warming may affect over-winter chill requirements of temperate tree fruits and require replacement by new cultivars or species. In the case of annual crops, modification of planting dates and use of varieties better adapted to the available growing season will be required, particularly in the case of potatoes. For annual and tree fruit crops, the search for more effective and environmentally friendly approaches for controlling more aggressive (or new) insects and weeds will be needed.

Overall, conventional and biotechnology-based breeding will be important to preserve the competitive position of existing commodities. Selection of materials from world regions where the developing future climate conditions already exist in present time is an option, recognizing that the current niche of successful commodities in the state is due to suitable current climatic conditions in eastern WA compared to other regions. Research in automation, sensors, information technologies, and overall improvement of agricultural management will be required to reduce costs. Agricultural research efforts should be targeted to prioritize research that helps to cope with potential negative effects of climate change and to capture the benefits of elevated CO_2, considering that adaptation to evolving future conditions is likely among the largest long-term challenges for agriculture.

Finally, an activity that should be urgently implemented by agricultural research and extension in the state is to maintain a state-of-the-art monitoring network and information center to gather and interpret data on the many manifestations of climate change impacts on agricultural production. This network is extremely important to track the actual speed of change and guide the basic and applied research that will be needed for adaptation.

5. Caveats of Projected Impact of Climate Change on Agriculture

This assessment of possible effects of climate change on Washington agriculture is based on computer simulation models, which are approximations of reality drawing from experimental research to represent the mechanistic processes that relate crop growth and yield and associated factors with climate. However, our projections of the direction and magnitude of yield changes for annual crops generally agree with previous studies. Projections for apples are more uncertain as tree fruit models are less developed and previous studies are not available.

We have selected 4 GCMs for this study out of 20+ available, encompassing the high and lower end of the range of expected warming. We found consistency in the ultimate effects of warming on agriculture regardless of the GCM used. However, changes in extreme heat and cold weather and extreme precipitation events will have impacts that are generally not well represented either by the GCMs themselves or the downscaling procedure that we used to relate the GCM output to local conditions. Other associated factors such as changes in cloudiness affecting solar radiation and changes in air humidity are not considered in our projections, and may have significant effects on future crop yields.

6. Conclusions

The impact of climate change on the agriculture of eastern Washington State is assessed in this study by focusing on the major commodities in terms of output value: Apples, potatoes, and wheat. Agricultural impacts depend on the direct effects of climate, but they also depend on increasing atmospheric CO_2 independent of CO_2's influence on climate. Increased CO_2 in the atmosphere can increase crop yields for some plants and also increase water use efficiency, which in turn may provide additional benefits in dryland crop yields. Projections presented assume that plants have adequate supply of nutrients and are well protected from pests and weeds, and for irrigated crops they assume adequate availability of water for irrigation. Crop response to climate change is assessed based on changes for 2020, 2040, and 2080 scenarios with respect to a baseline climate (1975-2005).

It is projected that the impact of climate change on selected but economically significant crops in eastern Washington will be generally mild in the short term (i.e., next two decades), but increasingly detrimental with time (potential yield losses reaching 25% for some crops by the end of the century). However, the projected elevated CO_2 is expected to provide significant mitigation of climate change effects, and in fact result in important yield gains for some crops. There is some debate about whether the CO_2 effect on plants will be temporary (perennial plants may adapt to new conditions or growth of plants in natural environments may be limited by other factors), but mounting experimental evidence involving well-managed agricultural crops show a definite beneficial effect of "CO_2 fertilization" on growth and yield of many crops, even for perennial crops such as fruit trees that are expected to be in production for many years.

Yields of dryland winter wheat are projected to increase (2 to 8%) for the 2020 scenario or remain generally unchanged or with some gains for the 2040 scenario because earlier maturity in response to warming will provide a degree of water stress avoidance. However, yield reductions (4 to 7%) are projected for the 2080 scenario in the higher precipitation region. When CO_2 elevation is added, yields are projected to increase by 13-15% (2020s) to 13-24% (2040s), reaching gains of 23% to 35% by the 2080 scenario, with the larger gains in drier sites. No change in spring wheat yields is projected for the 2020 scenario, but declines of 10% to 15% for the 2040 scenario, and 20% to 26% for the 2080 scenario are projected due to climate change. Increased CO_2 will compensate for decreased yields, leading to increases of 7% and 2% for the 2020 and 2040 scenarios at Pullman, but a 7% increase (2020s) followed by a 7% reduction (2040s) at Saint John. Earlier planting combined with CO_2 elevation is projected to increase yields by 16% for the 2020s.

Yields of irrigated potatoes are projected to decline by 9%, 15%, and 22% for the 2020, 2040, and 2080 scenarios, respectively, with smaller losses of only 2% to 3% for all scenarios when the effect of CO_2 is included. The development of varieties with a longer duration of green leaf area, combined with elevated CO_2, could potentially result in yield gains of ~15%. However, tuber quality is a concern due to tuber growth limitations under warmer conditions.

Without the effect of elevated CO_2, future climate change is projected to decrease apple production by 1%, 3%, and 4% for the 2020, 2040, and 2080 scenarios, respectively. When the effect of CO_2 is added, yields are projected to increase by 6% (2020s), 9% (2040s), and 16% (2080s). To realize potential yield gains and maintain fruit quality standards at higher yields will require management adaptations.

Caveats of the projection of climate change impacts on agriculture presented in this study are: a) possible changes in the frequency and persistence of extreme temperature (both frosts and heat waves) and precipitation events are not well represented in current climate projections, which could adversely affect crop yields, b) the extent to which the potential benefits of elevated CO_2 will be realized has a degree of uncertainty that should be considered by decision makers, and c) it is also possible that changes in impacts by pests, weeds and invasive species could affect agriculture in ways not described here.

References

Allen RG, Pereira LS, Raes D, Smith M (1998,) Crop evapotranspiration: Guidelines for computing crop water requirements. Irrig Drain Paper 56, FAO, Rome, Italy

Alva AK, Hodges T, Boydston RA, Collins HP (2002) Effects of irrigation and tillage practices on yield of potato under high production conditions in the Pacific Northwest. Commun Soil Sc Plant Anal 33:1451 – 1460

Beers EH, Brunner JF (1992) Implementation of the codling moth model on apples in Washington State, USA. Acta Phytopathologica et Entomologica Hungarica 27: 97– 102

Beers EH, Brunner JF, Willett M, Warner G (1993) Orchard pest management: A resource book for the Pacific Northwest. The Good Fruit Grower, Yakima, Washington

Bindi M, Fibbi L, Miglietta F (2001) Free Air CO2 Enrichment (FACE) of grapevine (Vitis vinifera L.): II. Growth and quality of grape and wine in response to elevated CO2 concentrations. Eur J Agron 14: 145–155

Boydston RA (2004) Managing volunteer potato (Solanum tuberosum) in field corn (Zea mays) with carfentrazone-ethyl and dicamba. Weed Technol 18: 83–87

Bridges DC (1992) Crop losses due to weeds in the United States. Weed Sci Soc Am, Champaign, IL, USA, 403 pp

Brown RA, Rosenberg NJ (1999) Climate change impacts on the potential productivity of corn and winter wheat in their primary United States growing regions. Clim Chang 41: 73–107

Castellvi F, Stöckle CO (2001) Comparing the performance of WGEN and ClimGen in the generation of temperature and solar radiation. Trans of ASAE 44:1683-1687

Cotrufo MF, Ineson P, Scott Y (1998) Elevated CO2 reduces the nitrogen concentration of plant tissues. Global Change Biol 4: 43-54

Dahlsten DL, Garcia R (eds) (1989) Eradication of exotic pests: Analysis with case histories. Yale University Press, NewHaven, Connecticut, 296 p

Duchêne E, Schneider C (2005) Grapevine and climatic changes: a glance at the situation in Alsace. Agron Sustain Dev 25: 93-99

Favis-Mortlock DT, Evans R, Boardman J, Harris TM (1991) Climate change, winter-wheat yield and soil-erosion on the English south downs. Agric Syst 37: 415-433

Ferris R, Ellis RH, Wheeler TR, Hadley P (1998) Effect of high temperature stress at anthesis on grain yield and biomass of field-grown crops of wheat. Annals of Bot 82: 631-639

Gent DH, Barbour JD, Grove GG, Mahaffee WF, Nelson ME, Ocamb CM, Peetz A, Turechek WW (2008) A decade of hop powdery mildew in the Pacific Northwest. Online. Plant Health Progress doi: (in press)

Greer DH, Wunsche JN, Halligan EA (2002) Influence of postharvest temperatures on leaf gas exchange, carbohydrate reserves and allocations, subsequent budbreak, and fruit yield of Braeburn apple (Malus domestica) trees. New Zealand J Crop Hort Sci 30: 175-186

Grove GG (2004) Perennation of Uncinula necator in vineyards of Eastern Washington. Plant Dis 88: 242-247

Grove GG, Boal RJ (1991) Overwinter survival of Podosphaera clandestina in eastern Washington. Phytopathol 81: 385-391

Harrison PA, Butterfield RE (1996) Effects of climate change on Europe-wide winter wheat and sunflower productivity. Clim Res 7: 225-241

Hatfield J, Boote K, Fay P, Hahn L, Izaurralde C, Kimball BA, Mader T, Morgan J, Ort D, Polley W, Thomson A, Wolfe D (2008) Agriculture. In: The effects of climate change on agriculture, land resources, water resources, and biodiversity. A Report by the U.S. Climate Change Science Program and the Subcommittee on Global Change Research. Washington, DC., USA, 362 pp

Idso SB, Kimball BA (2001) CO2 enrichment of sour orange trees: 13 years and counting. Env Exp Bot 46: 147-153

IPCC (2007) Climate change 2007: synthesis report. Intergovernmental Panel for Climate Change, Fourth Assessment Report

Jones GV (2005) Climate change in the western United States grape growing regions. Acta Horti. 689: 41-59

Kim HY, Lieffering M, Miura S, Kobayashi K, Okada N (2001) Growth and nitrogen uptake of CO2 enriched rice under field conditions. New Phytologist 150: 223–229

Kimball BA, Kobayashi K, Bindi M (2002) Responses of agricultural crops to free-air CO2 enrichment. Adv Agron 77: 293-368

Long SP, Ainsworth EA, Rogers A, Ort DR (2004) Rising atmospheric carbon dioxide: Plants FACE the future. Annu Rev Plant Biol 55: 591-628

Masle J, Doussinault G, Sun B (1989) Responses of wheat genotypes to temperature and photoperiod in natural conditions. Crop Sci 29: 712-721

Mote PW, Salathé Jr E P (2009) Future climate in the Pacific Northwest. Washington Climate Change Impacts Assessment: Evaluating Washington's future in a changing climate. In press

NASS (2006) Agricultural chemical usage 2005 fruit and nut summary. USDA/NASS/ERS

Nonhebel S (1996) Effects of temperature rise and increase in CO2 concentration on simulated wheat yields in Europe. Clim Chang 34: 73-90

Oechel WC, Cowles S, Grulke N, Hastings SJ, LawrenceB, Prudhomme T, Riechers G, Strain B, Tissue D, Vourlitis G (1994) Transient nature of CO2 fertilization in arctic tundra. Nature 371: 500-503

Olesen JE, Bindib M (2002) Consequences of climate change for European agricultural productivity, land use and policy. Eur J Agron 16: 239-262

Pannkuk CD, Stöckle CO, Papendick RI (1998) Validation of CropSyst for winter and spring wheat under different tillage and residue management practices in a wheat-fallow region. Agr Sys 57: 121-134

Parry ML, Rosenzweig C, Iglesias A, Livermore M, Fischer G (2004) Effects of climate change on global food production under SRES emissions and socio-economic scenarios. Glob Env Chang 14: 53–67

Peralta JM, Stöckle CO (2002) Nitrate from an irrigated crop rotation at the Pasco-Quincy area (Washington, USA) available for groundwater contamination: A long-term simulation study. Agr Ecosyst Env 88: 23-24

Pimental DL, Lach L, Zuniga R, Morrison D (2000) Environmental and economic costs associated with non-indigenous species in the Untied States. Biosci 50:53-65

Raese JT, Williams MW, Billingsley HD (1978) Cold hardiness, sorbitol, and sugar levels of apple shoots as influenced by controlled temperature and season. J Am Soc Hort Sci 103: 796-801

Riedl H, Croft BA, Howitt AJ (1976) Forecasting codling moth (Carpocapsa pomonella) phenology based on pheromone trap catches and physiological-time models. Can Entomol 108: 449-460

Rosenzweig C, Phillips J, Goldberg R, Carroll J, Hodges T (1996) Potential impacts of climate change on citrus and potato production in the US. Agr Sys 52: 455 479

Rosenzweig C, Iglesias A, Yang XB, Epstein P, Chivian E (2000) Climate change and U.S. agriculture: The impacts of warming and extreme weather events on productivity, plant diseases, and pests. Center for Health and the Global Environment, Harvard Medical School, Boston, Massachusetts

Schlenker W, Roberts M (2008) Estimating the impact of climate change on crop yields: The importance of nonlinear temperature effects. Working Paper 13799, National Bureau of Economic Research, Cambridge, MA (http://www.nber.org./papers/w13799)

Scott MJ, Vail LW , Jaksch JA , Stöckle CO, Kemanian, AR (2004) Water exchanges: tools to beat El Niño climate variability in irrigated agriculture. J Am Water Res Assoc 40: 15-31

Sievers FJ, Holtz HF (1922) The silt loam soils of eastern Washington and their management. State College of Washington Agricultural Experiment Station, Bulletin # 166

Steiner CM, Newberry G, Boydston R, Yenish J, Thornton R (2005) Volunteer potato management in the Pacific Northwest rotational crops. W.S.U. Ext Bull EB1993

Stinson KA, Bazzaz FA (2006) CO2 enrichment reduces reproductive dominance in competing stands of Ambrosia artemisiifolia (common ragweed). Oecologia 147: 155-163.

Stöckle CO, Williams JR, Rosenberg NJ, Jones CA (1992) A method for estimating the direct and climatic effects of rising atmospheric carbon dioxide on growth and yield of crops:Part I. Modification of the EPIC model for climate change analysis. Agric Sys 38:225-238

Stöckle CO, Martin S, Campbell GS (1994) CropSyst, a cropping systems model: water/nitrogen budgets and crop yield', Agric Sys 46: 335-359

Stöckle CO, Donatelli M, Nelson R (2003) CropSyst, a cropping systems simulation model.. Eur J Agron 18: 289-307

Stöckle CO, Kjelgaard J, Bellocchi G (2004,) Evaluation of estimated weather data for calculating Penman-Monteith reference crop evapotranspiration. Irr Sci 23: 39-46

Sutherst RW (1990) Impact of climate change on pests and diseases in Australia. Search 21:230–232

Thomson AM, Brown RA, Rosenberg NJ, Izaurralde RC, Benson V (2005) Climate change impacts for the conterminous USA: An integrated assessment Part 3 Dryland production of grain and forage crops. Clim Chang 69: 43–65

Timlin D, Lutfor R, Baker, SM, Reddy VR, Fleisher D, Quebedeaux (2006) Whole plant photosynthesis, development, and carbon partitioning in potato as a function of temperature. Agron J 98: 1195-1203

Tubiello FN, Rosenzweig C, Goldberg RA, Jagtap S, Jones JW (2002) Effects of climate change on US crop production: Simulation results using two different GCM scenarios. Part I: Wheat, potato, maize, and citrus. Clim Res 20: 259–270

Washington State Department of Agriculture (2008) Agr Pub 120-126 (R/1/08)

Welch SM, Croft BA, Brunner JF, Michels MF (1978) PETE: an extension phenology modeling system for management of multi-species pest complex. Environ Entomol 7: 482-494

Wolfe DW, Schwartz MD, Lakso AN, Otsuki Y, Pool RM, Shaulis NJ (2005) Climate change and shifts in spring phenology of three horticultural woody perennials in northeastern USA. Int J Biometeorol 49: 303-309

Ziska LH (2003) Evaluation of yield loss in field sorghum from a C3 and C4 weed with increasing CO2. Weed Sci 51: 914-918.

Photo credit, page 197: Climate Impacts Group, University of Washington

6: Salmon

Impacts of Climate Change on Key Aspects of Freshwater Salmon Habitat in Washington State

Nathan Mantua [1,2], Ingrid Tohver [1], and Alan Hamlet [1,3]

Abstract

This study evaluates the sensitivity of Washington State's freshwater habitat of Pacific Salmon (*Oncorhynchus spp.*) to climate change. Our analysis focuses on summertime stream temperatures, seasonal low flows, and changes in the frequency and magnitude of peak flow events because these physical factors are likely to be key pressure points for many salmon populations in Washington State. We evaluate the sensitivity of weekly summertime water temperatures and extreme daily high and low streamflows under multimodel composites for A1B and B1 greenhouse gas emissions scenarios. Simulations predict increasing water temperatures and increasing thermal stress for salmon in both western and eastern Washington state that are slight for the 2020s but increasingly large later in the 21st century. Streamflow simulations predict that the largest hydrologic sensitivities are for watersheds that currently have so-called *transient* runoff streamflows, those that are strongly influenced by a mix of direct runoff from autumn rainfall and springtime snowmelt. By the 2080s, the hydrologic simulations predict a complete loss of snowmelt dominant basins in WA, and only about 10 basins remaining in the north Cascades classified as transient snow basins. Historically transient runoff watersheds will trend towards rainfall dominant basins and experience longer summer low flow periods, increased streamflow in winter and early spring, declines in the magnitude of summer low flows, and increases in winter flooding. The combined effects of warming stream temperatures and altered streamflows will very likely reduce the reproductive success for many salmon populations in Washington watersheds, but impacts will vary according to different life history-types and watershed-types. Salmon populations having a stream-type life history with extended freshwater rearing periods (*i.e.* steelhead, coho, sockeye and stream-type Chinook) are predicted to experience large increases in hydrologic and thermal stress in summer due to diminishing streamflows and increasingly unfavorable stream temperatures. Salmon with an ocean-type life history (with relatively brief freshwater rearing periods) are predicted to experience the greatest freshwater productivity declines in transient runoff watersheds where future warming is predicted to increase the magnitude and frequency of winter flooding that reduces egg-to-fry survival rates.

[1] JISAO Climate Impacts Group, University of Washington, Seattle, Washington
[2] School of Aquatic and Fishery Sciences, University of Washington, Seattle, Washington
[3] Department of Civil and Environmental Engineering, University of Washington, Seattle, Washington

1. Introduction

Climate plays a crucial role in salmon ecology at every stage of their life cycle, but the relative importance of climatic factors is quite different for different salmon stocks. Key limiting factors for freshwater salmon productivity include thermal and hydrologic regimes; these depend on species, their life history, watershed characteristics, and to a great extent stock-specific adaptations to local environmental factors (*e.g.* Richter and Kolmes 2005, Beechie et al. 2008, Crozier and Zabel 2007, and Farrell et al. 2008). Those stocks that typically spend extended rearing periods in freshwater (steelhead, stream-type Chinook, sockeye and coho) are likely to have a greater sensitivity to freshwater habitat changes than those that migrate to sea at an earlier age (ocean-type Chinook, pinks, and chum). While it would be desirable to produce watershed-specific estimates of the aggregate effects of climate change on individual stocks of Pacific salmon (*Oncorhynchus spp*.) in Washington State watersheds, scientific understanding of the interactions between climate and salmon productivity at each stage of each stock's life cycle is not yet adequate to do so. Even in cases where it is possible to carry out stock-specific assessments, such undertakings are beyond the scope of this statewide analysis. Instead we focus on a few direct, well-understood mechanisms whereby more easily predicted physical properties of the *freshwater* habitat for salmon directly influence salmon reproductive success at certain stages of their life cycle. Those physical properties are stream temperature and the volume and time distribution of streamflow. We combine observations, statistical modeling, and hydrologic modeling to compare conditions of the past (1970-1999) with those under projected future climate scenarios for 30-year windows centered on the decades of the 2020s, 2040s, and 2080s.

The overarching question to be addressed in this study is: How will climate change alter the potential reproductive success of Washington State's salmon, and where and under what conditions is freshwater habitat for salmon most vulnerable to direct hydroclimate (rising water temperatures and altered flow) effects of climate change? Guided by the Independent Scientific Advisory Board's (ISAB 2007) and Crozier et al.'s (2008) reviews of climate change impacts on salmon productivity in the Columbia River Basin, we limit our study to focus on the following subsidiary questions:

- What will be the role of climate change in coming decades on summertime water temperatures?
- How will a changing climate affect summer low flows and flood peaks?
- How, and in which watersheds, will these hydrologic changes likely affect the reproductive success for salmon?

We use three approaches to address these research questions. First, we employ the statistical modeling approach of Mohseni et al. (1998) to relate past surface air temperatures to stream temperatures, and apply these relationships trained on past climate in conjunction with projections of future air temperatures to predict corresponding future stream temperatures. Second, hydrologic models driven by future scenarios of surface air temperature and precipitation provide projections for changes in the statistics of summer low flows and flood peaks (Elsner et al. 2009, this report). And third, the likely impacts of climate change on the reproductive

Table 1. Maximum weekly temperature* upper thermal tolerances for salmonids.

Species	Upper thermal tolerance
Cutthroat trout (O. clarki)	23.3 °C (73.9 °F)
Rainbow trout (steelhead) (O. mykiss)	24.0 °C (75.2 °F)
Chum salmon (O. keta)	19.8 °C (67.6 °F)
Pink salmon (O. gorbuscha)	21 °C (69.8 °F)
Coho salmon (O. kisutch)	23.4 °C (74.1 °F)
Chinook salmon (O. tshawytscha)	24 °C (75.2 °F)

*Based on the 95th percentile of maximum weekly mean temperatures where fish presence (juvenile or adult) was observed (Eaton and Scheller 1996).

success for salmon in Washington's watersheds are realized by combining salmon sensitivities described in the scientific literature with our scenarios for changes in the statistics of stream temperature and streamflows.

The sensitivity of stream temperature and streamflow to changes in climate vary within and between watersheds due to natural and anthropogenic factors that include watershed geomorphology, vegetative cover, groundwater inputs to the stream reach of interest, water resources infrastructure (dams and diversions), the amount and timing of streamflow diverted to out-of-stream uses, and the degree to which key hydrologic processes have been impaired by changes in watersheds.

Increasing summertime stream temperatures are likely to be a key pressure point for many salmon populations in Washington State. Following methods used in previous assessments of climate change impacts on stream habitat (Eaton and Scheller 1996, O'Neal 2002, Mohseni et al. 2003), here we evaluate the sensitivity of summertime weekly water temperature for reasons outlined below.

Water temperature is a key aspect of water quality for salmonids, and excessively high water temperature can act as a limiting factor for the distribution, migration, health and performance of salmonids (e.g. McCullough 1999, Richter and Kolmes 2005, EPA 2007, Farrell et al. 2008). For salmon, excessively warm waters can inhibit migration and breeding patterns, and reduce cold-water refugia and connectivity. When average water temperatures are greater than 15 °C (59 °F) salmon can suffer increased predation and competitive disadvantages with native and non-native warm water fish (EPA 2007). Water temperatures exceeding 21-22 °C (70-72 °F) can prevent migration. Furthermore, adult salmon become more susceptible to disease and the transmission of pathogens as temperatures rise, and prolonged exposure to stream temperatures across a threshold (typically near 21°C, but this varies by species) can be lethal for juveniles and adults (McCullough 1999) (see Table 1).

Previous studies have projected climate change impacts on weekly water temperatures in order to evaluate impacts on trout and salmon habitat in the U.S. O'Neal (2002) used 8 climate change scenarios with a 2090 summertime warming ranging from 2 to 5.5 °C to predict maximum weekly U.S. water temperatures. Locations that experienced a projected maximum weekly water temperature greater than the upper thermal tolerance limit for a species were considered lost habitat. The projected loss of salmon habitat in Washington ranged from 5 to 22% by 2090, depending on the climate change scenario used in the analysis.

The Washington Department of Ecology (DOE) established water temperature standards for salmon habitat at various stages of their life history in Chapter 173-201A of the Washington Administrative Code (WAC), and these were subsequently reviewed by the Environmental Protection Agency (EPA 2007). The DOE and EPA express temperature thresholds for salmon as the 7-day average of the daily maximum temperature (7DADMax). Among adult salmon, the 7DADMax is lethal at ~23 °C, migration is inhibited at ~24 °C, and the risk of disease is elevated at ~14 °C. The models we used in this study estimate *weekly average* temperatures (hereafter T_w) rather than 7DADMax, so we must use an appropriately adjusted criteria. The EPA (2007) determined that the 7DADMax is 3 °C warmer than T_w. Therefore we identify sites where T_w exceeds 21 °C (or 3 °C less than the 7DADMax criteria) as the critical threshold for migration barriers and an elevated risk to fish kills for salmon (EPA 2007). Also note that Washington's DOE adopted a 17.5 °C 7-DADMax (equivalent to a 14.5 °C T_w) criterion to protect waters designated for 'Salmon Spawning, Rearing, and Migration use' where spawning occurs after mid-September and egg emergence occurs before mid-June (EPA 2007).

Characteristics of seasonal and daily streamflow variations can also serve as limiting factors for freshwater salmon habitat (Rand et al. 2006, Beechie et al. 2006). Battin et al. (2007) found that of the factors they evaluated for climate change impacts on ocean-type Chinook in the Snohomish Basin, projected increases in extreme high flows by far had the greatest negative impact on the reproductive success of salmon. Studies by Beechie et al. (1994) and Reeves et al. (1989) indicate that the most important factors for juvenile coho freshwater survival are (1) the in-stream temperature during the first summer, combined with the availability of deep pools to mitigate high temperatures; and (2) temperature during the second winter, combined with the availability of beaver ponds and backwater pools to serve as refuges from cold temperatures and high streamflow events. Consequently, a particularly troublesome scenario for coho involves an increase in summer water temperature in combination with a decrease in summer streamflow.

The WAC Chapter 173 provisions for in-stream resources protection program include several of Washington's river basins with regard to the changing summer low flows and how they impact salmon. Among the provisions stated in these programs is the maintenance of minimum flows for migrating fish.

In order to evaluate the impacts of climate change on summer low flows and flood peaks, we quantify projected changes in the statistics of extreme high and low flows through an analysis of daily streamflows simulated by a hydrologic model under past and future climate scenarios (Elsner et al. 2009, this report). The shifts in precipitation and temperature resulting from climate change will have a multifaceted effect on the streamflow variability since the sources feeding into the rivers in Washington State differ. Relatively warm river basins where surface air temperatures remain above freezing for most or all of the winter are rain-dominant and are found near the coast or at lower elevations in western Washington. Washington's coldest river basins are found in the higher elevation catchments of the Columbia Basin and North Cascades. In these basins winter surface temperatures remain well-below freezing for most or all of winter and have annual flows dominated by spring-summer snowmelt. Washington also has many salmon-bearing watersheds where streamflow is strongly influenced by both direct runoff from rainfall and springtime snowmelt because surface temperatures in winter typically fluctuate around the freezing point; these are referred to as *transient runoff* basins. Over the course of a given winter, precipitation in transient watersheds frequently fluctuates between snow and rain depending on relatively small changes in air temperature. Transient basins are found on the west slopes of the Cascades, the Olympics, and at lower elevation catchments draining the east slopes of the Cascades (Beechie et al. 2006, Hamlet and Lettenmaier 2007). Flooding intensity and timing in transient river basins is therefore dependent on temperature changes, amount of winter snow accumulation and subsequent spring snowmelt, and large-scale fall-winter storms. Low-flows in Washington's watersheds typically occur at the end of the summer and beginning of the fall. Extreme low-flow events can occur with rising summer temperatures, increasing evaporation, and in combination with reduced springtime snow pack and/or decreasing summer precipitation.

As previously noted, climate also influences estuarine and marine habitat for salmon. Interested readers can find informative reviews of climate impacts on marine habitat for PNW salmon by Pearcy (1992), Loggerwell et al (2003), and ISAB (2007). However, an evaluation of the impacts of climate change on those habitats is beyond the scope of this study.

2. Data and Methods

2.1. Historical Water Temperature and Air Temperature Data

Stream temperature has been monitored in both large rivers and smaller streams in Washington State by several different agencies. We used three different data sources covering a variety of time periods in this study (see Appendix A). Continuous summertime stream temperature data for 126 stations covering parts of the 2000 to 2007 period were obtained from Washington's DOE (http://www.ecy.wa.gov/programs/eap/fw_riv/rv_main.html#4). Hourly water temperature data from 51 stations in the Columbia River Basin covering parts of the 1995-2008 period were obtained from the U.S. Army Corps of Engineers (USACE) Data Access in Real Time (http://www.cbr.washington.edu/dart/help/hgas_def.html). The U.S. Geological Survey (USGS) archives long-term daily water temperatures at various sites along the Columbia River Basin covering parts of the 1950-2000 period. Mean daily stream temperature data for 34 stations in the Columbia River Basin were obtained from the USGS archives (http://www.streamnet.org/online-data/temperature1.html). For the continuous

August Mean Surface Air Temperature and Maximum Stream Temperature, 1970-1999

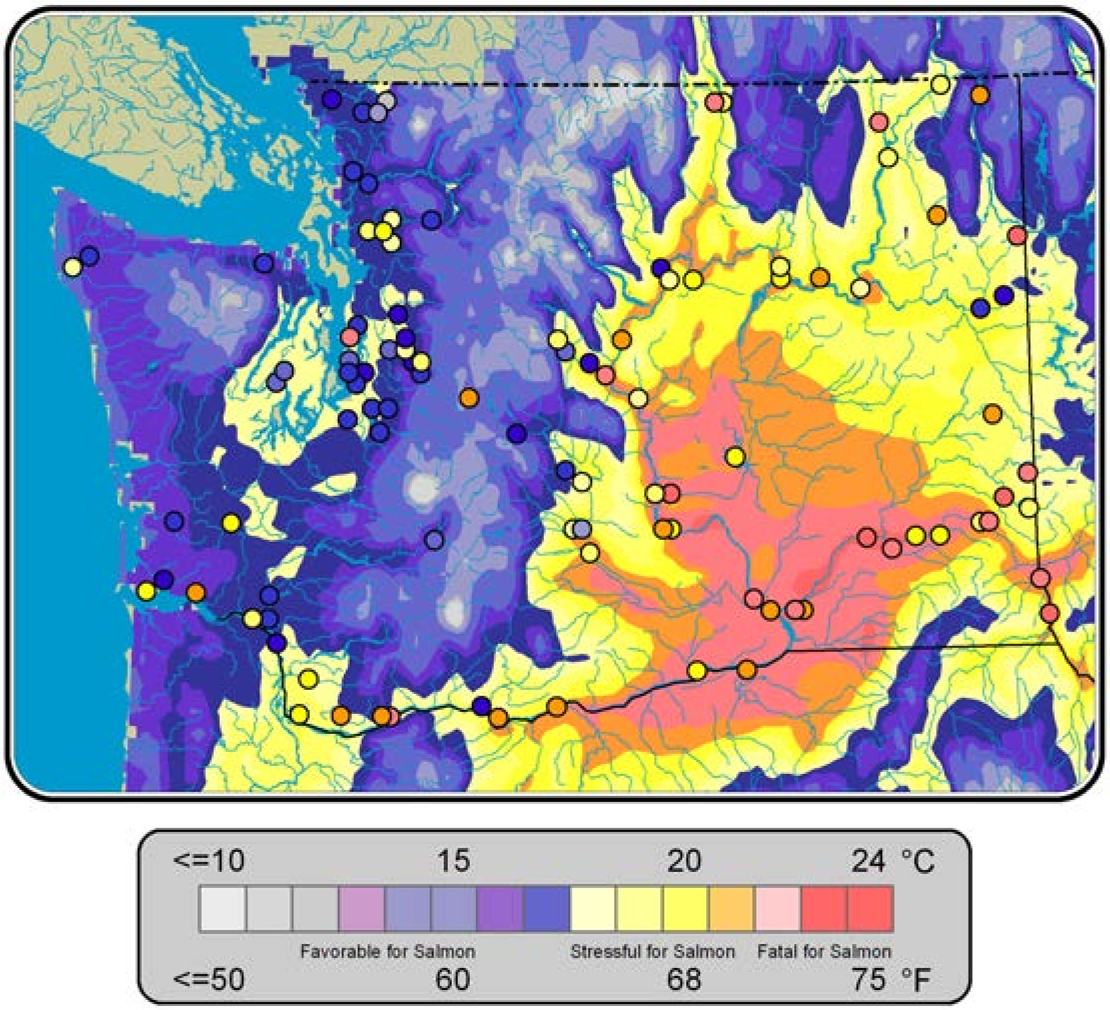

Figure 1. Color shading shows the historic (1970-1999) mean surface air temperatures for August, and shaded circles show the simulated mean of the annual maximum for weekly water temperatures for select locations.

and hourly data sets, daily average water temperatures were developed from the daily maximum and minimum temperatures. The daily averages were used to calculate mean weekly temperatures. The NOAA National Climate Data Center (NCDC) archives daily air temperature data for over 10,000 stations across the U.S. Station data for daily air temperature were matched to eight of the water temperature sites based on location (within 10 km) and data were downloaded from NCDC (http://cdo.ncdc.noaa.gov/CDO/dataproduct). We also used the downscaled, gridded, historic surface air temperatures at 1/16th degree latitude by longitude spatial resolution for the 1915-2006 period (Elsner et al. 2009, this report). Figure 1 shows August surface air temperatures averaged from 1970-99 that were derived from station data and mapped to the 1/16th degree grid used in this study.

2.2. Climate Change Scenarios

Our assessment of climate change impacts on stream temperature and streamflow in the 21st century originates from 19 of the 39 coarse-resolution (with typically 100-300 km grid-spacing) climate change scenarios for Washington State's surface air temperature and precipitation described by Mote and Salathé (2009, this report). The 19 scenarios used in this report consist of output from 10 climate models run under A1B emissions, and 9 models for B1 emissions. For our stream temperature modeling, we used air temperatures that were statistically downscaled from the global climate models to the 1/16th degree grid and from a monthly to daily timestep (Elsner et al. 2009, this report). Our streamflow analysis is based on outputs from a hydrologic model that was forced by both air temperature and precipitation that were downscaled from the global climate models using the so-called "delta method" approach, wherein the coarse spatial resolution monthly average changes between future and historic averages are used to adjust the 1/16th degree gridded historic daily time series in order to represent future climate.

For both stream temperature and streamflow, we focus on the sensitivity of freshwater habitat for salmon to the A1B and B1 scenarios for future greenhouse gas emissions (SRES 2000). The A1B emissions scenario can be considered a "medium" warming scenario, (it is not the warmest of all the IPCC scenarios), and refers to a future where population peaks mid-century and there is very rapid economic growth and a balanced portfolio of energy technologies including both fossil fuels and high efficiency technology that is adopted rapidly. The B1 emissions scenario has lower emissions than A1B that result in less warming, and could be considered the "low" warming scenario. B1 refers to a future where population is the same as A1B, but there are rapid economic shifts toward a service/information economy, the introduction of clean and resource-efficient technologies and emphasis on global solutions to economic, social, and environmental sustainability (SRES 2000).

Based on the average of the 19 scenarios, these models project increases in annual temperature for the Pacific Northwest, compared with the 1980s, of 1.2°C (2.2°F) by the 2020s, 1.9°C (3.4°F) by the 2040s, and 3.2°C (5.8°F) by the 2080s. Because the global climate models have just a few grid points that do a poor job resolving the topography in Washington State, the spatial gradients are very weak in the predicted *changes* for Washington's precipitation and surface air temperature. Changes in annual precipitation, averaged over all models, are small, but some models show large seasonal changes, especially toward wetter winters and drier summers. Most models predict summer warming exceeds the warming in other seasons, and the models with the most warming also produce the most summer drying (Mote and Salathé 2009, this report).

Based on the 10-model average for A1B emissions, Pacific Northwest summertime temperatures are projected to increase 1.7°C (3.0°F) by the 2020s, 2.7°C (4.9°F) by the 2040s, and 4.7°C (8.5°F) by the 2080s relative to the 1980s. The projections for summertime temperature increases from the 9-model average using B1 emissions are approximately 70% as large as those for the multi-model average using A1B emissions (Table 2). Also note that individual climate model projections for the same emissions

Table 2. Multi-model average projected changes in June-July-August PNW air temperature for A1B (10 models) and B1 (9 models) emissions. The statistically downscaled models represented here and used in our stream temperature modeling are: ccsm3, cgcm3.1 t47, cnrm cm3, echam5, echo g, hadcm, hadgem1 (A1B only), ipsl cm4, miroc 3.2, pcm1.

Scenario	2020s			2040s			2080s		
	Low	Avg	High	Low	Avg	High	Low	Avg	High
A1B	0.43°C (0.8°F)	1.7°C (3.0°F)	3.4°C (6.1°F)	1.3°C (2.3°F)	2.7°C (4.9°F)	5.1°C (9.1°F)	2.7°C (4.8°F)	4.7°C (8.5°F)	8.1°C (14.6°F)
B1	0.18°C (0.3°F)	1.2°C (2.2°F)	2.4°C (3.8°F)	0.2°C (0.4°F)	1.8°C (3.3°F)	3.7°C (6.6°F)	1.3°C (2.4°F)	2.9°C (5.2°F)	5.1°C (10.0°F)

scenario vary. For summertime temperature changes summarized in Table 2, the range of projected changes from individual models can be as extreme as 15% to 200% of the multimodel average.

As noted above, we use air temperatures derived from the statistically downscaled global climate model simulations to estimate summertime water temperatures for the 21st century, but in this study report only the multi-model averages for the A1B and B1 emissions scenarios, respectively.

Elsner et al. (2009, this report) used another downscaling approach, known as the *delta method*, in the hydrologic model simulations that generated the daily streamflow data analyzed in this report. The delta method simply applies changes in monthly average temperature and precipitation from global climate models to the full daily time series of historic meteorological fields for 1915-2006. Composite forcing fields on a 1/16th degree grid for A1B and B1 emissions scenarios were developed from multi-model weighted averages of air temperature and precipitation, respectively. These forcing fields were then used to drive the Variable Infiltration Capacity (VIC) hydrologic model simulations that produced daily time series of streamflow. Thus, the flood and low flow statistics from our analyses come from simulated streamflow data that came from simulations forced by three separate 92-year driving data sets for each of the emissions scenarios (A1B and B1), one representing the climate for each of the future time horizons centered on the 2020s, 2040s, and 2080s, respectively.

2.3. Non-linear Stream Temperature Regression Models

Mohseni (1998) used weekly average air temperature to predict weekly average water temperatures, and we use the same approach here using the data available for all of the sites (air and water temperatures). The regression models developed by Mohseni et al. (1998) show that the relationship between weekly air and water temperatures is best described by a nonlinear S-shaped function:

$$T_w = \mu + \frac{\alpha - \mu}{1 + e^{\gamma(\beta - T_{a_i})}} \tag{1}$$

where T_w is the estimated weekly average stream temperature, μ is the estimated minimum stream temperature (set to ≥ 0 since the rivers in this study never freeze), α is the estimated maximum stream temperature, γ is a measure of the steepest slope of the function, β indicates the air temperature at the inflection point, and T_a is the average weekly air temperature. To estimate the parameters of the nonlinear function the least squares method was applied, minimizing λ, the sum of the squared errors (ε) between the observed and fitted values for water temperatures:

$$\lambda = \sum_{i=1}^{n} \varepsilon_i^2 = \sum_{i=1}^{n} \left(T_{obs_i} - \mu - \frac{\alpha - \mu}{1 + e^{\gamma(\beta - T_{a_i})}}\right)^2 \tag{2}$$

Many climate variables other than air temperature also influence water temperatures, and some of the sites in this study undergo seasonal hysteresis, which involves a lag in stream temperature response to air temperature. For example, this phenomenon occurs when streams receive an influx of cold snowmelt water in the spring and maintain a cooler thermal regime despite warming air temperatures. The effects of this process are apparent during the fall and spring seasons when the data scatter is greater around the fitted model. In these cases, two regressions were applied to the data based on the weekly values separately for the fall and spring seasons. Of the estimated parameters from the two fitted models, the higher α, the lower μ, and average of the two γ and β parameters were used to calculate T_w (Mohseni et al. 1998), so that ultimately only one fitted model was applied to each site.

The Nash-Sutcliffe coefficient (NSC) (Nash and Sutcliffe, 1970) was used to determine the goodness of fit:

$$NSC = 1 - \frac{\sum_{i=1}^{n} (T_w - T_{obs})^2}{\sum_{i=1}^{n} (\overline{T}_{obs} - T_{obs_i})^2} \tag{3}$$

In streams where seasonal hysteresis was suspected of playing a role in water temperatures, the average NSC from the two fitted regressions was calculated and if it exceeded the NSC calculated for a single fitted function, the stream was assumed to exhibit hysteresis. Of the 211 stations modeled, only the 133 streams with NSC values ≥ 0.7 were included in this study (Mohseni et al. 1998). Of these sites, 12 demonstrated hysteresis and had higher NSC values when fit to two functions. The range of water temperature observations extended from less than one year to more than 30 years for some sites depending on the data source. Since we focus on summertime weekly average temperatures, we included only those sites where summertime temperatures were available (weeks 25 – 40). Because we are modeling weekly average temperatures, we feel justified in developing regression models with just one to a few years of stream temperature observations if, according to the NSC criteria employed here, we are able to develop a robust relationship between a location's weekly average air and water temperature. We also assume that the statistical relationship between weekly average air and water temperature are stationary, both for past and future years.

2.3.1. Model Validation and Application

The eight sites with paired observed air and water temperature data were used to validate the models. Weekly averages of observed air (NCDC station data in Appendix B) and stream temperatures were calculated for each site. Using the statistical programs R 2.7 and SAS 9.1, we estimated the model parameters for each test site by fitting the observed weekly air temperatures to the observed weekly water temperatures with the regression model (Equation 1) using the least squares method (Equation 2). Each test site was matched to the nearest grid in the 1/16^o downscaled dataset and the same method was applied using historic surface air temperature from this dataset (Elsner et al. 2009, this report). The model parameters for each site generated by (a) the observed air temperatures (station data) and (b) the downscaled historic air temperature data were similar enough to support the use of the downscaled historic air temperature dataset in the development of stream temperature regression models for all of the stream temperature observation sites. We also compared the NSC values generated by station data and downscaled air temperatures for the eight sites. The range of these NSC values are nearly identical, 0.79 – 0.99 and 0.80 – 0.99 for station and downscaled data, respectively. The averages of NSC values for these test sites are also comparable, 0.90 for station data and 0.88 for downscaled data.

All sites with observed water temperature data were matched to the nearest 1/16^o grid point in the downscaled dataset using ArcGIS 9.3. Model parameters were estimated using weekly surface air temperatures from the historic downscaled dataset for each site. The regression parameter of interest in this study is the α-value, or maximum temperature. The models estimated an α-value within 2 ^{o}C of the observed maximum temperature for 80% of the sites in this study. Similar to Mohseni et al. (1998), we found that the regression models more often underestimated the α-value in this study. We applied the regression model using the estimated parameters and the downscaled surface air temperatures for each climate change model (10 models for the A1B scenario and 9 models for the B1 scenario as made available by the IPCC) to estimate average weekly water temperatures for 19 future climate change scenarios at 133 sites. For each scenario, the projected weekly maximum water temperatures were identified for each model and averaged over the models into four 30-year intervals: 1970-1999, 2010-2039, 2030-2059, 2070-2099. Sites and time periods where weekly temperatures exceed 21 ^{o}C were flagged as indicators for potential migration barriers and extreme thermal stress for salmon, although it is important to keep in mind that not all these sites are in reaches that typically host juvenile or adult salmon during the warmest summer months.

2.4. Methods for Extreme High and Low Flow Analyses

The flood and low flow frequency statistics were calculated from Elsner et al's. (2009, this report) projected and historic (1915-2006) daily flow simulations at 97 sites in Washington State (listed in Appendix C). Flood frequency was calculated by ranking the annual maximum flows and fitting the Generalized Extreme Value distribution using the L-moments method (Wang 1997, Hosking and Wallis 1993, Hosking 1990). From the fitted probability distributions, the flood magnitudes with a 20-year return period were estimated for each time interval centered on the 1980s, 2020s, 2040s and 2080s. Beamer and Pess (1999) found that stocks of Chinook salmon in the Skagit and Stillaguamish rivers were unable to reproduce rapidly enough to "replace" themselves if peak flows during the intervals of egg incubation matched or exceeded the 20-year flooding event. The low flow statistic is the annual minimum 7-day consecutive lowest flow, to which the same probability distribution was fit as for flood flows. From the fitted distribution, we estimated 7Q2 and 7Q10, or the magnitude of the 2-year and 10-year return period 7-day low flow magnitudes, respectively, for each of the four 30-year time intervals. The results from these analyses were used to calculate the ratio of future to historic flooding and low flow magnitudes for each composite scenario/ time interval (e.g. "A1B 2020s", or "B1 2040s"). From the downscaled, derived historic air temperature data set, the average December/January/ February air temperatures (DJF) were calculated for each catchment for the 1970-1999 period to characterize wintertime temperature regimes. The projected return frequency of the historic 20-year flood was estimated and compared to each basin's DJF average temperature to typify each basin's sensitivity to warming temperatures.

3. Key Findings/Discussion

3.1. Summertime Stream Temperature Projections

Maximum weekly water temperatures in Washington State are typically observed from late July through late August, very much like the period of climatologically warmest air temperatures. In Figure 1 we show the downscaled historic averages for August surface air temperatures and simulated annual maximum weekly water temperatures for the 1970-99 period. Many of the interior Columbia Basin's water temperature stations modeled in this study have maximum weekly water temperatures that exceed 21°C. In reaches that typically host salmon in the warmest summer months these locations already have periods with episodes of extreme thermal stress for salmon. For instance, summer water temperatures in the mainstem Columbia River sometimes reach lethal limits for sockeye salmon (Naughton et al. 2005), and frequently pose thermal migration barriers for fall Chinook (Goniea et al. 2006) and summer steelhead (High et al. 2006). All but one of the extreme water temperature stations in our study are located in eastern Washington. The western Washington exception in our data set is for water temperatures at University Bridge between Portage Bay and Lake Union in Seattle, a location in the middle of a migration corridor for summer-running adult sockeye and Chinook.

Our stream temperature modeling predicts significant increases in water temperatures and thermal stress for salmon statewide for both A1B and B1 emissions scenarios. The projected annual maximum T_w patterns shown in Figure 2 indicate there will be large increases in the number of stations that are especially unfavorable for salmon (T_w > 21 °C). Figure 2 also shows the encroachment of summertime air temperatures (T_a > 18 °C) becoming the norm for western Washington by the 2040s, and for this period only the higher elevations of the Cascades and Olympics have temperatures like those characteristic of the western Washington lowlands in the 1980s.

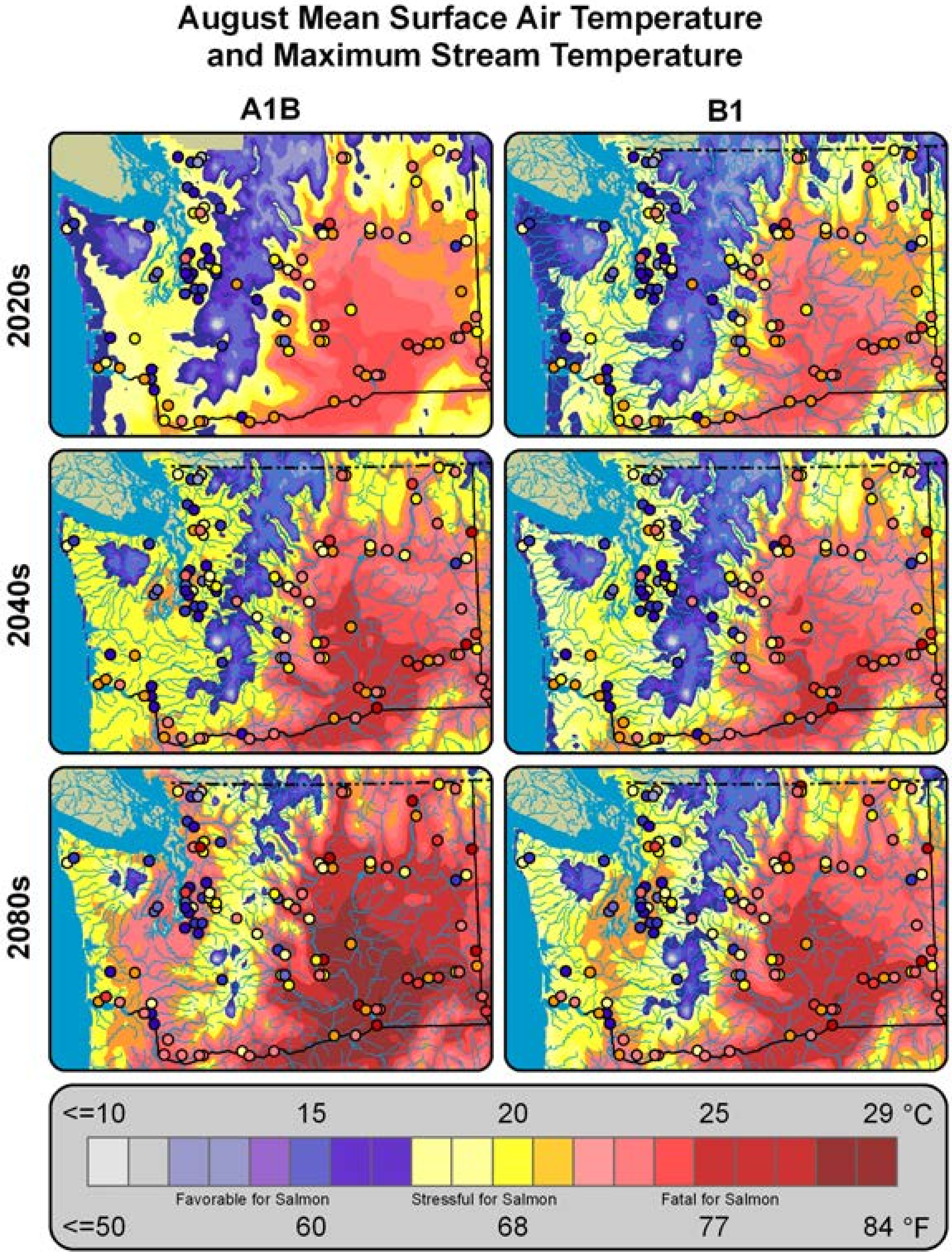

Figure 2. As in Figure 1, but here future climate scenarios for the 2020s, 2040s and 2080s are shown in the top, middle and bottom panels, respectively. Multi-model composite averages based on the A1B emissions are in the left panels, and those for B1 emissions are in the right panels.

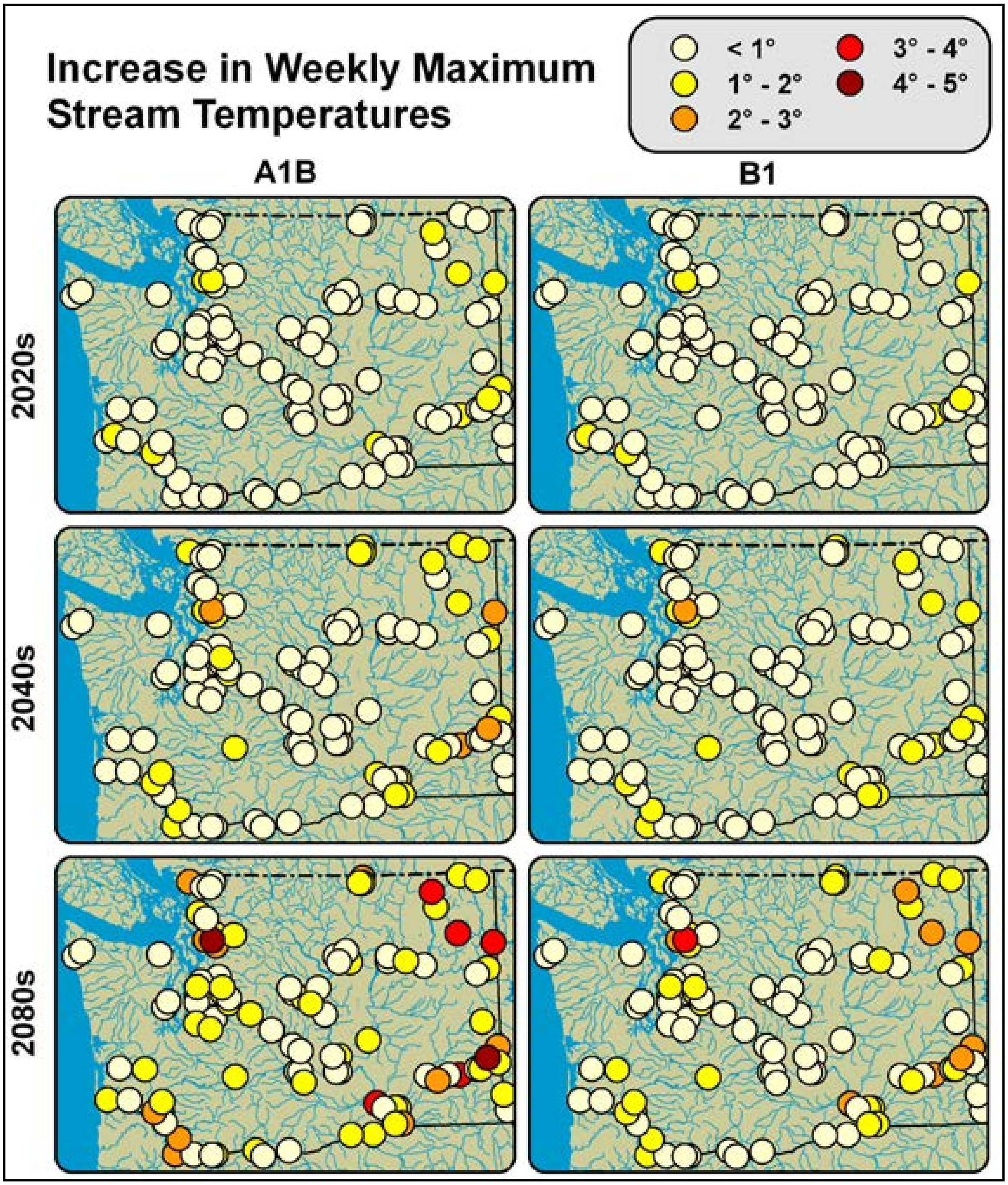

Figure 3. Simulated increases in the annual maximum of weekly water temperatures (°C) relative to the 1980s for select locations in Washington State. Top panels show simulated changes for the 2020s, middle panels for the 2040s, and bottom panels for the 2080s. Composite A1B emissions scenarios are in the left column, composite B1 emissions scenarios are in the right column.

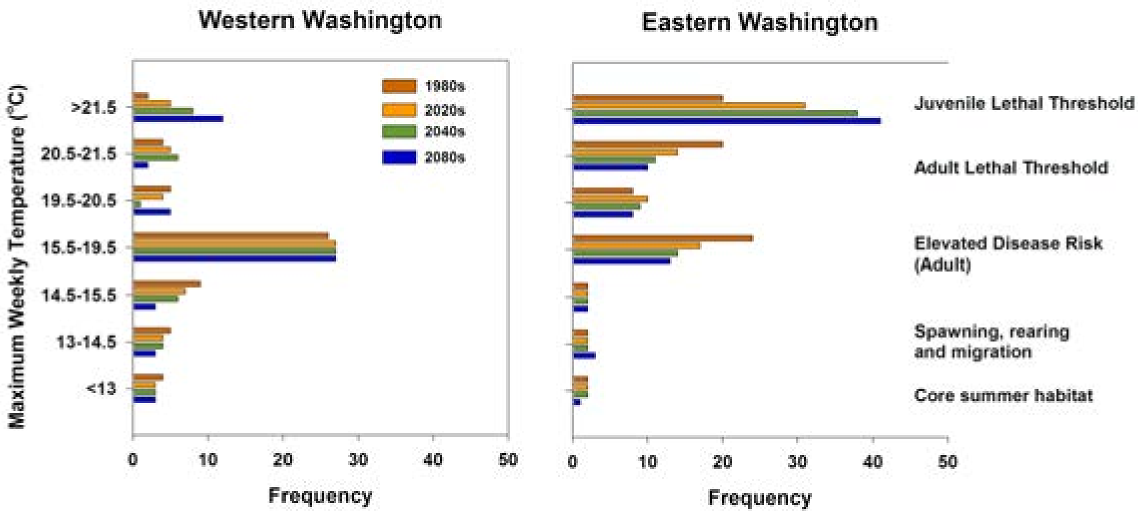

Figure 4. Histograms of maximum weekly water temperature in western and eastern Washington State for the 1980s, 2020s, 2040s, and 2080s under A1B emissions scenarios (data produced from B1 emissions scenarios not shown). Water temperature stations east of the Cascade crest and upstream of the Dalles, OR, are considered to be in eastern Washington, and all others in western Washington.

Future changes in the annual maximum T_w are shown in Figure 3. For both A1B and B1 emissions scenarios in the 2020s, annual maximum T_w at most stations is projected to rise less than 1 °C, but by the 2080s many stations on both the east and west side of the Cascades warm by 2 to 5 °C. Water temperatures projected under the A1B emissions scenarios become progressively warmer than those projected under the B1 emissions, and by the 2080s the differences are ~1 °C (recall that projected summertime air temperatures under A1B emissions are, on average, 1.8 °C warmer than those under B1 emissions for the 2080s).

For either scenario, the projected increases in water temperatures proceed at about an equal pace on both sides of the Cascades, however shifts to increasingly stressful thermal regimes for salmon are predicted to be greatest for eastern Washington where the historic baseline for water temperatures are substantially warmer than those in western Washington. The histograms in Figure 4 show that, in the 1980s, 31% of eastern Washington water temperature stations in our study had annual maximum T_w from 15.5-19.5°C, a category that indicates an elevated risk of disease for adult salmon. The fraction of stations in this already compromised category declines to 17% in the 2080s, while the percentage of stations in higher stress categories increases by an equivalent amount. For the 55 western Washington stations we examine, 80% had T_w < 19.5 °C in the 1980s, and this fraction declines to 65% of stations for the 2080s.

Climate change is also predicted to increase the frequency and persistence of thermal migration barriers and thermally stressed waters for salmon. The persistence of summertime water temperatures greater than 21 °C is predicted to start earlier in the year, and last later in the year (Figure 5). For most of the warmest stations we modeled T_w > 21 °C persisted for 1-to-5 weeks (and up to 10 weeks at the University Bridge site) in the 1980s (from late-July to mid-August). For the 2080s under A1B emissions, this period of extreme thermal stress and thermal migration barriers is projected to persist for 10-to-12 weeks (from mid-June until early-September) at

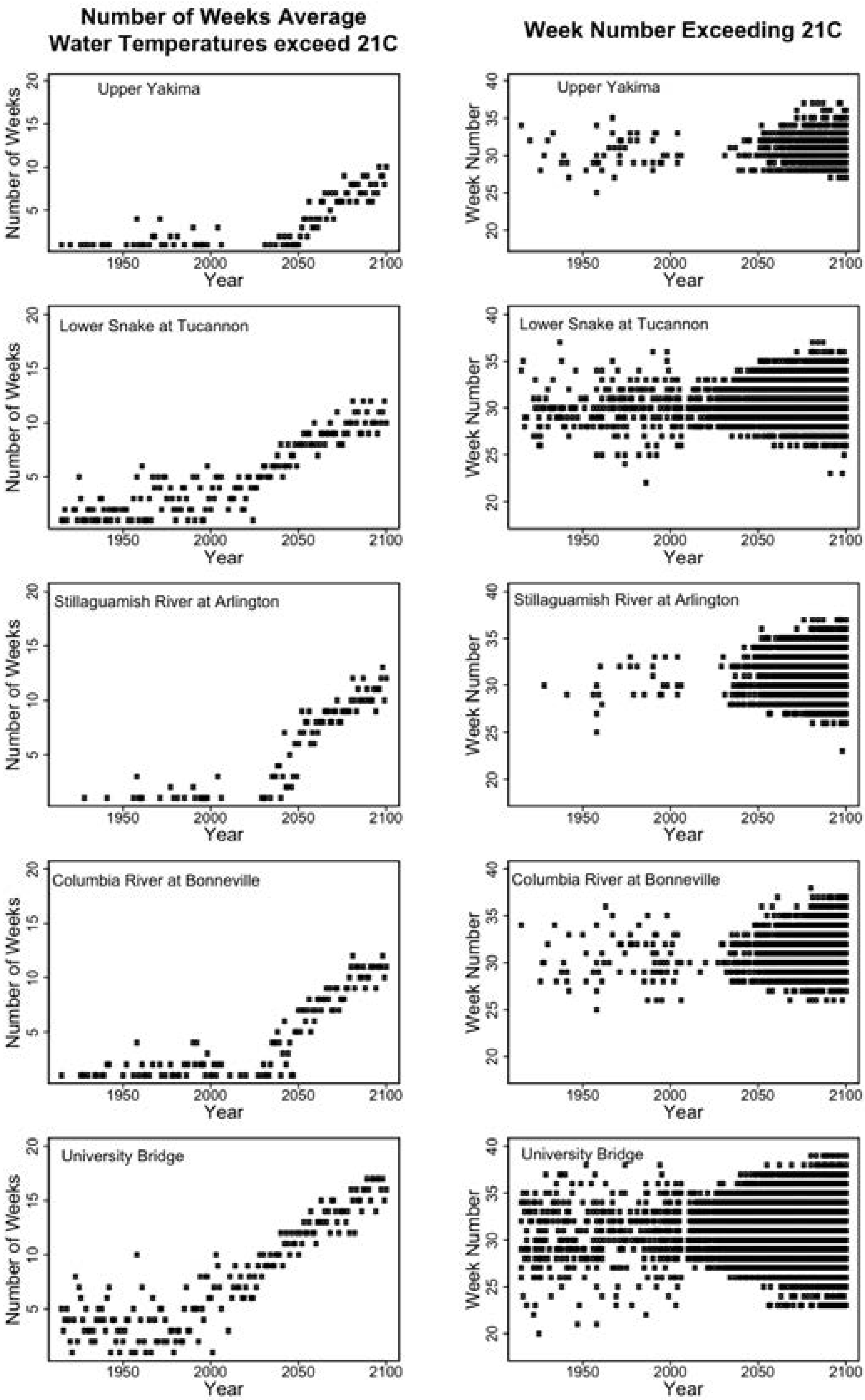

Figure 5. Composite A1B emissions scenarios for simulated number of weeks that T_w exceeds 21°C (left panels) and the week number that weekly water temperature exceeds 21°C (right panels) for: a) the Upper Yakima River, b) Lower Snake River at Tucannon, c) Stillaguamish River at Arlington, d) Columbia River at Boneville Dam, and e) University Bridge, between Portage Bay and Lake Union Seattle. Note that week 31 is apprximately the first week ofAugust.

many stations in eastern Washington and along the lower Columbia River, including the Upper Yakima River, the Columbia River at Bonneville Dam, and the Lower Snake River at Tucannon. This prolonged duration of thermal stress is also predicted for the Lake Washington/Lake Union ship canal (University Bridge). The expansion of the T_w > 21 °C season is predicted to increase considerably for the warmer streams in western Washington like the Stillaguamish River at Arlington. For this station the period of extreme thermal stress and thermal migration barriers last up to 13 weeks by 2100 and is centered on the first week of August.

Each of the stations discussed in the previous paragraph is located in a key migration corridor for summer-running adult salmon on their spawning migration, indicating that at least some salmon populations in each watershed will likely experience substantial increases in thermal migration barriers and thermal stress.

Overall, extended thermal migration barriers are predicted to be much more common in eastern Washington compared with western Washington (Figure 6). The rate of increase in the duration of the thermal migration barrier season is also sensitive to emissions scenarios – the A1B emissions pattern of change in the length of this season for the 2040s is quite similar to that for the B1emissions pattern in the 2080s.

3.2. Climate Change Impacts on Streamflow

3.2.1. Shifts Between Snowmelt, Transient, and Rain-dominant Watersheds

In Figure 7 we classify runoff in Washington's watersheds (at the Hydrologic Unit Code 4 level) for historic and future periods as either snowmelt dominant, transient, or rainfall dominant based on their basin-averaged ratio of simulated April 1st snowpack to October-March total precipitation. For the 1980s snowmelt basins (where this ratio > 0.4) prevail in Washington's North Cascades and the eastside central Cascades. Transient basins (mixed rain and snow basins where the ratio lies between 0.1 and 0.4) are found on the north Olympic Peninsula and the middle elevations of the Cascades and interior Columbia Basin. Rainfall dominant basins (where the ration < 0.1) are found in the low elevations of both eastern and western Washington. As projected climate warms for the 2020s, 2040s, and 2080s there is a clear transition for snowmelt basins to become transient basins, and transient basins to become rainfall dominant basins. By the 2080s, the hydrologic simulations predict a complete loss of snowmelt dominant basins in WA, and only about 10 basins remaining in the north Cascades classified as transient snow basins. Although the rate of transition is greater for the A1B emissions scenario, outcomes for the 2020s, 2040s and 2080s are very similar for the A1B and B1 scenarios, with differences in classification emerging for only a few specific basins in the 2040s and 2080s.

It is important to note that many large rivers which flow through WA, but whose basins are largely outside of the state (e.g. the Columbia, Snake, and Spokane Rivers), will show shifts towards transitional behavior, but will still be classified as snowmelt dominant for projected 21st century warming (Elsner et al. 2009, this report).

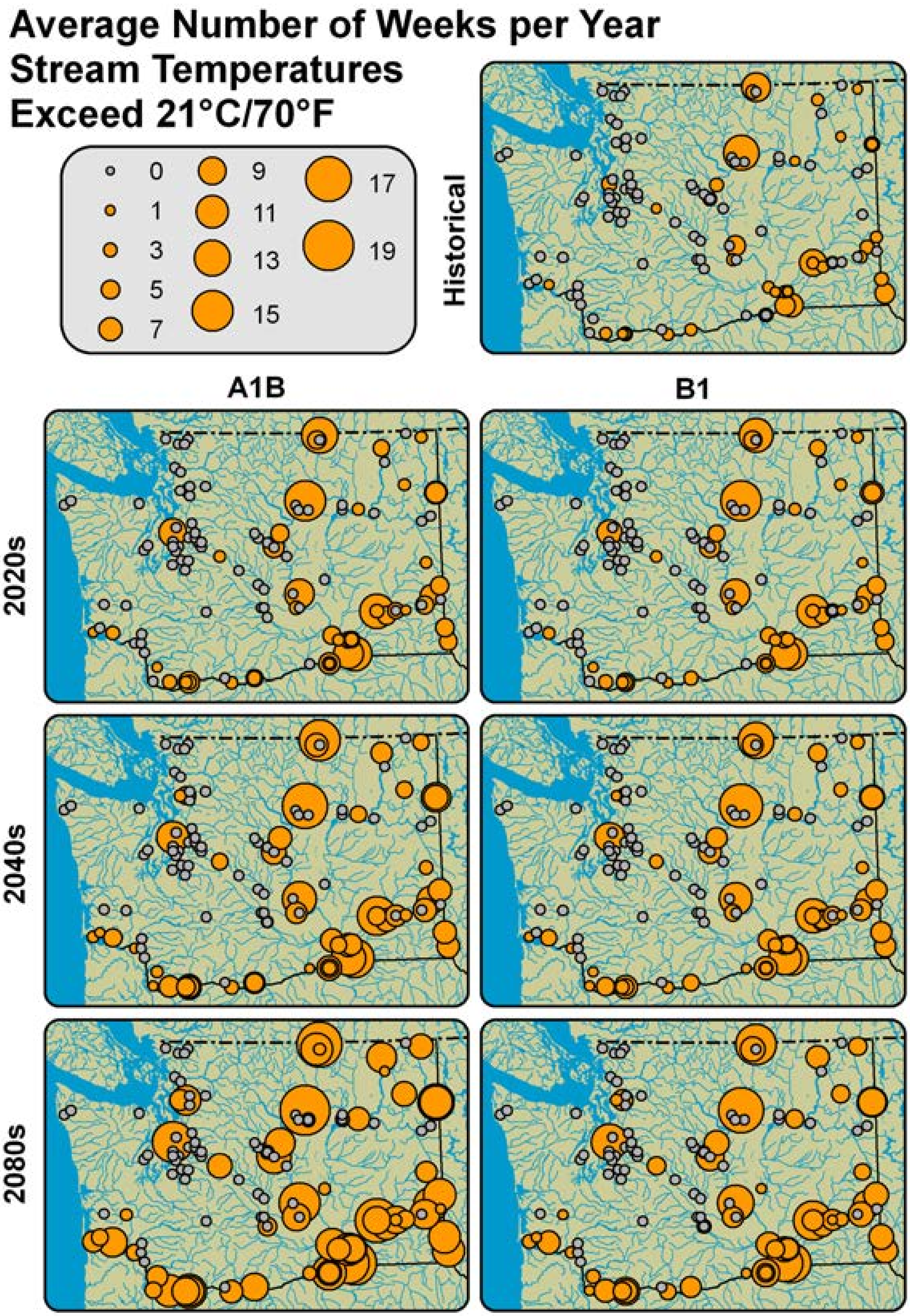

Figure 6. Simulated changes relative to the 1980s in the average number of weeks per year when $T_w >$ 21°C for select locations in Washington State. Top panels show simulated changes for the 2020s, middle panels for the 2040s, and bottom panels for the 2080s. Composite A1B emissions scenarios are in the left column, composite B1 emissions scenarios are in the right column.

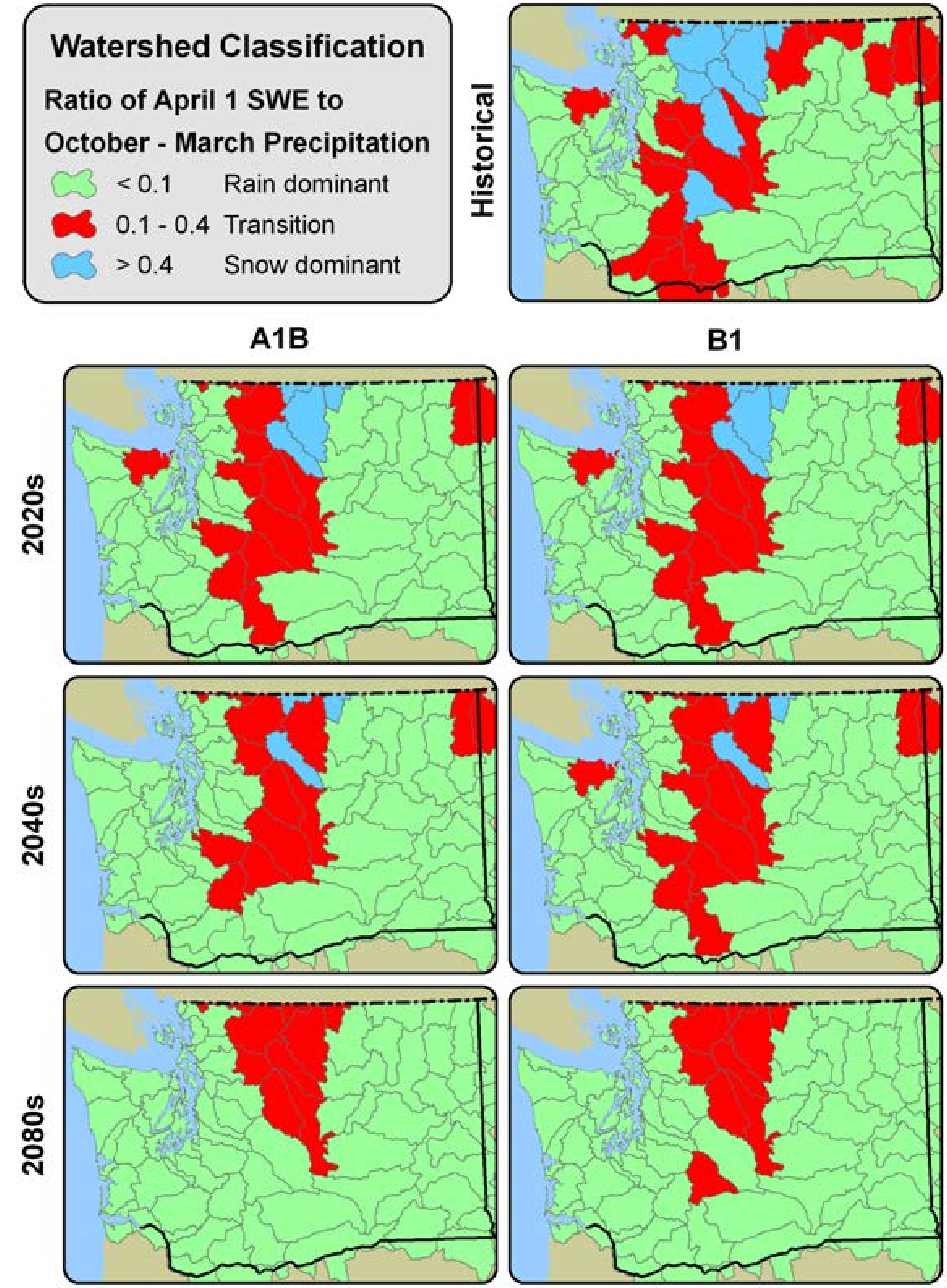

Figure 7. Watershed classification maps for simulated runoff in the historic period (1970-99), 2020s, 2040s, and 2080s. Simulations using A1B emissions are in the lower 3 rows of the left column, while those using B1 emissions scenarios are in the lower 3 rows of the right column.

3.2.2. The Statistics of Extreme High and Low Streamflow

The magnitude and frequency of flooding are predicted to increase most dramatically in the months of December and January for what are now Washington's transient runoff watersheds (Figure 8), which we now see are characterized by mean winter temperatures within a few degrees of 0 °C. Rain-dominant watersheds are predicted to experience small changes in flood frequency, and Washington's coldest snowmelt-dominated basins, where mean winter temperatures in the historic period were < -5°C, are predicted to experience a reduction in flooding that has historically been observed during exceptionally heavy snowmelt periods in late-spring and early-summer. Hydrological models indicate that warming trends will reduce snowpack (Elsner et al. 2009, this report), thereby decreasing the risk of springtime snowmelt-driven floods.

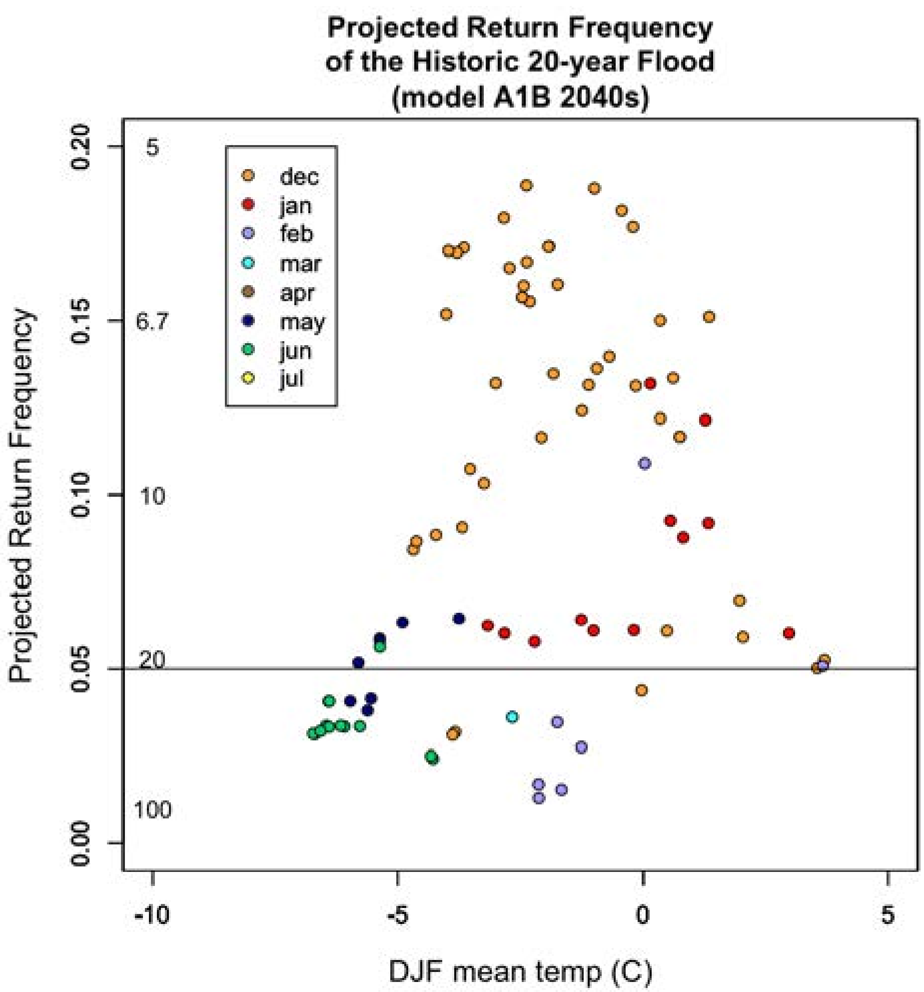

Figure 8. Projected return frequency of the historic 20 year flood magnitudes as a function of the DJF average temperatures in each basin. Color coding in the scatter plots identifies the month when flooding is projected to peak in the A1B 2040s simulation: orange = December, red = January, purple = February, light blue = March, brown = April, dark blue = May, green = June, and yellow = July. Projected return frequencies are based on climate change simulations for composite A1B emissions scenarios for the 30 year averages centered on the 2040s relative to those for the historic simulation period 1915-2006.

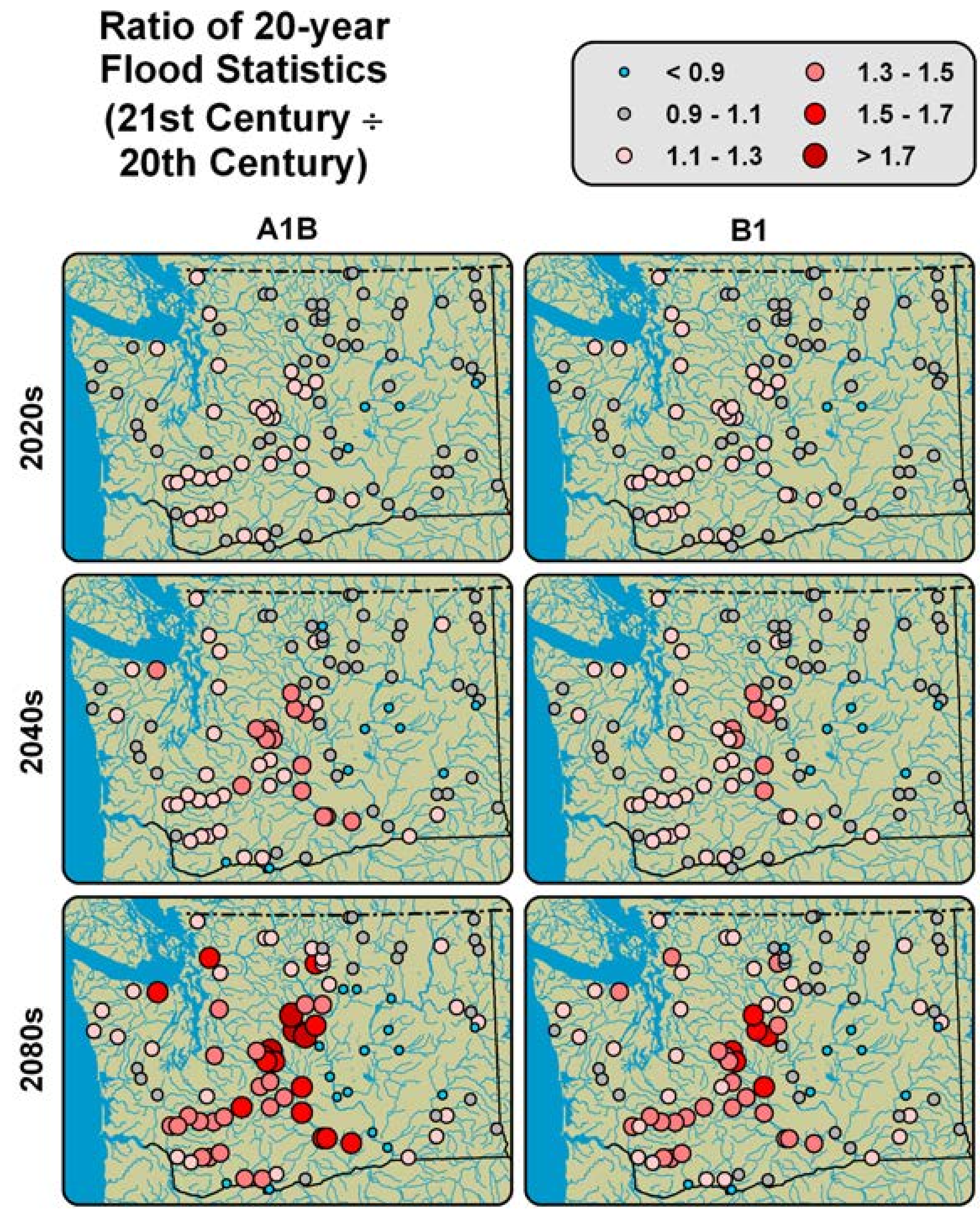

Figure 9. Ratio of the 20 year flood magnitudes for simulated future and historic streamflows at select locations. Top panels show simulated changes for the 2020s, middle panels for the 2040s, and bottom panels for the 2080s. Composite A1B emissions scenarios are in the left column, composite B1 emissions scenarios are in the right column.

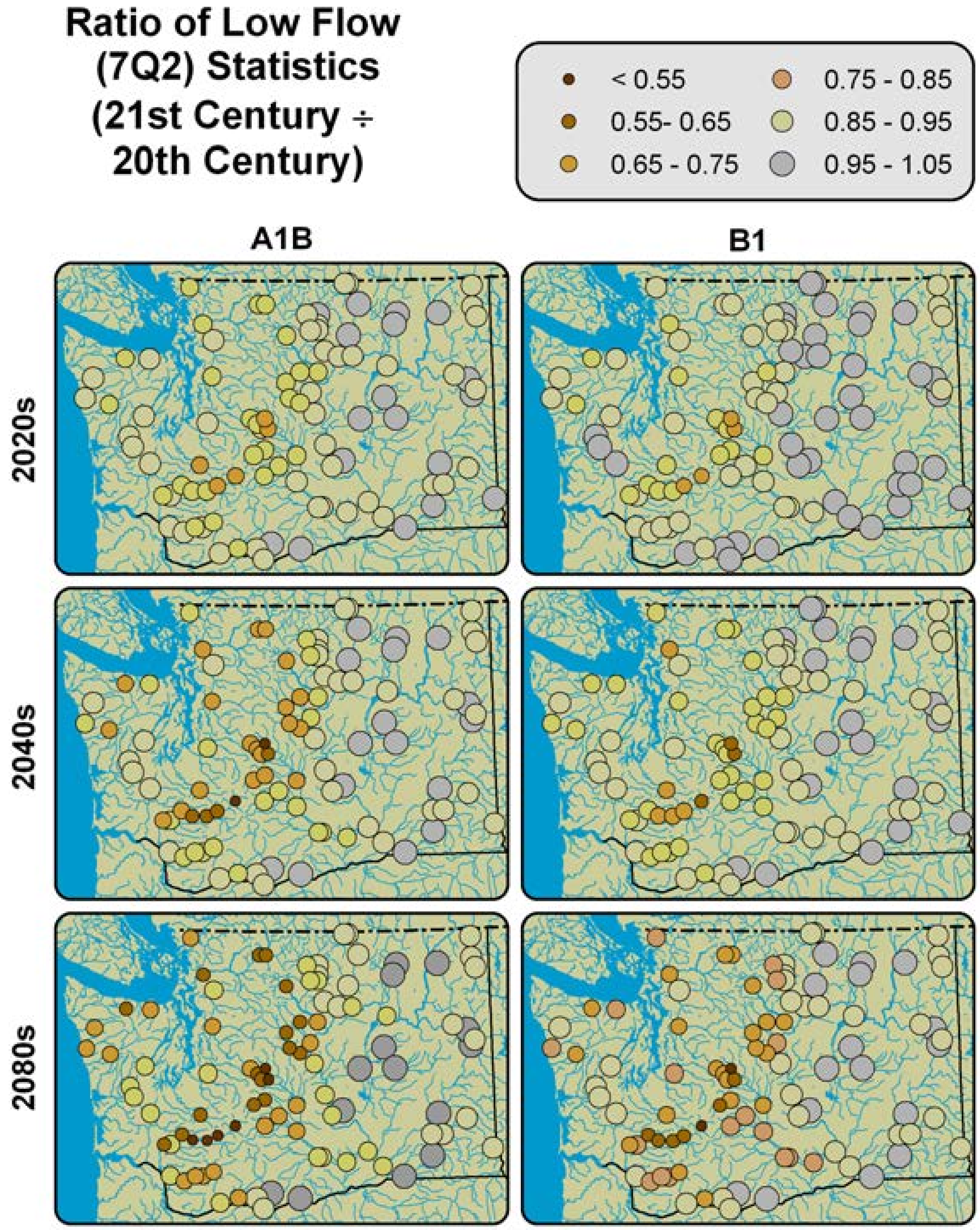

Figure 10. Ratio of low flow (7Q2) statistics for simulated future and historic streamflows at select locations. Top panels show simulated changes for the 2020s, middle panels for the 2040s, and bottom panels for the 2080s. Composite A1B emissions scenarios are in the left column, composite B1 emissions scenarios are in the right column.

Maps for projected changes in the return frequency of the historic 20-year flood are shown in Figure 9. The largest increases in flood return frequency are predicted for transient runoff catchments located in Puget Sound, the west slopes of the Cascades in southwest Washington and in the lower elevations on the east side of the Cascades. Hydrologic modeling predicts a pattern of increased flooding magnitudes in western Washington and decreased or unchanged flooding magnitudes in eastern Washington that becomes more distinct for the later decades of the 21st century. The shifts in flood risk in each basin tend to monotonically increase or decrease through time (not shown). In other words, the increases or decreases in flooding magnitude of each basin generally become larger, with the same sign from the 2020s to the 2080s, with the greatest impacts (either positive or negative) occurring at the end of the 21st century. Emissions scenarios also play a strong role in the rate of change in flooding magnitudes, with the pattern of changes for A1B emissions in the 2040s being similar to that for the B1 emissions in the 2080s (not shown).

Reductions in the magnitude of summer low flows are predicted to be widespread for Washington State's rain dominant and transient runoff river basins in southwest Washington, the Olympic Peninsula, and Puget Sound (Figure 10). Future estimates of the annual average low flow magnitude (7Q2, which is the 7 day average low flow magnitude with a 2 year return interval) are projected to decline by 0-50% by the 2080s under both the A1B and B1 emissions scenarios. The reduction in streamflow for more extreme (7Q10) low flow periods in rain dominant and transient runoff basins is also predicted to change by a similar amount, ranging from 5-40% (not shown). The magnitude of summer low flows are predicted to be relatively insensitive in most of the snowmelt dominated watersheds modeled in the interior Columbia Basin. However, the *duration* of the summer low flow period is projected to expand significantly in all watershed types (not shown, but see Elsner et al. 2009).

4. Assessment of Changes in Critical Temperatures and Streamflow for Washington's Salmon

Assuming that the capacity for and the rate of adaptation (either through phenological, phenotypic, or evolutionary responses) in present day salmon populations are less than the intensity and rate of climate change in the 21st century, our assessment points to widespread declines in the quality and quantity of freshwater habitat for Washington's salmon and steelhead populations. We summarize key climate change impacts on Washington's freshwater habitat for salmon in Figure 11, and also show how those impacts are phased with key life stages for a generic ocean-type and stream-type salmon life history, along with generic summer-run and winter-run steelhead life histories.

Significant increases in stream temperature alone point to significant increases in thermal stress for Washington's salmon populations having a stream-type life history that puts them in freshwater during summer for either spawning migrations, spawning, rearing, or seaward smolt migrations. Temperature impacts on adult spawning migrations are projected to be most severe for stocks having summertime migrations. These include summer-run steelhead, sockeye, and summer Chinook

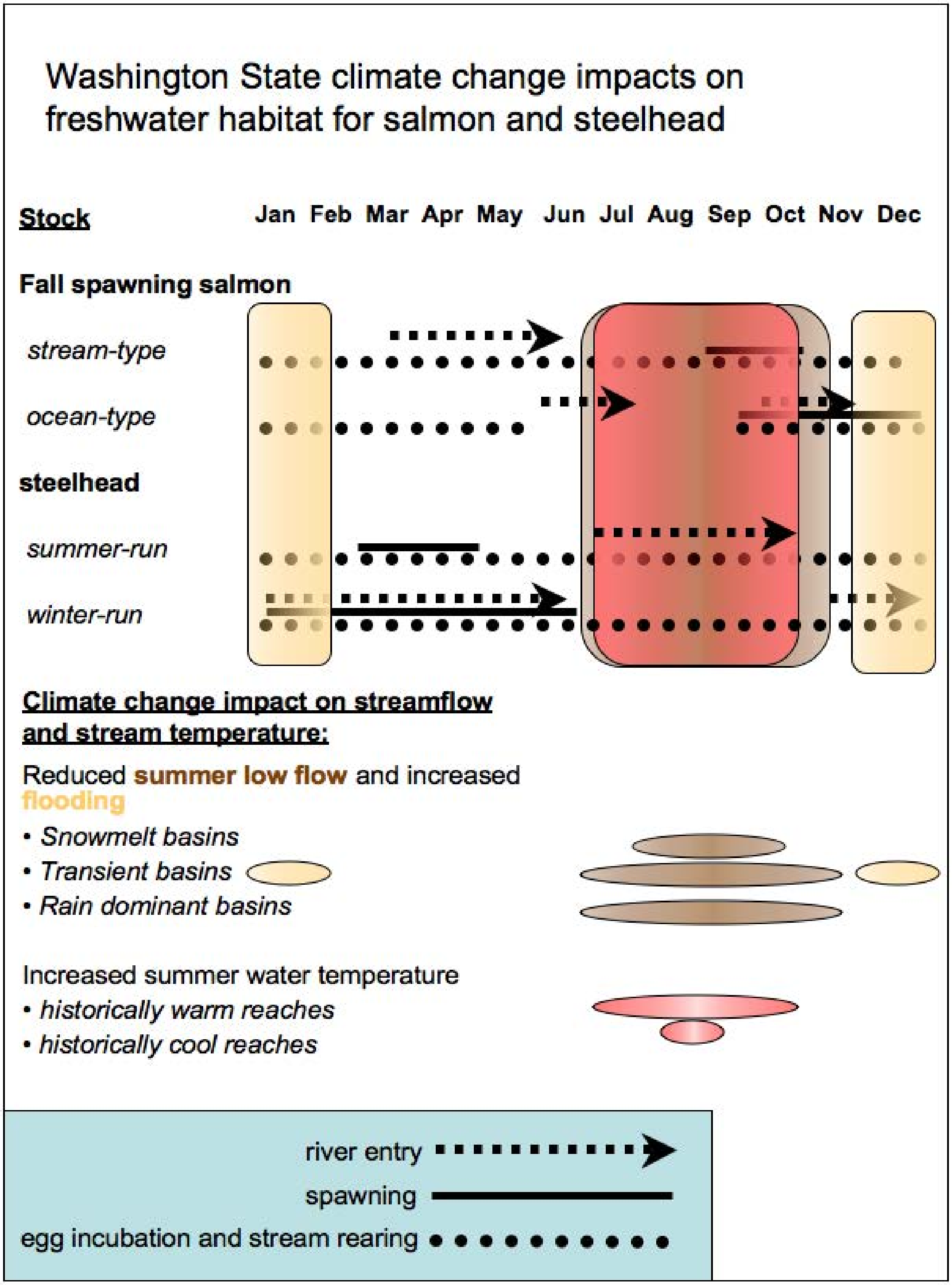

Figure 11. Summary of key climate change impacts on Washington's freshwater habitat for salmon and steelhead, how those impacts differ for streams with different hydrologic characteristics, and how the timing for different impacts compare with the life history for generalized salmon and steelhead life history types. Example life history stages are shown for adult river entry (broken arrows), spawning (solid lines), and egg incubation and rearing periods (dotted lines) for generalized stocks. Tan shading highlights periods of increased flooding, brown shading indicates periods with reduced summer/fall low flows, and red shading indicates periods with increased thermal stress.

populations in the Columbia Basin, and sockeye and Chinook in the Lake Washington system. Increased stream temperatures pose risks to the quality and quantity of favorable rearing habitat for stream-type Chinook, coho and steelhead (summer and winter run) throughout Washington because these stocks spend at least one summer (and for Washington's steelhead typically 2 summers) rearing in freshwater. Reductions in the volume of summer/fall low flows in transient and rainfall-dominated basins might also reduce the availability of spawning habitat for salmon populations that spawn early in the fall (e.g. Healey 1991). Predicted increases in the intensity and frequency of winter flooding in Washington's transient runoff basins will negatively impact the egg-to-fry survival rates for pink, chum, sockeye, Chinook, and coho salmon, and the parr-to-smolt survival rates for coho, stream-type Chinook, and steelhead. And reductions in springtime snowmelt may negatively impact the success of smolt migrations from snowmelt dominant streams where seaward migration timing has evolved to match the timing of peak snowmelt flows.

Summer chum salmon stocks in Hood Canal are listed as threatened under the federal Endangered Species Act, and these populations have a unique life history that makes them especially vulnerable to the impacts of climate change. Adults return to spawn in small shallow streams in late summer, and eggs incubate in the fall and early winter before fry migrate to sea in late winter. The predicted climate change impacts for the low elevation Hood Canal and Puget Sound streams used by summer chum include multiple negative impacts stemming from warmer water temperatures and reduced streamflow in summer.

The Lake Washington ship canal is among the most thermally impaired water bodies for salmon in western Washington. Extreme summertime water temperatures frequently inhibit the upstream migration of adult Chinook and sockeye, while elevated water temperatures in spring confer a competitive advantage to warm water predators, like smallmouth bass (*Micropterus dolomieui*), that can consume significant numbers of sockeye, coho, Chinook, and steelhead smolts on their seaward migrations through the ship canal (Tabor et al. 2004).

Because of the earlier timing of snowmelt and increased evaporation, most of Washington's river basins are projected to experience reduced streamflow in summer and early fall that results in an extended period of summer low flows, while rainfall-dominant and transient runoff basins are also projected to have substantially lower base flows. In combination with increased summertime stream temperatures, reduced summertime flow is likely to limit rearing habitat for salmon with stream-type life histories (wherein juveniles rear in freshwater for one or more years) and increase mortality rates during spawning migrations for summer-run adults.

5. Strategies for Mitigating the Impacts of Climate Change on Washington's Salmon

Generally speaking, a wide array of management options for mitigating the projected impacts of climate change on freshwater habitat for salmon exists, but many of those options will require trade-offs with other land and water uses in salmon watersheds. Options for mitigating future climate change impacts on salmon involve reducing the existing threats to their freshwater habitats caused by land and water use actions that impair natural hydrological processes. As shown in our analyses, the hydrologic processes that influence streamflow timing, volume, and stream temperature in Washington State streams are highly sensitive to projected changes in future climate. Many of the same hydrologic processes are also known to be highly sensitive to land and water use impacts.

Potential management options for mitigating stream temperature increases in response to climate change include reducing out-of-stream withdrawals during periods of high temperature and low streamflow, restoring floodplain functions that recharge aquifers, identifying and protecting thermal refugia provided by ground-water and tributary inflows, undercut banks and deep stratified pools, and restoring vegetation in riparian zones that provide shade and complexity for stream habitat. Restoring, protecting, and enhancing instream flows in summer are also key management options for mitigating the effects of projected trends toward warmer, lower streamflows as a consequence of climate change.

Similarly, management strategies to reduce the risks posed to salmon habitat by extremely high flow events in fall and winter include the protection and restoration of off-channel habitat in floodplains where fish can find refuge from high energy flows. Additional options include limiting the expansion of effective impervious area (Booth and Jackson 1997), and retaining forest cover (reviewed by Moore and Wondzell 2005).

In watersheds with large storage reservoirs there may be opportunities to change reservoir operations in ways that mitigate the impacts of climate change on flooding. Likewise, strategic use of cold-water releases may be able to mitigate climate change impacts on summer water temperature and seasonally low streamflow at key times.

It is important to recognize that, in many basins, climate change will likely increase the demand for surface water in summer for such uses as irrigation for agriculture and municipal water supplies. This situation will require that strategic policy thinking that recognizes trade-offs will have to be made between ecosystem protection and other water resource uses, and that clear decision guidance should be developed now in order to avoid protracted and potentially costly conflicts.

A particular challenge for watershed restoration efforts will be to match projects to both existing and future threats to salmon habitat. Battin et al's. (2006) study of climate change, restoration options, and their impacts on Snohomish ocean-type Chinook noted that most practical restoration actions are aimed at lower elevation floodplains, but that the most severe negative impacts for this stock were found in higher elevation spawning and rearing areas where the hydrologic sensitivity to climate change was greatest. In contrast, Martin (2006) suggests that thermal refugia will increasingly be found at the headwater reaches of Northwest streams, while future human population increases and the impacts on land and water use will be concentrated in low-elevation floodplains. He advocates renewed efforts to protect floodplains as migration corridors and to reconnect watersheds to largely protected headwater areas by removing dams and other barriers to upstream fish passage.

6. Research Gaps and Recommendations for Future Research

This analysis was based on a subset of single stations for streamflow and stream temperatures, yet these stations may not be representative of the complex and varied habitat features found within most salmon watersheds that provide critical refugia from stressful or even lethal water temperatures and streamflows. The widespread distribution and large magnitude of predicted negative impacts described in this study highlight an urgent need for mapping existing and potential thermal and hydrologic refugia in order to prioritize habitat protection and restoration efforts.

To date, there are few case studies aimed at understanding the impacts of climate change on restoration alternatives for specific watersheds and salmon stocks in Washington State. Yet, because salmon life histories are locally adapted and Washington's freshwater salmon habitat is diverse, such efforts should be given high priority where long-term investments in salmon habitat protection and restoration are considered. Battin et al.'s (2006) study of climate change and habitat restoration options for Snohomish Chinook provides an informative framework for carrying out such studies.

Because salmon life histories integrate across a complex network of freshwater, estuarine, and marine habitats, and because people compete directly and indirectly for resources that are important for salmon, an understanding of salmon ecology begs for integrated studies that cross multiple disciplines. For example, impacts of both climate change and ocean acidification on the ocean ecology of salmon are among the least understood, but possibly most important, aspects of salmon ecology in the coming decades (Fabry et al. 2008). Perhaps even more important for adaptation planning in Washington State are efforts to integrate so-called *human dimensions* of climate change into impacts studies for salmon. As noted by Miles et al. (1999), future climate change is likely to sharpen tradeoffs over water resources because it favors reductions in streamflows during summer when human demands and ecosystem needs for water are often greatest.

A better understanding for genetic and phenotypic adaptations in salmon is also needed to understand the capacity for adaptation, and whether adaptations might keep pace with future habitat changes (Crozier et al. 2008). Adaptive capacity may be among the most important issues facing Washington's salmonids yet this capacity is not well documented or understood. Most analyses of climate change impacts on salmon have assumed that the environmental sensitivities expressed by current populations will remain static in the future, yet this may not be the case. For example, summertime migrating stocks in already warm watersheds like Lake Washington sockeye will be faced with increasingly strong selection pressures that favor a shift in spawning migration timing away from what are projected to be increasingly hostile water temperatures. But climate change might produce conflicting selection pressures at other life stages that, in combination, may not lead to a viable life history pattern (Crozier et al. 2008).

An additional layer of uncertainty comes with the choice of downscaling methods used to create the surface air temperature and precipitation scenarios used in this work, and how well different downscaling approaches perform in estimating changes in the frequency and intensity of extreme events. For example, Salathé et al.'s (2009) regional climate modeling suggests that the statistically downscaled scenarios examined here likely underestimate the impacts of climate change on event-scale precipitation extremes and springtime surface warming in locations that lose their snow pack. These findings suggest that increased flooding frequency and magnitude in rainfall dominant and transient runoff watersheds may be more extreme than what we show in our analysis. Such changes in the frequency and intensity of extreme hydroclimate events will have important consequences for disturbance regimes that are important for in-stream habitat features and the reproductive success of salmon. Linking regional climate modeling to hydrologic modeling should be pursued to better evaluate the impacts of climate change on extreme events important for freshwater habitat for salmon.

7. Conclusions

Simulated stream temperatures under future climate scenarios highlight increased thermal stress on Washington's salmon populations in the warmest summer months. The distribution of stations, and the duration of time each year, where weekly water temperatures cause thermal migration barriers and increase the risk of fish kills (> 21 °C or 70 °F) are projected to expand with warmer summer temperatures. Generally speaking, the greatest thermal stresses are projected for watersheds in the interior Columbia Basin, while the least are projected for watersheds in western Washington. Among the sites modeled in this study, the Lake Washington ship canal stands out as the most thermally stressed water body in western Washington. Future climatic warming will exacerbate existing problems for both seaward migrating smolts and summer-run adult salmon (sockeye and Chinook) that spawn in the Lake Washington basin.

Our analysis of hydrologic model output identifies a mix of streamflow impacts on Washington's salmon watersheds that depend largely on a basin's present-day hydroclimate characteristics. Flood magnitudes and frequencies are predicted to increase most dramatically in winter months for Washington's transient runoff watersheds. Rain-dominant watersheds are predicted to experience small changes in flooding, while the coldest snowmelt-dominated basins (where winter temperatures were historically < -5°C) are predicted to experience a reduction in flooding that has historically been observed during exceptionally heavy snowmelt periods in late-spring and early-summer.

Our hydrologic simulations predict a complete loss of snowmelt dominant basins in WA by the 2080s along with a substantial reduction in the number and spatial distribution of transient snow basins. A reduction in the volume of summer low flows are predicted to be widespread for historically rain dominant and transient runoff river basins, which are mostly found in the Cascades, Olympics, and coastal and southwest Washington. The duration of the summer low flow period is projected to increase substantially for both transient and snowmelt dominant basins. For the interior Columbia River Basin, the combination of an extended period of summer and fall low flows and warmer water temperatures is very likely to be problematic for the many stream-type salmon and summer-run steelhead populations that migrate, spawn, and/or rear in freshwater during these periods.

In many cases, climate change promises to amplify many existing stresses on Washington's salmon in impaired watersheds, and at the same time will likely increase public and private demands for surface water in summer for such uses as irrigation for agriculture and municipal water supplies. In order to avoid protracted and potentially costly conflicts, this situation will require that strategic policy thinking that recognizes trade-offs will have to be made between ecosystem protection and other water resource uses, and that clear decision guidance should be developed before such conflicts become too extreme.

Acknowledgments

We thank Rob Norheim for creating the maps, Philip Mote for reading an early draft of this report and offering constructive comments, Robert Wissmar for discussions about this work, Kristian Mickelson for assistance with the flow frequency analysis, Dave Hallock for providing access to data from the DOE and Chris Holmes for providing data from the USACE, and 5 anonymous reviewers for their constructive comments on an early draft of this report.

References

Battin J, Wiley MW, Ruckelshaus MH, Palmer RN, Bartz KK, and Imaki H, and E Korb, (2007) Projected impacts of climate change on salmon habitat restoration. Proc of the Natl Acad of Sci of the U.S.A 104:6720-6725.

Beamer EM, Pess GR (1999) Effects of peak flows on Chinook (Oncorhynchus tshawytscha) spawning success in two Puget Sound river basins. In: Sakrison R, Sturtevant P (eds.) Watershed Management to Protect Declining Species. Am Water Resour Assoc, Middleburg, pp. 67-70.

Beechie TJ, Beamer EM, Wasserman L (1994) Estimating coho salmon rearing habitat and smolt production losses in a large river basin, and implications for habitat restoration. N Am J of Fish Manag 14:797-811.

Beechie TJ, Ruckelshaus M, Buhle E, Fullerton A, Holsinger L (2006) Hydrologic regime and the conservation of salmon life history diversity. Biol Conserv 130:560-572.

Beechie TJ, Moir H, Pess G (2008) Hierarchical physical controls on salmonid spawning location and timing. In: Sear D, DeVries P (eds.) Salmonid Spawning Habitat in Rivers: Physical Controls, Biological Responses, and Approaches to Remediation. Am Fish Soc, Symposium 65, Bethesda, Maryland, pp. 83-102.

Booth DB, and Jackson CJ (1997) Urbanization of aquatic systems—degradation thresholds, stormwater detention, and the limits of mitigation: Water Resources Bulletin, v. 33, p. 1077-1090.

Crozier LG, Zabel RW (2006) Climate impacts at multiple scales: evidence for differential population responses in juvenile Chinook salmon. J of Anim Ecol 75:1100-1109.

Crozier LG, Zabel RW, Hamlet A (2008) Predicting differential effects of climate change at the population level with life-cycle models of spring Chinook salmon. Glob Chang Biol 14:236-249.

Eaton JG, Scheller RM (1996) Effects of climate warming on fish thermal habitat in streams of the United States. Limnol Oceanogr 4l:109-1115.

Elsner MM, Cuo L, Voisin N, Hamlet AF, Deems JS, Lettenmaier DP, Mickelson KEB, Lee SY (2009) Implications of 21st century climate change for the hydrology of Washintgon State. Washington Climate Change Impacts Assessment: Evaluating Washington's future in a changing climate. (in press).

Environmental Protection Agency (2003) EPA Region 10 Guidance for Pacific Northwest state and tribal temperature water quality standards. U.S. EPA, Seattle, WA.World Wide Web (URL = www.epa.gov/r10earth/temperature.htm).

Environmental Protection Agency (2007) Biological evaluation of the revised Washington water quality standards. U.S. EPA, Seattle, WA.

Fabry, V. J., Seibel, B. A., Feely, R. A., and Orr, J. C. (2008) Impacts of ocean acidification on marine fauna and ecosystem processes. – ICES Journal of Marine Science, 65: 414–432.

Farrell AP, Hinch SG, Cooke SJ, Patterson DA, Crossin GT, Lapointe M, Mathes MT (2008) Pacific salmon in hot water: applying aerobic scope models and biotelemetry to predict the success of spawning migrations. Physiol and Biochem Zool 81(6): 697-708.

Goniea TM, Keefer ML, Bjornn TC, Peery CA, Bennett DH (2006) Behavioral thermoregulation and slowed migration by adult fall Chinook salmon in response to high Columbia River water temperatures. Transactions of the American Fisheries Society 135:408–419. DOI: 10.1577/T04-113.1

Hamlet AF, Lettenmaier DP (2007) Effects of 20th century warming and climate variability on flood risk in the western U.S. Water Resour Res 43: W06427. doi:10.1029/2006WR005099.

Healey MC (1991) in Pacific Salmon Life Histories, eds Groot C, Margolis L (Univ British Columbia Press, Vancouver, Canada) pp 313–393.

High, B., C.A. Perry, and D.H. Bennett. (2006) Temporary staging of Columbia River summer steelhead in cool-water areas and its effect on migration rates. Transactions of the American Fisheries Society 135: 519-528.

Hosking JRM (1990) L-moments: analysis and estimation of distributions using linear combinations of order statistics. J of the R Stat Soc, Series B 52:105-124.

Hosking JRM, Wallis JR (1993) Some statistics useful in regional frequency analysis, Water Resour Res 29(2):271-281.

Independent Scientific Advisory Board (ISAB) (2007) Climate Change Impacts on Columbia River Basin Fish and Wildlife. ISAB Climate Chang Rep. World Wide Web (URL = http://www.nwcouncil.org/library/isab/isab2007-2.htm)

Liang X, Lettenmaier DP, Wood EF, Burges SJ (1994) A simple hydrologically based model of land surface water and energy fluxes for general circulation models. J Geophys Res 14:415-428.

Logerwell EA, Mantua NJ, Lawson P, Francis RC, Agostini V (1993) Tracking environmental processes in the coastal zone for understanding and predicting Oregon coho (Oncorhynchus kisutch) marine survival. Fisheries Oceanography, 12(3): 1-15.

Martin J (2006) Climate and Development: salmon caught in the squeeze. In: Salmon 2100: the future of wild pacific salmon. Lackey R, Lach D, Duncan S (eds.) Am Fish Soc, 629 pp.

McCullough DA (1999) A review and synthesis of effects of alterations to the water temperature regime on freshwater life stages of salmonids, with special reference to Chinook salmon. Water Resour Assess, U.S. EPA 910-R-99-010, 291 pp., Seattle, WA.

McCullough DA, Spalding S, Sturdevant D, Hicks M (2005) Issue Paper 5: Summary of technical literature examining the physiological effects of temperature on salmonids. EPA-910-D-01-005, prepared as part of U.S. EPA Region 10 Temperature Water Quality Criteria Guidance Development Project (2001). World Wide Web (URL = http://yosemite.epa.gov/R10/WATER.

NSF/1507773cf7ca99a- 7882569ed007349b5/ce95a3704aeb5715882568c4007844 99).

Miles EL, Snover AK, Hamlet AF, Callahan BM, Fluharty, DL (1999) Pacific Northwest regional assessment: The impacts of climate variability and climate change on the water resources of the Columbia River Basin. Prepared for the Am Water Resour Assoc Specialty Conf on the Potential Consequences of Clim Variability and Chang to Water Resour of the U.S., Atlanta, GA.

Mohseni OS, Stefan HG, Erickson TR (1998) A Nonlinear Regression Model for Weekly Stream Temperatures. Water Resour Res 34:2685–2692.

Mohseni OS, Stefan HG, Eaton JG (2003) Global warming and potential changes in fish habitat in U.S. streams. Clim Chang 59:389-409.

Moore RD and Wondzell SM (2005) Physical hydrology and the effects of forest harvesting in the Pacific Northwest: a review. Journal of the American Water Resources Association, 41:753-784.

Mote PW, Salathé Jr EP (2009) Future climate in the Pacific Northwest. Washington Climate Change Impacts Assessment: Evaluating Washington's future in a changing climate (in press).

Nash JE, Sutcliffe JV (1970) River flow forecasting through conceptual models. J of Hydro 10:282-290.

Naughton GP, Caudill CC, Keefer ML, Bjornn TC, Stuehrenberg LC, Peery CA (2005) Late-season mortality during migration of radio-tagged sockeye salmon (Oncorhynchus nerka) in the Columbia River. Canadaian Journal of Fisheries and Aquatic Sciences 62:30-47.

O'Neal K (2002) Effects of global warming on trout and salmon in U.S. streams. Defenders of Wildlife, Washington, D.C. 46 pp.

Pearcy WM (1992) Ocean ecology of North Pacific salmonids. Washington Sea Grant, Seattle (USA). 179pp.

Rand PS, Hinch SG, Morrison J, Foreman MGG, MacNutt MJ, Macdonald JS, Healey MC, Farrell AP, Higgs DA (2006) Effects of river discharge, temperature, and future climates on energetics and mortality of adult migrating Fraser River sockeye salmon. Trans of the Am Fish Soc 135:655-667.

Reeves GH, Everest FH, Nickelson TE (1989) Identification of Physical Habitats Limiting the Production of Coho Salmon in western Oregon and Washington. Technical Report PNW-GTR-245, US Dep of Agric, For Service, Pacific Northwest Res Sn, Portland, OR.

Richter A, Kolmes SA (2005) Maximum Temperature Limits for Chinook, Coho, and Chum Salmon, and Steelhead Trout in the Pacific Northwest. Rev in Fish Sci, 13:1,23-49. DOI: 10.1080/10641260590885861

Salathé Jr, EP, Zhang Y, Leung LR, Qian Y (2009) Regional climate model projections for the State of Washington. Washington Climate Change Impacts Assessment: Evaluating Washington's future in a changing climate. (in press).

SRES (Special Report on Emissions Scenarios) (2000) Nakicenovic, Nebojsa and Swart, Rob (eds.), Cambridge University Press, Cambridge, United Kingdom, 612 pages. Intergovernmental Panel on Climate Change Special Report on Emissions Scenarios.

Tabor RA, Celedonia MT, Mejia F, Piaskowski RM, Low DL, Footen B, Park L (2004) Predation of juvenile Chinook salmon by predatory fishes in three areas of the Lake Washington basin. U.S. Fish and Wildlife Service, Western Washington Fish and Wildlife Office, Lacey, WA.

Wang QJ, (1997) LH moments for statistical analysis of extreme events. Water Resour Res,33(12):2841-2848.

Photo credit, page 225: Shutterstock.com

Appendix A: Washington State stream temperature stations used in this study.

Dataset[1]	Region[2]	Site/River Basin	Latitude	Longitude	alpha	beta	gamma	mu	nsc
USACE	UC	Albeni Falls Forebay Pend Orielle River	48.16	-117.09	23.1	12.18	0.27	5.63	0.82
USACE	UC	Albeni Falls Tailrace Pend Orielle	48.16	-117.09	31.05	15.09	0.14	0	0.94
USACE	UC	Anatone, WA. Snake River	46.16	-116.97	25.05	14.76	0.19	4.44	0.81
DOE	PS	Bertrand Creek at Rathbone Road	48.91	-122.53	19.11	17.44	0.5	11.41	0.91
DOE	PS	Big Mission Creek at Highway 300	47.41	-122.91	16.52	9.84	0.18	0	0.8
DOE	PS	Big Soos Creek near Auburn	47.28	-122.16	15.44	15.31	0.73	10.57	0.94
USACE	LC	Bonneville Forebay, Columbia River	45.66	-121.97	22.77	11.39	0.24	2.83	0.88
DOE	UC	Brender Creek near Cashmere	47.53	-120.47	18.87	17.21	0.24	8.73	0.86
DOE	LC	Burnt Bridge Creek at mouth	45.66	-122.66	24.42	20.26	0.24	11.93	0.8
USACE	LC	Cascade Island (below Bonneville)	45.66	-121.97	23.18	12.53	0.28	3.15	0.9
DOE	PS	Cedar River at Logan Street, Renton	47.47	-122.22	18.88	18.49	0.4	11.83	0.84
DOE	OP	Chehalis River at Dryad	46.66	-123.22	21.2	17.28	0.58	12.21	0.7
DOE	PS	Cherry Creek at Highway 203	47.78	-121.97	16.88	17.68	4.41	13.41	0.92
USGS	UC	Chief Joseph Dam Columbia River	47.97	-119.66	22.75	11.44	0.14	2.92	0.81
USACE	UC	Chief Joseph Forebay Columbia River*	47.97	-119.66	19.17	8.45	0.22	0	0.84
DOE	UC	Chumstick Creek near mouth	47.59	-120.66	13.38	19.37	0.64	9.69	0.96
DOE	UC	Chumstick Creek near Leavenworth	47.47	-120.34	13.15	16.83	27.3	10.88	0.91
USACE	UC	Boundary (US/Canada) Columbia River	48.97	-117.66	21.96	12.03	0.15	2.28	0.83
USGS	UC	Colville River	48.59	-118.09	21.98	12.58	0.17	0.67	0.88
DOE	UC	Colville River at Chewelah	48.28	-117.72	28.51	16.91	0.14	3.37	0.81
DOE	UC	Cowiche Creek at Powerhouse Road	46.66	-120.59	18.56	17.97	0.58	12.62	0.91
DOE	LC	Cowlitz River at Kelso	46.16	-122.91	16.71	16.54	0.6	11.92	0.76
DOE	UC	Crab Creek near Beverly	46.84	-119.84	25.05	14.28	0.23	0	0.93
USACE	LC	Camas/Washougal, WA. Columbia River	45.66	-122.34	22.43	12.74	0.32	5.13	0.87
DOE	UC	Deadman Creek near mouth	46.59	-117.78	27.08	26.07	0.22	11.71	0.91
DOE	UC	Deadman Creek at Holcomb Road	47.84	-117.22	21.36	12.85	0.13	0	0.93
DOE	PS	Des Moines Creek near mouth	47.41	-122.28	17.22	10.11	0.28	0	0.74
DOE	OP	Dickey River near La Push	47.97	-124.53	18.28	13.81	1.39	13.81	0.95
DOE	LC	Lewis River near Dollar Corner	45.84	-122.59	23.31	18.41	0.37	10.78	0.73
DOE	PS	Fauntleroy Creek near mouth	47.53	-122.34	14.49	17.73	0.72	12.32	0.85
USACE	UC	Grand Coulee Forebay Columbia River*	47.97	-118.97	19.64	9.85	0.26	2.39	0.86
USGS	UC	Franklin D. Roosevelt Lake	47.97	-118.97	22.31	11.49	0.15	2.99	0.81
USACE	UC	Grand Coulee Tailrace, Columbia River*	48.03	-118.97	19.18	10	0.23	2.86	0.79
DOE	PS	Griffen Creek at Highway 203	47.59	-121.91	17.44	18.8	0.54	11.77	0.82
USACE	UC	Ice Harbor Tailrace Snake River	46.22	-118.84	24.15	14.55	0.16	2.62	0.82
USACE	UC	Ice Harbor Forebay Snake River	46.22	-118.84	24.12	14.4	0.16	2.63	0.84
USACE	UC	John Day Forebay Columbia River	45.72	-120.72	22.17	14.01	0.26	5.34	0.85

Appendix A: Continued.

Dataset[1]	Region[2]	Site/River Basin	Latitude	Longitude	alpha	beta	gamma	mu	nsc
USACE	UC	John Day Tailrace Columbia River	45.72	-120.72	22.03	13.99	0.26	5.72	0.83
DOE	PS	Jim Creek at Whites Road	48.16	-122.03	20.91	17.84	0.39	11.48	0.79
DOE	PS	Jimmeycomelately Creek at Highway 101	48.03	-123.03	16.32	11.1	0.36	0	0.74
DOE	LC	Kalama River near Kalama	46.03	-122.84	17.33	17.6	0.85	12.18	0.71
DOE	UC	Kettle River near Barstow	48.78	-118.16	33.34	16.02	0.09	0	0.77
DOE	PS	Kimball Creek at Highway 202	47.53	-121.84	21.38	18.08	0.28	10.51	0.85
USGS	UC	Klickitat River at Klickitat	45.72	-121.28	19.74	12.3	0.15	0.46	0.94
DOE	PS	Laughing Jacobs Creek near Mouth	47.59	-122.03	15.17	13.51	0.21	8.67	0.97
USACE	UC	Lower Granite Tailrace Snake River	46.66	-117.47	20.29	11.62	0.21	2.78	0.86
USACE	UC	Little Goose Forebay Snake River	46.59	-117.97	24.03	13.68	0.16	1.17	0.81
USACE	UC	Little Goose Tailrace, Snake River	46.59	-117.97	21.49	14.38	0.21	4.7	0.79
DOE	PS	Little_Mission_Cr._@_Hwy_300	47.41	-122.91	12.1	6.8	0.22	0	0.9
USACE	UC	Lower Monumental Forebay Snake River	46.59	-118.34	23.26	14.3	0.18	2.84	0.81
USACE	UC	Lower Monumental Tailrace Snake River*	46.59	-118.34	24.27	13.96	0.23	4.18	0.86
USGS	LC	Lower Columbia	46.28	-123.84	21.73	10.98	0.37	3.81	0.83
USGS	LC	Lower Columbia at Clatskanie	46.16	-123.03	22.81	12.51	0.23	3.01	0.81
USGS	LC	Lower Cowlitz	46.28	-122.91	19.36	13.94	0.22	3.36	0.85
USGS	UC	Lower Crab	47.03	-119.34	22.41	9.83	0.13	0.08	0.88
USGS	UC	Lower Snake	46.28	-119.22	31.25	19.94	0.11	3.38	0.91
USGS	UC	Lower Snake near Asotin	46.22	-118.91	24.06	14.3	0.17	2.05	0.84
USGS	UC	Lower Snake near Tucannon	46.34	-117.03	23.73	13.06	0.17	1.57	0.84
USGS	UC	Lower Spokane	46.53	-118.16	23.7	13.72	0.17	1.87	0.85
USGS	UC	Lower Yakima	47.91	-118.34	19.77	12.18	0.19	0.73	0.81
USACE	UC	Lower Granite Forebay Snake River	46.66	-117.41	24.48	13.59	0.16	2.57	0.81
DOE	UC	Manatash Creek at Manatash Road	46.97	-120.66	15.17	14.72	0.64	9.48	0.97
DOE	PS	Maple Creek at mouth	48.91	-122.09	10.77	16.55	0.9	9.48	0.79
USACE	UC	McNary Tailrace Columbia River	45.91	-119.28	22.67	13.62	0.17	2.93	0.82
USACE	UC	McNary Forebay OR. Columbia River*	45.91	-119.28	22.16	11.96	0.22	2.58	0.86
USACE	UC	McNary Forebay WA. Columbia River	45.91	-119.28	23.12	13.96	0.17	3.04	0.82
USGS	UC	Methow River	48.03	-119.91	18.15	9.32	0.18	0	0.88
USGS	UC	Mid-Columbia near Lake Wallula	45.91	-119.66	22.58	14.14	0.16	2.7	0.8
DOE	PS	Miller Creek near mouth	47.47	-122.34	18.33	8.91	0.18	0	0.82
DOE	UC	Mission Creek near Cashmere	47.53	-120.47	37.01	23.62	0.08	0	0.92
DOE	UC	Moxee Drain at Birchfield Road	46.53	-120.47	22.61	10.6	0.16	0	0.84
USGS	UC	Naches River	46.66	-120.53	14.19	12.92	0.16	0	0.74
DOE	LC	Naselle River near Naselle	46.34	-123.72	39.37	22.65	0.26	9.24	0.75
DOE	PS	Newaukum Creek near Enumclaw	47.28	-122.03	15.13	14.52	0.67	9.6	0.94

Appendix A: Continued.

Dataset[1]	Region[2]	Site/River Basin	Latitude	Longitude	alpha	beta	gamma	mu	nsc
DOE	PS	Stillaguamish River at Cicero	48.28	-122.03	19.77	16.57	0.55	11.57	0.74
DOE	PS	Stillaguamish River near Darrington	48.28	-121.72	16.59	16.5	0.49	10.9	0.73
DOE	UC	Noname Creek near Cashmere	47.53	-120.47	19.35	17.21	0.21	8.46	0.85
DOE	PS	Nooksack River at North Cedarville	48.84	-122.28	15.66	16.84	0.61	11.15	0.76
DOE	PS	Nooksack River above Middle Fork	48.84	-122.16	12.42	16.21	4.22	10.63	0.9
USGS	UC	Okanogan River	48.97	-119.41	31.08	11.98	0.11	0	0.95
DOE	UC	Okanogan River at Oroville	48.09	-119.72	25.05	10	0.2	0	0.85
USGS	UC	Palouse River	46.91	-117.09	27.71	13.33	0.16	0	0.83
USACE	UC	Pasco, WA. Columbia River*	46.22	-119.09	21.54	13.91	0.27	2.4	0.92
DOE	UC	Paradise Creek at the Border	46.72	-117.09	24.2	2.44	0.07	0	0.78
DOE	PS	Patterson_Ck_near_Fall_City	47.59	-121.91	17.46	18.57	0.51	11.81	0.8
USGS	UC	Pend Orielle River	48.91	-117.34	24.35	9.97	0.16	0	0.87
DOE	UC	Peone (Deadman) Creek	47.78	-117.41	14.77	16.23	0.48	10.47	0.86
DOE	PS	Pilchuck Creek at Bridge 626	48.22	-122.22	23.97	15.2	0.25	7.33	0.75
DOE	UC	Pine Creek at Rosalia	47.22	-117.34	22.41	14.16	0.24	6.99	0.94
USACE	UC	Priest Rapids Forebay Columbia River*	46.66	-119.84	20.62	13	0.23	3.21	0.9
DOE	PS	Puyallup River at Puyallup	47.22	-122.34	17.6	11.58	0.22	0	0.89
DOE	PS	Raging River at mouth	47.59	-121.91	19.74	18	0.68	11.99	0.86
USACE	UC	Rock Island Forebay, Columbia River	47.34	-120.09	18.61	13.72	0.25	3.93	0.7
DOE	PS	Samish River near Burlington	48.53	-122.34	16.42	16.89	0.54	10.95	0.74
USGS	UC	Sanpoil River	47.97	-118.66	24.01	13.24	0.17	0	0.97
DOE	UC	Palouse River (South Fork) at Albion	46.78	-117.28	43.86	21.69	0.07	0	0.72
DOE	PS	Snoqualmie River at Bendigo	47.47	-121.78	17.3	5.89	0.13	0	0.71
DOE	PS	Snoqualmie at Valley Trail (RM 19)	47.53	-121.78	17.79	7.3	0.13	0	0.78
DOE	PS	Snoqualmie River at 468th Ave	47.47	-121.78	24.1	10.79	0.08	0	0.86
DOE	PS	Stillaguamish River at Arlington	48.22	-122.09	26.42	17.75	0.34	9.44	0.83
DOE	PS	Thornton Creek (South Fork) 107th Ave	47.72	-122.28	18.23	8.38	0.18	0	0.8
USGS	UC	Similkameen River	48.91	-119.41	22.78	12.7	0.16	0	0.88
DOE	UC	Similkameen River at Oroville	48.91	-119.47	24.49	11.67	0.18	0	0.86
DOE	PS	Skagit River above Sedro Woolley	48.47	-122.22	17.08	16.47	0.72	12.84	0.89
USACE	LC	Skamania, WA. Columbia River	46.28	-123.47	21.87	11.72	0.4	5.09	0.85
DOE	PS	Snoqualmie River above Carnation	47.53	-121.78	20.09	13.49	0.49	0	0.97
DOE	OP	Soleduck River near Forks	48.03	-124.41	16.5	15.6	3.02	13.4	0.96
DOE	PS	Stimson Creek at Highway 300	47.41	-122.91	14.09	8.48	0.21	0	0.8
USACE	UC	The Dalles Forebay Columbia River	45.66	-121.16	23.09	12.86	0.2	0	0.84
USACE	UC	The Dalles Tailrace Columbia River	45.66	-121.16	22.37	14.69	0.25	5.22	0.83
DOE	PS	Tolt River near Carnation	47.66	-121.91	18.69	17.77	0.36	10.92	0.89

Appendix A: Continued.

Dataset[1]	Region[2]	Site/River Basin	Latitude	Longitude	alpha	beta	gamma	mu	nsc
DOE	UC	Tucannon River at Powers	46.53	-118.16	27.97	17.09	0.12	2.56	0.71
USACE	PS	University Bridge Lake Union, Seattle	47.66	-122.34	24.1	13.37	0.3	6.8	0.92
DOE	PS	Union River near Belfair	47.47	-122.84	13.76	9.65	0.24	0	0.71
USGS	UC	Upper Columbia River at Entiat*	47.66	-120.22	22.69	10.4	0.18	1.62	0.93
USGS	UC	Upper Columbia River at Priest Rapids*	46.66	-119.91	22.31	11.63	0.19	1.41	0.92
USGS	LC	Upper Cowlitz River	46.59	-121.66	17.12	12.9	0.16	3.1	0.77
USGS	UC	Upper Yakima River	47.34	-121.41	22.54	6.42	0.23	1.38	0.92
USGS	UC	Walla Walla River	46.03	-118.78	30.41	17.43	0.16	3.63	0.93
DOE	UC	Walla Walla River near Touchet	46.03	-118.91	27.12	19.32	0.25	9.25	0.83
USACE	UC	Wanapum Forebay Columbia River*	46.84	-119.97	20.9	10.79	0.21	2.97	0.87
USACE	UC	Wanapum Downstream Columbia River*	46.84	-119.97	20.31	11.93	0.18	3.54	0.78
USACE	UC	Wells Forebay Columbia River*	47.97	-119.84	19.85	10.34	0.24	2.24	0.76
USACE	UC	Wells Tailrace Columbia River	47.97	-119.84	18.36	13.5	0.3	3.97	0.74
USGS	UC	Wenatchee River	47.47	-120.34	5.15	4.64	0.39	0	0.87
DOE	UC	Wenatchee River at Wenatchee	47.47	-120.34	24.16	14.08	0.21	0	0.93
DOE	UC	Wenatchee River near Leavenworth	47.66	-120.72	20.72	14.51	0.29	7.85	0.76
DOE	PS	White River at R Street	47.16	-122.09	17.64	17.74	0.52	10.99	0.8
DOE	UC	Wide Hollow Creek at Main Street	46.53	-120.47	21.8	8.19	0.12	0	0.85
DOE	OP	Willapa River near Willapa	46.66	-123.66	16.89	15.73	1	12.44	0.76
DOE	UC	Wilson Creek at Highway 871	46.91	-120.53	18.47	12.84	0.28	10.23	0.86
USACE	LC	Warrendale, OR. Columbia River	45.66	-122.03	22.24	10.2	0.26	3.09	0.88
DOE	UC	Yakima River near Cle Elum	47.16	-121.03	17.69	8.97	0.34	0	0.81

[1]Dataset refers to origin of data: Washington Department of Ecology (DOE), US Army Corps of Engineers (USACE), US Geological Survey (USGS).

[2]Region refers to Upper Columbia River and tributaries upriver of the Dalles (UC), Lower Columbia and tributaries downriver of the Dalles, OR (LC), Puget Sound (PS), Olympic Penisula (OP).

*Sites demonstrating hysteresis.

Appendix B: National Climatic Data Center meteorological stations with air temperatures and matching water temperature study sites.

Coop ID	NCDC Station Name	Matching study site
450844	Boundary Dam	Boundary (US/Canada) Columbia River
451630	Colville	Colville River at Chewelah
453883	Ice Harbor Dam	Ice Harbor Forebay Snake River
454841	Lower Monumental Dam	Lower Monumental Tailrace Snake River
455231	McNary Dam	McNary Forebay WA. Columbia River
457696	Skamania Fish Hatchery	Skamania, WA. Columbia River
457773	Snoqualmie Falls	Snoqualmie River at Carnation
459082	Wenatchee Pangborn AP	Wenatchee River at Wenatchee

National Climatic Data Center stations with air temperatures and matching study sites.

Appendix C: Locations with simulated streamflow used in this study.

River Basin/Site	Latitude	Longitude	Basin Area (mi^2)
Pend Orielle River at Albeni Falls	48.63	-117.13	24200
Nisqually River at Alder Dam	46.80	-122.31	286
Asotin Creek at Asotin	46.34	-117.06	323
Columbia River below Bonneville Dam	45.63	-121.96	240000
Pend Orielle River at US/Canada Boundary	49.00	-117.35	25200
Pend Orielle River near Ione	48.78	-117.42	24900
Bumping River	46.87	-121.29	71
Chehalis River near Grand Mound	46.78	-123.03	895
Chelan River at Chelan	47.83	-120.01	924
Chehalis River at Porter	46.93	-123.31	1294
Chewuch River at Winthrop	48.48	-120.19	525
Rufus Woods Lake at Bridgeport	47.99	-119.63	75400
Cle Elum River near Rosyln	47.24	-121.07	203
Columbia River at Clover Island	46.22	-119.11	104000
Colville River at Kettle Falls	48.59	-118.06	1007
Cowlitz River at Castlerock	46.27	-122.90	2238
Cowlitz River near Kosmos	46.47	-122.11	1040
Cowlitz River at Randall	46.53	-121.96	541
Cowlitz River at Packwood	46.61	-121.68	287
Crab Creek near Beverly	46.83	-119.83	4840
Crab Creek at Irby	47.36	-118.85	1042
Crab Creek near Moses Lake	47.19	-119.26	2228
Columbia River at Dalles	45.61	-121.17	237000
Skagit River at Diablo Dam	48.72	-121.13	1125
Dungeness River at Dungeness	48.14	-123.13	197
Elwha River near Port Angeles	48.06	-123.58	269
Entiat River near Ardenvoir	47.82	-120.42	203
Entiat River near Entiat	47.66	-120.25	419
Columbia River at Grand Coulee	47.97	-118.98	74700
Gorge Reservoir near Newhalem	48.70	-121.21	1159
Green River near Auburn	47.31	-122.20	399
Hangman Creek at Spokane	47.65	-117.45	689
Hoh River near Forks	47.81	-124.25	253
Snake River below Ice Harbor	46.25	-118.88	108500
Yakima River at Kachess Reservior	47.26	-121.20	64
Kalama River near Kalama	46.05	-122.84	202
Yakima River at Martin	47.32	-121.34	55
Little Klickitat River near Wahkiacus	45.84	-121.06	280
Klickitat River near Pitt	45.76	-121.21	1297
Lewis River at Ariel	45.95	-122.56	731
Lewis River near Cougar	46.06	-121.98	227
Snake River at Little Goose	46.50	-118.00	103900
Snake River at Lower Granite	46.60	-117.40	103500

Appendix C: Continued.

River Basin/Site	Latitude	Longitude	Basin Area (mi²)
Little Spokane River near Dartford	47.78	-117.50	698
Spokane River at Long Lake	47.84	-117.84	6020
Cowlitz River below Mayfield Dam	46.50	-122.60	1400
Methow River near Mazama	48.57	-120.38	373
Methow River near Pateros	48.08	-119.98	1772
Methow River at Twisp	48.37	-120.12	1301
Methow River at Winthrop	48.47	-120.18	1007
Cowlitz River at Mossyrock	46.53	-122.42	1170
Naches Rivernear Cliffdell	46.90	-121.02	390
Naches River near Naches	46.75	-120.77	941
Stillaguamish River near Arlington	48.26	-122.05	262
Nooksack River at Ferndale	48.85	-122.59	786
Okanaogan River at Malott	48.28	-119.70	8080
Okanogan River near Tonasket	48.63	-119.46	7260
Palouse River at Hooper	46.76	-118.15	2500
Columbia River below Priest Rapids Dam	46.63	-119.86	96000
Queets River near Clearwater	47.54	-124.31	445
Quinault River at Quinault Lake	47.46	-123.89	264
Yakima River at Rimrock Reservoir	46.66	-121.12	187
Columbia River below Rock Island Dam	47.33	-120.08	89400
Rock Creek at Old Highway 8 Bridge	45.75	-120.44	213
West Fork Sanpoil River near Republic	48.46	-118.75	308
Sanpoil River near Republic	48.48	-118.73	263
Satsop River at Satsop	47.00	-123.66	299
Similkameen River near Nighthawk	48.98	-119.62	3550
Similkameen River at Oroville	48.93	-119.44	3550
Skagit River near Mount Vernon	48.45	-122.33	3093
Skokomish River near Potlatch	47.31	-123.17	227
Snohomish River near Monroe	47.83	-122.05	1537
Spokane River at Spokane	47.66	-117.45	4290
Stehekin River at Stehekin	48.33	-120.69	321
Lewis River	46.05	-122.20	480
Touchet River at Bolles	46.27	-118.22	361
Toutle River near Silver Lake	46.33	-122.83	496
Tucannon River near Starbuck	46.50	-118.07	431
Twisp River near Twisp	48.37	-120.15	245
Walla Walla River at State Line	46.03	-118.73	1657
Columbia River at Wanapum Dam	46.90	-119.90	90700
Columbia River below Wells Dam	47.95	-119.87	86100
Wenatchee River at Monitor	47.50	-120.42	1301
Wenatchee River at Peshastin	47.58	-120.62	1000
Wenatchee River near Plain	47.76	-120.67	591
White River at Buckley	47.17	-122.02	427

Appendix C: Continued.

River Basin/Site	Latitude	Longitude	Basin Area (mi²)
White Salmon River near Underwood	45.75	-121.53	386
Wilson Creek near Almira	47.66	-118.93	327
Yakima River at Cle Elum	47.19	-120.95	495
Yakima River near Grandview	46.34	-120.20	5400
Yakima River at Union Gap	46.53	-120.47	3479
Yakima River at Easton	47.24	-121.18	~225
Yakima River at Kiona	46.25	-119.48	5615
Yakima River at Mabtom	46.23	-120.00	5359
Yakima River at Umtanum	46.86	-120.48	1594
Lewis River at Yale	45.96	-122.33	596
Yakima River near Parker	46.51	-120.45	3660

7: Forests

Forest Ecosystems, Disturbances, and Climatic Change in Washington State, USA

Jeremy S. Littell[1], Elaine E. Oneil[2], Donald McKenzie[1,3], Jeffrey A. Hicke[4], James A. Lutz[5], Robert A. Norheim[1,3], Marketa M. Elsner[1]

Abstract

Climatic change is likely to affect Pacific Northwest (PNW) forests in several important ways. In this paper, we address the role of climate in four forest ecosystem processes and project the effects of future climatic change on these processes. First, we analyze how climate affects Douglas-fir growth across the region to understand potential changes in future growth. In areas where Douglas-fir is not water-limited, future growth will continue to vary with interannual climate variability, but in places where Douglas-fir is water-limited, growth is likely to decline due to projected increase in summer potential evapotranspiration. Second, we use existing analyses of climatic controls on future potential tree species ranges to highlight areas where species turnover may be greatest. By the mid 21st century, some areas of the interior Columbia Basin and eastern Cascades are likely to have climates poorly suited to pine species that are susceptible to mountain pine beetle, and if these pines are climatically stressed, they may be more vulnerable to pine beetle attack. Climatic suitability for Douglas-fir is also likely to change, with substantial decreases in climatically suitable area in the Puget Trough and the Okanogan Highlands. Third, using regression approaches, we examine the relationships between climate and the area burned by fire in the PNW and in eight Washington ecosystems and project future area burned in response to changing climate. Area burned is significantly related to both temperature and precipitation in summer, but more physiologically relevant variables, such as water balance deficit, perform as well or better in models. Regional area burned is likely to double or even triple by the end of the 2040s, although Washington ecosystems have different sensitivities to climate and thus different responses to climatic change. Fourth, we evaluate the influence of climatic change on mountain pine beetle (MPB) outbreaks by quantifying both host-tree vulnerability and pine beetle adaptive seasonality. Host-tree vulnerability is closely related to vapor pressure deficit (VPD), and future projections support the hypothesis that summer VPD will increase over a significant portion of the range of host tree species. Due to the increased host

[1] JISAO Climate Impacts Group, University of Washington, Seattle, Washington
[2] Rural Technology Initiative, College of Forest Resources, University of Washington, Seattle, Washington
[3] USDA Forest Service Pacific Northwest Research Station, Seattle, Washington
[4] Department of Geography, University of Idaho, Moscow, Idaho
[5] College of Forest Resources, University of Washington, Seattle, Washington

vulnerability, MPB populations are expected to become more viable at higher elevations leading to increased incidence of MPB outbreaks The increased rates of disturbance by fire and mountain pine beetle are likely to be more significant agents of changes in forest structure and composition in the 21st century than species turnover or declines in productivity. This suggests that understanding future disturbance regimes is critical for successful adaptation to climate change.

1. Introduction

Global climate change is expected to affect Earth's ecosystems in many ways (IPCC Working Group II, 2007). Terrestrial ecosystems may experience widespread mortality of vegetation from the direct effects of changes in temperature and precipitation (Breshears et al. 2005, Lutz and Halpern, 2006, van Mantgem and Stephenson, 2007; van Mantgem et al. 2009) and from increased extent, intensity, and frequency of disturbance (McKenzie et al., 2004; Gedalof et al., 2005, Littell, 2006, Littell et al., in press). New ecosystem types, comprising heretofore rare or non-existent combinations of species, may succeed those no longer adapted to new climates, in turn changing landscape structure and spatial pattern across a range of scales (Davis 1986). Anticipating these changes is challenging, but necessary to support long-term planning, natural resources management, and maintenance of the myriad services that ecosystems provide.

In the Pacific Northwest (PNW) region of U.S. North America (here defined as Washington, Oregon, Idaho, and western Montana), forests, both on public and private lands, are a key natural resource. In Washington State alone, forests cover 8,926,490 ha (Figure 1), 52% of the total area of the state. Approximately 56% (~ 5 million ha) of this forested land is publicly owned, administered by federal (U.S. Departments of Agriculture and Interior) and state (WA Department of Natural Resources) agencies. The remainder is managed by tribal, private, and corporate landowners. Legal mandates and owner objectives for these lands vary, but all may be affected by a changing climate.

Conifer species dominate forest ecosystems within Washington State, with hardwood species abundant only in riparian areas that experience frequent flooding or other heavily disturbed areas such as avalanche chutes or recently logged sites. Forest composition varies with both elevation and position on a west-east (maritime-continental) gradient across the state. At a finer scale, orographic effects on species composition are apparent on the leeward versus windward sides of both the Olympic Mountains and the Cascade Range, where complex topography produces steep gradients in the biophysical environment across relatively short distances (Williams and Lillybridge, 1983; Franklin and Dyrness, 1988; Henderson et al., 1989, 1992; Williams et al. 1990; Lillybridge et al. 1995).

Research from many ecosystems around the world at many scales has documented climatic controls on vegetation (Davis and Botkin 1985, Overpeck et al. 1990, Guisan and Zimmerman 2000). Climatic *limiting factors* operate mechanistically through the interface between organisms and their environment. Plant performance is compromised when one or more resources (e.g., light, thermal energy, water, nutrients) are limiting. At

Figure 1. Forested areas of Washington State, and Bailey's ecosections used for sub-regional fire modeling.

broad scales, forests of western North America can be partitioned into two climatically mediated classes of limitation: energy-limited versus water-limited domains (Milne et al., 2002, McKenzie et al., 2003, Running et al., 2004, Littell and Peterson, 2005, Littell et al., 2008). Energy-limiting factors are chiefly light (e.g., productive forests where competition reduces light to most individuals or climates where cloud cover limits light) and temperature (e.g., high-latitude or high-elevation forests). Tree growth in energy-limited ecosystems appears to be responding positively to warming temperatures over the past 100 years (McKenzie et al., 2001).

In contrast, productivity in water-limited systems is expected to decline with warming temperatures, as increasing water balance deficit (the condition in which potential summer atmospheric and plant demands exceed available soil moisture) constrains photosynthesis across more of the West (Figure 2). There is evidence to support the hypothesis that CO_2 fertilization significantly increases water-use efficiency in plants (Boisvenue and Running, 2007) enough to partially offset future water demands (e.g., in model studies, Neilson et al., 2005, Lenihan et al., 2008), but conclusive results have not been forthcoming, and the overall expected change is decreasing water availability for plants in summer (Figure 2). Littell et al., (2008) found that most montane Douglas-fir (*Pseudotsuga menziesii*) forests across the northwestern United States appear to be currently water-limited; under all but the wettest climate projections water limitations will increase in both area and magnitude because increased potential evapotranspiration will exceed precipitation supply by more than it does currently.

Cool season surplus (runoff; precipitation and snow melt less plant use and soil water recharge) and summer water deficit can increase simultaneously in a warmer climate (Figure 2). In the base case (1980 - 1999 climate), precipitation is low during summer months, and winter temperatures are

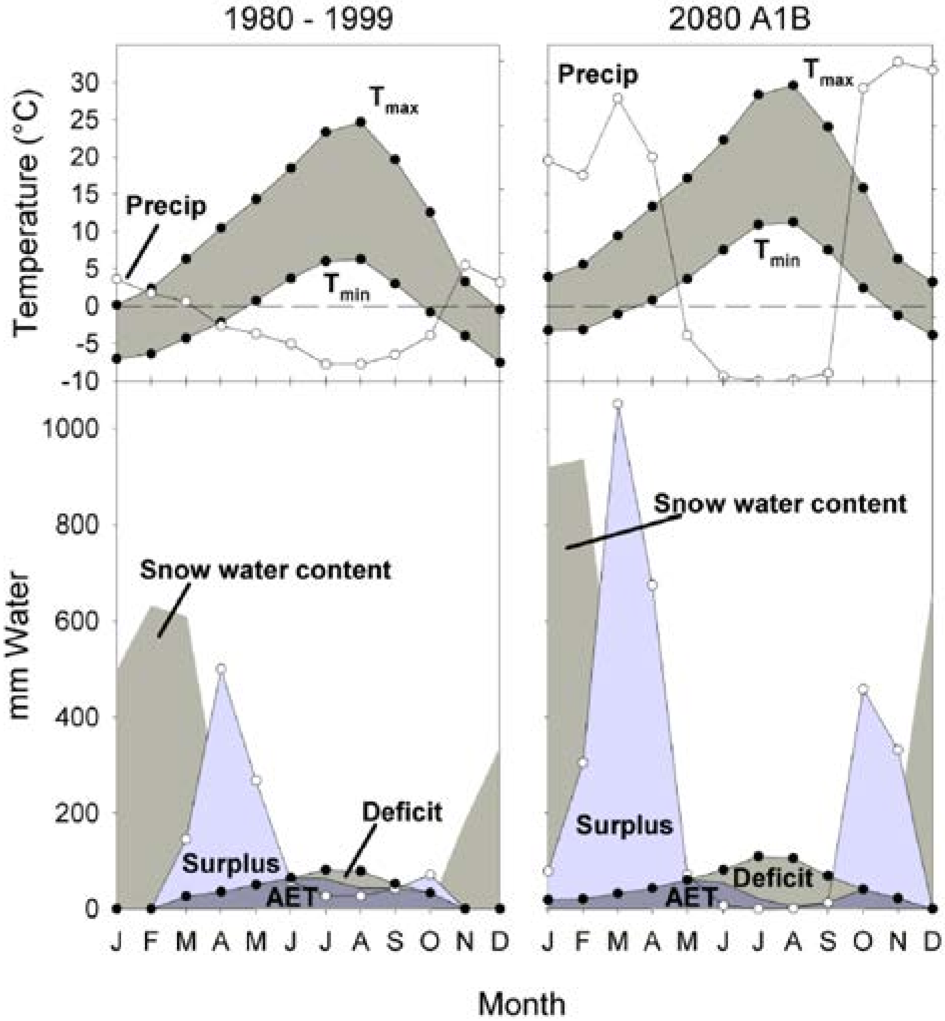

Figure 2. Physical (top) and biophysical (bottom) aspects of present and modeled future climate for a study plot in the Umatilla National Forest, SE Washington, slope 34 degrees, southwest aspect.

below freezing. Water supply (rain plus snowmelt) is less than evaporative demand (PET) from June through September. In the 2080 A1B composite scenario, summer precipitation is almost zero, and winter temperatures are no longer below freezing. Water supply is less than evaporative demand from May through October, resulting in a longer seasonal deficit. This is generally consistent with the findings of Elsner et al. (2009, this report), in which projected changes in winter temperature and precipitation result in decreased snowpack, summer temperatures increase, and summer soil moisture declines over much of the PNW.

Limiting factors can of course shift within a species range (Peterson and Peterson, 2001), or between seasons, as water demands abate and energy needs increase (Stephenson, 1990, 1998; Lutz, 2008). For example, in high-elevation or high-latitude arid forests (e.g., eastern slopes of the Sierra Nevada, Rocky Mountain Front Range, interior boreal spruce), short growing seasons limit energy inputs, but drought stress still occurs in summer. Similarly, climatic variability can alter the temperature and or precipitation such that limiting factors are exacerbated or mitigated for years or decades at a time; limiting factors can therefore also be transient, particularly for populations at the transition between energy and water limitation.

The effects of climatic change may be particularly strong in mountains, because warmer temperatures affect the depth and duration of snowpacks (Cayan, 1996; Mote et al., 2005; Knowles et al., 2006), which are key limiting factors for tree growth at high elevation (Peterson and Peterson, 2001; Nakawatase and Peterson, 2006; Case and Peterson, 2007). Population changes at upper treeline (e.g., Lloyd and Graumlich, 1997) and lower treeline (e.g., Allen and Breshears, 1998) are also linked to climatic variability, with the edge between forested ecosystems and other vegetation types (e.g., grassland, shrubland, or alpine meadows) clearly changing with decadal and centennial climate variability. Climatic influences are difficult to assess in mountainous areas, however, because complex topography produces steep gradients in the biophysical environment, and climate-monitoring stations are sparsely distributed, particularly at the highest elevations. (Thornton et al., 2000; Daly et al., 2008).

Two important disturbances in forests of the Pacific Northwest are wildfire and outbreaks of the mountain pine beetle (MPB -- *Dendroctonus ponderosae*). Wildfire has been linked to climatic variability via studies of Holocene charcoal sediments, fire-scar and stand-age reconstructions of fire history, and statistical models using 20th-century instrumental records (McKenzie et al., 2004 and references therein). Of particular concern are increases in fire area in a warming climate and the effects of extreme wildfire events on ecosystems (Gillett et al., 2004; Gedalof et al.,2005; Lutz, 2008; Littell et al., in press). For example, in 2006, the Tripod Complex Fire in north-central Washington burned over 80,000 ha, much of it higher severity than expected from historical fires.

Mountain pine beetle infestations have historically occurred frequently and extensively throughout the Pacific Northwest (Wellner, 1978; Logan and Powell, 2001). Climate change, in particular warming and drought, affects bark beetle life stage development rates, winter mortality, and host tree susceptibility (Logan and Powell, 2001; Carroll et al., 2004; Oneil, 2006). Across the West, stand structural conditions make host species susceptible to beetle attack (Hicke and Jenkins, 2008), future climate change is predicted to reduce the area of climate suitability for the MPB at low elevations, and increase climate suitability at higher elevations (Hicke et al., 2006).

Although the nature, timing, and impacts are only beginning to be understood, synergistic interactions between disturbances are producing larger effects than would occur from either disturbance independently (McKenzie et al., 2008). For example, MPB outbreaks have been linked to the increased likelihood of stand-replacing fire and changes in fire behavior, with the nature of the effect depending on the time since infestation (Lynch et al., 2006; Jenkins et al., 2008). Combined with increasing climatic stress on tree populations and growth, such disturbance interactions can alter forest structure and function more rapidly than could be predicted from models of species redistribution or disturbance alone. Simultaneous climatically driven shifts in the locations of species' optima, ecosystem productivity, disturbance regimes, and the interactions between them could reset forest succession over large areas and short time frames compared to changes observed during the 20th century. Yet there is still substantial uncertainty surrounding future climate and ecosystem responses, much less interactions between them, particularly at regional and sub-regional scales.

Planning for the impacts of climate change on forests requires better understanding of the role of climate in forest ecosystem processes. In this paper, we examine four key processes in forest ecosystems that we expect to change significantly across Washington State in a warming climate:

- Douglas-fir productivity and water limitation. Douglas-fir is one of the most widespread tree species in Washington, the most important by far economically, and possibly one of the more climate-sensitive species regionally. How will future changes in climate alter Douglas-fir productivity in different parts of its range? Can we further identify the geographic domain of future water limitation in Washington forests?
- Conifer species ranges. Management priorities for forest ecosystems in Washington depend on species composition. How will climate change affect species distributions, particularly in sensitive areas where species are near the edges of their climatic tolerances?
- Fire area burned. The area burned by fire is predicted to increase across western North America as a result of climate change, but what are the expectations for Washington State and their consequences?
- Mountain pine beetle outbreaks. In the last decade, MPB outbreaks have increased in the West and appear to be correlated with warmer temperatures and drought. What are the specific consequences within Washington State?

To answer these questions, we use historical climate data, statistical ecological models, and climate (regional and global) and hydrologic simulation models to quantify the magnitude and direction of climatic influences on each forest ecosystem process. We then examine the relative importance of each of these processes for the structure, composition, and extent of Washington State forests under different scenarios for climatic change (Mote and Salathé 2009, this report). We address both the magnitudes of effects and the temporal scales at which they operate because when the magnitude and direction of two different changes are equal, those that occur over shorter periods will appear more sudden and be more difficult to anticipate. We use both composite climate model output and scenarios based on individual climate models, statistically downscaled to 1/16th degree resolution (Salathé et al. 2007; Mote and Salathé 2009, this report, Elsner et al. 2009, this report), for future projections.

These four processes are by no means the only ones that will be affected by climate change; there is much that is left untreated by our emphasis on these four areas, and in most cases much more that could be said about the four we chose to emphasize. This assessment should be regarded as a first step, not an all-encompassing review.

2. Methods

2.1. Productivity: Douglas-Fir Growth and Changes in the Area of Water-Limited Forest

We explored the role of climate in the productivity of WA forests in two ways. First, we assessed potential changes in Douglas-fir growth for the period 1916-2003 (the period of time for which both tree cores and climate data exist) using growth increment measurements from 117 unmanaged stands in the Pacific Northwest (Littell et al., 2008). The sampled stands come from a wide range of local environments and represent a gradient of climatic conditions from maritime (e.g., western Olympics and western Cascades) to continental (e.g., eastern Cascades, north Idaho Panhandle, western Northern Rockies). We extended the work of Littell et al. (2008) by analyzing controls on absolute growth rather than focusing just on variability in growth. We developed stand-level basal area increment (BAI, a measure of annual radial growth) time series from 5-15 (mean = 10) canopy-dominant or co-dominant trees in each stand. Raw tree-ring series were measured to 0.02mm (Littell et al. 2008) and converted to BAI following Nakawatase and Peterson (2006). We used Pearson correlations to assess the relationship between annual mean basal area increment and regional time series of summer climate variables (1916-2003 driving data and output variables from the VIC hydrologic model - see Elsner et al. 2009, this report) previously linked to Douglas-fir growth: maximum temperature (Tmax), potential evapotranspiration (PET), actual evapotranspiration (AET), and water balance deficit (PET-AET).

Second, we evaluated the forested area in Washington that is currently energy-limited or marginally water-limited but likely to become severely water-limited during the mid 21st century. We defined severely water-limited forests as those forests where summer (JJA) PET exceeds annual precipitation; this is a conservative estimate of water limitation, but current areas of WA that meet this criterion are frequently ponderosa-pine woodland in transitional, low elevation forest habitat. This distinction of severe water limitation was made in order to emphasize the areas most likely to be impacted by changes in water deficit, but physiological limitations can occur before such limits are reached and the impacts are likely to be species dependent. We defined energy-limited forests as those where annual precipitation exceeds summer evapotranspiration. We used hydrologic simulations of current (1916-2006) and future (2020s, 2040s, and 2080s) annual PPT (precipitation) and summer PET (Elsner et al., 2009, this report) to map future conditions of water limitation.

2.2. Climate and Changes in Species Biogeography

We assessed the potential for climate to alter important PNW tree species distributions by using spatially explicit projections from recently published analyses of climate and species responses for western North America (Rehfeldt et al., 2006). Specifically, we were most concerned with the potential for climatic stress on regeneration or mortality in Douglas-fir forests and the potential for stress in three species susceptible to the mountain pine beetle (lodgepole pine, *Pinus contorta*; ponderosa pine, *Pinus ponderosa*; and whitebark pine, *Pinus albicaulis*) in the PNW. Other species range changes are also important, but a full assessment is beyond the scope of this project. We focused on Douglas-fir because it is widespread and economically important and on the pine species because of their potential for interaction with the mountain pine beetle, particularly in forests east of the Cascades. For each species, we used Rehfeldt et al. (2006) grid maps of potential future habitat based on climate and combined these to develop summary maps of areas where climate is likely to exceed

Rehfeldt et al.'s (2006) estimates of the tolerances of Douglas-fir. We used a similar approach to assess areas of change in pine species richness for the end of the 2040s-2060s (Rehfeldt's analyses are for the 2030s and 2060s). After Rehfeldt et al. (2006), we assumed that areas with ≥ 75% agreement among statistical climate/species models represented climatic conditions where the species was likely to occur. We assumed that areas with < 75% but ≥ 50% agreement were potential areas of future occurrence but where climatic variability might put the species at some risk, and we assumed that areas with <50% agreement were unlikely to have sustained climatic conditions appropriate for species persistence and regeneration after disturbance.

2.3. Climate and Area Burned by Fire

We developed statistical models that relate area burned to climate at two different spatial and temporal scales. Prior to the 1980s, fire data from federally protected lands were aggregated from 1916 at the state level and therefore prohibit analysis for sub-regional vegetation types or at fine spatial scales. After 1980, analysis is possible at finer scales and agency reporting was consistently carried out at the agency unit (e.g., a USFS National Forest district, USDOI National Park, USDOI Bureau of Indian Affairs reservation, or USBLM district). There is therefore a tradeoff between the ability to incorporate more climatic variability inherent in the longer state-based dataset and the ability to assess climate-fire relationships by vegetation type in the shorter agency-unit-based dataset. We chose to develop regional models for the period 1916-2006 to assess the role of climatic variability on fire area burned in the PNW, and to develop finer models for 1980-2006 at the level of Bailey's ecosections (Bailey, 1995) for the Pacific Northwest ecosystems in Washington: Coast Ranges / Olympic Mountains, Puget Trough / Willamette Valley, Western Cascades, Eastern Cascades, Okanogan Highlands, Palouse Prairie, Blue Mountains, and Columbia Basin.

For the regional analysis (1916-2006), climate variables were domain-averaged observed climate data (Tmax, Tmin, PPT, Mote and Salathé, 2009, this report). We used correlation analyses to identify potentially significant climatic drivers of area burned in the PNW, and these variables were iteratively entered as predictors in stepwise multiple linear regression models using AIC to arrive at the best model (Akaike Information Criterion – Akaike, 1974). AIC provides a metric, based on information theory, to optimize the tradeoff between model goodness-of-fit and parsimony (fewer parameters). The final regression maximized the variance explained by the model while retaining only multiple regression predictors significant at $\alpha = 0.1$ (usually 0.05). For ecosection analyses, the above procedure was repeated with ecosection-averaged climate variables (1980-2006, Tmax, Tmin, PPT, PET, AET, and PET-AET, or deficit, Elsner et al. 2009, this report) and for ecosection area-burned time series.

For both scales of inquiry, we then used future climate projections from the 2020s, 2040s, and 2080s in the regression equations to develop projected area burned for the region and for each ecosection in WA. For the regional climate modeling, we used the ECHAM5 and CGCM-t47 A1B projections (Mote and Salathé 2009, this report) and for sub-regional ecosection models, we used ecosection-average composite downscaled projections and hydrologic model output (Variable Infiltration Capacity, see Elsner et al. 2009, this report). Both methods superimpose the observed climate variability on future changes in mean values, so the extrapolated fire area burned assumes that the range of future interannual variability in climate is comparable to the 20th century. For the future regional area burned projections, we also calculated 95% exceedence probabilities (the probability that a given year would exceed the 95% quantile in the 1916-2006 record) for the 2020s, 2040s, and 2060s.

2.4. Climate and the Mountain Pine Beetle

2.4.1. Host Vulnerability

We used data on 20th century mountain pine beetle (MPB) outbreaks, climate conditions, and site and stand inventories to develop generalized linear models of the likelihood of successful attack by MPB for lodgepole pine forests of eastern Washington (Oneil 2006). We then projected these models onto future climate space to estimate the magnitude of future MPB impacts on Washington State forests.

To identify key variables associated with mountain pine beetle attack, we built upon the empirical predictive models of Oneil (2006), which found that vapor pressure deficit (VPD) variables, including average summer VPD, maximum VPD and length of time VPD exceeded certain thresholds were the best predictors of MPB attack for the epidemic starting in 2000. Summer VPD, the difference between the amount of water vapor held in the atmosphere at saturation vapor pressure and the amount of water vapor that could be held at average daylight temperature, was the best predictor of the number of MPB attacks during the warm dry summers of 2000 to 2003. These models took advantage of two extensive databases for eastern Washington, the Current Vegetation Survey (http://www.fs.fed.us/r6/survey/) and the Department of Natural Resources' Forest Health Aerial Survey (www.fs.fed.us/r6/nr/fid/as/index.shtml).

We explored generalized linear models of two types, the Poisson and negative-binomial families (Venables and Ripley, 2002), to estimate counts of the total number of attacks over the period of record (after Oneil, 2006). We tested a variety of predictors and interaction terms and retained the models with the minimum AIC (Akaike, 1974).

Projections of future climate for the host-vulnerability analysis were derived using methods described in the Scenarios chapter (Mote and Salathé 2009, this report) for composite future projections, because we needed daily data to compute some of the predictor variables used in Oneil (2006). The composite delta values (change in temperature, Tdelta and change in precipitation, Pdelta) for each time period and emission scenario were added to a historic time series (1980-2003) of daily weather data generated using the DAYMET model (www.daymet.org) -- the same data used to build the models in Oneil (2006). These results generated plot-specific estimates of climate conditions for the six scenarios: 2020s, 2040s, and 2080s for A1B and B1 emissions scenarios. We increased the historical Tmax and Tmin values equally by Tdelta, and averaged the resulting future Tmax and Tmin to obtain a daily average temperature.

From these, we calculated daily dewpoint temperature (Tdew), daily VPD, and daily Potential Evapotranspiration (PETday). For PETday, we used the methods of Lutz (2008), which correct for slope, aspect, and elevation. We also calculated the number of days VPD exceeds two different thresholds for each plot (hence the need for daily data). We used methods from Kimball et al. (1997) to adjust VPD estimates for arid and semi-arid regions where minimum daily temperature may not be sufficiently low to reach the dewpoint temperature.

We projected both models onto the future scenario composite data sets (Mote and Salathé 2009, this report), across our entire model domain (lodgepole and ponderosa pine forests of eastern Washington). Predicted values from the models, using the future data, were examined carefully to see if they suggested that we were extrapolating too far outside the ranges of the predictor variables used to build the models.

2.4.2. Adaptive Seasonality: Temperature Effects on the Lifecycle of the Mountain Pine Beetle

We evaluated the effects of changes in year-round (all seasons, hourly data) temperatures on the climatic suitability for mountain pine beetle outbreaks. The mountain pine beetle's life cycle is primarily controlled by temperature (Logan and Bentz, 1999; Powell and Logan, 2005). We employed a process model (developed from laboratory measurements of life-stage development rates as functions of temperature) that simulates the timing of all eight life stages of the mountain pine beetle (Bentz et al., 1991; Logan and Amman, 1986, Logan et al., 1995; Logan and Powell, 2001). The model computes a developmental index in each life stage by combining the annual course of hourly temperatures with the life-stage development rate. This index simulates life-stage development from egg through adult using input temperatures, and estimates time spent in each life stage.

"Adaptive seasonality" refers to beetle life cycle timing that is conducive to rapid reproduction, synchronized mass attacks on trees, and high survival rates in winter. This condition is predicted by the model when temperatures influence life-stage development rates such that: 1) the simulated population completes a life cycle in one year (instead of two); 2) the population is synchronized for mass attacks on host trees as indicated by a life cycle exactly one year long; and 3) adult emergence from brood trees occurs at a suitable time of year (late summer) to permit the most cold-resistant life stages to occur during winter. The model was successfully evaluated in a region in central Idaho that experienced a rapid increase in mountain pine beetle populations in the late 1990s (Logan and Powell, 2004). Long-term changes at coarse spatial resolution were evaluated with this model across the West by Hicke et al. (2006).

In this study, we used historical (1970-1999) temperatures to predict recent adaptive seasonality. We also estimated future (2070-2099) temperature suitability for two future climate scenarios (ECHAM5 and HADCM, A1B SRES scenario). Hourly temperatures were estimated from daily minimum and maximum temperatures by simulating a sawtooth pattern of hourly temperatures (Hicke et al., 2006).

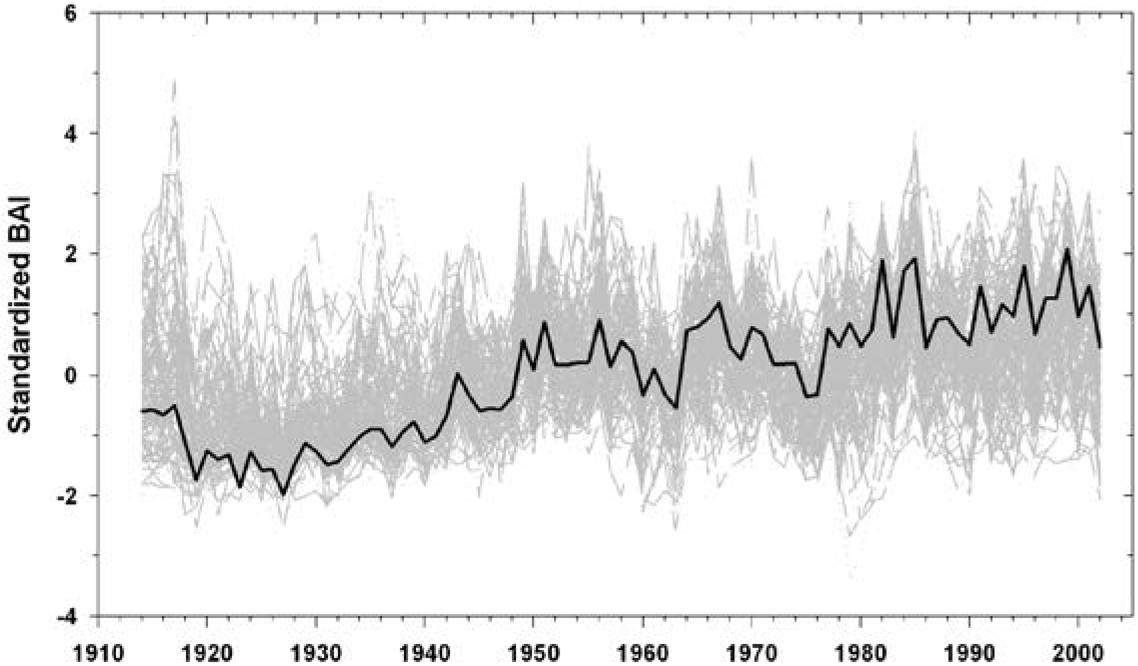

Figure 3. Douglas-fir network BAI time series 1914-2002. Gray traces represent plot-level time series, the black line is the mean of all series. Positive standardized BAI is higher than normal growth, negative standardized BAI is lower than normal growth. Trend and variability are both present.

3. Results

3.1. Productivity: Douglas-Fir Growth and Changes in the Area of Water-Limited Forest

Douglas-fir growth in the PNW was highly variable in space and time during the 20th century (Littell et al., 2008), and this variability was generally correlated with variables indicating water limitation (e.g., positively correlated with summer precipitation and actual evapotranspiration but negatively correlated with summer maximum temperature and potential evapotranspiration). The strength of the correlation between water deficit and tree growth depends on the location of the stand along a gradient of mean summer water deficit – the most water-limited stands had the greatest sensitivity. The mean BAI time series has a small but significant increasing trend of about 13 mm^2/yr/tree (Figure 3), and we could not attribute this growth trend to any single climatic factor, although there are weak but significant positive correlations with minimum temperature. The interannual *variability* about the trend in BAI (Figure 3) is not sufficiently explained by climatic variables to warrant statistical modeling of projected future productivity, but it is best correlated (r=0.42) with year prior July-August water balance deficit averaged over the sampled watersheds. The area of WA forest that is severely water-limited will increase by 32% in the 2020s, and an additional 12% in both the 2040s and the 2080s (all values relative to 20th century water-limited forests, Figure 4).

Figure 4. Increase in area of severely water-limited forests in WA. The Okanogan highlands and the foothills of the north-eastern Cascades contain most of the area that climate projections indicated will transition from energy- to water-limited forest by the 2080s.

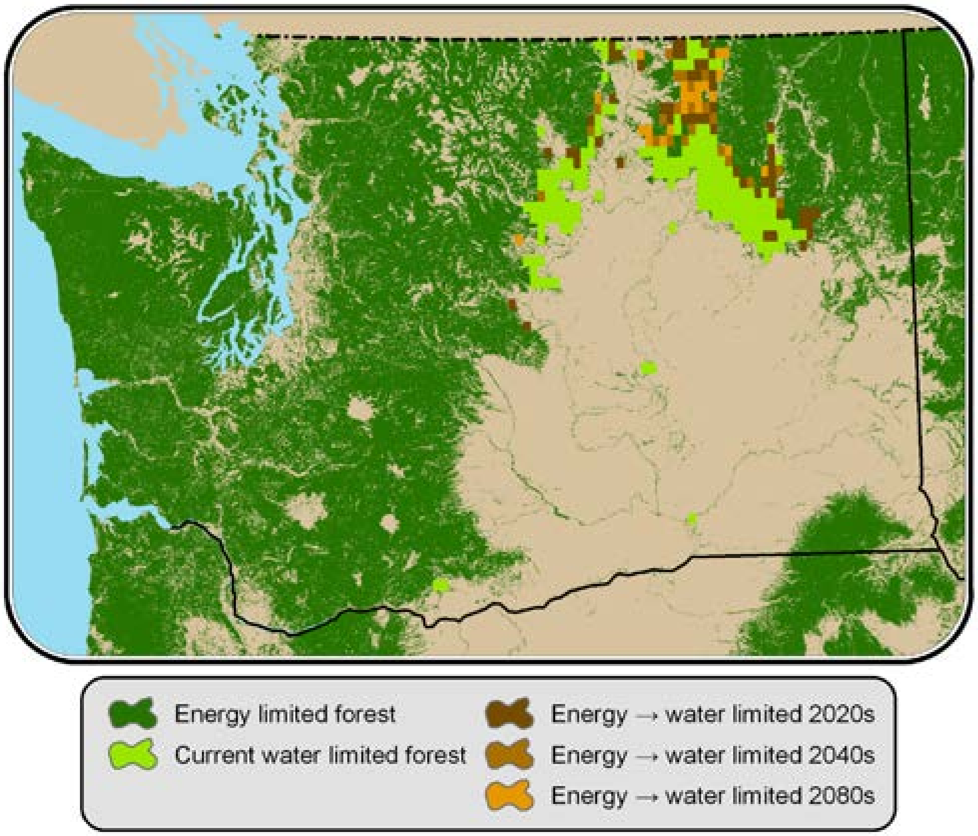

Figure 5. Change in area for which climate is suitable for Douglas-fir in the 2060s. Orange indicates area where fewer than 50% of the statistical models suggest climate appropriate for Douglas-fir presence in the 2060s. Dark green indicates areas where more than 75% of statistical models agree that climate is approrpriate for Douglas-fir. Data from Rehfeldt et al. (2006).

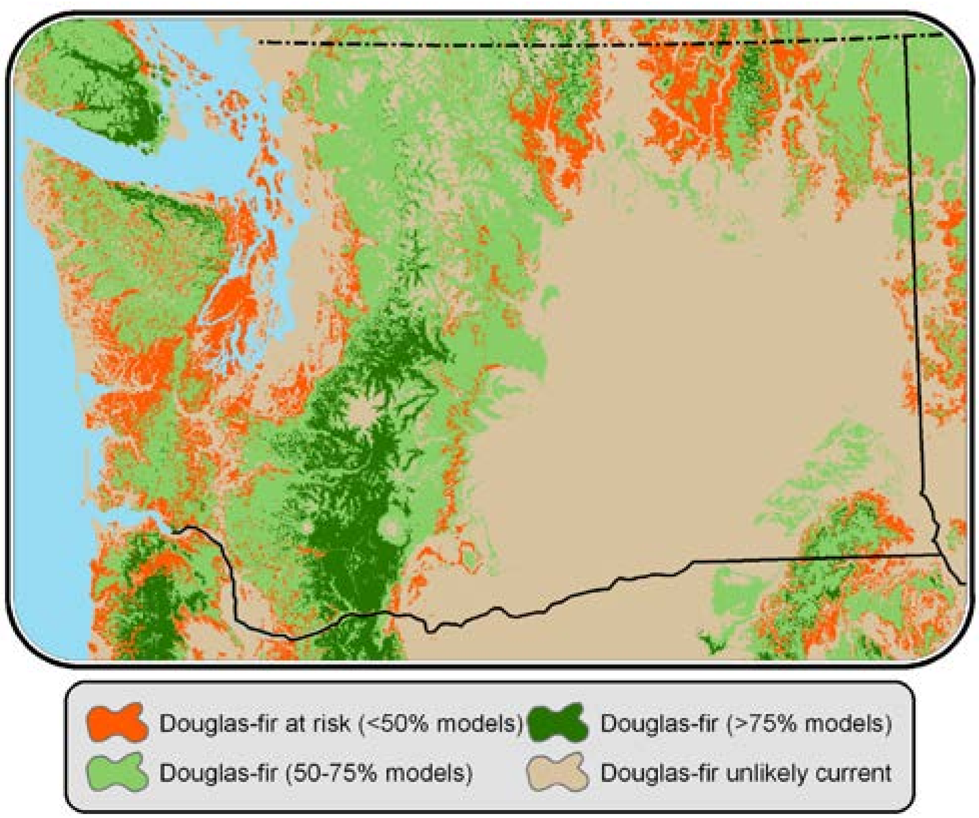

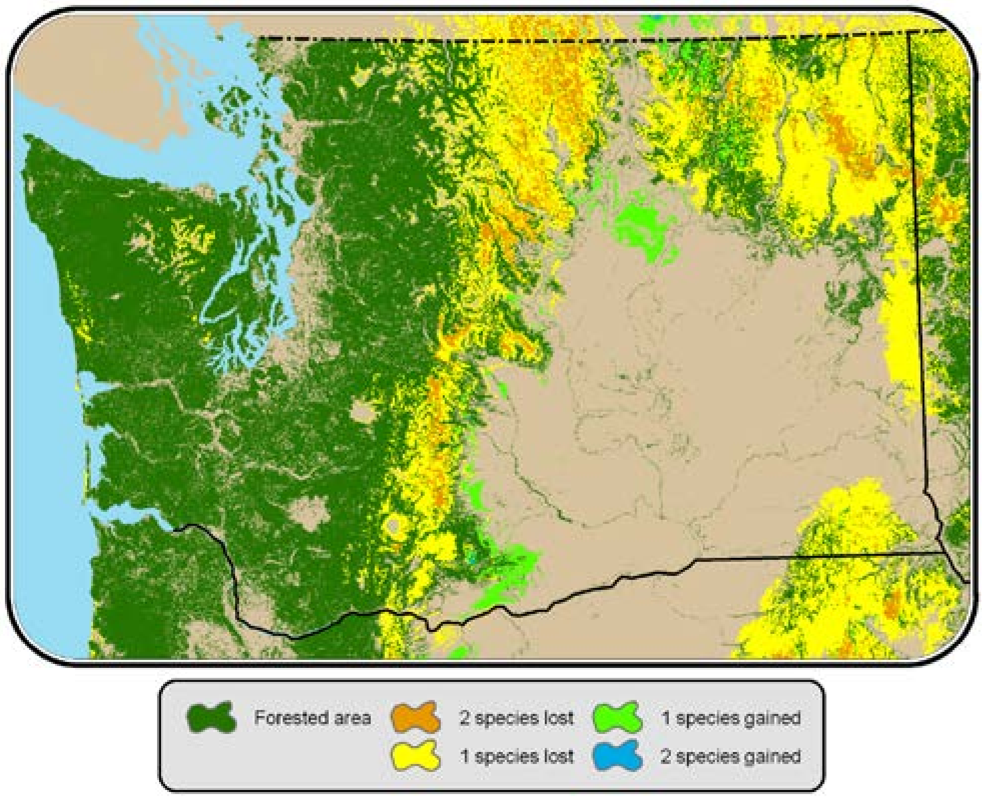

Figure 6. Change in number of pine species for which climate is suitable in the 2060s. Declines indicate places where climate is no longer suitable for species, while increases indicate places where climate is currently unsuitable and will become so. Areas in the Columbia Basin with gains projected by statistical models frequently already have patchy cover of ponderosa pine, whereas areas with gains at higher elevations in the Okanogan highlands likely represent upward migration of suitable climate for one or more pine species. Data from Rehfeldt et al. (2006).

3.2. Climate and Changes in Species Biogeography

By the end of the 2060s, independent species range modeling based on IPCC scenarios (a medium emissions scenario for both HadCM3 and CGCM2, Rehfeldt et al. 2006) suggests that climate will be sufficiently different from the late 20th century to constrain Douglas-fir distribution (Figure 5). This is probably due to increases in temperature and decreases in growing season water availability in more arid environments (e.g., in the Columbia Basin) but could be due to other variables in less arid parts of the species' range. About 32% of the area currently classified as appropriate climate for Douglas-fir would be outside the identified climatic envelope by the 2060s, and about 55% would be in the 50%-75% range of marginal climatic agreement among models. Only about 13% of the current area would be climatically suitable for Douglas-fir in >75% of the statistical species models. The decline in climatically suitable habitat for Douglas-fir is most wide-spread at lower elevations and particuarly in the Okanogan Highlands and the south Puget Sound / southern Olympics.

Climate is likely to be a significant stressor in pine forests in the Columbia Basin and eastern Cascades as early as the 2040s, particularly in parts of the Colville National Forest, Colville Reservation, and central Cascades (Figure 6). Of the area that is climatically suitable for at least one pine species, only 15% will experience climate consistent with no net loss of species; 85% will be outside the climatically suitable range for one or more current pine species (74% loss of one species, 11% loss of two species, <1% loss of three species).

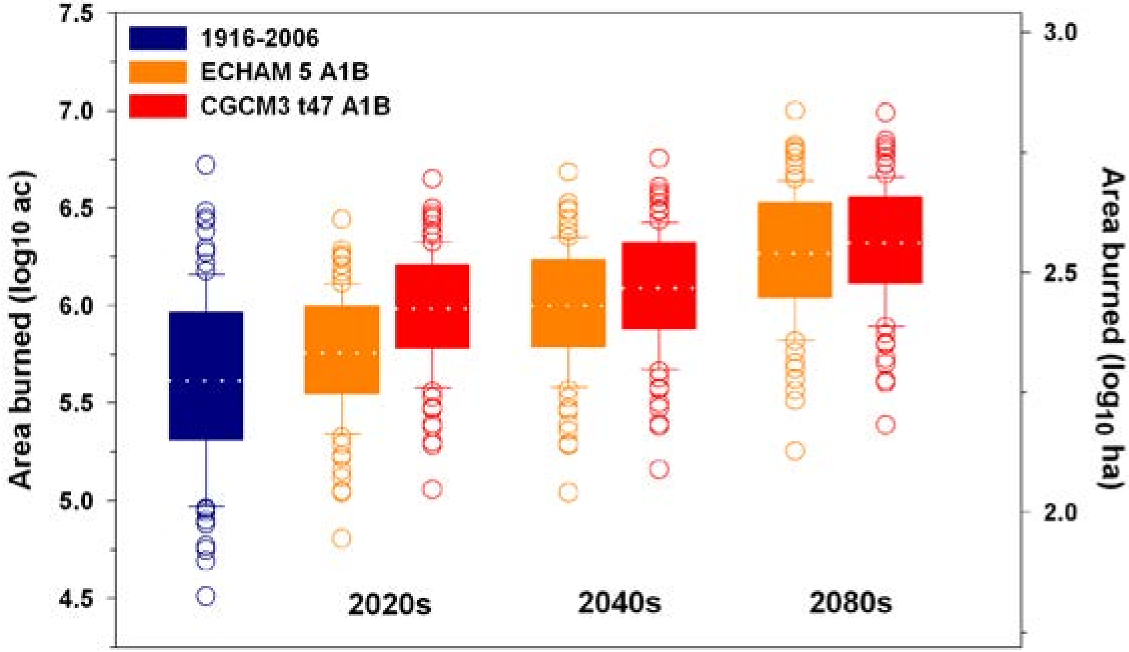

Figure 7. Changes in the distribution of annual area burned for the 2020s, 2040s, and 2080s for two "medium" scenario GCMs (Echam5 and CGCM_t47). The white dashed line inside each box indicates the median area burned. To compute actual area burned, use a value on the logarithmic Y-axis as a power of ten (e.g., 10^Y).

3.3. Climate and Area Burned by Fire

Regional fire models suggest that summer precipitation and temperature play a large role in the area burned by fire. About half the variance in annual regional area burned can be explained either by July and August temperature and precipitation or July and August water-balance deficit; the best model includes June-August total precipitation (negative relationship with fire), July-August average temperature (positive), and January precipitation (negative – total November to March precipitation performs similarly). Future fire projected from the best statistical model suggests a doubling or tripling of area burned by the 2080s (Figure 7). The median regional area burned, averaged over both GCMs, is projected to increase from about 0.5 million acres (0.2 M ha) to 0.8 million acres (0.3 M ha) in the 2020s, 1.1 million acres (0.5 M ha) in the 2040s, and 2.0 million acres (0.8 M ha) in the 2080s. The probability of exceeding the 95% quantile area burned for the period 1916-2006 increases from 0.05 to 0.48 by the 2080s (Table 1).

Sub-regionally, the strongest models occur in drier forest types and shrubland ecosystems (>55% variance explained by climate), whereas

Table 1. Modern and projected future exceedence probabilities for PNW regional area burned. 95% Exceedence (yr) refers to the count of years in a future record equivalent to the study record that would exceed the historical 1916-2006 95% quantile area burned; Exceedence (p) refers to the probability of a year exceeding the 1916-2006 95% quantile in the future.

	Modern*	**2020s**		**2040s**		**2080s**	
Exceedence		ECHAM5	CGCM3	ECHAM5	CGCM3	ECHAM5	CGCM3
95% (yr)	5	1	8	10	20	43	44
95% (p)	0.05	0.01	0.09	0.11	0.22	0.47	0.48
Number of yr > 1M ac	23	23	44	47	61	74	79
Number of yr > 3M ac	2	0	2	5	8	30	34

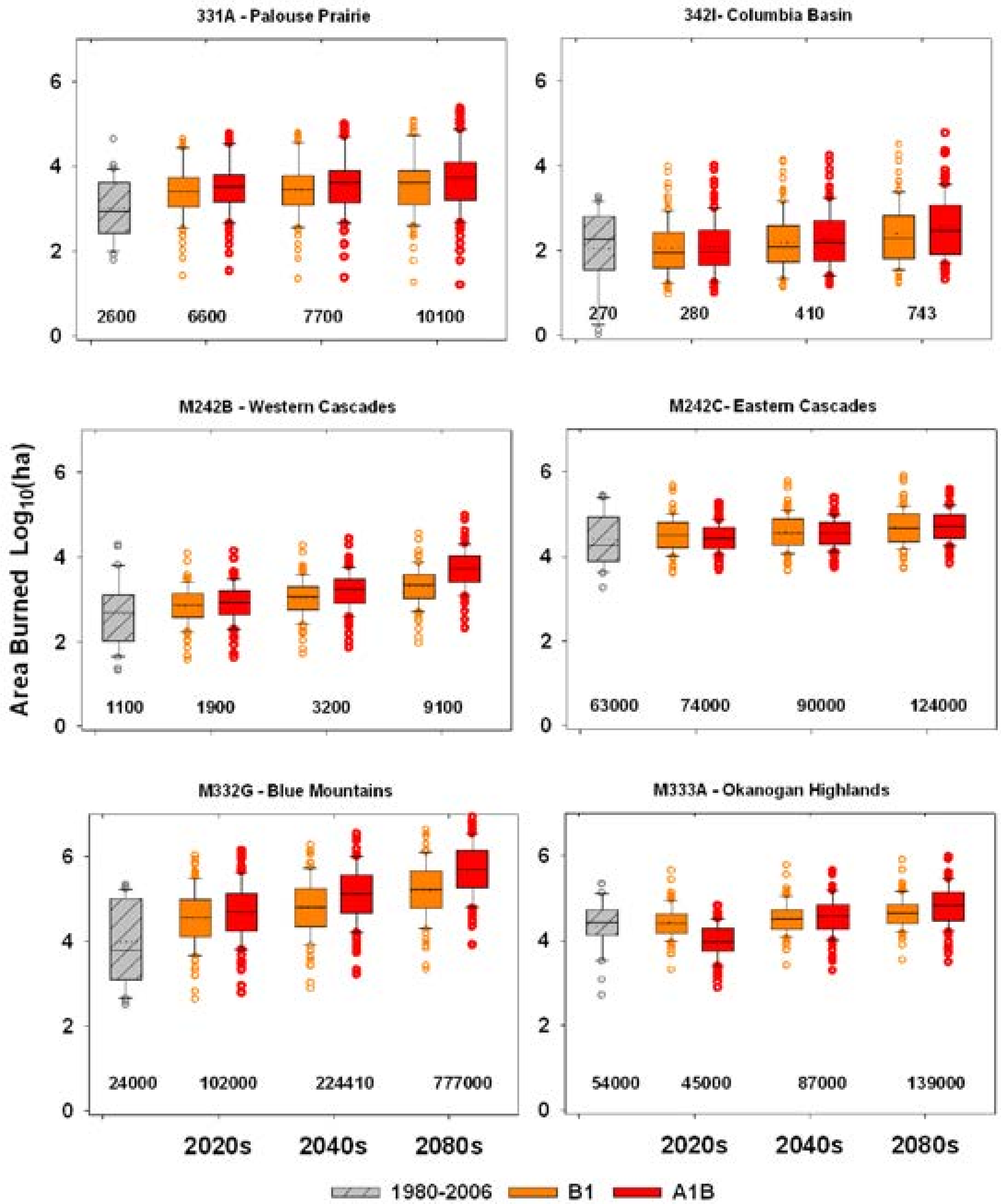

Figure 8. Projections of future area burned in WA ecosections for which statistical fire models could be constructed. All model projections were based on delta-method composite future climate (Mote and Salathé 2009, this report). The text numbers below each set of box-and-whiskers plots indicate the average of A1B and B1 future area burned estimates for the ecosections in acres.

west of the Cascades, the relationship between fire and climate is weaker and statistical models are difficult, if not impossible, to construct due to the low annual area burned. Models including potential evapotranspiration or deficit frequently performed better than those that relied on temperature, precipitation, and their interactions. Projections of future fire in the wetter ecosections generally have greater uncertainty, and other methods with a more mechanistic treatment of fire, weather, and climate will be required to fully understand the future role of fire in these ecosystems.

We were successful in developing statistical models of area burned for 6 of the 8 ecosections in Washington for the period 1980-2006; the Coast Ranges/Olympic Mountains and Puget Trough / Willamette valley sections had low annual area burned and low varaibility and did not yield strong regression models. The other six ecosections yielded regression models that explained between 50 and 65% of the variability in area burned. The most important explanatory variable in five of the eight models was either potential evapotranspiration or water balance deficit (PET-AET), and two models had July-August Tmax terms. Lagged precipitation terms and lagged inverse deficit terms (wetter) were important in the Columbia Basin, Palouse Prairie, and Okanogan Highlands. Future projections from these six models project mean area burned increases of between 0 and 600% depending on the ecosystem in question, the sensitivity of the fire model, emissions scenario and the time frame of the projection (Figure 8). By the 2040s, the area burned in non-forested ecosystems (Columbia Basin and Palouse Prairie) increased on average by a factor of 2.2. In forested ecosystems (Western and Eastern Cascades, Okanogan Highlands, Blue Mountains) the mean area burned increased by a factor of 3.8 compared to 1980-2006. Notably, the increase in area burned is accompanied by an increase in variability in some of the more arid systems – Palouse Prairie and Columbia Basin. The largest proportional increases are in the Western Cascades and Blue Mountains, although the Western Cascades model was the weakest statistically acceptable model, and the area burned is still small despite the large proportional increase. The Blue Mountains model was extremely sensitive, and projected area burned increased at a rate faster than any other ecosection.

Table 2. Expected water deficit and precipitation changes for six future scenarios and historical DAYMET-based calculations

		Scenario climate			% Change from 1980-1999			# Plots with deficit > 250mm
Scenario	Year	Mean water deficit (mm)	Annual PPT (mm)	Summer PPT (mm)	Mean water deficit	Annual PPT	Summer PPT	
A1B	2020	142	1242	34	294%	132%	29%	116
	2040	177	1935	17	367%	206%	15%	228
	2080	209	2831	12	432%	302%	11%	442
B1	2020	93	1604	88	193%	171%	75%	27
	2040	114	1756	70	236%	187%	60%	18
	2080	158	2199	29	326%	235%	25%	116
Historical	2000-03	96	767	60	199%	82%	51%	33
Historical	1980-99	48	937	118	100%	100%	100%	2

3.4. Climate and the Mountain Pine Beetle: Host Vulnerability and Adaptive Seasonality

Our analysis of host vulnerability identified a substantial change in the average water deficit across all sites within the current range of lodgepole pine (Table 2). Even though all future scenario projections indicate an increase in annual precipitation over the pre-2000 period average (Mote and Salathe 2009, this report), the summer water deficit increases two to three times because of reduced summer precipitation and increased temperature. This is consistent with hydrologic assessments suggesting reduced snowpack, reduced summer soil moisture, and increased PET (Elsner et al. 2009, this report). In Washington State, lodgepole pine is rarely found on sites with climatic water deficit > 250 mm (two of 1630 plots). In both the B1 and A1B climate scenarios, the climatic water deficit of plots currently occupied by lodgepole pine increasingly extends beyond the envelope where lodgepole pine currently exists. These projections of deficit suggest that areas with climatic conditions favorable for lodgepole pine will decrease considerably; 27% plots will be subject to more water stress than those under the most stress today.

Table 3. Summary statistics for the predictive model of MPB attacks. Two predictors were not significant at $\alpha = 0.05$, but were part of highly significant interactions.

Predictor	p-value
1) MaxVPD (when exceeds 2 kPa)	0.167
2) Pre-growing season PPT	0.393
3) AvgVPD (Jun, Jul, Aug)	0.031
4) DaysVPD exceeds 1.5 kPa	< 0.001
5) First DayVPD (exceeds 1.5 kPa)	< 0.001
6) Interaction of #1 and #3	0.024
7) Interaction of #4 and #5	< 0.001

These projections of deficit suggest that areas with climatic conditions favorable for lodgepole pine will become increasingly rare because trees will be subject to significantly more water stress with a correspondingly greater VPD. The best statistical model of MPB attack -- a negative-binomial family GLM -- found VPD-based variables and their interactions to be the most significant predictors of the number of attacks over the historical period of record, 2000-2003 (Table 3). Interpretation of the models is not straightforward, however, with five predictors and their interactions.

Plots of fitted values against MaxVPD and AvgVPD (not shown) suggest that the greatest likelihood of attack comes when mean conditions are hot and dry, but not exceptionally so, and there is a fairly short period of extreme VPD during which trees are extremely vulnerable because they are not physiologically adapted to maintain water balance under such conditions

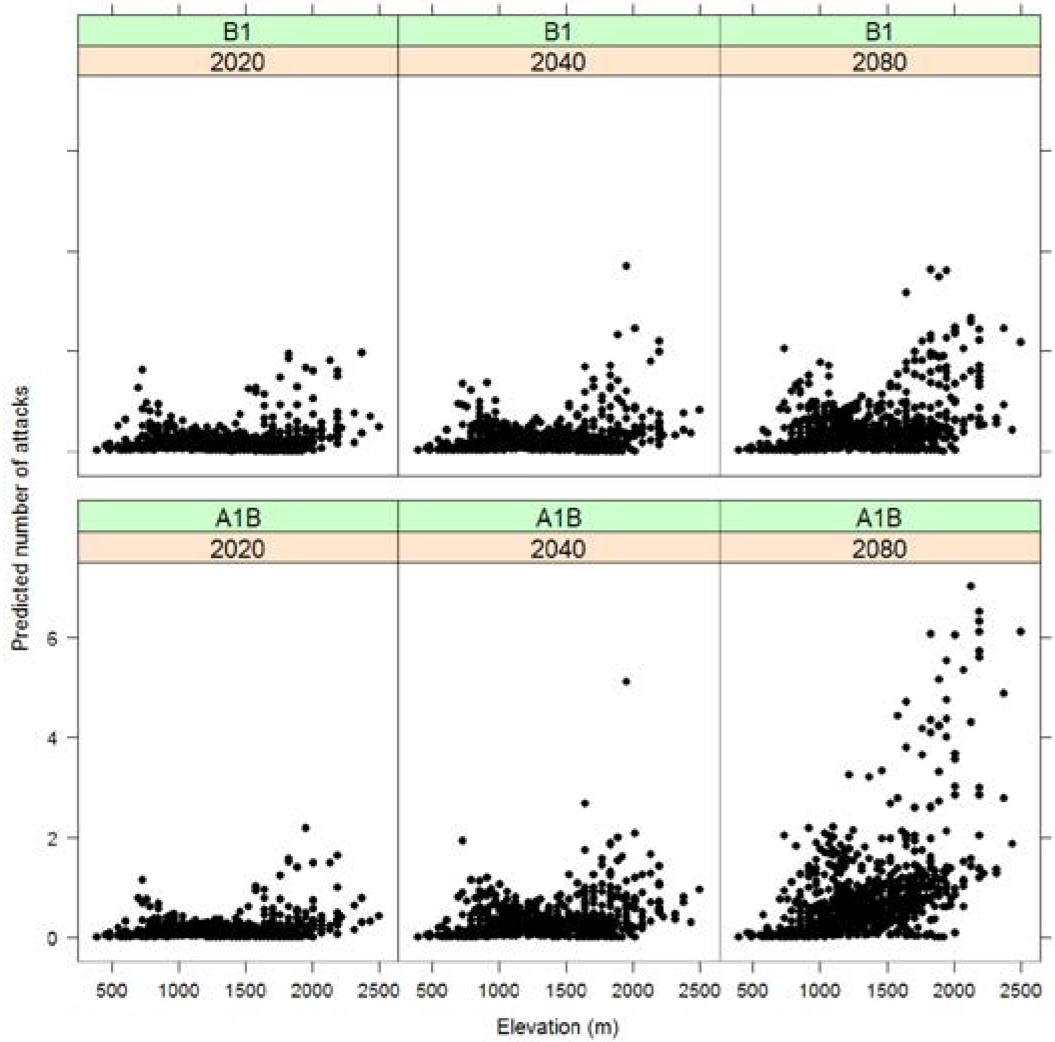

Figure 9. Changes in the number of predicted mountain pine beetle attacks (fitted values), with elevation, time, and emissions scenario. Models were fit for a 6-year period, so the maximum observed value of the response variable was 6. Note that predicted values are not integers because they are fit from a negative-binomial GLM.

(Running and Waring 1998), which is integral not only to survival but also to their capacity to repel beetle attacks (Delucia et al., 2000).

Projecting the model into the future clearly suggests that attacks will be concentrated at increasingly higher elevations (Figure 9) because the climate conducive to outbreaks effectively shifts to higher elevations. In conjunction with expected elevational shifts of host species (lodgepole pine and ponderosa pine), and predictions from the adaptive seasonality model (see below), we expect mountain pine beetle outbreaks to be a continuing concern.

Based on the adaptive seasonality modeling, however, the area suitable for these outbreaks will decrease (Figure 10). Temperatures are currently suitable for MPB outbreaks in large areas of the Olympic Mountains, northern Rocky Mountains, in a band of mid-elevation on the west and east sides of the Cascade Mountains, and to a lesser degree in the Blue Mountains of southeastern Washington. However, simulations using climate change scenarios for 2070-2099 predict that the region of climate suitability will move higher in elevation as the climate warms (Figure 10), thereby reducing the total susceptible area. At lower elevations, increasing temperatures will cause asynchrony in adult emergence through more rapid life stage development as well as cause emergence at inappropriate times

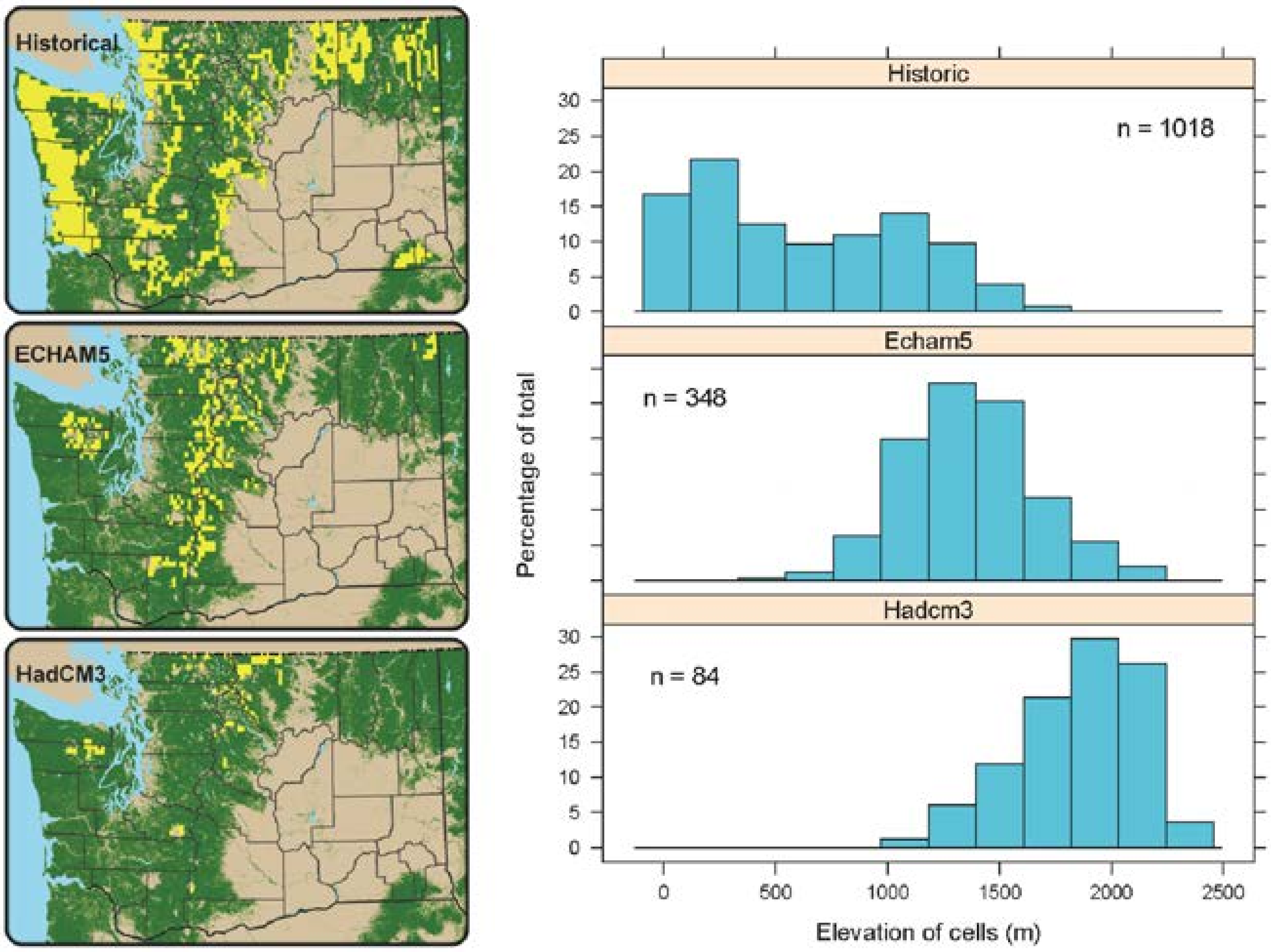

Figure 10. Adaptive seasonality of mountain pine beetle in Washington forests for historical (1970-1999), ECHAM5, and HadCM3 future scenarios for the 2080s (SRES scenario A1B). Yellow cells are suitable space for the beetle. Histograms show the change in elevation distribution across scenarios for suitable cells with n = total cells with suitable climate for the MPB.

of year, reducing populations and decreasing the efficacy of mass attacks (Logan and Bentz, 1999). Higher elevations will warm enough to allow synchronous population emergence during a one-year time frame. For the ECHAM5 climate model (moderate warming), temperature suitability will occur at high elevations in the Olympic and Cascade Mountains. The area of adaptive seasonality is greatly reduced in the Rocky Mountains and is eliminated in the Blue Mountains. For the HADCM3 climate model (greater warming), only a few areas of adaptive seasonality remain, in the highest elevations of the Olympic Mountains and highest and most northern Cascade Mountains. These areas of future adaptive seasonality coincide with the current distribution of whitebark pine, but are mostly above the current elevational range of other susceptible species.

It is important to recognize, however, that these figures are snapshots in time. In fact, outbreaks of mountain pine beetle could occur across the areas “traversed” by the beetle between now and the late 21st century as their climatic suitability moves upward in elevation. The low area of adaptive seasonality presented using the HadCM3 projection for the 2080s therefore belies the much larger area suitable for outbreaks in the interim. Furthermore, the average climate used does not capture interannual variability in future temperatures that may initiate outbreaks of mountain pine beetle earlier in time than suggested by these results.

4. Discussion

4.1. Importance of Disturbance as Principal Player in Forest Change

The direct impacts of climate on tree species (e.g., productivity, distribution) are important, but given the projected increases in fire area and MPB attacks at higher elevations, ecosystem changes caused by disturbance are likely to be greater, notwithstanding that disturbance has a more immediate impact on the ecological integrity of forest ecosystems and associated ecosystem services. It is likely in the future that the rate of forest change (forest type, species composition, productivity) in response to climate change will be driven more by disturbance than by gradual changes in tree populations (driven by impacts on life history characteristics and phenology) and will therefore be more rapid than climate-based analyses of future species range shifts indicate.

The combined projected increases in water limitation, area burned, increase in high elevation area of adaptive seasonality, and increase in host vulnerability suggest that few areas are immune to increasing disturbance. For example, although we were unable to build strong predictive models of future west-side fire, increasing summer Tmax and potential evapotranspiration suggest that large disturbances are likely in west-side forests that have not traditionally been thought of as "fire prone". Elsner et al. (2009, this report) found that west of the Cascade crest, summer soil moisture is likely to decline substantially due particularly to increasing temperature. Some global climate models project decreases in summer precipitation for the region, whereas others project little change – few suggest increased precipitation. This suggests that future climatic conditions will decrease fuel moisture, and it is therfore reasonable to expect increased fire activity. Evidence from stand age classes also indicates that fires much larger than those in the modern record occurred centuries in the past (Agee and Flewelling 1983, Henderson and Peter 1981). The impacts of increasing disturbance, whether east-side or west-side, are worthy of further study.

Some areas may also face novel disturbance interactions. For example, 20th century land management (younger stands and possible loss of genetic diversity) may exacerbate the effects of fire and insect disturbance. The increasing tendency toward water limitation on the edges of the Columbia Basin and the projections for modified climatic ranges for ponderosa pine, Douglas-fir, and lodgepole pine strongly suggest that post-disturbance regeneration will proceed along different successional trajectories and different genotypes or species will be favored.

The increase in area burned is a strong result, but statistical models of area burned have some important limitations. Area burned should not be expected to increase indefinitely – statistically or ecologically. At some point, forests have been disturbed and climate has changed to the point where the disturbance regime does not resemble the modeled relationships any longer. On the other hand, some ecosection models (e.g., Okanogan Highlands, Eastern Cascades) show evidence of hydroclimatic facilitation of fire, probably via increased fine fuels (Littell et al. in press), and future area burned could *decrease* if precipitation increases were insufficient to offset expected potential evapotranspiration or if summer precipitation decreased.

The climate models we used are a hedge against such uncertainties – they are the models best able to reproduce the region's observed climate and the average of many possible future realizations. However, the variablity in future fire regimes has been necessarily underestimated here by using the composite mean and not an ensemble composed of all the available future climate models

Most evidence suggests that mountain pine beetle attacks in the future are likely to be more successful and beetle populations will be moving to higher elevations. An important uncertainty here is the timing of species range changes and the timing of beetle populations range changes – for beetle attacks to achieve epidemic status, a sufficient population of well established mature trees must be present to sustain the insects. If the impacts of fire and species turnover proceed quickly, spatial heterogeneity of age classes on the landscape may reduce beetle impacts significantly.

The strength of the relationships between climate and fire and climate and mountain pine beetles supports a hypothesis of climate-driven disturbance as the primary mechanism of change in the future forests of Washington. We were not able to assess the interaction between fire and mountain pine beetles quantitatively, but it is likely, for example, that MPB outbreaks will affect fuel structure and availability to fire (Lynch et al. 2006). A process model that considers this interaction and any potential synergies for impacts to forest ecosystems would be useful to project future conditions. Such a model should consider the relative importance of the two disturbances in future synergistic interactions, which depends on the presence of suitable host species and the fire regimes expected in those forest types. For example, high elevation whitebark pine ecosystems may have severe MPB mortality in the future without greatly influencing the area burned by fire because fuel availiability would not necessarily change dramatically in such low-density forests. On the other hand, nearly pure lodgepole pine forests, which are already strongly fire dependent, will potentially have altered fuel characteristics conducive to relatively rapid rates of fire spread, thus increasing the potential size of fires. We also did not study disturbance effects on forest management goals, such as wildlife habitat, timber products, or other ecosystem services, but because the area susceptible to disturbance impacts will be large, and strategies to mitigate the potential resource risks will need to carefully consider potential novel effects of altered disturbance regimes.

4.2. Broad Characteristics of Future Forests in Washington

Increasing water limitation appears likely across a significant portion of the northern Columbia Basin and eastern Cascades, if other factors (e.g., CO_2 driven increases in water use efficiency) do not offset the climatically driven changes. Our definition of water limitation is conservative, and emphasizes the most severe limitation; much of the forested area we defined as energy limited in Washington is water limited for some portion of the year, but that limitation is not as severe as the areas highlighted in Figure 4. For those areas where annual precipitation is less than annual potential evapotranspiration (a less conservative definition of water limitation) there may still be important limitations on productivity and regeneration.

A caveat to the projections of future species-appropriate climate envelopes is that they fail to consider ecological factors that can exacerbate or mitigate the projected changes. For example, such models assume the climatic ranges they describe are equally applicable across all parts of a species' lifecycle, but the models are constructed on the presence or absence of established trees of many ages – not on seedlings, which are likely most susceptible to climate variability. We also do not consider the impacts of local soil limitations, nutrient limitations, changes in nitrogen deposition, all of which could affect productivity and species distribution locally in the future.

Many of Washington's future forests may look much like the forests that are currently present, but the most vulnerable forests may look radically different due to increased frequency and severity of disturbances. Eventually, species and stand densities that are resistant to increased summer water deficit and increased disturbance will be favored, and landscape structure and pattern will change. Particularly in places where vegetation types shift from forest to woodland or from tundra to forest, fire regimes will be influenced by the shift in vegetation; dynamic vegetation models that address the feedbacks between vegetation, climate, fire, and biogeochemistry are required to understand such processes. In the near term, however, such uncertainties are less important than the considerable impacts on Washington's current forest ecosystems.

All of the impacts assessed in this study are likely to occur by the 2040s at the northern edge of the Columbia Basin in the Okanogan highlands and in the northeastern North Cascades. The impacts of climate on fire regimes, insect attacks, tree water stress and both Douglas-fir and pine species' ranges will likely interact strongly in the north eastern Cascades, Okanogan Highlands, and Blue Mountains earlier rather than later in the 21st century. Although less area burned is projected in the western Cascades and the Olympics and there is less area dominated by pines susceptible to MPB, it would be a mistake to conclude that impacts and their interactions will not be important in those ecosystems. For example, Douglas-fir will be outside of its optimal climate range over considerable areas, and there are almost certainly thresholds of water deficit past which large areas of west side forests would be at risk for large fires. Such fires do not occur in the 20th century historical record, so statistical fire models are incapable of projecting them. However, even though we are unable to model large west-side fires, hotter and drier summers unequivocally increase the chance that such fires will occur.

4.3. Adaptation Options

Adaptation options depend greatly on the scale in question (Table 4, Millar et al., 2007; Joyce et al., 2008). Regional adaptation is necessarily an exercise in forest policy and planning as much as it is engaging in land-management actions; it must be sufficiently flexible to facilitate adaptation locally but also capable of organizing regional responses. Local adaptation must be tailored to local conditions to succeed (all adaptation is necessarily local), but decisions that determine local action may be made at the state or federal level, requiring a regional or national viewpoint. Furthermore, given climate change and globalization, adaptation proceeds in a context defined as much by regional and global pressures as by local conditions

Table 4. Examples of adaptation options (after Millar et al. 2007)

Adaptation strategy	Regional actions (policy)	Local actions (management)
Resist change	Minimize impacts of disturbance, suppress fire in systems where fire is rare, but maintain Wildland Fire Use (WFU)	Suppress wildfire in wildland-urban interface;
Promote resilience to change	Thin stands from below (to increase fire resilience); create uneven-aged structures or reduce density (to increase insect resilience)	Use large disturbances as opportunities to establish new genotypes, and forest heterogeneity and diversity
Allow forest ecosystems to respond to change	Plant new species expected to respond favorably to warmer climate	Use new genotypes, or even species, in forestry plantations

– no successful strategy can be crafted without awareness of these outside pressures.

Regional adaptation consists of strategies likely to promote conditions that increase the likelihood of a specific objective. Thinking about adaptation for forests is in many ways in its infancy, but examples might include stronger emphases on: reducing anthropogenic stresses on forest ecosystems, promoting resilience to likely impacts, landscape and biological diversity, planning for projected future conditions, and assessing the decision context in terms of barriers and opportunities that limit or facilitate local adaptation (Millar et al., 2007; Joyce et al., 2008).

Local adaptation consists of application of tools (existing or new) to affect conditions. First one must identify management objectives, assess capacity to alter conditions for the objectives, and then develop appropriate tools. For example, targeted thinning in drier forests in which fire suppression has led to fuel accumulations capable of sustaining a high severity fire (novel in those ecosystems) may increase the resilience of that forest to a fire. In wetter forests where 20th century harvest practices have decreased age class diversity and altered patch structure, targeted thinning and cutting could simultaneously create appropriate fuel breaks and increase canopy and age-class diversity. In water-limited forests, it is possible that tailoring stand density to the expected water conditions of the future will increase resilience to insect attack and climate change in general by increasing stand water supply to counteract the projected increased atmospheric demand. Clearly, some general guidelines exist.

The management implications of climate impacts to forests and the resulting need for planning for and adapting to those impacts in the state of Washington are manifold. Obvious implications are that "forest types", "communities", disturbance return intervals, and historic ranges of variability are all concepts that attempt to define the state of a forest, but that state is inherently dynamic and thus defies easy categorization – climate change will only increase the necessity of recognizing such dynamism in ecosystems. Reference conditions and historic ranges of variability are also concepts that will need to be re-evaluated as management tools because the trajectories of forest ecosystems will be away from conditions we are familiar with and future disturbance regimes will likely exceed the range of historic variability. All this does not mean that there is no utility in planning – quite the opposite. It means planning for expected conditions and what they mean for resource management – it may well mean changing the mandates and goals of land management agencies to reflect new conditions and priorities. It may also mean planning for unexpected conditions, and experimenting with novel ideas (or reviving old ideas) particularly when there is too much uncertainty in projections. It quite likely also means using available tools now (silviculture, cross-agency collaboration) while considering the barriers to using other tools (e.g., prescribed fire). In order to accomplish this, however, a concerted effort to increase communication between scientists, managers, and policy makers is required – the rates of change expected and the nature of the impacts will require broad collaboration.

5. Research Needs

5.1. Finer-Scale Climatic Projections in Mountain and Forest Ecosystems

Climate in the complex terrain associated with forest ecosystems is poorly understood. Much more needs to be known about how to downscale regional climate to local conditions and whether such downscaling will decrease the uncertainty forest managers face. In particular, will there be substantial differences in the way climate will change in different geographic areas (e.g., for maritime vs. continental) or different elevational zones. Current data resources and future scenarios are generally inadequate to assess impacts at scales useful for managers.

5.2. Understand the Geographic Distribution of Genetic Variability and Climatic Tolerances for Tree Species

Planning for future resilience and responses to disturbance require well developed knowledge of genotypic variability and sub-species climatic tolerances so that seed stock well adapted to likely future conditions can be selected. The geographic variability of sub-species genotypes and how those genotypes perform in different climatic conditions is poorly documented for most species. Some climatic changes could have substantial differences in their impacts on different species within the same stand due to differences in physiology, life history, morphology, etc., and the implications of these need to be better understood in the context of energy and water limitation.

5.3. Understand the Role of Climate in Tree Establishment Generally, but Particularly Post-Fire and at Lower Treeline, to Prioritize Post-Disturbance Treatments and Planting Efforts

The success of tree establishment after disturbance likely varies with climate, but the degree to which climate limits establishment is not well known. Most of the bioclimatic approaches to future vegetation response to climate change do not account for this potential sensitivity in early life-history stages and instead focus on climate relationships for established trees. Because establishment is more sensitive than persistence of established trees, it is likely that important tree species will fail to establish after disturbance when the climate has shifted sufficiently.

5.4. Move from Fire Area Burned to Landscape Fire Effects and Fire Severity

The area burned by fire is not the best metric of ecological impact – the role of future fire in forested landscapes depends as much or more on fire effects and fire severity as on the area burned. Physically based models at finer spatial scales are needed to address impacts of changing fire regimes on vegetation and watershed hydrology. Fire also has important implications for short-term hydrologic response after disturbance, which may include important feedbacks to biological effects in forest and aquatic systems.

5.5. Understand How Other Insects (e.g., Spruce and Fir Beetles) and Pathogens Respond to Climatic Change.

The mountain pine beetle is not the only insect species that may have greater impacts in a warming climate, and the role of climate in other insects' life cycles and host vulnerabilities must be better understood if we are to anticipate future impacts.

5.6. More Research on the Impacts and Benefits of Silvicultural Treatments on Fire Behavior and Stand Vigor is Needed

Forest managers need tools for climate change adaptation, and a tool that is available now is silviculture. Appropriate silvicultural prescriptions require knowledge of expected local impacts and stand and tree physiological thresholds that may not have historical analogues. The potential impacts identified in this paper point to two silvicultural research needs. First we must better understand the physiological response of mature trees to changing climate conditions to determine if silvicultural treatments could stem those impacts. Second we need to understand how different silvicultural treatments can be used in anticipation of different projected climatic changes. The impacts and benefits of silvicultural treatments on forest ecosystems processes such as fire severity are generally poorly quantified.

6. Conclusions

- Spatial patterns of productivity will change -- state-wide productivity may initially increase due to warmer temepratures but will then decrease due to increased drought stress. Douglas-fir productivity appears to vary with climate across the region and will potentially increase in energy-limited forests in the near term. Climatic variability will continue to mediate productivity.
- Species composition will be affected by climate, and the consequences for lower elevation forests and for species susceptible to mountain pine beetle are potentially substantial. Climate will be

inconsistent with the establishment of Douglas-fir, ponderosa pine, and lodgepole pine in many areas by the middle of the 21st century. Forest species composition will likely change chiefly in the wake of large disturbances and may be affected by climatic limitation of regenerating trees.

- Regional fire area burned may increase two- or three-fold. Fire regimes in different ecosystems in the PNW have different sensitivities to climate. Year-to-year variation will continue and potentially increase, and will also be a challenge for planning.

Due to climatic stress on host trees, mountain pine beetle outbreaks may increase in frequency and levels of tree mortality. Mountain pine beetles will reach higher elevations due to a shift in favorable temperature conditions in these areas as the region warms. Conversely, this species may become less of a threat at middle and lower elevations as the region warms, due to less favorable temperature conditions. Other insect species may emerge in areas that are no longer suitable for the mountain pine beetle.

Acknowledgments

Alan Hamlet, Richard Gwozdz, and Ingrid Tohver provided detailed comments on an earlier draft of the manuscript. We thank three anonymous reviewers for helpful suggestions.We would also like to thank G. Rehfeldt and N. Crookton for making their output for future species ranges publicly available.

References

Agee, JK, Flewelling R (1983) A fire cycle model based on climate for the Olympic Mountains, Washington. Proc Fire For Met Conf 7:32-37.

Akaike, H (1974) A new look at the statistical model identification. IEEE Trans Auto Control 19(6): 716–723.

Allen, CD, Breshears DD (1998) Drought-induced shift of a forest–woodland ecotone: Rapid landscape response to climate variation. Proc Natl Acad Sci USA 95:14839–14842.

Bailey RG (1995) Description of the ecoregions of the United States. USDA For Service Miscs Public 1391 (revis) Washington, DC.

Bentz BJ, Logan JA, Amman GD (1991) Temperature-dependent development of mountain pine beetle and simulation of its phenology. Can Entomol 123:1083-1094.

Boisvenue C, Running SW (2006) Impacts of climate change on natural forest productivity — evidence since the middle of the 20th century. Global Biogeochem Cycles 12:862–882.

Breshears DD, Cobb NS, Rich PM, Price KP, Allen CD, Balice RG, Romme WH, Kastens JH, Floyd ML, Belnap J, Anderson JJ, Myers OB, Meyer CW (2005) Regional vegetation die-off in response to global-change type drought. Proc Nat Acad Sci, USA 102:15144-15148.

Carroll AL, Taylor SW, Regniere J, Safranyik L (2004) Effects of climate change on range expansion by the mountain pine beetle in British Columbia. In: Mountain Pine Beetle Symposium: Challenges and Solutions. Nat Resour Can, Can For Serv, Pacific For Cent, Kelowna, BC, pp 223-232.

Case MJ, Peterson DL (2007) Growth-climate relations of lodgepole pine in the North Cascades National Park, Washington. Northwest Sci 81(1):62-75.

Cayan DR (1996) Interannual climate variability and snow pack in the western United States. J Climate 9(5):928-948.

Daly C, Halbleib M, Smith JI, Gibson WP, Doggett MK, Taylor GH, Curtis J, Pasteris PA (2008) Physiographically sensitive mapping of temperature and precipitation across the conterminous United States. Int J Climatol DOI: 10.1002/joc.1688.

Davis MB (1986) Climatic instability, time lags, and community disequilibrium. In: Diamond J, Case TJ, eds. Community Ecology. P. 269-284. Harper and Row. New York.

Davis MB, Botkin DB (1985) Sensitivity of cool-temperate forests and their fossil pollen record to rapid temperature change. Quaternary Res 23:327-340.

DeLucia EH, Maherali H, Carey EV (2000) Climate-driven changes in biomass allocation in pines. Global Change Biol 6(5):587-593.

Cushman SA, McKenzie D, Peterson DL, Littell JS, McKelvey KS (2007) Research agenda for integrated landscape modeling. USDA For Serv Gen Tech Rep RMRS-GTR-194. Rocky Mt Res Stn, Fort Collins, CO.

Elsner MM, Cuo L, Voisin N, Hamlet AF, Deems JS, Lettenmaier DP, Mickelson KEB, Lee SY (2009) Implications of climate change for the hydrology of Washintgon State. Washington Climate Change Impacts Assessment: Evaluating Washington's future in a changing climate. In press.

Franklin JF, Dyrness CT (1988) Natural vegetation of Oregon and Washington. Oregon State Univerity Press, Corvallis, OR.

Gedalof Z, Peterson DL, Mantua NJ (2005) Atmospheric, climatic, and ecological controls on extreme wildfire years in the Northwestern United States. Ecol Appl 15:154-174.

Gillett NP, Weaver AJ, Zwiers FW, Flannigan MD (2004) Detecting the effect of climate change on Canadian forest fires. Geophys Res Lett 31, L18211, doi:10.1029/2004GL020876.

Guisan A, Zimmermann NE (2000) Predictive habitat distribution models in ecology. Ecol Modell 135:147-186.

Henderson JA, Peter DH (1981) Preliminary plant associations and habitat types of the Shelton Ranger District, Olympic National Forest. USDA For Serv, Pacific Northwest Reg, Portland, OR 53 p.

Henderson JA, Peter DH, Lesher RD, Shaw DC (1989) Forested plant associations of the Olympic National Forest. USDA For Service, Pacific Northwest Res Stn R6-ECOL-TP-001-88, Portland, OR 502 p.

Henderson JA, Lesher RD, Peter DH, Shaw DC (1992) Field guide to the forested plant associations of the Mt. Baker-Snoqualmie National Forest. USDA For Service, Pacific Northwest Res Stn R6-ECOL-TP-028-91, Portland, OR.

Hessl AE, McKenzie D, Schellhaas R (2004) Drought and Pacific Decadal Oscillation affect fire occurrence in the inland Pacific Northwest. Ecol Appl 14:425-442.

Hicke, JA, Jenkins JC (2008) Mapping lodgepole pine stand structure susceptibility to mountain pine beetle attack across the western United States. For Ecol Manage 255:1536-1547.

Hicke JA, Logan JA, Powell J, Ojima DS (2006) Changing temperatures influence suitability for modeled mountain pine beetle (Dendroctonus ponderosae) outbreaks in the western United States, J Geophys Res B, 111, G02019, doi: 10.1029/2005JG000101.

IPCC (Intergovernmental Panel on Climate Change) (2007) Climate Change 2007: the Physical Science Basis. Summary for policymakers. http://www.ipcc.ch

IPCC (Intergovernmental Panel on Climate Change) (2007) Working Group II Report "Impacts, Adaptation and Vulnerability". http://www.ipcc.ch/ipccreports/ar4-wg2.htm

Jenkins MJ, Hebertson E, Page W, Jorgensen CA (2008) Bark beetles, fuels, fires and implications for forest management in the Intermountain West. For Ecol Manage 254(1):16.

Joyce LA, Blate GM, Littell JS, McNulty SG, Millar CI, Moser SC, Neilson RP (2008) National forests. Chapter 3 In: S.H. Julius, J.M. West (eds.), J.S. Baron, B.Griffith, L.A. Joyce, P. Kareiva, B.D. Keller, M.A. Palmer, C.H. Peterson, and J.M. Scott (authors), Preliminary Review of Adaptation Options for Climate-Sensitive Ecosystems and Resources. A report by the U.S. Climate Change Science Program and the Subcommittee on Global Change Research. U.S. Environmental Protection Agency, Washington, DC, USA, pp. 3-1 to 3-127.

Kimball JS, Running SW, Nemani R (1997) An improved method for estimating surface humidity from daily minimum temperature. Agric For Meteorol 85:87-98.

Knowles N, Dettinger MD, Cayan DR. 2006. Trends in snowfall versus rainfall in the western United States. J Climate 19:4545-4559.

Lenihan JM, Bachelet D, Neilson RP, Drapek RJ (2008) Simulated response of conterminous united states ecosystems to climate change at different levels of fire suppression, CO2 emission rate, and growth response to CO2. Global Planetary Change 64:16-25.

Lillybridge TR, Kovalchik BL, Williams CK, Smith BG (1995) Field guide to forested plant associations of the Wenatchee National Forest. USDA For Serv Gen Tech Rep PNW-GTR-359. Pacific Northwest Res Stn, Portland, OR, USA, 336 p.

Littell JS (2006) Climate Impacts to Forest Ecosystem Processes: Douglas-fir Growth in Northwestern U.S. Mountain Landscapes and Area Burned by Wildfire in Western U.S. Ecoprovinces. Ph.D. dissertation. University of Washington, Coll For Resources, Seattle, Washington, USA. 160 p.

Littell JS, Peterson DL (2005) A method for estimating vulnerability of Douglas-fir growth to climate change in the Northwestern US. Forestry Chron 81:369-374.

Littell JS, Peterson DL, Tjoelker M (2008) Douglas-fir growth-climate relationships along biophysical gradients in mountain protected areas of the northwestern U.S. Ecol Monogr 78(3): 349–368.

Littell JS, McKenzie D, Peterson DL, Westerling AL (2009) Climate and wildfire area burned in western U.S. ecoprovinces, 1916-2003. Ecol Appl (in press).

Logan JA, Bentz BJ (1999) Model analysis of mountain pine beetle (Coleoptera: Scolytidae) seasonality. Env Entomol 28:924-934.

Logan JA, Amman GD (1986) A distribution model for egg development in mountain pine beetle. Can Entomol 118:361-372.

Logan JA, Bolstad PV, Bentz BJ, Perkins DL (1995) Assessing the effects of changing climate on mountain pine beetle dynamics. In: Workshop on Interior West Global Climate. USDA For Serv, Fort Collins, CO pp 92-105.

Logan JA, Powell JA (2001) Ghost forests, global warming and the mountain pine beetle (Coleoptera: Scolytidae). Am Entomol 47:160-173.

Logan JA, Powell JA (2004) Modeling mountain pine beetle phenological response to temperature. In: Mountain Pine Beetle Symposium: Challenges and Solutions. Nat Res Can, Can For Service, Pacific For Cent, Kelowna, BC pp. 210-222

Lloyd AH, Graumlich LJ (1997) A 3,500 year record of changes in the structure and distribution of forests at treeline in the Sierra Nevada, California, U.S.A. Ecology 78:1199-1210.

Lutz JA (2008) Climate, fire, and vegetation change in Yosemite National Park. Ph.D. dissertation. University of Washington, Coll For Resources Seattle, Washington, USA. 169 p.

Lutz JA and Halpern CB (2006) Tree mortality during early forest development: a long-term study of rates, causes, and consequences. Ecol Monogr 76:257-275.

Lynch HJ, Renkin RA, Crabtree RL, Moorcroft PR (2006) The influence of previous mountain pine beetle (Dendroctonus ponderosae) activity on the 1988 Yellowstone fires. Ecosystems 9:1318–1327.

McKenzie D, Gedalof Z, Peterson DL, Mote PW (2004) Climatic change, wildfire, and conservation. Conserv Biol 18:890-902.

McKenzie D, Hessl AE, Peterson DL (2001) Recent growth in conifer species of western North America: assessing the spatial patterns of radial growth trends. Can J For Res 31:526-538.

McKenzie D, Peterson DL, Littell JS (2008) Global warming and stress complexes in forests of western North America. In S. V. Krupa (ed.), Developments in Environmental Science, Vol. 8, Wild Land Fires and Air Pollution, A. Bytnerowicz, M. Arbaugh, A. Riebau, and C. Anderson (eds.). Amsterdam, The Netherlands: Elsevier Science, Ltd. pp. 319-337.

McKenzie D, Peterson DW, Peterson DL, Thornton PE (2003) Climatic and biophysical controls on conifer species distributions in mountain forests of Washington state, USA. J Biogeogr 30:1093-1108.

Millar CI, Stephenson NL, Stephens SL (2007) Climate change and forests of the future: managing in the face of uncertainty. Ecol Appl 17:2145-2151.

Milne BT, Gupta VK, Restrepo C (2002) A scale-invariant coupling of plants, water, energy, and terrain. EcoScience 9:191–199.

Mote PW, Hamlet AF, Clark MP, and Lettenmaier DP. 2005. Declining mountain snowpack in western North America. Bull Am Meteorol Soc 86:39-49.

Mote PW, Salathé Jr EP (2009) Future climate in the Pacific Northwest. Washington Climate Change Impacts Assessment: Evaluating Washington's future in a changing climate. In press.

Nakawatase JM, Peterson DL (2006) Spatial variability in forest growth-climate relationships in the Olympic Mountains, Washington. Can J For Res 36: 77-91.

Neilson RP, Pitelka LF, Solomon AM, Nathan R, Midgley GF, Fragoso JMV, Lischke H, Thompson K (2005) Forecasting regional to global plant migration in response to climate change. BioScience 55:749-759.

Oneil EE (2006) Developing stand density thresholds to address mountain pine beetle susceptibility in eastern Washington forests. PhD Dissertation, University of Washington, Seattle, 99pp.

Overpeck JT, Rind D, Goldberg R (1990) Climate-induced changes in forest disturbance and vegetation. Nature 343:51-53.

Peterson DW, Peterson DL (2001) Mountain hemlock growth responds to climatic variability at annual and decadal scales. Ecology 82:3330-3345.

Powell JA, Logan JA (2005) Insect seasonality: circle map analysis of temperature-driven life cycles. Theor Pop Biol 67:161-179.

Rehfeldt GE, Crookston NL, Warwell MV, Evans JS (2006) Empirical analysis of plant-climate relationships for the western United States. Int J Plant Sci 167(6):1123–1150.

Running SW, Nemani RR, Heinsch FA, Zhao M, Reeves M, Hashimoto H (2004) A continuous satellite-derived measure of global terrestrial primary production. BioScience 54(6):547—560.

Running SW, Nemani RR, et al (1987) Extrapolation of synoptic meteorological data in mountainous terrain and its use for simulating forest evapotranspiration and photosynthesis." Can J For Res 17(6): 472-483.

Salathé Jr EP, Mote PW, Wiley MW (2007) Review of scenario selection and downscaling methods for the assessment of climate change impacts on hydrology in the United States Pacific Northwest. Int J Climatol 27:1611-1621.

Stephenson NL (1990) Climatic control of vegetation distribution: the role of the water balance. Am Nat 135:649-670.

Stephenson NL (1998) Actual evapotranspiration and deficit: biologically meaningful correlates of vegetation distribution across spatial scales. J Biogeogr 25, 855-870.

Thornton PE, Hasenauer H, White MA (2000) Simultaneous estimation of daily solar radiation and humidity from observed temperature and precipitation: an application over complex terrain in Austria. Agric For Meteorol 104:255-271.

Thornton PE, Running SW (1999). An improved algorithm for estimating incident daily solar radiation from measurements of temperature, humidity, and precipitation. Agric For Meteorol 93(4): 211-228

Thornton PE, Running SW, et al (1997). Generating surfaces of daily meteorological variables over large regions of complex terrain. J Hydrol 190(3-4): 214-251.

van Mantgem PJ, Stephenson NL (2007) Apparent climatically induced increase of tree mortality rates in a temperate forest. Ecol Lett 10:909-916.

van Mantgem PJ, Stephenson NL, Byrne JC, Daniels LD, Franklin JF, Fulé PZ, Harmon ME, Larson AJ, Smith JM, Taylor AH, Veblen TT (2009) Widespread increase of tree mortality rates in the western United States. Science Vol. 323: 521 – 524 DOI: 10.1126/science.1165000

Venables WN, Ripley BD (2002) Modern Applied Statistics with S. 4th edition. Springer, New York. 495 pp.

Waring RH, Running SW (1998) Forest Ecosystems: Analysis at Multiple Scales. Academic Press, New York. 370 pp.

Wellner CA (1978) Management Problems Resulting from Mountain Pine Beetles in Lodgepole Pine Forests, pp 9-15 in Theory and Practice of Mountain Pine Beetle Management in Lodgepole Pine Forests, Pullman, WA, For, Wildlife and Range Exp Stn, University of Idaho.

Williams CK, Lillybridge TR (1983) Forested plant associations of the Okanogan National Forest. USDA Forest Serv Tech Pap R6-ECOL-132b-1983. Pacific Northwest Res Stn, Portland, OR, USA, p. 140.

Williams CK, Lillybridge TR, Smith BG (1990) Forested plant associations of the Colville National Forest, field guide. USDA Forest Service, Pacific Northwest Res Stn, Portland, OR, USA, p. 133.

Photo credit, page 263: Climate Impacts Group, University of Washington

8: Coasts

Impacts of Climate Change on the Coasts of Washington State

Daniel D. Huppert[1], Amber Moore[1], Karen Dyson[1]

Abstract

Climate change on the Washington coast will trigger significant physical and chemical stressors: (a) inundation of low-lying areas by high tides as sea level rises; (b) flooding of coasts during major storm events, especially near river mouths; (c) accelerated erosion of coastal bluffs; (d) shifting of beach profiles, moving the position of the Mean High Water line landward; (e) saltwater intrusion into coastal freshwater aquifers; and (f) increased ocean temperature and acidity. Similar forces will be working everywhere, but shore areas will respond differently depending upon substrate (sand versus bedrock), slope (shallow versus steep cliffs), and the surrounding conditions (exposed versus sheltered from storms). We expect substantial impacts on coastal systems from bluff erosion, shifting beach berms, shoreline armoring, and inundation of coastal lands. Further, increased ocean temperatures and acidity will negatively impact shellfish aquaculture. As beaches adjust to sea level rise, coastal property lines and intertidal aquaculture leases will need to be carefully defined through modified property laws. We anticipate relatively minor impacts on coastal freshwater aquifers. Additional research is needed to develop a more comprehensive assessment of climate impacts on all coastal features in the state.

[1] School of Marine Affairs College of Ocean and Fishery Sciences, University of Washington, Seattle, Washington

1. Introduction

Washington State has more than 5000 km (3085 miles) of coastline (Table 1) with very diverse characteristics. The coastline can be divided into five regions: (1) the Pacific coast south of Point Grenville, (2) the Pacific coast north of Point Grenville, (3) the coast along the north shore of the Olympic peninsula and east through the Strait of Juan de Fuca, (4) the Puget Sound region, including Hood Canal, and (5) the San Juan Islands and the US portion of the Strait of Georgia (Figure 1). Sandy beaches with shallow slopes and high-energy waves are characteristic of the ocean shore in southwestern Washington, while Willapa Bay and Grays Harbor are shallow, protected bays with extensive mudflats. The coast north of Point Grenville and along north Olympic Peninsula coast has a mixture of steep rocky shores, estuaries, and sandy beaches and spits subject to high wind and waves. According to Johannessen and MacLennan, "the most prevalent shore type in Puget Sound is the bluff-backed beach – coastal bluffs fronted by narrow mixed sand and gravel beaches" (2007, p. v). Much of the San Juan Islands coast is hard, stable bedrock.

Table 1. Shoreline length for each segment of the Washington coast (adapted from Bailey et al., 1998 and ArcGIS measurements)

Coastal Segment	Shoreline Length
Puget Sound (including Hood Canal)	2411.6 km (1477.1 mi)
San Juan Islands and Georgia Strait	1302.9 km (807.8 mi)
North Olympic Peninsula Coast	325.4 km (202.4 mi)
Cape Flattery to the Point Grenville	267.1 km (166.0 mi)
Point Grenville to the Columbia R. -- "Southwest Coast"	695.3 km (432.0 mi)
Total	5002.3 km (3085.3 mi)

Long-term climate change is expected to result in sea level rise (SLR), and increased ocean temperature and acidity (Intergovernmental Panel on Climate Change 2007). Further, on the Pacific coast of Washington there is evidence that shifting storm tracks and increased wave heights have begun eroding beaches south of Point Grenville (Graham and Diaz 2001, and Allan and Komar 2006). While the same basic climate forces will be changing everywhere, each region, and related human activities, will respond to climate change in specific ways depending upon substrate (sand versus bedrock), slope (shallow versus steep cliffs), and the surrounding conditions (exposed shores versus sheltered bays and sounds).

The physical and chemical effects of climate change will manifest themselves in five primary ways:

Inundation. As the sea level rises (Mote, et al. 2008), the lowest lying shores will be regularly flooded by high tides. Coastal inundation is a gradual process on decadal time scales due to expanding volume of ocean water (called *eustatic* SLR), melting of glaciers, and local factors such as land subsidence and tectonic uplift (Snover et al., 2007).

Flooding. During major storm events, SLR will compound the effects of storm surges, which can contribute to more extensive coastal flooding. Also, changes in the seasonal pattern of rainfall or increased peak run-off from snow melting could lead to more serious coastal flood events, especially near rivers.

Erosion and Landslides. Although erosion on beaches and bluffs is a natural, on-going process, major episodes of erosion often occur during storm events, particularly when storms coincide with high tides. SLR will exacerbate the conditions that contribute to episodic erosion events, and this will accelerate bluff and beach erosion. Increased storm strength or frequency will exacerbate this. Climate change is also likely to increase

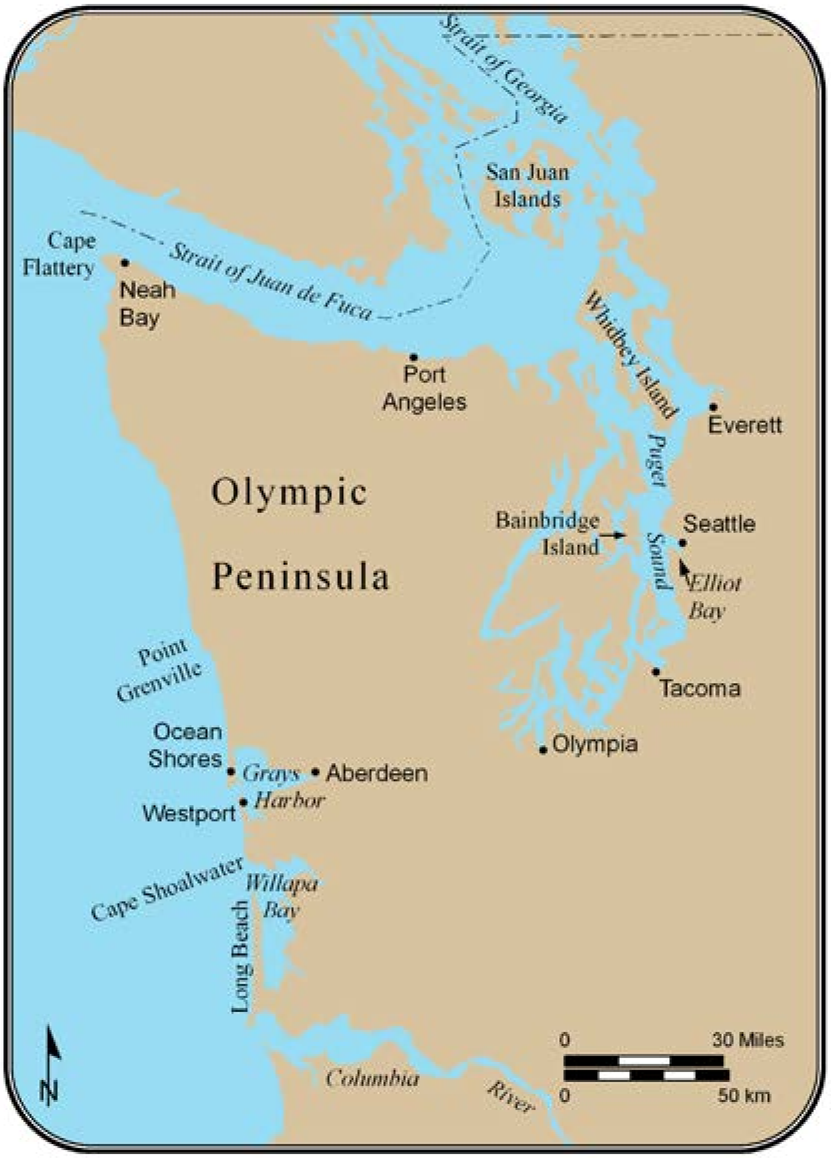

Figure 1. Washington coastal region

winter precipitation in the Pacific Northwest, which can contribute to landslides on bluffs saturated by rainfall or run-off.

Saltwater Intrusion. As the sea level rises, coastal freshwater aquifers will be subject to increased intrusion by salt water.

Increased Ocean Surface Temperature and Acidity. As the atmosphere warms, the ocean temperatures will increase. Additionally, absorption of carbon dioxide by the oceans leads to increasing acidity (lower pH).

Because Washington's coasts are heavily utilized for ports, home sites, public recreation, and shellfish aquaculture, these physical and chemical effects of climate change will pose significant challenges. To highlight expected climate change impacts, this chapter will focus on select locations in Puget Sound, Willapa Bay on the southwest Washington coast, and the San Juan Islands. Some general predictions are made about climate impacts in these study areas, and adaptation options and research gaps are discussed.

Table 2. Relative sea level rise projections for major geograpic areas of Washington State (adapted from Mote et al 2008)

SLR Estimate	By the year 2050			By the year 2100		
	NW Olympic Peninsula	Central & Southern Coast	Puget Sound	NW Olympic Peninsula	Central & Southern Coast	Puget Sound
Very Low	-5" (-12 cm)	1" (3cm)	3" (8cm)	-9" (-24cm)	2" (6 cm)	6" (16cm)
Medium	0 " (0 cm)	5" (12.5 cm)	6" (15 cm)	2" (4cm)	11" (29 cm)	13" (34 cm)
Very High	14" (35 cm)	18" (45 cm)	22" (55 cm)	35" (88cm)	43" (108cm)	50" (128cm)

2. Background

The scientific literature relevant to dynamics of change in Washington coastal areas describes (a) the nature and process of coastal erosion on beaches and bluffs (Shipman, 2004; Terich, 1987; Komar, 1998); (b) the roles of sea level changes and storm waves in accelerating shoreline erosion (e.g. Graham and Diaz, 2001; Allan and Komar, 2006; Mote et al., 2008; and Zhang, Douglas, and Leatherman, 2004); (c) long-term experience with saltwater intrusion into coastal freshwater aquifers, mainly as a result of excessive pumping for freshwater supply (e.g. Walters, 1971; and Jones, 1985); (d) effects of increased sea surface temperature on the frequency of harmful algal blooms (Moore et al., 2008); and (e) trends in and effects of ocean acidification (e.g. Doney, 2006 and Feely et al., 2008). The literature has also begun to document how climate change may exacerbate risks to human uses of coastal areas. A number of recent regional investigations and public workshops have addressed these issues. For example, the State of Washington has prepared documents describing the nature of climate change, regional vulnerabilities, and opportunities for adaptation (Snover et al., 2007). These sources of information, assessment, and policy investigations have been broadly surveyed and incorporated in the following sections. Based on that starting point, this chapter focuses on specific risks posed by climate change to the Washington coast.

Locally, *relative* SLR -- the combined effect of global SLR and local rates of vertical land movement -- drives many coastal impacts. Mote, et al (2008) explain that Western Washington is located on the edge of the North American continental plate with the Juan de Fuca oceanic plate subducting underneath, which produces gradual uplift in the northwestern part of the region. The northwestern Olympic peninsula has been rising at about 2 mm/yr. On the other hand, South Puget Sound has been subsiding at a rate of 2 mm/yr. Vertical land movement on most of Washington's coast and the rest of Puget Sound has been found to be less than 1 mm/yr. If these trends continue, relative SLR will be greatest in south Puget Sound and least on the northwest tip of the Olympic peninsula (See Table 2). Substantial and reliable scientific models do not back up these trends, which is a major reason for the wide range of projected SLR. As noted by Mote el al (2008), (1) they have not formally quantified the probabilities, (2) SLR cannot be estimated accurately at specific locations, and (3) these SLR projections are for advisory purposes and are not actual predictions.

Clearly, the regional impacts of climate change depend upon the patterns of coastal land use and development. The predominant land use in the Puget Sound is low-density housing (91% of shoreline properties classified as single-family homes), often located at the top of bluffs, which are typically protected by a form of shoreline defense (such as concrete bulkheads or riprap) (Gabriel and Terich, 2005). On the southwest Washington coast there are local, dense developments of beach homes and tourist businesses. Because the Puget Sound region is most densely inhabited region, human impacts are expected to be greatest there and least on the Olympic peninsula north of Point Grenville and in the San Juan Islands. Between those extremes lie the Strait of Georgia and southwest Washington coasts.

3. Approach/Methods Used

The background information identified above has been reviewed and assessed in the five Key Findings summarized in the following section. In addition, we include information gathered through conversations and interviews with personnel at State and local agencies who are dealing with some of the potential impacts of SLR, elevation of sea temperature and acidity, and saltwater intrusion of coastal aquifers. Our basic approach is (a) to select specific locales and impacts for study, (b) to characterize the understanding of the local circumstances and concerns related to these impacts, and (c) to note how the impacts on the local population, structures, public facilities, and economy depend upon how people adapt to the physical changes. We characterize the adaptation responses in three categories: (1) *accommodation*, which means continuing with current uses of the coastline despite the changes in coastal oceans and environments – for example, to accommodate to SLR by raising the height of piers and placing shoreline buildings on pilings; (2) *protection*, which involves building structures like seawalls and dikes that keep the sea from intruding on coastal areas; and (3) *retreat*, which involves abandoning coastal sites and moving to higher ground. Each of these adaptive responses is likely to be adopted within the Washington coastal areas.

Because available information is not adequate to examine climate impacts on the entire Washington coast, this study focuses on a few cases to illustrate the nature of the impacts and to highlight specific areas of the coast where these impacts will be a significant concern. his case study approach is necessarily somewhat anecdotal and incomplete. The principal outcome of this study is to push the existing knoledge a bit further in the direction of useful, integrated understaning of the threats posed by climate change on the Washington coast**.**

4. Key Findings

4.1. Impacts on Beaches and Sand Spits

Beach erosion is an on-going natural process. Beaches are nourished by sediment eroded from bluffs or provided by rivers. Sand eroded from beaches moves along the coast or is pushed offshore by high-energy waves. There is a constant dynamic tension between the natural processes of accretion and erosion. Here, we focus on the role of SLR in processes affecting beaches of Puget Sound and Willapa bay.

Figure 2. Seawalls protecting Bainbridge Island homes, which have been found to degrade nearshore habitat (The Seattle Times, 2008)

4.1.1. Washington Beaches and Sea Level Rise (SLR)

Puget Sound's shoreline, estimated at 2411 km (1477 mi) in length, has many facilities and residential developments that will be affected by SLR (Shipman 2004). SLR will increase erosion rates and coastal flooding on Washington's beaches and bluffs. Erosion tends to occur largely through infrequent, episodic events, such as high-energy storm waves coming on a high tide. Wave-induced erosion of the uplands can occur when waves reach the junction between the beach face and its backing feature, such as a sea cliff, dune, or shore armoring (Ruggiero et al., 1997). SLR will cause the landward migration of the shoreline as waves break higher on the beach profile.

Coastal development could be threatened by increased vulnerability of coastal property as SLR shifts shorelines and tides closer to homes and infrastructure. In the Puget Sound region, approximately 90% of Puget Sound's shorelines have single-family residences or are available for residential development (Taylor et al., 2005). In recent years, the Washington State Department of Fish and Wildlife has approved numerous residential bulkheads to armor the shoreline of Puget Sound (particularly around Tacoma, Olympia, and the coasts of Whidbey Island), despite the documented damage to nearshore habitats. (Johannessen and MacLennan 2007, p.15)

Ironically, shoreline armoring by sea walls, riprap, or revetments typically decreases the volume of sediment available to sustain beaches. Because wave energy reflected off coastal armor carries sediment offshore, and the armoring itself reduces erosion of protected bluffs, protected shores gradually lose sediment and shallow water habitat (Johannessen and MacLennan, 2007, p.13.). The resulting increased water depths and greater wave energy tends to weaken the protective structures. In addition,

Figure 3. Housing on Point Monroe, Bainbridge Island (Washington Department of Ecology, Washington Coastal Atlas)

the beaches of Puget Sound are critical habitat for juvenile fish (including salmonids) and shorebirds, and they support shellfish and epibenthic zooplankton, among other species. Aquatic vegetation dominates the base of the food web in these habitats and provides forage, refuge, and other functions for many marine species (Zelo et al., 2000). Beach erosion rates will vary depending on wave environment, geology, beach characteristics, and extent of shoreline armoring (Finlayson, 2006).

4.1.2. Expected Impacts on Washington Beaches

4.1.2a. Bainbridge Island

Bainbridge Island contains 85.2 km (53.3 mi.) of shoreline with 82% of the shorelines currently in residential, recreational, commercial, or industrial use. Bainbridge Island's shorelines are quite diverse, with conditions ranging from polluted urban waterfronts, to residential developments, to fairly uninhabited areas of shoreline with intact riparian habitats (NOAA, 2004). The majority of development is for single-family residences, but also includes parks, a fish-pen aquaculture center, a ferry terminal, and mixed-use developments. About 48% of the shoreline is armored (mostly vertical rip rap or concrete structures). Figure 2 illustrates a bulkhead protecting homes along Bainbridge Island's shoreline. About 27% of the shoreline has armoring that extends into the intertidal zone (NOAA, 2004). Where shoreline modification is extensive, the slope is gauged as unstable, while the areas with little shoreline modification have stable slopes.

Areas most susceptible to inundation are the uplifted beach terraces on the southern third of the island, and the majority of the bays and coves on the island (City of Bainbridge Island, 2007). Rolling Bay-Point Monroe on the northeastern shore runs 9.0 km (5.6 miles) encompassing Point Monroe, Point Monroe Lagoon, and Rolling Bay to Skiff Point. Areas like Point Monroe (Figure 3), where houses are situated on a small strip of beach with water on two sides, are especially at risk. While Point Monroe is primarily residential, its shore does include Fay Bainbridge State Park, which is a stretch of relatively undeveloped sandy beach with access for recreation. Many homes along the spit at Point Monroe are built on fill material (NOAA, 2004). A total of 291 modifications were recorded along the Point Monroe shorelines, at an average of 10 modifications per 1000 ft. (NOAA, 2004). These include protective structures at the waterline (112), docks (33), and overwater structures (28). NOAA (2004) recommends that unnecessary armoring structures, especially those that intrude into the intertidal zone, be modified or removed.

4.1.2b. Impacts on the Southwest Washington Beaches

The southwest Washington coast covers the northern three quarters of the Columbia River littoral cell, which stretches from Point Grenville south to Tillamook Head, Oregon. The Washington segment of the littoral cell contains three sub-cells stretching from the Columbia River to the entrance to Willapa Bay, from Willapa Bay to the Grays Harbor entrance, and from the Grays Harbor entrance to Point Grenville. The coast here is of two principle types, sandy beach and berms along the outer coast, and mudflats within the two bays. The ocean beaches and dunes reflect a high-energy coast that shifts seasonally as wave energy and direction vary. After jetties were constructed at the entrances to the Columbia River and Grays Harbor in the early 1900s, sediments were trapped behind the jetties, causing rapid beach accretion in the first half of the 20th century. But development of 11 major, mainstem dams on the Columbia River has reduced peak river flows and sediment discharges to the coast. Substantial recent evidence suggests a shifting regional trend towards erosion (Kaminsky, et al. 1998), which may be related to lower sediment budget and/or shifting storm tracks with larger, more energetic winter storm waves.

The Southwest Washington Coastal Erosion Project has identified several erosion “hot spots”. These are located at the south end of Ocean Shores; near the southern jetty at the Grays Harbor entrance north of Westport; at the north end of the Long Beach peninsula (Leadbetter Point); and just north of the Columbia River entrance near Fort Canby. Recently, the highest erosion rates occur at the north entrance of Willapa Bay (formerly known as Shoalwater Bay) the fastest-eroding beach on the Pacific coast, locally referred to as Washaway Beach (Daniels et al., 1998). Since the 1880s, it has been losing 19.7m (65ft) of beach a year on average. High erosion rates have also been observed at Ocean Shores, just north of Cape Leadbetter. Beach erosion appears to occur when large waves approach at a steeper angle from the south, especially during El Niño conditions, when winter sea level is as much as 0.3 m higher than July levels. Researchers also suspect that higher storm waves are reaching the southwest Washington coast due to a northward shift in the storm track as a consequence of broader global climate changes. Hence, there are at least three possible factors contributing to erosion along the beaches of southwest Washington, (a) reduced sediment supply; (b) gradual SLR as a longer-term factor, and (c) northward shift in Pacific winter storm tracks. Increased storm intensity may be an additional climate-related factor, but there is less than broad agreement among the climate scientists about the relative importance of these factors.

Economic impacts of episodic erosion events are illustrated by the events at Washaway Beach. Despite official warnings, and a decade-old building moratorium, people still continue to buy property there. More than 100 homes have fallen into the ocean in the last 20 years, including the entire town of North Cove (Martin, September 2007). Current residents of Washaway Beach are resigned to the fact that their homes will most likely be gone within a decade and that they will have to retreat due to the wave action and erosion, but they say that the view and location is worth the risk (Martin, September 2007). More than $24 million has been spent to protect nearby Highway 105 and $12 million has been spent to protect the Shoalwater Bay Indian reservation, which has seen a reduction of tribal lands and shellfish resources due to the rapid retreat of Cape Shoalwater. There are currently no plans to protect the property at Washaway Beach (Morton et al., 2007).

Ocean Shores has been actively eroding since the 1995/96 winter season. A temporary structure was emplaced to protect condominiums and infrastructure valued at more than $30 million (Kaminsky, 1998). While these examples of shoreline erosion occur without significant climate change, they illustrate the kinds of erosion events that may occur more frequently as SLR and increased winter storm waves attack other shoreline segments on the southwest Washington coast.

Within the shallow bays, the shorelines are relatively well protected from high-energy waves and major episodes of erosion. Extensive mudflats in both Willapa Bay and Grays Harbor have long been utilized for shellfish aquaculture, primarily oyster culture, which contributes significantly to the local economy. In Grays Harbor, the mudflats have been eroding and shrinking, perhaps due to higher currents flowing through the dredged and jettied entrance, which permits greater wave energy to enter the Bay. Again, higher sea levels and increased wave action due to shifting storm tracks, driven by global climate changes, could be a contributor to reduced habitat for shellfish in the Bay. (Kaminsky, personal communication 2009).

4.2. Bluff Erosion in Puget Sound

Bluff erosion is an on-going natural process that feeds sediment for beach formation, but also threatens property and human lives when buildings are close to the eroding bluffs (Figure 4). We examine the role of wave action and tides, and how this may change with SLR. Three case studies illustrate some of the different types of bluffs present in the Sound.

4.2.1. Sea Level Rise and Bluff Erosion

Wave action creates unstable bluff profiles through toe erosion, which "results in the loss of lateral support" for the bluff, and may lead to large slabs of the bluff failing (Baum, 1998). The steepening of bluff slopes increases the probability of bluff failure (Thurston County, 2005), and

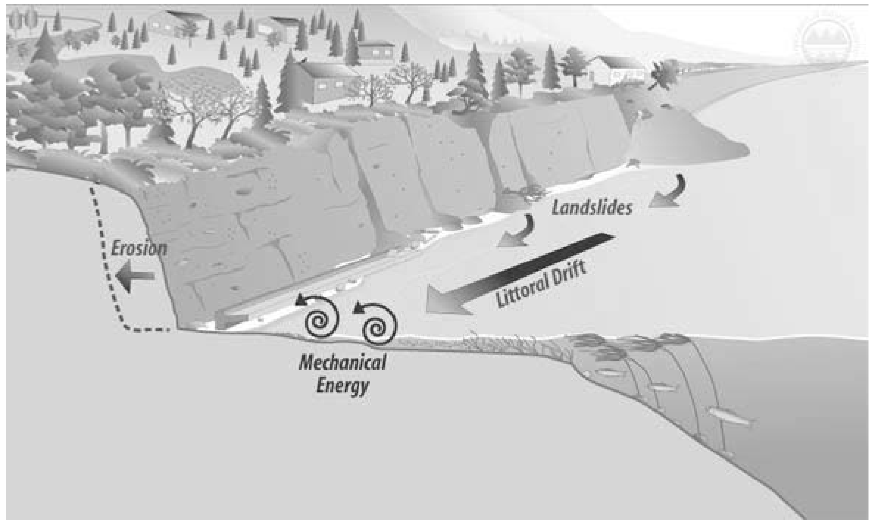

Figure 4. Bluff erosion process (Williams et al., 2006)

accelerates the long-term retreat of the bluff. Steeper, unstable bluffs are more susceptible to small landslides, which are often triggered by heavy rainfall and drainage failures (Terich, 1987). Elevated groundwater levels or seismic activity may also trigger large landslides (Shipman, 2004.). Therefore, bluff toe erosion "sets the stage" for slope failure, but rarely is it the direct cause of a coastal bluff landslide (Thurston County, 2005).

Among key factors in bluff erosion are storms with large waves, especially when combined with high tides or elevated sea levels associated with El Niño events (Shipman, 2004). The length of the fetch --the distance over which waves develop-- and wind speed during storms increases wave energy. For example, western Whidbey Island is subject to a very long fetch along the Strait of Juan de Fuca (Shipman, 2004). Furthermore, when storms occur at high tide, the wave action on bluffs is magnified. Increasing the sea level raises the high tide level. As a result, waves will be able to directly erode the toe of the bluff in its current position more often, increasing the frequency of landslides (Shipman, 2004). These factors could lead to complex changes in shorelines as SLR shifts the bluff/sea interface further inland. Eventually, the sediment supply from eroding bluffs should maintain the elevation of beaches as beach and bluff profiles move landward.

4.2.2. Examples of Bluff Erosion

4.2.2a. Western Whidbey Island

Island County is comprised of six islands with 354 km (221 mi) of shoreline, of which 51% is classified as "unstable" (Shipman, 2004). Whidbey Island is the largest and most populated island in Island County. Erosion rates in the county have been measured from a centimeter to more than 61 cm (2 ft) per year (Island County, 2006). The western shore of Whidbey Island has experienced many landslides. There is a large prehistoric landslide that extends about 2 km (1.25 mi) along the shoreline, which sometimes reactivates during wet weather (Shipman, 2004). Typical erosion rates are about 3 cm (1.2 in)/yr, which involves the loss of 1 meter of bluff or bank in a landslide every 33 years. Areas that have greater exposure and higher wave energy may exhibit erosion rates of several inches per year or more

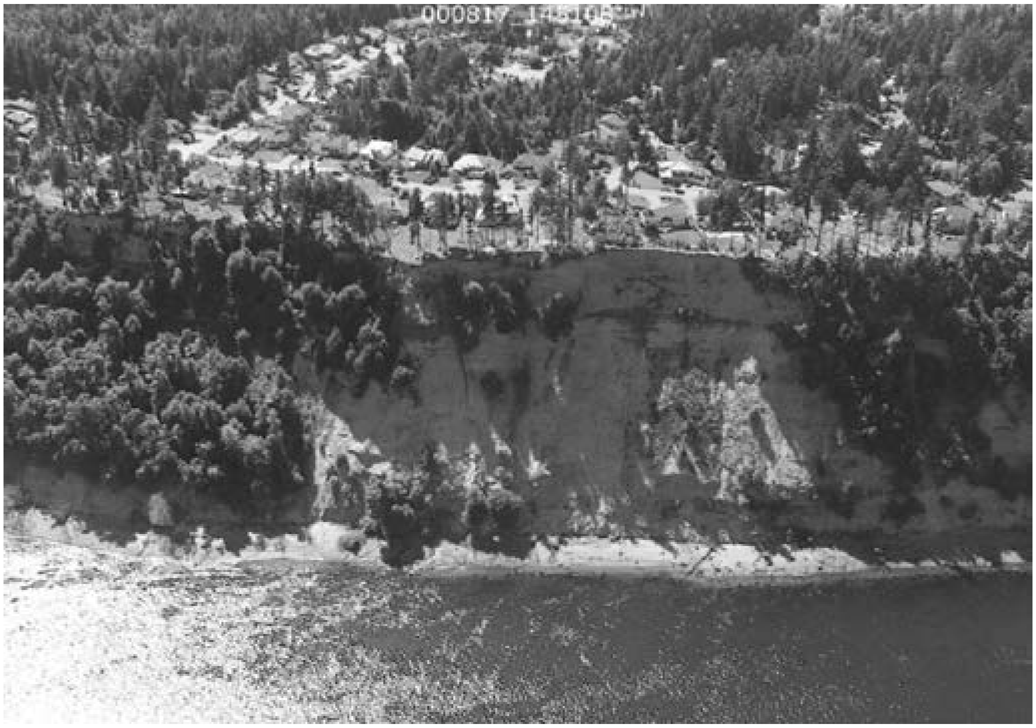

(Zelo et al., 2000). Recently, high waves have caused large amounts of erosion on Whidbey Island, particularly in drift cells on the southeastern portion of the island and on large spits on Cultus Bay (Johannessen and MacLennan, 2007). A recent risk assessment has shown that there is a 100% probability of a landslide somewhere, of some magnitude in a given year, though most will be small (Island County, 2006). As in most of Puget Sound, Whidbey Island bluffs are attractive sites for residential development (Shipman, 2007). As a result, when major bluff slides occur, homes are on the front lines, and residents may be forced to protect, accommodate, or retreat from their homes (Figure 5).

Figure 5. Houses on a bluff on western Whidbey Island. (http://apps.ecy.wa.gov/shorephotos/scripts/bigphoto.asp?id=ISL0354)

Many residential developments built on Whidbey Island in the 1950s and 1960s included construction of bulkheads at the base of high bluffs. These practices would not be allowed today, but the structures that are currently standing are allowed to remain. Regulation of construction on residential sites is not very restrictive, because the Shoreline Management Act (1971) exempts the construction of single-family residences and "normal protective bulkheads" from a Shoreline Substantial Development Permit (Zelo et al., 2000). There have been regular conversions of small houses into large homes, which are at greater risk of slide damage when they reside on unstable slopes (Shipman, 2004).

As SLR causes increased bluff erosion and landslides, these locations will be subject to increased hazards of damage. A preliminary analysis using Zillow (a web-based tool for estimating home value based upon tax assessments and home improvements, among other factors) shows that along a one mile long stretch of bluff along West Beach Road on northwest Whidbey Island, approximately $32 million worth of property could be involved (Barton and Frink, 2007). Many of these homes are less than a hundred feet from the current bluff edge, and are at risk for severe structural damage resulting from accelerated bluff erosion.

4.2.2b. Bainbridge Island

Bainbridge Island has 394 km (246 mi) of shoreline, 20% of which is classified as "unstable" (Shipman, 2004). Unlike Whidbey Island, where substantial waves arrive through the Strait of Juan de Fuca, Bainbridge Island is nestled inside Puget Sound where waves do not gather the same magnitude of energy. However, the bluffs on Bainbridge Island are still vulnerable to erosion. Bluff erosion rates average between 5.1 cm (2 in) and 15.2 cm (6 in) per year, depending on physical characteristics such as beach profile, substrate, and slope angle, as well as the presence or absence of human-built protective structures such as bulkheads (City of Bainbridge Island, 2007). As on Whidbey Island, bluff erosion events are episodic. After heavy rains and soil saturation, Bainbridge Island has experienced a number of bluff erosion events.

Rolling Bay Walk has been the site of a number of large bluff erosion events, including one in the spring of 1996 that pushed a house off of its foundation, and a series of slides in 1997 that overturned one house into the water, and damaged at least three more (Baum et al., 1998). Another area that has experienced bluff erosion is near Harvey Road. In the past decade, homeowners have reported a 2.5-3 m (8-10 ft) retreat at the base of the bluff. At least one of the homes is now within 6.1 m (20 ft) of the edge of the bluff, with others 12.1 m or 24.2 m (40 or 80 ft) from the retreating bluff line. Additionally, many auxiliary structures such as septic systems are threatened by bluff erosion (Shoreline Hearings Board, 2007).

4.2.2c. The San Juan Islands

The San Juan Islands, in contrast to the previous two cases, have very little bluff erosion. Although there is moderate fetch and storm wave energy in the north and south, the islands are comprised predominately of exposed bedrock coast (Shipman, 2004). This landscape was formed when glaciers scoured knobs and hills, exposing the bedrock. Only 3% of San Juan County's 602 km (376 mi) of shoreline is classified as "unstable" (Shipman, 2004). Therefore, due to "their resistant lithologies and the modest wave energy of the sound" in these areas, bluff erosion rates are negligible (Shipman, 2004). While there are some unstable bluffs vulnerable to erosion and landslides, the resistance of bedrock bluffs to wave action erosion makes it unlikely that an increase in SLR will significantly affect the bluff erosion patterns in the San Juan Islands.

4.3. Impacts on Ports and Harbors

Major ports and harbors in the State of Washington include the Ports of Seattle, Tacoma, Everett, Olympia, Grays Harbor, and Port Angeles. In addition, there are many smaller ports and marinas designed mainly for private pleasure craft. Because such facilities are adjacent to the shore, SLR will affect them all. The magnitude of impacts to the operation of ports and harbors due to SLR will depend upon a variety of factors. These include: the geomorphology of the land surrounding the port, whether the port is located near a river whose flow may be affected by climate change, the degree to which the transportation system surrounding the port will be impacted, and whether re-construction of piers and other structures can accommodate the expected level of SLR.

Most ports in Washington State are operated by local Port Authorities, organized at the county level, which can encompass a variety of administrative units. Due to limitations on time and resources available for this study, only the two large ports of Seattle and Tacoma are specifically considered below. Both of these are “landlord ports,” meaning that they lease terminals and shore-based equipment (e.g. container cranes) to shipping lines that operate the terminals. These two large ports handle most of the State’s freight and cruise ship traffic, and much of the commercial fishing fleet operating out of Puget Sound. The likely impacts depend upon the strategies adopted by the ports for adapting to SLR. Finally, it should be noted that the broader effects of SLR on the transportation networks would impact ports. Both the Seattle and Tacoma ports serve as points of freight transfer between ocean ships and land-based cargo carriers serving distant markets. Roughly 50% of the cargo moving through the Port of Seattle is destined for markets east of the Mississippi River. The ability of the ports to continue operation in the face of SLR depends upon the continued operation of trucking lines and railroads. Hence, we can broaden the concept of impacts to include any disabling of links in the transportation system that disconnects the ports from distant markets they are serving.

4.3.1. Port of Seattle

Freight terminals in the Port of Seattle line the edges of Elliot Bay and the Duwamish River estuary. Much of the land on which the piers and facilities reside was created by fill dirt brought from upland sites early in the history of Seattle. These sites are all within a few feet of the extreme high water mark. Hence, higher levels of forecasted SLR (> 0.91m or 3 ft) will pose a significant hazard to the continued operation of the port facilities. According to key staff at the port, they are considering a variety of strategies to accommodate to SLR, such as raising existing docks and designing floating terminals with ramps to the upland railroad yards. Some docks and cranes have already been raised in elevation to accommodate to SLR and the increasing size of ships. The main port complex in Elliot Bay is adjacent to railroad yards and the south Seattle industrial district which is located on very low elevation land. A significant rise in sea level would threaten to inundate the entire area, cutting the Port off from the requisite inland transportation facilities. Adding to this potential problem is the nearshore position of the Burlington Northern-Santa Fe railway line on the Puget Sound north of Seattle. Even if the Port were able to protect its current facilities from SLR, a break in the rail network could threaten its viability as a major container and bulk freight center.

Further, the Port’s Shilshole marina is just seaward of a significant bluff on the west side of the Sunset Cliffs neighborhood. It is surrounded by very low elevation land that could be inundated by just a few feet of SLR. There is little prospect of adapting this facility to significant SLR, short of installing a few feet of new fill dirt to raise the elevation of the adjacent land.

4.3.2. Port of Tacoma

The Port of Tacoma is a major freight transfer facility, bounded on the south by the Puyallup River and on the north by the Hylebos waterway. Just north of that waterway is a steep bluff topped by extensive housing developments. Current pier maintenance and re-construction plans will increase pier elevations by roughly 1.3 m (4.3 ft) to accommodate the higher levels of SLR predicted for the next century. Hence, the facilities operated by the Port and most of the Port's tenants will accommodate to SLR over the next century unless the actual levels of SLR exceed the predictions. However, the Port planners are aware that SLR, in combination with high river run-off, raises the threat of flooding along the Puyallup River to the south of the main body of freight terminals. This could inundate the intermodal rail yards upon which the transportation network depends. Additional protective structures, such as dikes along the riverbanks, may be needed under the high SLR scenarios.

4.4. Saltwater Intrusion in Coastal Aquifers

4.4.1. Hydrological Dynamics of Aquifers and Seawater

Under normal conditions, the movement of freshwater towards the sea prevents saltwater from contaminating the water in coastal aquifers, and the interface between freshwater and saltwater is below the land surface near the coast (USGS, 2004). Since freshwater is slightly less dense, it tends to float on top of saltwater when both are present in an aquifer. The bottom of the freshwater body floating on seawater within an aquifer is typically about 40 times as far below sea level as the top is above sea level. When freshwater is pumped from the aquifer, the underlying saltwater tends to rise 40 ft for every foot that the water table is lowered (Walters, 1971). The boundary between the freshwater and saltwater zones, known as the zone of diffusion or the zone of mixing (Kelly, 2005), will be pushed landward and upward as sea level rises, potentially making coastal aquifers more vulnerable to saltwater intrusion (Barlow, 2003).

Seawater typically contains about 35,000 mg/L of dissolved solids, including approximately 19,000 mg/L of chloride. Uncontaminated groundwater in most areas of coastal Washington usually contains less than 10 mg/L of chloride, and the EPA recommends that the chloride concentration of drinking water supplies be less than 250 mg/L (Dion and Sumioka, 1984). If saltwater intrusion into coastal aquifers occurs, the waters may not be suitable for drinking and irrigation, the high mineral content of the saltwater could cause corrosion of pipelines and well pumps, and the aquifer and its wells could become unusable if the intrusion becomes too severe (Island County Water Resources Management Plan, 2005).

In some areas of Washington State saltwater intrusion is already a concern due to excessive pumping of the aquifers. On Whidbey Island 72% of its residents rely on the groundwater (Island County Water Management Plan, 2005). In a study by Island County Environmental Health in 2005, areas containing wells were designated as low risk, medium risk, or high risk. Low risk wells within 0.8 km (½ mile) have chloride concentrations less than 100 mg/L; medium risk wells have chloride concentrations between 100 and 200 mg/L; and high risk areas have chloride concentrations greater than 200 mg/L. Out of 379 wells surveyed, 242 showed no evidence of intrusion, 101 showed inconclusive indications of intrusion, and 36 showed positive indications of intrusion. In preventing saltwater intrusion, the important factor is the water level in the area between the well and the shoreline, because saltwater intrusion would first occur along the shoreline and then move inland as the situation worsened. In addition, aquifers that are at critically low water elevation are at risk of saltwater intrusion if there is continued groundwater withdrawal (Kelly, 2005).

4.4.2. Likely Impacts of Sea Level Rise

While projected SLR could cause increased saltwater intrusion into coastal aquifers, expert opinion suggests that SLR will have only a minor effect. Aquifers act as a gradient to the sea, and the amount of water recharge from the surface will likely remain about the same. Hence, the amount of freshwater available is not expected to change. In the very near coastal areas, a rise of 0.3 - 0.9 m (1-3 ft) in the sea level will reduce the depth of the freshwater lens floating above the seawater by 0.3 – 0.9m (1-3 ft). Nearshore wells that already have intrusion problems may have trouble with more saline water, so those wells may need to be moved or reconstructed. But this will be a serious concern only in a very narrow range along the coast, where the freshwater lens is already very shallow, and there are few wells. Based upon our review of the saltwater intrusion problem on Whidbey Island, we conclude saltwater intrusion is not a major risk for Washington State aquifers.

4.5. Impacts on Shellfish Aquaculture

Washington currently has 106 commercial shellfish-growing areas and is the leading producer of commercially farmed bivalve shellfish in the United States, including 86% of the West Coast's production in 2000. Washington's shellfish farmers and harvesters sell shellfish products around the world, and support the economies of many rural western Washington communities ("Treasures of the Tidelands," 2003). Table 3 shows that the sale value of oysters, mussels, small clams, and geoduck clams from aquaculture in Washington is roughly $75 million a year.

4.5.1. Impacts of Sea Level Rise and Increased Sea Surface Temperature

SLR and increased sea surface temperature could impact the shellfish aquaculture industry in several ways. Negative effects of increased temperature could include reduced shellfish growth, reproduction, distribution, and health (Cheney and Dewey, 2006). SLR may affect

Table 3. Shellfish production in Washington State in 2006 (Cheney and Dewey, 2006)

	Oysters	Clams	Mussels	Geoduck	Total
Production (mil. lbs.)	77	7	1.5	.4	85.9
Sales Value (mil. $)	$57.75	$14	$1.73	$2.5	$75.98

coastal habitats in the Puget Sound through the inundation and shift of habitat types on existing beaches. SLR would have a minimal impact on mussel and oyster culture on rafts or other floating structures (Pacific Coast Shellfish Growers Association, 2008).

Most shellfish culture occurs on the intertidal substrate, where SLR will directly affect access to these lands through changes in the high and low tide ranges (Pacific Coast Shellfish Growers Association, 2008). If the aquaculture sites do not migrate landward, SLR reduces access to aquaculture beds because of increased water coverage. A 0.16 m (0.53 ft) rise in sea level could lead to an increase in water coverage and a reduction in harvest time of 13%, while a 0.31 m (1 ft) rise in sea level could lead to an increase in water coverage and a reduction in harvest time of 31% (Cheney and Dewey, 2006). The increased water coverage will reduce workdays for shellfish growers because they typically work at low tide. It is very difficult to plant, harvest, or tend partially or completely submerged oysters (Gordon et al., 2003). A further complexity is the issue of shoreline armoring, which affects the availability of tidelands for shellfish farming, as shoreline armoring tends to increase beach erosion and change the characteristic of the beach sediment.

Since SLR will shift beach profiles landward, there may be no reduction in sub-tidal habitat overall, but the optimal growing areas may be shifted off of the farmer's property or lease (Cheney and Dewey, 2006). At present, "average high tide" or "ordinary high water" is treated as a stable boundary line that separates upland property from inter-tidal areas used for shellfish aquaculture. In the future, however, SLR may create ambiguity in the definition of the property rights due to a shift in where the actual high tide occurs. The high tide with SLR will be further inland. One option would be to retain the definition of tidelands and shoreline property boundaries, but recognize explicitly that these boundaries are moving upland as sea level rises – an option entitled "rolling easements" (Titus, 1986).

4.5.2. Likely Impacts of Sea Surface Temperature and Harmful Algal Blooms

Harmful Algal Blooms (HABs) are blooms of algae that can produce potent natural toxins that cause harmful physiological effects (including illness or death) when they are concentrated within filter feeding shellfish and fish. Humans and other animals are exposed to the HAB toxins by ingesting the contaminated fish or shellfish and by consumption, aerosol inhalation, or skin contact with contaminated water. Paralytic shellfish poisoning (PSP) from dinoflagellates in the genus *Alexandrium* and amnesiac shellfish poisoning, caused by domoic acid created by diatoms *Pseudo-nitzschia,* are the primary problems on the West Coast (Horner et al., 1997). Other species of dinoflagellates can cause a range of illnesses, such as neurotoxic shellfish poisoning, diarrheic shellfish poisoning, and ciguatera fish poisoning. These also cause fish, bird, and marine mammal die-offs (Patz et al., 2006).

Over the past decade, evidence of a relationship between climate and the magnitude, frequency, and duration of HABs has suggested that the seasons when HABs occur may expand as a result of climate change. Sea surface temperature and upwelling have both been linked with HABs (Patz et al., 2006). Due to their physiological and ecological diversity HAB species will not exhibit a uniform response to changes in climate. Phytoplankton growth is typically influenced by temperature, light, and the availability of nutrients (Moore et al., 2008). Most marine HAB dinoflagellates are expected to be favored over other phytoplankton under future climate scenarios, because their ability to swim allows them to reach nutrients in the deeper parts of the upper stratified layer of the water column that diatoms and other phytoplankton cannot reach. It is not known if blooms originate at one or several sites, or whether isolated blooms develop in separate locations at the same time in response to similar hydrographic conditions. It is also difficult to determine if blooms develop offshore before they are detected in coastal waters (Horner et al., 1997).

The frequency and distribution of HABs has increased over the last 30 years, and human illness from algal sources has increased. In fact, the present variability and occurrence of HABs is unrivaled from those in the past 60 years (Patz et al., 2006). In Puget Sound *Alexandrium* species occur primarily in the late summer and early fall when the water temperatures reach their seasonal peak. Blooms of the dinoflagellates *Ceratium* species and *Akashiwo sanguinea* generally occur during the same period in shallow areas of southern Puget Sound. Increased mortality of oyster larvae and adults has been associated with these dinoflagellates, but there is no indication of a chemical toxin. The increased mortality could be due to mechanical damage or oxygen depletion caused by a bloom decay (Horner et al., 1997).

By the year 2100, surface air temperatures in the Puget Sound region could increase by as much as 6°C (10.8°F). Surface water temperatures are expected to follow this closely. This increase is a concern because water temperatures greater than 13°C (56.7°F) have been found to promote blooms. The rising air and water surface temperatures may also promote earlier and longer lasting HABs. The growth responses of HABs could also be influenced by interactions with other physical and biological aspects of the marine ecosystem, such as wind-driven upwelling at coastal margins.

Some toxic blooms are triggered by nutrients supplied by land runoff. Hence, shifts in the timing of runoff into coastal estuaries fed by snowmelt rivers could lead to changes in the timing and magnitude of stratification related to freshwater inputs and to nutrient loading and turbidity related to freshwater supplies, which could increase the frequency of blooms in coastal waters. Studies in Sequim Bay on the Strait of Juan de Fuca suggest that paralytic shellfish poisoning toxicity increases when the climate is warm and dry, and decreases when the climate is cold and wet (Horner et al., 1997). Even though there is a need for more data assessing the impacts of different climate change stressors on HAB species, current research findings suggest that HABs will occur more frequently and over wider ranges as a result of climate change.

4.5.3. Ocean Acidification

The oceans have absorbed approximately 127 billion metric tons (140 billion short tons) of carbon as carbon dioxide (CO_2) since the beginning of the industrial era. Hydrographic surveys and modeling studies have confirmed that the uptake of CO_2 by the oceans has resulted in a lowering of seawater pH by about 0.1 since the beginning of the Industrial Revolution (Feely et al., 2008). A drop by one pH unit corresponds to a ten-fold increase in the concentration of hydrogen ions, thus making the water more acidic (Doney, 2006). Lower pH levels have been found to decrease calcification rates in mussels, clams, and oysters because the reaction of CO_2 with seawater reduces the availability of carbonate ions that are necessary for $CaCO_3$ skeleton and shell formation for a number of marine organisms. Many species of juvenile shellfish may be highly sensitive to lower-than-normal pH levels, resulting in higher rates of mortality directly correlated with the higher CO_2 levels (Feely et al, 2008). A growing number of studies have shown that the survival of larval marine species, including commercial shellfish, is reduced by ocean acidification.

The range and magnitude of biological and socio-economic effects are not certain enough to quantify at this time, but they are thought to be substantial (NOAA, 2008). Acidity levels in upwelled waters off the Pacific Coast have already begun increasing faster than anticipated (Feely et al., 2008). Because these changes will be large and will occur quickly, and because human development has fragmented species into small and vulnerable populations, there is concern that future climate changes will be more stressful to species than past changes (Tangley, 1988). Hence, while there is great uncertainty about the future path of acidification and resulting impacts, there are also potentially great risks of significant changes in the species composition and vulnerability of ocean ecosystems that support shellfish.

An indication of the potential risks of increased ocean acidification and related water quality changes was recently documented in commercial and research shellfish hatcheries in Washington and Oregon. These facilities experienced poor egg survival and massive mortalities of larval and juvenile oysters during an extended period when low pH (7.5 to 7.8) water was entering their seawater intake lines. The mortalities are still unexplained, but the pH shift is one of a number of possible causal factors (personal communication with Dan Cheney, 2008).

5. Adaptation to Climate Change on the Coast

As noted earlier, adaptation to climate change can involve: (1) accommodation -- continuing, but altering, current uses of the coastline in response to changes in coastal oceans and environments; (2) protection -- fending off the impacts by building structures like seawalls and dikes that keep the sea at bay; and (3) retreat -- abandoning coastal sites and moving to higher ground. This section outlines some adaptations that could be adopted in response to SLR, increased storm strength, beach and bluff erosion, and increased temperature and acidity of ocean waters.

5.1. Beaches, Bluffs, and Sand Spits

Because flooding will be an increasing problem on river deltas, points, spits, barrier beaches, pocket beaches, and berms with low backshores, building on these properties will be increasingly risky. The greatest risk exists for structures located on top of beach berms since they can be hit by storm waves and beach debris. The Department of Ecology recommends

Figure 6. Failed bulkheads and large slide on Whidbey Island (Washington Department of Ecology http://www.ecy.wa.gov/programs/sea/pugetsound/building/bulkhead.html)

that anyone thinking of purchasing property in coastal regions should check with the local planning/zoning office to see if the area is a flood zone (Washington Department of Ecology, 2007). Further, to adapt to forecasted SLR, flood zone designations could be modified to incorporate the expected SLR of 0.15m to 0.36m (0.49 to 1.24 ft) by 2100 but which could reach an extreme of 1.4 m (4.6 ft) by 2100 if the accelerated melting of the Antarctic ice shelf and Greenland ice cap continues.

An estimated 1/3 of the total Puget Sound shoreline contains bulkheads and other hard coastal structures. As noted above, these can temporarily reduce upland erosion caused by wave action, but they can do little to prevent continued erosion of the seaward beaches, since wave reflection can enhance offshore sediment transport. This can undermine the bulkheads. Figure 6 depicts failed bulkheads and a large slide on Whidbey Island (Department of Ecology, 2007). Ultimately, owners of structures within the higher mean tide level generated by SLR may find that the best course of action is to retreat upland from their current location as the sea level rises or to build further from the edge of the bluffs.

5.2. Adaptation in Ports and Harbors

As noted in Section 4.3, Washington's ports and harbors will be impacted by the slow rise in sea level over the next century. In the Puget Sound, a port manager with low risk tolerance might want to plan for the higher 0.55m (1.8 ft) SLR by 2050 and the 1.28 m (4.2 ft) SLR by 2100. For most port facilities, the speed of SLR in combination with 30-40 year re-building cycles gives them the flexibility to adapt via raising and shifting piers and docks over time in response to observed and forecasted SLR. But, preserving shoreline facilities may be an inadequate adaptive response. As noted earlier, the Port of Seattle and surrounding lands would have to be elevated via additional fill dirt or protected via diking in order to adapt to significant SLR. Because property ownership in the port region is complex, a solution to the SLR threat would require a broad, well-coordinated plan of action by the Port authorities, railroads, city, county, State, and Federal agencies (especially the Department of Transportation and Army Corps of Engineers).

Another complication is in preserving the port's ability to function in the freight transportation network if SLR causes flooding of lands currently devoted to highways, railroads or storage areas. There would most likely need to be construction of new dikes and/or heightening of existing riverside dikes to prevent significant flooding of the lands needed by the freight handling facilities. No specific adaptation approaches have been developed here, but the need for organizing broader sets of interests (local, State, Federal, and industry) in designing port and transportation systems is strongly emphasized.

5.3. Saltwater Intrusion in Coastal Aquifers

Because we do not anticipate significant impacts of SLR on the coastal aquifers, there will be little adaptation needed in response to climate change here. A few wells may be located in the narrow band near the shore that could be affected by SLR. These wells will undoubtedly be abandoned and new wells drilled further inland.

5.4. Shellfish Aquaculture

Shellfish aquaculture will need to adapt to the three basic threats outlined earlier: (a) SLR causing a shift of shallow tidelands towards the upland shore, which is typically owned by shoreline property owners; (b) increased sea surface temperatures and acidification which may affect shellfish survival and growth; and (c) increased frequency of harmful algal blooms. One adaptive response to shifting tidelands has been identified as shifting of shoreline property lines as the mean high water mark moves inland. In fact, some US States already follow this principle. In Texas, when large hurricane or other events cause significant erosion of shorelines, the private property lines are shifted upland to preserve the public beaches and tidelands. This sort of adaptive response might be feasible in parts of Puget Sound and in the bays of southwestern Washington.

Increased temperatures and acidification present potentially difficult challenges to the rearing of current species and strains of shellfish. However, there may be sufficient genetic variability and tolerance for changes in water temperature and pH among shellfish to allow some room for adaptation. Specifically, shifting to more tolerant strains could be a successful strategy for maintaining shellfish production. We do not have sufficient information regarding these factors to confidently predict whether this approach would be successful.

Regarding increased HAB outbreaks, the State Department of Health may need to close recreational shellfish fisheries more often and monitor commercial shellfish harvests more closely in order to prevent adverse health impacts from HABs. If reliable, qualitative predictions of HAB risks can be developed then managers can be more prepared to respond quickly if HAB risks are "high" (Moore et al., 2008). This approach to adaptation is being discussed currently among scientists.

6. Research Gaps and Recommendations for Future Research

6.1. Beaches and Sand Spits

This report reviews potential climate change impacts at select sites within Washington's coastal region. Given that Washington has about 5,002 km (3085 mi) of coastline, however, it would be prudent to initiate broader monitoring and research on beaches in the future. Beach profiles should be monitored to contribute to better understanding of the dynamics of beach accretion and erosion. The sites mentioned in this paper should also be monitored closely. For instance, Whidbey Island's western shore could be monitored to determine if it does exhibit the predicted changes due to climate change. Over the years other shoreline segments within the Willapa Bay and Grays Harbor regions (and other shorelines with similar beach characteristics) should be assessed for shoreline erosion. For those areas where unnecessary armoring structures have been removed or modified, it should be determined whether reflective wave energy has been reduced and if natural sediment processes have been allowed to restore normal beach profiles. Both applied and basic research into movement of sediments and shifts in beach profiles should be priority research topics.

6.2. Puget Sound Bluffs

Shipman (2004) notes that, "Little systematic study of bluff recession rates has been carried out within the Puget Sound region, limiting knowledge of actual rates and understanding of the relative importance of different factors in determining rates" (p. 89). As with Washington's beaches, additional Puget Sound bluff sites should be incorporated into future studies in order to gain a more comprehensive look at the effects of climate change. More research could examine how auxiliary structures will be and are being threatened by beach and bluff erosion and the possible actions that can be taken in response. A comparison of erosion rates (historic and future projections) could then be used in choosing when and where to retreat from vulnerable bluff sites.

6.3. Ports and Harbors

Since our paper focuses on climate change at the ports of Seattle and Tacoma, additional research could focus on the ports of Everett, Olympia, Grays Harbor, and Port Angeles, as well as the smaller ports and marinas designed mainly for recreational purposes. Ideally, additional interviews would be conducted at each port and marina and a comparative study would be written detailing the effects of climate change on their infrastructure and potential responses and adaptations for each location.

6.4. Shellfish Aquaculture

As with the beaches and bluffs, there should be increased monitoring to gauge the extent that shellfish aquaculture sites follow inland tidelands with SLR. Further legal research and analysis could determine the extent of subsequent issues regarding property laws between shellfish farmers and shoreline property owners. More research should focus on climate change stressors that could have an impact on shellfish growth and mortality. For instance, the effects of increased sea surface temperature and ocean acidification on various strains of shellfish are not clearly understood. More research is also recommended on how HABs originate and develop, along with the impact of different climate change stressors on HAB species and on the physiology and ecology of HABs.

7. Conclusions

Overall, this brief survey of climate impacts on the coasts of Washington State has identified numerous possible routes by which climate can interfere with historical uses of the coast and has raised many questions requiring additional research. One conclusion is that SLR will cause shifts in the coastal beaches and increased erosion of unstable bluffs, and these effects will endanger housing and other structures built near the shore or near the bluff edges. State and local governments, as well as property owners, will need to engage in longer term planning and decision-making to determine whether to retreat from the endangered shores and bluffs or to invest in structural protection or adaptation projects. These conclusions extend to the numerous ports and marinas in the Puget Sound region, which must accommodate to SLR or retreat to higher ground if they are to continue to function as major transshipping points for US-Asia trade.

We found indications that shellfish may be harmed by increasing ocean temperatures and acidity, due to shifts in disease and growth patterns, and to more frequent HABs. Further, inter-tidal habitat for shellfish aquaculture will likely be slowly shifting shoreward as sea level rises. Adapting to these effects may involve both genetic research to select more resilient sub-species of shellfish and altered property boundaries to accommodate the shifting high tide lines. All of these conclusions are tentative, based upon current understanding of the underlying phenomena. Further research will be a necessary element of any longer-term, adaptive strategy for climate change in the region.

Acknowledgments

The authors want to acknowledge the important contributions and assistance provided by various individuals in the research reported here. Alexander (Sascha) Petersen was involved in the Climate Impacts Group research before this project was underway, and he assisted in our initial attempts to understand and depict the sea level rise impacts. Hugh Shipman and George Kaminsky (Washington Department of Ecology), and Tom Terich (Western Washington University) were instrumental in developing our perspectives on beach and bluff erosion. Doug Kelly (Island County) and Dave Nazy (Washington Department of Ecology) contributed to our understanding of the saltwater intrusion problem for coastal aquifers. Several people that helped us to understand the effects of sea level rise on ports include Sue Mauermann and Cindy Lin at the Port of Tacoma, and Burr Stewart and Eric Hanson at the Port of Seattle. Finally, effects of climate on shellfish and aquaculture were largely elucidated by the writings and presentations of Dan Cheney and Bill Dewey (Pacific Shellfish Institute) and Stephanie

Moore (NOAA, Northwest Fisheries Science Center and School of Oceanography, University of Washington). None of these individuals can be held responsible for any errors or misperceptions expressed in this paper.

References

Allan JC, Komar PD (2006) Climate controls on US west coast erosion processes. J Coast Res 22: 511-529.

Barlow PM (2003) Ground water in freshwater-saltwater environments of the Atlantic coast: U.S. Department of the Interior and U.S. Geological Survey Circular 1262: 1-113

Barton R, Frink L (2007) Algorithmic property valuation for Whidbey Island. Available online at: www.zillow.com

Bailey A, Berry H, Bookheim B, and Stevens D (1998) Probability-based estimation of nearshore habitat characteristics. In: Proceedings of Puget Sound Research ’98 Conference, Seattle, WA. Online at: http://www.dnr.wa.gov/Publications/aqr_nrsh_hab_estimate98.pdf

Baum R, Chleborad A, Schuster R (1998) Landslides triggered by the winter 1996-97 storms in the Puget Lowland, Washington. Accessed on 26 February 2008; Available online at: http://pubs.usgs.gov/of/1998/ofr-98-239/ofr-98-239.html

Cheney, D and Dewey B (2006) Shellfish and climate change: Ecological and economic effects. Powerpoint Presentation to the Washington State Climate Project. Pacific Shellfish Institute

City of Bainbridge Island (2007) Summary of new best available science: Geologically hazardous areas. Available online at: http://www.ci.bainbridge-sl.wa.us/documents/PCD _CAO_2007_05_BI_SummaryNewBAS_111407.pdf .

Daniels RC, Huxford RH, McCandless D (1998) Coastline mapping and identification of erosion hazard areas in Pacific County, Washington. Paper presented at the ESRI International Users Conference, San Diego, California

Dion NP, and Sumioka SS (1984) Seawater intrusion into coastal aquifers in Washington, 1978: U.S. Geological Survey Water-Supply Bull 56: 10 of 14 pgs.

Doney SC (2006) The dangers of ocean acidification. Sci Am (March) 294: 58-65

Feely RA, Sabine CL, Hernandez-Ayon JM, Ianson D, Hales B (2008) Evidence for upwelling of corrosive ‘acidified’ water onto the continental shelf. Sci Express (May): 1-4

Finlayson D (2006) The geomorphology of Puget Sound beaches. Puget Sound Nearshore Partnership. Technical Report 2006-02.

Gabriel AO, Terich TA (2005) Cumulative patterns and controls of seawall construction. Thurston County, Washington. J Coast Res 21: 430-440.

Gordon DG, Blanton NE, Nosho TY, Chew KK (2003) Heaven on the half shell. Portland: Westwinds Press

Graham NE, Diaz HF (2001) Evidence for Intensification of north pacific Winter Cyclones since 1848. Bull Amer Meteor Soc 82(9): 1869-1893.

Horner RA, Garrison DL, Plumley FG (1997) Harmful algal blooms and Red Tide problems on the U.S. West Coast. Limnol and Ocean 42: 1076-1088

Intergovernmental Panel on Climate Change (IPCC) (2007) Climate Change 2007: The Physical Science Basis. Contribution of working group I to the fourth assessment report. Cambridge University Press, Cambridge, United Kingdom and New York, NY, USA

Island County (2006) Multi-jurisdiction hazard mitigation plan: Island County profile and hazard identification and vulnerability assessment. December 2006. Online at http://www.islandcounty.net/gsa/des/documents/SECTION3V5_000.pdf.

Island County (2005) Island County water resource management plan final draft.

Johannessen J, MacLennan A (2007) Beaches and bluffs of Puget Sound and the northern straits. Puget Sound Nearshore Partnership, 1-34

Jones MA (1985) Occurrence of ground water and potential for seawater intrusion, Island County, Washington. US Geological Survey Water-Resources Investigations Rep. 85-4046, 6 p

Kaminsky G, Ruggiero P and Gelfenbaum G (1998) Monitoring Coastal Change in southwest Washington and Northwest Oregon during the 1997/98 El Nino. Shore and Beach (July):42-51.

Kelly D (2005) Seawater intrusion topic paper (final), Island County: WRIA 6 Watershed Planning Process, 1-30

Komar PD (1998) The Pacific Northwest coast. Duke University Press. Durham, North Carolina

Martin J (2007) Hungry sea devours dreams. The Seattle Times, September 14, Local news section. Online at: http://community.seattletimes.nwsource.com/archive/?date=20070914&slug=washaway14m.

Moore SK, Trainer VL, Mantua NJ, Parker D, Laws EA, Backer LC, Fleming LE (2008) Impacts of climate variability and future climate change on harmful algal blooms and human health. Environmental Health 7(Suppl 2): S4.

Morton RA, et al. (2007) Forcing of Large-Scale Cycles of Coastal Change at the Entrance to Willapa Bay, Washington. Marine Geol 246: 24-41

Mote P, Petersen A, Reeder S, Shipman H, and Whitely-Binder L (2008) Sea level rise in the coastal waters of Washington State. A report by the University of Washington Climate Impacts Group and the Washington Department of Oceanography

National Oceanic and Atmospheric Administration (May 2008) State of the science FACT SHEET: Ocean acidification. Available online at: http://www.pmel.noaa.gov/co2/OA/

National Oceanic and Atmospheric Administration (November 2004) Bainbridge Island nearshore habitat characterization and assessment: Management strategy prioritization, and monitoring recommendations. Available online at: http://ci.bainbridge-isl.wa.us/.

Pacific Coast Shellfish Growers Association (2008) Shellfish farming. Available online at: http://www.pcsga.org/ (accessed February 16, 2008)

Patz JA, Olson SH, Gray AL (2006) Climate change, oceans, and human health. Ocean 19: 52-59

Ruggiero P, et al. (1997) Extreme waves and coastal erosion in the Pacific Northwest. Paper presented at the Ocean Wave Measurements and Analysis, Proceedings of the 3rd International Symposium, Waves

Shipman H (2004) Coastal bluffs and sea cliffs on Puget Sound, Washington. In: Formation, evolution, and stability of coastal cliffs – status and trends, Hampton M, Griggs G (eds) U.S. Geological Survey Professional Paper 1693, 81-94.

Shorelines Hearings Board, State of Washington (2007) LEONEL S. and ISLE K. STOLLAR, husband and wife; PAUL B. and MARGERY M. GREENAWALT, husband and wife; PATRICK J. and SUZANNE C. MILLER, husband and wife; STEPHEN and FRANCINE SADOWSKY, husband and wife; and MARK and CHERYL VRIELING, husband and wife, Petitioners, v. CITY OF BAINBRIDGE ISLAND, and STATE OF WASHINGTON, DEPARTMENT OF ECOLOGY (October 25). Accessed on 26 February 2008 at:http://www.eho.wa.gov/searchdocuments/2007%20Archive/shb%2006-024,027%20final.pdf

Snover AK, Whitely Binder L, Lopez J, Willmott E, Kay J, Howell D, Simmonds J (2007) Preparing for climate change: A guidebook for local, regional, and state governments. In association with and published by ICLEI- Local Governments for Sustainability, Oakland, CA

Tangley L (1988) Preparing for climate change. BioScience 38: 14-18

Taylor K, Culverwell H, Cambalik J (2005) Educating shoreline landowners: Examples From King, Whatcom, Kitsap, Jefferson, Mason, and Pierce Counties; A perspective on approaches and effectiveness in eliciting on-the-ground change. Proceedings of the 2005 Puget Sound Georgia Basin Research Conference: 1-6

Terich TA (1987) Living with the shore of Puget Sound and the Georgia Strait. Duke University Press

The Seattle Times (2008) Accessed online at: http://seattletimes.nwsource.com/html/localnews/ 2004409777_growth_shorelines15m1.html)

Thurston County (2005) Best available science/guidance geologic hazard areas: Planning commission public hearing draft. Accessed on 26 February 2008; Online at: http://www.co.thurston.wa.us/permitting/Critical_Areas/Best_Science_Docs/BAS%20Draft%20-%20Geologic%20Hazard%20Areas%207-20-05.pdf

Titus JG (1986) Greenhouse effect, seal level rise, and coastal zone management. Coast Zone Manage J 14(3): 147-171.

"Treasures of the Tidelands." (2003) Shellfish Econom: 1-2

U.S. Geological Survey (2004) Estimating ground-water recharge from precipitation on Whidbey and Camano Islands, Island County, Washington, water years 1998 and 1999. Water-Resources Investigations Report 03-4101. Version 1.20. Online at: http://pubs.usgs.gov/wri/wri034101/.

Vedonck D (2006) Contemporary vertical crustal deformation in Cascadia. Technophysics 417: 221-250

Walsh TJ, et al. (2005) Tsunami hazard map of the Anacortes-Whidbey Island Area, Washington: Modeled tsunami inundation from a Cascadia Subduction Zone Earthquake. Washington State Department of Natural Resources. January

Walters L (1971) Reconnaissance of sea-water intrusion along coastal Washington, 1966-68: U.S. Geological Survey Water-Supply Bulletin 32: 51

Washington Department of Ecology (2007) Puget Sound shorelines. Accessed on March 3, 2008; Available online at: http://www.ecy.wa.gov/programs/sea/pugetsound/index.html.

Washington State Department of Ecology (2008) Washington coastal atlas https://fortress.wa.gov/ecy/coastalatlas/viewer.htm (accessed February 11, 2008)

Williams GD, Thom RM, Miller MC, Woodruff DL, Evans NR, Best PN (2003) Bainbridge Island nearshore assessment: Summary of best available science. PNWD-3233. Prepared for the City of Bainbridge Island: Bainbridge Island, WA, by Battelle Marine Sciences Laboratory: Sequim, WA

Zhang K, Douglas BC, Leatherman SP (2004) Global warming and coastal erosion. Clim Chang 64: 41-58

Zelo I, Shipman H, Brennan J (2000) Alternative bank protection measures for Puget Sound Shorelines. Shorelands and Environmental Assistance Program, Washington Department of Ecology

Photo credit, page 295: Climate Impacts Group, University of Washington

9: Stormwater Infrastructure

Precipitation Extremes and the Impacts of Climate Change on Stormwater Infrastructure in Washington State

Eric A. Rosenberg[1], Patrick W. Keys[1], Derek B. Booth[1,2], David Hartley[3], Jeff Burkey[4], Anne C. Steinemann[1,5], and Dennis P. Lettenmaier[1]

Abstract

Stormwater management facilities are important elements of the civil infrastructure that can be sensitive to climate change, particularly to precipitation extremes that generate peak runoff flows. The design and anticipated performance of stormwater infrastructure is based on either the presumed characteristics of a "design rainstorm" or the continuous simulation of streamflow driven by a time series of precipitation. Under either approach, a frequency distribution of precipitation is required, either directly or indirectly, together with an underlying assumption that the probability distribution of precipitation extremes is statistically stationary. This assumption, and hence both approaches, are called into question by climate change. We therefore examined both historical precipitation records and simulations of future rainfall to evaluate past and prospective changes in the probability distributions of precipitation extremes across Washington State. The historical analyses were based on hourly precipitation records for the time period 1949–2007 from weather stations surrounding three major metropolitan areas of the state: the Puget Sound region (including Seattle, Tacoma, and Olympia), the Vancouver (WA) region (including Portland, OR), and the Spokane region. Changes in future precipitation were simulated using two runs of the Weather Research and Forecast regional climate model (RCM) for the time periods 1970–2000 and 2020–2050, statistically downscaled from the ECHAM5 and CCSM3 Global Climate Model and bias-corrected against the SeaTac Airport rainfall record. Downscaled and bias-corrected hourly precipitation sequences were then used as input to the HSPF hydrologic model to simulate streamflow in two urban watersheds in central Puget Sound. Few statistically significant changes in extreme precipitation were observed in the historical records, with the possible exception of the Puget Sound. RCM simulations generally indicate increases in extreme rainfall magnitudes throughout the state, but the range of projections is too large to predicate engineering design, and actual changes could be difficult to distinguish from natural variability. Nonetheless, the evidence suggests that drainage infrastructure designed using mid-20th century rainfall records may be subject to a future rainfall regime that differs from current design standards.

[1] Department of Civil and Environmental Engineering, University of Washington, Seattle, Washington
[2] Stillwater Sciences, Santa Barbara, California
[3] Northwest Hydraulic Consultants, Seattle, Washington
[4] King County Water and Land Resources Division, Seattle, Washington
[5] Evans School of Public Affairs, University of Washington, Seattle, Washington

1. Introduction

Infrastructure is commonly defined as the various components of the built environment that support modern society (e.g., Choguill 1996; Hanson 1984). These encompass utilities, transportation systems, communication networks, water systems, and other elements that include some of the most critical underpinnings of civilization. Thus even modest disruptions to infrastructure can have significant effects on daily life, and any systematic change in the frequency or intensity of those disruptions could have profound consequences for economic and human well-being.

The elements of Washington's urban infrastructure are not equally vulnerable to weather conditions or climate regime, however, and several components (energy, water supply, and coastal facilities) are the subject of other reports in this volume (Hamlet et al. 2009, this report; Huppert et al. 2009, this report; Vano et al. 2009a, b, this report). Prior studies have considered the vulnerability of these and other infrastructure elements, and the daily news provides frequent examples of those elements of our Northwest cities that are most vulnerable to the vagaries of even present-day fluctuations in weather. The Chehalis River floods in December 2007, for example, resulted in the closure of Interstate 5, the state's major north–south transportation artery, for four days at an estimated cost of over $18M (WSDOT 2008).

In this paper, we focus on one element of the civil infrastructure, stormwater management facilities in urban areas. The relationship of this sector to climate, and particularly to precipitation extremes on which much of its facility design is based, is clear. Recent improvements in the ability to downscale the projections of global climate models to the local scale (Salathé et al. 2005) have made feasible the preliminary evaluation of climate change impacts on the spatially heterogeneous, rapidly fluctuating behavior of urban stormwater. Consequences of inadequate stormwater facilities can be severe, but adaptation strategies are available and relatively straightforward if anticipated well in advance (Kirschen 2004; Larsen 2007; Shaw 2005).

Historical management goals for urban stormwater have emphasized safe conveyance, with more recent attention also being given to the consequences of increased streamflows on the physical and biological integrity of downstream channels (Booth and Jackson 1997). Urbonas and Roesner (1993) classify drainage systems into two categories – minor, consisting of the roadside swales, gutters, and sewers typically designed to convey runoff events of 2- or 5-year return periods, and major, which include the larger flood control structures designed to manage 50- or 100-year events. While design events can be based on direct observations of runoff, they are more commonly based on precipitation events with equivalent likelihoods of occurrence, due to the limited availability of runoff observations in urban areas. Hence, while we give some consideration to modeled trends in runoff, the focus of this paper is on the precipitation events from which they result, and specifically those events of 1-hour duration (since many of the smaller watersheds have times of concentration of 1 hour or less) and 24-hour duration (which is that most commonly used for purposes of design).

It is worth noting that more complicated phenomena with implications for stormwater management, such as rain-on-snow events, are also subject to the effects of a changing climate. We do not consider trends in these phenomena, however, since our modeling approach is not well-calibrated for such conditions, which are not necessarily significant in the lowland urban areas that are the focus of our study. Nor do we consider changing patterns of development, which may also considerably impact runoff magnitudes, but are not related to climatic factors. Nonetheless, future changes in climate that may alter precipitation intensity or duration would likely have consequences for urban stormwater discharge, particularly where stormwater detention and conveyance facilities were designed under assumptions that may no longer be correct. The social and economic impact of increasing the capacity of undersized stormwater facilities, or the disabling of key assets because of more severe flooding, could be substantial.

This study thus addresses the following questions:

- What are the historical trends in precipitation extremes across Washington State?
- What are the projected trends in precipitation extremes over the next 50 years in the state's urban areas?

What are the likely consequences of future changes in precipitation extremes on urban stormwater infrastructure?

2. Background

Despite the inherent challenges in characterizing changes in extreme rainfall events, a number of studies have either assessed historical trends in precipitation metrics or investigated the vulnerability of stormwater infrastructure under a changing climate, as described below.

2.1. Historical Trends in Precipitation Extremes

Several studies have evaluated past trends in rainfall extremes of various durations, mostly at national or global scales. Karl and Knight (1998) found a 10% increase in total annual precipitation across the contiguous United States since 1910, and attributed over half of the increase to positive trends in both frequency and intensity in the upper ten percent of the daily precipitation distribution. Kunkel et al. (1999) found a national increase of 16% from 1931-96 in the frequency of 7-day extreme precipitation events, although no statistically significant trend was found specifically for the Pacific Northwest. A follow-up study that employed data extending to 1895 (Kunkel et al. 2003) generally reinforced these findings, but noted that frequencies for some return periods were nearly as high at the beginning of the 20th century as they were at the end, suggesting that natural variability could not be discounted as an important contributor to the observed trends.

Groisman et al. (2005) analyzed precipitation data over half of the global land area and found "an increasing probability of intense precipitation events for many extratropical regions including the United States." They defined intense precipitation events as the upper 0.3% of daily observations, and used three model simulations with transiently increasing greenhouse gases to offer preliminary evidence that these trends are linked to global warming. Pryor et al. (2009) analyzed eight metrics of precipitation in century-long records throughout the contiguous USA, finding that statistically significant trends generally indicated increases in intensity of events above the 95th percentile, although few of these were located in Washington State. However, Madsen and Figdor (2007), in a study that systematically analyzed trends from 1948 to 2006 by both state and metropolitan area, found a statistically significant increase of 30% in the frequency of extreme precipitation in Washington, and of 45% in the Seattle-Tacoma-Bremerton area. Interestingly, however, trends in neighboring states were widely incongruent, with a statistically significant *decrease* of 14% in Oregon and a non-significant increase of 1% in Idaho.

While these studies provide useful impressions of general trends in precipitation extremes, their results are not applicable to infrastructure design, which requires estimates of the distributions of extreme magnitudes instead of, for example, the number of exceedances of a fixed threshold. Relatively few such approaches have been explored to date, with the exception of Fowler and Kilsby (2003), which used regional frequency analysis to determine changes in design storms of 1, 2, 5, and 10 day durations from 1961 to 2000 in the United Kingdom. We take this approach one step further and analyze changes in design storms of sub-daily durations, as discussed in Section 3.

2.2. Future Projections and Adaptation Options

Only a few previous studies have evaluated the vulnerability of stormwater infrastructure to climate change, with considerable variation in their methodologies. Denault et al. (2002) assessed urban drainage capacity under future precipitation for a 440-ha (1080-ac) urban watershed in North Vancouver, Canada. Observed trends of precipitation intensity and magnitude for the period 1964–1997 were projected statistically to infer the magnitude of design storms in 2020 and 2050, and the consequences for urban discharges were modeled using the SWMM hydrologic model[1]. They evaluated only the potential impacts on pipe capacity, finding that flow increases were sufficiently small that few if any new problems were likely to be created. They also observed that any given watershed has unique characteristics that affect its ability to accommodate specific impacts, thus emphasizing the importance of site-specific evaluation. They also recognized that uniform climate changes could produce varying levels of impact on any individual municipality, because of differences in topography, watershed size, level of development, and(or) existing infrastructure drainage capacity.

Waters et al. (2003) evaluated how a small (23 ha [58 ac]) urban watershed in the Great Lakes region (Burlington, Ontario) would be affected by a 15% increase in rainfall depth and intensity. This increase was presumed from a literature review and prior analysis of other nearby catchments. Their study emphasized the adaptive measures that could be taken to absorb the increased rainfall, and they evaluated the efficacy of alternative

[1] http://www.epa.gov/ednnrmrl/models/swmm/

adaptations to projected flow increases using SWMM. Their recommended measures included downspout disconnection (50% of connected roofs), increased depression storage (by 45 m^3/impervious hectare), and increased street detention storage (by 40 m^3/impervious hectare).

Shaw et al. (2005) also emphasized the consequences of presumed increases in precipitation on flooding of stormwater systems, while relying on relatively simplistic projections of future precipitation. They defined low, medium and high climate-change scenarios, based on projections of temperature increase, and translated those temperature increases into linear increases in 24-hour rainfall events. Consequences on stormwater capacity for a small urban watershed in central New Zealand (the Wairau Valley watershed in North Shore City, North Island), using both event-based and continuous hydrologic models, were then evaluated for inadequate infrastructure capacity.

Watt et al. (2003) examined the multiple impacts that climate change could have on stormwater design and infrastructure in Canada, suggesting adaptive measures for urban watersheds with their associated advantages, disadvantages, and estimated costs. The authors also examined two case studies of adapting stormwater infrastructure to climate change; one was the study of Waters et al. (2003) and the other was a study of a residential area in urban Ottawa. They offered a useful qualitative rating system to compare the environmental, social, and aesthetic implications of different structural solutions to stormwater runoff management.

Crabbé and Robin (2006) studied the need for institutional "adaptation" to be better able to respond and adapt to climate change. The authors focused on the bureaucracies of Canada and the financial and physical responsibility that local municipalities will need to bear in adapting infrastructure to climate change. The review considered the institutional costs for preparing water-resources infrastructure for climate change, and the potential increases in both revenues and expenditures for local and regional governments. It also acknowledged institutional barriers, such as a lack of skilled scientists, over-dependence on engineering consultants, and reliance on management-by-crisis rather than long-term management and planning. The study offered potential approaches to solve these impediments, including easily understandable climate-change reporting, increased citizen participation, and financial assistance from regional governments.

These prior studies provide a good methodological starting point for identifying the most likely consequences of climate change on stormwater infrastructure, along with an initial list of potentially useful adaptation measures. Like those presented in Section 2.1, however, their greatest shortcoming uniformly lies in their rudimentary characterization of the precipitation regimes that drive the responses (see also Kirschen et al. 2004; Trenberth et al. 2003). Our report seeks to bridge this gap between presumptive (but poorly quantified) future climate change and the acknowledgment that infrastructure adaptation is generally less costly and disruptive if necessary measures are undertaken well in advance of anticipated changes.

We have approached this task both by analyzing the variability in historical precipitation extremes across Washington State and by utilizing regional climate model results, now available at a higher resolution than previously possible, to characterize future projections of precipitation extremes. We processed these results in a bias-correction and statistical-downscaling procedure to drive a continuous hydrologic model for prediction of urban streamflows in one region of the state, the central Puget Lowland. These results have allowed a preliminary evaluation of the implications of simulated precipitation extremes for urban drainage and urban flooding.

3. Historical Precipitation Analysis

As a precursor to investigating potential changes in future precipitation extremes as simulated by climate models, we examined whether such changes might already be occurring in the three major urban areas of Washington State. Three different analyses were applied to historical rainfall records, beginning in 1949, to look for such trends: (1) regional frequency analysis, (2) precipitation event analysis, and (3) exceedance-over-threshold analysis. In the *regional frequency analysis,* we used a technique adapted from the regional L-moments method of Hosking and Wallis (1997) to evaluate changes in rainfall extremes over the period 1956–2005 for a wide range of frequencies and durations. The *precipitation event analysis* used a method adapted from Karl and Knight (1998) to determine trends in annual precipitation event frequency and intensity, based on the occurrence of individual rainfall "events" of presumed one-day duration. Finally, the *exceedance-over-threshold analysis* examined the number of exceedances above a range of threshold values for the depth of precipitation, also on the basis of one-day rainfall events.

3.1. Regional Frequency Analysis

The precipitation frequency analysis (sometimes referred to as the index-flood approach) analyzed the annual maximum series for aggregates of hourly precipitation ranging from one hour to ten days for the three major urban areas in Washington State: the Puget Sound region (including Seattle, Tacoma, and Olympia), the Vancouver region (including Portland, OR), and the Spokane region. The approach entails fitting a frequency distribution to time series of annual precipitation maxima from a set of *multiple* stations within a region, rather than fitting the data from a single station to an individual distribution. The strength of this method is in the regionalization, allowing for a larger sampling pool of data points and a more robust fit to the probability distribution, resulting in estimates of extreme quantiles that are considerably less variable than at-site estimates (e.g., Lettenmaier et al. 1987). Data originated from National Climatic Data Center (NCDC) hourly precipitation archives and were extracted using commercial software provided by Earth Info, Inc. Stations selected for the analysis are shown in Figure 1 and listed in Table 1. The minimum requirement for inclusion was a reported period of record of 40 years. Years with more than 40% missing data in the fall and winter months were removed from the analysis, since precipitation events during these two seasons have the highest probabilities of being annual maxima, and so the precipitation that was recorded could misrepresent that year's true annual maximum.

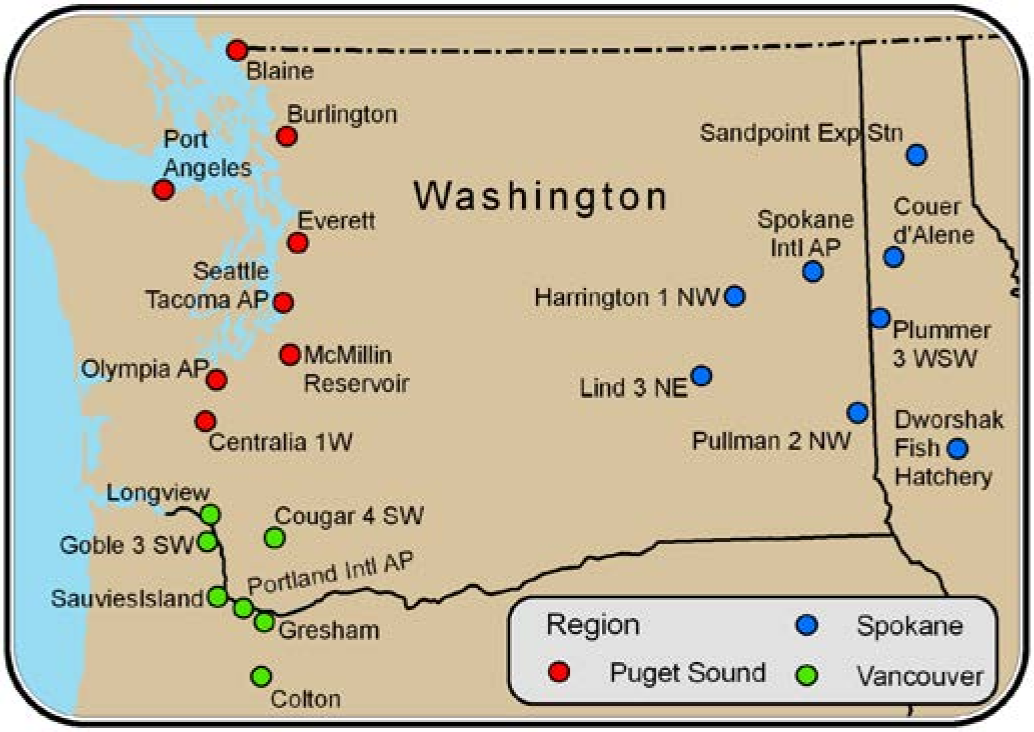

Figure 1. Locations of weather stations used in the regional frequency analysis, grouped by region.

A basic premise of regional frequency analysis is that all sites within a region can be described by a common probability distribution after site data are divided by their at-site means. These common probability distributions are referred to as regional growth curves. Design storms at individual sites can then be calculated by reversing the process, multiplying the regional growth curves by at-site means. The approach provides the advantage of greater sample sizes, which allow for more reliable estimation of long return-period events even if individual records are otherwise too short.

Annual maximum precipitation depths for multiple durations (1, 2, 3, 6, 12, and 24 hours; and 2, 5, and 10 days) were identified for each station and combined into pools in order to calculate regional L-moment parameters (Fowler and Kilsby 2003; Hosking and Wallis 1997). These parameters were then used to fit data to Generalized Extreme Value (GEV) distributions and to generate regional growth curves. We then analyzed for any historical trends in precipitation by dividing the precipitation record from each region into two 25-year periods (1956–1980 and 1981–2005). We investigated a finer division of the data into five 10-year periods, but the results were statistically inconclusive and so are not reported here. For each of the two 25-year periods, design storm magnitudes were determined at Seattle Tacoma (SeaTac), Spokane, and Portland International Airports based on the regional growth curves and the means at those stations. A bootstrap method (Efron 1979), whereby one year of record was removed at a time and growth curves refitted, was used to provide uncertainty bounds about the GEV distributions. Changes in design storm magnitudes were determined by comparing the distributions from each period. Statistical significance for differences in distributions was found using the Komolgorov-Smirnov test, for differences in means using the Wilcoxon rank-sum test, and for trends in the entire time series using the Mann-Kendall test, all at a two-sided significance level of 0.05.

Table 1. Stations used in the regional frequency analysis.

Region	Station	State	Co-op ID	Reported Period	# of Years Removed	Sample Size
Puget Sound	Blaine	WA	729	1949–2007	7	52
	Burlington	WA	986	1949–2007	5	54
	Centralia 1W	WA	1277	1968–2007	3	37
	Everett	WA	2675	1949–2007	4	55
	McMillin Reservoir	WA	5224	1949–2007	14	45
	Olympia AP	WA	6114	1949–2007	8	51
	Port Angeles	WA	6624	1949–2007	13	46
	Seattle Tacoma AP	WA	7473	1949–2007	0	59
Spokane	Couer d'Alene	ID	1956	1949–2007	20	39
	Dworshak Fish Hatchery	ID	2845	1967–2007	1	40
	Harrington 1 NW	WA	3515	1962–2007	5	41
	Lind 3 NE	WA	4679	1949–2007	5	54
	Plummer 3 WSW	ID	7188	1949–2007	12	47
	Pullman 2 NW	WA	6789	1949–2007	6	53
	Sandpoint Exp Stn	ID	8137	1960–2007	5	43
	Spokane Intl AP	WA	7938	1949–2007	0	59
Vancouver	Colton	OR	1735	1949–2007	2	57
	Cougar 4 SW	WA	1759	1949–2007	3	56
	Goble 3 SW	OR	3340	1949–2007	2	57
	Gresham	OR	3521	1949–2007	9	50
	Longview	WA	4769	1955–2007	10	43
	Portland Intl AP	OR	6751	1949–2007	0	59
	Sauvies Island	OR	7572	1949–2007	1	58

The summarized results (Table 2) present the average of changes in design storm magnitudes across all recurrence intervals (from 1.01-yr through 100-yr), which generally is about the same magnitude of change seen in the 2-year events. Changes at SeaTac were consistently positive, with the greatest increases seen at the 24-hour and 2-day durations. Changes at Spokane were mixed, while changes at Vancouver were mostly negative, with the notable exception of the 1- and 24-hour durations. None of the changes were found to be statistically significant, however, with the exception of the 2-day and (possibly) 24-hour durations at SeaTac.

A breakdown of changes by return period is provided for the 1- and 24-hour durations in Table 3, so chosen because of their relevance to urban stormwater infrastructure as indicated in Section 1. Included in the table are estimated return periods of the 1981–2005 events that are equal in magnitude to the 1956–1980 events having the return periods indicated in the first column. Rainfall frequency curves that illustrate the changes in 1- and 24-hour durations listed in Table 3 are shown in Figure 2. Shaded regions represent uncertainty bounds as determined by bootstrapping the historical data but do not necessarily indicate statistical significance or nonsignificance in changes.

In summary, the last half-century has seen significant increases in extreme precipitation in the Puget Sound region, with much more ambiguous changes in other parts of the state. For changes in the 24-hour duration at SeaTac, which come closest to attaining statistical significance, the largest change is seen at the 50-year return period, which increases in magnitude by 37%. Thus, what was a 50-year storm (i.e., having a 2% (1/50) chance of occurring in any given year) from 1956–1980 became an 8.4-year storm (i.e., having a 12% (1/8.4) chance of occurring in any give year) from 1981–2005, and is thus about six times as likely to occur. These results suggest that urban stormwater systems in the Puget Sound region probably have already experienced substantially increased peak discharges over the past half-century.

3.2. Precipitation Event Analysis

In addition to changes in extreme precipitation frequency distributions, it is also useful to recognize any trends in total annual precipitation, and to determine whether such trends are due to changes in storm frequency, storm intensity, or both. An analysis to determine these trends was performed on the NCDC precipitation data by adapting the method of Karl and Knight (1998), which requires a continuous precipitation record for its application. Thus, we used the single station in each of the urban areas analyzed in the previous section with the most complete record—the airport gauges at Seattle-Tacoma, Spokane, and Portland. Each had a common period

Table 2. Changes in average fitted annual maxima between 1956–1980 and 1981–2005, as determined by the regional frequency analysis at SeaTac, Spokane, and Portland Airports. Kolmogorov-Smirnov (top), Wilcoxon rank-sum (middle), and Mann-Kendall (bottom) p-values are provided in italics. Those p-values found to be significant at a two-sided α of 0.05 are indicated in bold.

	SeaTac	Spokane	Portland
1-hour	+7.2%	-1.0%	+4.4%
KS	*0.877*	*0.124*	*0.237*
rank-sum	*0.547*	*0.272*	*0.217*
MK	*0.192*	*0.892*	*0.137*
2-hour	+10.0%	-5.2%	-5.3%
KS	*0.877*	*0.649*	*0.990*
rank-sum	*0.534*	*0.409*	*0.846*
MK	*0.184*	*0.800*	*0.926*
3-hour	+14.2%	+0.3%	-6.6%
KS	*0.124*	*0.877*	*0.414*
rank-sum	*0.398*	*0.683*	*0.491*
MK	*0.166*	*0.704*	*0.404*
6-hour	+12.7%	+0.7%	-8.2%
KS	*0.649*	*0.414*	*0.237*
rank-sum	*0.438*	*0.600*	*0.130*
MK	*0.199*	*0.926*	*0.141*
12-hour	+18.7%	+14.9%	-5.2%
KS	*0.237*	*0.237*	*0.124*
rank-sum	*0.187*	*0.151*	*0.095*
MK	*0.226*	*0.070*	*0.113*
24-hour	+24.7%	+6.9%	+1.9%
KS	*0.237*	*0.649*	*0.414*
rank-sum	*0.052*	*0.567*	*0.332*
MK	*0.140*	*0.584*	*0.302*
2-day	+22.3%	+2.9%	-6.6%
KS	*0.124*	*0.990*	*0.414*
rank-sum	***0.023***	*0.923*	*0.151*
MK	***0.038***	*0.781*	*0.185*
5-day	+13.4%	-10.1%	-5.0%
KS	*0.237*	*0.124*	*0.649*
rank-sum	*0.082*	*0.146*	*0.362*
MK	*0.276*	*0.161*	*0.361*
10-day	+7.3%	-3.9%	-9.7%
KS	*0.124*	*0.877*	*0.237*
rank-sum	*0.146*	*0.541*	*0.146*
MK	*0.303*	*0.503*	*0.155*

Table 3. Distribution of changes in fitted 1- and 24-hour annual maxima from 1956–1980 to 1981–2005 at SeaTac, Spokane, and Portland Airports. Numbers in italics represent the return periods of the 1981–2005 events that are equal in magnitude to the 1956-1980 events having the return periods indicated in the first column. As an example, for the 1-hour storm at SeaTac, the 25-year event from 1956 to 1980 [having a 4% (1/25) chance of occurring in any given year] became a 16.7-year event from 1981 to 2005 [having a 6% (1/16.7) chance of occurring in any given year]. Average changes across all return periods are provided at the bottom, matching those reported in Table 2, with Kolmogorov-Smirnov (top), Wilcoxon rank-sum (middle), and Mann-Kendall (bottom) p-values provided in italics. None of the changes were found to be significant at a two-sided α of 0.05.

Return Period (yrs)	1-hour Storm			24-hour Storm		
	SeaTac	Spokane	Portland	SeaTac	Spokane	Portland
2	+3.6% 1.8	+7.7% 1.7	+3.8% 1.8	+22.8% 1.4	+8.7% 1.6	-2.2% 2.1
5	+3.5% 4.4	+2.9% 4.5	+4.5% 4.2	+30.2% 2.1	+7.5% 3.6	+5.3% 4.1
10	+5.8% 8.1	-3.1% 11.3	+5.0% 8.0	+33.3% 3.0	+5.9% 7.4	+10.3% 6.5
25	+11.0% 16.7	-12.6% 45.0	+5.7% 19.0	+35.8% 5.3	+3.4% 20.4	+16.8% 11.8
50	+16.2% 27.9	-20.2% 140.0	+6.3% 36.8	+37.0% 8.4	+1.2% 46.3	+21.7% 18.1
Average	+7.2%	-1.0%	+4.4%	+24.7%	+6.9%	+1.9%
KS	0.877	0.124	0.237	0.237	0.649	0.414
rank-sum	0.547	0.272	0.217	0.052	0.567	0.332
MK	0.192	0.892	0.137	0.140	0.584	0.302

of record from January 1, 1949 to December 31, 2007, for a total of 59 years.

The central concept in this approach is that once trends in total annual precipitation are determined, the relative influence of changes in event *frequency* and changes in event *intensity* can be identified. Trends in event frequency can be determined by defining a precipitation event as any nonzero accumulation over a specified time interval, and tallying their number in each period. The remainder of the trends in total annual precipitation can then be attributed to the trends in event intensity, defined as the amount of precipitation in a given event.

This approach provides the additional advantage of determining whether changes were due to trends in light precipitation events, trends in heavy precipitation events, or both. This is a consequence of breaking down each rainfall record into multiple intervals based on event magnitude. For this study, an event was defined as any measurable precipitation over a 24-hour period (midnight-to-midnight), although this requires an assumption that any day with nonzero precipitation is a single "event" (even though a single storm may have spanned the division between two days while lasting less than 24 hours, or there could have been two events in one day separated by one or more hours of no rain).

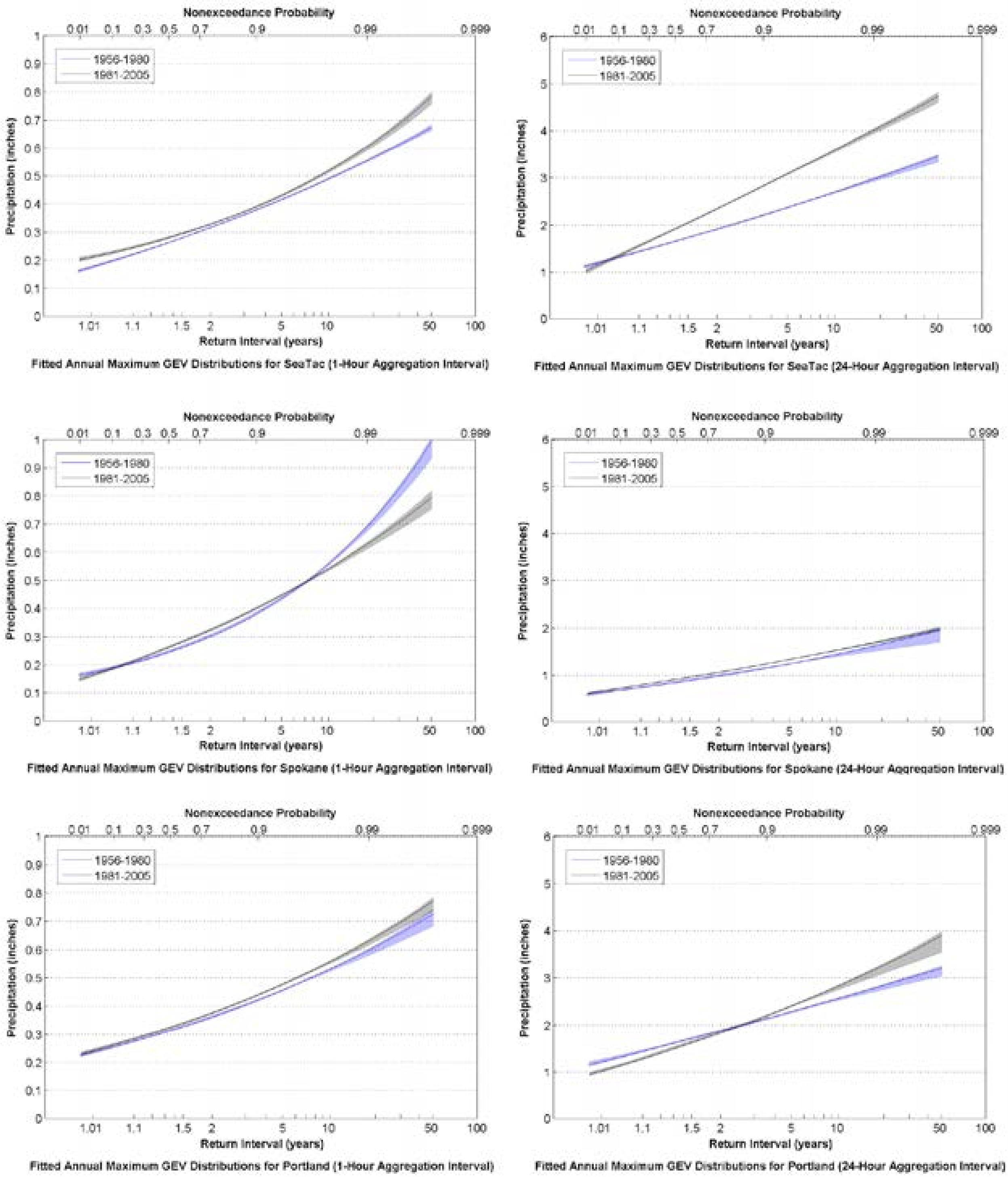

Figure 2. Changes in fitted 1- and 24-hour annual maximum distributions from 1956–1980 to 1981–2005. Uncertainty bounds as determined by a bootstrap method are indicated by the shaded areas. None of the changes were found to be significant at a two-sided α of 0.05, although the Wilcoxon rank-sum statistic for 24-hour distributions at SeaTac was significant at a two-sided α of 0.10. Changes at specific return periods are provided in Table 3.

The analysis is performed by first calculating both the total precipitation and the number of "events" for each year (as defined above), ranking those events from lowest to highest, and dividing them into 20 class intervals that each contain 1/20 of the total number of events for that year. Thus the first class interval is assigned the 5% of events with the lowest daily totals, the second class interval is assigned the 5% of events with the next lowest daily totals, etc. For each class, the average long-term precipitation per event (event intensity) is then calculated, and the trend in precipitation due to the trend in event frequency is calculated as:

$$b_e = \overline{P_e} b_f \ ,$$

where is the average long-term event intensity and is the percent change in the frequency of events, as determined by the slope of the linear regression line through a scatter plot of number of events vs. year. The trend in precipitation due to the trend in the annual intensity of events is then calculated as a residual using the expression:

$$b_i = b - b_e \ ,$$

where is the percent change in total precipitation, as determined by the slope of the linear regression line through a scatter plot of total precipitation versus year. Median and highest precipitation events are calculated regardless of class for each year, and trends again are determined by the slopes of their respective regression lines. All trends are divided by average values and multiplied by the 59-year period of analysis.

Results of the analysis are summarized at the annual level for all three stations in Table 4. Trends were tested for significance using the Mann-Kendall test at a two-sided significance level of 0.05. Although none

Table 4. Results of the precipitation event analysis from 1949 to 2007. Trends in annual precipitation are provided for the 59-year period as a percentage of the average annual precipitation, as are the portions of these trends due to trends in event frequency and event intensity. Trends in annual median and maximum event intensity are provided as a percentage of their respective long-term averages. Mann-Kendall p-values are provided in italics; none of the trends were found to be significant at a two-sided α of 0.05. An "event" is defined as any day with measurable (nonzero) precipitation.

	SeaTac	**Spokane**	**Portland**
Average annual number of events	154.5	110.2	152.1
Average annual precipitation (in)	38.2	16.5	36.6
Trend in annual precipitation *MK*	-8.9 % *0.219*	-13.0 % *0.055*	-8.3 % *0.202*
…due to trend in event frequency *MK*	-9.3 % *0.056*	-11.9 % *0.052*	-2.6 % *0.843*
…due to trend in event intensity *MK*	+0.4 % *0.628*	-1.1 % *0.433*	-5.7 % *0.239*
Trend in annual median event intensity *MK*	+4.6 % *0.917*	-1.4 % *0.437*	-2.7 % *0.420*
Trend in annual maximum event intensity *MK*	+39.0 % *0.174*	+9.1 % *0.527*	-2.3 % *0.798*

were found to be significant, trends were consistently negative for total precipitation and event frequency, and mostly negative for event intensity. As an example, at Spokane, total annual precipitation has decreased by 13.0% since 1949; 11.9% of this decrease was due to a decrease in event frequency, and the remaining 1.1% of this decrease was due to a decrease in event intensity. Trends in median event intensity were mixed, however, while trends in maximum event intensity were mostly positive.

Distributions of annual trends by class are presented in Figure 3, with the class interval containing the smallest 5% of events to the left of each graph and the class interval containing the largest 5% of events (i.e., extreme events) to the right. The sums of the trends in each class equal the cumulative values reported in Table 4. At SeaTac, for example, despite mostly negative trends in intensity for the lowest 19 class intervals, a relatively large increasing trend in the intensity of the extreme class interval causes the cumulative trend for intensity to be slightly positive. A closer inspection of the data behind these results at SeaTac reveals that 3 of the 4 highest 1-day totals since 1949 have occurred in the last five years.

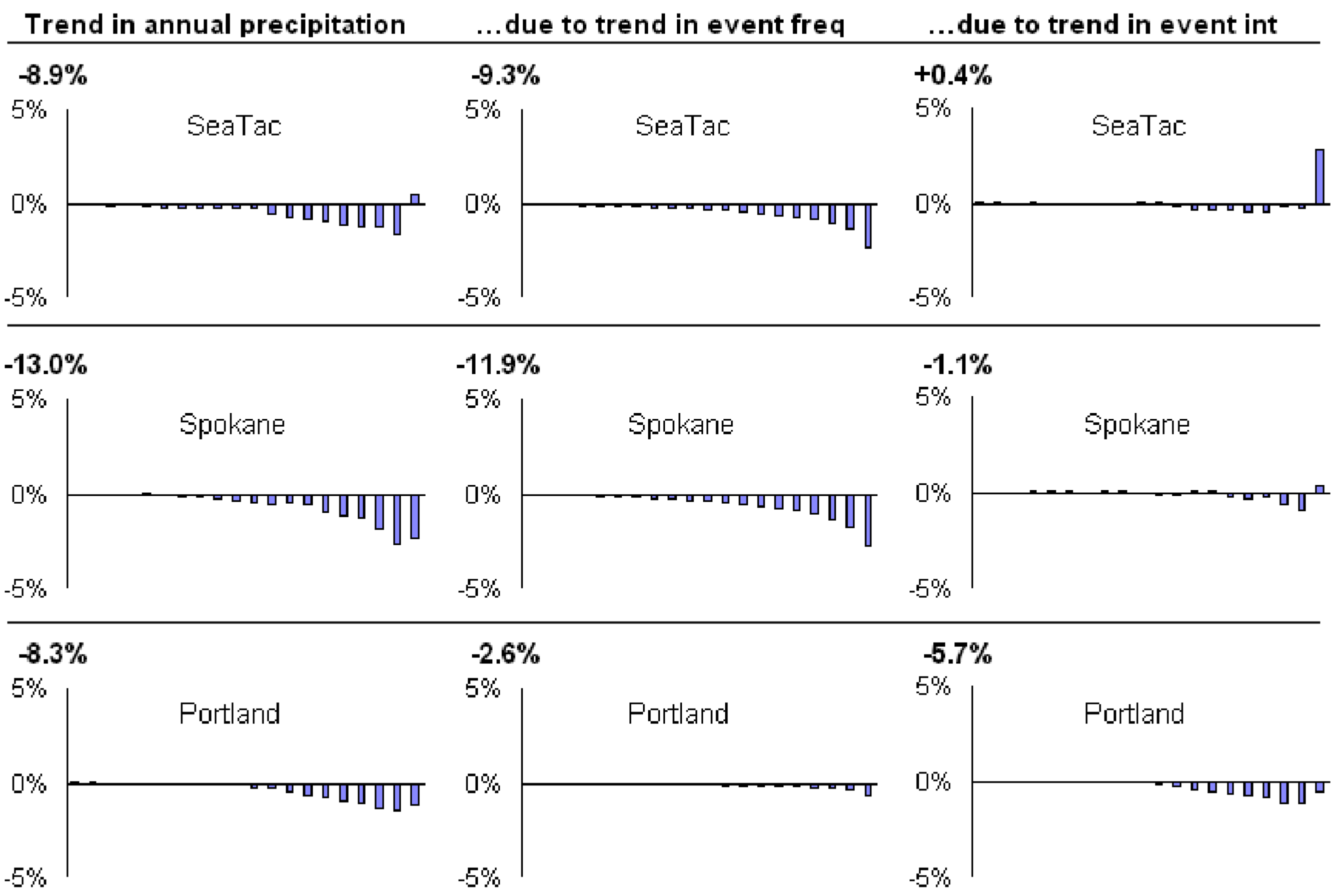

Figure 3. Distribution of trends reported in Table 4. At left are trends in annual precipitation; at center, the portion of the trends in annual precipitation due to trends in event frequency; at right, the portion of the trends in annual precipitation due to trends in event intensity. An "event" is defined as any day with measurable (nonzero) precipitation. Trends for individual class intervals are represented by the bars in each graph, with the class interval containing the smallest 5% of events at left and the class interval containing the largest 5% of events at right. Values above each graph show cumulative trends across all 20 class intervals.

3.3. Exceedance-Over-Threshold Analysis

In addition to the regional frequency and precipitation event analyses, examining the number of events exceeding a given threshold (e.g., 0.1 in, 0.2 in, etc.) throughout a precipitation record can provide more detailed information on historical changes in frequency. Such an "exceedance-over-threshold" analysis, distinct from a peak-over-threshold approach which then uses the magnitudes of these events to estimate design storms, was conducted for the three stations examined in Section 3.2. All recorded nonzero daily precipitation totals were again treated as single events. Trends were determined by linear regression and expressed as a percentage of the average annual number of exceedances over the 59-year period. The Mann-Kendall test was again employed to test for statistical significance at a two-sided significance level of 0.05.

As found in the precipitation event analysis, trends in the frequencies of exceedance (Table 5) were negative across all thresholds, suggesting a modest overall decrease in the number of rain events consistent with the decrease in event frequency found in Section 3.2. Statistically significant trends were found for events exceeding several of the thresholds, such as 0.2" at SeaTac displaying a 15% decrease over the 59-year period. This particular analysis does not consider exceedances of thresholds larger than 0.5" due to the small numbers of these that occur annually, which preclude any meaningful interpretation of trends regarding more extreme events.

3.3.1. Summary

Although the three components of the historical precipitation analysis demonstrate a high degree of variability in both time and space, a few patterns emerge from these analyses:

1. Results of the regional frequency analysis, which evaluated annual maxima, indicate consistently positive changes in precipitation extremes in the Puget Sound region, with significant increases occurring in 24-hour and 2-day storms. Results from Spokane and Portland-Vancouver, however, are more variable, and none of the changes in these regions are statistically significant.
2. Trends in the precipitation event and peak-over-threshold analyses are consistently negative in all three regions for both total precipitation and event frequency, though most are nonsignificant.
3. Overall, the rainfall record of the Puget Sound region suggests that total annual precipitation has decreased, but the magnitude of large, low-frequency events has increased across all durations. Spokane displays a similar pattern in total annual precipitation, but a less pronounced pattern in changes in event magnitude, which vary in sign depending on storm duration. Portland–Vancouver, in contrast, displays decreases in both total annual precipitation and extreme event magnitudes at most durations. The only statistically significant change with relevance to stormwater infrastructure, however, is the increase in magnitude of 24-hour extremes in the Puget Sound region.

Table 5. Results of the exceedance-over-threshold analysis from 1949 to 2007. Trends in the annual number of events exceeding the specified thresholds are provided for the 59-year period as a percentage of the average annual number of respective exceedances. Mann-Kendall p-values are provided in italics; those found to be significant at a two-sided α of 0.05 are indicated in bold. An "event" is defined as any day with measurable (nonzero) precipitation.

	0.1"	0.2"	0.3"	0.4"	0.5"
SeaTac	-10.9%	-15.0%	-15.8%	-13.1%	-12.4%
MK	*0.094*	***0.039***	***0.045***	*0.148*	*0.161*
Max	121	87	61	46	39
Min	68	40	25	12	9
Spokane	-14.8%	-15.1%	-21.2%	-23.9%	-17.7%
MK	***0.022***	*0.123*	*0.074*	*0.168*	*0.244*
Max	76	46	27	17	11
Min	38	19	8	2	2
Portland	-4.2%	-8.8%	-13.3%	-16.1%	-18.9%
MK	*0.356*	*0.153*	***0.038***	*0.141*	*0.187*
Max	116	92	69	51	41
Min	65	37	22	14	9

4. Modeled Trends in Future Extreme Precipitation

Urban watersheds are small and commonly provide rapid surface flow paths for runoff, thus responding very quickly to even short-duration events (Leopold 1968). Their discharge records reflect the influence of individual storm cells and localized bands of high-intensity rainfall, which can sometimes produce runoff responses that vary greatly over just a few kilometers (Gerstel et al. 1997). Thus the raw output from Global Climate Models (GCMs), on which most assessments of future climate are based, is not directly useable because the model grid resolution (100s of km) is much too coarse. For Washington State, however, two regional climate model simulations were performed to downscale the GCM output into hourly precipitation with spatial resolutions of 20 and 36 km (Leung et al. 2006; Salathé et al. 2008; Salathé et al. 2009, this report). Although these spatial and temporal scales are not ideal for capturing the behavior of urban runoff response, the use of nested model simulations to estimate annual maximum series of precipitation (as opposed to peak-over-threshold extremes only) represents a significant advance in our ability to understand precipitation at the local scales at which watersheds respond to intense rainfall.

The two regional climate model (RCM) simulations used here and described in Salathé et al. (2009, this report) use different IPCC (2007) GCM outputs as their boundary conditions. Because the RCM runs are linked via their boundary conditions to different GCMs that each predict future climate differently, and that also use slightly different global emissions scenarios, it is expected that they will also differ in their projections of future climate. Ideally, a multimodel ensemble at the regional scale, paralleling that being used for regional hydrologic analysis (e.g., Vano et al. 2009a, b, this report), would be available for our analyses. At present, however, this strategy is not computationally feasible (each RCM simulation required several months of computer time). Thus the results presented here can offer a sense of the likely direction and general magnitude of future changes in precipitation extremes, but reducing their substantial uncertainties must await additional RCM simulations that can be linked to the many other GCMs presently in existence.

4.1. RCM Summary

The two global climate models (GCMs) that were used to provide boundary conditions for the RCM simulations were the Community Climate System Model version 3.0 (CCSM3) under the A2 emissions scenario, and the Max Planck Institute's ECHAM5 under the A1B emissions scenario (Table 6). During the first half of the 21st century, atmospheric CO_2 concentrations are similar in both the A2 and the A1B emissions scenarios, and so differences in the RCM simulation results are most likely expressions of differences in the GCMs. Slight differences in spatial resolution may also influence these results, but they have not been systematically explored to date. Both CCSM3 and ECHAM5 are considered to be in the middle of the range of existing GCMs in their projections of precipitation for the Pacific Northwest (Mote et al. 2005).

The RCM employed to downscale both GCMs was the Advanced Research Weather Research and Forecasting (WRF) mesoscale climate model. The CCSM3/A2 WRF simulation was performed on a grid spacing of 20 km, while the ECHAM5/A1B WRF simulation had a grid spacing of 36 km. Both simulations were used to simulate hourly precipitation data for the time periods 1970–2000 (the "historical" period) and 2020–2050 (the "future" period). Annual maxima were derived from these "raw" data at grid points near each of the three airports in the urban regions of Washington State (SeaTac, Spokane, and Portland). Statistical significance for differences in distributions was found using the Komolgorov-Smirnov test, for differences in means using the Wilcoxon rank-sum test, and for trends in the entire time series using the Mann-Kendall test, all at a two-sided significance level of 0.05.

Table 6. Summary of emission scenarios, GCMs, and geographic coordinates of the downscaled precipitation records used for this study.

IPCC Emissions Scenario	Global Circulation Model (GCM)	Regional Climate Model (RCM)	RCM grid spacing for Washington State simulation	Lat-Long Coordinates of RCM output used for hydrologic modeling (see Figure 4)	
A2[1]	CCSM3	WRF	20 km	47.525°N	122.287°W
A1B[2]	ECHAM5	WRF	36 km	47.500 °N	122.345°W

[1]A2 simulations performed by Pacific Northwest National Laboratories

[2]A1B simulations performed by UW-CIG

Changes in average annual maxima between the two time periods are reported in Table 7. They suggest a likelihood of increasing precipitation intensities at all three locations, although their magnitudes vary considerably for the simulations. Significant changes were found at SeaTac under both simulations, at Spokane under the ECHAM5/A1B simulation for 24-hour storms, and at Portland under the CCSM3/A2 simulation for 1-hour storms. As in the historical analysis, a breakdown of changes by return period is provided for the 1- and 24-hour durations in Tables 8 and 9, respectively. Curiously, differences at SeaTac and Spokane for shorter duration storms are projected to increase under the CCSM3/A2 simulations but decrease under the ECHAM5/A1B simulations.

A closer inspection of results under the CCSM3/A2 simulations revealed that the vast majority of modeled future annual maxima are projected to occur in the month of November, a finding that was not replicated in the ECHAM5/A1B simulations. Quality control checks demonstrated that these elevated November projections are indeed present in the underlying GCM, but that they originated from the one ensemble member with the greatest divergence from the ensemble mean, which indicates more modest increases in autumn precipitation. Thus, these particular results must be interpreted as the combined influence of systematic climate change and internal climate variability. For a more complete discussion, see Salathé et al. (2009, this report).

In order to use the simulations to generate realistic estimates of future runoff, the raw model output for both periods were bias-corrected and statistically downscaled ("BCSD") to match the rainfall record at the SeaTac Airport precipitation gauge, as described in Section 4.2. The resulting sequence of hourly precipitation was then used as input to a continuous hydrological model to simulate runoff extremes in two urban watersheds in the central Puget Sound region (Section 5).

4.2. Bias Correction and Statistical Downscaling (BCSD)

Although the raw output from the RCM provides a broadly recognizable pattern of rainfall, even a cursory comparison of simulated and gauged records shows obvious disparities in both the frequency of rainfall events and the total amount of recorded precipitation. For example, from 1970 to 2000, the CCSM3/A2 simulation at the grid center closest to SeaTac Airport resulted in 11,734 hours of nonzero precipitation for a total of 225 inches during the month of January (annual averages of 379 hours and 7.3 inches), while the gauges at SeaTac recorded 4144 hours of nonzero precipitation for a total of 162 inches (annual averages of 134 hours and 5.2 inches). The need to remove systematic bias in RCM output has been explored by Wood et al. (2002) and Payne et al. (2004), who described the framework that was used to perform the bias correction used here, refined to be applicable to precipitation extremes. For this analysis we focused on only one region of Washington State, the central Puget Sound region, and we bias-corrected the simulated data month-by-month (rather than on an annual basis) to ensure that the dramatic seasonal differences that characterize rainfall in western Washington were preserved and represented accurately.

Bias correction was applied to the simulation record for the grid point

Table 7. Changes in the average modeled empirical annual maxima from 2020 to 2050 relative to the average modeled empirical annual maxima from 1970 to 2000, using raw RCM data. Kolmogorov-Smirnov (top), Wilcoxon rank-sum (middle), and Mann-Kendall (bottom) p-values are provided in italics. Those p-values found to be significant at a two-sided α of 0.05 are indicated in bold.

	CCSM3/A2			**ECHAM5/A1B**		
	SeaTac	**Spokane**	**Portland**	**SeaTac**	**Spokane**	**Portland**
1-hour	+16.2%	+10.3%	+10.5%	-4.6%	-6.6%	+2.1%
KS	***0.014***	*0.120*	*0.120*	*0.944*	*0.062*	*0.363*
rank-sum	***0.011***	*0.272*	***0.044***	*0.757*	*0.346*	*0.714*
MK	***0.015***	*0.220*	***0.004***	*0.388*	*0.504*	*0.183*
2-hour	+16.9%	+5.9%	+7.0%	-4.3%	-6.4%	+3.9%
KS	*0.062*	*0.062*	*0.062*	*0.944*	*0.778*	*0.944*
rank-sum	***0.013***	*0.163*	*0.076*	*0.811*	*0.473*	*1.000*
MK	***0.027***	*0.091*	***0.007***	*0.362*	*0.466*	*0.085*
3-hour	+17.5%	+6.3%	+6.5%	-4.0%	-5.8%	+2.9%
KS	***0.030***	*0.120*	*0.062*	*0.944*	*0.560*	*0.944*
rank-sum	***0.007***	*0.128*	*0.078*	*0.966*	*0.456*	*1.000*
MK	***0.020***	***0.044***	***0.009***	*0.395*	*0.416*	*0.174*
6-hour	+18.3%	+5.4%	+3.6%	+3.6%	-1.7%	+1.2%
KS	*0.120*	*0.216*	*0.062*	*0.560*	*0.560*	*0.998*
rank-sum	***0.019***	*0.231*	*0.147*	*0.439*	*0.588*	*0.966*
MK	*0.116*	*0.104*	*0.055*	*0.181*	*0.455*	*0.388*
12-hour	+15.9%	+5.5%	-0.5%	+9.1%	+12.1%	+2.1%
KS	*0.216*	*0.559*	*0.778*	*0.217*	*0.062*	*0.778*
rank-sum	*0.076*	*0.536*	*0.545*	*0.121*	*0.065*	*0.811*
MK	*0.331*	*0.568*	*0.375*	*0.106*	*0.080*	*0.331*
24-hour	+18.7%	+3.9%	+4.8%	+14.9%	+22.2%	+2.0%
KS	*0.216*	*0.778*	*0.363*	***0.006***	***0.013***	*0.778*
rank-sum	*0.052*	*0.944*	*0.346*	***0.022***	***0.023***	*0.933*
MK	*0.291*	*0.875*	*0.356*	***0.045***	***0.049***	*0.560*
2-day	+11.2%	+4.2%	+2.0%	+13.8%	+16.0%	+3.1%
KS	*0.120*	*0.363*	*0.363*	***0.030***	*0.363*	*0.560*
rank-sum	*0.143*	*0.855*	*0.318*	***0.034***	*0.159*	*0.844*
MK	*0.331*	*0.789*	*0.362*	*0.072*	*0.123*	*0.932*
5-day	+6.3%	+3.2%	+9.0%	+12.2%	+8.8%	+4.6%
KS	*0.559*	*0.944*	*0.120*	*0.120*	*0.560*	*0.944*
rank-sum	*0.318*	*0.933*	*0.181*	*0.050*	*0.278*	*0.833*
MK	*0.618*	*0.799*	*0.114*	*0.123*	*0.302*	*0.585*
10-day	+9.0%	+2.3%	+7.5%	+7.2%	+8.9%	+11.5%
KS	*0.216*	*0.944*	*0.363*	*0.216*	*0.120*	*0.363*
rank-sum	*0.177*	*0.704*	*0.200*	*0.190*	*0.200*	*0.402*
MK	*0.572*	*0.971*	*0.145*	*0.322*	*0.229*	*0.531*

Return Period (yrs)	CCSM3/A2			ECHAM5/A1B		
	SeaTac	Spokane	Portland	SeaTac	Spokane	Portland
2	+16.7%	+6.4%	+15.6%	-1.1%	-8.6%	-0.7%
	1.3	*1.7*	*1.3*	*2.1*	*2.6*	*2.0*
5	+15.8%	+5.1%	+8.7%	-5.5%	-10.1%	+4.3%
	2.6	*4.3*	*3.2*	*6.4*	*7.4*	*4.2*
10	+15.2%	+7.1%	+3.3%	-8.9%	-9.2%	+7.9%
	4.7	*8.1*	*7.9*	*16.1*	*14.5*	*6.9*
25	+14.3%	+12.6%	-3.9%	-13.4%	-6.2%	+13.1%
	11.1	*17.5*	*36.3*	*56.8*	*32.0*	*13.1*
50	+13.7%	+18.7%	-9.4%	-16.8%	-2.8%	+17.2%
	21.9	*30.3*	*149.2*	*153.3*	*55.9*	20.9
Average	+16.2%	+10.3%	+10.5%	-4.6%	-6.6%	+2.1%
KS	***0.014***	*0.120*	*0.120*	*0.944*	*0.062*	*0.363*
rank-sum	***0.011***	*0.272*	***0.044***	*0.757*	*0.346*	*0.714*
MK	***0.015***	*0.220*	***0.004***	*0.388*	*0.504*	*0.183*

Table 8. Distribution of changes in fitted 1-hour annual maxima from 1970-2000 to 2020-2050, using raw RCM data. Numbers in italics represent the return periods of the 1981-2005 events that are equal in magnitude to the 1956–1980 events having the return periods indicated in the first column. Average changes across all return periods are provided at the bottom, matching those reported in Table 7, with Kolmogorov-Smirnov (top), Wilcoxon rank-sum (middle), and Mann-Kendall p-values (bottom) provided in italics. Those p-values found to be significant at a two-sided α of 0.05 are indicated in bold.

Return Period (yrs)	CCSM3/A2			ECHAM5/A1B		
	SeaTac	Spokane	Portland	SeaTac	Spokane	Portland
2	+13.5%	-4.4%	+9.9%	+20.8%	+15.3%	-3.1%
	1.4	*2.3*	*1.6*	*1.3*	*1.5*	*2.2*
5	+13.1%	-2.8%	+5.9%	+18.5%	+28.7%	+1.9%
	3.2	*5.5*	*3.7*	*2.3*	*2.2*	*4.6*
10	+16.7%	+3.1%	+1.5%	+13.7%	+38.5%	+7.3%
	5.4	*9.0*	*8.9*	*4.4*	*3.0*	*7.1*
25	+24.3%	+15.0%	-4.8%	+5.9%	+52.1%	+16.0%
	9.9	*14.9*	*46.9*	*14.5*	*4.2*	*11.3*
50	+32.1%	+27.0%	-9.5%	-0.5%	+63.0%	+23.6%
	14.9	*20.4*	*335.4*	*53.0*	*5.3*	15.1
Average	+18.7%	+3.9%	+4.8%	+14.9%	+22.2%	+2.0%
KS	*0.216*	*0.778*	*0.363*	***0.006***	***0.013***	*0.778*
rank-sum	*0.052*	*0.944*	*0.346*	***0.022***	***0.023***	*0.933*
MK	*0.291*	*0.875*	*0.356*	***0.045***	***0.049***	*0.560*

Table 9. Distribution of changes in fitted 24-hour annual maxima from 1970–2000 to 2020–2050, using raw RCM data. Numbers in italics represent the return periods of the 2020–-2050 events that are equal in magnitude to the 1970–2000 events having the return periods indicated in the first column. Average changes across all return periods are provided at the bottom, matching those reported in Table 7, with Kolmogorov-Smirnov (top), Wilcoxon rank-sum (middle), and Mann-Kendall (bottom) p-values provided in italics. Those p-values found to be significant at a two-sided α of 0.05 are indicated in bold.

Figure 4. Locations of the two gridpoints used for BCSD, shown in relation to SeaTac Airport and the Thornton Creek and Juanita Creek watersheds (see Section 5).

from each of the two downscaled hourly WRF time series (1970–2000 and 2020–2050) that was closest to SeaTac Airport (Figure 4). For the RCM run forced by the CCSM3/A2 simulation (hereafter referred to as the "CCSM3" run), the grid point employed was 47.525°N, 122.287°W, corresponding to a location about 9 km NNE of SeaTac Airport. For the RCM run forced by the ECHAM5/A1B simulation (hereafter referred to as the "ECHAM5" run), the grid point employed was 47.500°N, 122.345°W, corresponding to a location about 7 km NNW of SeaTac Airport. For purposes of comparison, a separate bias correction was performed for each run at their next gridpoint to the south; results were very similar and are not reported here.

The bias correction procedure is based on probability mapping as described by Wilks (2006). The underlying principle acknowledges biases in RCM-simulated climate but anticipates that the simulation data may still provide useful signals if interpreted relative to the RCM climatology rather than the observed climatology (Wood et al. 2002). The monthly data for grid nodes were thus corrected so that they had the same probability distributions as the observed data from SeaTac airport, which were the same data used in the historical analyses described in Section 3.

The first step in the bias-correction procedure was to truncate simulated data for the 1970–2000 period so that each month had the same number of nonzero hourly values as the observed data from the SeaTac gauge. This was done to correct for the smooth manner in which the RCM simulates precipitation, which creates an unrealistically high number of miniscule hourly observations (what has been termed the "climate model drizzle problem"). Simulated data for the future period (2020–2050) were similarly truncated, using the same threshold hourly values resulting from matching the number of nonzero past values to that which was observed. Thus, using the example provided above, the 7590 (i.e., 11,734-4144) hours containing the smallest amounts of nonzero precipitation were eliminated from the 1970–2000 simulated record for the month of January, coinciding with a truncation threshold of 0.012 inches

The procedure was performed first for the historical period and then for the future period of each RCM run. In the example of January non-zero rainfall days, any hour during the month of January during the 2020–2050 simulated record with a nonzero precipitation of less than 0.012 inches was eliminated (6824 out of 10,322 hours). This process was repeated for each month Bias correction was then achieved by replacing RCM values with values having the same nonexceedence probabilities, with respect to the observed climatology, that the original RCM values had with respect to the RCM climatology (where the climatology is defined from the historical period of each data set). Monthly totals were first calculated (by year), and Weibull plotting position was employed to map those totals from the simulated empirical cumulative distribution function (eCDF) to monthly totals from the observed eCDF. Simulated hourly values were then rescaled to add up to the new monthly totals. These new hourly values were then mapped from their eCDF to the hourly values from the observed eCDF, and once again rescaled to add up to the monthly totals derived in the first mapping step. Values that fell outside the range of the simulated climatology, but within 3.5 standard deviations of the climatological mean, were corrected by assuming a lognormal distribution. Those that fell outside of 3.5 standard deviations of the climatological mean were corrected by simply scaling the mean of the observed climatology by its ratio with the mean of the simulated climatology.

Results of the bias-correction procedure were again tested for significance using the Komolgorov-Smirnov, Wilcoxon rank-sum, and Mann-Kendall tests at a two-sided α of 0.05. Overall, average biases in empirical annual maxima were reduced from -22.2% to +3.1% for the ECHAM5 run, and from +9.6% to +2.5% for the CCSM3 run (Table 10). Changes in the raw annual maxima between the 1970–2000 and 2020–2050 periods were largely preserved, although the procedure did have the effect of making some of the changes under the CCSM3/A2 simulation more statistically significant. Under the ECHAM5 run, the corrected empirical annual maxima display a decrease between the two 30-year periods by an average of 5.8 to 6.3% for 1-, 2-, and 3-hour durations, and an increase of 2.3 to 14.1% for the remaining durations. Under the CCSM3 run, the corrected empirical annual maxima show an increase of 13.7 to 28.7% across all

Table 10. Results of the bias-correction procedure for both RCM runs at SeaTac. The reported biases are those of the average modeled empirical annual maxima (both raw and corrected) relative to the average observed empirical annual maxima from 1970 to 2000. The reported changes are those of the average modeled empirical annual maxima from 2020 to 2050 relative to the average modeled empirical annual maxima from 1970 to 2000, using both raw and corrected data. Kolmogorov-Smirnov (top), Wilcoxon rank-sum (middle), and Mann-Kendall (bottom) p-values are provided in italics. Those p-values found to be significant at a two-sided α of 0.05 are indicated in bold.

	CCSM3/A2				ECHAM5/A1B			
	Bias		Change		Bias		Change	
	Raw	Cor	Raw	Cor	Raw	Cor	Raw	Cor
1-hour	-19.2%	-7.3%	+16.2%	+14.3%	-33.2%	-13.4%	-4.6%	-6.3%
KS			***0.014***	***0.002***			*0.944*	*0.944*
rank-sum			***0.011***	***0.013***			*0.757*	*0.554*
MK			***0.015***	***0.003***			*0.388*	*0.799*
2-hour	-2.6%	+4.1%	+16.9%	+22.8%	-21.2%	+3.9%	-4.3%	-5.8%
KS			*0.062*	***0.001***			*0.944*	*0.998*
rank-sum			***0.013***	***0.001***			*0.811*	*0.612*
MK			***0.027***	***0.001***			*0.362*	*0.623*
3-hour	+2.4%	+6.2%	+17.5%	+23.7%	-17.3%	+11.8%	-4.0%	-6.3%
KS			***0.030***	***0.002***			*0.944*	*0.778*
rank-sum			***0.007***	***0.000***			*0.966*	*0.573*
MK			***0.020***	***0.001***			*0.395*	*0.536*
6-hour	+8.8%	+6.6%	+18.3%	+24.3%	-17.3%	+12.8%	+3.6%	+2.3%
KS			*0.120*	***0.030***			*0.560*	*0.363*
rank-sum			***0.019***	***0.005***			*0.439*	*0.508*
MK			*0.116*	***0.044***			*0.181*	*0.185*
12-hour	+12.7%	+4.4%	+15.9%	+24.2%	-20.6%	+6.8%	+9.1%	+8.3%
KS			*0.216*	***0.030***			*0.217*	*0.216*
rank-sum			*0.076*	***0.009***			*0.121*	*0.151*
MK			*0.331*	*0.155*			*0.106*	*0.080*
24-hour	+11.0%	-1.9%	+18.7%	+28.7%	-22.7%	+3.4%	+14.9%	+14.1%
KS			*0.216*	***0.013***			***0.006***	*0.02*
rank-sum			*0.052*	***0.003***			***0.022***	***0.040***
MK			*0.291*	*0.085*			***0.045***	***0.034***
2-day	+19.4%	-1.1%	+11.2%	+24.0%	-22.7%	+1.2%	+13.8%	+14.1%
KS			*0.120*	***0.013***			***0.030***	***0.006***
rank-sum			*0.143*	***0.004***			***0.034***	***0.023***
MK			*0.331*	*0.099*			*0.072*	***0.033***
5-day	+29.0%	+7.1%	+6.3%	+13.7%	-22.4%	+1.1%	+12.2%	+11.5%
KS			*0.559*	*0.216*			*0.120*	*0.062*
rank-sum			*0.318*	*0.069*			*0.050*	*0.054*
MK			*0.618*	*0.437*			*0.123*	*0.072*
10-day	+25.1%	+4.6%	+9.0%	+18.0%	-22.4%	+0.3%	+7.2%	+7.8%
KS			*0.216*	***0.002***			*0.216*	*0.216*
rank-sum			*0.177*	***0.010***			*0.190*	*0.168*
MK			*0.572*	*0.078*			*0.322*	*0.193*
Average	+9.6%	+2.5%	-	-	-22.2%	+3.1%	-	-

durations. Time series of 24-hour annual maxima resulting from the bias-corrected data are plotted alongside those resulting from observed data in Figure 5. As shown, the means and ranges of the simulated data generally match those of the observed data from 1970 to 2000. The plots illustrate the wide interannual variation in annual maxima, which is not well captured in summary statistics like changes in means.

The results from our analysis of historical precipitation trends (Section 3) affirm an increase in the intensity of extreme events in the Seattle-Tacoma area. The magnitude of observed increases for the 24-hour storm over the past 50 years (24.7%) is comparable to the magnitudes of projected increases for the same duration over the next 50 years (14.1 to 28.7%, depending upon the data employed), all of which are statistically significant to some degree. This has potential implications for stormwater management, which is explored more directly in the next section.

5. Prediction of Future Changes in Urban Flood Extremes

Although our historical analysis focused on changes in precipitation across major urban areas of Washington State, the direct relevance of these changes to stormwater infrastructure is best displayed through predictions of future streamflows. As case studies, we selected two Seattle-area watersheds (Figure 4), Thornton Creek in the City of Seattle and Juanita Creek in the City of Kirkland and adjacent unincorporated King County, because they encompass physical and land-use characteristics typical of the central Puget Lowland. The Thornton Creek watershed is Seattle's largest watershed, with approximately 28.7 km^2 (11.1 mi^2) of mixed commercial and residential land use. Juanita Creek is a mixed-land-use 17.6 km^2 (6.8 mi^2) watershed that drains to the eastern shore of Lake Washington; its land cover is 34% effective impervious with 30% forest cover.

Hydrologic simulations of streamflows in these two watersheds were generated by the Hydrologic Simulation Program-Fortran (HSPF; Bicknell et al. 1996). HSPF, which was developed under contract to and is maintained by the U.S. Environmental Protection Agency, is a lumped-parameter model that simulates discharge at user-selected points along a channel network from a time series of meteorological variables (notably, rainfall, temperature, and solar radiation) and a characterization of hydrologic variables (such as infiltration capacity and soil water-holding capacity) that are typically averaged over many hectares or square kilometers. HSPF has enjoyed widespread application across western Washington since its first regional application in the mid-1980s (King County 1985), and the procedures for model set-up, initial parameter selection, and calibration are well established for the region (Dinicola et al. 1990, 2001).

The BCSD precipitation data for the periods 1970–2000 and 2020–2050, using the RCM grid points previously discussed (see Section 4.2; Table 6 and Figure 4), were input to HSPF to reconstitute historical streamflows and predict future streamflows in the Thornton Creek and Juanita Creek watersheds. Since the inputs to the hydrologic model for the two periods differed only in precipitation, any attribute of an altered hydrologic response that is not driven predominantly by rainfall (e.g., the dependence of low-flow extremes on evapotranspiration rates) would

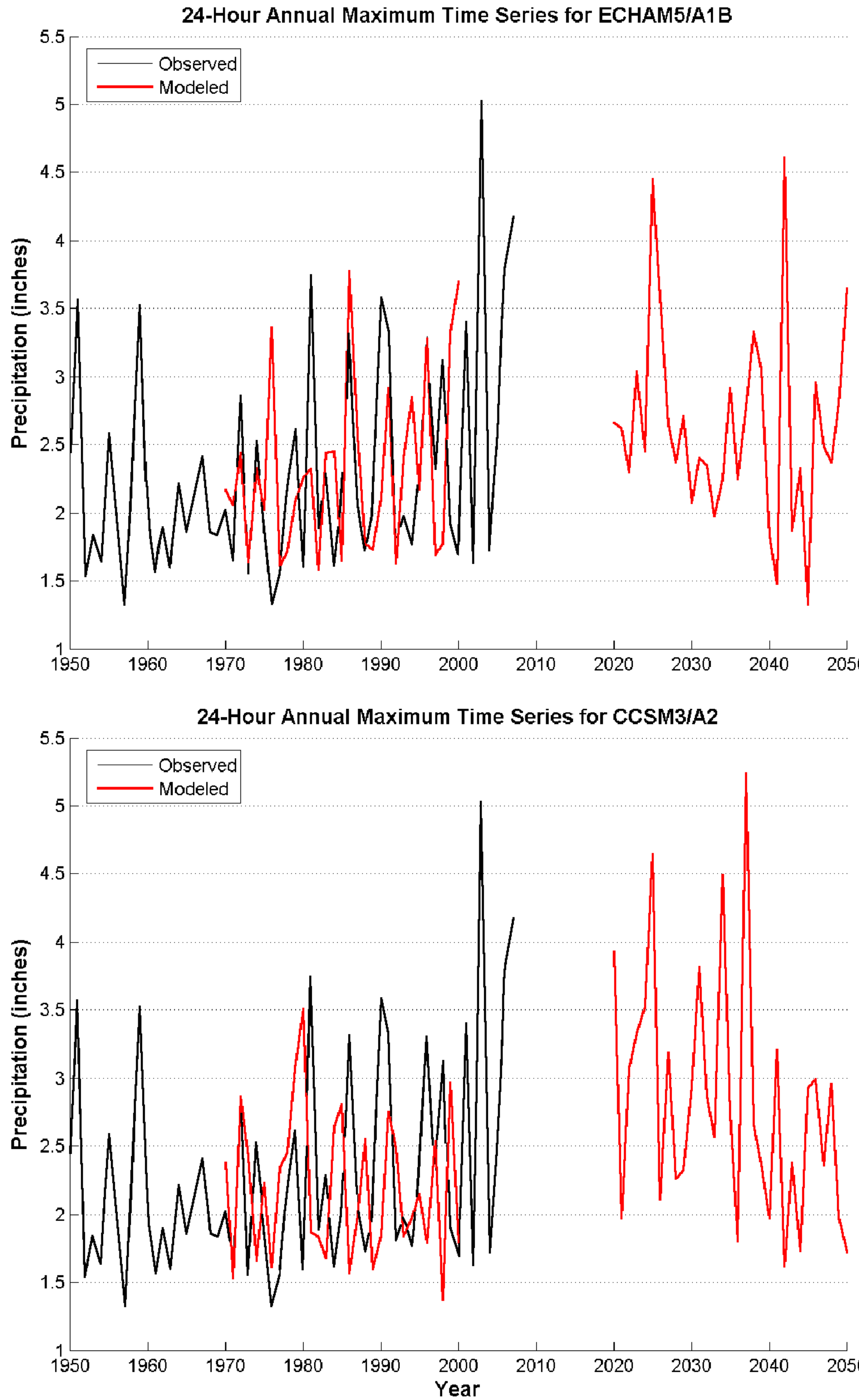

Figure 5. 24-hour annual maxima resulting from the bias-corrected data plotted on top of 24-hour annual maxima resulting from the observed data at SeaTac. As shown, the ranges and means of the simulated data generally match those of the observed data for the historical period (1970–2000).

not be plausibly represented and have not been explored here. These two case studies, however, offer some guidance on whether predicted runoff changes in urban and suburban areas present any critical areas of concern for stormwater managers.

5.1. Results

To parallel the approach of the BCSD analysis, HSPF was first employed to evaluate differences in 1970–2000 simulated flows as forced by both the historical rainfall record and the BCSD rainfall. Results from both the Thornton Creek and Juanita Creek modeling runs suggest streamflow biases of the same magnitude or less than those from the direct comparison of observed and simulated rainfall records (see Tables 11, 12, 13 and Figure 6). For the exploratory purposes that motivated the modeling, these differences were judged acceptable.

Streamflows were then simulated for both watersheds and each of the two RCM runs using the BCSD rainfall for the periods 1970–2000 and 2020–2050. Log-Pearson Type 3 distributions were fitted to the resulting annual maxima, and changes were tested for statistical significance using the Komolgorov-Smirnov, Wilcoxon rank-sum, and Mann-Kendall tests at a two-sided α of 0.05. Results at the mouths of both watersheds (Tables 11 and 12) indicate increases in streamflows for both RCM runs and all recurrence intervals. While these increases are more muted at the mouth of Juanita Creek, this is most likely the consequence of an extensive wetlands complex that serves to attenuate peak flows in that watershed.

Despite this relative uniformity, however, not every scenario is equally consistent. Statistically significant results using CCSM3-generated precipitation are systematically greater than those using ECHAM5, which are not significant. In addition, in the HSPF results for Kramer Creek, a 45-ha (120-ac) mixed commercial and residential subwatershed that constitutes less than 2% of the Thornton Creek watershed area, simulated changes in peak flow conflict in sign between the two scenarios. For the CCSM3-driven simulations, 2-yr through 50-yr peak flows are projected to rise by as much as 25% while the ECHAM5-driven simulations mostly indicate small *declines* (Table 13). Although only a single example, these are dramatically different, even contradictory results, suggesting that the present state of understanding is still highly uncertain, at least for small urban drainage basins of this scale.

We have explored predicted changes under both RCM runs for additional flow metrics beyond simply peak annual discharge, using selected indices of hydrologic alteration (IHA) that have likely ecological influence (Konrad and Booth 2002; Richter et al. 1996). These indices are generally grouped into those that assess the time of year for average or extreme flow events, the frequency and duration of flow pulses, and the rate and frequency of change in flow conditions. In general, these metrics did not change between the two modeled time intervals nearly as much as did the peak annual discharge (e.g., Table 11). As an example, the results on Juanita Creek for a "time-of-year" metric, the high pulse start date (Figure 7), are similar to most of the others: only modest differences are apparent between the two scenarios, and very limited differences between the two simulation periods.

Table 11. Comparisons of HSPF-simulated annual maximum streamflows at the mouth of Juanita Creek, as forced by bias-corrected data for 1970–2000 and 2020–2050 from each of the two RCM runs. Percent differences indicated are with respect to HSPF-simulated annual maximum streamflows as forced by observed data for 1970–2000. Kolmogorov-Smirnov (top), Wilcoxon rank-sum (middle), and Mann-Kendall (bottom) p-values are provided in italics at bottom, with those p-values found to be significant at a two-sided α of 0.05 indicated in bold.

Return Interval (yrs)	CCSM3-WRF				ECHAM5-WRF			
	Peak Flow Quantiles 1970-2000 (cfs)	% Diff with Obs	Peak Flow Quantiles 2020-2050 (cfs)	Change From 1970-2000	Peak Flow Quantiles 1970-2000 (cfs)	% Diff with Obs	Peak Flow Quantiles 2020-2050 (cfs)	Change From 1970-2000
2	230	+6%	289	+25%	224	+3%	252	+13%
5	285	+3%	358	+25%	287	+4%	318	+11%
10	318	+1%	400	+26%	330	+4%	358	+9%
25	358	-3%	451	+26%	383	+4%	405	+6%
50	386	-5%	488	+26%	424	+4%	438	+3%
KS *rank-sum* *MK*				***0.030*** ***0.002*** ***0.040***				*0.216* *0.147* *0.056*

Table 12. Comparisons of HSPF-simulated annual maximum streamflows at the mouth of Thornton Creek, as forced by bias-corrected data for 1970–2000 and 2020–2050 from each of the two RCM runs. Percent differences indicated are with respect to HSPF-simulated annual maximum streamflows as forced by observed data for 1970–2000. Kolmogorov-Smirnov (top), Wilcoxon rank-sum (middle), and Mann-Kendall (bottom) p-values are provided in italics at bottom, with those p-values found to be significant at a two-sided α of 0.05 indicated in bold.

Return Interval (yrs)	CCSM3-WRF				ECHAM5-WRF			
	Peak Flow Quantiles 1970-2000 (cfs)	% Diff with Obs	Peak Flow Quantiles 2020-2050 (cfs)	Change From 1970-2000	Peak Flow Quantiles 1970-2000 (cfs)	% Diff with Obs	Peak Flow Quantiles 2020-2050 (cfs)	Change From 1970-2000
2	118	+17%	187	+58%	107	+6%	134	+25%
5	186	+14%	292	+57%	173	+6%	225	+30%
10	238	+10%	364	+53%	227	+5%	296	+30%
25	312	+6%	458	+47%	309	+5%	399	+29%
50	373	+2%	529	+42%	381	+5%	485	+27%
KS *rank-sum* *MK*				***0.003*** ***0.001*** ***0.005***				*0.951* *0.624* *0.399*

Table 13. Comparisons of HSPF-simulated annual maximum streamflows at the mouth of Kramer Creek, as forced by bias-corrected data for 1970–2000 and 2020–2050 from each of the two RCM runs. Percent differences indicated are with respect to HSPF-simulated annual maximum streamflows as forced by observed data for 1970–2000. Kolmogorov-Smirnov (top), Wilcoxon rank-sum (middle), and Mann-Kendall (bottom) p-values are provided in italics at bottom, with those p-values found to be significant at a two-sided α of 0.05 indicated in bold.

Return Interval (yrs)	**CCSM3-WRF**				**ECHAM5-WRF**			
	Peak Flow Quantiles 1970-2000 (cfs)	% Diff with Obs	Peak Flow Quantiles 2020-2050 (cfs)	Change From 1970-2000	Peak Flow Quantiles 1970-2000 (cfs)	% Diff with Obs	Peak Flow Quantiles 2020-2050 (cfs)	Change From 1970-2000
2	7.0	+4%	8.8	+25%	6.6	-1%	6.7	+3%
5	8.6	+4%	10.6	+24%	8.3	0%	8.3	0%
10	9.5	+1%	11.7	+22%	9.4	0%	9.3	-2%
25	10.6	0%	12.8	+20%	10.9	+3%	10.4	-5%
50	11.4	-1%	13.5	+19%	12.0	+4%	11.2	-7%
KS *rank-sum* *MK*				***0.001*** ***0.001*** ***0.001***				*0.951* *0.898* *0.455*

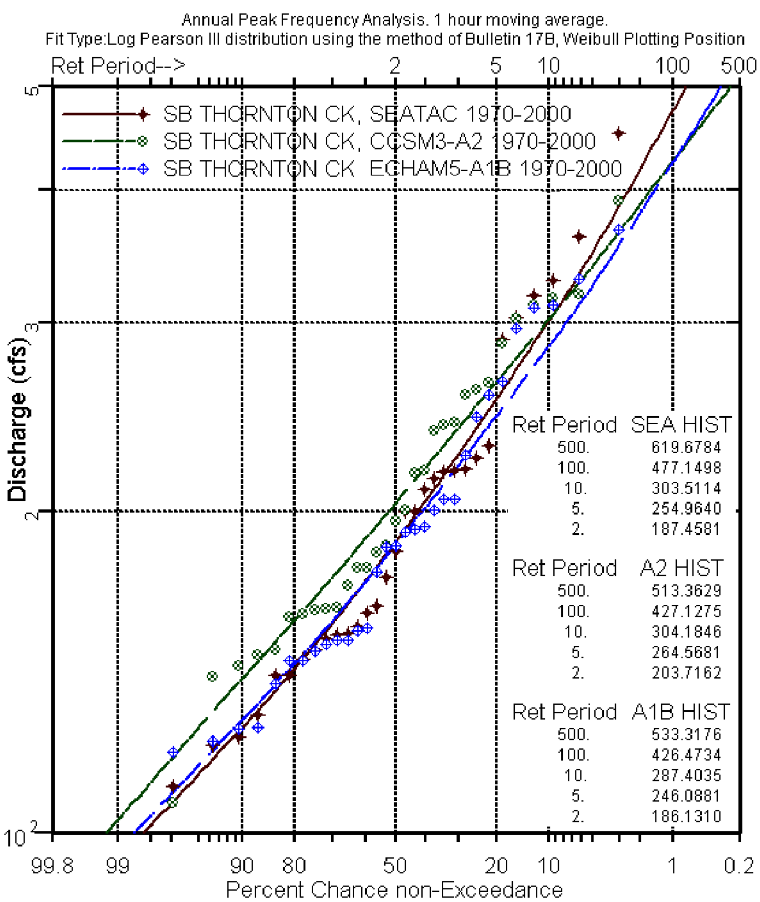

Figure 6. Example flood frequency curves for the South Branch Thornton Creek (930-ha drainage area), comparing HSPF-simulated results for the period 1970–2000 driven by the SeaTac rainfall record (red line and symbols) with the results driven by the BCSD rainfall from the two alternative climate scenarios (green and blue).

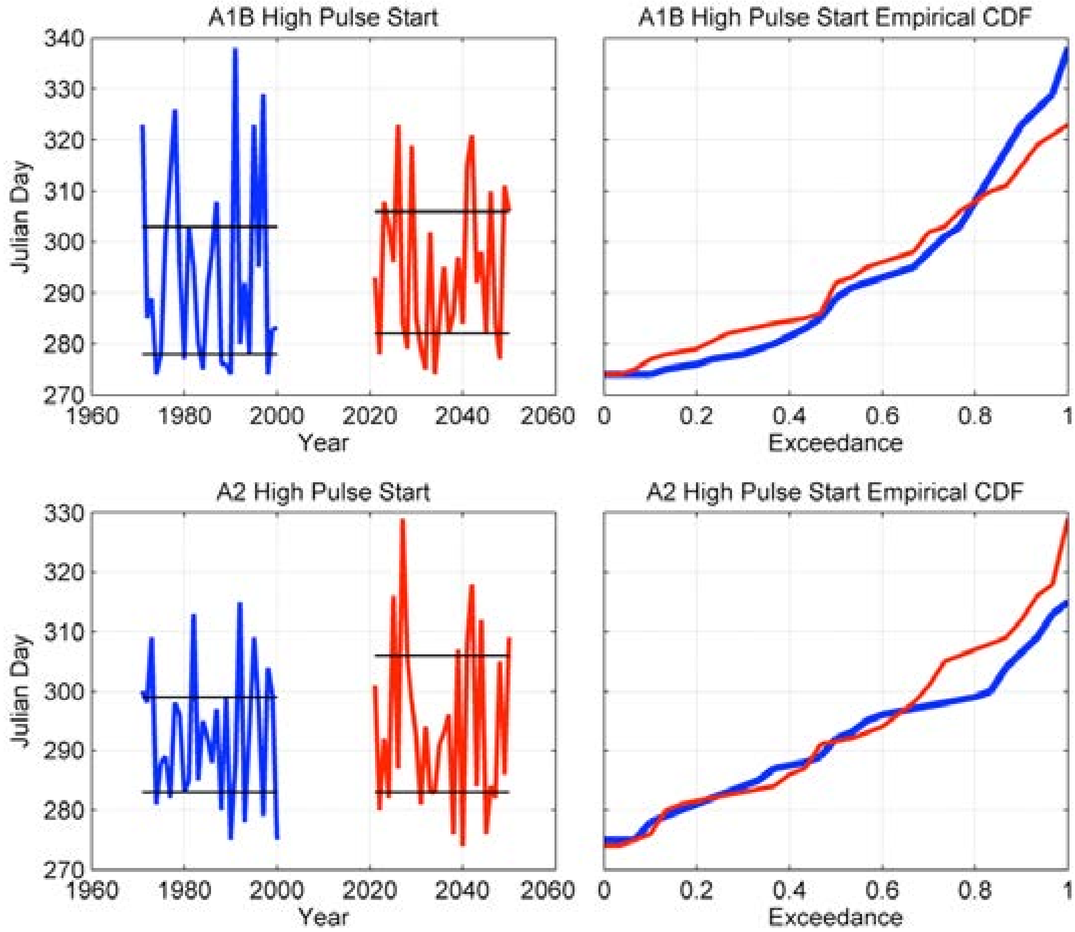

Figure 7. Example of an IHA metric (High Pulse Start Date) as simulated by the two GCM/emission scenarios for the periods 1970–2000 and 2020–2050 at the mouth of Juanita Creek. Differences between models, or between periods, are neither systematic nor particularly large.

In contrast, analysis of a common measure of stream-channel erosivity (aggregate duration of flow above a threshold discharge) displays a suggestion of systematic change between the present and future periods. The threshold discharge assumed in this study is 50% of the peak 2-year flow for the period 1970–2000, a credible index value for initiation of sediment transport in an alluvial gravel-bed channel (Booth and Jackson 1997). A single value, derived from the average of the three 1970–2000 simulations, was used as this "threshold discharge" for all duration analyses at a given stream location. Both GCM-driven simulations show consistent increases, with the largest change associated with the smallest watershed area (Table 14). Similar to other results comparing simulated 2020–2050 flows to those from 1970–2000, increases in erosivity predicted using the CCSM3 precipitation dataset are consistently more dramatic than those predicted using the ECHAM5 dataset. In comparison to streamflow simulation driven by the historical 1970–2000 rainfall record, however, both GCM-driven simulations consistently over-estimate high-flow durations by approximately one-third. Interestingly, the two different GCM-based simulations produce very consistent errors; apparently the bias-correction procedures does not adequately adjust the moderate levels of precipitation intensity that affect this flow statistic.

Table 14. Flow durations for Q > 50% of the 2-year discharge (percent of time exceedance), as predicted by HSPF at four locations along the channel network of Thornton Creek. The first column gives the time of exceedance using the historical record; the "1970–2000" column under each GCM shows the same metric using the BCSD simulated record (with simulation results about 1/3 higher, on average). The column labeled "Change" is the 2020–2050 value for this metric relative to the 1970–2000 durations using the BCSD rainfall record.

SeaTac Historical	CCSM3-WRF			ECHAM5-WRF		
1970-2000	1970-2000	2020-2050	Change	1970-2000	2020-2050	Change
Kramer Creek (0.45 km²)						
0.23%	0.28%	0.58%	+107%	0.29%	0.51%	+76%
South Branch Thornton Creek						
0.23%	0.28%	0.42%	+50%	0.29%	0.34%	+17%
North Branch Thornton Creek						
0.36%	0.45%	0.66%	+47%	0.46%	0.56%	+22%
Thornton Creek nr Mouth (28.7 km²)						
0.19%	0.24%	0.38%	+58%	0.24%	0.30%	+25%

6. Discussion

Our findings from the analyses of historical precipitation indicate that there have been shifts in the distributions of extreme precipitation events over the past half-century, but with substantial differences in different parts of the state. In the Puget Sound region, statistically significant increases were observed in annual maxima at the 24-hour duration, which is the interval most frequently used for the design of stormwater infrastructure. Annual maxima in the other two regions, however, display markedly different responses over the last 50 years, with mixed results in the Spokane region and consistently negative changes in the Portland-Vancouver region, none of which were statistically significant. Although prior studies have generally focused on trends in the *frequency* of extreme events, and not in *intensity* as we have done here, these results are generally consistent with those of Kunkel et al. (1999) and Pryor et al. (2009), both of which found rather ambiguous trends in the Pacific Northwest, as well as Madsen and Figdor (2007), which found significant upward trends in both Washington and Seattle, but conflicting trends in Oregon and Idaho. Anticipating uniform responses in the patterns of future rainfall across all of Washington State, therefore, is surely unwarranted—adaptations will need to be region-specific, because historical changes in rainfall are spatially variable even within the western half of the state.

Modeled trends in future extreme precipitation broadly extend the trends of the historical analyses. Two different GCMs provided the coarse-scale simulated climatic data used to generate downscaled precipitation results, and both agree in general trends and overall magnitude. The precise level of rainfall increases predicted by the two models, however, vary significantly, and actual changes may be difficult to distinguish from natural variability. Although the historical analyses suggest that the magnitude of future projected increases is plausible (and, in fact, consistent with past trends), the differences between the two model predictions are sufficiently large to carry significant consequences for their direct application in the design of stormwater facilities. Nonetheless, the evidence suggests that drainage infrastructure designed using mid-20th century rainfall records may be subject to a future rainfall regime that differs from current design standards.

Results of the hydrologic modeling on two urban watersheds in the central Puget Sound region affirm and extend both the broad trends and the substantial uncertainties evident in the precipitation simulations. For the two modeled watersheds, simulations provide general agreement that peak discharges will increase, although the range of predicted change (from a slight decrease to a near-doubling, depending on the selected recurrence interval, the watershed, and the underlying GCM simulation) are much too large on which to predicate engineering designs. The comparative simulation results are most confounding for the smallest watershed areas, wherein even the net direction of change (i.e., a future increase or a future decrease) is in part dependent on the choice of GCM model.

In part, these inconsistencies must reflect the inherent limitations of the present generation of downscaled rainfall data—for a small (and even not-so-small) urban watershed, an hourly time step is many times longer than the lag-to-peak of the basin (the time between the maximum rainfall intensity and the maximum stream discharge), and so the rainstorms that give rise to the largest discharges in these flashy systems will be simulated poorly (if at all). However, within-watershed comparisons demonstrate that the differences in the two GCMs, which themselves span only a modest range of the entire ensemble of global climate models, display sufficient variability to preclude their present use as a basis for the design of stormwater facilities.

7. Conclusions

- **Few statistically significant changes in extreme precipitation have been observed to date in the state's three major metropolitan areas, with the possible exception of the Puget Sound.** Nonetheless, drainage infrastructure designed using mid-20th century rainfall records may be subject to a future rainfall regime that differs from current design standards.
- **Projections from two regional climate model (RCM) simulations generally indicate increases in extreme rainfall magnitudes throughout the state over the next half-century, but their projections vary substantially by both model and region, and actual changes may be difficult to distinguish from natural variability.**
- **Hydrologic modeling of two urban creeks in central Puget Sound suggest overall increases in peak annual discharge over the next half-century, but only those projections resulting from one of the two RCM simulations are statistically significant.** Magnitudes of projected changes vary widely, depending on the particular basin under consideration and the choice of the underlying global climate model.

8. Research Gaps and Recommendations for Future Research

Our assessment of future streamflows, and the magnitude of peak discharges on which the design of stormwater infrastructure is based, suggest that concern over present design standards is warranted and that some adaptation to changing conditions is already probably prudent (particularly in the Puget Sound region, where regional downscaling and simulations of future streamflow were conducted). However, this analysis is based on just two GCMs and so is at most suggestive. For a more complete understanding of how precipitation extremes are likely to change in the future, the methods employed in the precipitation distribution analysis should be used to explore a larger sample of simulated future climate data. Additional model simulations, based on a larger ensemble of GCMs and emission scenarios, are needed to develop a more robust set of conclusions and provide additional information for evaluating alternative stormwater-facility design standards.

Acknowledgments

This study was conducted under the auspices of the University of Washington's Climate Impact Group, with primary funding received from the Washington State Legislature. Additional support was also provided by Seattle Public Utilities and Northwest Hydraulic Consultants (to DH), King County Water and Land Resources Division (to JB), and Stillwater Sciences (to DBB). We would also like to acknowledge the encouragement and insights of Paul Fleming and Gary Schimek (City of Seattle).

References

Bicknell BR et al. (1996) Hydrological Simulation Program – Fortran: User's manual for Release 11. US Environmental Protection Agency, Environmental Research Laboratory, Office of Research and Development, Athens, Georgia

Booth DB, Jackson CR (1997) Urbanization of aquatic systems - degradation thresholds, stormwater detention, and the limits of mitigation. J Am Water Resourc Assoc 22(5)

Choguill CL (1996) Ten steps to sustainable infrastructure. Habitat Int 20(3) 389-404

Crabbé P, Robin M (2006) Institutional adaptation of water resource infrastructures to climate change in eastern Ontario. Clim Chang Doi: 10.1007/s10584-006-9087-5

Denault C, Millar RJ, Lence BJ (2002) Climate change and drainage infrastructure capacity in an urban catchment. Annual conference of the Canadian Society for Civil Engineering, Montreal, Quebec, Canada

Dinicola et al. (1990) Characterization and simulation of rainfall-runoff relations for headwater basins in western King and Snohomish Counties, Washington. US Geological Survey Water-Resources Investigation Report 89-4052

Dinicola et al. (2001) Validation of a numerical modeling method for simulating rainfall-runoff relations for headwater basins in western King and Snohomish Counties, Washington. US Geological Survey Water-Supply Paper 2495

Efron B (1979) Bootstrap methods: another look at the jack-knife. Annals of Stat

Fowler HJ, Kilsby CG (2003) A regional frequency analysis of United Kingdom extreme rainfall from 1961 to 2000. Int J Climatol

Gerstel WJ, Brunengo MJ, Lingley WS Jr, Logan RL, Shipman H, and Walsh TJ (1997) Puget Sound bluffs: the where, why, and when of landslides following the 1996/97 storms. Wash Geol 25(1):17-31

Groisman PY, Knight RW, Easterling DR, Karl TR, Hegerl GC, Razuvaev VN (2005) Trends in intense precipitation in the climate record. J Clim 18(9):1326-1350

Hamlet AF, Lee SY, Mickleson KEB, Elsner MM (2009) Effects of projected climate change on energy supply and demand in the Pacific Northwest. Washington Climate Change Impacts Assessment: Evaluating Washington's future in a changing climate. In press

Hanson R (ed) (1984) Perspectives on urban infrastructure. Committee on National Urban Policy, National Research Council, Washington DC. National Academies Press, 216 pp

Hosking JRM, Wallis JR (1997) Regional frequency analysis: an approach based on L-moments. Cambridge University Press, New York

Huppert DD, Moore A, Dyson K (2009) Impacts of climate change on the coasts of Washington State. Washington Climate Change Impacts Assessment: Evaluating Washington's future in a changing climate. In press

Intergovernmental Panel on Climate Change (IPCC) (2007) Climate change 2007: synthesis report. contribution of working groups I, II and III to the fourth assessment report of the Intergovernmental Panel on Climate Change [core writing team Pachauri RK, Reisinger A eds.] Geneva, Switzerland

Karl TR, Knight RW (1998) Secular trends of precipitation amount, frequency, and intensity in the United States. Bull Am Meteorol Soc

King County (1985) Juanita Creek basin plan. King County Department of Public Works, Surface Water Management Division, Seattle, Washington

Kirschen P, Ruth M, Anderson M, Lakshmanan TR (2004) Infrastructure systems, services and climate change: Integrated impacts and response strategies for the Boston metropolitan area. Tufts University: Climate's Long-term impacts on metro Boston (CLIMB). USEPA Grant Number R.827450-01, final report (see http://www.aia.org/SiteObjects/files/CLIMB%20Executive%20Summary.pdf). Accessed 6 Dec 2008

Konrad CP, Booth DB (2002) Hydrologic trends associated with urban development for selected streams in the Puget Sound basin, western Washington. US Geological Survey Water Resources Investigations Report No. 4040

Kunkel KE, Andsager K, Easterling DR (1999) Long-term trends in extreme precipitation events over the conterminous United States and Canada. J Clim 12:2515-2527

Kunkel KE, Easterling DR, Redmond K, Hubbard K (2003) Temporal variations of extreme precipitation events in the United States: 1895-2000. Geophys Res Lett 30(17):1900

Larsen P, Goldsmith S (2007) How much might climate change add to future costs for public infrastructure? Institute of Social and Economic Research, University of Alaska Anchorage. UA Research Summary No. 8

Leopold LB (1968) Hydrology for urban land planning – a guidebook on the hydrologic effects of urban land use. Geological Survey Circular 554

Leung LR, Kuo YH, and Tribbia J (2006) Research needs and directions of regional climate modeling using WRF and CCSM. B Am Meteorol Soc 87:1747-1751

Lettenmaier DP, Wallis JR, Wood EF (1987) Effect of regional heterogeneity on flood frequency estimation. Water Resourc Res 23(2): 313-324

Madsen T, Figdor E (2007) When it rains, it pours: global warming and the rising frequency of extreme precipitation in the United States. Report prepared by Environment America Research and Policy Center, Boston

Mote P, Salathé E, Peacock C (2005) Scenarios of future climate for the Pacific Northwest. Report prepared by the Climate Impacts Group, Center for Science in the Earth System, Joint Institute for the Study of the Atmosphere and Oceans, University of Washington, Seattle, available at http://cses.washington.edu/db/pdf/kc05scenarios462.pdf

Payne JT et al. (2004) Mitigating the effects of climate change on the water resources of the Columbia River Basin. Clim Chang 62(1-3) 233-256

Pryor SC, Howe JA, Kunkel KE (2009) How spatially coherent and statistically robust are temporal changes in extreme precipitation in the contiguous USA? Int J Clim 29:31-45

Richter BD, Baumgartner JV, Powell J, and Braun DP (1996) A method for assessing hydrologic alteration within ecosystems. Conserv Biol 10:1163-1174

Salathé EP (2005) Downscaling simulations of future global climate with application to hydrologic modeling. Int J Climatol

Salathé EP, Steed R, Mass CF, and Zahn P (2008) A high-resolution climate model for the U.S. Pacific Northwest: Mesoscale feedbacks and local responses to climate change. J Climate 21:5708-5726

Salathé, EP., Y. Zhang, L.R. Leung, Y. Qian. (2009) Regional climate model projections for the State of Washington. Washington Climate Change Impacts Assessment: Evaluating Washington's Future in a Changing Climate. In Press.

Shaw H, Reisinger A, Larsen H, Stumbles C (2005) Incorporating climate change into stormwater design – why and how? South Pacific Conference on Stormwater and Aquatic Resource Protection, Ministry for the Environment, Auckland, New Zealand

Trenberth K, Dai A, Rasmussen RM, Parsons DB (2003) The changing character of precipitation. Bull Am Meteorol Soc 84(9): 1205-1217

Urbonas BR, Roesner LA (1993) Hydrologic design for urban drainage and flood control. In: Maidment DR (ed) Handbook of hydrology, McGraw-Hill, New York

Vano JA, Voisin N, Cuo L, Hamlet AF, Elsner MM, Palmer RN, Polebitski A, Lettenmaier DP (2009a) Multi-model assessment of the impacts of climate change on water management in the Puget Sound region, Washington, USA. Washington Climate Change Impacts Assessment: Evaluating Washington's future in a changing climate. In press

Vano JA, Voisin N, Scott M, Stockle CO, Halmet AF, Mickleson KEB, Elsner MM, Lettenmaier DP (2009b) Multi-model assessment of the impacts of climate change on water management and agriculture of the Yakima River basin, Washington, USA. Washington Climate Change Impacts Assessment: Evaluating Washington's future in a changing climate. In press

Waters D, Watt WE, Marsalek J, Anderson BC (2003) Adaptation of a storm drainage system to accommodate increased rainfall resulting from climate change. J Environ Plan and Manag 46(5): 755–770

Watt WE, Waters D, Mclean R (2003) Climate variability and urban stormwater infrastructure in Canada: Context and case studies. Toronto-Niagara Region Study Report and Working Paper Series, Meteorological Service of Canada, Waterloo, Ontario, Canada

Wilks DS (2006) Statistical methods in the atmospheric sciences, Second Edition. Academic Press

Wood AW, Maurer EP, Kumar A, Lettenmaier DP (2002) Long-range experimental hydrologic forecasting for the eastern United States. J Geophys Res

Washington State Department of Transportation (WADOT) (2008) Storm-related closures of I-5 and I-90: Freight Transportation Economic Impact Assessment Report. Washington State Department of Transportation WA-RD 708.1

Photo credit, page 321: Shutterstock.com

10: Public Health Impacts

Public Health Impacts of Climate Change in Washington State: Projected Mortality Risks Due to Heat Events and Air Pollution

J. Elizabeth Jackson, MA[1,2]; Michael G. Yost, PhD[3]; Catherine Karr, MD, PhD, MS[4,3]; Cole Fitzpatrick, MA[3]; Brian K. Lamb, PhD[5]; Serena H. Chung, PhD[5]; Jack Chen, PhD[6]; Jeremy Avise, PhD[7]; Roger A. Rosenblatt, MD[1]; Richard A. Fenske, PhD[3]

Abstract

Climate change is likely to have serious and long-term consequences for public health. Among these are illness and mortality related to heat and worsening air quality In this study we examined the historical relationship between age- and cause-specific mortality rates and heat events at the 99th percentile of humidex values in the greater Seattle area (King, Pierce and Snohomish counties), Spokane County, the Tri-Cities (Benton and Franklin counties) and Yakima County from 1980 through 2006; the relative risk of mortality during heat events compared with more temperate periods were then applied to population and climate projections for Washington State to calculate number of deaths above the baseline (1980-2006) expected to occur during projected heat events in 2025, 2045 and 2085. We also estimated excess deaths due to ground-level ozone concentrations for mid century (2045-2054) in King and Spokane counties. Estimates were based on current (1997-2006) ozone measurements and mid-21st century ozone projections, using estimates from the scientific literature to determine the effect of ozone on overall and cardiopulmonary mortality. For the historical heat analysis, relative risks derived for the greater Seattle area showed a significant dose-response relationship between duration of the heat event and the daily mortality rate for non-traumatic deaths for persons aged 45 and above, typically peaking at four days of exposure to humidex values above the 99th percentile. Three different warming scenarios were considered, including high, low and moderate estimates. In the greater Seattle area, the largest number of excess deaths in all years and scenarios was predicted for persons aged 65 and above. Under the middle scenario, this age group is expected to have 96 excess deaths in 2025, 148 excess deaths in 2045 and 266 excess deaths in 2085 from all non-traumatic causes. Daily maximum 8 hour ozone concentrations are forecasted to be 16-28% higher in the mid 21st century

[1]Department of Family Medicine, University of Washington, Seattle, Washington
[2]Department of Sociology, University of Washington, Seattle, Washington
[3]Department of Environmental & Occupational Health Sciences, University of Washington, Seattle, Washington
[4]Department of Pediatrics, University of Washington, Seattle, Washington
[5]Laboratory for Atmospheric Research, Department of Civil and Environmental Engineering, Washington State University, Pullman, Washington
[6]Institute for Chemical Process and Environmental Technology, National Research Council Canada, Ottawa, ON, Canada
[7]Atmospheric Modeling and Support Section, California Air Resources Board, Sacramento, California

compared to the recent decade of 1997-2006. We estimated that the total non-traumatic ozone mortality rate by mid-century for King County would increase from baseline (0.026 per 100,000; 95% confidence interval 0.013-0.038) to 0.033 (0.017-0.049). For the same health outcome in Spokane County, the baseline period rate was 0.058 (0.030- 0.085) and increased to 0.068 (0.035 -0.100) by mid-century. The cardiopulmonary death rate per 100,000 due to ozone was estimated to increase from 0.011 (0.005-0.017) to 0.015 (0.007-0.022) in King County, and from 0.027 (0.013-0.042) to 0.032 (0.015-0.049) in Spokane County. Public health interventions aimed at protecting Washington's population from excessive heat and increased ozone concentrations will become increasingly important for preventing deaths, especially among older adults. Furthermore, heat and air quality related illnesses that do not result in death, but are serious nevertheless, may be reduced by the same measures.

1. Introduction

Climate change is likely to have serious and long-term consequences for public health. Researchers have identified a number of broad health issues associated with climate change, such as severe weather events, worsening air pollution, infectious diseases related to changes in vector biology, food and water contamination and shortages, as well as more indirect impacts such as food security, large-scale migration and civil conflict (Frumkin et al. 2008). These authors emphasize that the health effects of climate change will vary by region, population group, and capacity for public health responses. Recent reviews of the impacts of climate change have documented variability in mortality and morbidity for the United States (Patz et al. 2001), and globally (Patz et al. 2005).

This report was not able to address many of these very important issues, although we hope to do so in subsequent work. Instead, our worked has focused on two key public health concerns related to climate change: heat-related illness and worsening air quality (Luber et al. 2008; Kinney 2008). Annual average temperatures in the United States and globally are rising, although the effects vary from region to region. It is estimated that 400-700 people die from documented thermal stress, or hyperthermia, each year in the United States (Bernard and McGeehin 2004). Because the immediate cause of death is usually some form of cardiovascular failure, and hyperthermia is often not noted on the death certificate as an underlying factor, the number of heat-related deaths is underestimated (Wolfe et al. 2001; CDC 2006).

Relatively short but intense heat waves over the last 30 years have been responsible for hundreds of deaths in the United States and Canada, and thousands of deaths in Europe (Jones et al. 1982; Semenza et al. 1996; Whitman et al. 1997; Naughton et al. 2002; Kaiser et al. 2007). Climate projections suggest that these events will become more frequent, more intense and longer lasting in the remainder of the 21st century (Meehl and Tebaldi 2004). The greatest impacts will be in cities with milder summers, less air conditioning and higher population density (McGeehin and Mirabelli 2001). An aging population also will put more people at risk (Smoyer et al. 2000).

Retrospective epidemiological research has identified groups most likely to be harmed by heat waves and suggests strategies to mitigate these harms through public interventions. The groups at greatest risk include the following: children, due to slower adaptation during exercise (AAP 2000); the elderly, due to changes in the physiological ability to maintain normal body temperature (Borrell et al. 2006; Basu et al. 2005; CDC 2005); poor and socially isolated populations, due to less access to mitigation measures (Greenberg et al. 1983; McGeehin et al. 2001; Browning et al. 2006); some urban dwellers, due to heat island effects and lack of vegetation (Grimmond and Oke 1999; DeGaetano and Allen 2002); outdoor laborers, due to extended exposures and lack of access to drinking water and shade (Greenberg et al. 1983; WA Dept Labor and Industries 2008); people with chronic illnesses (e.g., diabetes, heart disease), due to increased vulnerability to sustained heat (Medina-Ramon et al. 2006); and the mentally ill, due to behavioral factors and the effects of psychoactive medications (Kaiser et al. 2001).

Methods used for estimating mortality due to heat generally rely on an analysis of regional weather data in combination with daily mortality data. This typically requires large, dense urban areas for daily values to be sufficiently stable to support analyses. Most such studies consider the effects of both temperature and humidity. Studies of heat-related mortality in Philadelphia and Toronto have used synoptic climate modeling to identify regional conditions associated with elevated mortality (Kalkstein et al. 1996; Pengelly et al. 2005; Cheng et al. 2005). Regional and temporal differences in the effect of heat on mortality have been identified (Kalkstein and Davis 1989; Davis et al. 2003).

In addition to heat, adverse effects of climate change on air quality have recently come under investigation. The primary ambient air pollutants of concern for public health risk in Washington State include both fine particulate matter and ozone. An expanding evidence base regarding the relationship of these pollutants to adverse health outcomes has resulted in lowering of the concentrations of these pollutants in federal standards (U.S. EPA 2006, U.S. EPA 2008), Despite overall improvement in regional air quality over the decade, adoption of these more protective federal standards make it likely that future climate change related increases in ozone or PM2.5 could lead to more days of exposure above health-based guidelines for Washington residents (PSCAA, 2007).

The influence of meteorology on ozone and particulate matter concentrations is well documented (EPRI 2005, Bernard 2001). There is considerable evidence that ozone concentrations would increase in the United States as a result of climate change, if precursor emissions were held constant; data regarding influences of climate change on particulate matter are far fewer, precluding clear conclusions (CCSP 2008). For both of these pollutants regional-specific assessments of potential health impacts are few (Knowlton et al. 2004).

While ozone and fine particulate matter are associated with multiple health outcomes, including increases in prevalence, clinical utilization, and severity of cardiac and respiratory disease, most studies have focused on premature mortality as an endpoint. This reflects recognition of this endpoint as the most serious outcome, as well as its status as the most accessible and reliable health outcome for which data are available for evaluation in large population based studies. Numerous epidemiologic studies in the United States and abroad have identified increased premature mortality in association with increased ozone exposure (Bell 2004b). The robustness of this evidence base, including several recent multi-city and meta-analyses, has been noted in a recent National Academy of Sciences report (NRC 2008). While the effect estimates vary somewhat by study design and region, the studies viewed as a whole provide a pattern of consistency with generally comparable magnitude of effect estimates.

Increasingly, region-level modeling of ozone and other air pollutants under climate change scenarios is being conducted (Weaver et al, 2009). In the Pacific Northwest regional projections of future air quality at the resolution of approximately county level scales (36 km horizontal grids) have been developed. We sought to integrate knowledge of the concentration-mortality response with Washington State ozone pollution projections to provide an initial quantitative assessment of potential mortality impacts in the mid 21st century. Specifically, we estimated the excess mortality due to climate-related ambient ozone concentrations in Spokane County and King County, Washington for the recent decade (1997-2006) and mid century decade (2045-2055).

Increased levels of $PM_{2.5}$ are an important factor in poor air quality conditions in the State of Washington. Climate change, however, has not been shown conclusively to be a significant factor in projecting future $PM_{2.5}$ levels. In an attribution study of various contributions to future air quality projections, Avise et al (2008) showed that projected changes in weather patterns for the 2050s produced an insignificant (0.2 µg/m3) reduction in $PM_{2.5}$ for EPA Region 10 (Alaska, Idaho, Oregon, Washington). Nevertheless, future changes in local and Asian emissions are projected to increase $PM_{2.5}$ levels by 2 µg/m3 (from a current value of 4 µg/m3) over the same period in this region, and interaction between this increase and climate change may have an amplified impact on human health in the future. Such interactions are beyond the scope of the current project but merit future research given the increasing evidence for adverse public health consequences of $PM_{2.5}$ exposure.

This study had three goals. First, we determined the historical relationship between extreme heat events and mortality in different regions of Washington State, for selected age groups and causes of death. Second, we used these findings to predict the number of excess deaths by age group and cause during projected heat events in years 2025, 2045 and 2085. Finally, we used estimates of the relationship between ozone concentration and mortality available from the scientific literature to predict the number of excess deaths in mid-century (2045-2054) due to ozone under a changing climate, assuming a growing population.

2. Methods

2.1. Estimates of Relative Risk of Mortality Due to HeatEvents, 1980-2006

Four study areas were selected for the heat event analysis (Figure 1): greater Seattle area (King, Pierce and Snohomish counties); Tri-Cities

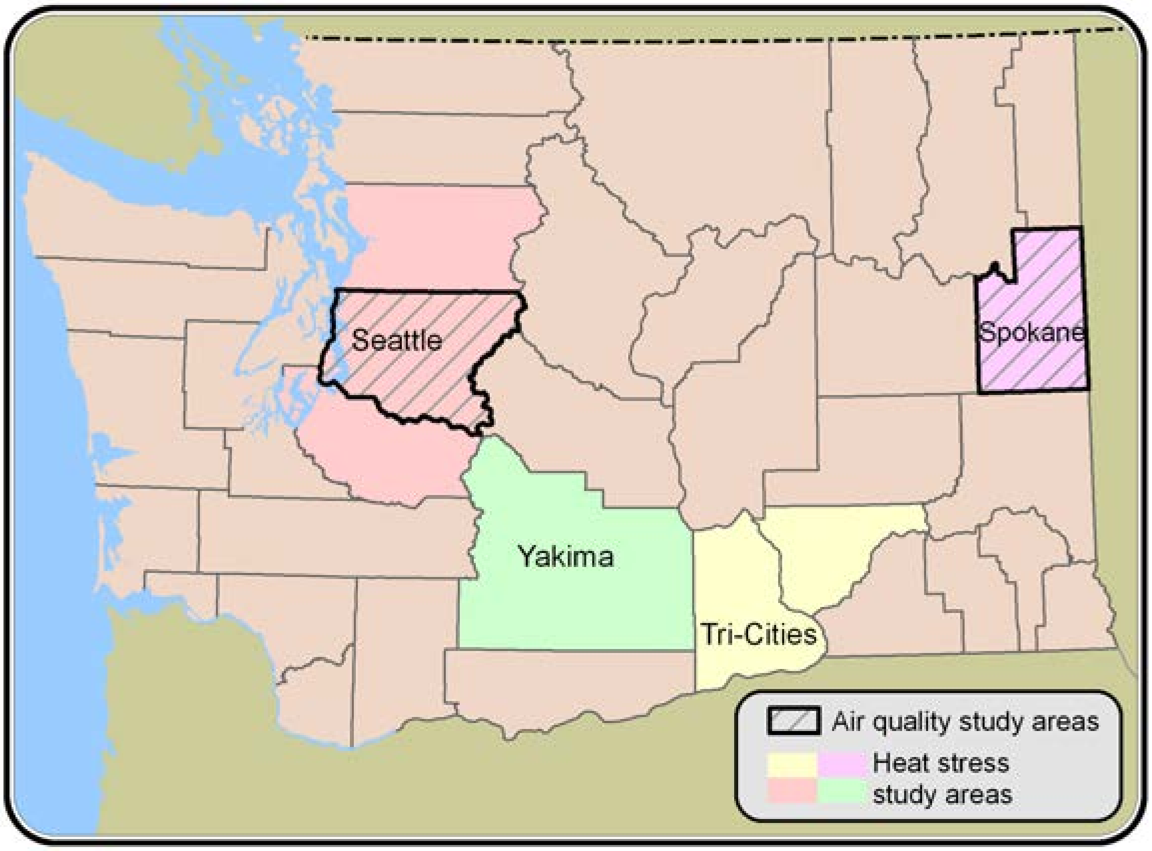

Figure 1. Map of study areas.

(Benton and Franklin counties); Spokane County; Yakima County. Daily historic weather data were drawn from the 16th degree downscaled models (Elsner et al. 2009, this report; Mote and Salathé 2009, this report). Grid points falling within study area counties (grid size ~7.2 km by 4.8km) were identified by spatially joining the grid points and county boundaries using ESRI ArcMap software. The humidex, a measure of the combined effect of heat and humidity on human physiology (Masterton and Richardson 1979, Environment Canada 2008), and has been used in other mortality studies and as a basis for declaring heat warnings (Smoyer-Tomic and Rainham, 2001). The humidex value was calculated for each grid point from daily maximum temperature and relative humidity data using the following formula:

$$\text{Humidex} = T + 5/9 * (v - 10)$$

where: $v = \text{vapor pressure} = (6.112 \times 10^{(7.5*T/(237.7 + T))}) * H/100)$

T= air temperature (degrees Celsius), H= humidity (%)

Grid point humidex values were averaged across all grids in each county to yield a county-level humidex value for each day from January 1, 1970 to December 31, 2006. Thresholds at the humidex 99th percentile were identified for this entire historical period in each study area. After finding the 99%tile value, we then determined which months in the historical record had heat events and used observation frame for the analysis. This approach allowed us to unambiguously define both the humidex threshold and the months for observing heat events. The duration of events was determined the weather event. Heat events were defined as one or more consecutive days of the humidex above these thresholds; the number and duration of heat events were counted in each study area over the period. Since only daily observations of mortality were available, it was not possible or necessary to resolve the heat event time periods to less than 1 day intervals.

Annual county population estimates by age group from 1980 through 2006 were obtained from Washington State's Office of Financial Management (OFM 2008a). Complete mortality data from 1980 through 2006 were obtained from the Washington State Department of Health. Computerized mortality data was not available for earlier periods prior to 1980. Daily numbers of deaths for each year were aggregated by cause, age group, and county of residence.

Heat has been cited frequently as a contributing factor in deaths due to failure of the circulatory and respiratory systems, Therefore, the following cause-of-death categories were examined: all non-traumatic causes (ICD-9: 001-799; ICD-10: A00-R99), circulatory (ICD-9: 390-459; ICD-10: I00-I99, G45, G46), respiratory (ICD-9: 460-519; ICD-10: J00-J99), cardiovascular (ICD-9: 393-429; ICD-10: I05-I52), and ischemic (ICD-9: 410-414; ICD-10: I20-I25); cardiovascular and ischemic are subsets of circulatory. The ICD grouping used are from a study of heat- and air quality-related mortality in Toronto (Cheng et al. 2005). Heat events have been shown to present increased risks for older persons, so data were examined according to the following age categories: 45 years and older, 64 years and older and 85 years and older.

Observed and expected crude daily mortality rates for age and cause-of-death specific groupings were calculated for heat event days (days 1 to day 5+) and non-heat event days (day 0) during the years from 1980-2006. Only data in the months of May – September between 1980 and 2006 were used in the analysis. Daily mortality observed during heat events in the months of May- September were accumulated in 5 time periods of roughly 5-year duration: 1980-1984; 1985-1989; 1990-1994; 1995-1999; and 2000-2006. Mortality was computed in six age-specific categories of 0-4, 5-14, 15-44, 45-64, 65-84, and 85+ years. The deaths occurring in each consecutive day of a heat event were counted for each study area, and classified according to the duration of heat exposure prior to the day of death for heat event days 1 through day 5+ of heat events. The average daily mortality rates on days between May and September with no defined heat event (designated as day 0) were treated as the baseline mortality rates for each time period. Expected values for the number of deaths in each day of a heat event in an annual period were calculated by applying the average daily mortality rate for non-heat event days to the number of days observed in each heat event during a specific time period. The total observed and expected deaths were then summed for each exposure duration category for all heat events. The mortality relative risks by heat event duration, specific age and disease categories were computed from the ratios of observed over expected duration-specific mortality. Calculating separate relative risks for each elapsed day of a heat event (starting with day 1 of the heat event) allows evaluation of the influence of a single day versus more prolonged heat events on mortality.

Confidence intervals were computed assuming Poisson intervals for the observed number of cases as recommended by the Washington State Department of Health (DOH 2002). Exact 95% confidence intervals were computed using Poisson distribution percentiles when the number of observed deaths was <500; for >500 observed deaths, intervals were computed using a normal approximation method (Breslow and Day 1987). This procedure was repeated separately for each heat study area in order to control for regional differences in the effect of heat events on mortality. Given the smaller population in Eastern Washington, a combined analysis of Benton, Franklin, Spokane and Yakima county study areas also was performed.

2.2. Population Projections for Washington State in the 21st Century

Projected county population estimates by age group were obtained from the Washington Office of Financial Management for the years 2005-2030 (OFM 2008b). In predicting future excess deaths during extreme heat events, population was held constant at 2025 projected estimates, allowing differences in excess deaths between years to be interpreted as the component due to climate change. For the analysis of excess deaths related to ozone concentrations, calculated total and age-group populations were calculated by extending the Office of Financial Management linear projections to 2045 through 2054. Washington State population forecasts are developed from a cohort component demographic forecast model that accounts for births, deaths and net migration. Projected births are derived from a natural change model component of the childbearing population, applying historical trends in fertility rates by county. Annual deaths, in terms of life expectancy generally follow national trends, and survival expectations are adjusted to follow Social Security Administration projections in 2007. Migration is the most important variable component of the population forecasts. The state's future net migration is based on an econometric model where Washington's relative attractiveness to job seekers is weighed against the attractiveness of California and other state destinations. A historical comparison of the actual and fitted net migration for 1978-2008 using OFM's migration model found an R^2 of 0.91, indicating reasonably good agreement.

2.3. Projected Excess Mortality Due to Heat Events

Projected heat events were determined for three years: 2025, 2045 and 2085. Three climate change scenarios were selected for high, moderate and low summer (May-Sept.) warming, for a total of nine modeled future heat regimes. The low scenario chosen was the PCM1-B1 model, the high scenario chosen was the HADCM-A1B model, and the middle scenario was the mean of the two composite models using either the A1B or B1 emissions scenario (Salathé et al., 2009, this report). Expected monthly temperature deviations in Celsius for each scenario and time period were added to the observed daily temperature and relative humidity distributions in each study area from 1970 to 1999; the daily humidex was then calculated for each of the new temperature distributions. Historical humidex thresholds at the 99th percentile were applied to the estimated future distributions, and the number and duration of expected heat events in 2025, 2045 and 2085 were calculated for each scenario.

Projections of heat-related mortality applied the baseline mortality rate and duration-specific relative risks derived from the historical analysis to the expected future population structure and expected number and duration of heat events in each of three heat scenarios for 2025, 2045 and 2085. Excess deaths, which are the number of expected deaths above the baseline number of deaths, were calculated for each heat scenario for each year. The use of a 30-year baseline allowed us to calculate mean annual excess deaths in a sample of 30 simulated years for each region and year.

2.4. Projected Excess Mortality Due to Air Pollution

We adapted a health risk assessment modeling approach described by Knowlton et al. (2004) in their effort to assess ozone mortality impacts in the northeastern United States. We selected two populous but distinct climatological areas of the State for this initial assessment. Using the following formula, we estimated ozone related mortality for King County and Spokane County in the recent decade (1997-2006) and at mid-century (2045-2054):

$$M = (P/100{,}000) * B * CR * E$$

where M is the excess mortality due to ozone, P is the estimated population in the county for the period of interest, B is the baseline county-level mortality rate, CR is the concentration-response function that describes the expected change in daily mortality per incremental increase in ozone, and E is the concentration of ozone during the period of interest. We calculated overall non-traumatic mortality as well as mortality specific to cardiopulmonary causes.

The population (P) data were derived from annual population size estimates available from the U.S. Census for King and Spokane County for 1997-2006 and projections of the annual population for these counties in 2045-2054, as described above. The mean of each decade's annual averages was calculated. These data demonstrated that from the period of 1997-2006 to mid-century (2045-2054), the annual average population size for King County is expected to increase from 1,758,260 to 2,629,160 (50% increase). In Spokane County, the population is expected to grow from 424,636 to 712,167 (68% increase).

The county-level non-traumatic (categorized as above) and cardiopulmonary (ICD-9: 393-429, 460-519; ICD-10: I05-I52, J00-J99) mortality rates were calculated by dividing the daily average number of total non-traumatic deaths and cardiopulmonary deaths in the baseline decade of each county by its annual population average. For 1997-2006, the mean daily total non-traumatic and cardiopulmonary death rates per 100,000 for King County were 1.55 and 0.57, respectively. For Spokane County, these rates were 2.03 and 0.78, respectively.

We examined concentration-response (CR) functions for ozone based on three meta-analyses, two multi-city time series, and one case-crossover study of populations in the United States, all of which were reviewed in a recent National Academy of Science report which summarized estimates of the percentage increase in mortality from short-term increases in ozone (NAS 2008). We decided to apply the analysis by Bell et al. (2004b) to our data. This analysis included data and methods developed for the National

Mortality and Morbidity Air Pollution Study (NMMAPS). This landmark study estimated a national average relative rate of mortality (non-injury mortality and cardiopulmonary mortality) associated with short-term average ambient ozone concentrations in 1987-2000 based on 95 large U.S. urban communities made up of almost 40% of the U.S. population (including Spokane and Seattle). Of note, the city-specific estimates for King and Spokane County within the NMMAPS analyses were nearly identical to the combined multi-city concentration-response function employed in this assessment, further supporting its appropriateness. Estimates available per 24-hour average ozone concentration were converted to 8-hour maximum concentrations based on the recommended ratio of 8-hour ozone to a 24-hour average of 1.53 (NAS 2008). The concentration-response for ozone-related non injury mortality and cardiopulmonary mortality derived from this analysis was 0.80% (95% confidence interval 0.41%-1.18%), and 0.98% (0.47%- 1.50%), respectively per 10 parts per billion (ppb) increase in 8-hour maximum daily ozone concentration over the previous week.

Exposure to ozone ($E_{1997\text{-}2006}$) in the recent decade of each county was assessed based on 8-hour maximum daily ozone (ppb) concentration data drawn from the Washington State Department of Ecology state monitoring network for each county for the months May-September (warm season) from 1997-2006. A warm season "baseline" decadal daily average was calculated.

We then estimated future comparable measurements of ozone in the mid-century decade ($E_{2045\text{-}2054}$). To accomplish this, we derived the change (delta) in ozone concentration predicted from a modeling framework which calculated both daily 8 hour maximum concentrations for the baseline decade of this century (1990-1999) as well as for 2045-2054. Specifically, daily 8 hour maximum daily average ozone concentration for May-September of the mid-century decade (2045-2054) were derived by coupling a global climate model projection with regional meteorology and chemistry models for the 36 km grids that coincide with King and Spokane Counties.

The modeling framework is described in detail in Chen et al 2008 (online discussion paper under review). Briefly, the regional Mesoscale Meteorological model version 5 (MM5) was used to downscale the Parallel Climate Model (PCM) to produce regional meteorological fields which were used to drive the Community Multi-scale Air Quality (CMAQ) model, which downscaled the Model for Ozone and Related Chemical Tracers, version 2.4 (MOZART2 outputs) and accounted for regional pollutant emissions to predict photochemical ozone and PM levels. The MM5/CMAQ modeling treats increased ozone formation under climate change as a direct effect of increasing temperature as well as broad indirect effects. The 2050's projections were based on the IPCC A2 scenario, changes in U.S. emissions due to population growth and economic expansion, and alterations in land use/land cover that can affect both meteorological conditions and biogenic emissions important for ozone formation. Future chemical boundary conditions were obtained through downscaling of MOZART-2 based on the IPCC A2 emissions scenario. Projected changes in U.S. anthropogenic emissions are estimated using the EPA Economic Growth Analysis System (EGAS), and changes in land-use are projected using data from the Community Land Model (CLM) and the Spatially Explicit Regional Growth Model (SERGOM).

It is important to recognize that the county monitoring data are influenced by fresh nitrogen oxide emissions largely derived from traffic sources which cause titration (loss) of ozone in the urban areas, while the model results, based upon 36 km grids, tend to minimize this effect since the NOx emissions are diluted significantly due to the size of the grid. This is clear from evaluation of the modeling system which consistently shows that the model overestimates low ozone levels. Consequently, urban monitors will record relatively low ozone concentrations while nearby more rural monitors will record higher ozone concentrations. The model results will not correctly reflect these differences. This is clear from evaluation of the modeling system which consistently shows that the model overestimates low ozone levels (Chen et al., 2008).

Because of this bias in the model, we employed the model results in a relative sense where the change in predicted ozone levels between the baseline period and the future decade were added to the baseline measured values at each site to yield an estimate of future levels. This is essentially the same approach that EPA uses for analysis of ozone control strategies where it is recognized that the models perform better in predicting the change in ozone due to a control compared to predictions of absolute levels.

3. Results

3.1. Estimates of Excess Mortality Due to Heat Events, 1980-2006

The heat study areas accounted for approximately two-thirds of Washington State's population in 2006; King, Pierce and Snohomish counties combined made up just over half of the state's 2006 population of 6.3 million (Table 1). Persons aged 85 and over made up approximately one percent of the total population in most study areas, and one half of one percent in the Tri-Cities region in 1980; by 2006 this age group had roughly doubled in all areas as a proportion of total population. Among study areas, the mean daily maximum humidex from May to September, 1970-2006, was lowest in the greater Seattle area (23.2°C, 73.8°F) and highest in the Tri-Cities (28.1°C, 82.6°F). The 99th percentile for the annual daily maximum humidex ranged from 10°C to 12°C (18-20°F) higher than the May-September mean daily maximum. Number of heat events above the 99th percentile averaged 1.6 to 1.8 per year, with a mean duration of 2.0 to 2.3 days, and maximum duration from 6 days (greater Seattle area) to 10 days (Yakima).

Residents of the greater Seattle area experienced 14,250 deaths from all non-traumatic causes in all months of 1980, and 19,341 in 2006; in the Spokane, Tri-Cities and Yakima areas combined, there were 4,676 deaths from non-traumatic causes in 1980, and 6,264 in 2006 (not shown in tables). Annual mortality rates by non-traumatic causes in all study areas ranged from 36 to 130 per 100,000 for persons aged zero to 14 and from 36 to 58 per 100,000 for those aged 15 to 44. Deaths for specific causes (e.g. ischemic disease) in these age groups were on the order of 20 per 100,000 or fewer annually in all study areas.

Mortality rates for all non-traumatic causes, circulatory causes and respiratory causes increased with age, and were highest for persons 85 years of age or older. In the greater Seattle area, the non-traumatic annual

Table 1. Baseline climate and population parameters 1980-2006.

	Greater Seattle Area	Spokane	Tri-Cities	Yakima
Counties included	**King, Pierce, Snohomish**	**Spokane**	**Benton, Franklin**	**Yakima**
1980 Population				
Total	2,236,898	367,867	157,983	187,226
45 to 64	395,521	62,823	25,928	32,670
65 to 84	184,078	35,232	9,141	19,009
85 and above	20,398	4,221	739	1,912
2006 Population				
Total	3,488,123	471,872	242,781	251,381
45 to 64	847,217	113,889	55,611	52,829
65 to 84	288,330	46,746	19,633	22,134
85 and above	51,580	9,502	2,774	4,493
Humidex, °C (°F)				
Mean daily high, May-Sep	23.2(73.8)	26.2(79.2)	28.1(82.6)	24.9(76.8)
99th pctl of daily high, annually	33.6(92.5)	38.1(100.6)	38.3(100.9)	35.5(95.9)
Heat events above 99th pctl				
Mean annual number	1.7	1.8	1.6	1.6
Mean(max) duration in days	2.2(6)	2.0(9)	2.2(9)	2.3(10)

mortality rate among those aged 85 and above was 14,937 per 100,000 in 1980 and 12,460 per 100,000 in 2006; in the other study areas combined there were similar rates in this age group: 14,871 per 100,000 and 12,517 per 100,000 in 1980 and 2006, respectively. Annual mortality rates for all causes but respiratory were higher for all age groups in 1980 than in 2006. About half of all non-traumatic deaths in 1980, and about one third in 2006, were from circulatory causes, the bulk of these from cardiovascular causes. Only about one-tenth of non-traumatic deaths occurred due to respiratory causes annually (not shown in tables).

In the greater Seattle area, risk of death due to all non-traumatic causes and circulatory causes rose for the overall population aged 45 years and above beginning on day 1 of heat events, peaked on day 4, and declined slightly for days 5 and beyond (Table 2a; Figure 2). The highest relative risk (RR) estimated for non-traumatic deaths was 1.3 (95% confidence interval (CI): 1.2-1.5) for persons aged 65 and above, and 1.5 for those aged 85 and above (95% CI: 1.2-1.8). Relative risk of death due to circulatory causes followed a similar pattern for persons aged 65 and above, and 85 and above, with the highest effect observed in association with 4 days of exposure (RR=1.4, 95% CI: 1.1-1.7, and 1.5, 1.1-2.0, respectively) (Figure 3). Risk of death from non-traumatic and circulatory causes was significantly elevated for all ages on most days of heat events. Duration-specific relative risks due to respiratory causes were less likely to reach statistical significance and were based on smaller sample sizes (Figure 4); the risk was greatest on day 3 for persons aged 45 and over (RR = 1.4; 95% CI: 1.1-1.7) and 65 and over (RR = 1.4; 95% CI: 1.1-1.8). However, the highest estimates were observed on day 5 for all age ranges, and confidence intervals suggest the possibility of substantially elevated risks on day 5 and beyond for anyone aged 45 and above (RR = 1.5; 95% CI: 0.9-2.3), and particularly

Table 2a. Mortality relative risks for selected causes and age groups by heat event duration, greater Seattle area vs. Spokane, Tri-Cities & Yakima combined, 1980-2006† number designations.

	Greater Seattle Area					Spokane, Tri-Cities, Yakima				
Day of heat event	1	2	3	4	5+	1	2	3	4	5+
All non-traumatic causes										
aged 45+	**1.0**	**1.2**	**1.1**	**1.3**	**1.2**	1.0	1.1	1.1	1.0	1.0
	(1,1.1)	(1.1,1.3)	(1,1.2)	(1.1,1.5)	(1,1.4)	(0.9,1.1)	(1,1.2)	(1,1.3)	(0.8,1.3)	(0.9,1.3)
aged 65+	**1.1**	**1.2**	**1.1**	**1.3**	**1.2**	1.0	1.1	1.1	1.1	1.0
	(1,1.1)	(1.1,1.3)	(1,1.2)	(1.2,1.5)	(1,1.4)	(0.9,1.1)	(0.9,1.2)	(0.9,1.3)	(0.8,1.3)	(0.8,1.2)
aged 85+	**1.1**	**1.3**	**1.3**	**1.5**	1.1	1.0	1.1	1.1	1.1	1.0
	(1,1.1)	(1.2,1.5)	(1.1,1.5)	(1.2,1.8)	(0.8,1.5)	(0.8,1.1)	(0.9,1.3)	(0.8,1.5)	(0.7,1.6)	(0.6,1.4)
Circulatory										
aged 45+	1.0	**1.2**	**1.2**	**1.3**	1.1	1.0	1.1	1.1	1.0	1.1
	(1,1.1)	(1.1,1.3)	(1,1.3)	(1.1,1.6)	(0.8,1.3)	(0.9,1.1)	(0.9,1.2)	(0.9,1.4)	(0.7,1.4)	(0.8,1.4)
aged 65+	**1.1**	**1.2**	**1.2**	**1.4**	1.1	1.0	1.1	1.2	1.1	1.0
	(1,1.2)	(1.1,1.3)	(1,1.3)	(1.1,1.7)	(0.9,1.4)	(0.9,1.2)	(0.9,1.3)	(0.9,1.5)	(0.8,1.5)	(0.7,1.4)
aged 85+	1.1	**1.4**	**1.3**	**1.5**	1.2	1.1	1.1	1.2	1.1	1.1
	(1,1.2)	(1.2,1.6)	(1.1,1.6)	(1.1,2)	(0.8,1.7)	(0.9,1.3)	(0.8,1.4)	(0.8,1.8)	(0.6,1.8)	(0.6,1.7)
Respiratory										
aged 45+	1.0	**1.3**	**1.4**	1.1	1.5	0.9	1.0	0.9	0.6	0.8
	(0.8,1.1)	(1.1,1.5)	(1.1,1.7)	(0.7,1.7)	(0.9,2.3)	(0.7,1.1)	(0.7,1.4)	(0.5,1.5)	(0.2,1.3)	(0.3,1.5)
aged 65+	1.0	**1.3**	**1.4**	1.2	1.6	0.8	1.0	1.0	0.5	0.8
	(0.8,1.1)	(1,1.5)	(1.1,1.8)	(0.7,1.8)	(0.9,2.5)	(0.6,1.1)	(0.7,1.4)	(0.6,1.7)	(0.1,1.4)	(0.3,1.6)
aged 85+	0.8	1.3	1.3	1.4	1.5	0.6	1.3	0.7	0.8	0.6
	(0.6,1)	(0.9,1.7)	(0.9,2)	(0.6,2.7)	(0.5,3.2)	(0.3,1)	(0.7,2.2)	(0.1,2)	(0.1,2.9)	(0.1,2.3)

† Bolded relative risk values are significantly greater than 1 ($p < .05$)

for persons aged 65 and above (RR = 1.6; 95% CI: 0.9-2.5). The overall relative risk of death for non-traumatic causes was 1.1 for persons aged 65 and above and 1.2 for persons aged 85 and above (which can also be expressed as elevated risks of death during heat events of 10% and 20%, respectively), compared with more temperate periods; overall RRs were similar for circulatory causes (not shown in tables).

Relative risks were derived for Eastern Washington study areas combined as a group (Table 2a). For residents of these areas, the risk of death by any cause on any given day of a heat event was not significantly elevated for any age group. However, risk estimates for death due to all non-traumatic causes, and for circulatory causes specifically, initially increased as the duration of heat event increased, rising from approximately 1.0 on day 1 to 1.1-1.2 on days 2-3, and falling back to about 1.0 on day 5 and beyond, for all age ranges. Non-traumatic death risk estimates on days 2 and 3 for persons aged 45 and above approached statistical significance (RR = 1.07 95% CI: 0.96-1.19 and 1.12 95% CI: 0.96-1.31, respectively). Relative risks were more variable for death due to respiratory causes, and followed no clear pattern. The overall relative risk of death for non-traumatic causes was 1.03 for persons aged 65 and above and 1.02 for persons aged 85 and above, for elevated risks of death during heat events of 2% and 3%, respectively, compared with more temperate periods. For circulatory causes, overall relative risks were 1.06 for persons aged 65 and over and 1.10 for those aged 85 and over, indicating elevated risks during heat wave of 6% and 10%, respectively (not shown in tables).

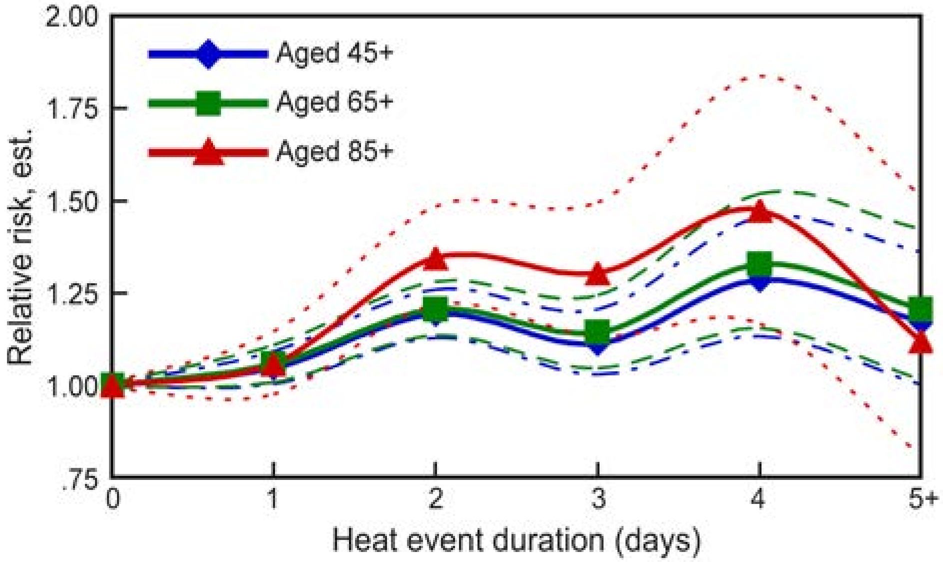

Figure 2. Mortality relative risk estimates (solid lines) for all non-traumatic causes (ICD-9: 001-799; ICD-10: A00-R99) by heat event duration (99th percentile), Greater Seattle Area (King, Pierce and Snohomish counties), 1980-2006. Dotted lines show estimated 95% confidence limits.

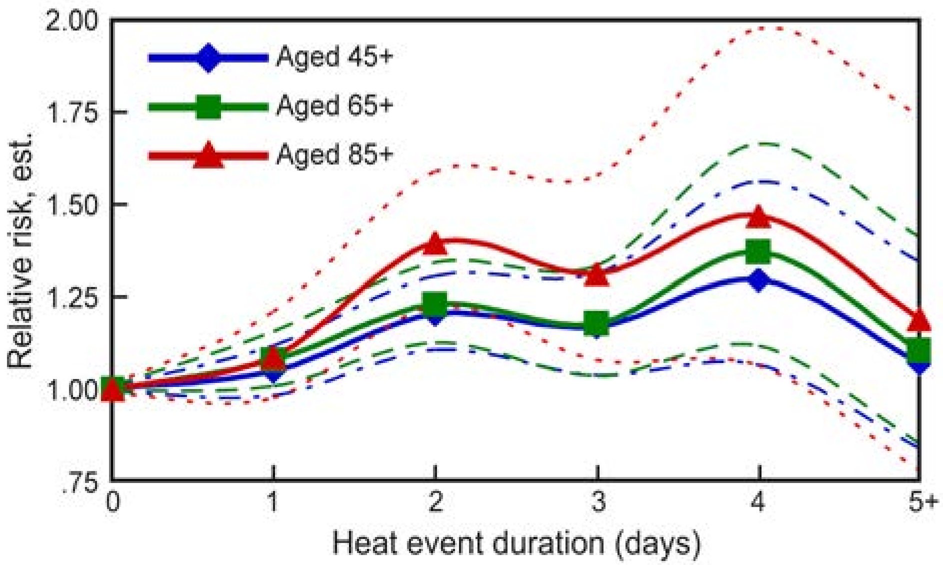

Figure 3. Mortality relative risk estimates (solid lines) for circulatory causes (ICD-9: 390-459; ICD-10: I00-I99, G45, G46) by heat event duration (99th percentile), Greater Seattle Area (King, Pierce and Snohomish counties), 1980-2006. Dotted lines show estimated 95% confidence limits.

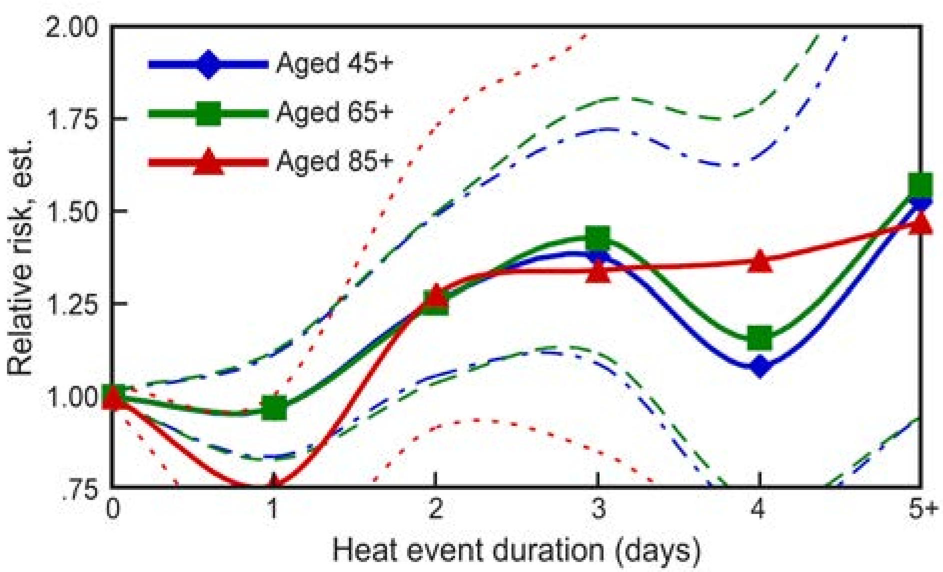

Figure 4. Mortality relative risk estimates (solid lines) for respiratory causes (ICD-9: 460-519; ICD-10: J00-J99) by heat event duration (99th percentile), Greater Seattle Area (King, Pierce and Snohomish counties), 1980-2006. Dotted lines show estimated 95% confidence limits.

Table 2b. Mortality relative risks for selected causes and age groups by heat event duration, Spokane, Tri-Cities & Yakima, 1980-2006.

	Spokane					Tri-Cities					Yakima				
Day of heat event	1	2	3	4	5+	1	2	3	4	5+	1	2	3	4	5+
All non-traumatic causes															
aged 45+	1.0	1.1	1.1	0.9	0.9	1.1	1.1	1.0	1.0	1.3	1.0	1.0	1.1	1.2	1.3
	(0.9,1.1)	(0.9,1.3)	(0.9,1.4)	(0.6,1.3)	(0.6,1.1)	(0.9,1.3)	(0.8,1.4)	(0.7,1.5)	(0.6,1.6)	(0.8,2.1)	(0.8,1.1)	(0.8,1.3)	(0.8,1.5)	(0.8,1.7)	(0.9,1.8)
aged 65+	1.0	1.1	1.1	0.9	0.9	1.0	1.1	1.2	1.1	1.1	0.9	1.0	1.1	1.2	1.2
	(0.9,1.1)	(0.9,1.3)	(0.9,1.4)	(0.6,1.3)	(0.6,1.2)	(0.8,1.2)	(0.8,1.5)	(0.7,1.8)	(0.6,1.9)	(0.6,2)	(0.8,1.1)	(0.8,1.2)	(0.8,1.5)	(0.8,1.8)	(0.8,1.7)
aged 85+	1.0	1.1	1.1	1.0	0.9	1.0	1.0	1.5	0.7	1.5	0.9	0.9	1.0	1.4	1.0
	(0.8,1.2)	(0.8,1.4)	(0.7,1.6)	(0.5,1.7)	(0.5,1.5)	(0.7,1.4)	(0.6,1.7)	(0.7,2.9)	(0.2,2.2)	(0.4,3.7)	(0.7,1.3)	(0.6,1.4)	(0.5,1.7)	(0.7,2.5)	(0.4,2.1)
Circulatory															
aged 45+	1.0	1.1	1.1	0.9	0.8	1.1	1.1	1.1	1.3	1.4	1.0	0.9	1.2	1.0	1.4
	(0.9,1.2)	(0.9,1.4)	(0.8,1.5)	(0.5,1.5)	(0.5,1.2)	(0.9,1.4)	(0.7,1.6)	(0.6,2)	(0.6,2.4)	(0.5,2.6)	(0.8,1.2)	(0.6,1.2)	(0.8,1.8)	(0.5,1.8)	(0.8,2.1)
aged 65+	1.1	1.1	1.1	1.0	0.8	1.0	1.2	1.3	1.3	1.0	1.0	0.9	1.2	1.1	1.3
	(0.9,1.2)	(0.9,1.4)	(0.8,1.6)	(0.6,1.7)	(0.5,1.3)	(0.7,1.3)	(0.8,1.7)	(0.7,2.3)	(0.6,2.6)	(0.3,2.4)	(0.7,1.2)	(0.6,1.3)	(0.7,1.8)	(0.5,1.9)	(0.7,2.1)
aged 85+	1.1	1.1	1.2	1.0	0.8	1.2	0.8	1.7	0.9	1.8	1.0	1.0	1.0	1.2	1.4
	(0.8,1.4)	(0.8,1.6)	(0.7,2)	(0.4,2.1)	(0.3,1.6)	(0.8,1.8)	(0.3,1.7)	(0.6,3.8)	(0.1,3.1)	(0.4,5.2)	(0.7,1.5)	(0.6,1.7)	(0.4,2)	(0.4,2.8)	(0.5,3.1)
Respiratory															
aged 45+	0.9	1.0	0.9	0.2	0.9	0.8	1.7	1.4	1.3	0.0	0.7	0.5	0.7	0.8	0.8
	(0.7,1.3)	(0.6,1.6)	(0.4,1.8)	(0,1.2)	(0.3,1.9)	(0.4,1.5)	(0.8,3.2)	(0.3,4)	(0.2,4.9)	(0,3.4)	(0.3,1.2)	(0.1,1.3)	(0.1,2.1)	(0.1,2.9)	(0,2.5)
aged 65+	0.9	1.1	1.0	0.0	0.8	0.8	1.7	1.6	1.6	0.0	0.6	0.3	0.8	0.9	0.9
	(0.6,1.3)	(0.7,1.6)	(0.4,2)	(0,0.9)	(0.3,1.9)	(0.3,1.5)	(0.8,3.4)	(0.3,4.6)	(0.2,5.7)	(0,4)	(0.3,1.2)	(0,0.9)	(0.2,2.3)	(0,3.3)	(0.1,3.3)
aged 85+	0.6	1.3	0.8	0.0	0.5	0.4	2.5	0.0	0.0	0.0	0.7	0.8	0.8	2.6	1.3
	(0.2,1.1)	(0.5,2.5)	(0.1,2.7)	(0,2.6)	(0,2.6)	(0,2.1)	(0.5,7.2)	(0,7.6)	(0,11.3)	(0,17.4)	(0.1,1.9)	(0.1,2.8)	(0,4.2)	(0.3,9.4)	(0,7.1)

Relative risks of death during heat events were examined for all three eastern study areas individually as well (Table 2b). No statistically significant excess risk for the cause- and age-groups considered was observed and confidence intervals were much wider due to smaller population size, although a few patterns emerged. In Spokane, relative risks for non-traumatic cause-of-death remained close to 1.0, but for all age ranges, wherein point estimates for the relative risks were was approximately 1.0 on day 1, they increased to 1.1 on days 2 and 3 (95% CI: 0.9-1.4 for ages 45+ and 65+) and then decreased to 0.9 on day 5 and beyond. Relative risks for circulatory cause-of-death followed a similar pattern. In the Tri-Cities, elevated relative risk of death by all non-traumatic or circulatory causes for persons 45 years of age and older approached statistical significance on day 1 (RR = 1.1; 95% CI: 0.9-1.3 and RR = 1.1; CI: 0.9-1.4, respectively). In Yakima, relative risk of death for all non-traumatic causes or by circulatory causes peaked on day 5 for persons aged 45 and above (RR = 1.3 and 1.4; 95% CI: 0.9-1.8 and 0.8-2.1, respectively). In general, although not statistically significant, the estimates suggested an increased risk of death for all non-traumatic causes and circulatory causes among persons aged 45 and above.

Table 3. Projected climate and population parameters

	Greater Seattle Area			Spokane			Tri-Cities			Yakima		
	2025	2045	2085	2025	2045	2085	2025	2045	2085	2025	2045	2085
Population (in thousands)												
Total	4,091	4,910	6,542	561	684	933	293	355	480	287	346	463
45 to 64	980	1,082	1,242	131	147	176	62	78	110	59	69	87
65 to 84	638	1,005	1,765	86	130	223	36	51	82	33	46	73
85 and above	73	105	161	11	13	18	4	8	15	5	6	7
Low summer warming												
Mean high humidex, °C (°F),	24.0	24.4	25.1	26.9	27.2	27.8	28.7	29.0	29.6	25.6	25.9	26.5
May-September	(75.2)	(75.9)	(77.2)	(77.2)	(81.0)	(82.0)	(83.7)	(84.2)	(85.3)	(78.1)	(78.6)	(79.7)
Mean annual heat events	2.6	3.1	3.8	2.5	2.9	3.2	2.5	2.9	3.3	2.5	3.0	3.4
Mean(max) event duration in days	2.2(6)	2.3(7)	2.3(8)	2.3(9)	2.6(9)	2.7(9)	2.4(9)	2.5(12)	2.6(13)	2.4(11)	2.5(13)	2.6(13)
Moderate summer warming												
Mean high humidex, °C (°F),	24.8	25.8	27.5	27.6	28.5	30.1	29.4	30.2	31.7	26.2	27.1	28.6
May-September	(76.6)	(78.4)	(81.5)	(81.7)	(83.3)	(86.2)	(84.9)	(86.4)	(89.1)	(79.2)	(80.8)	(83.5)
Mean annual heat events	3.6	4.7	7.2	3.2	4.1	6.0	3.2	4.2	5.9	3.2	4.3	5.9
Mean(max) event duration in days	2.3(7)	2.6(14)	2.9(18)	2.6(9)	3.0(14)	3.4(17)	2.7(13)	3.0(14)	3.6(17)	2.8(13)	2.9(14)	3.5(17)
High summer warming												
Mean high humidex, °C (°F),	26.3	28.1	31.3	29.0	30.6	33.5	30.6	32.2	34.8	27.5	29.1	31.8
May-September	(79.3)	(82.6)	(88.3)	(84.2)	(87.1)	(92.3)	(87.1)	(90.0)	(94.6)	(81.5)	(84.4)	(89.2)
Mean annual heat events	5.8	8.8	10.1	4.8	6.6	8.4	4.9	6.9	8.9	5.2	6.8	9.4
Mean(max) event duration in days	2.7(18)	3.2(18)	6.1(57)	3.4(16)	3.8(17)	5.6(50)	3.5(16)	3.9(24)	5.6(50)	3.4(17)	3.9(24)	5.4(42)

3.2. Projected Mortality Due to Heat Events: 2025-2085

Projected population and climate factors are shown in Table 3. Population projections for Washington State indicate an expected increase in total population between 2006 and 2025 of 14% to 21%. The group expected to grow fastest in all areas are persons aged 65 to 84; this age group is expected to grow by 121% in the greater Seattle area, by 84% in Spokane and the Tri-Cities, and by 49% in Yakima. The expected number and duration of heat events above the humidex historical 99^{th} percentile thresholds will also increase. Under the moderate warming scenario, the greater Seattle area can expect 3.6 heat events with a mean duration of 2.3 days, and in 2085 this will increase to 7.2 heat events of 2.9 days mean duration. Spokane can expect approximately 3.2 heat events of 2.6 days mean duration in 2025, and 6.0 heat events of 3.4 days mean duration in 2085.

The mean numbers of excess deaths that can be expected annually from heat events above the 99^{th} percentile are presented in Table 4 for the greater Seattle area and for Spokane, the Tri-Cities and Yakima combined, holding population constant at 2025 projected levels. Holding the population level constant allows for the comparison of excess deaths

Table 4. Projected Annual Excess Deaths by Cause and Age Group for Low, Middle and High Warming Scenarios

	Low			Middle			High		
	2025 mean (se)	2045 mean (se)	2085 mean (se)	2025 mean (se)	2045 mean (se)	2085 mean (se)	2025 mean (se)	2045 mean (se)	2085 mean (se)
Greater Seattle Area									
Non-traumatic deaths									
aged 45+	68(10)	89(12)	107(13)	101(12)	156(17)	280(22)	211(20)	401(26)	988(32)
aged 65+	64(9)	84(11)	102(12)	96(12)	148(17)	266(21)	200(19)	382(25)	956(32)
aged 85+	32(4)	40(5)	48(6)	46(5)	68(7)	117(8)	89(8)	160(9)	304(8)
Circulatory deaths									
aged 45+	34(5)	43(6)	52(6)	49(6)	72(7)	124(8)	95(8)	170(9)	326(8)
aged 65+	35(5)	45(6)	54(6)	51(6)	75(8)	130(9)	99(9)	178(10)	351(9)
aged 85+	20(3)	26(3)	31(3)	30(3)	44(5)	76(5)	58(5)	105(6)	215(5)
Respiratory deaths									
aged 45+	9(1)	11(2)	14(2)	13(2)	22(3)	44(5)	31(4)	66(6)	218(11)
aged 65+	8(1)	11(2)	13(2)	13(2)	22(3)	42(5)	30(4)	64(6)	213(11)
aged 85+	1(0)	2(0)	2(1)	2(1)	4(1)	8(1)	6(1)	14(2)	53(3)
Spokane, Tri-Cities, Yakima									
Non-traumatic deaths									
aged 45+	12(2)	15(2)	17(2)	17(2)	24(2)	37(2)	31(2)	45(2)	76(2)
aged 65+	9(1)	11(1)	13(1)	13(1)	18(2)	27(2)	23(2)	32(1)	45(2)
aged 85+	1(0)	1(0)	1(0)	1(0)	2(0)	3(0)	3(0)	4(0)	4(1)

† Population held constant at 2025 projections

due to heat events alone, without introducing uncertainty in the population projections beyond 2025, which are increasingly speculative. Under a climate scenario that yields relatively low summer (May-Sept.) warming, during heat events the greater Seattle area can expect 68 excess deaths in 2025, and 89 excess deaths in 2045 and 107 excess deaths in 2085 from all non-traumatic causes among persons 45 years of age and older, than during more temperate periods. Under the moderate warming scenario, which is also the most reliable estimate, Seattle can expect 101 excess deaths in 2025, 156 excess deaths in 2045 and 280 excess deaths in 2085 from all non-traumatic causes among adults 45 and above. Under the highest warming scenario, 211 excess deaths in 2025, 401 excess deaths in 2045 and 988 excess deaths in 2085 are expected during extreme heat in the same cause- and age-group. The bulk of all non-traumatic deaths will happen in persons 65 years old or older, with approximately one third to one half of these occurring among those aged 85 and above. Under the moderate scenario, just under half of all excess deaths in the greater Seattle area will occur by circulatory failure, and about 1 in 7 will be due to respiratory failure.

In the combined eastern study areas, 12 to 31 excess deaths by non-traumatic causes in persons aged 45 and older are expected in 2025, depending on the scenario. By 2085, this same age-cause group is expected to yield between 17 and 76 excess deaths. As in Seattle, most non-traumatic deaths among the population aged 45 and above will occur among persons aged

Table 5. Baseline decade (1997-2006) and mid-century decade (2045-2054) estimates of population size, daily ozone concentration, mortality rate due to ozone, and excess deaths due to ozone (May-September).

Estimates	**King County**		**Spokane County**	
May -September	1997-2006	2045-2054	1997-2006	2045-2054
O_3 (ppb)[1]	20.7	26.5	35.5	41.6
Population	1,758,260	2,629,160	424,636	712,617
O_3 Non Traumatic Mortality rate (95% CI)[2]	0.026 (0.013- 0.038)	0.033 (0.017 -0.049)	0.058 (0.030-0.085)	0.068 (0.035-0.100)
O_3 Cardiopulmonary mortality rate (95% CI)[2]	0.011 (0.005-0.017)	0.015 (0.007-0.022)	0.027 (0.013-0.042)	0.032 (0.015-0.049)
O_3 Non traumatic deaths (95% CI)3	69 (35-102)	132 (68-196)	37 (19-55).	74 (38-109).
O_3 Cardiopulmonary deaths (95% CI)[3]	31 (15-47)	59 (28-90)	18 (9-27)	35 (17-54)

[1]Average daily maximum 8 hour ozone concentration
[4]Rate expressed per 100,000 for May-September with 95% confidence interval
[5]Number of deaths May-September

65 and above; however, comparatively few deaths are expected to occur in persons 85 years of age or older, even though the proportion of the population aged 85 and older is similar between regions.

3.3. Projected Excess Mortality Due to Air Pollution

Using the modeling framework, the delta or forecasted change in ozone for the mid century was calculated and determined to be +5.8 ppb in King County and +6.1 ppb in Spokane County. This was then applied to the baseline decade measurements made at monitoring stations. Baseline decade summertime (May-Sept.) average 8 hour average maximum daily ozone concentrations for King County based on regulatory monitoring measurements were 20.7 ppb for 1997-2006. So, applying the model delta, the future ozone concentrations in the mid century are forecasted to be approximately 26.5 ppb, a 28% increase. In Spokane County, the measured ozone concentrations were higher than in King County, with a 35.5 ppb average 8 hour maximum ozone concentration based on regulatory monitor data for 1997-2006. Applying the model delta predicts future ozone concentration at approximately 41.6 ppb in Spokane County, a 17% increase.

Using the health risk assessment framework, estimates of the total ozone related non-traumatic mortality and cardiopulmonary mortality as rates (per 100,000) and numbers of death for each county for each decade were summarized (Table 5). We estimated that the total non traumatic ozone mortality rate in the recent and mid-century period for King County will increase from 0.026 (95% confidence interval 0.013-0.038) to 0.033 (95% confidence interval 0.017-0.049) (Table 1). For the same health outcome in Spokane County, the rate is 0.058 (0.030-0.085) in the recent decade and increases to 0.068 (0.035-0.100) in the mid century. The estimated annual number of May-September excess deaths in King County due to ozone in 1997-2006 is 69 (95% CI 35-102). Using projections of the future population size and ozone concentration increase this to 132 (95% CI 68-

195). For Spokane County the warm season excess deaths due to ozone in the recent decade are estimated to be 37 (95% CI 19-55). In mid-century this is predicted to be 74 (95% CI 38-109).

The cardiopulmonary death rate per 100,000 due to ozone was estimated to increase from 0.011 (95% CI 0.005-0.017) to 0.015 (0.007-0.022) in King County comparing the recent decade to mid-century. In Spokane, the daily cardiopulmonary death rate attributed to ozone increases from 0.027 (95% CI 0.013-0.042) to 0.032 (95% CI 0.015-0.049) across the decades. This translates to an estimated annual number of May - September excess deaths in King County due to ozone in 1997-2006 of 31 (95% CI 14.7-47) and an increase in mid century to 59 (95% CI 28-90). For Spokane, the estimated baseline deaths due to ozone is 18 (95% CI 9-27) and in the mid century is estimated to increase to 35 (95% CI 17-54).

4. Discussion

4.1. Mortality and Heat Events

In the greater Seattle area there is a clear relationship between heat events and elevated risk of mortality for persons aged 45 and above. The elevated risk is apparent for non-traumatic causes in general, and for circulatory and respiratory causes specifically. The majority of circulatory deaths are due to cardiovascular causes; an analysis of cardiovascular deaths (not presented) showed that the relative risks associated with circulatory cause-of-death were driven primarily by cardiovascular deaths. Respiratory deaths were too small in number to allow for an analysis of more specific causes. The highest relative risks were for persons aged 65 and above; relative risks for persons aged 45 to 64 were smaller (not presented) and this age group contributed relatively few excess deaths in the historical period (not shown). Analyses of age groups younger than 45 were inconclusive, as there were insufficient numbers of deaths to produce stable relative risk values (not presented). We did not attempt to extend the mortality analysis beyond the duration of the heat event itself. This approach may have missed some latent deaths if they occurred after the heat event ended. However, by limiting the analysis just to the heat event, the calculated risk estimates should be conservative because they would tend to understate the deaths attributable to the event.

In the Spokane, Tri-Cities and Yakima study areas, separately or combined, only a few, isolated relative risks were statistically significant. Some patterns in relative risk, however, suggest real differences in mortality rates during heat events, but with samples perhaps too small to support statistical significance.

Projected annual numbers of excess deaths in the greater Seattle area were substantial under some conditions; even under moderate summer (May-Sept.) warming, the area can expect around 100 excess non-traumatic deaths in 2025 and more than 150 excess in 2045. The projections for the eastern study areas combined were much smaller. Even when projected population is taken into account, excess deaths per 100,000 were much lower in Spokane, Tri-Cities and Yakima than in the greater Seattle area. This could be explained in a number of ways. The urban heat island effect may be stronger in the more densely settled Seattle area. To the extent that socioeconomic inequality is greater in urban portions of the Seattle area, this may explain the higher relative risks for mortality during heat waves.

Perhaps the best possible explanation is the greater market penetration of residential air conditioning in Spokane, Tri-Cities, and Yakima in comparison to the greater Seattle area. According to a corresponding study by Elsner et al. (2009), market penetration of residential air conditioning is significantly higher in the study areas east of the Cascade Mountains. As of 1980, the Spokane (24%), Tri-Cities (54%), and Yakima (21%) study areas had significantly higher percentages of residential air conditioning than the greater Seattle area (8%). According to projections for 2020, the disparity will grow even more as the Seattle study area (10%) will still have significantly lower percentages of residential air condition than the Spokane (41%), Tri-Cities (68%), and Yakima (30%) study areas. This association between lowered risks for heat related illness and higher prevalence of residential air conditioning has also been cited by a number of authors (McGeehin et al. 2001; Chestnutt et al. 1998) as a mitigating factor on heat related illness during heat events.

The numbers of excess deaths shown in Table 4 are estimates averaged across 30 annual climate scenarios. The variability in the estimates, due to the changing frequency and duration of heat events in the annual scenarios, is reflected in the standard error term for each value. We acknowledge that in using the inter-annual variation as a measure of uncertainty, not all sources of uncertainty may have been included, and therefore the standard errors likely will be artificially small. Although variability in the climate data contributes much to uncertainty in these estimates, we did not account for additional uncertainty due to the underlying risk estimates. In some cases, age-specific mortality rates for some disease categories are very close to baseline, and may not indicate a net excess. For example, the projections for circulatory deaths in the greater Seattle area show slightly fewer excess deaths in the 45+ category than in the 65+ category, because the overall point estimates indicate a small protective effect for the 45-64 age group (data not shown). This probably reflects statistical uncertainties in the age-specific relative risk calculations, which have some confidence limits which overlapped unity. However in the remaining categories where the relative risk estimates were significantly elevated, there are consistent trends in excess deaths across projection scenarios.

A limitation of this analysis was the use of the county as the geographic level at which mortality data were linked with climate data. This decision was driven by the ready availability of both death certificate and population data at that level, and the substantial difficulty of creating smaller areas of analysis that were geographically stable (and therefore containing a consistent population base) for each year over the historical period. The necessity of averaging climate variables over a comparatively large area meant that local extremes in temperature and humidity were dampened, and the estimated effect of heat on mortality may have been attenuated. However, this suggests that our analysis yielded conservatively-biased estimates of the relationship between heat and mortality, and that the actual effects may be larger.

In addition, the reliability of the projections for excess deaths in each of the nine future heat regimes depends upon the reliability of both climate projections and population projections. The middle 2025 scenario, combining the closest time period with the average climate scenario, is the most reliable of the nine simulations. Excess death estimates using the low and high warming scenarios must be interpreted cautiously, as extremes bracketing the best estimate. Estimates of excess deaths for 2045 and 2085 were made using 2025 projected populations. To the extent that population continues to grow beyond 2025, particularly if more growth occurs in higher age ranges, excess death estimates will be conservative.

Other issues that should be mentioned concern our use of ICD-9 and ICD-10 codes to categorize deaths by cause. First, ICD-9 and ICD-10 codes are not perfectly comparable, so cause-specific rates may appear to change between years when different coding schemes were in use for no other reason than deaths are grouped somewhat differently in each system. However, we did not aim to analyze changing mortality rates over time, so the change in coding scheme is not central to the analysis. Second, since deaths are not classified as being caused by heat, some inference is necessary in choosing cause-of-death groupings that are believed to be influenced by heat. Since we cannot precisely isolate cause of deaths that are due solely or substantially to heat, inaccurate cause of death information could create potential non-differential misclassification and estimates of the effect of heat on mortality are potentially conservatively biased.

Finally, the analytic method we chose relies upon a dense population with substantial numbers of deaths each day. Members of smaller, more isolated populations may also experience elevated risk of mortality during heat events, perhaps to an even greater extent than in larger, central populations, perhaps due to increased exposure or lack of access to cooling. This analysis is not sensitive enough to determine relative risks for smaller, rural locales.

4.2. Mortality and Ozone

We assessed the potential health impacts of ozone related climate change at a locally relevant regional scale, the county, for two highly populated regions of Washington State; King and Spokane counties. Given the assumptions of our models, increases in projected ozone concentrations will increase the mortality rate due to this pollutant in both areas. The higher ozone concentrations and underlying mortality rates observed in Spokane County yield higher current and future decade mortality rates due to ozone in this eastern Washington setting. However, the relative change in ozone related mortality is predicted to be greater in King County, due to a larger relative change (increase) in predicted ozone concentrations for this Western Washington region in mid-century.

The availability of regionally downscaled climate models and meteorological and air pollution models provides an opportunity for this initial public health assessment of climate change and ozone in Washington State. However, the models and subsequent estimates are subject to influence based on assumptions for the underlying components and the scope of available data sources. We applied a single climate change scenario-ozone model to forecast future ozone concentrations that incorporates the range of influences on ozone formation through both direct and indirect meteorological changes. Previous application of climate change related ozone forecasting and subsequent health impact have relied on ozone projections focused on the direct impacts of climate change and do not incorporate land use/land cover projections, anthropogenic emission changes, and future boundary conditions (Knowlton et al. 2004; Bell et al.2007).

We used a concentration response function from the NMMAPS study. Several features support its selection. The effect estimates fall within the range of those reported among the National Academy of Sciences recent review of U.S. based studies that include multiple cities or meta analyses where the point estimates ranged between 0.46% - 1.50 % increase in mortality per 10 ppb increase in 8 hour ozone concentrations, with the lower and upper bounds of the confidence intervals ranging from 0.23%-2.10 % (Thurston 2001, Levy 2001, Stieb 2002, Bell 2004, Bell 2006, Schwartz 2006, NAS 2008). NMMAPS and the studies cited include temperature and particulate matter air pollution in the ozone concentration-response model, to remove confounding by the influence of these factors on mortality.

There is an ongoing need for better data on the portion of mortality that represents people who are at risk of death within a few days irregardless of ozone exposure - the so-called "harvesting effect". However, the current evidence suggests that mortality due to ozone is not restricted to this subgroup of individuals (NRC 2008). While individuals within the population with pre-existng disease, particularly cardiopulmonary conditions and at extremes of the age range are likely more vulnerable to the effects of increasing ozone, the distribution of ozone-mortality effects on subpopulations are not well characterized unlike the overall (population-weighted) average concentration effects such as applied in this study.

In the first study of this kind to apply regional climate model outputs to county level public health risk assessment for ozone mortality (Knowlton, 2004), the estimated 1990s baseline decade (1990s) ozone mortality for 31 northeast U.S. counties were between 5 and 123 (for June- August period). This was calculated based on modeling the baseline 1990s decade ozone concentrations using a regional climate ozone model under the IPCC A2 scenario. Our baseline 1990s ozone mortality estimates for King and Spokane County yield comparable findings (69 and 37, respectively for May-September period), although our baseline decade ozone concentrations were based on regulatory monitoring network measurements, rather than application of the regional model for the 1990s. We predict slightly larger increases between our measurements in the current decade and the mid century modeled projections, a +6.1 ppb change for Spokane County and +5.8 ppb for King County compared to more modest increases of 1-4 ppb in the northeastern county based analysis. This likely reflects that the climate change ozone model employed by Knowlton et al did not incorporate land use/land cover projections, anthropogenic emission changes, and future boundary conditions (Knowlton et al. 2004; Bell et al. 2007) which would be expected to increase future ozone concentrations above the influence of more direct effects of climate on ozone.

The application of projected population increases on mortality rates had a strong influence on future mortality projections. This demonstrates the relative public health impact that even modest increases in ozone concentrations may have as the population grows but also underscores the uncertainties inherent in risk assessment such as this. In the future, we plan to employ both alternative models of climate change-ozone concentrations with differing underlying assumptions as they become available for our region.

6. Research Gaps and Recommendations for Future Research

Social and economic factors have been shown to influence mortality during periods of excessive heat (Greenberg et al. 1983; McGeehin et al. 2001; Browning et al. 2006). A logical next stage in the study of the effect of heat events on mortality in Washington State would be to consider socioeconomic factors that shape exposure to heat and mitigation of the effects of heat, in particular, race/ethnicity, income and occupation. Moreover, we were unable to study the mitigating influence of such things as distribution of residential air conditioning or access to cooling at work or leisure; such access is unlikely to be equally distributed across the state or adequately available to persons most at risk of serious illness or death.

A refinement of the estimated relationship between heat events and mortality could be made by reducing the size of the geographic unit used to link climate variables with mortality, so that a more precise approximation of the local heat history surrounding the decedent could be made. If fatalities were geocoded to census blocks then climate variables at the grid level could be assigned to specific blocks individually, rather than averaged over a much larger area. In addition, a variety of block-level contextual factors (e.g., neighborhood characteristics) available from Census data that might be relevant to heat-related mortality risk could be linked and analyzed in concert with other factors.

Finally, this analysis considered only fatalities, the end stage of a progression of heat-induced morbidity that many individuals will not reach. A more sensitive and perhaps more revealing analysis of the effects of heat on the health and welfare of a population would consider other outcomes, such as emergency room and hospital admissions for heat-related illnesses, and even lost income and productivity due to illness.

Complexities not considered in the analysis of ozone and mortality include differences within population subgroups regarding vulnerability, housing characteristics, and activity patterns which may vary in the future. As the climate warms, people may spend more time indoors or in air conditioned settings which will decrease exposure. We applied a single baseline mortality rate based on current decade but this may change due to medical advances, access to medical care and changes in other risk factors such as smoking and diet, and aging of the population. Some acclimatization may occur but quantifying this is outside the scope of this study. We focused on short term mortality increases due to increased ozone, but other important but less severe health conditions that are known to be influenced by short term increases in ozone include hospitalization for asthma and other chronic respiratory disease, lost work and school days due to respiratory symptoms. The adverse health consequences of chronic elevated ozone exposure on health is less well-studied although an expanding literature suggests such exposure increase the prevalence of asthma and asthma symptoms (McConnell 2002, Lin 2008).

In regard to ozone and mortality, the following issues need to be addressed:

- Development of a range of climate - ozone projections reflecting different assumptions regarding population growth, emission changes, and land use changes would allow consideration of the range of potential changes in ozone concentration and the influence of potential future policy-making options on those changes.
- Consideration of other important health outcomes and medical/public health system burdens due to increases in ozone such as asthma hospitalizations, asthma prevalence, and cardiovascular disease events should be applied to future policy-making options
- Development of robust models forecasting regional scale changes in particulate matter (e.g. PM2.5) and application in health risk studies in Washington State would further enhance climate-preparedness efforts.
- Better understanding of the effects of ozone on vulnerable subpopulations such as those with pre-existing diseases and differing age groups, particularly the very young and elderly.

Finally, a great deal more study is needed to understand the multiple effects of climate change on incidence of death or illness from causes not considered in this focused initial effort. For example, the currently observed wintertime increases in cardiopulmonary disease may be lessened with future decreases in wintertime temperatures. Characterizing this will be helpful to fully understand the global context of climate change and health in the population.

These include food- and water-borne illnesses, vector-borne disease, and exposure to risk of traumatic injury and death from extreme weather events such as flooding, storm surges and sea-level rise.

7. Conclusions

Heat stress is a significant factor in mortalities during the warmer months in Washington State, especially for persons aged 65 and above. As summer (May-Sept.) heat increases and the population grows, Washington can expect an increase in the number of heat-related deaths annually. More research should be done to explore other important factors influencing the effect of heat on mortality in Washington, including individuals' socioeconomic status and access to cooling in very hot weather.

In the last decades, overall ambient air quality has improved in Washington State through regulatory policy but health impacts continue and climate change related effects may threaten gains that have been made. A better understanding of climate change impacts on ambient air quality is critical to prepare for and alleviate potential worsened public health consequences.

References

American Academy of Pediatrics, Committee on Sports Medicine and Fitness (2000) Climatic heat stress and the exercising child and adolescent. Pediatrics 106:158-159

Avise J, Chen J, Lamb B, Wiedinmyer C, Guenther A, Salathé E, and Mass C (2008) Attribution of projected changes in US ozone and PM2.5 concentrations to global changes. Atmos Chem Phys Discuss J1 - ACPD 8:15131-15163

Basu R, Dominici F, Samet JM (2005) Temperature and mortality among the elderly in the United States: A comparison of epidemiologic methods. Epidemiology 16:58-66

Bell, ML, Samet JM, Dominici F (2004a) Time-series of particulate matter. Annu Rev Public Health 25:247-80

Bell, ML, McDermott A, Zeger SL, Samet JM, Dominici F (2004b) Ozone and short-term mortality in 95 urban communities, 1987-2000. JAMA 292:2372-78

Bell ML, Goldberg R, Hogrefe C, Kinney PL, Knowlton K, Lynn B, Rosenthal J, Rosenzweig C, Patz JA (2007) Climate change, ambient ozone, and health in 50 US cities. Climatic Change 82:61–76

Bernard SM, McGeehin MA (2004) Municipal heat wave response plans. AJPH 94:1520-1522

Bernard SM, Samet JM, Grambsch A, Ebi KL, Romieu I (2007) The potential impacts of climate variability and hange on air pollution-related health effects in the United States. Environ. Health Perspect 109:199-209 (Supplement 2)

Borrell C, Mari-Dell'Olmo M, Rodriguez-Sanz M, Garcia-Olalla P, Cayla Ja, Benach J, Muntaner C (2006) Socioeconomic position and excess mortality during the heat wave of 2003 in Barcelona. European J Epidemiology 21:633-640

Breslow NE and Day NE (1987) Statistical Methods in Cancer Research: Volume II: The Design and Analysis of Cohort Studies. Lyon, International Agency for Research on Cancer

Browning CR, Wallace D, Feinberg SL, Cagney KA (2006) Neighborhood social processes, physical conditions, and disaster-related mortality: The case of the 1995 Chicago heat wave. Am Sociol Rev 71:661-678

California Air Resources Board (2008) Methodology for Estimating Premature Deaths Associated with Long-term Exposure to Fine Airborne Particulate Matter in California. Accessed 24 October 2008 at http://www.arb.ca.gov/research/health/pm-mort/pm-mort_final.pdf

CCSP: Climate Change Science Program (2008) Analyses of the effects of global change on human health and welfare and human systems. A Report by the U.S. Climate Change Science Program and the Subcommittee on Global Change Research. [Gamble JL (ed.), Ebi KL, Sussman FG, Wilbanks TJ (Authors)] U.S. Environmental Protection Agency, Washington, DC, USA

CDC: Centers for Disease Control and Prevention (2005) Heat-related mortality--Arizona, 1993-2002, and United States, 1979-2002. Morbidity and Mortality Weekly 54:628-630

CDC: Centers for Disease Control and Prevention (2006) Heat-related deaths--United States, 1999-2003. Morbidity and Mortality Weekly Report 55:796-798

Changnon SA, Kunkel KE, Reinke BC (1996) Impacts and responses to the 1995 heat wave: A call to action. Bull Am Meteorol Soc 77:1497-1506

Chen J, Avise J, Lamb B, Salathé E, Mass C, Guenther A, Wiedinmyer C, Lamarque J-F, O'Neill S, McKenzie D, and Larkin N (2008) The Effects of Global Changes upon Regional Ozone Pollution in the United States. Atmos Chem Phys Discuss 8:15165-15205

Cheng CS, Campbell M, Li Q, Li G, Auld H, Day N, et al. (2005) Differential and

Combined Impacts of Winter and Summer Weather and Air Pollution due to Global Warming on Human Mortality in South-central Canada. Toronto Public Health, Toronto, Canada. Accessed July 21, 2008 at http://www.toronto.ca/health/hphe/pdf/weather_air_pollution_impacts.pdf

Chestnutt LG, Breffle WS, Smith JB, Kalkstein LS (1998) Analysis of differences in hot-weather-related mortality across 44 U.S. metropolitan areas. Environ Sci Poly 1:59-70

Davis RE, Knappenberger PC, Novicoff WM, Michaels PJ (2003) Decadal changes in summer mortality in U.S. cities. Int.J.Biometeorol. 47(3):166-175

DeGaetano AT, Allen RJ (2002) Trends in Twentieth-century temperature extremes across the United States. J of Climate 15:3188-3205

DOH: Washington Department of Health (2002) Guidelines for Using Confidence Intervals for Public Health Assessment. Washington State Department of Health, Olympia, WA. Accessed November 30, 2008 at http://www.doh.wa.gov/data/guidelines/guidelines.htm

Elsner MM, Cuo L, Voisin N, Hamlet AF, Deems JS, Lettenmaier DP, Mickelson KEB, Lee SY (2009) Implications of 21st century climate change for the hydrology of Washington State. Washington Climate Change Impacts Assessment: Evaluating Washington's Future in a Changing Climate. In Press

Environment Canada (2008) Humidex Brochure/Fact Sheet. Accessed November 30, 2008 at http://www.msc.ec.gc.ca/cd/brochures/humidity_e.cfm

EPRI (2005) Interactions of Climate Change and Air Quality: Research Priorities and New Directions. Electric Power Research Institute. http://www-as.harvard.edu/chemistry/trop/publications/Air_Climate_Workshop1.pdf

Frumkin H, Hess J, Luber G, Malilay J, McGeehin M. (2008) Climate change: the public health response. AJPH 98:435-445

Greenberg JH, Bromberg J, Reed CM, Gustafson TL, Beauchamp RA (1983) The epidemiology of heat-related deaths, Texas--1950, 1970-79, and 1980. AJPH 73:805-807

Grimmond CSB and Oke TR (1999) Heat storage in urban areas: Local-scale observations and evaluation of a simple model. J Appl Meteorol 38:922-940

Jones TS, Liang AP, Kilbourne EM, Griffin MR, Patriarca PA, Wassilak SG, Mullan RJ, Herrick RF, Donnell Jr, HD, Choi K, Thacker SB (1982) Morbidity and mortality associated with the July 1980 Heat Wave in St Louis and Kansas City, Mo. JAMA 247:3327-3331

Kaiser R, Rubin CH, Henderson AK, Wolfe MI, Kieszak S, Parrott CL, Adcock M (2001) Heat-related death and mental illness during the 1999 Cincinnati heat wave. Am J Forensic Med Pathol 22:303-307

Kaiser R, Le Tertre A, Schwartz J, Gotway CA, Daley WR, Rubin CH (2007) The effect of the 1995 heat wave in Chicago on all-cause and cause-specific mortality. AJPH 97:S158-62 (Supplement 1)

Kalkstein LS, Davis RE (1989) Weather and Human Mortality: An Evaluation of Demographic and Interregional Responses in the United States. Annals of the Association of American Geographers 79(1):44-64

Kalkstein LS, Jamason PF, Greene JS, Libby J, Robinson L (1996) Philadelphia Hot Weather-Health Watch/Warning System: Development and Application, Summer 1995. Bulletin of the American Meteorological Society 77(7):1519-1528

Karl T, Knight R (1997) The 1995 Chicago heat wave: How likely is a recurrence? Bull Am Meteorol Soc 78:1107-1119

Kinney PL (2008) Climate change, air quality, and human health. Am J Prevent Med 35:459-467

Knowlton K, Rosenthal JE et al. (2004) Assessing Ozone-Related Health Impacts under a

Changing Climate. Environ Health Perspect 112:1557–1563

Lin S, Liu X, Le LH , Hwang SA (2008) Chronic exposure to ambient ozone and asthma hospitalizations among children. Environ Health Perspect 116:1725–1730

Luber G, McGeehin M (2008) Climate change and extreme heat events. Am J Prevent Med 35:429-435

Masterton JM, Richardson FA (1979) A method of quantifying human discomfort due to excessive heat and humidity. Downsview, Ontario, Canada:AES, Env. Canada, CLI 1-79.

McConnell R, Berhane K, Gilliland F, London SJ, Islam T, Gauderman WJ, et al. (2002) Asthma in exercising children exposed to ozone: a cohort study. Lancet 359:386–391

McGeehin MA, Mirabelli M (2001) The potential impacts of climate variability and change on temperature-related morbidity and mortality in the United States. Environ Health Perspect 109:185-189 (Supplement 2)

Medina-Ramon M, Zanobetti A, Cavanagh DP, Schwartz J (2006) Extreme temperatures and mortality: Assessing effect modification by personal characteristics and specific cause of death in a multi-city case-only analysis. Environ Health Perspect 114:1331-1336

Meehl GA, Tebaldi C (2004) More intense, more frequent, and longer lasting heat waves in the 21st century. Science 305:994-997

Mote PW, Salathé Jr. EP (2009) Future climate in the Pacific Northwest. Washington Climate Change Impacts Assessment: Evaluating Washington's Future in a Changing Climate. In Press

Naughton MP, Henderson A, Mirabelli MC, Kaiser R, Wilhelm JL, Kieszak SM, Rubin CH, McGeehin MA (2002) Heat-related mortality during a 1999 heat wave in Chicago. Am J Prevent Med 22:221-227

NRC: National Research Council (2008) Estimating Mortality Risk Reduction and Economic Benefits from Controlling Ozone Air Pollution. Decreasing Tropospheric Ozone Exposure. National Academies Press, Washington, DC

OFM: Washington State Office of Financial Management (2008a). Age and Historical Data. Accessed on November 30, 2008 at http://www.ofm.wa.gov/pop/historical.asp

OFM: Washington State Office of Financial Management (2008b). Estimates and Forecasts. Accessed on November 30, 2008 at http://www.ofm.wa.gov/pop/stfc/default.asp

Patz J, Campbell-Lendrum D, Holloway T, Foley JA (2005) Impact of regional climate change on human health. Nature 438:310-317

Patz JA, McGeehin MA, Bernard SM, Ebi KL, Epstein PR, Grambsch A, et al. (2001) The potential health impacts of climate variability and change for the United States. Executive summary of the report of the health sector of the U.S. national assessment. [Electronic version]. Journal of Environmental Health 64(2), 20-28

Pengelly D, Cheng C, Campbell M (2005) Influence of Weather and Air Pollution on Mortality in Toronto. Toronto Public Health, Toronto, Canada. Accessed July 21, 2008 at http://www.toronto.ca/health/hphe/pdf/weather_air_pollution_summary_june_2005.pdf.

PSCAA: Puget Sound Clean Air Agency (2007) Air Quality Data Summary. Accessed November 30, 2008 at http://www.pscleanair.org/news/library/reports/2007AQDSFinal.pdf

Salathé Jr, EP, Zhang Y, Leung LR, Qian Y (2009) Regional Climate Model Projections for the State of Washington. Washington Climate Change Impacts Assessment: Evaluating Washington's Future in a Changing Climate. In Press

Semenza JC, Rubin CH, Falter KH, Selanikio JD, Flanders WD, Howe HL, Wilhelm JL (1996) Heat-related deaths during the July 1995 heat wave in Chicago.

N.Engl.J.Med. 335(2):84-90

Smoyer KE, Rainham DC, Hewko JN (2000) Heat-stress-related mortality in five cities in Southern Ontario: 1980-1996. Int J Biometeorol 44:190-197

Smoyer-Tomic, KE, Rainham DCG (2001), Beating the Heat: Development and Evaluation of a Canadian Hot Weather Health-Response Plan, Environmental Health Perspectives V109(12).

USEPA: Environmental Protection Agency (2004) Air Quality Criteria for Particulate Matter. Volume II. EPA/600/P-99/002bF

USEPA: Environmental Protection Agency (2005) Air Quality Criteria for Ozone and Related Photochemical Oxidants: Volume II, January. EPA/600/R-05/004bA

USEPA: Environmental Protection Agency (2006) PM National Ambient Air Quality Standards for Particulate Matter; Final Rule October 17, 2006. Federal Register 71(200). http://www.epa.gov/ttn/naaqs/standards/pm/data/fr20061017.pdf

USEPA: Environmental Protection Agency (2008) PM National Ambient Air Quality Standards for Ozone; Final Rule March 27, 2008. Federal Register 73(60). http://www.epa.gov/EPA-AIR/2008/March/Day-27/a5645.pdf

WA Dept of Labor and Industries (2008) Outdoor Heat Exposure Rule. Washington Administrative Code 296-62-095. Accessed 30 November 2008 at http://www.lni.wa.gov/safety/topics/atoz/heatstress/

Weaver CP et al (2009) A Preliminary Synthesis of Modeled Climate Change Impacts on U.S. Regional Ozone Concentrations. Submitted to Bull. Amer. Meteorol. Soc

Whitman S, Good G, Donoghue ER, Benbow N, Shou W, Mou S (1997) Mortality in Chicago attributed to the July 1995 heat wave. AJPH 87:1515-1518

Wolfe MI (2001) Heat-related mortality in selected United States cities, summer 1999. Am J Forensic Med Pathol 22:352-357

Photo credit, page 355: Shutterstock.com

11: Preparing for Climate Change

Preparing for Climate Change in Washington State

Lara C. Whitely Binder[1] with contributions from Jennifer Krencicki Barcelos[2], Derek B. Booth[3], Meriel Darzen[2], Marketa McGuire Elsner[1], Richard Fenske[4], Thomas F. Graham[2], Alan F. Hamlet[5], John Hodges-Howell[2], Daniel D. Huppert[6], J. Elizabeth Jackson[7], Catherine Karr[8], Patrick W. Keys[5], Jeremy S. Littell[1], Nathan Mantua[1], Jennifer Marlow[2], Don McKenzie[9], Michael Robinson-Dorn[2], Eric A. Rosenberg[5], Claudio O. Stöckle[10], Julie A. Vano[5]

Abstract

Climate change is expected to bring potentially significant changes to Washington State's natural, institutional, cultural, and economic landscape. Addressing climate change impacts will require a sustained commitment to integrating climate information into the day-to-day governance and management of infrastructure, programs, and services that may be affected by climate change. This paper discusses fundamental concepts for planning for climate change and identifies options for adapting to the climate impacts evaluated in the Washington Climate Change Impacts Assessment. Additionally, the paper highlights potential avenues for increasing flexibility in the policies and regulations used to govern human and natural systems in Washington.

[1] JISAO Climate Impacts Group, University of Washington, Seattle, Washington
[2] Kathy and Steve Berman Environmental Law Clinic, University of Washington, Seattle, Washington
[3] Stillwater Consultants, Berkeley, California
[4] Department of Environmental and Occupational Health Sciences, University of Washington, Seattle, Washington
[5] Department of Civil and Environmental Engineering, University of Washington, Seattle, Washington
[6] School of Marine Affairs, University of Washington, Seattle, Washington
[7] School of Public Health and Community Medicine, University of Washington, Seattle, Washington
[8] Department of Pediatrics, University of Washington, Seattle, Washington
[9] College of Forest Resources, University of Washington, Seattle, Washington
[10] Department of Biological Systems Engineering, Washington State University, Pullman Washington

1. Introduction

Climate change is expected to bring significant changes to Washington State. As described in accompanying papers, Washington's natural, institutional, cultural, and economic systems (collectively referred to herein as "human and natural systems") face potentially unprecedented challenges from the combined effects of a changing climate, population growth, and growing demands on resources. Addressing these challenges will require a sustained commitment to preparing for the impacts of climate change (adaptation) and reducing greenhouse gases (mitigation).

This paper provides a starting point for climate change planning in Washington State by highlighting major considerations for adaptation planning as a whole and for the specific sectors analyzed as part of the Washington Climate Change Impacts Assessment (the Washington Assessment). Sections 2 and 3 explain what adapting to climate change means and why adaptation is necessary at the state and local level. Section 4 describes Washington State's efforts to date with state-wide adaptation planning and discusses possible adaptation strategies and actions related to the analyses conducted for the Washington Assessment. Section 5 suggests several approaches for incorporating rapidly evolving climate conditions and climate science into Washington State policy making. Finally, Section 6 describes next steps and research recommendations.

2. What Constitutes Climate Change Adaptation?

Adapting to climate and climate variability is not a new activity for human and natural systems. Reservoirs are constructed in response to seasonal variations in streamflow. Levees are built to reduce flood risk. Ecosystems shift over time to compensate for changes in temperature or sea level. The need for more systematic adaptation is increasing, however, as evidence that climate change is occurring continues to grow and as it becomes clear that substantive reductions in greenhouse gas emissions will not be made in time to avoid many projected climate change impacts (IPCC 2007).

The need to adapt to climate is based on the vulnerability of human and natural systems to climate impacts, which is a function of a system's

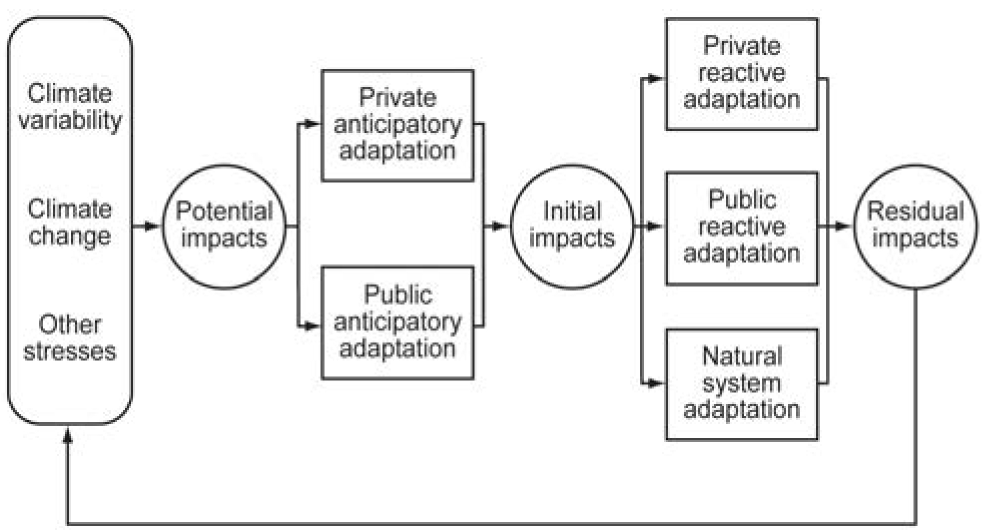

Figure 1. The role of anticipatory and reactive adaptation in addressing climate impacts (Klein 2003, figure used with permission)

sensitivity, exposure, and adaptive capacity to climate (Box 1). Breaking this down further, IPCC 2007 (Chapter 19) identified the following seven key components that influence vulnerability to climate change: 1) the magnitude of impacts (e.g., scale and intensity), 2) the rate and timing of impacts (e.g., fast vs. slow; near-term vs. long-term), 3) the persistence and reversibility of impacts, 4) the likelihood of impacts, 5) the potential for adaptation, 6) distributional aspects of impacts and vulnerabilities (e.g., across regions and population groups), and 7) the importance of the system(s) at risk.

It is important to note that vulnerability to climate impacts also may be affected by changes in non-climatic stresses such as population growth, increasing resource demands, changes in global economic markets, competition from invasive species, and development in or near sensitive habitats. Adapting to climate change likely will be more effective when adaptation efforts address both the climatic and non-climatic stresses affecting a system's vulnerability. For example, efforts to address climate change impacts on Pacific Northwest salmon likely will be more successful if other stresses related to habitat loss, hydropower operations, and salmon hatchery management practices are also considered part of the adaptation "portfolio."

But what does it mean to adapt to climate change? Definitions of adapting to climate change vary in detail but are generally based on the concept of making adjustments in physical, ecological, economic, and social systems to compensate for climate impacts (Smit et al. 2000, Adger et al. 2005, IPCC 2007). The goal of these adjustments is making human and natural systems more *resilient* to the impacts of climate change. A resilient system is one that has the capacity to "absorb and rebound from weather extremes, climate variability, or change and continue functioning" (Luers and Moser 2006; also Turner et al. 2003, IPCC 2007).

Adapting to climate change can be done in anticipation of climate change impacts (anticipatory adaptation) or in response to climate events (reactive adaptation), as illustrated in Figure 1. Anticipatory adaptation occurs when governments, businesses, and private citizens take proactive steps to reduce the negative consequences of projected climate change impacts. Anticipatory adaptation can also be used to maximize the benefits of climate change, such as a longer growing season or increased winter hydropower production.

Because it is impossible to anticipate perfectly how climate change will affect human and natural systems, and because natural systems cannot anticipate climate change impacts, reactive adaptation also will occur. Reactive adaptation may be an acceptable strategy in cases where the risks associated with responding reactively to climate impacts are considered acceptable. However, relying exclusively on reactive adaptation can be problematic (Smith 1997). First, reactive adaptation may be "too little too late" given that some climate change impacts, such as the loss of a species,

Box 1: Basic Concepts in Adaptation Planning

Sensitivity: The degree to which a system is affected, either negatively or positively, by climate variability or change. The effect may be direct (e.g., a change in crop yield in response to a change in the mean, range, or variability of temperature) or indirect (e.g., damages caused by an increase in the frequency of coastal flooding due to sea-level rise) (IPCC 2007).

Exposure: The nature and degree to which a system is exposed to significant climatic variations (IPCC 2001). Exposure to climatic stresses may vary by geography, elevation, length of time, and other factors.

Vulnerability: The extent to which a natural or social system is susceptible to sustained damage from weather extremes, climate variability, and change (and other interactive stressors) (Luers and Moser 2006).

Adaptive capacity: The ability of a system to adjust to climate stresses (including weather extremes, climate variability, and climate change) so that potential damages are reduced, consequences coped with, or opportunities maximized (IPCC 2007).

Table 1. Examples of adaptive capacity building (Luers and Moser 2006; Snover et al. 2007; UKCIP, undated)	
Increase access to information about climate and climate impacts	• Increase staff access to science experts and peer-reviewed science and policy publications • Host brown bag seminars, department meetings, and scientific briefings for staff • Include climate impacts/adaptation information in websites, newsletters, fact sheets, utility inserts, brochures • Include information on climate impacts and adaptive planning activities in public meetings
Increase technical capacity to incorporate information on climate impacts	• Collect data and improve monitoring to fill critical information gaps • Conduct research, or partner with organizations to fund needed research on climate impacts • Increase training opportunities and access to technologies that support adaptation needs • Increase partnerships with organizations that can support adaptation needs • Hire expertise in areas that support adaptation needs • Dedicate new or existing staff time to overseeing adaptation activities
Increase legal and administrative capacity to adapt to climate change	• Develop adaptation planning strategy to guide adaptation activities • Assess regulatory, institutional, and cultural barriers to implementing adaptation actions • Modify regulations, policies, administrative procedures, etc. to remove or minimize identified barriers • Improve guidance/best management practices to incorporate adaptive planning objectives • Provide the necessary financial resources to support adaptive planning

may be irreversible. Second, reactive adaptation is likely to cost more than anticipatory adaptation (idem, Luers and Moser 2006, IPCC 2007, Repetto 2008). This may be particularly true when dealing with long-lived infrastructure that is difficult to retrofit or relocate in response to climate impacts, or when the potential to implement more cost-effective anticipatory adaptation measures becomes permanently constrained by present-day activities (IPCC 2007). Finally, reactive adaptation may run the risk of being short-sighted by focusing on resolving the crisis at hand, e.g., a single drought or coastal erosion event, and not addressing the underlying current and projected problems that contribute to the crisis, e.g., over-allocation of water resources or development in unstable coastal areas (Smith 1997). Consequently, adapting to climate change will ultimately involve both anticipatory and reactive adaptation actions.

Whether anticipatory or reactive, adaptive planning involves two general categories of activity: building adaptive capacity and implementing adaptive actions (UKCIP, undated). Building adaptive capacity focuses on increasing institutional capacity to handle the impacts of climate change, i.e., to deliver adaptive actions. Building adaptive capacity recognizes that there are institutional, legal, cultural, technical, fiscal, or other barriers to planning for climate change that need to be addressed if a community is going to effectively adapt to climate change. Building adaptive capacity can occur regardless of the amount of uncertainty that exists around specific climate change projections (e.g. whether sea level rise increases

4 cm [2 in] or 34 cm [13 in]). As such, these steps represent "no regrets" strategies (Section 4.9) for adapting to climate change. General examples of activities that may build adaptive capacity are provided in Table 1; additional examples related to the eight sectors analyzed for the Washington Assessment are included in Table 2, located at the end of this paper.

Adaptation actions are actions taken to address specific climate vulnerabilities or opportunities. Examples of adaptation actions include improving drought planning, promoting new irrigation technologies to improve water use efficiency, managing forest density to reduce vulnerability to forest fires, and opening additional cooling centers during extreme heat events. A more extensive list of possible adaptation actions relevant to the eight sectors evaluated in the Washington Assessment is found in Table 2, located at the end of this paper.

Understanding what adaptation is also means understanding what it is not. Adapting to climate change is not about completely insulating communities and natural systems from all climate impacts; this is an unattainable goal. While many impacts can be anticipated and significantly minimized through adaptive planning, it is not possible to anticipate perfectly how climate will change and how these changes will manifest themselves at specific locations and points of time. Surprises are unavoidable. Consequently, the goal of adaptive planning is better framed as increasing the resilience of human and natural systems to climate impacts by eliminating or minimizing the negative consequences of climate change on these systems.

Second, adapting to climate change is not a one-time activity. Climate will continue to change as will Washington's communities, economies, social preferences, and policies and regulations. The assumptions that shape adaptation planning must be periodically revisited and adjusted to reflect these changes. Therefore, adapting to climate change must be seen as a "…continuous set of activities, actions, [and] decisions" undertaken by individuals, groups, and governments rather than a one-time activity (Adger et al. 2005).

3. Why Adapt to Climate Change at the State and Local Level?

State and local efforts to prepare for climate change are relatively new yet gaining ground quickly. As of September 2008, eight states – Washington, Oregon, California, Alaska, Florida, Maryland, New Hampshire, and Massachusetts – were developing state-level adaptation plans (Pew 2008). Six additional states (Arizona, Utah, Colorado, North Carolina, South Carolina, and Vermont) had recommended developing adaptation plans within their state mitigation plans. Numerous county and local governments around the country, including Washington's City of Olympia, King County, and City of Seattle, are also developing adaptation plans (Box 2).

Box 2. The CASES Database

Understanding how state and local governments are approaching the task of adapting to climate change is often helpful for building public and political support for adaptation, understanding the range of activities that constitute adapting to climate change, and learning from the experiences of other state and local governments who have started the process of adapting to climate change. Knowing which state and local governments are working on climate change adaptation and where to find information on their efforts can be challenging, however.

To help address this challenge and support state and local adaptation planning, the Climate Impacts Group is developing the CASES (Climate Adaptation caSE Studies) database. CASES is a user-driven, searchable database that will provide basic information on state and local adaptation planning efforts. Users will be able to query the database by location and/or any other combination of search options, including population size, impact concerns, and adaptation activities. CASES reports will include a summary of adaptation planning activities within a community and contact information for requesting additional information. The database is expected to "go live" with an initial set of case studies. Users will help grow the database over time by submitting case studies on their own adaptation work to the database. Funding for the development of CASES was provided by Washington State as part of the Washington Climate Change Impacts Assessment.

Adapting to climate change at the state and local level is prudent for several reasons (Snover et al. 2007, Smith 1997, Box 3). First, significant regional-scale climate change impacts are projected. Furthermore, because of lags in the global climate system and the long lifetime for key greenhouse gasses in the atmosphere, impacts over the next few decades are virtually certain. Impacts in the second half of the 21st century are also certain, but the magnitude of those impacts will be greatly influenced by the success or failure of efforts to reduce greenhouse gas concentrations both in the near-term and over time.

As described in accompanying papers, Washington State is projected to experience a wide range of climate change impacts (absent adaptation) by mid-21st century, including:

- An increase in average annual temperature of 1.8°C (3.2°F) by the 2040s (Mote and Salathé 2009, this report);
- A 37-44% decline in spring snowpack by the 2040s (Elsner et al. 2009, this report);
- A 13-16% decrease in summer hydropower production by the 2040s and a 363-555% increase in summer cooling demands, which is related to warmer summer temperatures as well as population growth and building trends (Hamlet et al. 2009, this report);
- Changing yields for dryland winter wheat (+13 to +24%), irrigated potatoes (-2% to -3%), and irrigated apples (+9%) by the 2040s *assuming continued availability of water to irrigated crops and benefits from the carbon dioxide* (*CO_2*) *fertilization effect* (Stöckle et al. 2009, this report). Average yield for cherries and apples decrease 40-50% by 2070 for junior water rights holders in the Yakima Basin despite the CO_2 fertilization effect when climate change-related declines in summer water supply are accounted for (Vano et al. 2009b, this report);
- A quadrupling of the duration of temperatures causing migration barriers and thermal stress for salmon (temperatures greater than

Box 3. Primary Reasons for Planning for Climate Change at the State and Local Level

1. Significant regional-scale climate change impacts are projected.
2. State and local governments, businesses, and residents are on the "front line" when it comes to dealing with climate impacts.
3. Decisions with long-term impacts are being made every day, and today's choices will shape tomorrow's vulnerabilities.
4. Significant time is required to motivate and develop adaptive capacity, and to implement changes.
5. Preparing for climate change may reduce the future costs of climate impacts and responses.
6. Planning for climate change can benefit the present as well as the future.

70°F) in the interior Columbia Basin by the 2080s (Mantua et al. 2009, this report);

- A tripling in the area burned by fire in the interior Columbia Basin risk by the 2040s (Littell et a. 2009, this report);
- Increasing coastal threats associated with higher mean sea level, increased coastal storm strength and flooding, increased beach and bluff erosion, and increased ocean temperatures and acidity (Huppert et al. 2009, this report);
- Projected increases in extreme rainfall magnitudes throughout the state by mid-century, although the projections vary substantially by both model and region (Rosenberg et al. 2009, this report); and
- An additional 156 deaths annually among persons aged 45 and above during heat events in 2045 in the greater Seattle, Washington, area alone, as well as an additional 132 deaths between May and September annually due climate change impacts on air quality (Jackson et al. 2009, this report).

The impact of these projected changes on Washington's human and natural systems could be significant if steps are not taken to eliminate, reduce, or otherwise accommodate the changes.

Second, Washington's residents, businesses, and local and state governments are on the "front line" when it comes to dealing with climate impacts. Climate change is driven by the global accumulation of greenhouse gases in the atmosphere but the impacts of this global-scale problem will be felt most acutely at the state and local level. State and local governments, businesses, and private citizens will be forced to deal with the physical impacts of climate change and the associated economic costs of lost productivity, damaged infrastructure, and increasing emergency response costs, among others. At its core, adapting to climate change is an inherent part of providing for the safety, health, and welfare of a community.

Third, decisions with long-term impacts are being made every day, and today's choices will shape tomorrow's vulnerabilities. State and local governments regularly make decisions that have long-lasting implications for climate vulnerability, including decisions related to land use planning and development, habitat management, flood control, erosion control, water supply, and infrastructure design. Excluding the potential impacts of climate change in these types of decisions can increase vulnerability to climate change. For example, developing property in an area that is likely to experience more flooding as a result of climate change increases the risk of flood damage to the new structures.

Fourth, significant time is required to motivate and develop adaptive capacity, and to implement changes. Evaluating and integrating information on climate change impacts into decision making does not happen quickly. Significant time is required to develop the necessary support for examining how climate change may affect specific resources or activities; for identifying and addressing where legal, institutional, and cultural barriers to using climate information in decision making exist; and for implementing strategies that reduce vulnerability to climate change impacts.

Fifth, preparing for climate change may reduce the future costs of climate impacts and responses. Efforts taken now to reduce vulnerability to climate change impacts may lead to future cost savings through damage avoidance and/or by avoiding the need to retrofit for climate resilience. For example, updating coastal setback requirements or modifying land use planning to eliminate certain types of land uses within the flood zone are likely to be more cost-effective when done proactively rather than reactively. The suite of adaptation choices also may be greater when preparing for, rather than reacting to, climate change.

Finally, planning for climate change can benefit the present as well as the future. Climate change is likely to intensify existing stresses by increasing the frequency, duration, and extent of events that contribute to present-day problems, such as flooding, drought, and forest fire risk. Most adaptation activities aimed at addressing projected climate change impacts are likely to provide benefits today, meaning that communities do not have to wait until the 2020s or the 2050s to realize the benefits of adaptation activities. For example, expanding an existing water conservation program in anticipation of increasing drought risk will help mitigate present-day droughts as well.

While the reasons for preparing for climate change are clear, adaptive planning to date has been inhibited by many real and perceived barriers. These include the following (Luers and Moser 2006; Snover et al. 2007; IPCC 2007; Ligeti et al. 2007; Repetto 2008; UKCIP, undated).

Information Barriers. Updated information on climate impacts and adaptation planning may be hard to find, out of date, and/or difficult to apply directly to state and local government management needs. For example, the geographic scope of available impacts assessments (such as a region of the country or a particular sub-basin) may not match the needs of individual decision makers, who would ideally like to know how climate change will affect their specific community or management domain with as much detail as possible. Additionally, the technical nature of climate information can make it difficult to interpret the relevance of available climate information to state and local planning needs.

Dealing with Uncertainty and Perceptions of Risk. Decision makers may feel there is too much uncertainty about the timing and extent of climate impacts, or the risks associated with implementing certain adaptation actions, to begin adapting to climate change. Additionally, decision makers may not feel that the impacts and associated risks are significant enough to require a change from "business as usual."

Issue Fatigue and Disconnected Time Horizons. Decision makers are often contending with multiple pressing issues related to present-day problems. Incorporating climate change impacts into already complex decision-making environments can be difficult, particularly given the long-term nature of the climate change problem. This challenge may become even more pronounced if projected impacts are not expected to occur until after a decision maker's term has expired or they have retired. Additionally, decision makers may find it hard to rationalize the near-term costs of specific adaptation options relative to the future (long-term) costs of inaction. The division of responsibilities between short-term and long-term planning, and the location of these responsibilities in different departments, may contribute to the problem of disconnected time horizons (Luers and Moser 2006).

Technical, Fiscal, and Human Resource Constraints. A lack of staff, fiscal, and technical resources for adaptive planning can limit adaptive planning efforts.

Regulatory and Institutional Barriers. Regulations, policies, and procedures may include provisions that limit the ability of institutions or individuals to implement adaptive actions. In some cases, regulatory programs or limits may actually promote actions that increase vulnerability to climate impacts (e.g., flood insurance programs that allow for development in floodplains). Institutional barriers may include problems coordinating across different levels of government, departments, or disciplines; lack of internal and/or external support for acting on climate change; and turnover of staff and elected officials. Institutional responses to risk taking also may create barriers. In general, staff are not punished when things go wrong if they followed existing guidelines. This encourages reliance on past information even when decisions made on the basis of past information may not be consistent with future needs.

Lack of "Peer" Examples for Adaptive Planning. In some cases, the perception that few, if any, "peer" communities (i.e., communities of similar size or geographic location) are planning for climate change may create a barrier to planning for climate change.

Reducing the barriers to adaptive planning will take time. Many may be addressed in substantive ways by building and maintaining adaptive capacity, as described in Section 2. Focusing early adaptation actions on low-regrets and no-regrets strategies (see Section 4.9) also may be effective for gaining early momentum on adaptive planning. Most important, however, is recognizing that while these barriers exist (and likely will always exist to some degree), the need to begin preparing for climate change impacts remains clear.

4. Adaptation Options for Washington State

Washington's commitment to adapting to climate change was formalized on February 7, 2007, when Governor Christine Gregoire signed the Washington Climate Change Challenge (Executive Order 07-02). In addition to establishing greenhouse gas reduction goals for the state, Executive Order 07-02 committed the state to determining what steps the State could take to prepare for the impacts of climate change. Five multi-stakeholder Preparation and Adaptation Working Groups (PAWGs) focusing on public health, agriculture, coasts and infrastructure, forestry, and water supply and management were assembled to develop the adaptation recommendations. The PAWG recommendations, released February 2008, varied by sector but addressed the following common themes (Ecology and CTED 2008):

- Enhancing emergency preparedness and response;
- Incorporating climate change and its impacts into planning and decision-making processes;
- Restoring and protecting natural systems and natural resources;
- Building institutional capacity and knowledge to address impacts associated with climate change;

- More effectively managing and sharing best available data; and
- Educating, informing and engaging landowners, public officials, citizens and others.

The Washington Assessment complements the State's effort with the PAWGs by providing updated and expanded details on the potential impacts of climate change in Washington. Adaptation options relevant to the scope of the analyses conducted for the Washington Assessment are described in the following sections and aggregated in Table 2, located at the end of this paper.

Note that the Washington Assessment does not provide a detailed list of specific policy changes that could be made, nor have the various studies in this report analyzed the effectiveness of the identified adaptation strategies and options on projected climate change impacts for each sector. The Washington Assessment should be viewed as starting point for initiating a more systematic review of adaptation needs, as recommended in Section 6**.** This could be done with continued involvement from the PAWGs and/or through a combination of intra- and inter-agency working groups convened to evaluate what adaptation options are needed and how they can be implemented.

4.1. Hydrology and Water Resources

Washington's water resources are highly sensitive to climate change, as described in Elsner et al. 2009, this report; Vano et al. 2009 a,b, this report. This sensitivity is largely dominated by the state's reliance on snowpack for much of its water supply. Although specific impacts will vary by watershed, climate change is projected to contribute to lower spring snowpack, higher winter streamflows, earlier peak spring runoff, and lower summer streamflows. These changes are most pronounced in relatively warm mid-elevation watersheds (such as those originating on the west slopes of the Cascades) where projected warming shifts more winter precipitation to rain rather than snow.

In the absence of adaptive responses, the projected hydrologic changes are expected to result in reduced water supplies in Seattle, Tacoma, and Everett, and increased impacts to irrigators with junior water rights in the Yakima basin (Vano et al. 2009a,b, this report). Regional hydropower production, flood control operations, and instream flow in the Columbia River basin will be materially affected by streamflow timing shifts that accompany regional warming, requiring operational changes (Lee et al. 2009) and different approaches to energy planning (Hamlet et al. 2009, this report).

Impacts on the high flow side of the spectrum are also projected. Increases in winter precipitation combined with regional warming are projected to increase flooding in many river basins in Washington (Mantua et al. 2009, this report). Changes in hydrologic extremes (floods and droughts) impact both human systems (Rosenberg et al. 2009, this report) and aquatic ecosystems (Mantua et al. 2009, this report), particularly in the context of Pacific Northwest salmon recovery activities.

Non-climatic factors are likely to compound projected hydrologic impacts. Patterns of development, such as location of new communities in a flood plain, may escalate flood risk by increasing community exposure to flooding. Loss of riparian habitat due to development, timber production, or other non-climatic factors may intensify projected impacts related to low streamflow, warmer summer water temperature, and damaging winter high flows.

Population growth will also add stress to water supplies. The majority of Washington's population (both current and projected) lives west of the Cascades in vulnerable areas affected strongly by loss of snowpack and increased flood risk. Likewise Washington's key agricultural areas are located in sensitive watersheds with limited reservoir storage. Finally, energy policies that place increased emphasis on renewable energy sources such as hydropower may effectively increase the stresses associated with projected losses in summer hydropower production (Hamlet et al. 2009, this issue).

The rapidly evolving impacts of climate change on the hydrologic cycle will require new approaches to water management, and greater flexibility in the way we conserve and manage our water resources and prepare for emergencies such as floods and droughts (Hamlet et al. 2009, in review). Strategies for adapting to reductions in summer water availability and increasing summer drought stress include expanding and diversifying existing water supplies, developing new or alternate water supplies, reducing demand/improving efficiency, implementing operational changes, increasing the ability to transfer water between uses and users, and increasing drought preparedness (Table 2, located at the end of this paper).

Adaptation actions to reduce increased winter flood risk include infrastructure changes such as strengthened dikes and levees, increased reservoir storage, restoration of hydrologic function in floodplains, operational approaches such as improved flood forecasting and adaptation of reservoir management policies, improved emergency management systems, and altered land use policies and flood insurance programs that take into account the changing risks of extreme events. Changes in ecosystem management and salmon habitat restoration plans will also be needed to adapt to changing high flow risks.

Most of the adaptation strategies identified in Table 2 are already familiar to water resources planners and managers, or are extensions of existing water planning and management strategies. This supports the argument that adapting to climate change can make use of existing tools and approaches (Snover et al. 2007), although which tools are used and how they are used may differ once projected climate change impacts are taken into account. It is worth noting that, in the context of water supply, demand management strategies such as conservation often emerge as low cost (often lowest cost) adaptation strategies, whereas adaptation strategies based on large scale infrastructure changes are often the highest cost (Hamlet et al. 2009, in review).

Barriers to adaptation in the water sector include institutional or legal constraints that ultimately prevent meaningful changes in water policy, water allocation, or water resources management from occurring (Gamble et al. 2003). Functional linkages between science (in this case climate change science) and water resources planning and management practice are frequently missing or are outdated. Perceptions of professional risk in the water resources management community are an obstacle to the acceptance of changes that are currently outside of accepted professional practice (e.g. scenario-based planning based on climate and hydrologic model simulations). Planning horizons are often too short to meaningfully encompass climate change impacts, and the policy sector is often unresponsive to the gradual nature of the changes. Instead changes in water management or water policy often follow crises. In the case of climate change impacts, these crises may occur decades in the future with the result that policy makers and planners ignore projected climate change impacts and focus on present difficulties. Polarization in communities focusing primarily on mitigation and those focusing primarily on adaptation has been a source of confusion in the media that limits the effectiveness of both groups. However, effective adaptations strategies can also have a positive impact on mitigation efforts (e.g., water conservation efforts may ultimately reduce the amount of total power required to treat and pump water). Together these efforts can result in greater flexibility in managing water resources into the future.

4.2. Energy

As shown in Hamlet et al. 2009 (this report), energy demand for heating and cooling is projected to increase due to the combined effects of population growth and warmer regional temperatures. Heating energy demands are projected to increase in the region by 35-42% by the 2040s despite reductions in heating days[1] due due to warming. Cooling energy demands in the region are expected to increase significantly, rising 363-555% by the 2040s relative to the late 20th century.

Increased heating energy demands will affect both direct fossil fuel use (e.g. natural gas use for space heating) and demand for electrical power from hydropower and other sources. Growing cooling energy demands, on the other hand, will primarily increase demand for electric power since air conditioning technology is predominantly powered by electricity. Increasing cooling energy demands will also indirectly affect fossil fuel use associated with non-renewable power sources as the energy industry looks to increase capacity in response to growing demands. Increases in air conditioning use in the Pacific Northwest are likely to intensify these impacts and increase peak electrical power loads in summer.

Climate change will also affect hydropower production. Hydropower accounts for roughly 70% of the electrical energy production in the Pacific Northwest and is strongly affected by climate-related changes in annual streamflow amounts and seasonal streamflow timing. Winter (December-February) regional hydropower supplies are projected to increase by about 4% by the 2040s, which will offset increases in heating energy demand to a certain extent. However, summer (July-September) regional hydropower

[1] Cooling and heating degree days are measurements used in the energy market to estimate demand. In the United States, a cooling degree day is counted for each degree the average temperature for a day moves above 75°F (24°C). For example, if the average temperature for the day was 80°F (27°C), that would count as 5 cooling degree days. One heating degree day is counted for each degree that average daily temperature falls below 65°F (18°C).

supply is projected to *decrease* by about 15% by the 2040s, exacerbating the projected growth in cooling energy demands. Total annual hydropower production is expected to decline by about 3% (*idem*).

Adapting to these changes will be needed, especially in summer. Impacts in summer are expected to be much more severe due to strongly increasing demand for electrical power, expected increases in air conditioning use and associated peak demands, and substantially reduced supplies from regional hydropower resources during the peak air conditioning months. Adaptation options for increasing energy supply include expanding the capacity of conventional, alternative, and renewable energy supplies in both winter and summer in anticipation of increased demand, and increasing local transmission capacity and peaking generation capacity in anticipation of projected increases in peak summer loads (Table 2, located at the end of this paper). Changes in water management policy to allow for increased summer hydropower generation may partially compensate for lost generating capacity. Increasing summer hydropower production may also help offset projected impacts to salmon (Mantua et al. 2009, this report) by increasing summer streamflow volumes as more water is passed through hydropower dams to generate electricity. The increase in summer production would potentially come at a loss for winter production, however, as reservoir levels are drawn down for summer production rather than being carried over into winter. Regional capacity constraints in the winter may be eased by importing energy from California and the Southwest, where excess capacity is expected to increase with winter warming.

Reducing energy demand in winter and summer will also be critical adaptation strategies. Options include establishing more stringent energy efficiency standards for new construction and appliances (including increased state-wide heating and air conditioning efficiency and insulation standards), promoting increased use of high efficiency air conditioning technology (e.g. geothermal air conditioning systems), reducing heat island effects in urban settings via "green roofs" or other approaches, implementing water and energy conservation programs, and increasing application of renewable energy sources such as solar hot water heating and photovoltaic panels in residential and commercial buildings.

Barriers to adaptation in the energy sector include limited (and fully allocated) hydropower resources and current limitations on the ability to increase renewable resources to meet projected changes in demand. Although increased hydropower production in summer may be technically feasible, losses of summer recreation opportunities on reservoirs and tradeoffs with winter hydropower production are likely to occur. The need to balance greenhouse gas mitigation activities with the need for increased generation capacity will require difficult tradeoffs between acquiring additional capacity to meet projected demand and portfolio standards for renewables imposed by the policy sector.

4.3. Agriculture

Stöckle et al. (2009, this report) indicate that, with the possible exception of winter wheat, the main agricultural commodities in eastern Washington will be affected by future climate, even as soon as the next few decades.

However, elevated atmospheric carbon dioxide (CO_2) may compensate for the effect of warming and result in yield gains. Adapting agriculture to changing conditions will be critical to managing climate change and capturing the potential benefits of elevated CO_2. Changes in the relative importance of the region's commodities, adoption of new crops and varieties, changes in management, and research will play an important role for adaptation.

Adapting to evolving future climatic conditions is among the significant long-term challenges for the agriculture in the state. Conventional or biotechnology-based plant breeding research will be needed for this task. Overall advances in agricultural technology will be also needed to reduce costs and improve crop yields and quality. Research in automation, sensors, and overall improvement of decision-making tools for management will also be important (Table 2, located at the end of this paper). Maintaining a state-of-the art monitoring network and information center for evaluating the manifestations of climate change and guiding basic and applied research for adaptation would be beneficial.

Apples and other temperate tree fruits are projected to benefit from warmer weather combined with elevated CO_2, but management and varieties will need to constantly adapt to harvest the benefits of future conditions. Eventually, warming will affect over-winter chill requirements of temperate tree fruits requiring substitution. In the case of annual crops, modification of planting dates and use of varieties better adapted to the available growing season will be required, particularly in the case of potatoes. For annual and tree fruit crops, the search for more effective and environmentally friendly approaches for controlling more aggressive (or new) insects and weeds will be needed.

Impacts to Washington agriculture will also depend on changes to agricultural areas outside of Washington, which was beyond the scope of Stöckle et al. (2009, this report). It is difficult to predict the economic environment under which agriculture will operate as we move through the century. Increasing global population is projected to reach nine billion people by mid-21st century and the rapid development of highly populated countries such as China and India will ensure increasing demand for agricultural products. The diversification of the state's agriculture may be an important factor for adaptation. Conventional and biotechnology-based breeding may further help the competitive position of existing commodities in the state as well as facilitate adaptation to climate change as already discussed. Finally, consequences of climate change appear less severe for higher latitude regions like Washington than agricultural areas further south, potentially increasing the competitive position further.

4.4. Salmon

As shown in Mantua et al. (2009, this report), the hydrologic processes that influence the timing, volume, and temperature of streamflow in Washington State are highly sensitive to projected changes in future climate. Changing thermal and hydrologic regimes will likely have a wide range of impacts on freshwater ecosystems, favoring some species while having negative impacts on others. While the magnitude of streamflow and stream temperature impacts varies by location, many salmon populations are expected to experience greater thermal stress in the summer due to warmer summer water temperatures and lower summer streamflows. In watersheds where streamflow is now strongly influenced by a mix of rainfall and snowmelt-driven runoff, winter flood events are predicted to increase. Winter floods can reduce the reproductive success of salmon by damaging eggs while they are incubating in nests (redds), and by reducing the overwinter survival for rearing fry and parr. Taken together, the analysis points to reduced reproductive success for many salmon populations in Washington State (*idem*).

While salmon populations are affected by many non-climatic stresses (e.g., dams, other habitat loss, hatcheries, harvest and pollution), Mantua et al. (2009, this report) clearly demonstrates that adaptation in the salmon sector will require addressing factors that influence the timing, volume, and temperature changes projected for Washington's lakes and streams. Potential adaptation options for offsetting water temperature increases include reducing out-of-stream water withdrawals during periods of high temperature and low streamflow; identifying and protecting thermal refugia provided by ground-water inflows, undercut banks, and deep stratified pools; and restoring vegetation in riparian zones that provide shade and complexity for stream habitat (Table 2, located at the end of this paper). Protecting and/or restoring instream flows in summer is also a key adaptation option for reducing the future impacts of climate change.

Adaptation strategies for reducing the risk posed by flooding in fall and winter include protecting and restoring off-channel habitat in floodplains. In watersheds with large storage reservoirs, there may be opportunities to change reservoir operations in ways that compensate for climate change impacts on summer water temperature and seasonally low streamflow by augmenting flows with relatively cold water released from reservoirs at key times. However, climate change is also likely to increase the demand for surface water in summer for such uses as irrigated agriculture and municipal water supplies. This situation will require strategic policy thinking that recognizes the trade-offs that will have to be made between ecosystem protection and other water resource uses, and development of clear decision guidance to avoid protracted and potentially costly conflicts. Modified flood control operations in watersheds with dams may also provide a means for reducing the projected impacts of climate change on flooding.

4.5. Forests

Littell et al. (2009, this report) show that climate change will have potentially profound impacts on Washington's forest ecosystems. Warmer temperatures and declining snowpack are projected to increase water stress on forests, increase forest fire risk, and increase in the frequency of mountain pine beetle outbreaks. Productivity of Douglas-fir, a commercially important species, will vary more with water stress east of the Cascades and possibly at middle to upper elevations, where stands are more sensitive to drought than at the most productive lower-elevation sites west of the Cascade crest. However, productivity is ultimately projected to decline statewide later in the century with increased temperatures and drought stress.

Eastside forests will be the most vulnerable in the short term, as they are already periodically affected by severe disturbances worsened by drought stress. Both fire and insect disturbance may vary in extent and severity due to non-climatic factors such as stand dynamics and fuel buildup (or reduction) from fire management. Forest management will need to anticipate new landscape patterns that emerge from climate-disturbance interactions.

Adaptation options for the forest sector can be viewed differently at different scales (Millar et al. 2007, Joyce et al. 2008). For example, regional adaptation involves planning that is sufficiently flexible to facilitate appropriate local actions but also capable of organizing regional responses to broader impacts. Examples of regional-scale adaptation strategies include a stronger emphasis on maintaining mixed landscape structure, maintaining species diversity and within-species diversity, increasing forest resilience to drought stress and severe disturbance by managing density, improving information used in forest management to facilitate planning for projected conditions, and evaluating the barriers and opportunities that limit or facilitate local adaptation (Table 2, located at the end of this paper).

Local adaptation must be tailored to local conditions to succeed. One must identify specific management objectives, such as reduced risk of fire or insect outbreaks, characteristics of landscape pattern, or habitat needs for threatened species; assess the capacity to alter conditions to meet the objectives, e,g, by achieving target densities or basal area; and then implement the appropriate treatments that will allow objectives to be met. For example, targeted thinning may increase the resilience of drier forests in which fire suppression has caused a shift toward fuel structures susceptible to crown fires. In wetter forests where 20th century timber management has decreased age class diversity and altered patch structure, targeted thinning could simultaneously create appropriate fuel breaks and increase canopy and age-class diversity. In water-limited forests, tailoring stand density to the expected water conditions of the future will likely increase resilience to insect attack and climate change in general.

Two of the key barriers to adaptation in the forest sector are mixed land ownership (and management mandates/missions) and the need for a wide range of ongoing ecosystem services from forests. For example, federal forests (both wilderness and multiple-use), state forests, and private forests have different mandates for management, making integrated planning at the spatial scales of landscapes and watersheds more difficult. The global timber economy and local forest-reliant communities make adaptation decisions more complex and introduce unexpected pitfalls. On the other hand, barriers might in some cases be turned into opportunities; for example, if national economic priorities called for carbon-smart biomass use that also provided incentives for thinning vulnerable forests to densities more resilient to climatic change. Ongoing dialogues among stakeholders directed toward anticipating both climatic and non-climatic stressors will be needed.

4.6. Coasts

Climate change is projected to bring higher mean sea level, increased coastal storm strength and flooding, increased beach and bluff erosion, and increased ocean temperatures and acidity to Washington's coastal environment (Huppert et al. 2009, this report). Current projections for changes in mean sea level range from 4 cm (2 in) to 34 cm (13 in) by 2100 in moderate scenarios, but could reach an extreme of 128 cm (50 in) by 2100 if the accelerated melt rates observed in Greenland and Antarctica between 2002 and 2006 were to continue through the 21st century (Mote et al. 2008). How these changes affect a given location or coastal use will vary depending on the physical characteristics of the coast and the influence of human activities in that area (e.g., whether the beach is armored or not).

Adaptation strategies must recognize the dual nature of coast impacts. Adapting to coastal impacts will require adapting to more frequent or more severe short-term problems such as increasing episodic coastal flooding and storm damage while also taking into account the long-term problem of increasing mean sea level, which threatens to permanently inundate low-lying areas. Adaptation to climate change can take three forms. Accommodation involves altering current uses of the coastline in response to changes in coastal oceans and environment, such as by raising the height of piers and placing shoreline buildings on pilings. Protection involves fending off the impacts by building structures like seawalls and dikes that keep the sea from intruding on coastal structures. Retreat involves avoiding the harmful effects of rising sea level by abandoning coastal sites and moving to higher ground (Table 2, located at the end of this paper).

Beaches, Bluffs, and Sand Spits. Washington's beaches, bluffs, and spits are vulnerable to increased flooding and increased shoreline erosion due to sea level rise. Building on these properties will be increasingly risky. Bulkheads and rock walls can temporarily reduce upland erosion caused by wave action, but they can do little to prevent continued erosion and sliding of the seaward bank, since waves rebound off the breakwater and increase the rate of beach erosion. Beach armoring can cause two negative effects that act to reduce the beach area: stopping the sediment from bluff erosion from adding to the beaches and moving the sand offshore (Johannessen and MacLennan, 2007). Flood zone designations could be modified to incorporate the expected sea level rise. Coastal communities may also choose to reduce development in coastal hazard areas. Alternatives to bulkheads should be considered where shoreline erosion is a problem. Setback policies and the redesignation of property lines that are to move with rising mean high water, called rolling easements by Titus (1998), can also be employed to accommodate sea level rise. Ultimately, however, communities and residents may decide to retreat upland from their current location as the sea level rises (Chrisman-Glass, 2009).

Ports and Harbors. For most port facilities, the slow speed of changes in mean sea level in combination with 30 to 40 year re-building cycles gives port facilities the flexibility to adapt by raising and shifting piers and docks over time. However, a much greater challenge is preserving a port's ability to function in the freight transportation network if sea level rise causes flooding of adjacent transportation corridors (highways, railroads) or storage areas. Because most Washington ports are inside of Puget Sound, they are protected from acute storm damage caused by waves. Some ports will have to deal with episodic flooding, in estuaries at river mouths. For example, the Port of Tacoma may have increasing problems with access to container and other terminal yards when the Puyallup river floods. Maintaining access to port facilities may require new dikes or raising existing dikes to prevent significant flooding of the lands needed by freight handling facilities. Because the set of interests is great, and property ownership in the region is complex, adapting to these risks will require a broad, well-coordinated plan of action by Port authorities, railroads, cities, counties, and state and federal agencies.

Shellfish Aquaculture. Shellfish aquaculture will need to adapt to three basic threats: (a) sea level rise causing a shift of shallow tidelands towards the upland shore, much of which is privately owned; (b) increased sea surface temperatures and acidification which may affect shellfish survival and growth; and (c) increased frequency of harmful algal blooms (HABs). One adaptive response to shifting tidelands is shifting shoreline property lines as the mean high water mark moves inland. In fact, some U.S. states already follow this principle. In Texas, when large hurricane or other events cause significant erosion of shorelines, the private property lines are shifted upland to preserve public beaches and tidelands.

Breeding or shifting to more tolerant strains of shellfish may facilitate adaptation to increased temperatures and acidification, although we do not have sufficient information regarding these factors to confidently predict whether this approach would be successful. Finally, the potential for more HAB outbreaks will require closer monitoring of shellfish tissue and water quality by the State Department of Health and NOAA. If reliable, qualitative predictions of HAB risks can be developed and managers can then be more prepared to respond quickly if HAB risks are "high" (Moore et al., 2008). This approach to adaptation is being discussed currently among scientists.

4.7. Urban Stormwater Infrastructure

Flooding is a pervasive problem in urban areas, often leading to property damage, public health threats (when combined with sanitary sewage), and disruptions to transportation systems. One need only look at the last three years to appreciate the devastation such events can cause in Washington State (Mapes 2009).

Although the link between flooding and precipitation is obvious, it is important to recognize that floods are not exclusively dependent upon climatic factors. Of equal (if not greater) significance are patterns of urban development - both in the watersheds that give rise to runoff volumes in response to large storms and across the floodplains that have always conveyed high waters. These considerations, and their relationship with changing precipitation patterns, are not specifically addressed in this report. However, the results of Rosenberg et al. (2009, this report) indicate that the magnitudes of extreme precipitation events have increased in the Puget Sound over the past 50 years, with more ambiguous changes in other parts of the state. Furthermore, simulations of future precipitation suggest that these magnitudes could continue to increase over the next 50 years, although specific projections vary widely by simulation, and actual changes may be difficult to distinguish from natural variability.

The existing literature proposes a variety of possible adaptation actions that could be employed, in part or in whole, to address the impacts of climate change on urban stormwater infrastructure (e.g., Crabbé and Robin 2006, Waters et al. 2003, Table 2, located at the end of this paper). The most common actions advocate recasting design storms and/or design flows and resizing pipes or stormwater facilities to reflect a new (or anticipated) discharge. This approach presupposes a known target discharge, presumably based upon a defensible, broadly accepted model of future climate. A key finding of Rosenberg et al. (2009, this report) is that such knowledge does not presently exist. Even if more confident projections do indicate that current systems will be undersized (and the evidence in the Puget Sound region is that some may already be), the costs associated with upgrading our infrastructure are likely to be prohibitive, particularly in densely developed areas where there may be limited space to put more robust systems in place.

More practical management options (with or without specific recommendations for redesigning infrastructure) are those that emphasize local-scale on-site management of stormwater volumes, which are capable of reducing discharges that flow into these downstream conveyance systems. These strategies, collectively termed "Low Impact Development" in the Puget Sound (PSAT 2005), "Green Infrastructure" by the EPA (PGI 2008), and "Sustainable Urban Drainage" in the United Kingdom (Woods-Ballard et al. 2007), are likely to perform most successfully in the face of a changing climate. In part, this is because their designs are inherently resilient, typically accommodating large stormwater volumes. Total storm volumes also are projected to change more modestly than storm intensities in this region (Salathé et al. 2009, this report). Examples of these "facilities" include green roofs, permeable pavements, vegetated swales, rain gardens, and pocket wetlands. Such approaches provide greater intrinsic opportunities for adaptation than those that depend solely on precise determination of rainfall depths and durations, particularly given the widely varying projections of future short-term rainfall intensities.

Fundamentally, accounting for future increases in stormwater runoff is still a matter of risk, with or without the consideration of climate change. Where large capital projects are proposed, robust decision-making can factor in both historical and projected trends in precipitation to help determine what is cost-effective over the design lives of the projects. Specific design adjustments, however, necessarily will vary with location and the risk tolerance of the decision maker.

4.8. Human Health

Jackson et al. (2009, this report) analyzed climate change impacts on heat- and air quality-related mortality. The analysis found that excess deaths have resulted from heat events for residents in the greater Seattle area (King, Pierce and Snohomish counties). This pattern was not demonstrated for Spokane County, the Tri-Cities (Benton and Franklin counties), and Yakima County, perhaps because of the relatively small populations in these regions, but also because people in these regions may have already implemented successful adaptations. With increasing temperatures predicted throughout the state during the 21st century, increasing excesses in mortality due to heat seems likely in all of these regions unless appropriate prevention and intervention strategies are implemented. More heat events are also likely to result in increased illness and hospitalization, and loss of income and productivity through illness and death. Climate change will also likely degrade air quality. Ground level ozone concentrations are projected to increase in King and Spokane counties due to increases in warm season air temperatures (May-September). These increases could easily overwhelm air quality improvements made over the last several decades.

Persons who are particularly vulnerable to heat stress and poor air quality include the elderly, the very young (such as infants), the infirm, the economically disadvantaged, and those who labor outdoor. Effective adaptation strategies must take into account the particular needs of these groups. For example, the elderly are at increased risk to heat stress due to the combined effects of chronic illness, medication use, social isolation, and lack of mobility. Effective adaptation actions could focus on notifications and door-to-door transportation services to cooling centers (Table 2, located at the end of this chapter). Adaptation options for vulnerable groups such as outdoor laborers may prove more problematic. While the state has guidelines for preventing heat-related illness, the major challenge is the effective implementation of these practices in the face of the practical realities of farming and of the economic forces that can drive workers to exert themselves beyond healthy limits.

Washington faces serious barriers to the adoption of truly effective adaptation strategies. Growing population and urbanization likely will increase the frequency of extreme heat events by reducing the number of trees and extent of green space, as well as through extensive use of asphalt and concrete, creating what is known as the urban health island effect (i.e., temperatures in urban centers are increased relative to surrounding areas). In the case of air quality, the major problem is pollution from vehicular derived emissions. It is not clear what the proper combination of incentives and disincentives might be to move communities toward low or zero emission vehicles, or to transition large numbers of people to mass transit. Many other factors will influence future air quality, including decisions about land use and forestry practices, transportation, industrial emissions, fire management, and regulatory standards. All of these have implications for energy consumption and emissions, which will in turn impact air quality.

Addressing these challenges will require partnerships among scientists, policymakers, and the public. More immediately, public health measures could include improved use of early warning systems for extreme heat events and alert systems for high air pollution days; offering free public transportation on high ozone or particulate matter days; and increased public education that focuses on the risks and signs of heat exposure, and that emphasizes behavior changes that can reduce exposures to air pollutants.

4.9. No Regrets, Low Regrets, and Win-Win Strategies

As Washington decision makers begin assessing how to move forward on adapting to climate change in Washington State, strategies for prioritizing early actions on climate change will need to be considered. One approach is identifying “no regrets,” “low regrets,” and “win-win” (or “co-benefit”) strategies (de Loë et al. 2001,Willows and Connell 2003, Snover et al. 2007, Luers and Moser 2007).

No regrets, low regrets, and win-win strategies describe approaches to acting on climate change that balance the need for adaptive action with uncertainty and risk. No regrets actions provide benefits in current and future climate conditions even if no climate change occurs. For example, improved drought planning provides benefits for managing present-day drought regardless of what happens to drought risk in the future. However, if drought risk increases as projected with climate change, the benefits from improved drought planning will be even greater.

Low regrets actions provide important adaptation benefits at relatively little additional cost or risk. For example, a community planning flood levee upgrades may increase the height of the levees in anticipation of greater flood risk if the benefits of the increased levee height exceed the marginal cost of the increase.

Finally, win-win (or co-benefit) actions reduce the impacts of climate change while providing other environmental, social, or economic benefits. For example, implementing coastal setback requirements or rolling easements[2] (Titus 1998, Chrisman-Glass 2009) to address the potential threats of sea level rise on coastal properties may also provide benefits to nearshore habitat by giving these habitats room to migrate inland as sea level rises.

Implementing no regrets, low regrets, and win-win strategies can help build early momentum on adaptation planning while also producing potentially significant cost savings. Care must be taken, however, not to consider a community adapted to climate change based solely on the implementation of no cost or low cost adaptation actions. Implementing no cost or low cost adaptation actions is likely to address the “low hanging fruit”, potentially leaving important determinants of vulnerability to climate change as issues that must still be resolved. Adapting to climate change will require difficult choices; making and implementing these choices will take time, underscoring the need to begin adaptive planning sooner rather than later.

5. Policy Formulation in a Changing Climate

As noted in Section 2 and reflected in Section 4, climate change will require building adaptive capacity and delivering adaptive actions to address the challenges and opportunities presented by climate change. These two general categories of activity can happen simultaneously, although in

[2] Setback, or retreat, policies generally condition the use of property in areas vulnerable to erosion and flooding and prohibit new construction seaward of a setback line. A “rolling easement” is a device that allows publicly owned tidelands to migrate inland as the sea rises, thereby preserving ecosystem structure and function. Thus, rolling easements transform static property lines into ones where private property must yield the right of way to naturally migrating shorelines.

some cases it may be necessary to address specific capacity needs before certain adaptation actions can be fully undertaken.

One component of increasing adaptive capacity is increasing flexibility in institutions and decision processes so the public and private sector can more readily adjust to climate impacts as they occur. The need for more flexibility is well recognized in climate change literature (Smith and Lenhart 1996; Fankhausera et al. 1999; Smith et al. 2000). Though Washington agencies currently enjoy some flexibility when determining, issuing, and applying regulations, more flexibility may be needed to accommodate uncertainties associated with climate change as well as uncertainties in non-climatic stresses, such as changes in population growth, economic trends, resource demands, the legal landscape, and economic trends. Without more flexibility, the institutions, laws, and policies used to govern human and natural systems may become increasingly constrained in their ability to effectively manage climate change impacts.

This section briefly considers some of the broader, systemic options for increasing flexibility in Washington State policy-making. These options include, but are not limited to, building social capital; broader use of market mechanisms, conditional permitting, adaptive management, and the precautionary principle; and increasing legislative flexibility in the courts.

With the possible exception of building social capital, which is a fundamental component for all government action, none of the options provided are offered as "one size fits all" answers to increasing flexibility and building adaptive capacity. When, where, and under what conditions these options are applied will vary in ways yet to be determined depending on 1) the nature of the decisions being made and the individuals or institutions implementing those decisions, 2) how risks are perceived, and 3) existing barriers to adaptive planning, among other factors. Additional research is needed in this area.

More importantly, increasing flexibility is an objective that needs to be pursued judiciously. Important questions must be considered: What does "increased flexibility" really mean? Where and when is it required? What are the potential consequences of increasing flexibility? In some cases, the needed flexibility may exist but there may be a lack of political will to implement the needed changes. These questions are not easily answered and will need to be evaluated as adaptive planning progresses in Washington State.

5.1. Building Social Capital

Social capital can be defined as the social skills, informal networks, levels of trust, and values within an organization, community, or society that allow people to work together for mutual benefit (Putnam 2000, Pelling and High 2005, Luers and Moser 2006). Adger (2003) describes social capital as the "necessary glue for adaptive capacity, particularly in dealing with unforeseen and periodic hazard events." Building social capital between public agencies and their stakeholders may be one of the most beneficial, and yet most difficult to evaluate, courses of action for increasing flexibility in decision-making processes. The means for building social capital will vary but include transparency in decision making (e.g. Washington State's commitment in 2007 to keep PAWG and related mitigation working group meetings open to the public via toll free conference call lines), outreach and education, and building sustained partnerships.

Social capital must also be built between regulatory agencies. Climate change impacts reflect a complex combination of both climatic and non-climatic stresses that often extend beyond the jurisdiction of individual agencies. Effectively addressing the complex challenges presented by climate change will likely require more coordinated responses between agency jurisdictions. A diverse set of institutions and agencies must learn to integrate their practices and work collaboratively in areas that were previously the responsibility of one particular agency. It will be necessary to build cooperative mechanisms and mandates into current agency structures to facilitate efficient information, jurisdiction, and resource sharing.

5.2. Market Mechanisms

Market mechanisms provide an alternative approach to technological mandates and environmental regulation for achieving environmental protection. Market mechanisms often use market-based approaches in conjunction with government policy to provide financial incentives for innovation or behavior change. Market mechanisms are the core of environmental trading programs designed to limit activities found to have negative impacts on the environment (e.g., the emerging carbon trading market), or to facilitate the transfer of limited resources between users (e.g., water markets).

Market mechanisms provide flexibility by generally allowing users to choose individualized pathways toward meeting regulatory goals, although it is common for limits to be placed on some aspects of the market system. In the context of climate change, market mechanisms selectively apply (in theory) the best practices of the current economic system to leverage efficiency, innovation, and capital to achieve adaptation goals. Water markets, for example, may aid climate change adaptation by providing incentives for improved water use efficiency. Surplus water is then available, at the discretion of the water rights owner, to sell or lease to municipal governments or conservation organizations for meeting growing demands for municipal and industrial water supply and habitat conservation (Adler 2008, Medellin-Azuara et al. 2008). A study of climate change impacts on California's water supply assessed the economic value of this optimization of water use through markets at $142 million/year in 2050 (Medellin-Azuara et al. 2008).

There are notable limitations associated with adopting new market mechanisms. First, rights must be well-defined, enforceable, and transferable for markets to be effective. Second, determining how marketable rights are priced and whether those rights include the value of ecosystem services such as clean water, habitat preservation, and other public goods that may be affected by market activities can be difficult. Other important questions to be answered include who owns the rights; who benefits from the sale if there are payments for public goods; and how low-income buyers or sellers fare under new markets (Ruhweza and Waage 2007). Perhaps most importantly, developing new markets requires buy-in from businesses, policy makers, and consumers alike. Businesses, consumers, regulators, and government entities would need to fundamentally adjust to "free goods" becoming "scarce assets". Education in the new models will be crucial.

5.3. Conditional Permitting

Conditional permitting increases regulatory flexibility by allowing specified activities or uses to occur within defined limits. Conditional permitting, or conditioned rights, is a common tool of governance. For instance, intellectual property rights expire after pre-determined periods of time because it is thought that perpetual patents negatively impact economies and encourage monopolies. Nuisance law requires that landowners refrain from activities interfering with another's use and enjoyment of their own land. Climate change may create new needs and opportunities for conditional permitting, including, for example, setback policies and rolling easements in coastal areas.

5.4. Adaptive Management

The term "adaptive management" has been used traditionally to describe an approach to natural resource management that is based on the understanding that ecosystems function in ways that are unpredictable and therefore uncertain (Holling 1978, Walters and Holling 1990, Tarlock 1994)[3]. Climate change adds to this uncertainty. Management of these systems is improved under an adaptive management framework by allowing for changes throughout a program's implementation as new information is acquired.

Precedent for expanding adaptive management in Washington law is found in Washington State's Growth Management Act (GMA). The GMA suggests the use of adaptive management as an interim approach for managing scientific uncertainty, stating that "management, policy, and regulatory actions are treated as experiments that are purposefully monitored and evaluated to determine whether they are effective and, if not, how they should be improved to increase their effectiveness" (WAC 365-195-920). The Code goes on to note that effective implementation of an adaptive management program requires a willingness by cities and counties to fund the research component of an adaptive management program, modify decisions on the basis of new information, and commit to the "appropriate timeframe and scale necessary to reliably evaluate regulatory and nonregulatory actions affecting critical areas protection and anadromous fisheries" *(idem)*.

Washington's GMA code highlights two fundamental components to adaptive management. The first is the concept of iteration, or the idea that an adaptive management program should incorporate cyclical feedback

---

[3] More generally (and particularly in the context of climate change), adaptive management can also refer to implementing adaptation actions now to address the obvious risks of climate change while deferring action in other areas where the risk of deferring action is acceptable (UKCIP, undated). In this case, as with the more traditional definition of adaptive management, consistent monitoring and reevaluation of new information is integral to determining when action must ultimately be taken.

rather than operate in a strictly linear manner. This cyclical feedback loop will place greater emphasis on the use of "Best Available Science."

The second important component is social and institutional learning through a strong monitoring, evaluation, and reporting program. Monitoring, evaluation, and reporting are essential for adapting management practices to a changing climate as many of the changes themselves likely will be incremental and discernible over longer periods of time. Monitoring, evaluation, and reporting are important tools for identifying when current policies or programs become ineffective, obsolete, or require tweaking to fulfill their mandates. An additional benefit is that new information can improve the baseline used in future decision making. Monitoring can also provide good quality, publicly available data that others can use to learn from predecessors and thus lower costs (Ruhl 2005). Consequently, specific attention should be paid to ensuring that monitoring and assessment are maintained as part of an adaptive management approach.

The practice of adaptive management has not been without challenges, however. Noted problems include difficulties developing acceptable predictive models for policy comparison (often complicated by a lack of data on key process or difficulties validating data); difficulty implementing large-scale management experiments because of the costs and risks; a mismatch between the length of the adaptive management process and short funding cycles; agency and stakeholder impatience with the slow pace of adaptive management; and a lack of leadership for monitoring and coordinating efforts (Halbert 1993, McLain et al. 1996, Walters 1997, Levine 2004). Consequently, adaptive management to date has been more influential as an idea rather than as a practical management tool (Lee 1999).

5.5. The Precautionary Principle

What we know, and don't know, about climate change impacts on Washington State involves risk. Under circumstances involving great risk - whether related to climate change or other hazards - a more precautionary approach may be warranted, even if some of the cause and effect relationships are not fully established scientifically (Barrieu and Sinclaire-Desgagné 2006).

The precautionary principle provides flexibility by allowing decision makers to take a more proactive stance on risk reduction. The precautionary principle differs from adaptive management in its inherent acceptance of scientific uncertainty at the outset. The approach asks "how much harm can be averted" rather than "how much harm is allowable" (Seattle Precautionary Principle Working Group 2004).

Washington State has at least two programs that recognize the precautionary principle concept. The Department of Ecology's Persistent Bioaccumulative Toxins (PBT) program explicitly adopted the precautionary principle as one of the policy's ten guiding principles for addressing PBTs (Gallagher 2000). The GMA, previously noted for its suggested use of adaptive management, also suggests a "precautionary or no risk approach" in situations when there is incomplete scientific evidence about whether a development or land use action could harm established critical habitat areas (WAC 365-195-920(1)). However, the language in the statute is advisory language that does not impose any serious mandate on the decision makers.

It is worth emphasizing that the precautionary principle does not necessitate a "zero-risk" or "zero-harm" response (Seattle Precautionary Principle Working Group 2004; Foster et al. 2000). Rather, the approach advocates considering a range of alternatives that balance known and unknown risks against a number of decision criteria, including scientific information, the costs and benefits of the actions (or non-action), and risk tolerance.

5.6. Legislative Flexibility and the Courts

Courts review agencies' interpretations of statutes, promulgation and application of rules and standards, and the constitutionality of agencies' founding and enabling acts. Consequently, courts play an important role in determining the flexibility that state and local agencies have in responding to environmental uncertainty. Legislatures, in turn, can influence how the courts assess the flexibility that agencies have in responding to environmental uncertainty by giving agencies broad enough statutory authority to respond to new contingencies.

Courts have shown a willingness to allow agencies flexibility in the face of uncertainty. For example, in *Postema v. Pollution Control Hearings Board* (142 Wash.2d 68, 91, 11 P.3d 726 (2000)), the Supreme Court of Washington held the Department of Ecology did not need to engage in formal rulemaking in order to apply new standards based on changes in science or technology. The federal precedent cited in *Postema* indicates that courts may give some latitude to agencies responding to evolving circumstances as new contingencies are encountered. However, to help achieve this judicial tolerance of agency flexibility, the legislature must be careful to give an agency broad enough statutory authority to respond to new contingencies.

6. Conclusions

Adapting to climate change will ultimately require more systematic integration of governance levels, science, regulation, policy, and economics to effectively deal with the wide range of impacts projected for Washington State. This integration will be shaped through formal mechanisms such as the development or modification of laws, regulations, and policies, and through legal proceedings in the courts. Integration also will evolve through more subtle changes in institutional culture, channels of communication, and modes of interaction that build trust between government agencies and their stakeholders.

This paper discusses fundamental concepts for planning for climate change and identifies options for adapting to the impacts evaluated in the Washington Assessment. Additionally, the paper highlights potential avenues for increasing flexibility in the policies and regulations used to govern human and natural systems in Washington. The paper should not be viewed as an ending point for the discussion on adaptation needs in Washington State, however. That discussion is, in fact, just beginning.

Areas of future research to support adaptive planning include research on institutional capacity needs and regulatory barriers to adaptation in Washington agencies. Improving institutional capacity to better understand

and incorporate climate change impacts into planning is a "no regrets" strategy that yields benefits regardless of how much warming is realized or whether precipitation decreases or increases, for example. An analysis of institutional capacity should assess how the Department of Ecology and other state agencies might be able to improve institutional capacity for adapting to climate change. This includes looking at:

- specific information needs;
- additional training/skills needs;
- specific regulatory, institutional, or other barriers to addressing climate change impacts; and
- additional coordination needs between departments and agencies, including federal, regional, and local agencies.

Identification of regulatory/policy barriers will be particularly beneficial. From this initial analysis, a series of white papers discussing identified barriers and options for addressing these barriers could be developed.

Additional research on the use of "best available science" in decision making is also suggested. Washington Administrative Code (WAC) 365-195-900–925 (procedural criteria for the Growth Management Act) is the only place where best available science is specifically elaborated upon in Washington law. The WAC is designed to assist local governments in evaluating science and deciding when they are in possession of the best science available. The recurring need for updated information on climate impacts and other related information will place a heavier reliance on the use of best available science in the policies used to govern human and natural systems. An evaluation of the successes and failures in using best available science in programs like the Growth Management Act may provide useful guidance on how to best integrate evolving climate change science into decision making. Finally, additional research on building social capital and the potential application of market mechanisms, conditional permitting, and other mechanisms for increasing flexibility in Washington State policy-making is needed.

Washington State faces unprecedented economic challenges, however. A significant budget deficit looms and deep cuts will be required to balance the state budget. Despite these challenges, preparing for climate change can continue from its important beginnings in the 2007 PAWG process. Many of the actions recommended by the PAWG process as well as others provided within this report require nominal fiscal resources. These include, but are not limited to, identifying and eliminating legal and administrative barriers to planning for climate change; increasing technical capacity within state and local governments to incorporate climate information into decision making; and public outreach and education. Furthermore, many adaptive actions may create cost savings through damage avoidance (e.g., by modifying development plans in areas likely to experience greater flooding) or delayed infrastructure upgrades (e.g., by reducing per capita water use through improve conservation and water use efficiencies). Finally, many of the changes required to develop a more climate-resilient Washington will take time to implement. Waiting for climate change to "arrive" will be too late in some cases and significantly more costly in other cases.

Table 2. Options for adapting to the impacts identified in the Washington Climate Change Impacts Assessment enhancing or supplementing Washington's Preparation/Adaptation Working Group recommendations, released February 2008

Sector	Adaptation Strategy	Examples of Adaptation Actions and Activities that Build Adaptive Capacity
Hydrology and Water Mngmt.	Expand and diversify existing water supplies	• Connect regional water systems to utilize overall water supply more efficiently • Enhance existing groundwater supplies through aquifer storage and recovery • Purchase existing water rights to meet changing supply needs • Add capacity to existing reservoirs by raising dam height
	Develop new or alternate water supplies	• Develop new sustainable groundwater sources • Construct new surface water reservoirs • Develop advanced wastewater treatment capacity for water reuse ("gray water" or "purple pipe") • Implement new technologies such as reverse osmosis for desalination (coastal areas only) • Encourage rainwater harvesting to provide water supply for residential and commercial buildings
	Reduce demand/ improve efficiency	• Increase water conservation measures • Price water to encourage conservation in summer • Reduce outdoor landscape water demands (e.g., promote drought tolerant landscaping) • Update building codes to require highest efficiency plumbing fixtures (e.g. dual flush toilets) • Provide financial incentives (e.g., tax breaks, rebates) for switching to more efficient manufacturing processes, irrigation practices, and appliances • Reduce system losses (repair pipes, line irrigation canals)
	Implement operational changes	• Rebalance flood control rule curves and reservoir refill schedules • Allocate increased storage for instream flow • Improve hydrologic forecasting and use of forecasts • Increase use of optimization in reservoir management to rebalance systems • Shift hydropower generation schedules to emphasize summer energy production • Revise maintenance schedules to conserve water (e.g. seasonal pipe and reservoir flushing schedules) • Use existing flood irrigation systems to recharge soil moisture and groundwater during winter
	Increase ability to transfer water between uses and users	• Use water banks, water pools, and water markets to facilitate the reallocation of water resources in times of shortage • Remove obstacles to flexible water reallocation in existing water law and water policy • Factor in climate change impacts in renegotiations of transboundary water agreements where applicable
	Increase drought preparedness	• Improve drought forecasting capability • Update drought management plans to recognize changing conditions • Increase emergency aid assistance for droughts • Improve coordination between stakeholders during drought
	Reduce winter flood impacts	• Strengthen dikes and levees where appropriate • Increase reservoir storage • Revise flood control rule curves • Restore hydrologic function in floodplains • Improve flood forecasting and emergency management systems • Alter land use policies and flood insurance programs to incorporate the changing risks of extreme events

Table 2. Options for adapting to the impacts identified in the Washington Climate Change Impacts Assessment enhancing or supplementing Washington's Preparation/Adaptation Working Group recommendations, released February 2008

Sector	Adaptation Strategy	Examples of Adaptation Actions and Activities that Build Adaptive Capacity
Energy	Increase energy supply	• Increase the capacity of conventional, alternative, and renewable energy supplies in both winter and summer • Increase local transmission capacity and peaking generation capacity in anticipation of projected increases in peak loads in summer • Increase winter transfers of excess energy capacity in California and the Southwest, where excess capacity is expected to increase with warming. • Implement changes in reservoir management policies to increase hydropower production in summer.
	Decrease energy demand	• Establish more stringent energy efficiency standards for new construction and appliances, including increased state-wide heating and air conditioning efficiency and insulation standards • Implement energy conservation programs • Implement water conservation programs (reduces energy use via reductions in hot water use) • Promote use of high-efficiency heating and air conditioning technologies (e.g., geothermal air conditioning systems) • Promote use of "green roofs" and other strategies to reduce urban cooling loads • Promote the use of renewable energy sources such as solar hot water heating and photovoltaic panels in residential and commercial buildings to reduce summer energy demand and peak loads.
Agriculture	Adjust production to reflect changing conditions	• Change planting dates • Change planting varieties to include crops that are better suited to projected climate conditions • Improve approaches to insect and weed management
	Improve agricultural water supply and use	• Promote new irrigation technologies to improve water use efficiency • Promote water conservation • Use market forces to distribute water • Diversify and expand water supplies and infrastructure
	Improve information and technology used in managing agriculture	• Maintain well-funded monitoring network and information center for data collection on impacts to agriculture • Support research on biotechnology-based breeding to increase the number of crop varieties that are suitable for projected climate conditions • Increase research on automation, sensors, and overall improvement of agricultural management practices to reduce costs and compensate for yield losses
Salmon	Reduce summer stream temperatures and protect (and sustain) minimum instream flows in summer	• Reduce out-of-stream withdrawals during periods of high temperature and low streamflow • Identify and protect thermal refugia provided by groundwater flows, undercut banks, and deep stratified pools • Restore riparian zones that provide shade and complexity for stream habitat • Modify reservoir operating rules to mitigate impacts on summer low flows and water temperature
	Reduce peak winter flows	• Protect and restore off-channel habitat in floodplains • Modify reservoir operating rules to mitigate impacts on winter flooding

Table 2. Options for adapting to the impacts identified in the Washington Climate Change Impacts Assessment enhancing or supplementing Washington's Preparation/Adaptation Working Group recommendations, released February 2008

Sector	Adaptation Strategy	Examples of Adaptation Actions and Activities that Build Adaptive Capacity
Forests	Maintain mixed landscape structure	• Expand or adjust protected areas to incorporate greater diversity of topographic and climatic conditions to allow for shifts in species distributions in response to climate change • Tailor timber harvest or prescribed burning to create a mosaic of patch sizes and age classes • Avoid creating monoculture forests or forests lacking structural diversity (e.g., homogeneous stands or large clearcuts)
	Maintain species diversity and within-species diversity	• Expand or adjust protected areas to incorporate greater diversity of topographic and climatic conditions to allow for shifts in species distributions in response to climate change • Plant tree species or varieties known to have a broad range of environmental tolerances • Reduce potential for invasive species
	Reduce the impact of climatic and non-climatic stressors	• Manage forest density to reduce susceptibility to severe fire, insects outbreaks (whether natives or invasives), and drought, by establishing or enhancing structural prescriptions • Manage forests for changing fire regimes so that the risk of extreme fire events in minimized
	Improve information used in forest management	• Incorporate understanding of elevation-specific climate sensitivities into management strategies • Actively monitor trends in forest conditions, including drought stress, insects, and invasive species
Coasts	Accommodate coastal impacts	• Incorporate climate change impacts into design requirements for coastal structures • Modify flood zone designations to incorporate projected sea level rise • Increase (or initiate) use of setbacks and rolling easements to allow for inland migration of wetlands, salt marshes, and other critical habitat systems, including shallow tidelands used in shellfish production. • Reduce sources of nutrients that contribute to harmful algal blooms (HABs) and increase HAB monitoring to help ensure continued viability of recreational and commercial shellfish harvests
	Protect high value coastal uses	• Construct new dikes/raise existing dikes to protect high-value areas • Increase partnerships across government levels to manage impacts to ports and supporting transportation systems
	Retreat from high-risk coastal areas	• Reduce development on beaches and bluffs likely to be threatened by sea level rise. • Where protection of property is not feasible, abandon coastal sites and move to higher ground
Urban Stormwater Infrastructure	Increase resiliency of stormwater management strategies	• Where long-lived capital projects depend on a specified design capacity, integrate specific design adjustments appropriate for the location of the project, the risk tolerance of the decision maker, and anticipated costs of increasing capacity or volume. • Promote the use of stormwater-management strategies that emphasize the management of stormwater volumes (e.g., Low Impact Development strategies), rather than strategies that that depend on precise determination of rainfall depths and durations (e.g., engineered stormwater detention ponds)

Table 2. Options for adapting to the impacts identified in the Washington Climate Change Impacts Assessment enhancing or supplementing Washington's Preparation/Adaptation Working Group recommendations, released February 2008

Sector	Adaptation Strategy	Examples of Adaptation Actions and Activities that Build Adaptive Capacity
Human Health	Reduce impacts of extreme heat events	• Open additional cooling centers during extreme heat events and improve transportation services to cooling centers for vulnerable populations • Increase public education on risks associated with heat stress and ways to reduce impacts • Improve use of early warning systems for extreme heat events • Increase use of shade trees to reduce temperatures in urban areas • Improve guidelines for providing cooling to outdoor laborers, as well as guidelines for when outdoor work or activities should be postponed or avoided
	Reduce the impacts of ozone/particulate matter pollution	• Increase public education on risks associated with high air pollution and ways to reduce impacts • Improve use of early warning systems for poor air quality days • Increase availability and use of mass transit to reduce auto emissions (e.g., free or reduced public transportation fees on high ozone or high particulate matter days)

References

Adger NW (2003) Social capital, collective action, and adaptation to climate change. Econ Geogr 79(4): 387-404

Adger WN, Arnell N, Tompkins EL (2005) Successful adaptation to climate change across scales. Glob Environ Change Doi:10.1016/j.gloenvcha.2004.12.005

Adler JH (2008) Water marketing as an adaptive response to the threat of climate change. Case Western Reserve University Case Legal Studies Research Paper 08-08, available at http://papers.ssrn.com/sol3/papers.cfm?abstract_id=1097594 Accessed 8 Feb 2009

Barrieu P, Sinclaire-Desgagné B (2006) On precautionary policies. Manag Science 52(8): 1145-1154

Chrisman-Glass E (2009) The legal implications of sea level rise in Washington. White Paper prepared for the Climate Impacts Group, University of Washington, Seattle

Crabbé P, Robin M (2006) Institutional adaptation of water resource infrastructures to climate change in eastern Ontario. Clim Change Doi: 10.1007/s10584-006-9087-5

de Loë RC, Kreutzwiser RD, Moraru L (2001) Adaptation options for the near term: climate change and the Canadian water sector. Glob Environ Change 11(3): 231-245

Ecology and CTED (Washington State Department of Ecology and Washington State Department of Community, Trade and Economic Development) (2008) Leading the way: preparing for the impacts of climate change in Washington, recommendations of the Preparation and Adaptation Working Groups, in Leading the way on climate change: the challenge of our time, Interim Report. Publication #08-01-008, Washington State Department of Ecology, Lacey, Washington, pp. 95-169

Elsner MM, Cuo L, Voisin N, Hamlet AF, Deems JS, Lettenmaier DP, Mickelson KEB, Lee SY (2009) Implications of 21st century climate change for the hydrology of Washington State. Washington climate change impacts assessment: evaluating Washington's future in a changing climate. In Press

Foster KR, Vecchia P, Repacholi MH (2000) Science and the Precautionary Principle. Science Doi: 10.1126/science.288.5468.979

Fankhausera S, Smith JB, Tol RSJ (1999) Weathering climate change: some simple rules to guide adaptation decisions. Ecol Econ 30(1): 67-78

Gallagher MJ (2000) Proposed strategy to continually reduce Persistent, Bioaccumulative Toxins (PBTs) in Washington State. Publication #00-03-054, Washington State Department of Ecology: Lacey, Washington

Gamble JL, Furlow J, Snover AK, Hamlet AF, Morehouse BL, Hartmann H, Pagano T (2002) Assessing the impact of climate variability and change on regional water resources: the implications for stakeholders. In Water: Science, Policy, and Management, R. Lawford et al., editors, AGU Press Monograph

Halbert CL (1993) How adaptive is adaptive management? Implementing adaptive management in Washington State and British Columbia. Rev in Fish Sci 1:261-283.

Hamlet AF, Lee SY, Mickleson KEB, Elsner MM (2009) Effects of projected climate change on energy supply and demand in the Pacific Northwest. Washington climate change impacts assessment: evaluating Washington's future in a changing climate. In Press

Hamlet AF, Mote PW, Snover AK, Miles EL (2009, in review) Climate, water cycles, and water resources management in the Pacific Northwest. Chapter 6 in Snover AK, Miles EL, and the Climate Impacts Group, Rhythms of change: an integrated assessment of climate impacts on the Pacific Northwest, MIT Press, Cambridge

Holling CS (1978) Adaptive environmental assessment and management. Blackburn, Camden

Huppert DD, Moore A, Dyson K (2009) Impacts of climate change on the coasts of Washington State. Washington climate change impacts assessment: evaluating Washington's future in a changing climate. In press

IPCC (2007) Climate change 2007: impacts, adaptation and vulnerability. Contribution of Working Group II to the Fourth Assessment Report of the Intergovernmental Panel on Climate Change, Parry ML, Canziani OF, Palutikof LP, van der Linden PJ, Hanson CE (eds), Cambridge University Press, Cambridge

Jackson JE, Yost MG, Karr C, Fitzpatrick C, Lamb BK, Chung S, Chen J, Avise J, Rosenblatt RA, Fenske RA (2009) Public health impacts of climate change in Washington State: projected mortality risks due to heat events and air pollution. Washington climate change impacts assessment: evaluating Washington's future in a changing climate. In press

Joyce LA, Blate GM, Littell JS, McNulty SG, Millar CI, Moser SC, Neilson RP (2008) National forests. Chapter 3 in Julius SH, West JM (eds.), Baron JS, Griffith B, Joyce LA, Kareiva P, Keller BD, Palmer MA, Peterson CH, Scott JM (authors), Preliminary review of adaptation options for climate-sensitive ecosystems and resources. A report by the U.S. Climate Change Science Program and the Subcommittee on Global Change Research, U.S. Environmental Protection Agency, Washington, DC, USA, pp. 3-1 to 3-127

Lee KN (1999) Appraising adaptive management. Conserv Ecol 3(2): 3

Lee SY, Hamlet AF, Fitzgerald CJ, Burges SJ, Lettenmaier DP (2009) Optimized flood control in the Columbia River Basin for a global warming scenario, ASCE J. Water Res Plan and Manag (in review)

Levine J (2004) Adaptive management in river restoration: theory vs. practice in western North America. Water Resources Center Archives. Restoration of Rivers and Streams. Paper levine. Available at: http://repositories.cdlib.org/wrca/restoration/levine Accessed 2 Feb 2009

Ligeti E, Penney J, Wieditz I (2007) Cities preparing for climate change: a study of six urban regions. Clean Air Partnership, Toronto, Canada

Littell JS, Oneil EE, McKenzie D, Hicke JA, Lutz J, Norheim RA, Elsner MM (2009) Forest ecosystems, disturbance, and climatic change in Washington State, USA. Washington climate change impacts assessment: evaluating Washington's future in a changing climate. In press

Luers AL, Moser SC (2006) Preparing for the impacts of climate change in California: opportunities and constraints for adaptation. White Paper prepared for the California Energy Commission (Energy Commission) and the California Environmental Protection Agency (Cal/EPA)

Mantua N, Tohver IM, Hamlet AF (2009) Impacts of climate change on key aspects of freshwater salmon habitat in Washington State. Washington climate change impacts assessment: evaluating Washington's future in a changing climate. In press

Mapes L (2009) When disaster becomes routine: crisis repeats as nature's buffers disappear. The Seattle Times 12 Jan 2009

McLain RJ, Lee RG (1996) Adaptive management: promises and pitfalls. Environ Manag 20: 437-448

Medellín-Azuara J, Harou JJ, Olivares MA, Madani K, Lund JR, Howitt RE, Tanaka SK, Jenkins MW, Zhu T (2008) Adaptability and adaptations of California's water supply system to dry climate warming. Clim Change 87 (Suppl 1): S75–S90

Millar CI, Stephenson NL, Stephens SL (2007) Climate change and forests of the future: managing in the face of uncertainty. Ecol Appl 17:2145-2151.

Moore, SK, Trainer VL, Mantua NJ, Parker D, Laws EA, Backer LC, Fleming LE (2008, in press) Impacts of climate variability and future climate change on harmful algal blooms and human health. Environ. Health

Mote PW, Petersen A, Reeder S, Shipman H, Whitely Binder LC (2008) Sea level rise scenarios for Washington State. Report prepared by the Climate Impacts Group, Center for Science in the Earth System, Joint Institute for the Study of the Atmosphere and Oceans, University of Washington, Seattle, Washington and the Washington Department of Ecology, Lacey, Washington

Mote PW, Salathé Jr EP (2009) Future climate in the Pacific Northwest. Washington climate change impacts assessment: evaluating Washington's future in a changing climate. In press

Pelling M, High C (2005) Understanding adaptation: what can social capital offer assessments of adaptive capacity? Glob Environ Change 15: 308-319

Pew Center on Global Climate Change (2008) Adaptation planning: what U.S. states and localities are doing. Washington, D.C. (originally published November 2007, updated September 2008)

PGI (Partners for Green Infrastructure) (2008) Managing wet weather with green infrastructure. available at: http://www.epa.gov/npdes/pubs/gi_action_strategy.pdf Accessed 9 Feb 2009

PSAT (Puget Sound Action Team) (2005) Low impact development: technical guidance manual for Puget Sound. Publication No PSAT 05-03, available at: http://www.psp.wa.gov/downloads/LID/LID_manual2005.pdf Accessed 15 Jan 2009

Putnam RD (2000) Bowling alone: the collapse and revival of American community. Simon and Schuster, New York

Repetto R (2008) The climate crisis and adaptation myth. Yale School of Forestry and Environment Studies Working Paper No. 13, New Haven, Connecticut

Rosenberg EA, Keys PW, Booth DB, Hartley D, Burkey J, Steinemann AC, Lettenmaier DP (2009) Precipitation extremes and the impacts of climate change on stormwater infrastructure in Washington State. Washington climate change impacts assessment: evaluating Washington's future in a changing climate. In press

Ruhl JB (2005) Regulation by adaptive management - is it possible? 7 Minn. J.L. Sci. & Tech. 21

Ruhweza A, Waage S (2007) The state of play: payments for ecosystem services in East and Southern Africa, available at: http://ecosystemmarketplace.com/pages/article.opinion.php?component_id=5108&component_version_id=7498&language_id=12) Accessed 12 Dec 2008

Salathé Jr, EP, Zhang Y, Leung LR, Qian Y (2009) Regional climate model projections for the State of Washington. Washington climate change impacts assessment: evaluating Washington's future in a changing climate. In press

Seattle Precautionary Principle Working Group (2004) A policy framework for adopting the precautionary principle, available at http://www.iceh.org/pdfs/CHE-WA/PrecautionaryPrinciple/PPWhitePaper.pdf Accessed 12 Dec 2008

Secunda J, Susskind LF (1999) "Improving" Project XL: helping adaptive management to work within EPA. 17 UCLA J. Envtl. L. & Pol'y 155, FN 20 (1999) (citing Wilkens & Hunt, Supra n.11, at 483, 521)

Smit B, Burton I, Klein RJT, Wandel J (2000) An anatomy of adaptation to climate change and variability. Clim Change Doi: 10.1023/A:1005661622966

Smith JB (1997) Setting priorities for adapting to climate change. Glob Environ Change 7(3): 251-264

Smith JB, Lenhart SS (1996) Climate change adaptation policy options. Clim Res 6: 193-201

Smith B, Burton I, Klein RJT, Wandel J (2000) An anatomy of adaptation to climate change and variability. Clim Change 45(1): 223-251

Snover AK, Whitely Binder LC, Lopez J, Willmott E, Kay JE, Howell D, Simmonds J (2007) Preparing for climate change: a guidebook for local, regional, and state governments. ICLEI - Local Governments for Sustainability, Oakland

Stöckle CO, Higgins S, Nelson RL, Keller M, Whiting M, Brunner J, Grove G, Boydston R, Painter P, Gallinato S, Huggins D (2009) Assessment of climate change impact on dryland and irrigated agriculture in eastern Washington. Washington climate change impacts assessment: evaluating Washington's future in a changing climate. In press

Tarlock D (1994) The non-equilibrium paradigm in ecology and the partial unveiling of environmental law, 27 Loy. L.A.L. Rev. 1121

Titus JG (1998) Rising seas, coastal erosion, and the takings clause: how to save wetlands and beaches without hurting property owners. 57 Maryland Law Rev. 1279: 1316

Turner II BL, Kasperson RE, Matson PA, McCarthy JJ, Corell RW, Christensen L, Eckley N, Kasperson JX, Luers A, Martello ML, Polsky C, Pulsipher A, Schiller A (2003) A framework for vulnerability analysis in sustainability science. Proc. Nat'l. Acad. Sci. 100(14): 8074-8079

UKCIP (United Kingdom Climate Impacts Programme) (undated) Identifying Adaptation Options. Available at http://www.ukcip.org.uk/images/stories/Tools_pdfs/ID_Adapt_options.pdf Accessed 2 Feb 2009

Vano JA, Voisin N, Cuo L, Hamlet AF, Elsner MM, Palmer RN, Polebitski A, Lettenmaier DP (2009a) Climate change impacts on water management in the Puget Sound region, Washington, USA. Washington climate change impacts assessment: evaluating Washington's future in a changing climate. In press

Vano JA, Scott M, Voisin N, Stöckle CO, Hamlet AF, Mickelson KEB, Elsner MM, Lettenmaier DP (2009b) Climate change impacts on water management and irrigated agriculture in the Yakima River Basin, Washington, USA. Washington climate change impacts assessment: evaluating Washington's future in a changing climate. In press

WAC (Washington Administrative Code) 265-195-920, available at http://apps.leg.wa.gov/WAC/default.aspx?cite=365-195 Accessed 10 Dec 2008

Walters C (1997) Challenges in adaptive management of riparian and coastal ecosystems. Conserv Ecol 1(2): 1

Walters CJ, Holling CS (1990) Large-scale management experiments and learning by doing. Ecology 71(6): 2060-2068

Waters D, Watt WE, Marsalek J, Anderson BC (2003) Adaptation of a storm drainage system to accommodate increased rainfall resulting from climate change. J Environ Plan and Manag 46(5) 755–770

Willows R, Connell R (eds) (2003) Climate adaptation: risk, uncertainty, and decision-making. UK Climate Impacts Programme, Oxford, England

Woods-Ballard B, Kellagher R, Martin P, Jefferies C, Bray R, Shaffer P (2007) The SUDS Manual. CIRIA, London

Image credit, page 383: see inside front cover for satellite image information.

CLIMATE IMPACTS GROUP

Climate Science
in the Public Interest